

# Kidney: Non-Neoplastic Diseases

# 23

Neeraja Kambham

## CHAPTER CONTENTS

### **Renal biopsy, 937**

Handling of the biopsy, 937

Biopsy interpretation, 938

### **Normal structure of the glomerulus, 938**

### **Classification of glomerular disease, 940**

### **Glomerular lesions associated with the nephrotic syndrome, 940**

Minimal change disease, 940

Focal segmental glomerulosclerosis, 942

C1q nephropathy, 945

Membranous glomerulonephritis, 945

Diabetic nephropathy, 948

Amyloidosis, 950

Fibrillary glomerulonephritis, 954

Immunotactoid glomerulopathy, 954

Light chain deposition disease, 954

Heavy chain deposition disease, 956

Proliferative glomerulonephritis with monoclonal immunoglobulin G deposits, 956

Congenital nephrotic syndrome, 957

### **Glomerular lesions associated with the syndrome of acute nephritis, 958**

Diffuse endocapillary proliferative glomerulonephritis, 958

C3-related glomerular diseases and membranoproliferative glomerulonephritis, 960

Diffuse mesangiproliferative glomerulonephritis, 964

Crescentic glomerulonephritis, 966

Lupus nephritis, 969

### **Glomerular lesions associated with vascular diseases, 973**

Systemic vasculitis, 973

Hemolytic uremic syndrome and thrombotic thrombocytopenic purpura, 976

Systemic sclerosis, 978

### **Renal diseases of pregnancy, 979**

Preeclampsia, 979

### **Hereditary glomerular diseases, 980**

Alport syndrome, 980

Thin basement membrane nephropathy, 981

Fabry disease, 982

Nail–patella syndrome, 983

Collagen type III glomerulopathy, 983

Fibronectin glomerulopathy, 983

### **Renal transplant pathology, 984**

Allograft rejection, 984

The Banff classification, 986

Cyclosporine A (cyclosporin) toxicity, 987

Tacrolimus (FK506) toxicity, 988

Polyomavirus nephropathy, 988

### **Tubulointerstitial diseases, 989**

Acute tubular necrosis, 989

Acute and chronic pyelonephritis, 990

Acute allergic tubulointerstitial nephritis, 992

Immunoglobulin G4–related tubulointerstitial nephritis, 992

Analgesic abuse nephropathy, 992

Heavy metals nephrotoxicity, 993

Nephrolithiasis and nephrocalcinosis, 993

Light chain cast nephropathy, 994

### **Renal vascular disease, 995**

Renal arteriolar disease, 995

Renal arterial disease, 996

### **Radiation nephropathy, 998**

Hematopoietic stem cell transplantation–associated thrombotic microangiopathy, 998

### **Cystic diseases of the kidney, 998**

Multicystic renal dysplasia, 998

Autosomal dominant polycystic kidney disease, 999

Autosomal recessive polycystic kidney disease, 1000

Nephronophthisis, 1000

Autosomal dominant tubulointerstitial kidney disease, 1001

Medullary sponge kidney, 1001

Acquired renal cystic disease, 1001

Simple cysts, 1002

## Abstract

A renal biopsy is an important tool in the evaluation of a patient with medical kidney disease. There is extensive overlap of clinical manifestations of a variety of kidney diseases, and the pathologic examination of tissues using light microscopy, immunofluorescence microscopy, and electron microscopy enables a renal pathologist to render an accurate diagnosis. Unfortunately, the host response to a variety of injurious agents also shows significant morphologic overlap. Hence, the renal biopsy interpretation should not be performed in a clinical vacuum and the value of timely communication with the nephrologist can never be underestimated. A thorough and systematic evaluation of various compartments, that is, glomeruli, tubules, interstitium, and blood vessels, points to the primary site of injury. The glomerular diseases are traditionally classified based on the presenting clinical syndrome, laboratory investigations, and morphologic pattern. Over the last two decades, many scientific advances have helped us gain insights into the relevant pathophysiological mechanisms, and these etiologic factors are being increasingly utilized in the classification of diseases. Better understanding of specific diseases such as focal segmental glomerulosclerosis, membranous glomerulonephritis, membranoproliferative glomerulonephritis, atypical hemolytic uremic syndrome, immunoglobulin (Ig)G4-related tubulointerstitial nephritis, and autosomal dominant tubulointerstitial kidney disease can aid in identifying more specific therapeutic targets. An allograft biopsy is the gold standard for assessment of graft dysfunction and institution of appropriate therapy. In addition to rejection, infections and drug toxicities can be diagnosed on biopsy and the extent of irreversible chronic changes can be estimated. Better laboratory tools and morphologic assessment methods have helped characterize the diagnostic and prognostic features of antibody-mediated rejection.

## Keywords

Glomerulonephritis,  
Vasculitis,  
Thrombotic microangiopathy,  
Renal transplant pathology,  
Kidney rejection,  
Polyomavirus nephropathy,  
Tubulointerstitial nephritis,  
Renal cystic diseases,  
Medical kidney disease,  
Renal biopsy

## Renal Biopsy

Renal biopsy is an important tool used in the evaluation of patients with renal disease.<sup>1-3</sup> Utilizing this procedure, it is possible to establish an accurate diagnosis, obtain critical information on the evolution and prognosis of the disease process, and develop a rational approach to the treatment of a renal disorder.<sup>4-6</sup> Even in advanced stages of kidney damage, a biopsy can provide clues regarding the possibility of recurrence of the disease following transplantation. The renal biopsy is also important in the management of the transplant recipient, representing the most accurate method for determining the presence of antibody- or T cell-mediated rejection, acute tubular injury, calcineurin inhibitor nephrotoxicity, or the development of de novo or recurrent glomerulonephritis in the allograft.

Renal disease is usually manifested by a limited number of symptoms that are commonly grouped in clinical syndromes, that is, nephrotic syndrome, persistent proteinuria, acute nephritic syndrome, persistent or recurrent hematuria, asymptomatic renal insufficiency, hypertension, rapidly progressive renal failure, acute renal failure, and chronic renal failure. Given the fact that the kidney reacts to a variety of injurious agents with a limited number of histopathologic patterns of injury, a given clinical syndrome can be associated with several histopathologic patterns, while a single histopathologic pattern may be linked to more than one syndrome. The accurate interpretation of a renal biopsy requires detailed knowledge of the structure and function of the normal kidney, as well as an understanding of the clinical, morphologic, and histopathogenic aspects of renal disease. To evaluate a kidney biopsy, the pathologist should correlate the clinical and laboratory information with light microscopic, immunofluorescence, and ultrastructural findings.

## Handling of the Biopsy

Most renal biopsies are done by either the percutaneous route using a cutting needle or by direct exposure of the kidney (open biopsy, often a wedge sampling of outer cortex). Most centers use 16–18-gauge needles for adults and 18-gauge needles for children less than 8 years of age. The specimen should be divided for light microscopy, immunofluorescence, and electron microscopy. Ideally, two biopsy cores should be obtained when a needle biopsy is performed. From the first core, two or more samples measuring 0.5–1 mm in thickness are taken from each end with a fresh razor or scalpel blade and placed in a cold solution of 2% glutaraldehyde in phosphate or cacodylate buffer for electron microscopy studies while the remaining tissue is placed in saline. If the second core is adequate, samples should also be taken from each end for electron microscopy, while the remainder is snap frozen in liquid nitrogen or in isopentane cooled on dry ice for immunofluorescence. For light microscopy, the tissue that was placed in saline should be transferred to a fixative, most common being 10% buffered formalin. If only one core is obtained, material should be taken from each end for electron microscopy and the remainder divided for light microscopy and immunofluorescence. If the core is too small, the specimen should be divided for electron microscopy and immunofluorescence studies since most of the light microscopic information can be obtained from the study of semi-thin sections of the plastic-embedded tissue processed for electron microscopy. Longitudinal division of the cores should be avoided. The triaging of the biopsy sample should ideally ensure that all three portions include cortex. On gross examination of the cores under dissecting microscope or loupe (magnifying device), glomeruli in well-preserved cortex appear as pale or congested bulges; however, this may not be evident when cores with sclerotic glomeruli or fibrotic interstitium are examined.

## Light Microscopy

A variety of fixatives have been recommended for the light microscopic study of renal biopsies. Zenker, Helly, Bouin, and Van der Griff fixatives are sometimes used and many pathologists feel that mercuric solutions provide the best architectural and cytologic detail. However, 10% neutral formalin can also provide good morphologic detail while also preserving the sample for future immunohistochemical studies or immunofluorescence microscopy on paraffin-embedded tissues, if needed.<sup>7,8</sup> To evaluate for glycogen or crystals of urate, uric acid, and other water-soluble substances, tissue should be fixed in ethanol. A panel of hematoxylin and eosin (H&E), periodic acid–Schiff (PAS), methenamine silver, and trichrome stains are recommended for the routine evaluation of renal biopsies, but from the practical point of view, PAS is the most useful, is easiest to perform, and can also provide most of the information obtained from other stains. It is recommended that the biopsy core be serially sectioned (2–3  $\mu$ m thick) and that three to four tissue sections be placed on each slide. At regular intervals, one slide is stained with H&E, one with PAS, one with trichrome, and another with silver stain. By following this procedure, the maximum number of glomeruli can be examined. The remaining unstained slides are saved in case special stains or immunohistochemical stains are needed.

## Electron Microscopy

There is a general misconception that electron microscopy is a complex and time-consuming procedure. In fact, satisfactory processing methods have been developed that require less than 5 hours.<sup>9</sup> Many fixatives have been developed for this procedure, each of which has specific advantages. Some pathologists prefer a primary fixation in osmium tetroxide for the optimal demonstration of deposits and basement membrane structure, but glutaraldehyde fixation with post-osmification is more convenient and is suitable as a routine procedure. For tissue embedding, various epoxy resins with comparable characteristics are available and their selection is a matter of personal preference. Semi-thin (1  $\mu$ m thick) sections obtained from the plastic-embedded tissue blocks are stained with toluidine blue or methylene blue and carefully studied as they can yield a great deal of information, especially when examined at high magnification (Fig. 23.1).<sup>10</sup> Thin sections from the blocks selected for ultrastructural study are double-stained with uranyl acetate and lead citrate for electron microscopic examination.

## Immunofluorescence Microscopy

Direct immunofluorescence performed on frozen sections is the simpler, faster, and most satisfactory method for the routine evaluation of a renal biopsy, but indirect methods may be used for extra sensitivity or for a specific antibody. The portion of the biopsy specimen selected for immunofluorescence is oriented in standard frozen section embedding compound on a piece of cork and is snap frozen by immersion in a beaker containing either isopentane or methylbutane surrounded by liquid nitrogen or dry ice. Frozen sections of 2–4  $\mu$ m thick are cut and stained with specific antibodies and examined under ultraviolet light using either transmitted or incident illumination, and the reactions are graded subjectively using a scale of 0 to 3+ (or 4+, depending on individual labs) and recorded by photography. The antibodies that are most commonly used are those against immunoglobulin (Ig)G, IgA, IgM, kappa and lambda light chains, C1q, C3, C4, and fibrinogen or fibrin. Immunostaining for a variety of other antigens can also be performed for selective diagnostic purposes. For example, C4d is very useful for the diagnosis of antibody-mediated acute allograft rejection.<sup>11,12</sup> IgG subclass

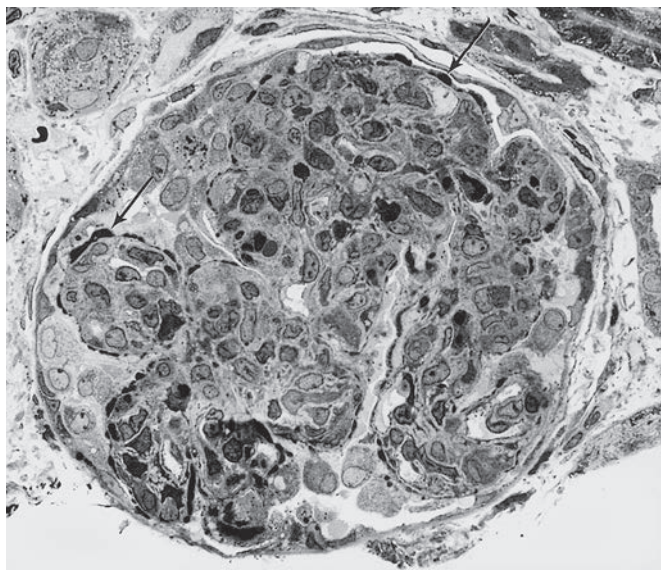


**Figure 23.1** Plastic-embedded semi-thin section stained with toluidine blue showing numerous humps along the capillary walls (arrows) and obliteration of the glomerular capillary loops by endocapillary cell proliferation in a case of poststreptococcal glomerulonephritis.

identification (IgG1, IgG2, IgG3, IgG4) and phospholipase A2 receptor 1 (PLA<sub>2</sub>R) staining is helpful in the diagnosis of primary membranous nephropathy.

In those cases in which glomeruli are not present in the portion of the submitted biopsy specimen, immunofluorescence studies can be successfully performed on pronase predigested tissue sections prepared from the portion of the biopsy allocated for light microscopy.<sup>8</sup> It should be mentioned, however, that immunofluorescence for detecting C3 on these specimens is less sensitive when compared with that performed on frozen tissue sections. In addition, anti-glomerular basement membrane (GBM) disease cannot be diagnosed by this pronase method due to high background staining.

Immunohistochemical studies can also be performed on formalin-fixed, paraffin-embedded biopsy specimens. In addition to extensive panel needed in the evaluation of incidental solid tumors or hematolymphoid neoplasms, the commonly used immunohistochemical stains in the context of medical renal biopsies include BK (or SV40) stain in the diagnosis of BK polyomavirus nephropathy,<sup>13,14</sup> adenovirus stain, cytomegalovirus stain, and C4d and amyloid A stain. Epstein–Barr virus (EBV) *in situ* hybridization is helpful in suspected cases of post-transplant lymphoproliferative disorders.

## Biopsy Interpretation

Although potentially challenging, the diagnosis of renal biopsy specimens is based on the same foundation of careful observation and clinicopathologic correlation that is used in other areas of pathology. A knowledge of normal morphology is essential for the recognition of any alteration that may occur in the various components of the kidney. Obtaining adequate clinical history is crucial to any renal biopsy interpretation. A checklist that can be used during the biopsy evaluation is provided in Table 23.1.

A renal biopsy must contain glomeruli to be considered adequate, but there is disagreement over the number of glomeruli required to make a diagnosis. The definition of adequacy largely depends on the disease under consideration. In disorders characterized by irregular or crescentic proliferation, the assessment should be based on a minimum of 10 glomeruli, whereas, in diffuse lesions (such as

membranous glomerulonephritis [MGN]), the identification of specific features in a single glomerulus may be sufficient, especially if ultrastructural studies are also performed. While there is often a variation in the severity of a specific lesion among different glomeruli, even in diffuse processes, a good guideline to follow is that at least 5–10 glomeruli should be examined to properly assess the extent of the disease.

## Normal Structure of the Glomerulus

Since most of the changes seen in renal biopsies occur in the glomerulus, we will briefly review the morphology of this structure. The glomerulus is a vascular structure composed of a tuft of specialized capillaries that arise from the afferent arteriole to form lobules, then rejoin the vascular pole to drain into the efferent arteriole. Normally, the lobules are poorly defined, but they are highlighted in some disease processes. Each lobule consists of a cluster of capillaries supported by the mesangium, which forms the centrolobular or axial framework of the glomerular tuft. The tuft of capillaries lies within the lumen of the expanded proximal end of the nephron, or Bowman space, which is lined on its parietal aspect by a layer of attenuated epithelial cells overlying a thick basement membrane. Together, the latter two structures make up the **Bowman capsule**, which is continuous at the vascular pole of the glomerulus with the adventitia of the afferent and efferent arterioles. At the urinary pole, the basement membrane of the Bowman capsule merges with that of the proximal tubule. Each glomerulus measures approximately 200 µm in diameter, but they are all not of the same size. Those located in the juxamedullary area are about 20% larger than those elsewhere in the cortex. The cellularity of the glomerulus varies in different diseases, and an accurate assessment requires histologic preparations of 2–4 µm thickness. The presence of more than three cells in an individual glomerular mesangial region away from the vascular pole is considered hypercellularity.

The walls of the glomerular capillaries are clothed by a reflected layer of cells of the Bowman capsule. These highly specialized epithelial cells are known as podocytes (visceral epithelial cells) because they have numerous tiny foot processes that rest on the basement membrane that separates them from the attenuated, fenestrated endothelium of the capillaries. The GBM is a trilaminar structure composed of a central electron-dense zone, or lamina densa, bordered by two narrow electron-lucent layers: the lamina rara interna and the lamina rara externa. The major components of the GBM are type IV collagen, laminin, heparan sulfate proteoglycans, and entactin, but minor amounts of other proteins have also been found.<sup>15</sup>

The principal function of the glomerulus is filtration, and the GBM is the main component of the filtration barrier. In normal adults, the GBM measures 310–380 nm in thickness; it is somewhat thinner in children (and achieving adult thickness by 10–12 years age), and slightly thicker in males than in females.<sup>16</sup> The GBM does not completely surround the capillary lumen since the vessel is attached to the mesangium, which consists of mesangial cells embedded in a basement membrane-like material, the mesangial matrix (Fig. 23.2). By electron microscopy, the mesangial matrix appears more fibrillar than the GBM. It is composed of collagen types IV, V, and VI, fibronectin, laminin, entactin, and sulfated glycosaminoglycans, including heparan sulfate and chondroitin sulfate.<sup>17</sup> The mesangial cells have cytoplasmic processes that contain  $\alpha$ -smooth muscle actin,  $\alpha$ -actinin, and myosin filaments, characteristics shared by smooth muscle cells, pericytes, and myofibroblasts.<sup>16,18,19</sup> Mesangial cells thus possess contractile properties and are probably involved in the regulation of blood flow through the glomeruli and modulation of the filtration process.<sup>20</sup> They produce growth factors that allow normal cell turnover.<sup>19</sup> Mesangial cells may also have some phagocytic

**Table 23.1** Biopsy evaluation checklist

	<b>LIGHT MICROSCOPY</b>	<b>IMMUNOFLUORESCENCE</b>	<b>ELECTRON MICROSCOPY</b>
Glomeruli	Size and cellularity Segmental or global changes Mesangium Leukocytes Capillary walls/lumens Necrosis Thrombi (type) Adhesions to Bowman capsule Deposits (type and location) Crescents (type and %) Sclerosis (distribution and %)	Positive/negative reaction Reagent Igs, complement, fibrin, etc. Distribution (mesangium, capillary wall, intracapillary globules) Pattern (linear or granular or smudgy) Intensity Necrosis, cellular crescents or intracapillary thrombi on fibrin stain	Basement membrane (thickness, density, contours, disruptions) Cellular changes Mesangium Deposits (type, location, and substructure) Inclusions in endothelial cells
Tubules	Necrosis Reparative changes Dilation Casts (type) Crystals Cellular inclusions Vacuolization Basement membrane	Reactions and pattern Intensity	Cellular changes Inclusions Basement membrane Deposits (type and location)
Blood vessels	Intimal thickening (type) Elastica changes Media hypertrophy Hyalinosus Thrombi Necrosis Inflammation Juxtaglomerular apparatus	Reactions and distribution Thrombi or vasculitis on fibrin stain	Intimal and medial changes Deposits
Interstitium	Edema Inflammation and fibrosis (cell type and %)	Reactions and distribution	Cellular infiltrates Deposits

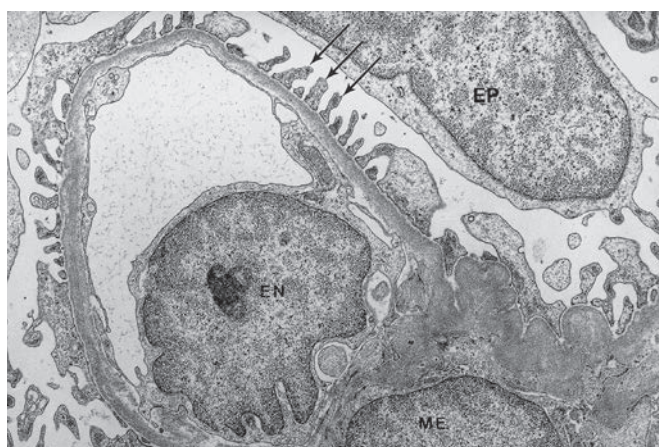


**Figure 23.2** Electron Micrograph of Normal Glomerulus Showing the Relationship of Different Cell Types. The epithelial aspect of the basement membrane is covered by foot processes (arrows) and the capillary lumen lined by attenuated endothelium. EN, Endothelial cell; EP, epithelial cell; ME, mesangium (x13,000).

activity and play a role in the clearance of debris, including immune deposits from the mesangium.<sup>21</sup> Although obvious ultrastructural differences exist between the endothelial and mesangial cells, these differences are not always evident in glomerular diseases, and the distinction between the endothelium and the mesangium is usually based on the location of these structures in the glomerulus.

The visceral epithelial cells/podocytes are involved in basement membrane synthesis and, by their unique structure, play an important role in glomerular permeability. These cells cover the GBM on its urinary side and are attached to it by cytoplasmic extensions or foot processes that, under the scanning electron microscope, appear as a complex of interdigitating structures originating from different epithelial cells (Fig. 23.3). The foot processes are approximately 25–60 nm apart, with a connecting slit-pore diaphragm 4–7 nm thick that shows similarities with tight and adherens junctions. Several molecules identified in podocyte foot processes and slit diaphragms over the last two decades contribute to the structural integrity and permselectivity of the filtration barrier.<sup>22</sup> Bowman capsule limits the urinary space and is lined by a layer of flattened parietal epithelial cells that express cytokeratin proteins. In contrast, the visceral epithelial cells do not immunoreact for cytokeratin but do for vimentin and desmin.<sup>23</sup> Recent evidence suggests that parietal epithelial stem

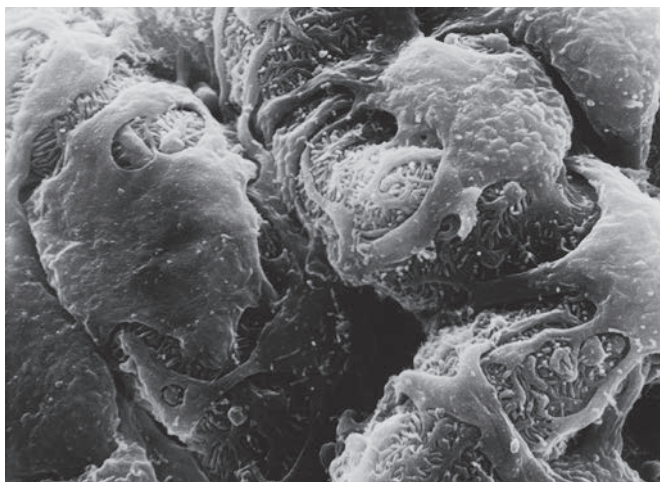


**Figure 23.3** Scanning electron micrograph showing the capillary loops covered by visceral epithelial cells and interdigitating foot processes (x8000).

#### Box 23.1 Classification of glomerular disease by distribution

Classification of disease distribution when many glomeruli are considered

Focal: disease affecting only some of the glomeruli

Diffuse: disease affecting most or all glomeruli

Classification of disease distribution when single glomeruli are considered

Segmental: a lesion involving only a part of the glomerulus

Global: a lesion involving the entire glomerulus

cells are critical in glomerular repair and maybe involved in the regeneration of podocytes and tubular epithelial cells.<sup>24,25</sup>

## Classification of Glomerular Disease

Glomerulonephritis is a term denoting an inflammation of the glomerulus, while glomerulopathy is an all-embracing term for disorders affecting this structure. In glomerular diseases, other parts of the nephron may also be involved, but the diagnosis hinges on the identification of a derangement of the normal glomerular configuration. While the changes may be recognizable by routine light microscopy, the findings from immunofluorescence are often significant. Electron microscopy is always informative and is sometimes the only means whereby the structural changes can be detected and defined. The damage to the glomeruli may take the form of definable morphologic patterns, and subdivisions in the character or distribution of the glomerular lesions are used to classify glomerulonephritis. Although there is general agreement on the definitions applied to the distribution of glomerular lesions (Box 23.1), more specific categorizations are sometimes controversial.

In this chapter, glomerular lesions are subdivided into those associated with the nephrotic syndrome or persistent proteinuria, those seen in acute nephritis or hematuria, and lesions associated with vascular diseases, such as systemic vasculitis, hemolytic uremic syndrome (HUS), and systemic sclerosis. Separate sections, including those describing tubulointerstitial lesions, renal vascular disorders, cystic diseases, and the interpretation of biopsies of transplanted kidneys, will be presented.

## Glomerular Lesions Associated With the Nephrotic Syndrome

The nephrotic syndrome is clinically characterized by the occurrence of massive proteinuria, hypoproteinemia, edema, and hyperlipidemia. Damage to the filtration barrier of the glomerulus allows proteins, particularly albumin, to be filtered into the urine. The criterion for the syndrome is the excretion of more than 3.5 g of protein in a 24-hour period. A spectrum of morphology has been correlated with the syndrome, but some glomerular lesions are not accompanied by significant inflammatory or proliferative response within the glomerulus, including primary nephrotic syndrome with minimal change disease (MCD), MGN, diabetes mellitus, amyloidosis, and various forms of congenital nephrotic syndrome. The major histologic, electron microscopic, and immunofluorescence findings in each of these conditions are summarized in Table 23.2.

### Minimal Change Disease

MCD (also known as nil lesion, and minimal change nephrotic syndrome) is the most common cause of idiopathic nephrotic syndrome in children, accounting for 80%–90% of all cases of idiopathic nephrotic syndrome in childhood,<sup>26,27</sup> and 10%–15% of adult cases.<sup>28,29</sup> Most of the affected children are under the age of 6 years at initial diagnosis, the majority being 3 or 4 years old.<sup>26,27</sup> There appears to be a male predominance, especially in children, where the male to female ratio is 2 to 3:1.<sup>30</sup> MCD is more common among whites, Asians, and Hispanics than blacks.<sup>31</sup> While MCD is idiopathic in 80%–90% of children, in a minority of cases it has been associated with viral infections, recent immunizations, ingestion of heavy metals (e.g., mercury or lead), allergies to some foods, dust, bee stings, and poison ivy, and drug reactions to a variety of agents, including lithium, interferon, and pamidronate. While the exact mechanism of MCD development is unclear, the final common event likely involves podocyte injury. In adult patients, especially the elderly, MCD can manifest as a hypersensitivity reaction to the use of nonsteroidal anti-inflammatory drugs.<sup>32</sup> In these cases, the disease is often accompanied by renal insufficiency and the development of acute interstitial nephritis.<sup>33</sup> In most of these patients, cessation of the offending medication results in resolution of the proteinuria. MCD has also been reported in association with lymphoid malignancies, usually Hodgkin lymphoma.<sup>34</sup> Remission of the nephrotic syndrome has been obtained in these cases with the cure of the lymphoma. Other neoplastic diseases that might cause MCD include leukemias, carcinomas, and thymomas, among others. MCD is a now well-defined renal manifestation of lupus nephritis or may be seen in recipients of hematopoietic stem cell transplantation.<sup>35,36</sup> De novo MCD has been reported in patients with post-transplant nephrotic syndrome.<sup>37</sup> None of the recipients had focal segmental glomerulosclerosis (FSGS) as a primary disease. The pathogenesis of idiopathic MCD remains unknown, but it has been suggested that a circulating factor/s produced by T lymphocytes that damage one or more elements of the glomerular permeability barrier is responsible for the proteinuria seen in this condition.<sup>38,39</sup> Patients with MCD do show T-cell subset abnormalities, and elevated levels of interleukin-13 (IL-13) were demonstrated during relapses.<sup>40</sup> IL-13 has been shown to increase the expression of CD80 in podocytes. CD80, in turn, has been identified in the urine of patients of MCD and appears to be a potential diagnostic biomarker.<sup>41</sup> Various injurious stimuli appear to activate the podocyte enzymatic pathways, resulting in disruption of actin cytoskeleton and slit diaphragm. In addition to structural disruption of the permeability barrier, the loss of podocyte negatively charged glycocalyx may contribute to the selective leakage of anionic plasma proteins such as albumin.

**Table 23.2** Glomerular lesions associated with the nephrotic syndrome

DISEASE	LIGHT MICROSCOPY	IMMUNOFLUORESCENCE	ELECTRON MICROSCOPY
Minimal change disease	Normal; minimal or no mesangial prominence	Usually negative for Ig and C3	Extensive foot process effacement
Focal and segmental glomerulosclerosis	Focal and segmental glomerulosclerosis	Nonspecific trapping of IgM and C3 in sclerosed segments	Extensive foot process effacement
C1q nephropathy	Mesangial hypercellularity common, $\pm$ focal segmental glomerulosclerosis	C1q mesangial granular deposits	Mesangial deposits
Membranous glomerulopathy	Uniform capillary wall thickening, sometimes with spike and dome pattern	IgG and C3 granular deposits along capillary wall (IgM, IgA, C1q in membranous lupus nephritis)	Four stages of subepithelial and intramembranous deposits
Diabetic nephropathy	Nodular and diffuse mesangial sclerosis; insudative lesions	IgG linear staining along capillary walls and tubular basement membranes	Diffuse thickening of basement membranes; increased mesangial matrix
Amyloidosis	Mesangial, capillary wall, and vascular amorphous deposits; weak PAS; methenamine silver negative; Congo red positive with apple-green birefringence	Based on subtype, smudgy staining for Ig light or heavy chains, amyloid AA, or other	Fibrils 8–10 nm in diameter
Light chain deposition disease	Mesangial widening and deposition of PAS-positive material	Kappa or lambda light chain restricted; granular mesangial and linear basement membranes	Finely granular material along the basement membranes, mesangium
Heavy chain deposition disease	Mesangial widening and deposition of PAS-positive material	Isolated heavy chain-restricted (frequently $\gamma$ ); granular mesangial and linear basement membranes	Finely granular material along the basement membranes, mesangium
Fibrillary glomerulonephritis	Mesangial widening and occasional hypercellularity, capillary wall thickening	Variable IgG, C3, occasional IgM, IgA; frequently polypic	Fibrils 16–20 nm in diameter
Immunotactoid glomerulopathy	Mesangial widening and occasional hypercellularity, capillary wall thickening	Variable IgG, C3, occasional IgM; frequently monotypic with light chain restriction	Fibrils 30–50 nm in diameter, often in parallel bundles
<b>Congenital Nephrotic Syndrome</b>			
Finnish type	Tubular ectasia, microcysts, glomerular sclerosis	Nonspecific trapping of IgM and C3	Diffuse foot process effacement
Diffuse mesangial sclerosis	Mesangial consolidation, pseudocrescents, fetal glomeruli	Negative or nonspecific trapping of IgM and C3	Diffuse foot process effacement

MCD typically presents with heavy proteinuria, often of selective type, leading to the nephrotic syndrome. Microscopic hematuria is seen in less than 15% of patients,<sup>42</sup> but macroscopic hematuria is rare. Blood pressure is usually normal at onset, and less than 20% of patients have hypertension.<sup>43</sup> Given the high probability that nephrotic syndrome in a child is due to MCD, pediatric patients are treated empirically with steroids and do not undergo a renal biopsy unless the nephrotic syndrome is steroid resistant. Complete remission is common within 8 weeks of starting corticosteroid therapy.<sup>26,27</sup> After withdrawal of the steroids, however, about half of the patients have intermittent relapses, a phase which may last for up to 10 years. The relapses are usually steroid responsive and the disease does not progress to chronic renal failure. Patients who achieve only partial remission with corticosteroid therapy may benefit from immunosuppressive drugs such as cyclophosphamide or cyclosporine.<sup>29</sup> Newer agents such as anti-CD20 and anti-CTLA-4 (cytotoxic T-lymphocyte-associated protein 4) antibodies are being tested in such patients.<sup>44,45</sup> The

development of azotemia should suggest an incorrect diagnosis and should raise the possibility of missed FSGS. Relapse is uncommon after a disease-free interval of 2 years.

The glomeruli in MCD appear normal or show minimal abnormality by light microscopy (Fig. 23.4). The glomerular capillaries are patent, and there is no increase in the thickness of the capillary walls, but podocyte hypertrophy may be appreciated. Some cases may show minor degrees of mesangial enlargement with a minimal increase in mesangial matrix and cellularity. The convoluted tubules may present focal vacuolization due to the accumulation of large amounts of lipid and protein transport droplets. Because of these light microscopic features and the finding of lipoid particles (oval fat bodies) in the urine of these patients, Munk in 1913 proposed the term lipoid nephrosis for this condition.<sup>46</sup> Only after ultrastructural studies were done in such cases was it established that the glomeruli, rather than the tubules, were the primary site of pathology. It should be borne in mind that biopsies from adult or elderly patients may

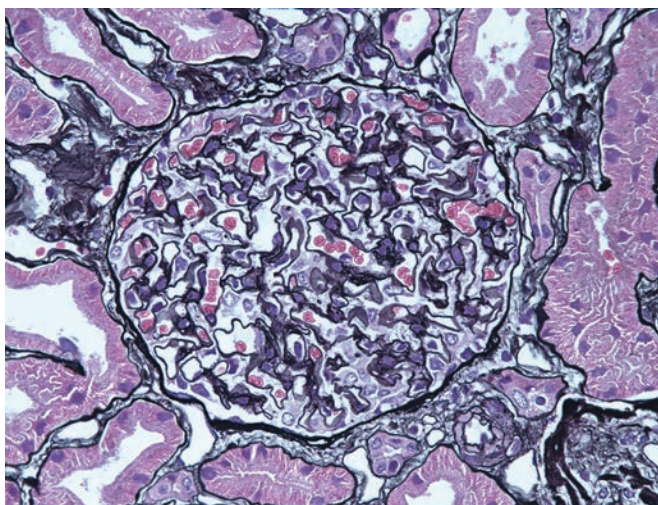


**Figure 23.4** Glomerulus From a Patient With Minimal Change Disease. The glomerulus is normocellular, the capillary loops are patent, and the basement membrane is normal in thickness.

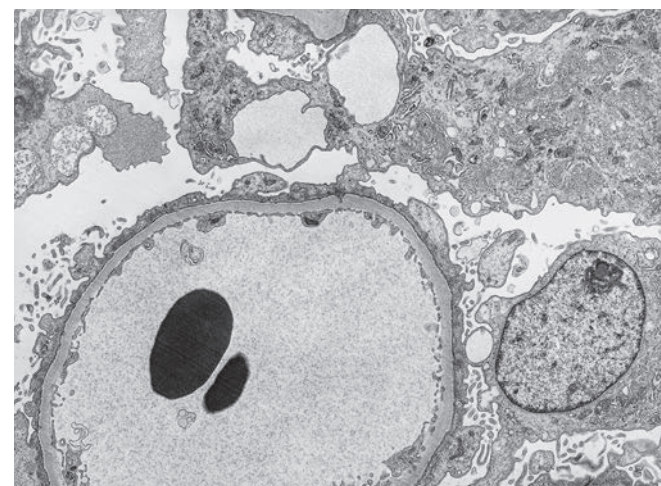


**Figure 23.5** Portion of a glomerulus from a patient with minimal change disease showing obliteration of foot processes. The visceral epithelial cell cytoplasm shows microvillus and cyst formation (x8400).

not be entirely normal on light microscopy and can show a variety of preexisting pathologies such as age-related glomerulosclerosis, hypertensive arteriosclerosis, chronic tubulointerstitial damage, or mild diabetic nephropathy.

The characteristic ultrastructural appearance of the glomeruli is of total foot process effacement with the basement membrane being covered by sheets of cytoplasm. Loss of the visceral epithelial processes is accompanied by distortion of the filtration slits, with a decrease in the number of slit diaphragms.<sup>47</sup> Visceral epithelial cells/podocytes show prominent intracytoplasmic organelles, suggesting increased cytoplasmic activity, and frequently contain cystoplasmic cysts/vacuoles. Numerous microvilli (i.e., villous projections of podocyte cytoplasm into urinary space) are often seen in MCD (Fig. 23.5). There is a frequent increase in the density of the cytoskeleton, especially actin filaments, in the cytoplasm adjacent to the basement membrane, but no electron-dense deposits are present. Lower degrees of podocyte foot process effacement may be observed in MCD patients with partial response to therapy.

Immunofluorescence studies are almost invariably negative for immunoglobulin and complement, but small amounts of IgM and C3 can occasionally be seen in cases with mesangial prominence. Albumin can be demonstrated as fine droplets in the cytoplasm of the proximal tubule cells when the tissue is stained for this protein (Fig. 23.6).

Because a biopsy is susceptible to sampling error, it should be kept in mind that lesions that affect only some glomeruli, such as FSGS, can lead to a misdiagnosis of MCD. Conversely, since tubular atrophy (TA) and interstitial scarring are not features of MCD, a diagnosis of FSGS should be considered if these findings are seen on a biopsy, especially in a child. It has been recently proposed that reduced expression of dystroglycan and CD44 observed in MCD can help differentiate it from FSGS, but further confirmation is needed.<sup>48,49</sup>

### Focal Segmental Glomerulosclerosis

FSGS, as a disease entity, is a clinicopathologic syndrome characterized by proteinuria, commonly in the nephrotic range, a high incidence of progressive renal failure, and focal and segmental sclerotic glomerular lesions. The segmental sclerosis results from an increase in mesangial matrix, causing obliteration of the glomerular capillaries.

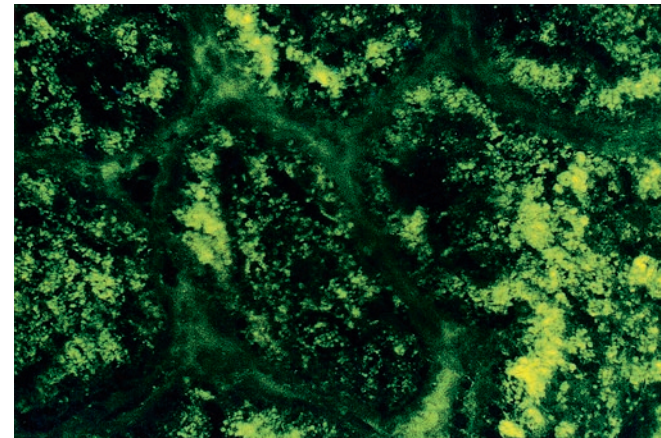


**Figure 23.6** Immunofluorescence preparation demonstrating numerous albumin-positive resorption droplets in the proximal tubular epithelial cells.

Five histologic subtypes have been described, including collapsing variant, "tip" lesion, cellular variant, perihilar lesion, and FSGS-NOS (not otherwise specified) variant.<sup>50,51</sup> This histologic classification is hierarchical and is referred to as "Columbia classification of FSGS." The presence of even a single collapsing lesion qualifies for a diagnosis of collapsing variant of FSGS. In the absence of a collapsing FSGS lesion, a "tip lesion," if present, trumps other variants. The next lesion in the hierarchy is cellular FSGS, followed by perihilar and NOS variants. Although the FSGS lesion identified in the biopsy may change over time in an individual patient, these morphologic variants do have clinical relevance.<sup>52-54</sup> The patients with collapsing FSGS have poor outcomes while patients with a "tip" variant respond well to immunosuppressive therapy, akin to MCD. Perihilar variants often point to a structural adaptive response to renal parenchymal loss or glomerular hyperfiltration due to a variety of other etiologies; the renal presentation is usually subnephrotic proteinuria rather than a full nephrotic syndrome as would be more common with collapsing and tip variants.

From an etiologic standpoint, FSGS may be primary or secondary to various forms of injuries or pathogenic mechanisms. The morphologic variants of FSGS are not helpful in distinguishing primary

from secondary FSGS and a biopsy diagnosis of FSGS should prompt an evaluation of etiology. The pathogenesis of primary FSGS is unknown, but it appears to be the result of circulating "permeability" factor(s), possibly a lymphokine or a cytokine, which leads to epithelial cell injury resulting in segmental scar and ultimately glomerular obsolescence.<sup>55</sup> The potential circulating permeability factors include cardiotrophin-like cytokine 1 and urokinase plasminogen activator receptor, but they have not been shown to be entirely sensitive or specific.<sup>52,56</sup>

FSGS can be secondary to a variety of conditions including drugs, viral infections, healed glomerulonephritis, and structural adaptive responses. In addition, genetic associations with either autosomal dominant or recessive mode of inheritances are being increasingly recognized as a cause of FSGS.<sup>52,57,58</sup> Mutations have been detected in several podocyte genes encoding proteins in the slit diaphragm, cytoskeleton, mitochondria, transcription, and DNA repair. Several patients with FSGS who would have been previously categorized as a "idiopathic" FSGS might in fact have a genetic form of FSGS.<sup>52,59</sup> Even in cases without a single gene mutation, there appears to be a familial susceptibility to developing FSGS. Recent studies have established a strong association between apolipoprotein L1 (*APOL1*) gene and FSGS in blacks.<sup>60,61</sup> The risk alleles G1 and G2 are more commonly seen in blacks and are also linked to higher rates of progressive kidney disease. The *APOL1* gene product is expressed in podocytes and platelets and although the exact mechanism of kidney disease causation is unknown, the risk alleles appear to confer an evolutionary protection against *Trypanosoma brucei* infections.<sup>60</sup>

The glomerular lesion of secondary FSGS can be histologically identical to that seen in primary FSGS and can occur in a variety of clinical settings with a clinical presentation indistinguishable from that of primary FSGS. Since the pathogenetic mechanisms involved in these disorders and their treatment differs significantly from that of primary FSGS, it is of paramount importance that they be excluded before a diagnosis of primary FSGS is made.<sup>62-64</sup> In **Box 23.2** are listed the conditions most commonly associated with FSGS which should be excluded before making the diagnosis of primary FSGS.

Primary FSGS is responsible for approximately 10%–15% of the cases of nephrotic syndrome in children and 20%–30% in adults. It constitutes the predominant cause of idiopathic nephrotic syndrome in adult patients, especially in blacks.<sup>65</sup> Nephrotic range proteinuria is common and the clinical manifestation can be an abrupt onset of nephrotic syndrome or insidious onset of subnephrotic proteinuria. Examination of the urinary sediment will often lead to the detection of microscopic hematuria. Forty to 60% of patients have been shown to develop end-stage renal disease (ESRD) within 10–20 years,<sup>66,67</sup> and recurrence following transplantation has been reported in 30%–40% of patients, often within weeks, leading to graft loss.<sup>68-72</sup> The response to steroid therapy is limited, often prompting a second line of aggressive immunosuppressive therapy and plasmapheresis that aids the removal of the circulating permeability factor.

Pathologically, in primary or secondary FSGS, the segmental sclerosis, collapse, or obliteration of capillary lumen (i.e., depending on the morphologic variants) usually affects one or more lobules of the glomerular tuft. Early lesions may show an increased mesangial matrix and mild mesangial hypercellularity; only when the sclerosis is advanced do these areas become hypocellular, often with adhesions to the Bowman capsule (Fig. 23.7). The visceral epithelial cells can line the sclerotic segments and these adhesions, and hence the term "podocyte capping." The loops in the sclerosed areas are distorted, and they may contain hyaline material (hyalinosis), which is thought to represent plasmatic insudation, and lipid-laden "foam" cells.<sup>73</sup> These findings in the absence of collapsing, cellular and tip variant features (described later) and present in a nonperihilar distribution define a FSGS-NOS subtype.<sup>50,58</sup>

**Box 23.2** Focal segmental glomerulosclerosis: etiologic classification

Primary (idiopathic) FSGS

Secondary FSGS

Genetic

Mutations in podocyte genes *NPHS1* (nephrin), *NPHS2* (podocin), *PLCE1* (phospholipase C  $\epsilon$ 1), *ACTN4* ( $\alpha$ -actinin 4), *CD2AP* (CD2-associated protein), *WT1* (Denys-Drash syndrome),

Mutations in basement membrane genes *COLA3*, *COLA4* (Alport syndrome), genes encoding  $\beta_4$  integrin and laminin  $\beta_2$

Mitochondrial cytopathies

Others

Viral infections

HIV-1, parvovirus B19, cytomegalovirus, simian virus 40, Epstein-Barr virus

Drugs

Heroin, interferon  $\alpha$  and  $\beta$ , lithium, bisphosphonates, sirolimus, calcineurin inhibitors, anabolic steroids

Glomerulonephritis

Healed focal segmental glomerular lesions

Mediated by adaptive-functional responses

Reduced renal mass and/or nephrons: unilateral renal agenesis, dysplasia/hypoplasia, oligomeganephropenia, prematurity/low birth weight, partial cortical necrosis, surgical renal ablation, reflux nephropathy, any advanced renal disease with reduction in functional nephrons

Initially normal renal mass: hypertension, morbid obesity, cyanotic congenital heart disease, glycogen storage diseases, sickle cell anemia

Modified from D'Agati VD, Kaskel FJ, Falk RJ. Focal segmental glomerulosclerosis. *N Engl J Med*. 2011;365(25):2398-2411.

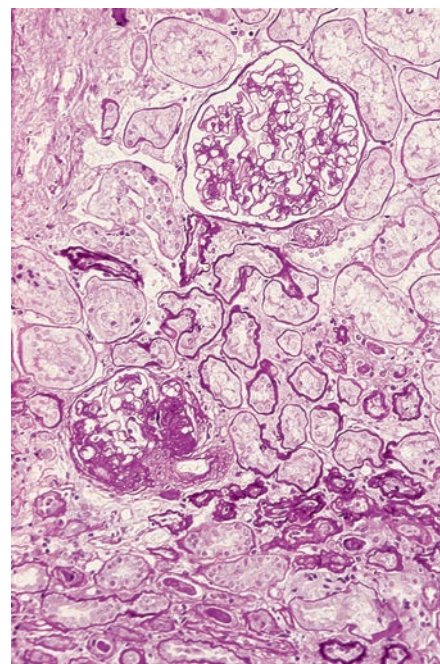


**Figure 23.7** Biopsy From a Patient With Focal and Segmental Glomerulosclerosis. One of the glomeruli shows segmental sclerosis, while the other appears unremarkable. Tubular atrophy is also seen (periodic acid-Schiff stain; PAS).

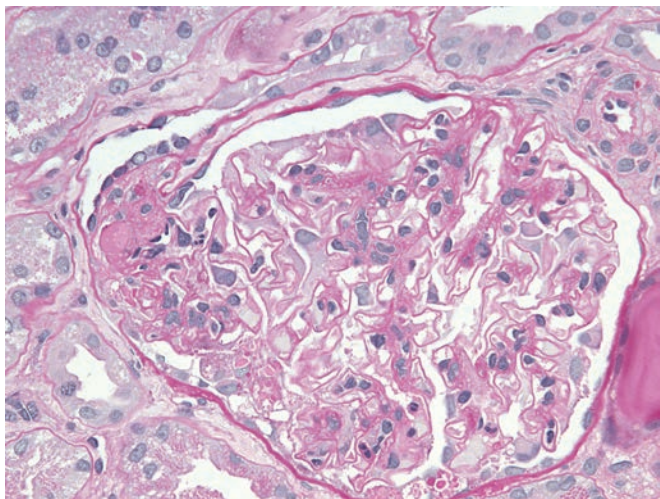


**Figure 23.8** Tip variant of focal segmental glomerulosclerosis shows Bowman capsular adhesion and hyaline insudation at the tubular pole. The adjacent podocytes also show hypertrophy with cytoplasmic protein droplets (PAS).

On occasion, sclerosis or consolidation is seen in the portion of the glomerulus opposite the hilus forming an adhesion in the vicinity of the opening of the Bowman space into the proximal tubule (glomerular tip lesion).<sup>74</sup> The consolidated portion of the capillary tuft in "tip" lesion may display endothelial swelling and entrapped foam cells (Fig. 23.8). The visceral epithelial cells overlying the involved segment are enlarged and vacuolated and often contain intracytoplasmic hyaline droplets. Some lesions are less cellular with an increase in mesangial matrix. The sclerotic segments in "perihilar" variant are localized next to the vascular pole, and it is a typical finding in secondary forms of FSGS attributable to adaptive functional response. The most controversial and least common subtype is the "cellular" variant in which the segmental lesion demonstrates intracapillary hypercellularity, and sometimes foam cells and karyorrhexis; hyperplasia of overlying podocytes is quite common. The collapsing FSGS lesion is described in detail in the subsequent section.

The extent of capillary tuft affected by sclerosis increases with eventual global sclerosis as the disease progresses. Areas of TA are common, and while this finding is not by itself diagnostic of FSGS, it should raise the possibility in biopsies which otherwise show MCD.<sup>75</sup> Interstitial fibrosis (IF) accompanies tubular loss and atrophy, and the extent of the tubulointerstitial damage is a prognostic indicator of the disease.<sup>64,76,77</sup> Since the glomerular injury in FSGS typically begins in the corticomedullary region, the lesion can be missed if this population of glomeruli is not included in the biopsy.

As FSGS represents podocyte injury, the most significant ultrastructural feature to be evaluated is podocyte foot process effacement, especially in capillary loops (and glomeruli) unaffected by sclerosis. Extensive podocyte foot process effacement is a feature of primary FSGS and is often seen in collapsing, tip, and cellular FSGS subtypes. Some secondary forms of FSGS and perihilar morphologic variants typically have less degree of foot process effacement.<sup>53,78,79</sup> A variable increase in mesangial matrix is customary in all glomeruli, and some degree of mesangial hypercellularity is not uncommon. In sclerosed segments, the GBMs are often folded and focally thickened; on occasion, foci of podocyte cell membrane detachment from GBM are seen and intervening space can accumulate multilayered basement membrane-like material and cellular debris. The hyaline deposits are composed of finely granular material that has a similar appearance

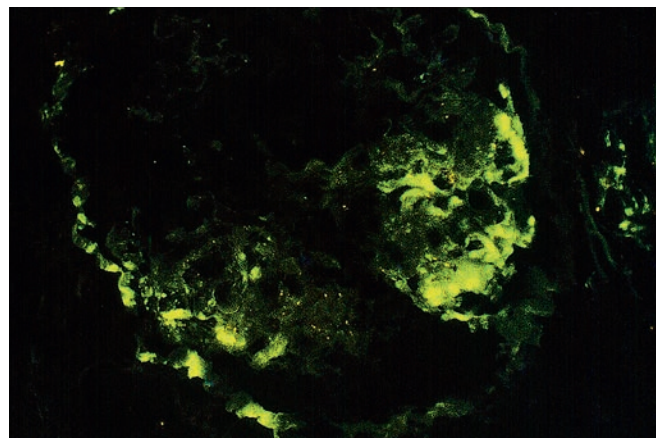


**Figure 23.9** Immunofluorescence microscopy demonstrating segmental deposition of IgM in a biopsy from a patient with focal and segmental glomerulosclerosis (anti-IgM).

and electron density to that of the insudative material seen in diabetic nephropathy. These insudations are predominantly subendothelial and located in the areas of segmental sclerosis; immunofluorescence studies show that they contain IgM and C3 (Fig. 23.9), but no immunoglobulin or complement deposition is seen in unaffected glomeruli.

### Collapsing Glomerulopathy

Collapsing glomerulopathy is a clinically and pathologically distinct variant of FSGS that is characterized by the widespread collapse of glomerular capillary loops, and predominance in blacks attributable to the *APOL1* risk alleles.<sup>50,60,80</sup> Patients usually present with abrupt onset of nephrotic syndrome or nephrotic range proteinuria and renal impairment. An idiopathic form of collapsing FSGS<sup>81,82</sup> has poor prognosis with rapid loss of renal function and virtually no response to immunosuppressive therapy.<sup>83</sup> A circulating permeability factor might be responsible as evidenced by a rapid recurrence in an allograft.<sup>84</sup> Collapsing FSGS can be a secondary process associated with intravenous (IV) drug abuse and/or human immunodeficiency virus (HIV) infection.<sup>85-87</sup> This variant of FSGS constitutes about 80%–85% of the glomerular changes reported in HIV-infected patients.<sup>88</sup> Collapsing glomerulopathy has also been reported in association with some autoimmune diseases, lymphoproliferative disorders, drugs such as bisphosphonates and interferons, severe allograft ischemia, and non-HIV viral infections, such as hepatitis C, cytomegalovirus, and parvovirus B19.<sup>52,85,89,90</sup> Treatment of the underlying cause is helpful in inducing remission in these secondary forms.

The characteristic histologic feature is a predominantly collapsing type of focal glomerulosclerosis that is segmental and often global. The segmental sclerosis is characterized by localized hypertrophy and hyperplasia of the epithelial cells overlying the collapsed segment (Fig. 23.10).<sup>91</sup> These cells are often swollen and vacuolated and may contain abundant resorption droplets. The presence of even a single glomerulus with collapsing FSGS lesion is adequate for this diagnosis. The hyperplastic epithelial cells in this lesion represent either a proliferation of dysregulated podocytes or migrated parietal epithelial cell in response to injury.<sup>92-94</sup> Relative to the extent of glomerular sclerosis, tubulointerstitial injury is more severe in collapsing glomerulopathy than in typical FSGS. The tubular epithelial cells may present degenerative changes and the tubular lumens are often markedly dilated and show extensive proteinaceous cast formation.

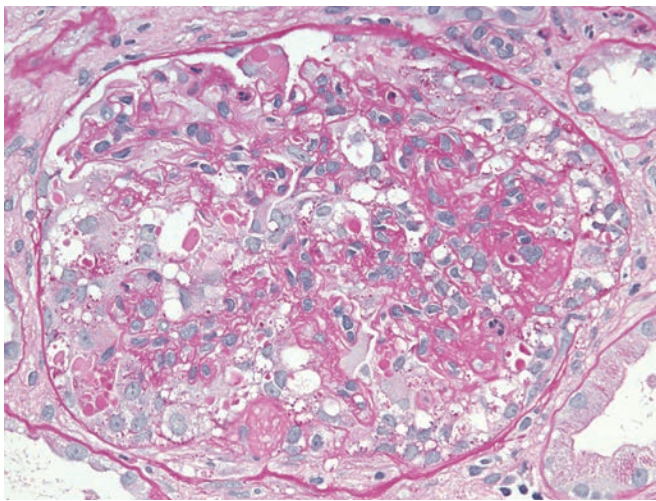


**Figure 23.10** Collapsing variant of focal segmental glomerulosclerosis lesion is characterized by the retracted glomerular basement membrane and hyperplastic overlying podocytes obliterating the Bowman space. The podocytes have prominent cytoplasm protein droplets (PAS).

The interstitium often exhibits a prominent inflammatory infiltrate mainly composed of lymphocytes.

The most common immunofluorescence finding in the glomeruli in patients with collapsing glomerulopathy is IgM and C3 in a segmental distribution in the lesional glomerulus. Less commonly, C1q may also be localized. The podocyte protein resorption droplets are highlighted by IgG, IgA, and albumin. The changes seen by electron microscopy are generally those of typical FSGS, and the podocyte foot processes are extensively effaced. The GBM is diffusely wrinkled in areas of collapse. A distinctive but nonspecific feature is the finding of endothelial tubuloreticular inclusions in over 90% of patients with HIV-associated collapsing glomerulopathy.<sup>95,96</sup> These structures are rarely seen in idiopathic collapsing glomerulopathy or in collapsing glomerulopathy associated with other causes. Numerous endothelial tubuloreticular inclusions are also seen in patients with systemic lupus erythematosus (SLE) or in patients treated with interferon alpha.

### C1q Nephropathy

C1q nephropathy is a relatively uncommon and controversial immune complex-mediated glomerulopathy that is characterized by the presence of dominant or codominant C1q deposition in the mesangium. Patients may present with nephrotic syndrome or mild proteinuria with or without hematuria.<sup>97–100</sup> The condition typically affects adolescents and young adults and appears to be more common in blacks than in whites.<sup>99,101,102</sup> C1q nephropathy with normal histology or mesangial proliferation responds to corticosteroids, but FSGS histology is associated with poorer outcome.<sup>103</sup> Progression to renal failure is slow, and it has been estimated that the 5-year renal survival rate is about 78%.<sup>101</sup> It is not entirely clear as to whether C1q nephropathy is a specific clinical entity or is part of the clinicopathologic spectrum of MCD and FSGS.<sup>102,104</sup>

Light microscopic findings vary from slight to marked mesangial hypercellularity with an increase in mesangial matrix, with or without segmental glomerulosclerosis. Electron microscopy studies invariably demonstrate mesangial immune complex deposits. Subendothelial or subepithelial deposits are uncommon. On immunofluorescence, C1q is often accompanied by IgG, IgM, and C3; IgA has been reported in about 60% of the cases.<sup>100</sup> The main differential diagnosis of C1q

### Box 23.3 Entities associated with membranous glomerulopathy

#### Autoimmune disease

Autoantibodies to phospholipase A2 receptor (~80% of “primary” MGN)

Autoantibodies to THSD7A (~10% of “primary” MGN)

Systemic lupus erythematosus, mixed connective tissue diseases, Sjögren syndrome, rheumatoid arthritis, IgG4-related systemic disease, sarcoidosis, Hashimoto thyroiditis, Graves disease, Weber-Christian panniculitis, myasthenia gravis, bullous pemphigoid, autoimmune enteropathy, primary biliary cholangitis

#### Infections

Hepatitis B, hepatitis C, syphilis, Epstein–Barr virus, malaria, leprosy, tuberculosis, schistosomiasis, filariasis, hydatid disease, enterococcal endocarditis, brucellosis, staphylococcal infection

#### Neoplastic diseases

Carcinoma (lung, gastrointestinal tract, breast, prostate, kidney), seminoma, lymphoma (especially non-Hodgkin), leukemia, melanoma

#### Drugs and toxic agents

Nonsteroidal anti-inflammatory drugs, D-penicillamine, bucillamine, anti-tumor necrosis factor agents, organic gold, probenecid, captopril, trimethadione, lithium, clomethiazole, diclofenac, hydrocarbons, formaldehyde, solvents, mercury

#### Alloimmune etiology

*De novo* MGN due to chronic antibody-mediated rejection, graft versus host disease in hematopoietic stem cell transplantation, neutral endopeptidase directed response in neonatal MGN, replacement therapy with recombinant aryl sulfatase and  $\alpha$ -glucosidase

#### Miscellaneous associations

Sickle cell disease, diabetes mellitus, Kimura disease, sclerosing cholangitis, antiglomerular basement membrane disease, cryoglobulinemia, Guillain–Barré syndrome

MGN, Membranous glomerulonephritis; THSD7A, thrombospondin type-1 domain-containing 7A.

nephropathy is lupus nephritis which can also have prominent C1q deposition in the mesangium together with immunoglobulins and C3. Clinical presentation, serologic evidence, extraglomerular deposits, and presence of tubuloreticular inclusions help differentiate between class II lupus nephritis and C1q nephropathy.

### Membranous Glomerulonephritis

MGN (a.k.a. membranous nephropathy) is a glomerular disease of diverse etiology characterized by subepithelial immune complex deposits and variable basement membrane thickening, without infiltration by inflammatory cells. MGN accounts for 20%–30% of all cases of idiopathic nephrotic syndrome in adults<sup>105</sup> and 1%–9% in children.<sup>106</sup> In large majority of cases, this condition occurs in a primary (“idiopathic”) form, but the disease has been related to a wide variety of conditions (secondary) in approximately 20%–25% of adults and 80% of children with MGN (Box 23.3).<sup>107</sup> Over 85% of cases of secondary MGN are caused by infection, neoplasia, or SLE. The most common causes worldwide are malaria and schistosomiasis, while SLE, neoplasia, hepatitis B infection, and drugs are the most frequent in the United States.<sup>107</sup> Rare familial cases of MGN, probably related to a genetically transmitted mechanism, have been reported.<sup>108</sup>

The pathogenetic mechanism that leads to the immune complex localization in the subepithelial aspect of the GBM, especially in primary forms, is being increasingly understood. Two mechanisms presumed responsible for the development and localization of the deposits along the GBM are that of *in situ* immune complex formation in the subepithelial capillary wall or that of circulating immune complexes being deposited in that location. Experimental studies suggest that in most cases, the immune complexes are formed *in situ* by the binding of circulating antibodies with antigens that are normally present in the glomerulus or with extrinsic antigens that have previously been planted as free antigens in the subepithelial area.<sup>109</sup>

Primary human MGN appears to be largely an autoimmune disease with *in situ* glomerular immune complex formation. Over 70%–80% of primary MGN patients have autoantibodies directed against PLA<sub>2</sub>R expressed in podocytes and proximal tubules.<sup>110,111</sup> These circulating PLA<sub>2</sub>R autoantibodies are IgG4 subtype and the plasma levels correlate with disease activity and therapeutic response,<sup>112</sup> and may predict the risk of post-transplantation recurrence.<sup>113</sup> Genome-wide association studies have strongly linked the disease to specific HLA-DQA1 and PLA2R alleles. Individuals with at risk polymorphisms may have increased propensity to present the autoantigen, precipitating MGN.<sup>114</sup> Approximately 5%–10% of patients with primary MGN have autoantibodies (IgG4 subtype) to a recently described second podocyte antigen, thrombospondin type-1 domain-containing 7A (THSD7A), further expanding the role of autoimmunity in these patients.<sup>115,116</sup>

In a subset of patients with MGN, alloimmune response appears to play a role in developing MGN. Neutral endopeptidase (NEP), expressed in podocytes and proximal tubular brush border, has been identified as the target antigen of antibodies deposited in the subepithelial space in patients with antenatal MGN.<sup>117</sup> In these cases, it is likely that the anti-NEP antibodies produced by the mother are transplacentally transferred to her child with genetic deficiency of NEP.<sup>118</sup> Some patients with Pompe disease and mucopolysaccharidosis IV receiving recombinant  $\alpha$  glucosidase and aryl sulfatase B, respectively, also develop alloimmune responses resulting in MGN.<sup>114</sup> Lastly, *de novo* MGN in allografts also appears to be an alloimmune response.

Conditions associated with secondary MGN include chronic infections, neoplasms, autoimmune diseases (SLE, rheumatoid arthritis, IgG4-related systemic disease), drugs, and sarcoidosis. Drugs commonly associated with MGN include nonsteroidal anti-inflammatory drugs, penicillamine, gold, lithium, mercury, captopril, and anti-tumor necrosis factor agents. In some instances of secondary MGN, hepatitis B antigens (HBsAg, HBcAg, and HBeAg), virus-like particles (hepatitis C), tumor antigens, thyroglobulin, and DNA-containing material have been identified in the immune complexes, but it is unclear if these antigens are indeed pathogenic.<sup>119</sup> Exogenous antigen such as cationic bovine serum albumin (BSA) derived from milk has been identified within subepithelial deposits in young children with MGN.<sup>120</sup> These children have no other evidence of milk allergy but have anti-BSA antibodies in circulation. Secondary forms of MGN typically lack circulating PLA<sub>2</sub>R, but a small subset of patients with hepatitis B, hepatitis C, malignant neoplasm, and sarcoidosis have circulating serum PLA<sub>2</sub>R. While this may be coincidental, it also raises the possibility that "primary" MGN is triggered by an underlying disease. In both primary and secondary forms, complement is activated at the capillary wall site and appears to have a role in the development of the proteinuria.

The incidence of MGN in different populations varies; there is a particularly high frequency in Japanese children<sup>121</sup> and in certain African populations,<sup>122,123</sup> probably related to a high incidence of hepatitis B infection and parasitic infestations. Although MGN may occur at any age, it is rare in children and adolescents. Eighty to

90% of the patients are over the age of 30 at the time of diagnosis, with a peak incidence in the fourth and fifth decades.<sup>124</sup> The disease is twice as common in males. Sixty to 80% of patients have the nephrotic syndrome at onset, and others are usually referred for investigation of asymptomatic proteinuria or an abnormal urinalysis.<sup>125</sup> The proteinuria is usually nonselective, but a highly selective proteinuria is seen in about 20% of cases.<sup>124</sup> Macroscopic hematuria is rare, but as many as 90% of patients have microscopic hematuria at some time during the course of the disease.<sup>124,126</sup> Hypertension is usually found after renal insufficiency has developed, but it can be seen in 30% of the patients at presentation.<sup>107</sup> Rare cases with circulating anti-GBM antibody and/or antineutrophil cytoplasmic antibody (ANCA) have also been reported.<sup>125</sup> Serum levels of C3, as well as other components of complement, are normal; however, if reduced, this suggests a secondary form of the disease.

The natural history and overall prognosis of MGN can be significantly affected by the underlying disease and the way it is treated. When MGN is secondary to drugs, toxic substances, or infections, removal of the etiologic agent will often result in the disappearance of the clinical symptoms and resolution of the renal lesion. The nephrotic syndrome may abate and the glomerular changes regress after resection and treatment of a malignant tumor. In patients with membranous lupus nephritis, the course is indolent, whereas those who develop a superimposed anti-GBM antibody disease undergo a rapid progression to renal failure. Most patients with primary MGN present with chronic proteinuria and have recurrent episodes of nephrotic syndrome persisting over many years. Only 20%–25% of these patients progress to renal failure terminating in ESRD.<sup>127</sup> Partial or complete spontaneous remission has been reported in 20%–65% of cases.<sup>127,128</sup> The likelihood of spontaneous remission is greatly increased in children<sup>106</sup> and in patients who presented with proteinuria without the nephrotic syndrome and in whom the biopsy demonstrated a stage I glomerular lesion.<sup>129</sup> Recurrence or *de novo* development of MGN after renal transplantation can occur. The recurrence rates have ranged from 10% to 30% in different series, while the *de novo* rate is more common, accounting for about twice as many cases of MGN in transplant recipients.<sup>130</sup>

The structural features of the glomerular capillary wall have been used to define four histopathologic stages of the disease.<sup>131</sup> In **stage I**, the glomeruli appear normal by light microscopy, and there are no significant changes in the thickness of the basement membrane. At this early stage, an incorrect diagnosis of MCD is possible if the biopsy is only studied by light microscopy. With the electron microscope, these cases show sparse immune complex deposits between the epithelial cell cytoplasm and the lamina densa of the basement membrane, but the latter appears homogeneous and uniform in thickness. The deposits can be irregular, dome shaped, or appear as small humps with a well-defined line between the lamina densa and the epithelial cell. Foot processes over the deposits are obliterated, but they often appear normal elsewhere (Fig. 23.11).

In **stage II**, the capillary walls are thickened and many subepithelial deposits are present, separated by extensions of basement membrane (Fig. 23.12A). The deposits do not stain with silver impregnation techniques, but the extensions of basement membrane do, thus creating the impression that the capillary loop is covered by spikes (see Fig. 23.12B). These spikes have been shown to be composed of type IV collagen and noncollagenous extracellular matrix components, including laminin, heparan sulfate, proteoglycans, and vitronectin. The epithelial foot process effacement is extensive throughout the loops.

When the disease is more advanced (**stage III**), the deposits are encircled by a newly formed basement membrane (Fig. 23.13). The capillary walls are markedly thickened and the capillary lumina

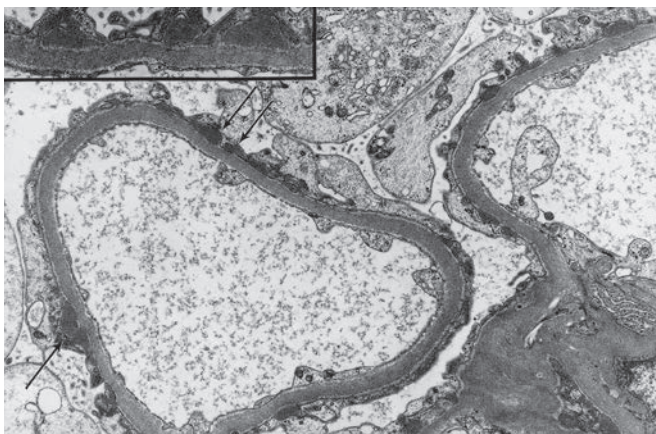


**Figure 23.11 Membranous Glomerulonephritis, Stage I.** Basement membrane is normal thickness. Small subepithelial deposits (arrows) are separated from the basement membrane by a thin clear zone (inset). The epithelial foot processes are obliterated ( $\times 6000$ ; inset  $\times 9100$ ).

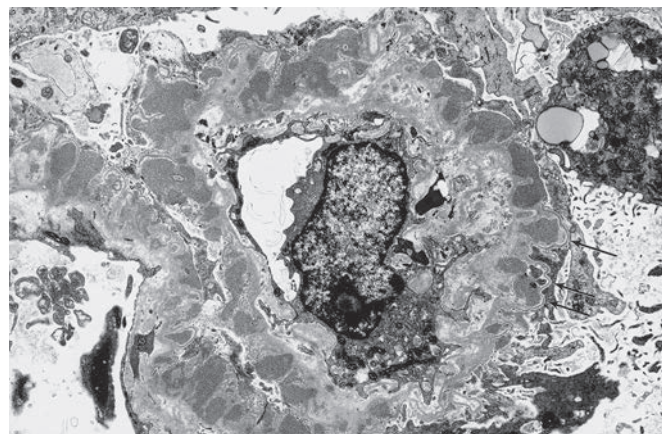


**Figure 23.13 Membranous Glomerulonephritis, Stage III.** The basement membrane is markedly thickened and the deposits appear surrounded by a newly formed basement membrane (arrows) ( $\times 6900$ ).

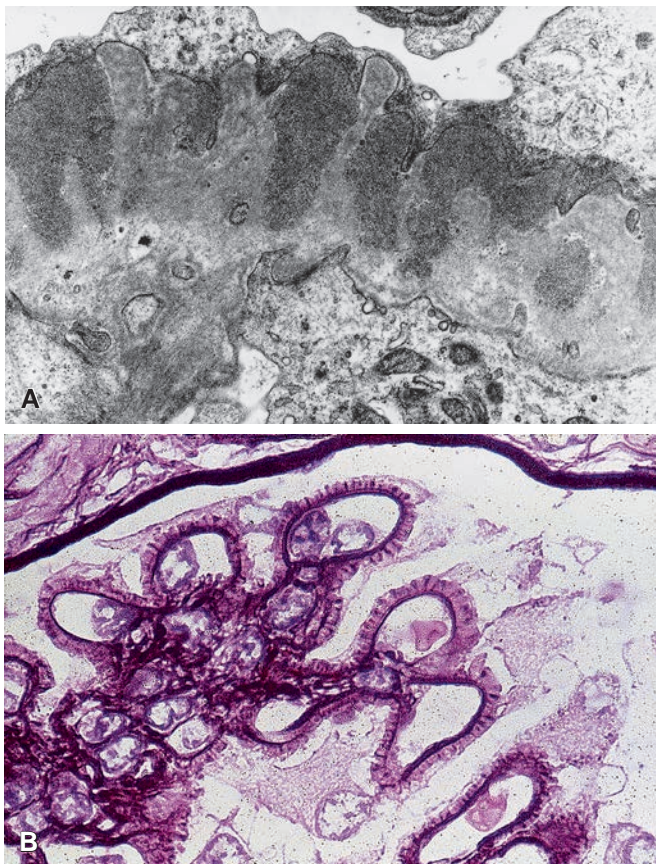


**Figure 23.12 A, B, Membranous glomerulonephritis, stage II.** Subepithelial deposits are separated by projections of the basement membrane ( $\times 18,000$ ). B, Silver preparation showing spike formation along the thickened basement membrane (methenamine silver).

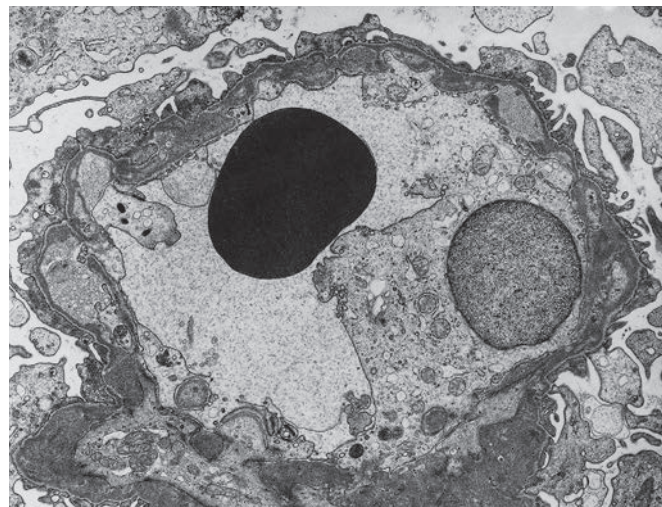


**Figure 23.14 Membranous Glomerulonephritis, Stage IV.** The basement membrane is markedly irregular and most of the deposits have been reabsorbed, leaving large electron-lucent areas ( $\times 9360$ ).

membranous bodies that are probably formed by degeneration of entrapped cellular components.

During the late stage of the disease (stage IV), deposits gradually lose their electron density and the basement membrane becomes vacuolated, folded, and thickened. Deposits may no longer be evident (Fig. 23.14). Capillary lumina become obliterated, and the glomerular tufts show segmental or global sclerosis. TA and vascular sclerosis can be prominent, making the diagnosis difficult. In the end-stage of the disease, the differential diagnosis includes various types of chronic glomerulonephritis. Although the degree of proteinuria does not parallel the stages of the renal lesion, stage I carries a better prognosis than more advanced disease and spontaneous remission is more likely. However, there seems to be no difference in prognosis between stages II, III, and IV. Histologic progression can occur without clinical progression, and clinical remission can occur in the absence of histologic regression.<sup>107</sup>

Immunofluorescence microscopy in all stages of MGN reveals a generalized, peripheral granular pattern of IgG, C3, kappa and lambda, sometimes with IgM (Fig. 23.15). The reaction for IgA is usually absent, and if it is strong and associated with the early components

narrowed. The basement membrane shows a reduplicated or moth-eaten appearance with PAS and silver stains. By electron microscopy, many of the deposits in stage III disease have a rarefied appearance that indicates resolution, and small spherical structures, which have been confused with virus particles, may be present during dissolution of the deposits. Individual deposits may also contain striated

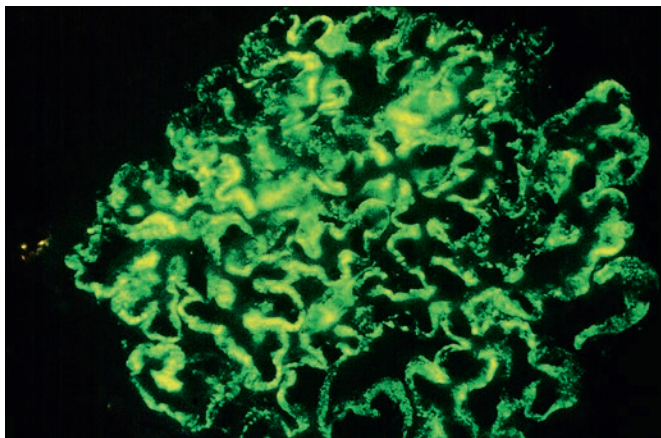


**Figure 23.15** Immunofluorescence preparation of membranous glomerulonephritis showing peripheral granular deposits of IgG (anti-IgG).

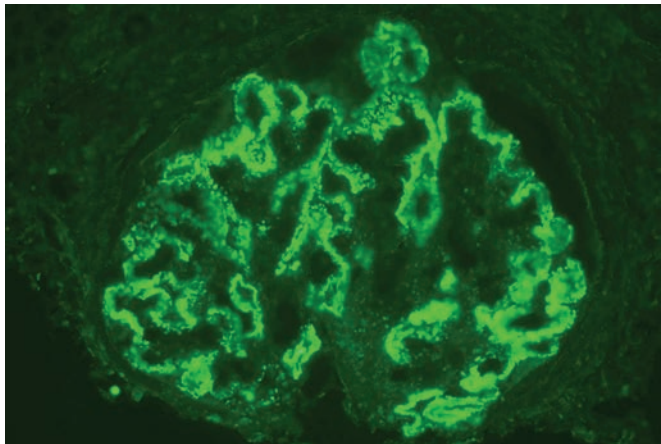


**Figure 23.16** Diffuse granular capillary wall staining with antibody to PLA2R supports a diagnosis of primary membranous nephropathy (anti-PLA2R).

of complement (C1q and C4), the possibility of lupus MGN must be considered. Although not evaluated on routine diagnostic studies, there is strong reactivity for terminal complement components (i.e., C5b–C9 membrane attack complex). Extraglomerular deposits have only rarely been reported in primary MGN.<sup>126</sup> The finding of granular deposits along the tubular basement membrane (TBM) should always raise the possibility of membranous lupus nephritis.<sup>132</sup> MGN with anti-TBM antibodies typically have linear TBM staining for IgG and sometimes with C3. Although not entirely sensitive or specific, with regards to IgG subclass staining, primary MGN deposits are mainly IgG4+, while membranous lupus nephritis deposits are positive for IgG1–IgG4 with IgG3 dominance. Primary MGN deposits stain for PLA2R by immunofluorescence microscopy and can be positive despite the lack of circulating antibodies as in early remission stage (Fig. 23.16).<sup>133,134</sup> Hence, renal biopsy is considered a sensitive tool for diagnosing primary MGN. Recurrent MGN in post-transplantation biopsies is also characterized by deposits that are IgG4 dominant and PLA2R positive. In contrast, *de novo* MGN deposits are IgG1 dominant and PLA2R negative.<sup>135,136</sup> *De novo* MGN is often associated with chronic antibody-mediated rejection (AMR) and hence is considered an alloimmune phenomenon.

Notable morphologic characteristics of MGN throughout its evolution are the absence of mesangial hypercellularity and a lack of inflammatory cells within the glomeruli. On occasion, however,

mesangial hypercellularity can occur, especially in patients with secondary forms of MGN, such as SLE, hepatitis B, or gold- or penicillamine-associated disease. In addition to epimembranous and intramembranous deposits, small amounts of immune complex deposition may be seen in the mesangial and/or subendothelial areas.<sup>137</sup> Margination of leukocytes in the glomerular capillaries may be an indication of renal vein thrombosis.<sup>138</sup> Crescent formation is uncommon and if focal, should suggest secondary MGN (e.g., due to SLE) or a superimposed disease. Diffuse fulminant crescentic disease is a rare and late consequence of the superimposition of anti-GBM or ANCA disease.<sup>125</sup> Rarely, patients with MGN have tubulointerstitial nephritis (TIN) because of antitubular basement membrane antibodies. These patients are almost invariably children, present with nephrotic syndrome and Fanconi syndrome and progress to ESRD.<sup>139</sup>

## Diabetic Nephropathy

Diabetic nephropathy is a clinical syndrome characterized by persistent proteinuria, hypertension, and progressive decline in renal function. It is considered to be the leading cause of ESRD, accounting for approximately 40% of the new cases in the United States undergoing long-term dialysis.<sup>140</sup> It is estimated that 20%–40% of all diabetic patients will develop diabetic nephropathy.<sup>141</sup> In type 1 diabetes, the cumulative incidence of diabetic nephropathy is about 25% after 25–40 years of disease.<sup>142</sup> Evidence suggests that the risk of overt nephropathy and progression to ESRD is similar in type 2 diabetes.<sup>143</sup> Microalbuminuria is the earliest manifestation of diabetic nephropathy but cannot be detected by standard urine dipstick method. Proteinuria, usually of nonselective type, is the most consistent overt manifestation of diabetic nephropathy. The nephrotic syndrome has been reported in 6%–40% of the cases and constitutes a sign of poor prognosis. About 28%–48% of patients may present with moderate microscopic hematuria. Hypertension is a late complication seen with advanced renal failure. The rate of progression to end-stage kidney disease is dependent on a variety of factors including genetics, environmental factors, therapeutic interventions, and comorbidities. Blacks and Native Americans with type II diabetes mellitus are at greater risk of developing diabetic nephropathy.

The development of diabetic nephropathy is related to multiple factors, and inadequate glycemic control is one of the most important. Persistent hyperglycemia causes accumulation of advanced glycosylated end products in various organs including kidney with resultant injury, tissue remodeling, and extracellular matrix deposition. It also causes defects in mitochondrial electron transport, increased production of reactive oxygen species, and increased oxidative stress. Many cellular proteins, including GBM collagen and matrix proteins, are affected. Inherited risk factors such as certain polymorphisms in genes involved in the renin angiotensin system and insulin resistance appear to play a role.<sup>144</sup>

Diabetic microangiopathy occurring throughout the body is the most characteristic morphologic change in the diabetic, and its hallmark is an increase in the amount of vascular basement membrane material. There are no significant morphologic differences in the renal lesions caused by type 1 and type 2 diabetes.<sup>145</sup> All areas of the kidney may be affected by diabetes, but the most striking lesions are found in the glomeruli and blood vessels, including diffuse glomerulosclerosis, nodular glomerulosclerosis, and the so-called insudative lesions (fibrin caps, capsular drops, and arteriolar hyalinosis).<sup>146</sup> Diabetic glomerulosclerosis is the general term for all of these lesions, and they are considered to be an expression of the microangiopathy.

Diffuse glomerulosclerosis, the most common lesion in diabetic nephropathy, is characterized by a diffuse increase in the mesangial

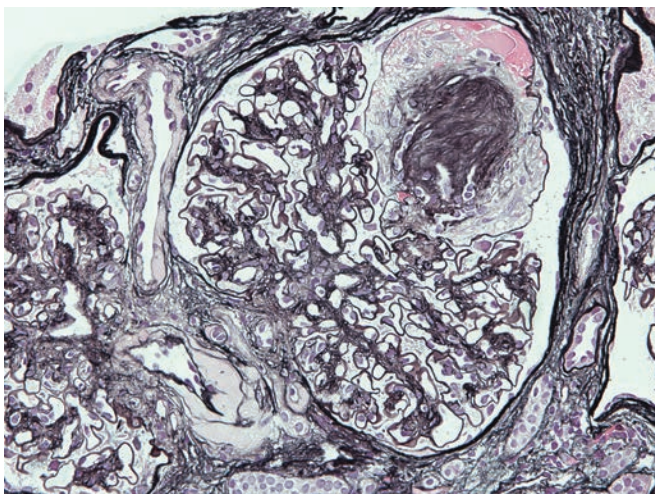


**Figure 23.17** Diabetic glomerulosclerosis with segmental mesangial Kimmelstiel-Wilson nodule and adjacent microaneurysm. Other mesangial areas have mild diffuse mesangial sclerosis. Arteriolar hyaline insudation is seen near the vascular pole (methenamine silver stain).

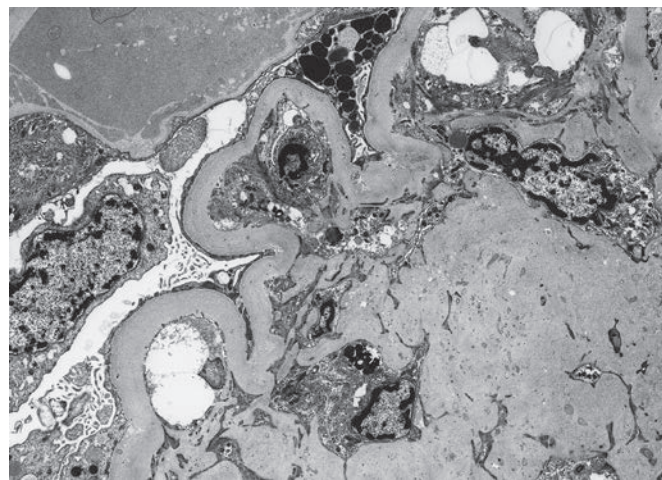


**Figure 23.18** Nodular Diabetic Glomerulosclerosis. The massive enlargement of the mesangium is due to an increase in mesangial matrix. The basement membrane is markedly thickened and a capsular drop is present at the left upper corner of the figure ( $\times 4400$ ).

matrix and thickening of the capillary walls (Fig. 23.17). Thickening of the GBM is the most consistent finding in diabetic nephropathy and is often seen in both diffuse and nodular glomerulosclerosis. Although minor degrees of basement membrane thickening are not specific for diabetes, measurement of the basement membrane width is the most effective way to quantitate early diabetic glomerular lesions. In advanced stages, the GBM may be many times its normal thickness, often with accentuation of the normal fibrillar structure. The GBM thickening and mesangial changes can be seen by electron microscopy before the damage is visible by light microscopy. The earliest structural alteration in diabetic glomerulopathy that can be quantified is increased thickness of the GBM, which can be documented as early as 1.5–2.5 years after the onset of type I diabetes mellitus. A clear increase in the mesangial matrix and cellularity can be detected on light microscopy as early as 5–7 years after the onset of diabetes mellitus<sup>147</sup> or within 2–5 years following renal transplantation.<sup>148</sup> Recently, a histologic classification of diabetic nephropathy has been proposed, but its clinical utility has not yet been validated.<sup>149</sup>

Nodular glomerulosclerosis (Kimmelstiel-Wilson lesion) is the characteristic histopathologic lesion in diabetic glomerulosclerosis. It consists of large acellular nodules located in the intercapillary regions (see Fig. 23.17). These nodules vary in size and often have a laminated appearance. They are eosinophilic, argyrophilic, and PAS positive and blue with trichrome stain. Ultrastructurally, the nodules are composed of masses of extracellular mesangial matrix (Fig. 23.18). Both the mesangial widening and the nodules are the result of an increase in the synthesis and/or decrease in the degradation of the mesangial matrix.<sup>146</sup> The capillary loops that surround the nodules may have narrow lumens because of the expansion of the mesangium, but they can also be aneurysmally dilated and some have peripheral mesangial extensions. Focal areas of mesangiolysis may also be present. Diffuse and nodular diabetic glomerulosclerosis can be found together, not only in the same patient, but also in the same glomerulus. Although nodular glomerulosclerosis is virtually pathognomonic of diabetic nephropathy, identical light microscopic lesions can be found in cases of light chain deposition disease (LCDD). In the latter condition, however, the nodules are composed of granular electron-dense material that shows light chain restriction with antibodies to kappa and lambda light chains. Nodular

glomerulosclerosis mimicking diabetic nephropathy has rarely been reported in patients without manifested diabetes, but with longstanding hypertension and/or smoking history, and is referred to as “idiopathic” nodular glomerulosclerosis.<sup>150</sup> Diffuse nodular deposits of amyloid can sometimes be confused with diabetic glomerulosclerosis by light microscopy, but the ultrastructural identification of amyloid fibrils will establish the diagnosis.

Insudative lesions are the least specific of the glomerular changes in diabetes. Ultrastructurally, they are seen to be masses of electron-dense material, often containing lipid droplets. Common locations of these lesions are the periphery of the loop in a subendothelial location (fibrin caps), within the basement membrane of the Bowman capsule (capsular drops), or in the mesangium or GBM. In blood vessels, they are more extensive in the subintima and media but can also involve the adventitia. This insudative lesion, known as hyalinosis, can affect the afferent and efferent arterioles and may ultimately replace the smooth muscle cells. The severity of the arteriolar hyalinosis correlates significantly with the percentage of sclerosed glomeruli, suggesting that the vascular lesion contributes to the ischemic global glomerulosclerosis. Histochemical and immunofluorescence studies indicate that the insudative material represents infiltration by constituents of the plasma, including proteins, lipids, and mucopolysaccharides.

Atubular glomeruli can also be found in diabetic glomerulosclerosis as a late manifestation of the disease, predominantly in patients with proteinuria.<sup>151</sup> Atubular glomeruli are defined as those glomeruli that have open glomerular capillaries but have lost their connection with the proximal tubule and are presumably nonfunctioning. Although accurate identification of these glomeruli requires serial sections, small glomeruli surrounded by tissue with marked tubular loss are most probably atubular.

The most characteristic tubular change is diffuse thickening of the tubular basement membrane. When the disease is advanced, there is also TA and interstitial scarring that may be accompanied by chronic inflammatory infiltrate. The presence of interstitial neutrophils or tubular neutrophil casts should raise concern for superimposed acute pyelonephritis. Glycogen vacuolization of the renal proximal tubular epithelial cells (Armanni-Ebstein lesion), associated with uncontrolled hyperglycemia, was common in the past, but is rarely seen today. Approximately a third of renal biopsies

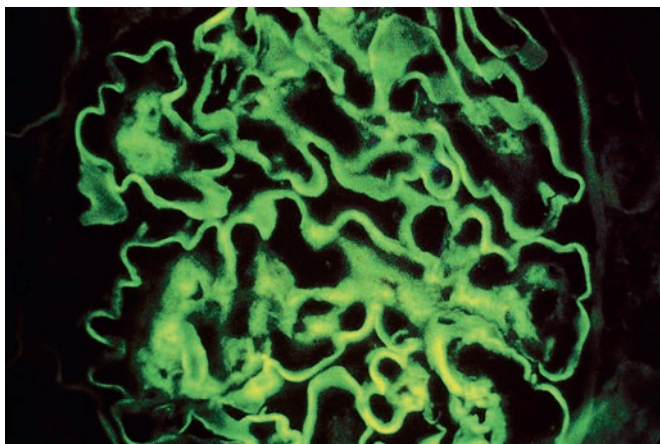


**Figure 23.19** Diabetic glomerulosclerosis with linear staining for IgG along the glomerular basement membrane (anti-IgG).

with diabetic nephropathy have superimposed glomerular disease,<sup>152</sup> and this list includes membranous nephropathy, IgA nephropathy (IgAN), postinfectious glomerulonephritis (especially IgA-dominant variant described later), and others. Cellular crescents are rare in diabetic glomerulosclerosis, but foci of organizing fibroepithelial crescents occur with superimposed ANCA-mediated glomerulonephritis,<sup>153</sup> and their presence is associated with aggressive clinical course.<sup>154</sup>

Diffuse linear reaction for IgG along the glomerular capillary, tubular, and Bowman capsular basement membranes is the most characteristic immunofluorescence finding in diabetic nephropathy (Fig. 23.19). Less intense reaction in a similar distribution may also be seen for IgM, fibrin, and albumin, but staining for C3, if present, is often granular. These linear reactions are unrelated to either the duration or the severity of the glomerular lesions and evaluation studies do not show specific antibody activity to basement membrane antigens. Insudative lesions may react with a variety of reagents but most frequently contain IgM and C3.

## Amyloidosis

The term amyloidosis designates a heterogeneous group of disorders characterized by the extracellular deposition of nonbranching linear fibrils with a mean diameter of 10 nm and a  $\beta$ -pleated sheet configuration on x-ray diffraction analysis. It is this configuration that is responsible for the tinctorial and optical characteristics seen on Congo red staining, which produces the typical apple-green birefringence seen on tissue sections when they are examined under polarized light. Amyloid itself does not have a consistent chemical composition but is instead a group of proteins that share common physical characteristics. At present, more than 30 structurally unrelated proteins have been identified as amyloid precursors associated with human disease, but most forms are localized with rare or no involvement of kidney (Table 23.3).<sup>155–157</sup> In addition to the fibrillary protein, amyloid deposits contain nonfibrillary proteins, including glycosaminoglycans, apolipoprotein E (Apo E), and amyloid P component. The amyloid P component (also known as serum amyloid P or SAP) is a 25-kDa glycoprotein member of the pentraxin family that includes C-reactive protein. Amyloid P component is present in all types of amyloid, accounting for about 15% of their mass. It is believed that amyloid P component may prevent degradation of the amyloid fibrils once they are formed.<sup>158</sup> Better understanding of the amyloid fibril composition, formation, and stabilization has helped the emerging field of targeted therapies in amyloidosis.<sup>159</sup>

The classification of amyloidosis is based on the type of precursor protein that forms the amyloid fibrils and the distribution of the amyloid deposits as to whether it is systemic or localized (see Table 23.3). By convention, the amyloid fibril type is designated A for amyloid, followed by an abbreviated form of the name of the fibril protein. **Amyloid light-chain (AL) amyloidosis** (formerly known as “primary” or “associated with multiple myeloma”) is the most common form of systemic amyloidosis in the Western world.<sup>157</sup> In this type of amyloidosis, the amyloid fibrils are composed of the N-terminal residues of the variable region of an immunoglobulin light chain. The specific amino acid sequences and post-translational modifications of light chains confer the amyloidogenicity. A minority have overt multiple myeloma, while others have monoclonal spike in the serum and/or urine. The amyloidogenic light chains are more frequently lambda than kappa type, in contrast to normal or cast nephropathy light chains.<sup>160</sup> Rarely, the amyloid deposits are derived from monoclonal immunoglobulin light and heavy chains or just heavy chains, and the disease is referred to as AHL amyloidosis or AH amyloidosis, respectively.

**Amyloid A (AA) amyloidosis** (formerly known as secondary amyloidosis) is a rare complication of persistent inflammation that may develop in patients affected by chronic rheumatic diseases, long-lasting infections, inflammatory bowel disease, periodic fever syndromes, familial Mediterranean fever, and malignancies.<sup>161–163</sup> It is the most common type of amyloidosis in the parts of developing world with endemic tuberculosis and leprosy. In this type of amyloidosis, the AA amyloid deposits are formed by the N-terminal proteolytic fragments of the acute-phase reactant serum amyloid A (SAA), a polymorphic apolipoprotein of high density that, upon chronic inflammatory stimuli, may reach persistently high plasma concentrations.<sup>164,165</sup> Certain polymorphisms in SAA gene appear to confer increased risk of developing AA amyloidosis in patients.<sup>163</sup>

**Hereditary systemic amyloidosis** is a diverse group of autosomal dominant, late-onset (sometimes sixth or seventh decade of life) disorders that occurs much less frequently than AL or AA amyloidosis. These amyloidoses are caused by mutations in the genes coding for some plasma proteins, including transthyretin, apolipoprotein A-I, apolipoprotein A-II, apolipoprotein A-IV, fibrinogen A  $\alpha$ -chain, gelsolin, cystatin C, and lysozyme.<sup>166</sup> Specific amino acid substitutions allow each of these soluble circulating proteins to be prone to aggregate and form amyloid fibrils in organs and tissues. The natural history of these conditions varies by the protein, as well as the tissue distribution. For example, transthyretin amyloidosis, which is the most common form of hereditary systemic amyloidosis, typically affects the peripheral and autonomic nervous systems, manifesting as progressive sensory–motor neuropathy, gastrointestinal and bladder dysfunction, impotence, and orthostatic hypotension, whereas apolipoprotein A-I, apolipoprotein A-II, apolipoprotein A-IV, fibrinogen  $\alpha$ -chain, and lysozyme amyloidosis are more often associated with a marked visceral burden of amyloid that clinically results in progressive kidney and liver disease.<sup>162</sup>

Familial Mediterranean fever is a common form of the nephropathic familial amyloidoses. The deposits of amyloid in this condition consist of amyloid AA, and, in contrast to other forms of familial amyloidosis which are autosomal dominant, familial Mediterranean fever is associated with autosomal recessive inheritance.<sup>167</sup> Mutations in *MEFV* gene encoding pyrin/marenostrin result in activation of IL-1 $\beta$  pathway with subsequent elevations of SAA levels, especially during febrile episodes. Other related periodic fever syndromes due to mutations in genes encoding cryopyrin, and tumor necrosis factor also cause autoinflammation with eventual precipitation of AA amyloid.<sup>163</sup>

A subtype of amyloidosis of ill-defined etiology is ALECT2, characterized by accumulation of leukocyte chemotactic factor 2.<sup>168,169</sup> No mutation in *LECT2* gene has been identified, but all sequenced

**Table 23.3** Amyloid fibril proteins and their precursors in humans

AMYLOID PROTEIN	PRECURSOR PROTEIN	DISTRIBUTION	RENAL BIOPSY FEATURES OR ASSOCIATED CONDITION
<b>Neoplasm-Associated (AL) Amyloidosis</b>			
AL	Immunoglobulin light chain	Systemic or localized	Glomerular, interstitial, and vascular deposits; multiple myeloma, B-cell lymphoma
AH	Immunoglobulin heavy chain	Systemic or localized	Glomerular, interstitial, and vascular deposits; multiple myeloma, B-cell lymphoma
<b>Chronic Inflammation-Associated Amyloidosis</b>			
AA	(Apo) serum AA	Systemic	Chronic infections or inflammation. Seen in hereditary inflammatory syndromes (Familial Mediterranean fever, hyper-IgD syndrome, familial cold urticarial, Muckle-Wells syndrome)
<b>Hereditary (or Mutation Associated) Amyloidosis</b>			
ATTR	Transthyretin	Systemic	Predominantly glomerular deposits or limited to medullary interstitium
AApoAI	Apolipoprotein AI	Systemic	Arterial and medullary interstitial deposits in kidney; localized deposits in aorta, meniscus
AApoAI	Apolipoprotein AI	Systemic	Medullary interstitial and vascular deposits
AGel	Gelsolin	Systemic	Glomerular deposits
ALys	Lysozyme	Systemic	Glomerular and vascular deposits
AFib	Fibrinogen alpha-chain	Systemic	Only glomerular deposits that stain for fibrinogen
ACys	Cystatin C	Systemic	Cerebral vessels (no renal involvement)
ALECT2	Leukocyte chemotactic factor 2	Localized	Glomerular, cortical interstitial and vascular deposits. No mutation, only a common polymorphism in <i>LECT2</i> gene identified
ABri	ABriPP	Systemic	Familial dementia
<b>Other Types of Amyloid Deposition</b>			
AApoAIV	Apolipoprotein AIV	Systemic	Sporadic, associated with aging
ATTR	Transthyretin	Systemic	Nonfamilial senile form
A $\beta$ <sub>2</sub> M	$\beta_2$ -Microglobulin	Systemic or localized	Hemodialysis associated; localized form in joints
ADan	ADanPP	Localized	Familial dementia (Danish type)
A $\beta$	A $\beta$ protein precursor (A $\beta$ PP)	Localized	Alzheimer disease, associated with aging

*Continued*

**Table 23.3** Amyloid fibril proteins and their precursors in humans—cont'd

AMYLOID PROTEIN	PRECURSOR PROTEIN	DISTRIBUTION	RENAL BIOPSY FEATURES OR ASSOCIATED CONDITION
APrP	Prion protein	Localized	Spongiform encephalopathies
ACal	(Pro) calcitonin	Localized	Medullary thyroid carcinoma
AIAPP	Islet amyloid polypeptide	Localized	Islet of Langerhans; Insulinomas
AANF	Atrial natriuretic factor	Localized	Cardiac atria
APro	Prolactin	Localized	Aging pituitary, Prolactinomas
Alns	Insulin	Localized	Iatrogenic
AMed	Lactadherin	Localized	Senile aortic, arterial media
AKer	Kerato-epithelin	Localized	Cornea, familial
ALac	Lactoferrin	Localized	Cornea (trichiasis)
AOaap	Odontogenic ameloblast-associated protein	Localized	Odontogenic tumors
ASemi	Semenogelin I	Localized	Seminal vesicle
ATau	Tau	Localized	Alzheimer disease, frontotemporal dementia, aging, other cerebral conditions

Modified from Westermark P, Benson MD, Buxbaum JN, et al. A primer of amyloid nomenclature. *Amyloid*. 2007;14:179–183.

cases show a specific polymorphism. Produced in the liver, LECT2 is a plasma cytokine that increases the phagocytic and bacteriocidal activity of macrophages. ALECT2 is typically seen in elderly individuals of Mexican ancestry, although other ethnic populations can be affected. These patients often have comorbidities such as diabetes mellitus and hypertension.

Another form of amyloidosis is **dialysis-related amyloidosis**, a serious complication in patients undergoing long-term dialysis that is caused by the deposition of fibrillar  $\beta_2$ -microglobulin (amyloid  $\beta_2$ M).<sup>170</sup> This type of amyloid has a predilection for musculoskeletal deposition.  $\beta_2$ -Amyloid can cause carpal tunnel syndrome and a destructive arthropathy of medium-sized and large joints, especially of the shoulders and knees. Visceral amyloid deposition occurs late, usually after 15 years of hemodialysis, and may involve the heart, liver, lungs, and gastrointestinal system.<sup>162</sup> End-stage kidneys may also be involved by  $\beta_2$ -microglobulin amyloidosis, but this has no clinical significance.

Nonselective proteinuria, with or without the nephrotic syndrome, is the most common manifestation of renal involvement by amyloidosis. Approximately 25% of the patients with AL amyloidosis have the nephrotic syndrome at diagnosis, and a total of about 40% will develop the syndrome during the course of the disease.<sup>171</sup> Over 90% of patients with AA amyloidosis have renal insufficiency or nephrotic syndrome at diagnosis; however, the degree of proteinuria does not correlate with the extent of the amyloid deposition in the kidney. The prognosis for a patient with renal amyloidosis is poor, especially in those with AL amyloidosis.<sup>171,172</sup>

Because the kidney is frequently affected in AL, AA, and several familial amyloidoses, a kidney biopsy is often a method by which the disease is identified.<sup>173,174</sup> Amyloid can be found anywhere in the kidney but especially accumulates in glomeruli. Deposition is initially mesangial, producing diffuse widening of axial areas but progressively involves the capillary walls (Fig. 23.20A and B).

Substantial mesangial deposition can produce nodules that may resemble those of diabetic glomerulosclerosis or LCDD. However, in amyloidosis, because the nodules are composed of amyloid protein rather than mesangial matrix, PAS staining is weak and trichrome stain is grayish blue in mesangium. Diffuse spread throughout the glomerulus can produce a picture reminiscent of membranous nephropathy, especially with the formation of basement membrane spicules. Amyloid deposition in the tubulointerstitium produces TA and IF, and in a small percentage of patients (~10%), the glomerular deposits are absent and amyloid is restricted to the tubulointerstitium or blood vessels. Several differences have been described in the distribution of amyloid deposits in various subtypes. For example, ALECT2 primarily affects cortical interstitium along with glomeruli and blood vessels, but the medulla is spared; AFib- $\alpha$  exclusively involves glomeruli and AApoAI/AII/AIV affects medullary interstitium with relative glomerular sparing.<sup>157</sup> Histochemical techniques used for the diagnosis of amyloid include Congo red and thioflavin T stains (Fig. 23.21A and B). Thioflavin T is extremely sensitive but not entirely specific, whereas the production of an apple-green color by polarized light in Congo red-stained sections is accepted as the most reliable light microscopic method for diagnosis. Each technique requires a critical amount of amyloid before a positive reaction can be elicited. Because of this, small amounts of amyloid may be missed and, even more important, neither technique is effective with very thin sections. The staining should be performed on sections cut at least 8  $\mu$ m thick and always with appropriate controls. The fibrils of AL and AA amyloidosis can be distinguished by pretreating tissue sections with potassium permanganate before the Congo red staining. Under these conditions, AA amyloid fibrils lose their affinity for the Congo red stain, and the birefringence is lost, whereas AL amyloid is not affected. This technique, however, is not as reliable as immunostaining with currently available AA antibodies.

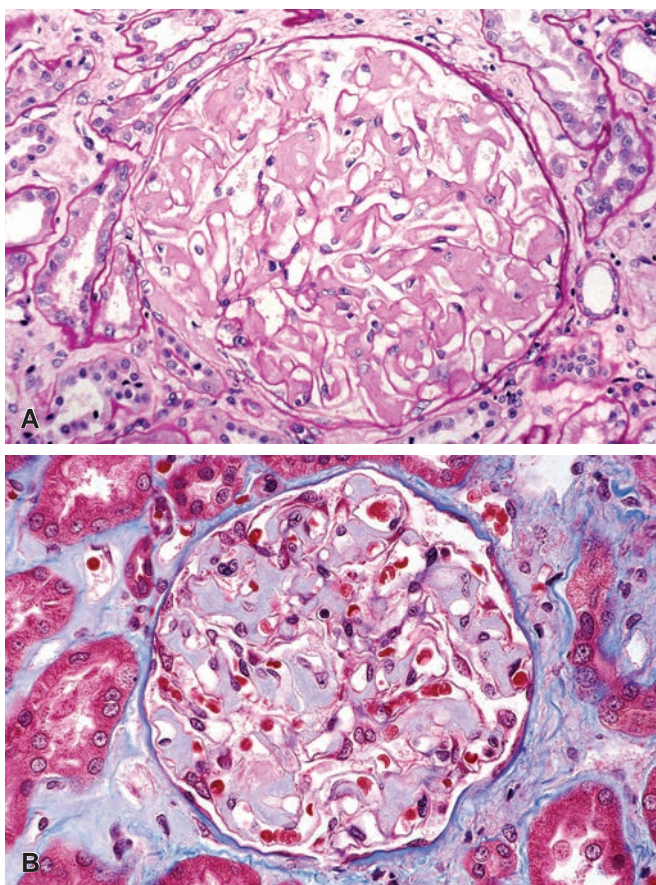


**Figure 23.20** Acellular Amorphous Deposits of Amyloid in the Mesangium With Patchy Glomerular Capillary Wall Extension. **A**, These deposits are weakly PAS positive in comparison to the Bowman capsule. **B**, Amyloid deposits have a grayish blue appearance on trichrome stain.

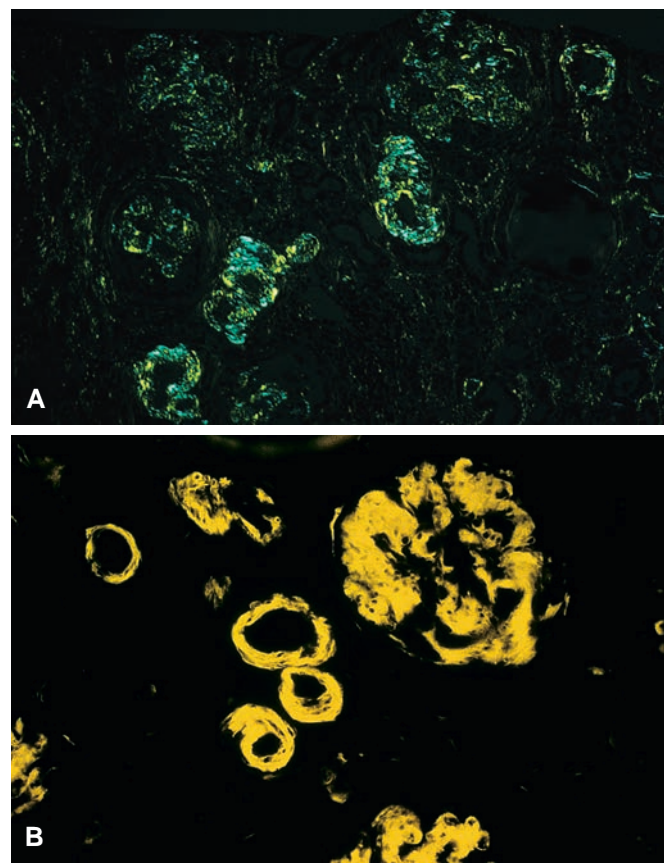


**Figure 23.21** **A**, Deposits of amyloid exhibiting birefringence under polarized light (Congo red stain). **B**, Fluorescence of amyloid under ultraviolet light (thioflavin T stain).

In the early stages of renal involvement when histochemical preparations fail to detect the deposits of amyloid, electron microscopy is the only method available to establish the diagnosis. Ultrastructurally, the amyloid fibrils in tissue sections form random aggregates of rigid, nonbranching fibrils measuring 8–10 nm in diameter (Fig. 23.22). Initially, the amyloid is seen in mesangium and the deposition subsequently extends into the subendothelial zone and through the basement membrane. When amyloid penetrates the basement membrane, epithelial foot processes are effaced and are often separated from the membrane.

Because the amyloidogenic light chain in AL amyloidosis is produced by clonal plasma cells, immunofluorescence or immunoperoxidase studies will show restrictive immunoreactivity for either kappa or, more frequently, lambda light chain. It should be emphasized, however, that a negative reaction for both light chains does not exclude the diagnosis of AL amyloidosis. This is because the main constituent of amyloid deposits in some cases of AL amyloidosis is the light chain variable region alone and the commercially available antibodies are typically raised against the light chain constant region.<sup>175</sup> Monoclonal heavy chain staining (IgG, IgA, or IgM) may instead be seen in AH amyloidosis or may be present in addition to light chain restriction, as in AHL amyloidosis. Sometimes the “stickiness” of amyloid causes nonspecific immunoglobulin staining and an erroneous subtyping of amyloid deposits.<sup>175</sup> Amyloid A usually can be demonstrated by the currently available anti-AA protein

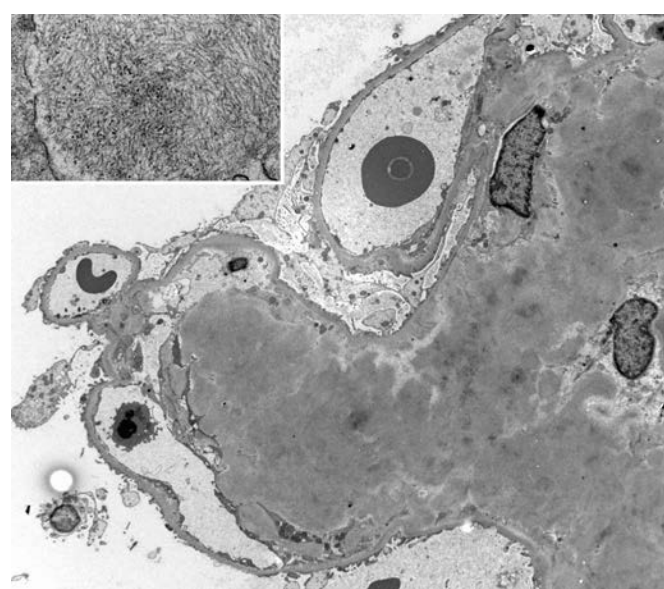


**Figure 23.22** Portion of a glomerulus with large amounts of mesangial deposits of amyloid. The typical fibrillary ultrastructural appearance of the amyloid fibrils is shown at high magnification ( $\times 5000$ ; inset  $\times 54,000$ ).

antibodies. Since amyloid P component is present in all types of amyloid, it can be used as a pan-amyloid marker to highlight the extent of amyloid deposition. It is important to keep in mind, however, that amyloid P component is not specific for amyloid and is present in the organized deposits of immunotactoid glomerulopathy<sup>176</sup> and in normal GBM and blood vessels<sup>177</sup>; therefore, a positive stain does not denote the presence of true amyloid deposition, and it is necessary to establish the presence of amyloid by a positive Congo red stain.

Other less common amyloid subtypes such as LECT2, ApoAI, ApoAI, and transthyretin can be characterized by performing immunohistochemical stains. However, the list of amyloid subtypes is quite extensive, and given the limited renal biopsy material, it is now standard of care to perform mass spectrometry on laser microdissected amyloid deposits on paraffin sections. Approximately 90% of renal amyloidosis cases belong to either AL or AA type. An initial panel of immunofluorescence and/or immunohistochemistry can be performed to evaluate for AL and AA amyloidosis and failure to subtype the amyloid with this initial testing should prompt mass spectrometry analysis.<sup>175</sup>

### Fibrillary Glomerulonephritis

Fibrillary glomerulonephritis is characterized by extracellular deposition of nonbranching, randomly arrayed fibrils approximately 10–30 nm in diameter.<sup>178–180</sup> Reported in just 0.5%–1.0% of the cases in three large series of native kidney biopsies,<sup>180–182</sup> it most commonly affects middle-aged adults but can also occur in older individuals and children as young as 10 years of age.<sup>181,183</sup> It is more common in whites than in blacks (ratio 8.3:1) and affects females more often than males (1.8:1).<sup>181,184</sup> Patients typically present with heavy proteinuria, often in the nephrotic range.<sup>181</sup> Microscopic hematuria is common, but on occasion gross hematuria may occur. About 75% of patients develop hypertension, sometimes severe.<sup>182,184</sup> Low serum complements are only rarely encountered in fibrillary glomerulonephritis. No specific serum or urine protein abnormalities have been recorded, and the patients have a low incidence of associated lymphoproliferative malignancy. The prognosis for patients with fibrillary glomerulonephritis is poor. Roughly half of these patients progress to ESRD within 2 years of the initial diagnosis.<sup>181,182</sup> Fibrillary glomerulonephritis has been reported to recur in almost a third of the patients who undergo renal transplantation.<sup>184–186</sup>

The light microscopic findings of fibrillary glomerulonephritis can be variable. Common features include mesangial hypercellularity, mesangial expansion with amorphous PAS-positive material, and thickening of the glomerular capillary walls (Fig. 23.23A). The overall appearance of the lesions can resemble mesangial proliferative, membranoproliferative, focal and diffuse proliferative, and MGN. Crescents are not uncommon and can occur in about one-fourth to one-third of cases. An important characteristic of these amorphous deposits is that they do not stain with Congo red or thioflavin T stains (thus differentiating them from amyloid fibrils) and they are observed in the absence of circulating cryoglobulins.

Ultrastructurally, the deposits can be found in all glomerular compartments, including the mesangium, GBM, and subendothelial and subepithelial areas. The fibrillary deposits in fibrillary glomerulonephritis are randomly oriented and measure 10–30 nm in diameter (see Fig. 23.23B). In rare cases of fibrillary glomerulonephritis, fibrils have been reported in the peritubular capillary walls and in the tubular basement membrane.<sup>187,188</sup> Patients usually exhibit extensive effacement of the podocyte foot processes, a finding that correlates with severe proteinuria observed in these patients. Immunofluorescence microscopy most often reveals IgG and C3 in a distribution that corresponds to the fibrillary deposits (see Fig. 23.23C). On occasion, small amounts of IgM and IgA can also be seen.<sup>181</sup> With

regards to IgG subclasses deposited, IgG4 is the dominant one, often in combination with IgG1.<sup>181</sup> Both kappa and lambda light chains are detected in most cases of fibrillary glomerulonephritis. Light chain restriction is seen in approximately 15% of patients with fibrillary glomerulonephritis.

### Immunotactoid Glomerulopathy

Although initially described together with fibrillary glomerulonephritis, immunotactoid glomerulopathy is recognized as a distinct entity. When strict diagnostic criteria are used, immunotactoid glomerulopathy is exceedingly rare, occurring with only one-tenth the frequency of fibrillary glomerulonephritis.<sup>181</sup> Although the clinical presentation of immunotactoid glomerulopathy is quite similar to that of fibrillary glomerulonephritis, these conditions differ in that immunotactoid glomerulopathy tends to occur in older individuals and is more likely to have an associated monoclonal gammopathy or lymphoproliferative malignancy, serum M-spike, and a worse long-term survival.<sup>180</sup> Approximately 40% of immunotactoid glomerulopathy patients have associated hypocomplementemia suggestive of complement activation by pathogenic immunoglobulins. The light microscopy findings are variable and amorphous Congo red negative deposits are often seen in the mesangium and capillary walls. The immunotactoid deposits consist of microtubular structures with a hollow core ranging from 30 to 50 nm in width and arranged in parallel or stacked arrays.<sup>178–180</sup> Vast majority of immunotactoid deposits (in 70%–90% of patients) are composed of monoclonal light chains, most often kappa type. When such monotypic deposits are seen in immunotactoid glomerulopathy, the IgG deposits often belong to IgG1 subclass.

### Light Chain Deposition Disease

LCDD is a rare systemic disorder caused by the overproduction and extracellular deposition of monoclonal immunoglobulin light chain.<sup>189,190</sup> A minority of cases may also have heavy chain determinants, and these cases are regarded as having light and heavy chain deposition disease (LHCDD).<sup>189</sup> On rare occasion, isolated heavy chain is deposited (HCDD, discussed later), and all these disorders with similar pathology constitute monoclonal immunoglobulin deposition disease (MIDD).<sup>191</sup> Although the principal clinical manifestations are dominated by renal disease, patients may present secondary symptoms produced by cardiac, hepatic, or neural damage.<sup>192</sup> In addition, abnormal light chains can be deposited in many other organs, including the skin, spleen, thyroid gland, adrenal glands, gastrointestinal tract, and lungs.<sup>192</sup>

LCDD has many histologic features in common with AL amyloidosis; however, in contrast to amyloidosis where the deposits are fibrillar, LCDD deposits are granular, do not stain with Congo red or thioflavin T, and do not contain amyloid P protein.<sup>193,194</sup> Also, while the deposits in amyloidosis consist mainly of lambda light chains, 80% of LCDD cases are composed of kappa light chains. The pathogenic light chains in LCDD have unique alterations in the complementarity-determining and framework portions of the variable region.<sup>189,195</sup> Males are more frequently affected, with a ratio of approximately 2:1.<sup>191</sup> About 60%–70% of the reported patients with LCDD have had well-documented multiple myeloma or another lymphoplasmacytic disorder at the time of, or subsequent to, the diagnosis of the nephropathy.<sup>191,196</sup> Although 15%–20% of patients lack monoclonal light chains in serum or urine by immunofixation method, abnormal serum free light chain ratio is detectable in all patients with LCDD and LHCDD.<sup>191</sup> Serum complement levels are typically normal unless associated with monoclonal heavy chains (as in LHCDD). LCDD occurs more frequently in middle aged to

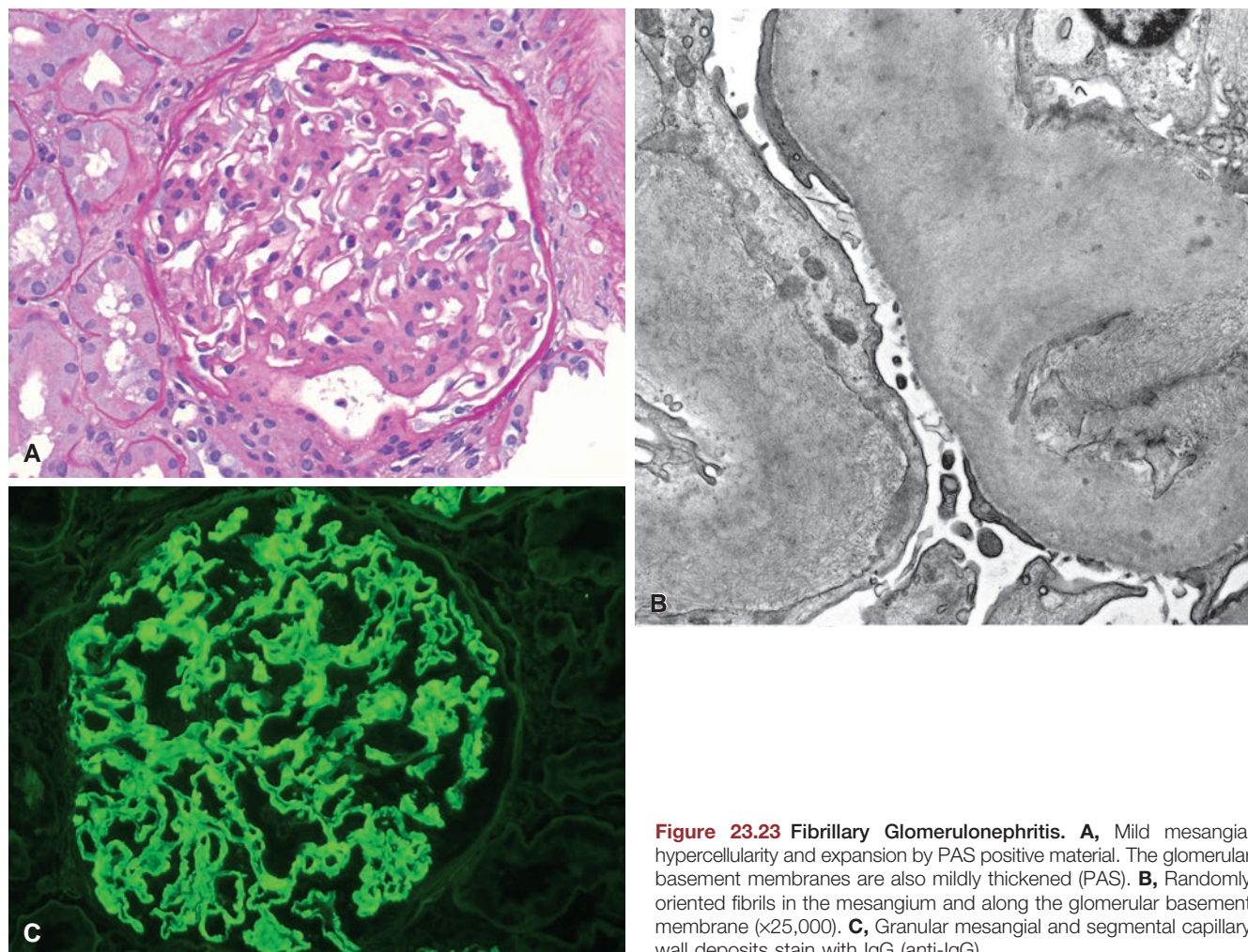


**Figure 23.23 Fibrillary Glomerulonephritis.** **A**, Mild mesangial hypercellularity and expansion by PAS positive material. The glomerular basement membranes are also mildly thickened (PAS). **B**, Randomly oriented fibrils in the mesangium and along the glomerular basement membrane ( $\times 25,000$ ). **C**, Granular mesangial and segmental capillary wall deposits stain with IgG (anti-IgG).

older individuals, but it has been reported in older children.<sup>197</sup> Most patients present with renal failure associated with heavy and nonselective proteinuria, reaching nephrotic range in over a third.<sup>191</sup> Concurrent cast nephropathy has been diagnosed in a third of patients with LCDD and the presenting feature is typically acute renal failure.<sup>189</sup> Microscopic hematuria is common. Renal insufficiency can progress to an end-stage kidney disease, at which time the patient will require dialysis or renal transplant. Without effective treatment to reduce light chain production, LCDD almost invariably recurs after renal transplantation, and the recurrence may occur within weeks to years after transplantation.<sup>198</sup> The prognosis for patients with LCDD is generally poor, and death is often attributed to cardiac disease or complications of infection.<sup>199</sup> The 5-year survival is approximately 70% but is less if there is coexisting multiple myeloma or light chain cast nephropathy.

Affected glomeruli are enlarged, and the deposition of the markedly PAS-positive material produces capillary wall thickening and nodular expansion of the mesangium. The extent of glomerular involvement can vary in a biopsy from minimal mesangial expansion to a fully developed nodular glomerulosclerosis that resembles diabetic glomerulosclerosis,<sup>193</sup> but other morphologic features characteristic of diabetes, such as severe arteriolar hyalinosis, fibrin

caps, and capsular drops are absent (Fig. 23.24). Although the pathogenesis of the glomerulosclerosis in LCDD is not entirely clear, experimental studies have shown that mesangial cells exposed to light chains obtained from a patient with LCDD produce transforming growth factor  $\beta$  (TGF- $\beta$ ), which triggers the production of matrix proteins, such as type IV collagen, laminin, and fibronectin.<sup>174,200,201</sup> The tubular basement membranes are thickened and present a homogeneous glassy appearance. Light chain-restricted casts are found in rare cases with concurrent cast nephropathy, and a minority of patients have concurrent AL amyloidosis.<sup>189</sup>

Immunofluorescence microscopy demonstrates linear staining of the monoclonal light chain along the glomerular and tubular basement membranes, as well as the vessel wall; mesangial deposits are also highlighted by the monoclonal light chain (Fig. 23.25). Electron microscopy studies reveal a continuous deposition of a powdery electron-dense material in the GBM, the mesangium, and along the tubular and vascular basement membranes (Fig. 23.26A).<sup>190</sup> Ultrastructurally, the material differs from dense deposit disease (DDD) in that it is finely granular, relatively homogeneous in thickness, and distributed along the inner aspect of the GBM and in the outer aspect of the tubular basement membrane (see Fig. 23.26B).

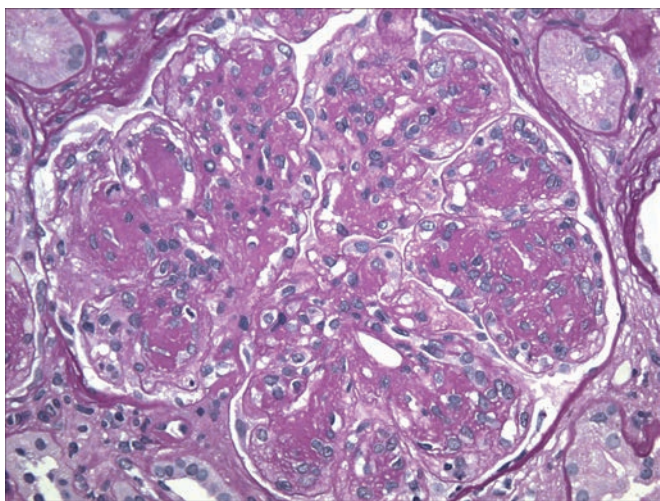


**Figure 23.24** Biopsy from a patient with light chain deposition disease showing nodular mesangial lesions resembling those of diabetes mellitus.

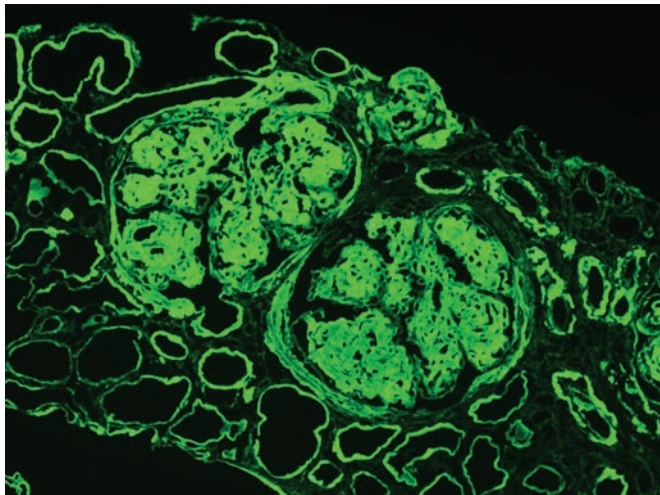


**Figure 23.25** Light Chain Deposition Disease. Immunofluorescence preparation demonstrating reactivity for kappa light chain along the glomerular basement membrane, mesangium, Bowman capsule, tubular basement membrane and vessel walls (anti-kappa).

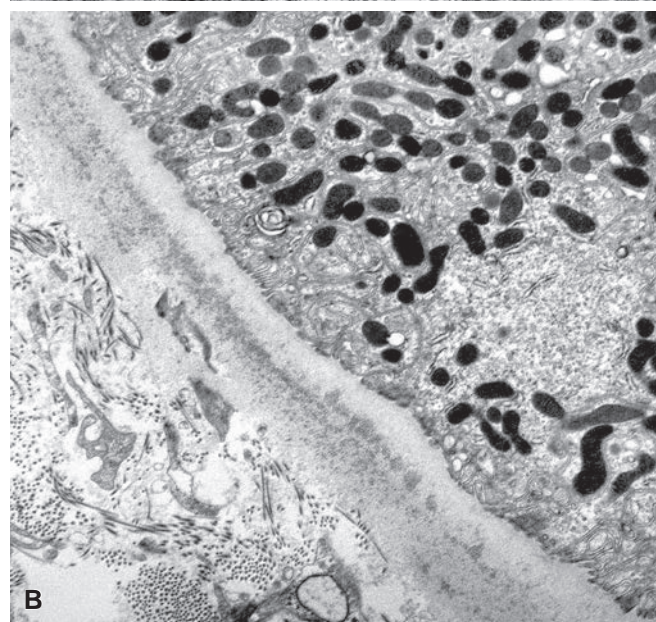
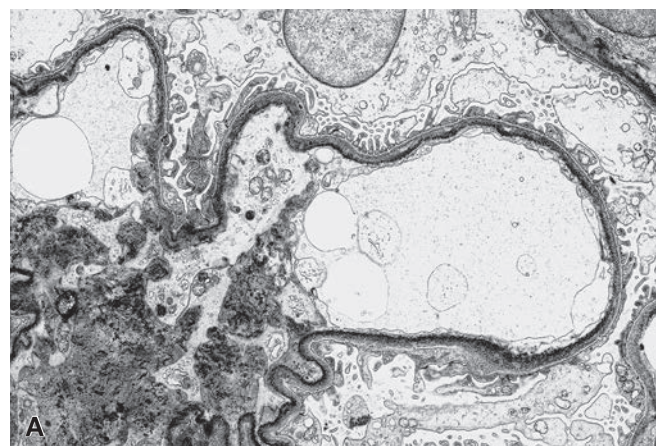


**Figure 23.26** Light Chain Deposition Disease. **A**, Subendothelial and mesangial deposition of granular electron dense material ( $\times 7000$ ). **B**, Similar granular electron-dense deposits are seen along the outer aspect of tubular basement membrane ( $\times 8000$ ).

for the heavy chain occurs along the glomerular, tubular, and vascular basement membranes and in the mesangium.<sup>202</sup>

## Heavy Chain Deposition Disease

Heavy chain deposition disease (HCDD) is much less common than LCDD.<sup>191,195</sup> It is characterized by systemic deposition of a monoclonal immunoglobulin heavy chain. The deposited heavy chain is gamma in most cases, and all subclasses of gamma heavy chain have been reported to participate in the disease. A deletion of the first constant domain (CH1) of the heavy chain has been reported in all documented cases and is likely necessary for the secretion of a free heavy chain by a plasma cell clone of HCDD.<sup>189</sup> The clinical manifestations and histologic features of HCDD are quite similar to those of LCDD.<sup>189,191,202</sup> In contrast to amyloidosis and LCDD, patients with HCDD often manifest hypocomplementemia, possibly due to the complement-fixing properties of IgG subclass deposited.<sup>203</sup> The diagnosis of HCDD can be done by the immunofluorescent demonstration of positivity for heavy chains (usually gamma, IgG) and negativity for both kappa and lambda light chains. The reactivity

## Proliferative Glomerulonephritis With Monoclonal Immunoglobulin G Deposits

Proliferative glomerulonephritis with monoclonal immunoglobulin G deposits (PGNMIGD) is a recently described, rare proliferative glomerular disease with monoclonal immunoglobulin G deposits.<sup>204</sup> It is often seen in middle aged or older individuals, with a female predominance. Over two-thirds of these patients present with nephrotic syndrome and renal impairment, while others have less degrees of proteinuria and hematuria. Despite having monoclonal IgG deposits on kidney biopsy, monoclonal gammopathy is seen in less than 30% of patients and underlying multiple myeloma is rare. A minority of patients (~25%) have reduced serum complement levels, but there is no clinical or serologic evidence of connective tissue disorder or cryoglobulinemia. While some patients may respond to steroids or other immunosuppressive therapy such as rituximab,

PGNMIGN is typically a slowly progressive kidney disease that recurs in allografts.<sup>205</sup> The light microscopic findings are quite variable with membranoproliferative pattern being the most common; endocapillary proliferation, crescents, membranous, mesangiocapillary, and segmental sclerosis patterns have also been described.<sup>204,206</sup> Immunofluorescence microscopy reveals granular mesangial and capillary wall deposits composed of IgG and C3 with associated light chain restriction (IgG3κ most common); IgM and C1q may sometimes be seen. PGNMIGD is defined by IgG subclass restriction and cannot be rendered without immunofluorescence microscopy analysis of IgG subclasses (IgG1–4). IgG3 deposition is most common (followed by IgG1) in PGNMIGD, and its frequent association with hypocomplementemia is possibly related to its complement-fixing abilities and nephritogenicity. Ultrastructural examination localizes the deposits to mesangium and subendothelium with occasional subepithelial deposits identified. Extraglomerular deposits and organized substructure are not typical features of this entity.

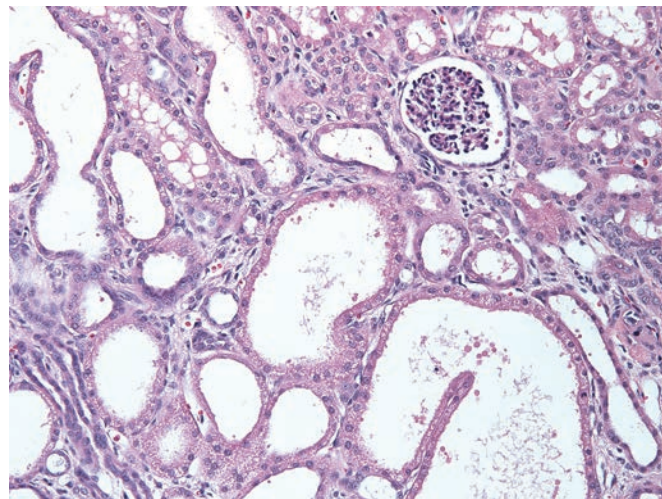


**Figure 23.27** Microcystic dilation of proximal tubules and interstitial scarring in a 1-year-old child with congenital nephrotic syndrome, Finnish type.

### Congenital Nephrotic Syndrome

The nephrotic syndrome is uncommon in the first year of life<sup>207</sup> but is being increasingly recognized that in majority of cases, it is caused by mutations in just one of four genes.<sup>208</sup> The term congenital nephrotic syndrome encompasses a heterogeneous group of conditions but is reserved for patients who present clinical symptoms of nephrotic syndrome at birth or within the first 3 months of life. Two distinct inherited types have been recognized: congenital nephrotic syndrome of the Finnish type and diffuse mesangial sclerosis (DMS). Neither form responds to steroids or immunosuppressive therapy, and renal transplantation is the only way to prolong and improve the quality of life. A renal biopsy is essential to differentiate these two types of congenital nephrotic syndrome from other renal disorders of the neonatal period, including MGN (associated with congenital syphilis or mercury intoxication), congenital toxoplasmosis, HIV (especially in the offspring of narcotic addicts), malaria, cytomegalovirus infection, and MCD.<sup>209–211</sup> In the absence of infections, routine molecular testing of steroid-resistant congenital and infantile nephrotic syndrome is now standard clinical practice.<sup>212</sup>

### Congenital Nephrotic Syndrome of the Finnish Type

Congenital nephrotic syndrome of the Finnish type is a rare autosomal recessive disease caused by mutations of the *NPHS1* gene located on chromosome 19q13.1.<sup>213,214</sup> This gene encodes nephrin protein that is an integral component of the podocyte slit membrane and plays a crucial role in normal glomerular filtration.<sup>215,216</sup> The estimated incidence of the disease in the genetically isolated population of Finland is approximately 1:10,000 newborns,<sup>217</sup> but it has been reported, though with much less frequency, throughout the world in families with no known Finnish ancestry.<sup>43</sup> More than 70 mutations in *NPHS1* gene have been identified worldwide, and majority are frameshift mutations (Fin-major) leading to complete absence of nephrin expression and an early onset severe nephrotic syndrome with rapid progression to end-stage kidney disease. The Fin-minor nonsense mutations result in truncated or nonfunctioning nephrin protein with less severe disease.

The diagnosis may be suspected in utero from the characteristic family history and the finding of elevated alpha-fetoprotein levels in the amniotic fluid and maternal serum, but this is neither highly specific nor sensitive. More recently, *NPHS1* gene sequencing for known and novel mutations is being performed for the prenatal diagnosis of the disease. The disease manifests in the fetal stage with heavy proteinuria in utero. At birth, the patients have large placentas, proteinuria, edema, and a high susceptibility to infections.<sup>43</sup>

Premature birth, mild abnormalities in face and limbs, and poor somatic development are common findings. The nephrotic syndrome often makes its appearance during the first days of life and does not respond to steroid therapy. The disease is progressive during the first 2 years of life, and kidney transplantation is the only successful life-saving treatment. The nephrotic syndrome recurs post transplantation in 20%–30% of cases and is attributed to circulating antinephrin antibodies, detected especially in patients with Fin-major mutations.<sup>218,219</sup>

The most striking histologic feature is ectasia of the proximal and distal tubules with flattening of the tubular epithelium (Fig. 23.27). The glomeruli show minimal changes early on but subsequently develop varying degrees of mesangial proliferation, sclerosis, and dilation of the Bowman space. There may also be an increased number of immature glomeruli. Progressive renal disease is associated with increased TA and IF. Obliteration of epithelial foot processes and other podocyte changes seen in MCD are observed by electron microscopy. Immunofluorescence is usually negative for immunoglobulins and complement components, but mesangial and capillary staining for IgM and C3 have been reported in partially sclerosed glomeruli.

### Diffuse Mesangial Sclerosis

DMS is a rare condition characterized by the early onset of severe proteinuria, characteristic glomerular morphology, and rapid progression to end-stage renal failure before the age of 3 years.<sup>220</sup> DMS can occur in an isolated form or associated with some well-characterized syndromes. Denys–Drash syndrome (DDS), a rare autosomal dominant disorder, is characterized by early onset nephrotic syndrome, male pseudohermaphroditism, and Wilms tumor. Incomplete forms of the syndrome, consisting of glomerulopathy associated with either genital abnormality or Wilms tumor, have also been described. Mutations of the *WT1* suppressor gene located on chromosome 11p13 have been demonstrated in nearly all patients with the complete or incomplete forms of the syndrome.<sup>221,222</sup> Other syndromes described with glomerular pathology of DMS include Galloway–Mowat syndrome (*WDR73* gene mutation), Pierson syndrome (*LAMB2* gene mutation), and a familial steroid resistant nephrotic syndrome (with mutations in *PLCE1* gene), all with autosomal recessive modes of inheritance.<sup>208,223</sup> Young children with Galloway–Mowat syndrome

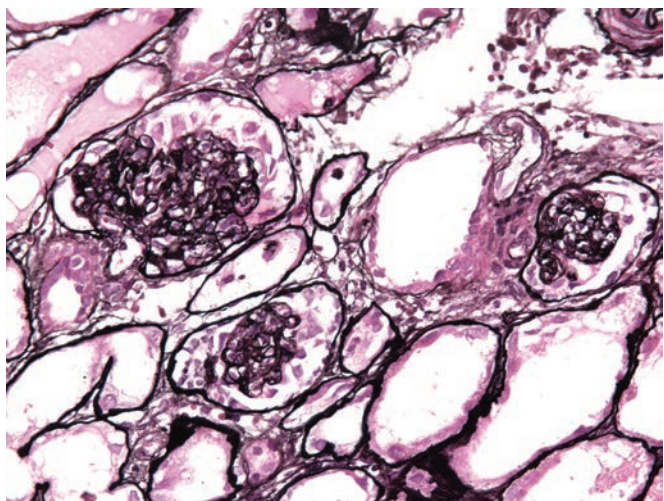


**Figure 23.28** Mesangial sclerosis and consolidation with prominent overlying podocytes are typical for diffuse mesangial sclerosis (methenamine silver).

have microcephaly and seizures in addition to steroid-resistant nephrotic syndrome. Ocular abnormalities such as microcoria, neurologic deficits, and congenital nephrotic syndrome characterize Pierson syndrome. The proteins encoded by all these candidate genes have a role in either podocyte differentiation or function of glomerular filtration barrier. A genetic basis for the sporadic cases of DMS is very much plausible but is unclear in most instances. On rare occasions, cytomegalovirus inclusions were identified in newborns with congenital nephrotic syndrome and glomerular changes of DMS.<sup>209</sup>

In patients with DMS, the nephrotic syndrome can develop as early as first week of life, but it is more likely to appear after the third month. In contrast to the Finnish type, the nephrotic syndrome in DMS is not associated with a large placenta, premature birth, or low birth weight. DMS does not recur after transplantation.<sup>220</sup>

By light microscopy, the glomeruli in early DMS show prominent crowded podocytes reminiscent of fetal appearance. Pseudocrescents with proliferating visceral and parietal epithelial cells have been observed.<sup>43</sup> Subsequently, the glomeruli display increased mesangial sclerosis and consolidation (Fig. 23.28). In advanced stages, there is marked TA with IF. The findings by electron microscopy are extensive obliteration of the epithelial foot processes, basement membrane thickening and lamellation, and an increase in the mesangial matrix. By immunofluorescence, deposition of IgM, C3, and C1q is demonstrable in the sclerotic mesangial areas.

### Glomerular Lesions Associated With the Syndrome of Acute Nephritis

Another major clinical presentation of patients with glomerular lesions is the acute nephritis syndrome. Patients with this syndrome present with hematuria, azotemia, oliguria, and mild to moderate hypertension. Urinalysis reveals an “active” sediment, which consists of the presence of red blood cells, leukocytes, and red blood cell casts. Proteinuria is common but is rarely in the nephrotic range. Edema, when present, is usually mild and is frequently manifested by facial puffiness. Variants of the clinical syndrome include milder forms with microscopic hematuria and non-nephrotic proteinuria, on occasion associated with mild hypertension, and a fulminant form known as rapidly progressive glomerulonephritis. As with the nephrotic syndrome, the histopathologic lesions that can give rise to this clinical presentation are varied.

### Diffuse Endocapillary Proliferative Glomerulonephritis

Diffuse endocapillary (or intracapillary) proliferative glomerulonephritis is a term used to describe lesions characterized by both mesangial and endothelial proliferation. Although this category has become virtually synonymous with acute poststreptococcal glomerulonephritis, it may occur after infections caused by other bacteria including staphylococci, meningococci, pneumococci, *Klebsiella*, *Salmonella*, enterococci, *Brucella*, *Leptospira*, and mycobacteria.<sup>224,225</sup> It can also arise as a complication of rickettsial infections; viral diseases including hepatitis B, varicella, mumps, measles, cytomegalic virus, and infectious mononucleosis; and parasitic conditions such as malaria, trichinosis, and toxoplasmosis.<sup>226</sup>

### Acute Poststreptococcal Glomerulonephritis

Poststreptococcal glomerulonephritis is primarily a disease of childhood, usually occurring between the ages of 5 and 15 years, but it can affect individuals of any age.<sup>227</sup> Approximately 5% of the patients are younger than 2 years of age.<sup>225</sup> Males are affected more commonly than females, with a ratio of 2:1.<sup>226,227</sup> Significantly higher incidence of poststreptococcal glomerulonephritis is seen in less developed countries when compared to the Western world and may even be underestimated due to subclinical cases.<sup>228</sup> The disease profile in developed countries is often different, more frequently affecting elderly individuals with comorbidities.<sup>227</sup>

In the classic form, the disease occurs within 1–4 weeks after infection with a nephritogenic strain of group A  $\beta$ -hemolytic streptococci. The rheumatogenic strains of group A  $\beta$ -hemolytic streptococci (causing rheumatic fever) differ from the nephritogenic strains by the surface M proteins. Primary infections may be either pharyngeal or, less commonly, cutaneous. The principal serotypes implicated in glomerulonephritis are streptococci of group M types 12, 4, 1, and 49.<sup>226</sup> The risk for developing glomerulonephritis after infection with a nephritogenic streptococcus is variable, depending on a variety of host and virulence factors, but the overall risk is estimated to be about 15%.<sup>229</sup> The clinical, morphologic, and serologic findings indicate that poststreptococcal glomerulonephritis is an immune complex disease, and the main target antigens implicated thus far include “streptococcal pyrogenic exotoxin B” (SPEB) and “nephritis-associated plasmin receptor.”<sup>230</sup> SPEB is a cationic protein that co-localizes in the subepithelial deposits and both antigens promote plasmin activity, contributing to glomerular tissue injury. In addition, the circulating antigen-antibody complexes deposit in subendothelium, activate the alternative and possibly lectin complement pathway, and trigger an inflammatory response.<sup>228</sup>

Clinically, this disease is manifested by a rather abrupt onset of gross hematuria, edema, proteinuria, hypertension, and impaired renal function.<sup>228,231</sup> Antibodies to certain streptococcal antigens, such as antistreptolysin O (ASO), are elevated, but this finding may not be helpful in diagnosis due to the ubiquitous nature of streptococcal infections. The serum levels of hemolytic complement activity and C3 protein are abnormally reduced early in course of the disease, but the values return to normal in less than 8 weeks. During the acute episode of poststreptococcal glomerulonephritis, 2%–5% of the patients die as a result of complications such as pulmonary edema, hypertensive encephalopathy, or rapidly progressive renal failure due to crescentic glomerulonephritis; and these figures are much higher in elderly patients.<sup>228,232</sup> The long-term prognosis of patients with acute poststreptococcal glomerulonephritis is good, especially in children, with only a small number of patients progressing to chronic renal failure many years after the acute episode.<sup>225,233</sup> Recovery in adults is less predictable than in children, especially

with persistent proteinuria or when the initial episode is associated with severe renal impairment and nephrotic syndrome.<sup>226,227,230</sup> Progression of renal disease is more common in patients who develop crescentic glomerulonephritis. Since the clinical syndrome of acute poststreptococcal glomerulonephritis may be quite distinctive and the overall prognosis is excellent, biopsies are not commonly performed unless atypical features complicate the presentation, such as nephrotic syndrome, anuria, acute renal failure, persistent or severe hypertension, or lack of recovery after 6 weeks. On long-term follow-up, approximately 17% of the patients have persistent mild proteinuria, microhematuria, or hypertension.<sup>230</sup> Recent studies have indicated an overlap between atypical postinfectious glomerulonephritis and C3 glomerulonephritis (C3GN), as several of these patients with persistent late symptoms have alternative complement pathway abnormalities.<sup>234</sup> In addition, it appears that streptococcal infections may act as a trigger for precipitating C3 glomerulopathy in a genetically predisposed individual.<sup>235,236</sup>

Light microscopic examination of biopsies taken within a few weeks of onset of disease shows diffuse enlargement of the glomerular tufts that tend to narrow the Bowman space. Glomerular intracapillary cellularity is increased due to mesangial proliferation and, to a lesser extent, proliferating and swollen endothelial cells. This results in narrowing of the capillary lumina and accentuation of the lobular glomerular pattern. Infiltration by leukocytes can contribute to the capillary obstruction as well, and, when prominent, the term *exudative* glomerulonephritis has been used (Fig. 23.29). Accompanying the polymorphonuclear leukocytes are mononuclear cells and, on occasion, eosinophils. Segmental necrosis and thrombosis with crescent formation are uncommon findings but indicate poor prognosis.

The most characteristic ultrastructural feature in the early stages of the disease is the presence of subepithelial, dome-shaped, electron-dense deposits called humps (Fig. 23.30). The deposits are separated from the lamina densa by a recognizable lamina rara externa, and the foot processes of the podocytes overlying the humps are usually obliterated. In general, there is a correlation between the number of humps and the degree of polymorphonuclear cell infiltration, but the humps may occur in loops devoid of leukocytes. Intramembranous deposits, some of them in continuity with the humps, and small subendothelial and mesangial deposits are not uncommon.

Immunofluorescence studies during the acute phase of the disease typically reveal granular staining for IgG and C3 along the capillary

loops where the humps are located (Fig. 23.31). Small amounts of IgM and IgA may be found. Properdin is frequently present and this, coupled with the strong reactivity for C3 and the absence of C1q and C4 in the deposits, suggests involvement of the alternative complement pathway.

Serial biopsies show a gradual resolution of the glomerular changes. Cellularity decreases and the humps generally disappear in 6–8 weeks, though they can be identified up to 6 months after the onset of the disease. During the resolving phase, the basement membrane may show focal irregularities with decreased electron density, the capillary lumina become patent, and the endothelial swelling and polymorphonuclear leukocytic infiltration disappear. Electron-dense deposits either are no longer visible or are confined to the mesangium.<sup>228</sup> IgG may not be demonstrable, and C3 staining gradually disappears from the periphery and becomes restricted to the mesangial areas. Complete restoration to normal histology occurs as early as 6 months and certainly within 2–3 years. In a small

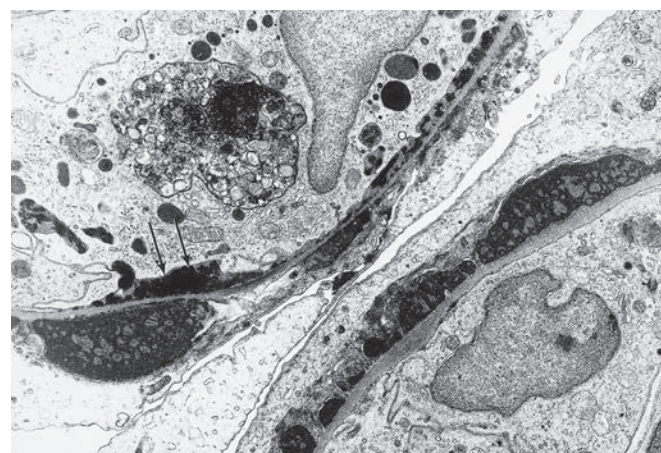


**Figure 23.30** Biopsy From a Patient With Acute Poststreptococcal Glomerulonephritis. There are numerous humps along the basement membrane. The capillary loops are obliterated by cell proliferation and inflammatory cells. Small amounts of fibrin are present in the subendothelial areas (arrows) (x9800).

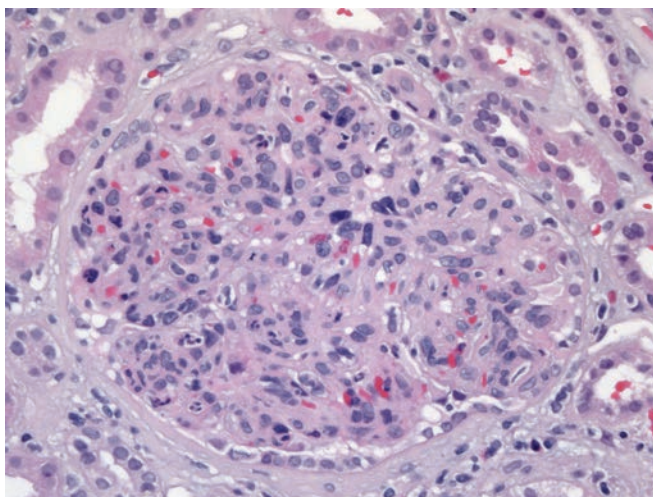


**Figure 23.29** Diffuse Proliferative Glomerulonephritis. There is marked hypercellularity due to an increase in mesangial and endothelial cells and infiltration by inflammatory cells.

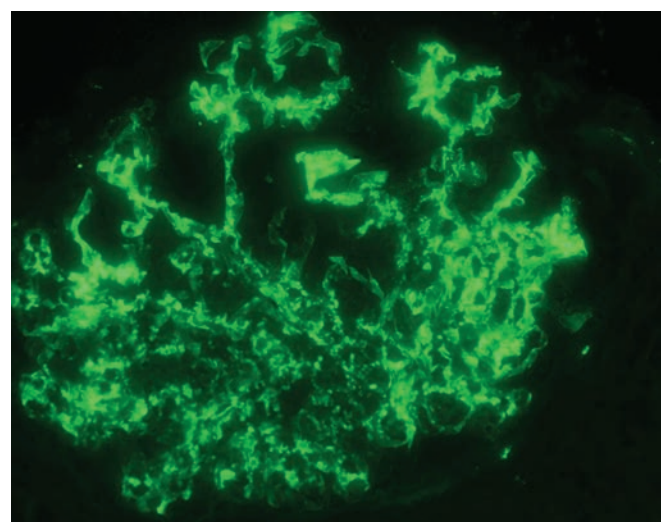


**Figure 23.31** Poststreptococcal Glomerulonephritis. The coarse granular immunostaining for C3 along the capillary loops corresponds to the humps seen by electron microscopy (anti-C3).

percentage of cases, mesangial hypercellularity, mesangial deposits, and increased mesangial matrix may persist for years after the acute episode, and the mesangial prominence tends to be focal and segmental.

### IgA-Dominant Staphylococcal Infection-Associated Glomerulonephritis

Infection-associated glomerulonephritis in the developed countries is being increasingly caused by *Staphylococcus aureus*, especially the drug-resistant strains.<sup>237,238</sup> Unlike poststreptococcal glomerulonephritis, staphylococcal infection-associated glomerulonephritides are more common in the elderly population (over 60 years of age) with comorbidities such as diabetes mellitus, drug abuse, alcoholism, and malignancy.<sup>228,238</sup> The underlying infection is typically ongoing (rather than "post-infection") and is often brought to attention by the kidney disease. The characteristic feature of this entity is IgA-dominant or co-dominant immune deposits that are seen in addition to C3.<sup>227,239,240</sup> The IgA-dominant host immune responses appear to play a role in this morphologic variant of infection-associated glomerulonephritis. It has been postulated that the *S. aureus* enterotoxins and possibly other antigens function as "superantigens," capable of binding directly to the major histocompatibility complex (MHC) class II molecules on antigen presenting cells without the required intracellular antigen processing to form receptor-fitting peptides.<sup>241,242</sup> In addition, these superantigens bind to T-cell receptors, causing massive T-cell activation, proliferation, and cytokine release. These events in turn trigger polyclonal B-cell activation, and patients with *S. aureus* infections were shown to have polyclonal elevation of serum IgA and IgG. The most common presentation is acute renal injury, proteinuria often in the nephrotic range, and hematuria.<sup>239,243</sup> There appears to be a male predominance, and two-thirds of the patients have mild hypocomplementemia. A small percentage of patients may present with lower extremity rash, reminiscent of Henoch-Schönlein purpura (HSP).<sup>226,244</sup> Reported underlying infections have included osteomyelitis, pneumonia, septic arthritis, empyema, sinusitis, and endocarditis, among others. The latent period between the onset of infection and renal manifestations appears to be 4–5 weeks, but in most cases the infection is not recognized until the time of the kidney biopsy. Treatment of underlying infection is the main form of therapy and overall, the prognosis is inferior to poststreptococcal glomerulonephritis, possibly related to the patient's age and associated comorbidities.

The glomerular changes on biopsy can be variable,<sup>226</sup> ranging from mild mesangial hypercellularity to diffuse endocapillary proliferation and on occasion, crescents; exudative features are not uncommon, although seen less frequently than in poststreptococcal glomerulonephritis. There is usually accompanying acute tubular injury and interstitial inflammation, but vasculitis is not a feature observed on kidney biopsy. In patients with diabetes mellitus, subtle changes of glomerular endocapillary proliferation may be masked by prominent Kimmelstiel-Wilson nodules.<sup>245</sup> The electron-dense deposits are primarily in the mesangium and parmesangium, but occasional subendothelial deposits are not uncommon. The subepithelial "humps," the hallmark of infection-related glomerulonephritis, are seen in less than 50% of patients. When present, these subepithelial deposits are often smaller and less "hump"-like. The glomerular immune deposits are composed predominantly of IgA and C3 with less intense or absent IgG. Light chain  $\kappa$  and  $\lambda$  staining is usually seen, and  $\lambda$  can be more intense than  $\kappa$ . These immunofluorescence findings can lead to a misdiagnosis of IgAN, especially in the absence of obvious infection or if the skin rash is reminiscent of HSP. Distinguishing between these two entities is extremely important as immunosuppression for a presumed IgAN will exacerbate

an unrecognized infection. Low serum complement levels and subepithelial humps, if present, indicate infection-associated glomerulonephritis rather than IgAN.<sup>226,246</sup>

### C3-Related Glomerular Diseases and Membranoproliferative Glomerulonephritis

Membranoproliferative glomerulonephritis (MPGN; also known as mesangiocapillary glomerulonephritis) is a term used to designate a distinctive histopathologic pattern of glomerular injury characterized by a combination of mesangial cell proliferation with lobular accentuation (Fig. 23.32) and capillary wall thickening with double contours and extension of the mesangial cell cytoplasm into the periphery of the loop (Fig. 23.33). Based on the ultrastructural morphology and distribution of the deposits, MPGN was traditionally subdivided into two major types: in the first (type I), the deposits are primarily subendothelial (Fig. 23.34); in the second (type II), the deposits are extremely dense and lie within the basement membrane. However, only a minority of later group (about 25%) exhibit the membranoproliferative pattern, and hence the preferred

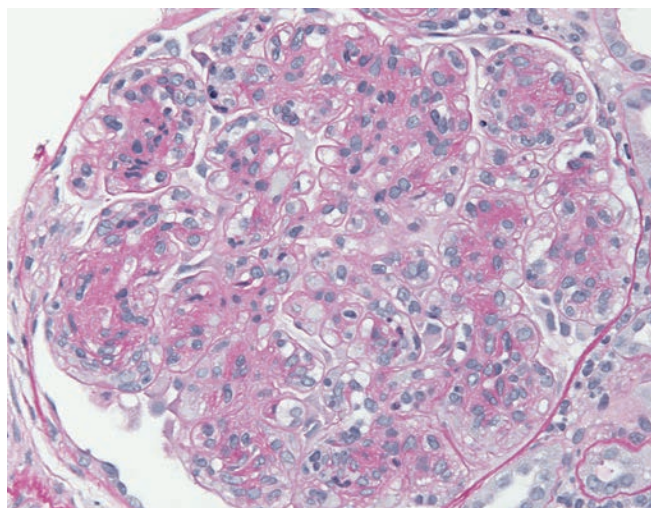


**Figure 23.32 Membranoproliferative Pattern Glomerulonephritis.** There is an increase in lobulation, diffuse mesangial hypercellularity, and thickening of the capillary walls.

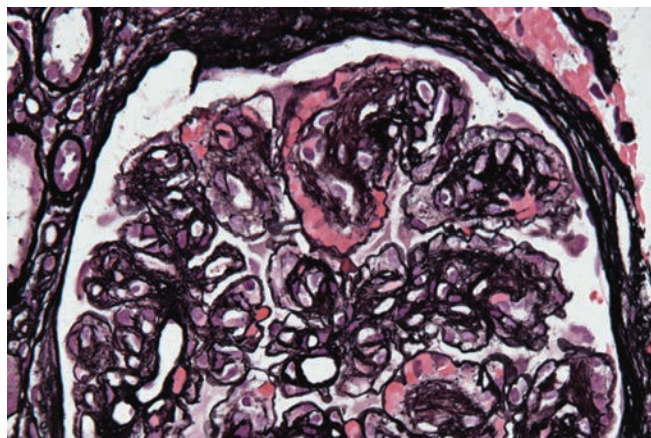


**Figure 23.33** Silver preparation showing marked increase in mesangial matrix in the centrilobular areas with peripheral extension of the mesangium producing a double contour (membranoproliferative) pattern in the loops (methenamine silver).

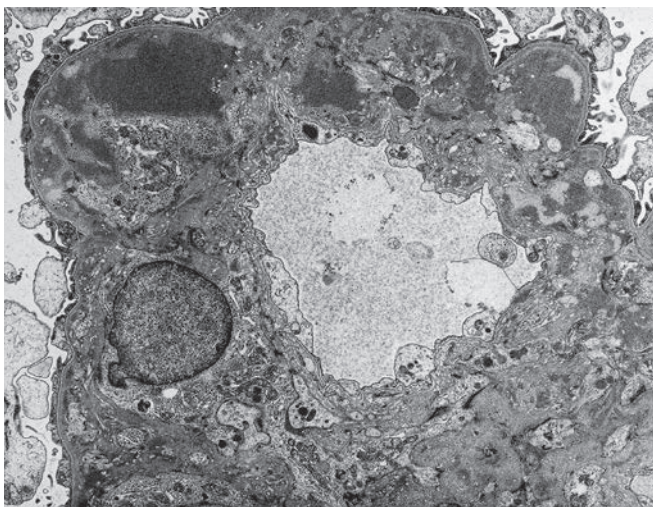


**Figure 23.34** Glomerular capillary loop from a patient with membranoproliferative pattern glomerulonephritis showing peripheral extension of the mesangium into capillary loop, basement membrane duplication, and subendothelial deposits ( $\times 5400$ ).

and currently used term DDD instead of MPGN type II.<sup>247</sup> In addition, other variants referred to as type III, which show either extensive disruptions of the lamina densa or frequent subepithelial deposits, have been described.<sup>248–250</sup>

Although the traditional subdivision of MPGN implied various morphologic patterns of a single clinicopathologic entity, the conditions do not share a common pathogenesis and they are linked only by the morphologic similarities on routine light microscopy. Recent studies have helped gain insight into the pathophysiological mechanisms of "MPGN" and related entity of C3GN.<sup>251–253</sup> Although the classification scheme is evolving, these disorders fall broadly into two categories (Box 23.4).<sup>254,255</sup> The first, *C3 glomerulopathy*, consists of glomerular diseases with prominent C3 deposition with little or no immunoglobulin deposition. It encompasses DDD, C3GN, and familial forms of MPGN and is associated with dysregulation of alternative complement pathway. A subset of previously designated MPGN type I and type III belongs to C3 glomerulopathy category under this new classification. The second group, *idiopathic MPGN with prominent immune complex deposition* (in addition to C3), includes approximately 70% of type I and 60% type III MPGN, as defined by the traditional classification.<sup>256</sup> Several patients in the second group also appear to have alternative complement pathway abnormalities, posing a challenge for an immunofluorescence-based classification system.<sup>254</sup>

### C3 Glomerulopathy

C3 glomerulopathy is characterized by abnormal persistent activation of alternative complement pathway and predominant glomerular deposition of C3, with a proposed definition of C3 immunofluorescence intensity  $\geq 2$  levels (scale 0–3+) above immunoglobulins or C1q.<sup>254</sup> These patients often have genetic abnormalities of, or circulating autoantibodies directed against, complement components.<sup>251,257,258</sup> Serum C3 levels are often reduced, and histology is variable, including some with membranoproliferative features. The main entities in this category are DDD and C3GN. Others include familial forms with type III MPGN features caused by an abnormal complement factor H-related protein (CFHR3-1), and an autosomal dominant form with mutations in CFHR5 (see Box 23.4).<sup>253,259</sup> It is interesting that some patients with "atypical" postinfectious

### Box 23.4 C3-related glomerular diseases and membranoproliferative glomerulonephritis (MPGN)

#### C3 glomerulopathy (isolated/predominant C3 deposits)

Dense deposit disease (previous term type II MPGN)

C3 glomerulonephritis

Familial C3 glomerulopathy (abnormal CFHR3-1 protein, type III MPGN features)

CFHR5 nephropathy (mutations in CFHR5 gene)

#### Idiopathic MPGN (immune complex deposition; C3 and immunoglobulin deposition)

MPGN type I morphology

MPGN type III morphology

#### Secondary causes of MPGN morphology

##### Infections

Hepatitis B and C, endocarditis, visceral abscesses, shunt nephritis, malaria, schistosomiasis, mycoplasma, HIV, and Epstein–Barr virus infections

##### Immunologic and systemic disorders

Systemic lupus erythematosus, scleroderma, Sjögren syndrome, rheumatoid arthritis, sarcoidosis, mixed essential cryoglobulinemia with or without hepatitis C infection, ulcerative colitis, sickle cell disease

##### Dysproteinemia

MGUS, type I cryoglobulinemia, Waldenström macroglobulinemia, fibrillary glomerulonephritis, immunotactoid glomerulopathy

##### Neoplastic diseases

Carcinoma, chronic lymphocytic leukemia, non-Hodgkin lymphoma, melanoma

##### Hereditary diseases

$\alpha 1$ -Antitrypsin deficiency, complement deficiency, hereditary angioedema, Wiskott–Aldrich syndrome, Sherwood–Proesmans syndrome, autosomal recessive MPGN type I

##### Miscellaneous

Drug abuse (heroin, pentazocine), Kartagener syndrome, Turner syndrome, Down syndrome, transplant glomerulopathy, chronic thrombotic microangiopathy

CFHR, Complement factor H-related protein or gene; MGUS, monoclonal gammopathy of undetermined significance; MPGN, membranoproliferative glomerulonephritis.

glomerulonephritis (with or without documented infection) also have mutations in complement genes or have related autoantibodies.<sup>234</sup> It has been suggested that an infection or other triggers unmask a C3GN in a predisposed individual.<sup>235,236</sup> Novel treatment approaches are being developed to treat C3 glomerulopathy, hence the importance of accurate diagnosis.<sup>260,261</sup> Plasma infusions and plasmapheresis aim to correct complement deficiencies or remove circulating autoantibodies. Inhibition of alternative complement pathway (C5 inhibition) and restoration of normal functional state may also be effective in these patients.

#### Dense Deposit Disease

DDD, previously termed as type II MPGN, is a C3 glomerulopathy characterized by a unique broad, linear intramembranous electron-dense deposits. DDD is rare and has been estimated to affect two to three people per one million population.<sup>261,262</sup> Both sexes are equally affected, with the diagnosis usually made in children between the ages of 5 and 15 years.<sup>263</sup> Affected patients typically present with nephrotic proteinuria, hematuria, and renal insufficiency. Most patients with DDD have hypocomplementemia and continue to have low levels of complement throughout the course of the disease. C4 levels are usually normal.<sup>264</sup> Over 80% of patients with DDD

are positive for serum C3 nephritic factor (C3NeF), an autoantibody directed against C3bBb, a convertase of the alternative pathway of complement cascade. Because C3NeF can be found in idiopathic MPGN and C3GN (previously type I and III MPGN), a definitive diagnosis of DDD depends on the ultrastructural demonstration of dense deposits within the GBM. Other unusual aspect of DDD is its association with macular degeneration and acquired partial lipodystrophy (loss of subcutaneous fat in upper half of the body) in approximately 3%–5% of cases. Patients with these conditions were found to have hypocomplementemia and C3NeF regardless of whether or not they develop DDD.<sup>265–269</sup>

DDD has a poor prognosis and in about 50% of the cases, the lesion slowly progresses to an end-stage kidney within 10–15 years of diagnosis. Abrupt decline in renal function can be seen with crescentic disease. On rare occasions, there have been reports of morphologic regression.<sup>270–272</sup> Recurrence after renal transplantation occurs in virtually all renal allografts.<sup>273</sup> Chronic activation of alternative complement pathway is the culprit and is mediated in most instances by C3NeF that inhibits the activation blocker, C3 convertase. Other less common autoantibodies documented in DDD are against factor H, factor B, and C3. Genetic predisposition plays a role and mutations in *CFH* gene have been detected in 17% of patients. Certain allelic variants of *CFH*, *CFI*, *C3*, and *CFHR5* and *C3* mutations have been associated with DDD.<sup>257,258,262</sup> It appears that infections, chemotherapy, and other unknown factors may precipitate DDD in these predisposed patients. Interestingly, adults with DDD may have coexistent monoclonal gammopathy, and the pathogenic light (or heavy) chains interfere with the control of the alternative complement pathway.<sup>274</sup>

On light microscopy, the general morphologic features can be quite variable. In a study of a large series of renal biopsies, nearly half showed mild, mesangial hypercellularity, whereas only about 25% had the typical membranoproliferative pattern (see Figs. 23.32 and 23.33). Approximately 17% had a crescentic glomerulonephritis pattern (Fig. 23.35), and 12% had an acute proliferative and exudative pattern that could be easily confused with postinfectious glomerulonephritis.<sup>247</sup> A feature that establishes the diagnosis is an eosinophilic, refractile, and ribbon-like thickening of the basement membrane, which is most pronounced along the GBM, although it can be seen in the Bowman capsule and in the tubular basement membrane. The deposited material is strongly PAS positive, stains blue with Masson trichrome, is pale on Jones stain, and can easily be recognized by its dark color on toluidine blue-stained

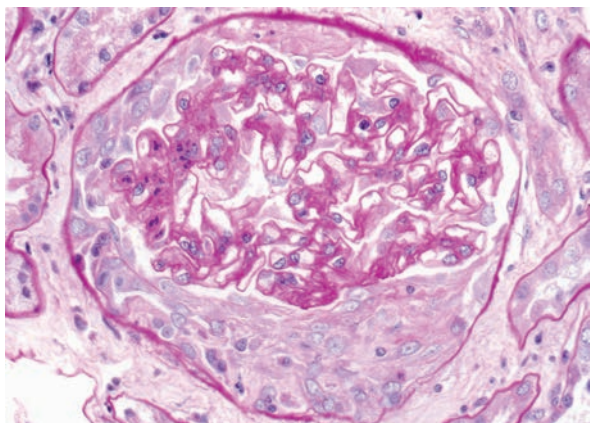


**Figure 23.35** Dense deposit disease has variable histologic manifestations. Crescent formation with mild segmental mesangial expansion by inflammatory cells in a young patient (PAS).

plastic-embedded tissue sections. Ultrastructurally, the material is extremely electron dense and lacks the prominent granularity of immune complex deposits. It is centrally positioned within the lamina densa of basement membrane but may vary in thickness or be focally discontinuous (Fig. 23.36A). Similar deposits can be found in the mesangium as homogeneous nodules or, less frequently, subepithelial humps.<sup>275</sup> These deposits can be seen in choroidal blood vessels and ocular Bruch membrane. The immunofluorescence pattern is typical and diagnostic. A linear or double-contoured staining for C3 along the glomerular capillary walls is associated with a bright nodular or ring-like reaction in the mesangium (see Fig. 23.36B). A focal and often discontinuous linear C3 reaction can be seen in the Bowman capsule and in some tubular basement membranes. Immunoglobulin and early components of complement are usually absent and if present, significantly less intense than C3. Using laser-capture mass spectrometry, it has been found that these deposits are composed of C3 and other late complement components, CFHP1, clusterin, vitronectin, and unsaturated lipids associated with ApoE among others.<sup>276</sup>

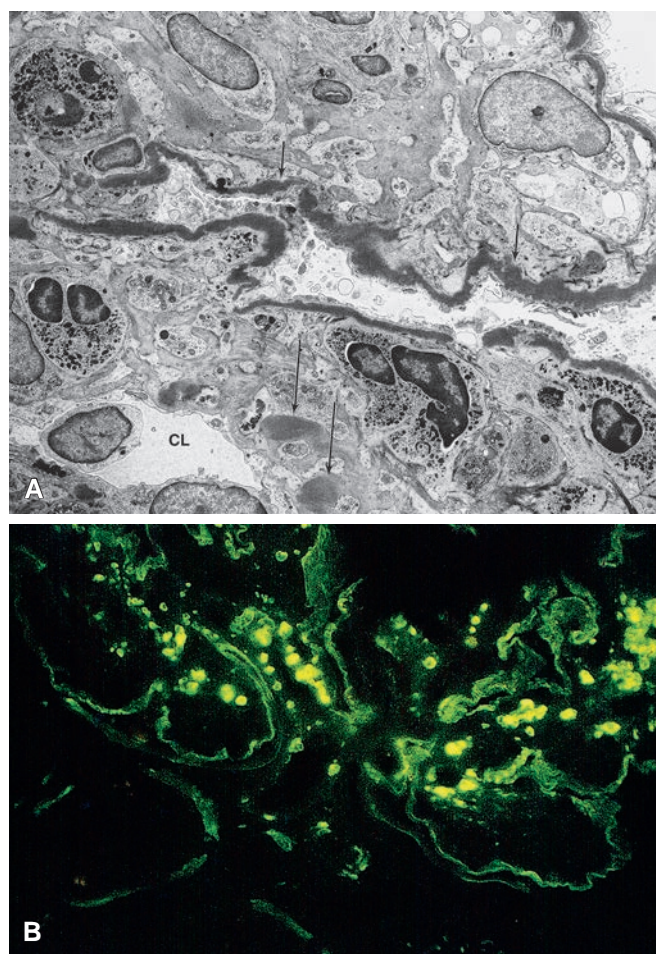


**Figure 23.36** **A**, There is homogeneous, highly dense material within the lamina densa (short arrows) and nodular deposits (long arrows) of the same electron density in the mesangium. The capillary lumen (CL) in the left lower portion of the figure is narrowed due to peripheral extension of the mesangium. Numerous neutrophils are also present (x4000). **B**, Immunofluorescent staining for C3 showing weak linear staining along glomerular capillary and tubular basement membranes (right lower corner) and bright granular deposits in the mesangium, some of which have a ring-like pattern.

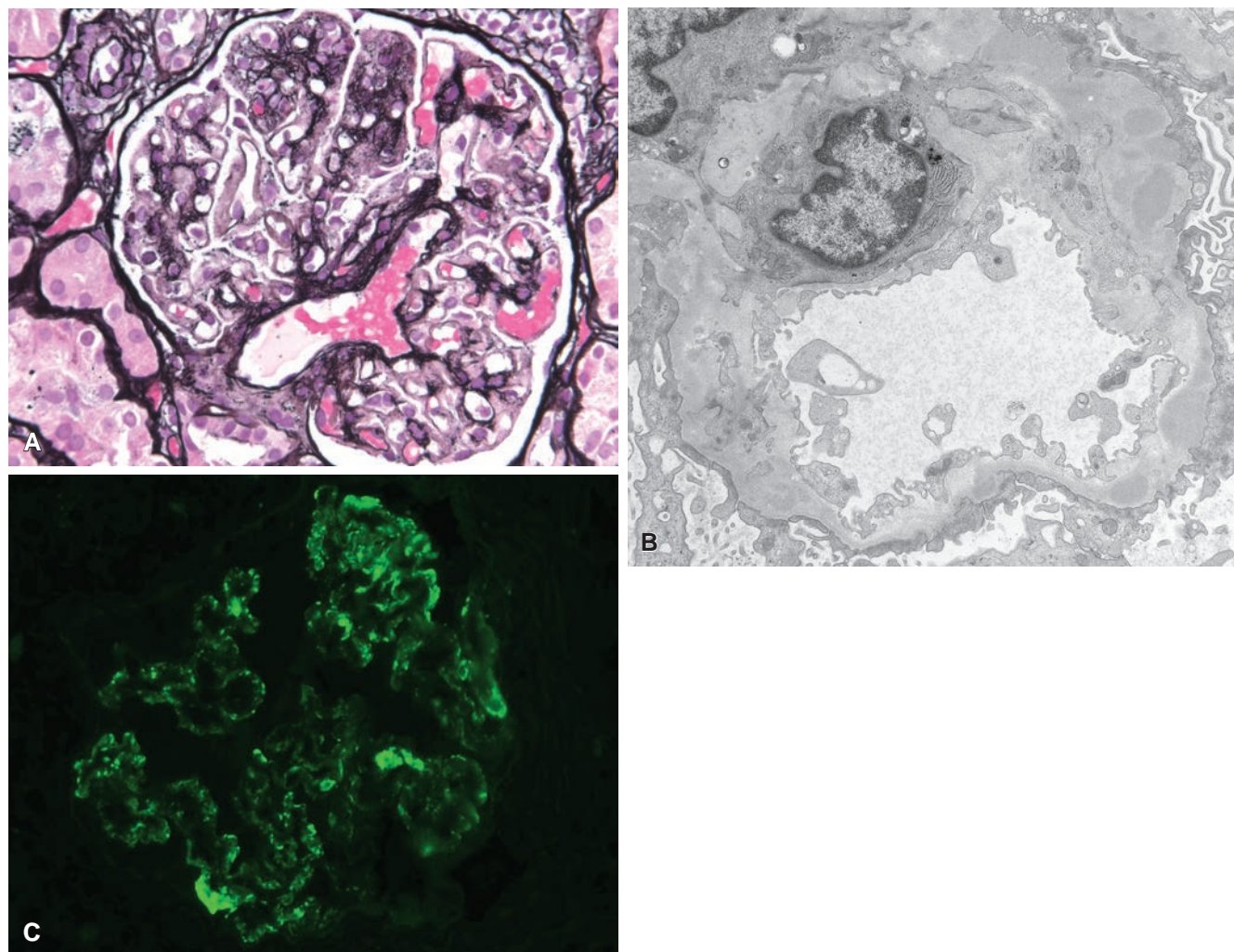


**Figure 23.37 C3 Glomerulonephritis.** **A**, Segmental mesangial proliferation and glomerular basement membrane thickening (methenamine silver). **B**, Intramembranous and subepithelial electron-dense deposits with focal glomerular basement membrane duplication ( $\times 7000$ ). **C**, Granular segmental mesangial and capillary wall deposits with C3. No immunoglobulin staining was observed by immunofluorescence (anti-C3).

### C3 Glomerulonephritis

C3GN is a type of C3 glomerulopathy characterized by isolated C3 deposits, minimal or no immunoglobulin deposition, and dysregulated alternative complement pathway. However, unlike DDD, the electron-dense deposits are amorphous and not as electron dense, broad, or linear. It includes majority of cases previously designated as type I and III MPGN and other glomerulonephritides without membranoproliferative morphology.<sup>254,256,277</sup> Patients with C3GN are often adults, with a mean age of 30 years at presentation, but it has been reported in children as young as 7 years and elderly individuals older than 70 years. The renal manifestations are variable, ranging from mild proteinuria to nephrotic syndrome. Microscopic hematuria, hypertension, and renal insufficiency are frequently present. Serum complement C3 levels are low in approximately 40% of patients, but C4 is typically normal.<sup>278</sup> C3NeF is detectable in approximately 45% of patients. Older individuals with C3GN can also have circulating monoclonal immunoglobulins, although a direct pathogenic link to C3GN has not been established. The light microscopic findings of C3GN are variable, ranging from minimal changes to diffuse proliferative to membranoproliferative patterns

(Fig. 23.37A).<sup>256</sup> Crescents are occasionally present and proliferative glomerulonephritis can also show exudative features, reminiscent of postinfectious glomerulonephritis.<sup>234</sup> The chronic tubulointerstitial damage typically ranges from mild to moderate depending on the chronicity of the disease. Ultrastructurally, amorphous deposits are predominantly in the mesangium and the capillary wall deposits can be in subendothelial, and/or subepithelial and intramembranous (type I or III MPGN pattern described in the next section) (see Fig. 23.37B). By mass spectrometry, these deposits are composed of alternative and terminal complement pathway components, identical to DDD.<sup>277</sup> As mentioned earlier, the glomerular deposits stain strongly for C3 with little or no immunoglobulin (see Fig. 23.37C).<sup>254</sup>

A diagnosis of C3GN (and DDD) should prompt thorough investigation for complement factor levels (factor H, factor I, factor B, membrane attack complex), anti-factor H autoantibodies and alternative complement pathway functional and hemolytic assays.<sup>254</sup> Mutations in genes encoding complement regulatory factors (factor H, factor I, CD46, CFHR5) and certain complement factor alleles that confer higher risk of developing disease have also been

documented in C3GN. Patients can have more than one acquired or inherited abnormality related to C3GN.<sup>277</sup>

### Membranoproliferative Glomerulonephritis With Immune Complexes

This group of diseases is characterized by mesangial hypercellularity and GBM duplication, with prominent C3 and immunoglobulin (and/or C1q) deposition, indicative of both classical and alternative complement pathway activation.<sup>254,279</sup> Extrapolating the historical data of type I MPGN, it likely accounts for approximately 5% of ESRD cases secondary to glomerulonephritis. Membranoproliferative pattern with immune complexes can be primary/idiopathic or more commonly, secondary to chronic infections, monoclonal gammopathy, systemic autoimmunity, and hereditary diseases (see **Box 23.4**). It is also believed that the majority of cases once thought to be "idiopathic" are associated with hepatitis C infection.<sup>280</sup> Further, recent advances in elucidating the pathogenetic mechanisms of MPGN, especially C3 glomerulopathy, has altered the prevalence of "idiopathic" MPGN. It is now a *diagnosis of exclusion*, especially in adults, and perhaps will become an increasingly uncommon diagnosis in the future.<sup>279,281</sup> Based on the historical data, primary/idiopathic form of the disease, affects primarily children and young adults, with 90% of patients being between 8 and 16 years of age at the time of diagnosis.<sup>275,282</sup> Onset before the age of 4 years is rare. Clinical presentation varies, and there does not appear to be a gender predominance. At least 50% of the patients present with nephrotic syndrome, and 25% may present with a combination of asymptomatic hematuria and asymptomatic proteinuria. Finally, up to one-third of patients may present with acute nephritic syndrome associated with abnormal urinary sediment, hypertension, and renal insufficiency.<sup>275,282,283</sup>

About two-thirds of the patients have hypocomplementemia with marked variation of its level over the course of the disease. The predominant complement depletion is C3, but early (i.e., C1q, C4, and C2) and terminal (C5, C6, C7, and C9) components of the classic pathway of complement activation maybe reduced as well. Components of the alternative pathway (i.e., factor B), are also frequently low,<sup>284</sup> and C3Nef is detected in more than half of patients with type I MPGN. Mutations in alternative complement pathway genes (*CFH* and *CFI*) have been detected in a minority of these patients (with type I pattern), blurring the line between the categories of C3 glomerulopathy and MPGN with immune complexes.<sup>257</sup> It has been speculated that in these cases, the underlying genetic or acquired complement dysregulation is triggered or exacerbated by the immune complex deposition.<sup>251</sup> Historically, the clinical course of "primary/idiopathic" MPGN is usually indolent but relentless, progressing to renal failure over a period of 10 or more years.<sup>285</sup> The disease has been reported to recur in 30%–50% of the patients who undergo renal transplantation<sup>273,286</sup> and the risk of recurrence appears to be higher in patients with low serum complement levels.<sup>287</sup>

On light microscopy, the glomeruli appear diffusely enlarged, with thickening of the capillary walls and prominent mesangial proliferation that produces lobulation of the tuft (see **Fig. 23.32**). Mesangial matrix accumulates in the center of the lobules, forming nodules resembling diabetic glomerulosclerosis. In addition to the lobular pattern, exudative, crescentic, and focal segmental histologic variants have been described.<sup>283</sup> In sections stained with PAS or Jones methenamine silver stain, continuation of the mesangial matrix can be seen to surround capillary loops, producing a double contour or "tram-track" pattern (see **Fig. 23.33**). Within the double contours, hyaline material corresponding to subendothelial deposits are often prominent. The presence of hyaline thrombi within the capillary lumens should raise the possibility of cryoglobulinemia or lupus nephritis.

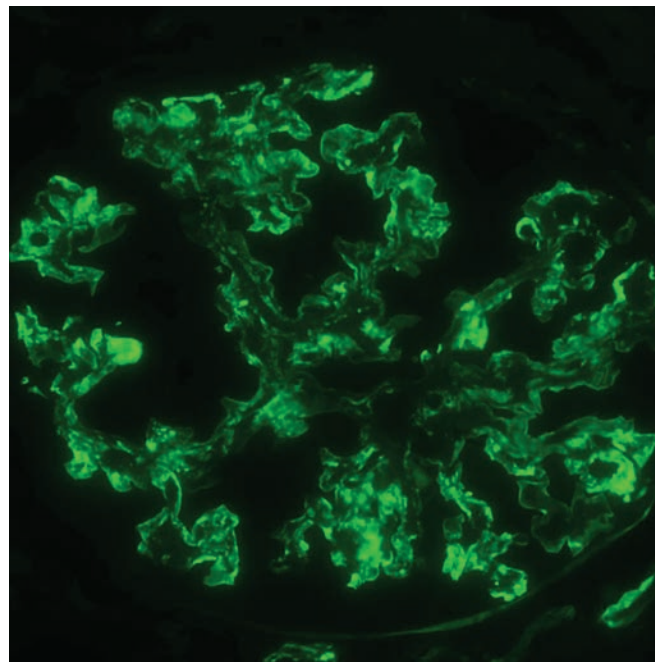


**Figure 23.38** Membranoproliferative Glomerulonephritis With Immune Complexes. Immunofluorescence preparation demonstrating immunoreactivity for IgG (and C3) in the mesangium and along patchy capillary loops (anti-IgG).

Immunofluorescence usually demonstrates a granular reaction for IgG and C3 along the capillary walls and mesangium (Fig. 23.38). In addition, IgM, C1q, and C4 can be present. Electron microscopy demonstrates that the mesangial areas are enlarged by cellular proliferation and accumulated matrix, and that the capillary lumina are reduced by a combination of peripheral mesangial expansion and interposition of cells and matrix beneath the endothelium. Typically, there is a continuous layer of mesangial cytoplasm around the entire capillary with an irregular layer of new matrix underlying the intact basement membrane. Electron-dense deposits in type I MPGN pattern are typically seen in the mesangial and subendothelial regions (see **Fig. 23.34**). Type III pattern MPGN is a very uncommon and controversial variant of MPGN, of which two morphologic subtypes have been defined. In the first subtype, referred to as the Burkholder variant, the glomerular lesion presents combined features of MPGN type I and MGN.<sup>249</sup> Ultrastructural examination of the capillary walls demonstrates mesangial interposition, subendothelial deposits, and numerous subepithelial deposits associated with basement membrane spikes. In the second subtype described by Anders and associates in 1977, the glomerular lesion resembles a hybrid between type I and type II MPGN.<sup>248,250,288</sup> Despite the pathologic differences, both variants of type III MPGN are clinically similar and do not differ significantly from MPGN type I.

### Diffuse Mesangiproliferative Glomerulonephritis

Diffuse proliferation of the mesangial cells and matrix without significant involvement of capillary walls or lumina occurs in a variety of renal diseases, including IgAN, HSP, SLE, and the resolving stage of postinfectious glomerulonephritis. The differential diagnosis of these conditions requires correlation of the light, electron, and immunofluorescent microscopic findings with the patient's clinical data. Only IgAN is discussed in this section.

## IgA Nephropathy

IgAN (previously called Berger disease) is defined by the predominant deposition of IgA in the glomerular mesangium. The distribution of IgAN varies greatly among different geographic regions of the world. It is the most common primary glomerular disease diagnosed in some Asian countries, including Japan, mainland China, and Singapore, accounting for about one-third of all renal biopsy diagnoses in these regions, 20% in Europe, and 10% in the United States.<sup>289,290</sup> The cause of these wide differences in incidence has partially been attributed to differences in the indication for renal biopsy in Asia when compared to the United States. Familial clustering has been reported in approximately 10% of the patients.<sup>291–293</sup> The familial forms of IgAN follow autosomal dominant transmission with incomplete penetrance. The first-degree relatives without clinical evidence of IgAN have high levels of galactose-deficient IgA (GD-IgA). Genome-wide associated studies using single nucleotide polymorphisms have revealed several susceptibility loci, the most common being MHC locus on 6p21.<sup>294</sup> These studies have also highlighted the role of mucosal defense systems and alternative complement pathway in the pathogenesis of IgAN.<sup>295</sup>

The diagnosis of IgAN is primarily based on the demonstration of IgA deposits in the mesangium, a feature seen in association with several conditions. HSP nephritis and IgAN are two closely related conditions that form part of the syndrome.<sup>296</sup> Mesangial IgA deposition has also been described in association with a variety of diseases, including chronic liver disease, inflammatory bowel disease, connective tissue disorders, neoplastic diseases, and viral and bacterial infections (Box 23.5).<sup>297</sup> IgAN results from the deposition of circulating immune complexes in the glomerular mesangium, leading to the activation of the complement cascade via the alternative pathway. The deposited IgA in idiopathic form is predominantly aberrantly glycosylated polymeric IgA1.<sup>298,299</sup> The serum levels of this GD-IgA are elevated in IgAN patients and this is reportedly an independent

risk factor for progression of renal disease.<sup>300</sup> It appears that GD-IgA serves as an autoantigen and the subsequent immune complex deposition stimulates mesangial cell proliferation.

IgAN can occur at any age, but it is more common in the second and third decades.<sup>301</sup> It is uncommon in children under the age of 10.<sup>297</sup> Males are affected two to six times more often than females. Most patients are diagnosed upon detection of microscopic hematuria during routine physical examination. About less than half the patients have a history of recurrent episodes of macroscopic hematuria, one-third of which occurred synchronously or within a few days after a respiratory or, less commonly, a gastrointestinal or urinary tract infection.<sup>297,302</sup> This may be related to increased host IgA response to mucosal antigens. Patients often have proteinuria, which is usually mild though it can on occasion be severe. Roughly 5%–10% develop the nephrotic syndrome. It is currently estimated that 25%–40% of the cases slowly progress to chronic renal failure over a period of 20 years.<sup>303</sup> About 60% of the patients who received transplants experienced recurrence of the disease in the donor kidney and a small percentage of them lose their graft to recurrent disease.<sup>304</sup>

It is now recognized that IgAN may display a wide variety of histologic patterns, ranging from normal or nearly normal to a diffuse crescentic glomerulonephritis.<sup>289,290</sup> Widening of the mesangium by increased matrix and hypercellularity is the most common microscopic finding (Fig. 23.39). The mesangial involvement is often uneven and varies among the glomeruli and glomerular lobules. Healing of the focal proliferative lesion may lead to FSGS. Glomerular scarring is associated with TA and IF. Various classification systems, such as Haas and more recently Oxford, are used to score and characterize the histologic features, and several studies have validated these systems in predicting the renal outcomes.<sup>305–308</sup> By electron microscopy, it is possible to demonstrate mesangial deposits in all glomeruli, indicating that the lesion is diffuse, not focal (Fig. 23.40). On occasion, small subendothelial or subepithelial deposits may also be found, especially in patients with more severe disease.

The immunofluorescence pattern parallels the distribution of the deposits seen by electron microscopy. There is strong diffuse mesangial reactivity for IgA, and it can extend into the capillary loops (Fig. 23.41). IgG is also common and may rival IgA in intensity. About one-third of the cases show weak reactivity for IgM and fibrinogen. C3 reactivity is strong, with a pattern identical to immunoglobulins, but no reactivity for either C1q or C4 is seen, indicating that the complement is activated via the alternative pathway. Deposits of IgA are not limited to the glomeruli in IgAN. They can also be demonstrated in the blood vessels of the superficial dermis of normal-appearing skin in patients with IgAN without systemic manifestations of HSP.<sup>309,310</sup> These findings, together with the

### Box 23.5 Entities associated with secondary IgA nephropathy

#### Liver diseases

Alcoholic cirrhosis, viral hepatitis, toxic liver disease, cystic fibrosis

#### Gastrointestinal diseases

Crohn disease, ulcerative colitis, celiac disease

#### Infectious diseases

HIV infection, tuberculosis, brucellosis, leprosy, *Staphylococcus aureus*, *Mycoplasma pneumoniae*, *Clostridium difficile*, *Yersinia enterocolitica*

#### Rheumatologic diseases

Rheumatoid arthritis, ankylosing spondylitis, psoriatic arthritis, Behcet disease, Reiter syndrome

#### Neoplastic diseases

Various carcinomas, including squamous cell carcinomas, small cell lung carcinoma, renal cell carcinoma, and a variety of adenocarcinomas, non-Hodgkin lymphoma, polycythemia vera, mycosis fungoides/Sézary syndrome

#### Skin diseases

Dermatitis herpetiformis, psoriasis

#### Miscellaneous diseases

Sarcoidosis, silicosis, bronchiolitis obliterans, uveitis with retinal vasculitis

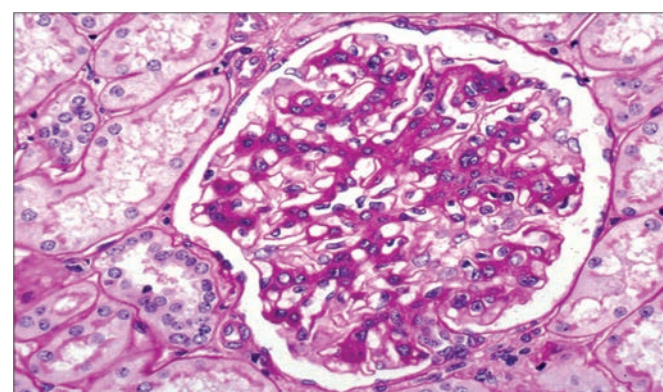


**Figure 23.39** Mesangial enlargement with increase in mesangial matrix and cellularity in IgA nephropathy (PAS).

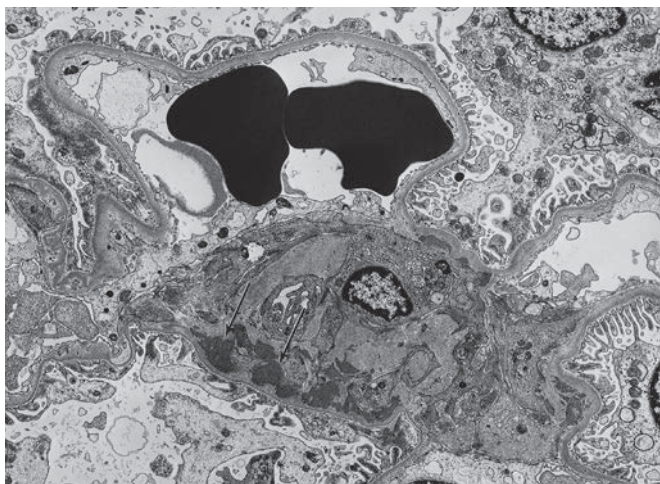


**Figure 23.40** Portion of a glomerulus from a patient with IgA nephropathy showing paramesangial electron-dense mesangial deposits (arrows) ( $\times 6000$ ).

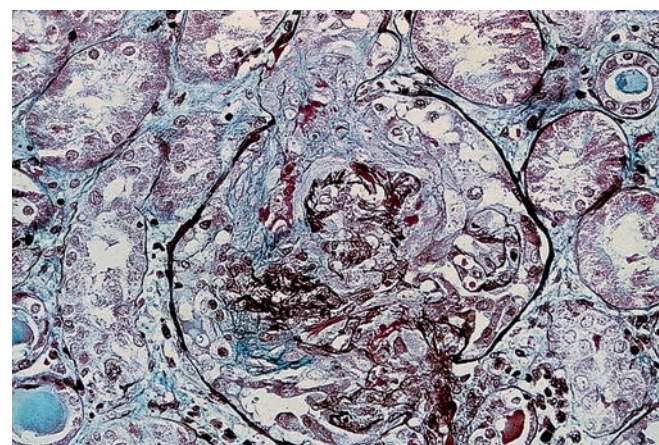


**Figure 23.42** Silver-stained histologic preparation of a glomerulus with epithelial crescent obliterating the Bowman space and extending into the proximal tubule. The glomerular tuft is entrapped in the crescent.

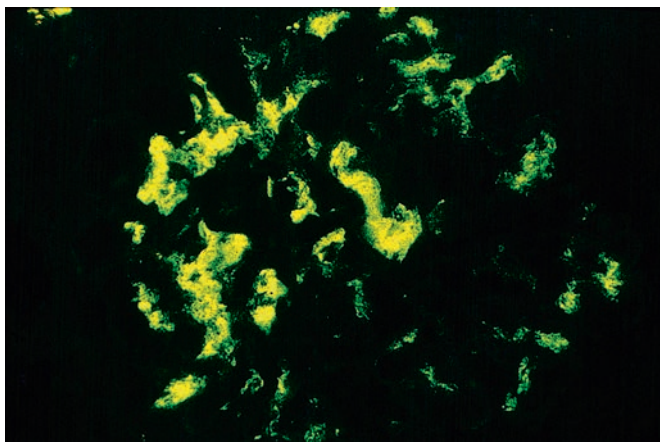


**Figure 23.41** Immunofluorescence preparation of a glomerulus demonstrating mesangial deposits of IgA (anti-IgA).

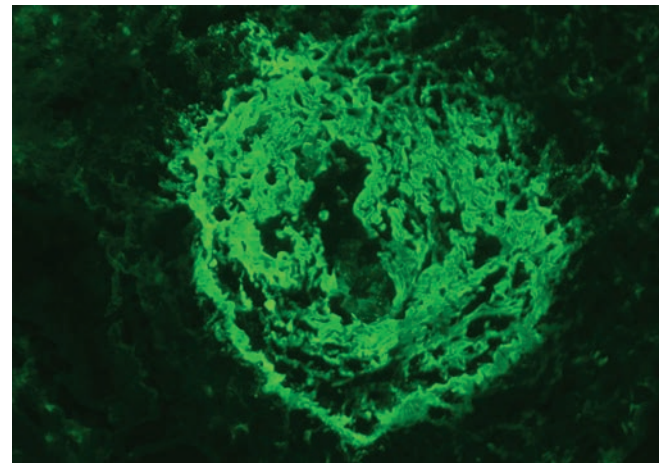


**Figure 23.43** Immunofluorescent preparation showing massive fibrin deposition within the crescent and glomerular capillary tuft (anti-fibrinogen).

phenotypic and pathogenetic similarities shared by these conditions, suggest that HSP may be a systemic form of primary IgAN or, conversely, that IgAN is a renal-limited form of HSP.<sup>311,312</sup>

### Crescentic Glomerulonephritis

*Crescentic glomerulonephritis* is a histopathologic term used to designate a severe form of glomerulonephritis in which 50% or more of the glomeruli are involved by epithelial crescents. This type of glomerular injury is associated with a clinical syndrome known as rapidly progressive glomerulonephritis that is characterized by the rapid and progressive loss of renal function accompanied by hematuria, red cell casts in urine, variable degrees of proteinuria, and severe oliguria. Untreated, this disease can result in death within weeks. The terms *crescentic glomerulonephritis* and *rapidly progressive glomerulonephritis* are often used interchangeably. Like *crescentic glomerulonephritis*, *extracapillary proliferative glomerulonephritis* is a pathologic term for this lesion which indicates that the cell proliferation is primarily in the Bowman space. All three of the previous terms are considered proper designations for this form of glomerular injury.

Studies using cell markers showed that the crescents are composed of a mixed population of cells primarily consisting of glomerular

epithelial cells and macrophages. It has been postulated that crescent formation results from disruption of the glomerular capillaries that allows leukocytes, fibrin, and other plasma proteins to escape into the Bowman space, where they induce epithelial cell proliferation and macrophage maturation that together produce cellular crescents (Fig. 23.42). This is supported by the invariable immunofluorescent finding of fibrin in active crescentic glomerulonephritis (Fig. 23.43) and the demonstration of GBM ruptures that are better visualized on silver-stained histologic preparations or by electron microscopy (Fig. 23.44). As the disease progresses, the extracapillary proliferating cells are transformed into fibroepithelial crescents which incorporate fibroblasts and collagen. Over time, the sclerosis progresses and the glomeruli become completely scarred.

Crescentic glomerulonephritis can be caused by a wide variety of diseases either restricted to the kidney or systemic. Using immunofluorescence and electron microscopy techniques, three main categories that reflect different pathogenic mechanisms have been identified: (1) anti-GBM glomerulonephritis; (2) immune complex crescentic glomerulonephritis; and (3) pauci-immune crescentic glomerulonephritis, usually associated with ANCA (Table 23.4). In each group, the disease may be associated with a known disorder or may be idiopathic.

### Antiglomerular Basement Membrane Disease

This form of glomerulonephritis is characterized by the immunofluorescent demonstration of linear deposits of IgG and, in many instances, C3 along the GBM. Anti-GBM disease is a rare autoimmune disease and accounts for 15% of the cases of crescentic glomerulonephritis.<sup>313</sup> It can occur as a renal-limited disease or as a pulmonary renal syndrome induced by a cross reaction of the anti-GBM antibodies with pulmonary basement membranes (Goodpasture syndrome). The incidence of anti-GBM disease has two peaks with respect to patient age.<sup>314,315</sup> The first is in the second and third decades of life, has a male predominance, and a higher frequency of pulmonary involvement (Goodpasture syndrome). The second occurs in the

sixth and seventh decades, has a female predominance, and is more often a renal-limited disease.

Renal anti-GBM disease is typically characterized by an abrupt onset of acute glomerulonephritis with severe oliguria or anuria.<sup>315</sup> On rare occasions, however, the onset is more insidious and the patient may remain essentially asymptomatic until the development of uremic symptoms. Patients with Goodpasture syndrome present with glomerulonephritis and pulmonary involvement, which is more often in the form of severe pulmonary hemorrhage. A preceding upper respiratory infection has been documented in about one-fourth of these patients. Pulmonary hemorrhage has also been observed after exposure to various inhalants, particularly hydrocarbons and there is an association with cigarette smoking. The circulating anti-GBM antibodies can be detected by enzyme immunoassay, but the titers do not correlate with disease severity. Treatment includes cytotoxic agents and plasmapheresis, but serum creatinine at presentation greater than 5 mg/dL is associated with poor prognosis.

The principal antigen to which anti-GBM antibodies react is localized to the carboxyl terminus of the NC1 domain of the  $\alpha 3$  chain of type IV collagen (Goodpasture epitope).<sup>316,317</sup> It has been suggested that hydrocarbons inhibit the enzyme that catalyzes the formation of sulfilimine bonds between collagen hexamers, thus causing conformational change, neo-epitope exposure, and subsequent autoantibody formation against the Goodpasture antigen.<sup>318,319</sup> Genetic predisposition may play a role, and there is a strong association between certain HLA class II antigens and risk of developing anti-GBM nephritis.

Anti-GBM disease can complicate other diseases. It can arise de novo following renal transplantation in patients with Alport syndrome (AS)<sup>320,321</sup> and has been reported in association with membranous nephropathy preceding, concurrent with, or following this disease.<sup>322,323</sup> Up to one-third of the patients with anti-GBM disease have circulating ANCA, especially with specificity for myeloperoxidase (MPO).<sup>324-326</sup>

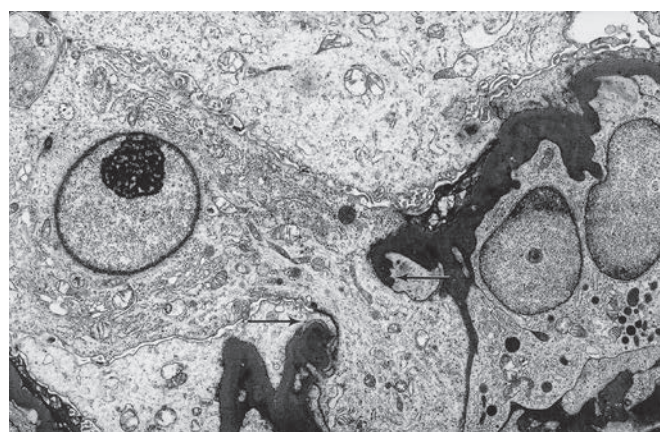


**Figure 23.44** Disruption of the glomerular basement membrane (arrows) in a case of crescentic glomerulonephritis (x9000).

**Table 23.4** Differential diagnosis of crescentic glomerulonephritis

CATEGORY	ANTI-GLOMERULAR BASEMENT MEMBRANE NEPHRITIS	PAUCI-IMMUNE GLOMERULONEPHRITIS	IMMUNE COMPLEX-MEDIATED GLOMERULONEPHRITIS
Light microscopy	No mesangial or endocapillary proliferation in unaffected glomeruli or tufts	No mesangial or endocapillary proliferation in unaffected glomeruli or tufts	Variable mesangial or endocapillary proliferation typically present
IF (other than fibrinogen in glomerular necrosis)	Linear lace-like staining in GBM ( $\pm$ TBM)	Absent ( $\pm$ nonspecific C3 in glomerular tuft)	Present (varies based on the disease entity)
Electron-dense deposits (on EM)	Absent	Absent	Present
Serology	Anti-GBM antibodies +	ANCA + (in 85% of patients)	ANA, ds-DNA, ASO, cryoglobulins, etc. (based on entity)
Comments	No small vessel vasculitis unless associated with ANCA	Vasculitis may be present	Vasculitis present, but less common than in pauci-immune GN
Other associations and examples	Goodpasture syndrome with pulmonary involvement	Microscopic polyangiitis, granulomatosis with polyangiitis, eosinophilic granulomatosis with polyangiitis	Examples include lupus nephritis, IgA nephropathy, infection-associated GN, cryoglobulinemic GN, membranoproliferative GN

ANA, Antinuclear antibodies; ANCA, antineutrophil cytoplasmic antibodies; ASO, antistreptolysin O; EM, electron microscopy; GBM, glomerular basement membrane; GN, glomerulonephritis; IF, immunofluorescence microscopy; TBM, tubular basement membrane.

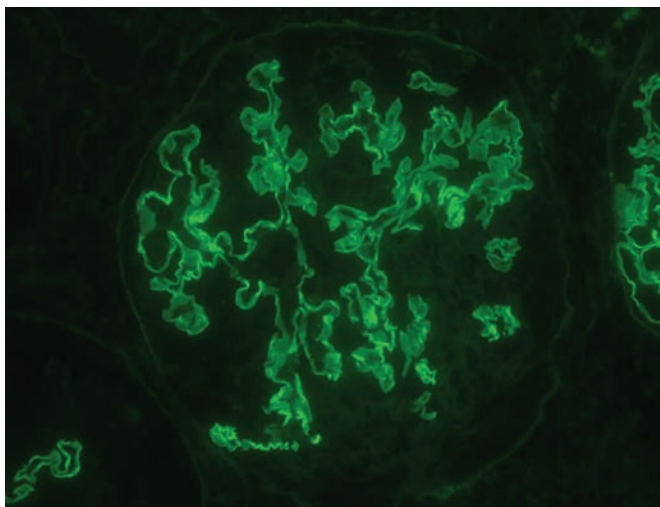


**Figure 23.45** Continuous linear IgG reactivity along the capillary walls in a case of anti-GBM glomerulonephritis (anti-IgG).

The presence of ANCA in patients with anti-GBM disease is associated with small vessel vasculitis in various organs in addition to lung and kidney.

The typical light microscopic lesion in renal anti-GBM disease is that of a necrotizing glomerulonephritis with crescent formation either in a focal or diffuse pattern. In the involved areas, the glomerular capillaries are disrupted and clusters of granulocytes are often present, but there is minimal intracapillary cell proliferation. The uninvolved segments may appear normal or slightly infiltrated by leukocytes or mononuclear inflammatory cells. The most severely involved glomeruli may exhibit extensive necrosis, disruption of the Bowman capsule, and intense periglomerular inflammation with multinucleated giant cells. Electron microscopy may demonstrate the presence of a subendothelial lucent zone near foci of necrosis, but this is not a constant or specific feature. Disruptions of the GBM and fibrin deposition can also be seen. An important negative ultrastructural finding in anti-GBM disease is the absence of electron-dense deposits.

Immunofluorescence studies demonstrate a continuous linear immunostaining of the glomerular capillaries for IgG, often accompanied by a focal linear staining for C3 and in several instances both  $\kappa$  and  $\lambda$  (Fig. 23.45). Distal tubules also express  $\alpha_3$  chain, and hence, linear tubular basement membrane staining with IgG is not uncommon. It must be kept in mind that a similar IgG immunofluorescence pattern of GBM can be seen in other glomerular lesions, including diabetic nephropathy and HCDD, so it is necessary to confirm the diagnostic impression with the demonstration of circulating anti-GBM antibodies. It is helpful to note that diabetic nephropathy is usually associated with strong linear staining of all basement membranes with albumin in addition to IgG; HCDD has diffuse linear staining of vascular and tubular basement membranes, in addition to GBM, with IgG.

### Immune Complex Crescentic Glomerulonephritis

Immune complex crescentic glomerulonephritis represents about 25% of all cases of crescentic glomerulonephritis.<sup>313</sup> It occurs most frequently as a complication of any of the immune complex glomerulonephritides, including postinfectious glomerulonephritis, MPGN, cryoglobulinemic glomerulonephritis, SLE, IgAN, and HSP (Fig. 23.46). In a minority of the cases of immune complex crescentic glomerulonephritis, the underlying cause cannot be determined.

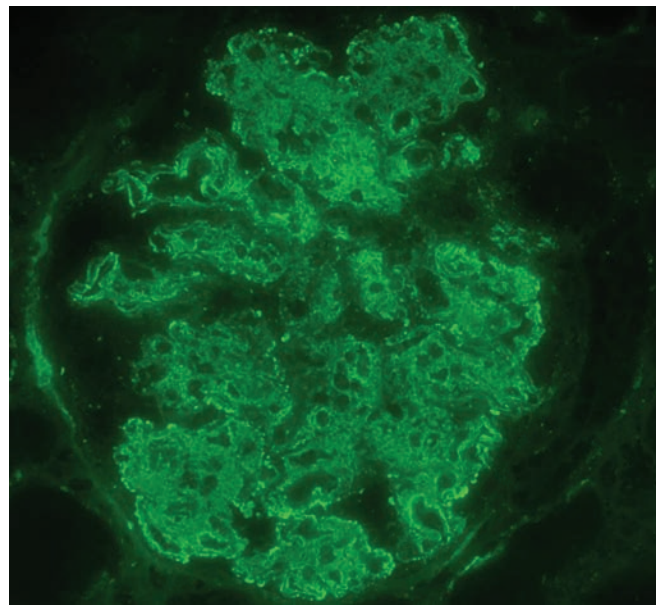


**Figure 23.46** Coarse granular deposits of IgG are prominent in the mesangium and along the capillary walls in a patient with crescentic lupus nephritis (anti-IgG).

These patients are diagnosed as having idiopathic immune complex glomerulonephritis, and underlying infection should always be excluded in these cases. The prognosis of idiopathic immune complex crescentic glomerulonephritis, although poor, is better than that of anti-GBM disease.<sup>313</sup>

The light microscopic features of immune complex crescentic glomerulonephritis depend upon the underlying glomerular disease. The glomerular segments adjacent to the crescents usually present some degree of necrosis, but this is not as extensive as that seen in anti-GBM or pauci-immune glomerulonephritis. An important finding that can help distinguish immune complex crescentic glomerulonephritis from both anti-GBM and pauci-immune crescentic glomerulonephritis is the presence of various combinations of capillary wall thickening and mesangial/endocapillary cell proliferation, features that are typically absent in the latter two types of crescentic glomerulonephritis (Fig. 23.47).<sup>313</sup> Electron microscopy and immunofluorescence allow the confirmation of immune complex deposits, thus establishing the diagnosis of immune complex crescentic glomerulonephritis. The diagnosis of a specific category of immune complex crescentic glomerulonephritis can usually be achieved by the careful correlation of the patient's clinical and laboratory data with light, immunofluorescence, and electron microscopic findings.

### Pauci-Immune Crescentic Glomerulonephritis

Pauci-immune crescentic glomerulonephritis is characterized by the absence or minimal staining for immunoglobulin by immunofluorescence. It is the most common form of crescentic glomerulonephritis diagnosed by renal biopsy (about 60% of the cases), more frequently affects elderly individuals, and is equally distributed between the genders.<sup>313,327</sup>

Pauci-immune crescentic glomerulonephritis can occur as a renal-limited disease or as a component of systemic necrotizing small vessel vasculitis. Constitutional symptoms include fever, arthralgias, and myalgias, and the extrarenal manifestations in systemic disease vary by the organ/s affected. Patients with pauci-immune

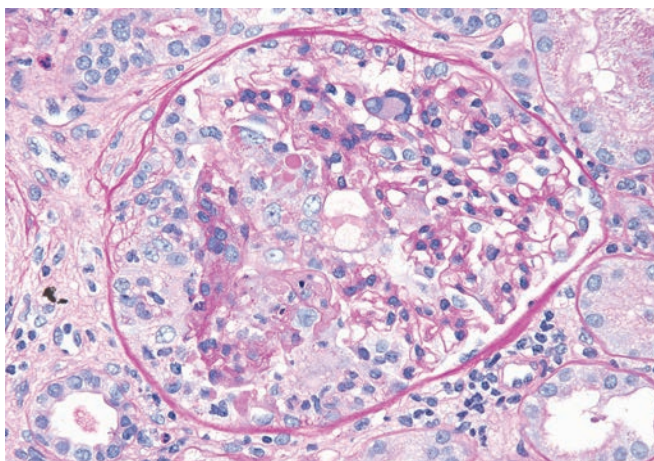


**Figure 23.47** Destruction of the capillary tuft by a cellular crescent in a patient with pauci-immune glomerulonephritis. It is characterized by the absence of deposits on immunofluorescence, and note the lack of mesangial or endocapillary proliferation in preserved portions of the capillary tuft.

centric glomerulonephritis tend to respond better to treatment than those with anti-GBM glomerulonephritis and, therefore, have a better prognosis. Treatment options for remission induction include steroids, cyclophosphamide, and rituximab, and disease relapses are not uncommon.<sup>328–330</sup>

Approximately 80%–90% of pauci-immune crescentic glomerulonephritis cases occur in ANCA-positive patients.<sup>328</sup> ANCAs have been recognized as serologic markers for pauci-immune glomerulonephritis with or without evidence of extrarenal disease.<sup>331,332</sup> By indirect immunofluorescence with ethanol-fixed neutrophils as substrate, two distinct immunostaining patterns have been recognized: cytoplasmic (C-ANCA) and perinuclear (P-ANCA). Enzyme-linked immunosorbent assay (ELISA) has shown that most C-ANCA- and P-ANCA-positive sera recognize proteinase 3 (PR3), which is a serine protease of 29 kDa, and MPO, respectively. Both are localized to the azurophilic granules of the neutrophils and monocytes, are translocated to the cell surface during cell activation, and are thus able to interact directly with circulating ANCA. Subsequent activation of cell signal transduction pathways and alternative complement pathway facilitate leukocyte adhesion to endothelial cells and vessel damage. Patients with pauci-immune crescentic glomerulonephritis without evidence of extrarenal vasculitis most often have P-ANCA/MPO-ANCA, those with granulomatosis with polyangiitis (GPA) most often have C-ANCA/PR3-ANCA, while those with microscopic polyangiitis have approximately an equal incidence of P-ANCA and C-ANCA.<sup>328</sup> The potential triggers for ANCA production include immune dysregulation, molecular mimicry of microbial factors, and drugs such as prothiouracil, hydralazine, penicillamine, minocycline, and others. Genetic predisposition may play a role as evidenced by HLA class II associations, frequency of certain gene polymorphisms and presence of epigenetic alteration of MPO and PR3 surface expression.<sup>333</sup> Approximately 10%–20% of pauci-immune glomerulonephritis patients lack ANCA, and other less frequent autoantibodies may have potential pathogenic role.<sup>334,335</sup> These include anti-LAMP2 (lysosomal-associated membrane protein-2), anti-moesin, and anti-plasminogen antibodies. Serum complement levels are typically normal in pauci-immune glomerulonephritis, but recent studies have highlighted the role of alternative complement pathway in the pathogenesis of this disease.<sup>336</sup> Cell mediated immune mechanisms also seem to play a role in the development of crescentic lesions.<sup>328</sup>

The light microscopic appearance of pauci-immune crescentic glomerulonephritis is indistinguishable from that of anti-GBM disease (see Fig. 23.47). Immunofluorescence studies may reveal small irregular focal staining for C3. Fibrinogen is frequently found in the crescents or in the necrotic areas of the glomerular tuft. Electron microscopy often demonstrates ruptures of the GBM as well as fibrin deposition. The absence of immune complex deposits differentiates pauci-immune crescentic glomerulonephritis from immune complex crescentic glomerulonephritis.

### Lupus Nephritis

SLE is a multisystem, autoimmune disease with a broad range of clinical presentation that has a high morbidity and mortality. The American Rheumatism Association has established diagnostic criteria for this condition based on clinical and serologic manifestations.<sup>337</sup> SLE can affect adults as well as children; two-thirds of patients present symptoms between 16 and 30 years of age. In children, SLE usually occurs in adolescence; it is uncommon before the age of 10 and very rare before the age of 5.<sup>338,339</sup> It is 10 times more common in females than males, with black females being affected more frequently than white. A drug-induced lupus-like disease, most commonly linked with hydralazine, procainamide, isoniazid, methyldopa, chlorpromazine, and quinidine, has also been recognized.<sup>340,341</sup> The renal lesions in these cases are similar to those seen in spontaneous SLE.

Serum antinuclear antibodies (ANAs) are detected in over 95% of patients and their presence is a sensitive marker of SLE, while anti-double-stranded DNA and anti-Sm antibodies are more specific markers. Other notable antibodies detected in SLE patients include antiphospholipid antibodies, ADAMTS13, and lupus anticoagulant.<sup>342</sup> There is a genetic predisposition for developing SLE, and recent genome-wide association studies have identified polymorphisms in several immunity-related genes that confer an increased risk.<sup>343,344</sup> This extensive loss of self-tolerance to a variety of intrinsic antigens in genetically susceptible individuals can be triggered by environmental factors such as ultraviolet light, estrogens, and drugs.

Immune-mediated nephritis is a common complication of SLE. The immune deposits in the kidney (and elsewhere) are derived from either circulating complexes or from an *in situ* combination of antigen and antibody.<sup>342</sup> Complement activation follows along with inflammatory response and organ damage. Immune-complex deposition is the most common form of glomerular injury, but immune deposits are absent in lupus-associated thrombotic microangiopathy (TMA) and podocytopathies (such as MCD) and the injury in these settings is antibody mediated. It appears that the tubulointerstitial inflammation in SLE is more T-cell mediated.

Clinical evidence of renal involvement, as determined by urinalysis, or impaired renal function is seen in approximately 40%–80% of unselected patients with SLE. It is likely, however, that clinical assessment underestimates the actual frequency since histologic evidence of renal disease may be present even when the urinalysis is essentially normal. The clinical spectrum of lupus nephritis is wide, encompassing the acute nephritic syndrome, the nephrotic syndrome, acute and chronic renal failure, and isolated abnormalities in the urinary sediment. The most constant feature found in nearly all patients with clinical lupus nephritis is proteinuria. Microscopic hematuria is almost always present, but rarely does it develop in isolation; macroscopic hematuria is rare.

A kidney biopsy is essential in the renal assessment of patients with SLE and is indicated in all patients with abnormalities of urine sediment or renal function. In patients with these abnormalities, the clinical presentation does not accurately predict the disease

**Table 23.5** International Society of Nephrology/Renal Pathology Society classification of lupus nephritis

CLASS	PATHOLOGY DIAGNOSIS	DESCRIPTION
I	Minimal mesangial LN	Normal by LM, mesangial deposits by IF and EM
II	Mesangial proliferative LN	Mesangial proliferation on LM, mesangial deposits by IF and EM
III	Focal LN (<50% of glomeruli)	Active or chronic lesions by LM in <50% glomeruli, usually subendothelial (in addition to mesangial) deposits by IF and EM
III (A)	Active lesions	Active lesions include endocapillary proliferation, cellular crescents, karyorrhexis/necrosis, neutrophils, and wire loops
III (A/C)	Active and chronic lesions	
III (C)	Chronic lesions	Chronic lesions include segmental or global glomerulosclerosis attributable to LN, and fibrous crescents
IV	Diffuse LN (≥50% of glomeruli)	Active or chronic lesions by LM in >50% glomeruli, usually subendothelial (in addition to mesangial) deposits by IF and EM
IV (A)	Active lesions	Subclassification of active lesions as S (segmental) or G (global) based on extent of glomerular tuft affected
IV (A/C)	Active and chronic lesions	
IV (C)	Chronic lesions	Subclassification of chronic lesions as S (segmental) or G (global) based on extent of glomerular tuft affected
V	Membranous LN	Subepithelial deposits present by LM, IF, and EM; can co-exist with class III or IV
VI	Advanced sclerosing LN (≥90% globally sclerosed glomeruli without residual activity)	Global glomerulosclerosis attributable to LN

EM, Electron microscopy; IF, immunofluorescence microscopy; LN, lupus nephritis.

severity and the renal biopsy findings provide prognostic information and aid in the formulation of the treatment plan.

The pathologic findings of lupus nephritis are extremely diverse and may occur in all four renal compartments: glomeruli, tubules, interstitium, and blood vessels. This diversity may be the result of differences in the immune response in different patients or in the same individual over time. Standardized histologic classification of lupus nephritis developed by the International Society of Nephrology (ISN)/Renal Pathology Society (RPS)<sup>345</sup> provides clear definitions for diagnostic categories based on quantitative assessment of individual histologic lesions. This classification has preserved some of the basic structure of earlier WHO classifications<sup>346–348</sup> but has successfully eliminated some of the ambiguities that existed in the WHO classifications. The ISN/RPS classification defines six major classes (Table 23.5) and several published studies have shown a significant improvement in interobserver reproducibility and in predicting renal outcome when this classification is used.<sup>349–352</sup>

As per the ISN/RPS classification, class I (minimal mesangial lupus nephritis) comprises those cases in which the glomeruli appear normal by light microscopy but show immune complex deposits by immunofluorescence and/or electron microscopy. Patients with class I nephritis usually manifest mild microscopic hematuria and/or mild proteinuria, and renal function is typically normal.

Class II (mesangial proliferative lupus nephritis) is defined by any degree of mesangial hypercellularity and/or mesangial matrix expansion as seen by light microscopy, accompanied by the demonstration of mesangial immune complex deposits by immunofluorescence and electron microscopy (Fig. 23.48). The classification allows for the presence of rare minute subepithelial or subendothelial deposits identifiable only by electron microscopy or immunofluorescence, but not by light microscopy. Clinically, majority of patients have mild renal involvement as demonstrated by an inactive urine sediment. Less than 50% of the patients have mild hematuria and/or

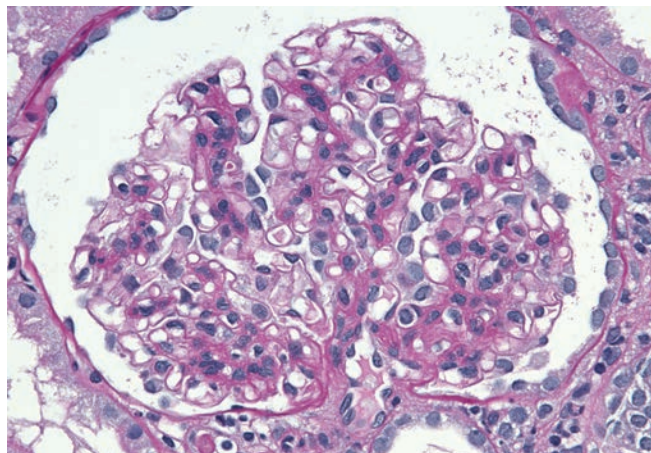
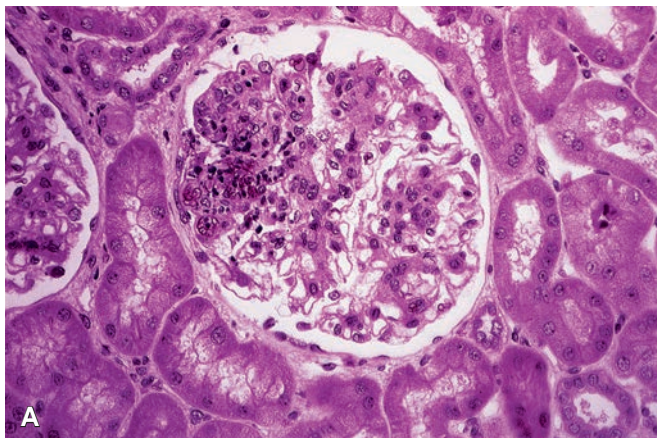


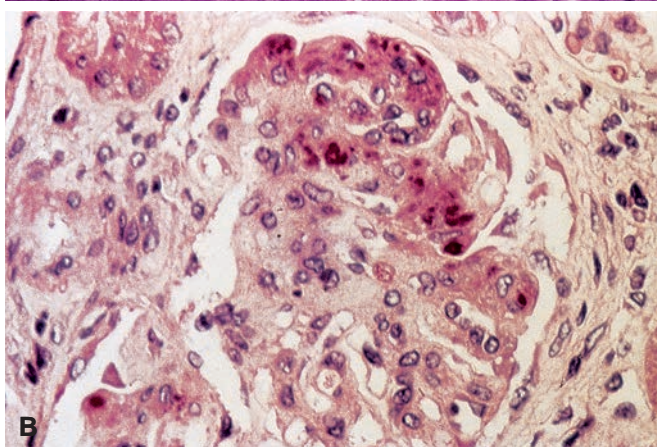
**Figure 23.48 Lupus Nephritis, ISN/RPS Class II.** There is mild diffuse mesangial hypercellularity and an increase in matrix. Mesangial deposits can be identified by immunofluorescence and electron microscopy.

proteinuria, which usually does not exceed 1 g per 24 hours. The nephrotic syndrome is exceedingly rare, and, when present, it may be a manifestation of concomitant MCD.<sup>353,354</sup>

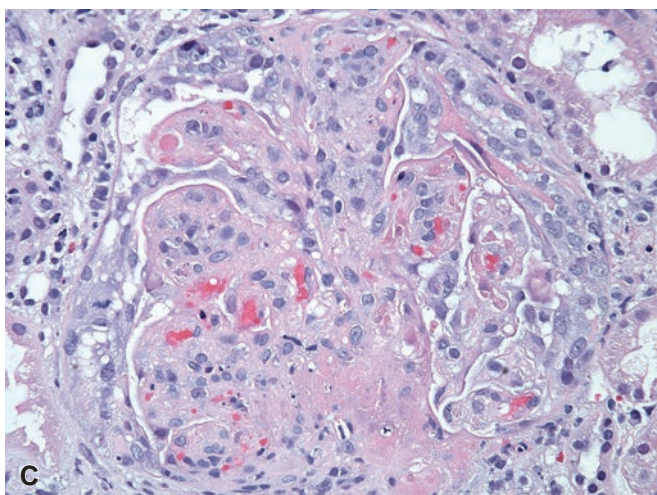
Class III (focal lupus nephritis) is defined as focal segmental and/or global endocapillary, and/or extracapillary glomerulonephritis affecting less than 50% of the glomeruli. The biopsy may reveal a variable admixture of proliferative, necrotizing, and sclerosing lesions. The less affected glomeruli usually exhibit a diffuse mesangial prominence as seen in class II. The segmental proliferative lesions may be associated with leukocyte infiltration, fibrinoid material, and necrotic debris (Fig. 23.49A). Focal areas of necrosis containing fragmented nuclei known as hematoxylin bodies may be present (see Fig. 23.49B). These structures are considered pathognomonic



A



B



C

**Figure 23.49** Lupus Nephritis, International Society of Nephrology/Renal Pathology Society Class III. **A**, There is focal and segmental glomerulonephritis characterized by segmental necrosis, adhesions to the Bowman capsule, and leukocytic infiltration. **B**, A glomerulus with a well-circumscribed area of necrosis containing numerous small hematoxylin bodies. **C**, Glomerulus with necrosis, fibrin extravasation, and a cellular crescent.

of lupus nephritis but are found in only 1%–2% of renal biopsies from these patients.<sup>342</sup> They range considerably in size from minute fragments to round masses approximately the size of the nucleus and have a characteristic lilac tinge on H&E-stained sections.<sup>342,355</sup> The segmental necrotic lesions may be associated with cellular crescent formation (see Fig. 23.49C) and tend to resolve by segmental sclerosis

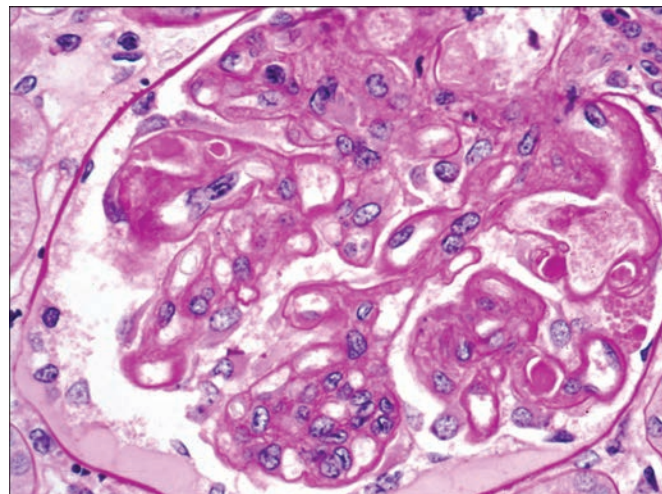


**Figure 23.50** Lupus Nephritis, ISN/RPS Class IV. Glomerulus from a patient showing several wire loops (subendothelial deposits) and intraluminal hyaline thrombi (deposits) (PAS).

with focal capsular adhesions or the development of fibrous crescents. Despite the focal nature of the lesion by light microscopy, immunofluorescence generally reveals a more diffuse deposition of immunoglobulins and complement. Electron microscopy often demonstrates deposits in the mesangial and subendothelial regions, and, less frequently, in the subepithelial areas. In the ISN/RPS classification, III (A) refers to active lesions, III (C) refers to healed, chronic, inactive lesions, and III (A/C) indicates a combination of active and chronic lesions. The proportion of glomeruli affected by active or healed lesions should be included in the diagnostic report. The clinical picture of patients with class III lupus nephritis is quite variable. Approximately half of the patients have active urinary sediment, and about 50% have proteinuria, which may be in the nephrotic range in up to one-third of the cases. Renal insufficiency is rather uncommon and occurs in 10%–25% of the patients.

Class IV (diffuse lupus nephritis) is defined as diffuse segmental and/or global endocapillary and/or extracapillary glomerulonephritis affecting 50% or more of the glomeruli included in the biopsy. The lesions in this class are identical to class III but tend to be diffuse and more global, and the immune complexes are more abundant. It has been suggested that classes III and IV lupus nephritis are ends of a pathologic continuum since the differences between these classes are quantitative rather than qualitative. The immune deposits in the subendothelial areas may produce marked thickening of the capillary walls to form the characteristic “wire loop” lesions (Fig. 23.50). On occasion, the capillary lumina can be occluded by massive deposition of immune complexes (“hyaline thrombi”). Immunofluorescence studies often reveal more than one class of immunoglobulin in a coarse granular pattern in the mesangium and peripheral capillary walls in all glomeruli. IgG is almost invariably present, but IgM and IgA are also frequently found. Both C3 and C1q are frequently found and the staining for C1q is particularly strong. When all immunoglobulins and complement components are present, the pattern is often referred to as “full house,” an immunofluorescent profile seen in all lupus classes and is considered characteristic of lupus nephritis (Fig. 23.51). Reactivity for fibrin and fibrinogen are commonly seen in crescentic and necrotizing lesions. Electron microscopy demonstrates large subendothelial electron-dense deposits usually accompanied by mesangial and sometimes subepithelial and/or intramembranous deposits (Fig. 23.52A). Subendothelial deposits are primarily found in proliferative lupus nephritis (classes III and

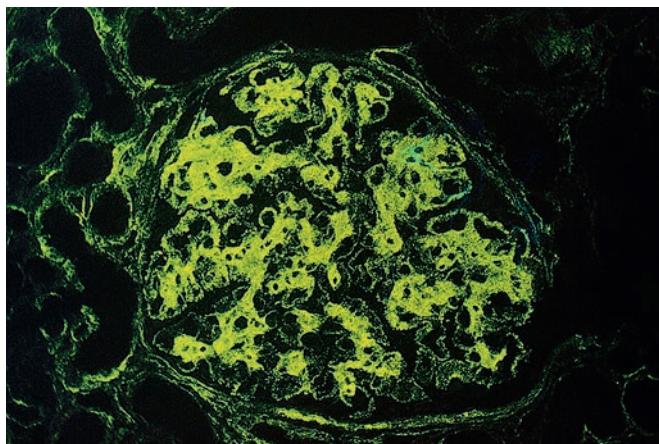


**Figure 23.51** Immunofluorescence showing large amounts of granular immune complex deposits not only in the mesangium and glomerular capillary loops, but also along tubular basement membranes, interstitium, blood vessels, and Bowman capsule (anti-IgG).

IV) and are considered to be a marker of activity.<sup>356</sup> On occasion, electron-dense deposits may show a distinctive fingerprint-like crystalline pattern, possibly representing cryoglobulins (see Fig. 23.52B).<sup>357</sup> This substructure, although nonspecific for lupus nephritis, are usually associated with class IV lesion. The endothelial cells may be swollen and contain tubuloreticular inclusions (see Fig. 23.52C). Studies have demonstrated that these *myxovirus-like* structures are inducible *in vitro* in normal lymphocytes on exposure to interferon alpha, earning them the descriptive term “interferon footprints.”<sup>358</sup> The ISN/RPS classification subdivides class IV lupus nephritis into those cases with diffuse segmental versus diffuse global proliferations. The designation IV-S is used if over 50% of the involved glomeruli exhibit segmental lesions; the designation of IV-G is used if over 50% of affected glomeruli show global lesions. This subdivision is rather arbitrary and of unclear significance but was included to further investigate possible differences in outcome and pathogenesis between these subgroups.<sup>359</sup> The clinical symptoms in patients with class IV lesions are quite severe and may include nephrotic range proteinuria and active urine sediment. Without therapy, these patients are considered to have the worst prognosis since a high percentage progress rapidly to renal failure.

Class V (membranous lupus nephritis) is defined by the presence of global or segmental continuous subepithelial immune complex deposits or their morphologic sequelae by light microscopy. The membranous changes may occur alone or with a background of mesangial hypercellularity and mesangial immune complex deposits. Small subendothelial deposits can be identified by immunofluorescence or electron microscopy but not by light microscopy. The peripheral glomerular capillary walls often appear diffusely thickened (Fig. 23.53) and the so-called spike and dome pattern may be demonstrated on silver methenamine stain. By electron microscopy, the GBM shows the same ultrastructural stages seen in idiopathic MGN. However, in contrast to this condition, mesangial deposits are commonly found in membranous lupus nephritis patients. Virtually all patients have proteinuria at presentation, and 60%–70% have the nephrotic syndrome. About 50% of the patients have hematuria.

Class VI (advanced sclerosing lupus nephritis) is defined by global glomerulosclerosis affecting over 90% of the glomeruli without residual activity. In less advanced lesions, mesangial and endocapillary hypercellularity may be seen and small amounts of immune complex deposits can be detected by immunofluorescence or electron

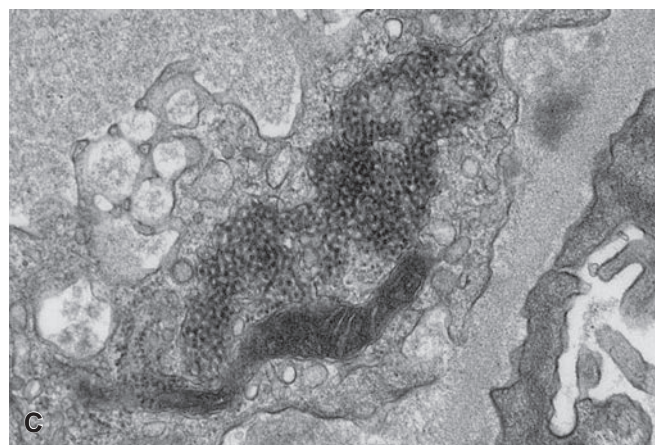
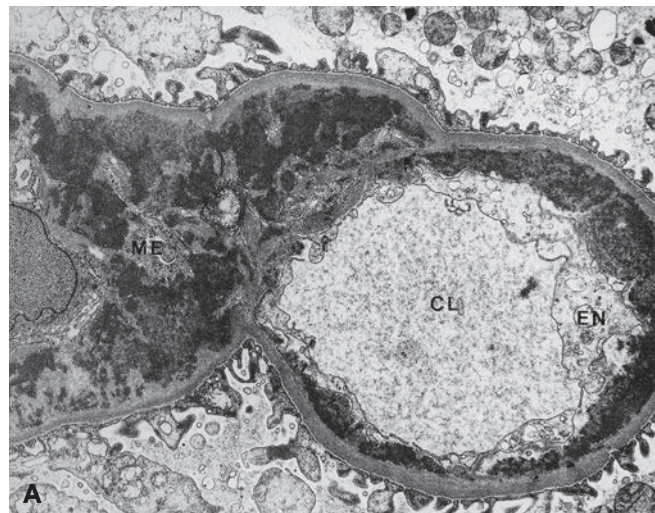


**Figure 23.52** **A**, Capillary loop showing marked accumulation of deposits in the mesangium and subendothelial regions. The deposits in the latter location represent the wire loop seen by light microscopy. CL, Capillary lumen; EN, endothelial cell; ME, mesangium ( $\times 7000$ ). **B**, Subendothelial deposits displaying a fingerprint-like pattern ( $\times 77,000$ ). **C**, Tubuloreticular inclusions in an endothelial cell ( $\times 30,000$ ).

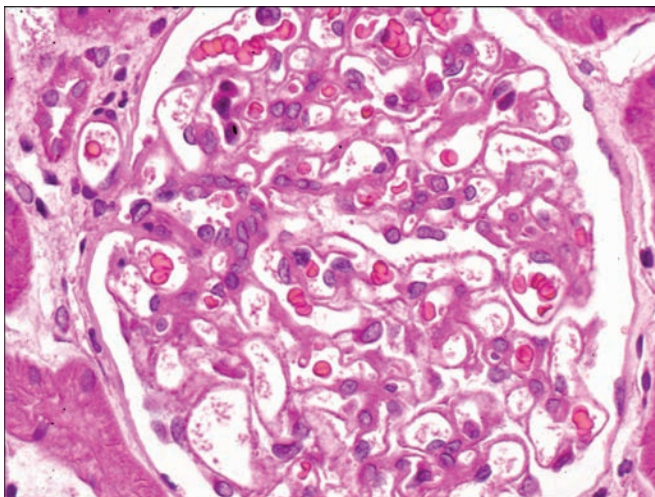


**Figure 23.53 Lupus Nephritis, ISN/RPS Class V.** The capillary walls are thickened and the mesangial matrix is segmentally increased.

microscopy in the mesangium and thickened capillary walls. Severe TA, IF, inflammation, and arteriosclerosis are usually present. Patients with class VI lesions often have significant proteinuria and severe renal insufficiency and are unlikely to respond to immunosuppressive therapy.

While most cases of lupus nephritis fall into the above categories, some overlap between classes exists. The most common involves classes III and V, and IV and V, and have been designated as combined classes III + V, and IV + V. The transformation of lupus nephritis lesions from one class to another is not uncommon over the course of the disease. It has been reported in 10%–50% of patients who undergo successive renal biopsies,<sup>360,361</sup> and it has occurred between all morphologic types: focal to diffuse,<sup>362</sup> focal to membranous, diffuse to membranous,<sup>363</sup> membranous to diffuse proliferative, and membranous to membranous with focal proliferative lesions.<sup>361,364,365</sup>

Tubulointerstitial inflammation can be found in all classes of lupus nephritis, even in those with minimal glomerular lesions.<sup>360</sup> Severe active TIN is most frequently seen in patients with classes III and IV lupus nephritis, is important in disease progression, and should be adequately assessed.<sup>366,367</sup> In most instances, the interstitial infiltrate is composed of mononuclear leukocytes, including lymphocytes, monocytes, and plasma cells, although neutrophils and eosinophils can sometimes be seen. In severe cases, there is inflammatory infiltration of the tubules and the tubular epithelial cells present degenerative and regenerative changes. Tubular casts made of neutrophils, erythrocytes, and shed tubular epithelial cells may be seen in the most severe cases. In about 50% of the patients, immunofluorescence and electron microscopy can demonstrate granular immune deposits along the peritubular capillaries, basement membranes of the proximal convoluted tubules, and interstitium (see Fig. 23.51). These deposits occur more frequently in diffuse lupus nephritis than in the focal variant but may also be found in patients with membranous and mesangial proliferative forms. Lupus nephritis is one of the few renal diseases in which immune deposits can be found not only in the glomeruli but also in the extraglomerular sites. The severity of the tubulointerstitial inflammation roughly correlates with the glomerular proliferative lesions; however, a few cases of severe tubulointerstitial damage without the significant glomerular disease leading to acute renal failure have been reported.<sup>368,369</sup>

Renal vascular lesions are relatively common in SLE and can assume a variety of morphologic forms, including uncomplicated

vascular immune deposits, noninflammatory necrotizing vasculopathy, true vasculitis with leukocyte infiltration and necrosis of the vessels walls, and TMA. All these vascular changes are signs of poor prognosis and, thus, should be recognized but are not currently included in histologic classification or activity and chronicity indices.<sup>370</sup>

Some authors have proposed that histologic indices derived from the semiquantitative analysis of activity and chronicity in renal biopsies of patients with SLE have a prognostic value and can serve as a therapy guide.<sup>371</sup> The activity index is calculated by the assessment of the following six histologic parameters: glomerular endocapillary proliferation, glomerular leukocyte infiltration, wire loop deposits and hyaline thrombi, glomerular fibrinoid necrosis and karyorrhexis, cellular crescents, and interstitial inflammation. The severity of each of these features is scored on a scale of 0 to 3+, and the fibrinoid necrosis/karyorrhexis and cellular crescents scores are doubled. Thus, the maximum activity score is 24. The chronicity index is computed by the sum of individual scores (0–3+) of the following four parameters: global glomerulosclerosis, fibrous crescents, TA, and IF. Thus, the maximum chronicity score is 12. Although the validity and the reproducibility of activity and chronicity indices have been questioned,<sup>372</sup> these indices help guide the management of individual cases as they provide useful information about the efficacy of therapy and the potential reversibility of the renal lesions.

Although in the past the recurrence of lupus nephritis after renal transplantation was reported to be rare, affecting only 1%–4% of the allografts, more recent studies indicate that the recurrence rate is higher (ranging from 8% to 30%) than was previously believed.<sup>373–375</sup>

## Glomerular Lesions Associated With Vascular Diseases

### Systemic Vasculitis

Vasculitis may occur in a variety of conditions, particularly in connective tissue diseases such as SLE and rheumatoid arthritis, and in hypersensitivity reactions caused by infections and drug reactions. Vasculitis may also occur as the primary manifestation of a variety of clinical conditions known as idiopathic systemic vasculitides. Clinical symptoms depend on the organ distribution, the size of the affected vessels, and the severity of the inflammation. The kidneys can be affected in different ways in systemic vasculitis. Large vessel vasculitides, such as giant cell (temporal) arteritis and Takayasu disease, can produce narrowing of the renal arteries, resulting in renal ischemia and hypertension. Medium-sized vessel vasculitides, such as polyarteritis nodosa (PAN) and Kawasaki disease, can affect intrarenal arteries and cause infarction and hemorrhage, whereas in small vessel vasculitides, such as microscopic polyangiitis (previously microscopic polyarteritis), GPA (previously Wegener granulomatosis), eosinophilic GPA (previously Churg–Strauss syndrome), HSP, and cryoglobulinemic vasculitis, the renal involvement is often manifested by glomerulonephritis.<sup>376</sup>

The vasculitides differ not only in their clinical and pathologic characteristics but also in their presumed pathogenesis. The large vessel vasculitides are supposedly caused by cell-mediated immune reactions to poorly defined (auto) antigens.<sup>377</sup> Immune complexes are involved in the pathogenesis of some small vessel vasculitides, such as HSP and cryoglobulinemia, whereas vasculitic lesions associated with microscopic polyangiitis, GPA, and eosinophilic GPA lack immune complexes and because of this, are collectively designated pauci-immune necrotizing vasculitides. Pauci-immune vasculitides are characterized by the presence of ANCA, which are valuable serologic markers for the diagnosis and monitoring of this group of vasculitides.<sup>378,379</sup> There is also evidence that ANCA are directly involved in the pathogenesis of these conditions.<sup>380,381</sup> Some of the

diseases in which vasculitis appears to be the primary histopathologic lesion will be discussed in this section.

### Polyarteritis Nodosa

PAN is a primary vasculitis of largely unknown etiology that affects muscular medium-sized arteries and produces lesions of varying stages (acute and healed) with aneurysm formation. The kidneys and gastrointestinal tract are among the organs most commonly affected, while the lungs are usually spared. The clinical manifestations are related to ischemia and disease severity of the involved organ.<sup>382</sup> Peripheral neuropathy has been reported in approximately 75% of the cases.<sup>383</sup> The estimated incidence is two to three cases per million.<sup>384</sup> Males are affected twice as often as females, and the peak incidence is in the sixth decade of life. There is no serum marker for PAN and, by disease definition, there should be no glomerular or other capillary involvement in classic PAN.<sup>376</sup> ANCA serology is typically negative unless there is a rare clinical overlap with microscopic polyangiitis.<sup>385</sup> About one-third of the patients may be carriers of the hepatitis B virus.<sup>386,387</sup> It has also been reported in hepatitis C and HIV-infected patients.<sup>388</sup> Recently mutations in *CECR1*, a gene encoding adenosine deaminase 2, an adenosine inactivating extracellular enzyme, have been detected in familial form of PAN with autosomal recessive inheritance.<sup>389</sup>

The kidneys are involved in 80%–90% of the cases.<sup>382</sup> Renal infarctions occur frequently and may be manifested by loin pain and hematuria. Hypertension is common and may be severe or malignant.<sup>390</sup> The renal lesion in PAN is a necrotizing vasculitis that involves medium-sized muscular arteries, such as the renal, interlobar, and arcuate arteries (Fig. 23.54). The lesions are quite focal and tend to localize to the bifurcations, and weakening of the vessel wall leads to the formation of aneurysmal dilations, detectable on Doppler ultrasonography or CT angiography. The inflammatory process may involve part of or the entire vessel wall and is characterized by fibrinoid necrosis and leukocytic infiltration, sometimes associated with intraluminal thrombosis. The acute phase evolves into a healing phase in which the necrosis subsides and the leukocytic inflammation is replaced by mononuclear infiltrate. In the healed stage, there is fibrosis of the media and perivascular tissue, disruption of elastic lamina, and recanalization of the thrombosed vessels.<sup>391,392</sup>

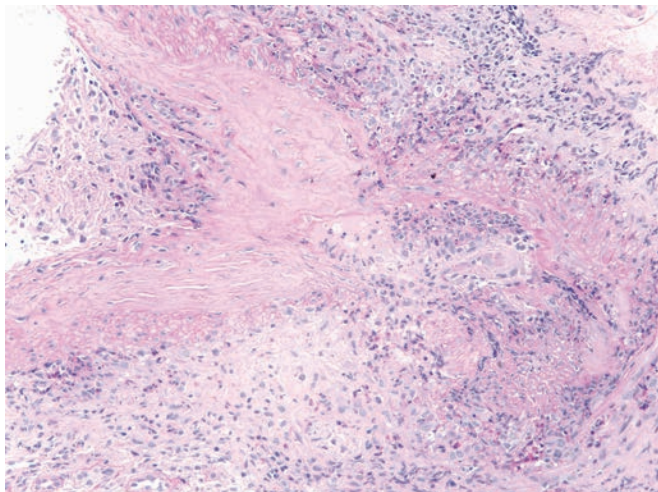


**Figure 23.54** Transmural vasculitis and fibrinoid necrosis involving a medium-sized artery, likely an interlobar artery, in polyarteritis nodosa. The glomeruli sampled in the kidney biopsy lacked crescents.

Because of the focal nature of the vessel lesion and involvement of medium-sized vessels, evidence of vasculitis may not be seen on a needle biopsy. The glomeruli show changes associated with ischemia consisting of variable degrees of collapse and sclerosis of the tufts; glomerular necrosis or crescents are not a feature of typical PAN. Immunofluorescence and electron microscopy typically do not reveal evidence of immune complex deposits.<sup>391</sup>

### Microscopic Polyangiitis

Microscopic polyangiitis, formerly known as microscopic polyarteritis, is a necrotizing systemic vasculitis with few or no immune complexes (pauci-immune) that affects small vessels (capillaries, venules, and arterioles) (Fig. 23.55). Involvement of small and rarely medium-sized arteries can also occur, but this is not a constant feature.<sup>393</sup> Because of the absence of arterial involvement in many cases, and the frequent involvement of venules, arterioles, and capillaries (including glomeruli), the term microscopic polyangiitis is now considered more appropriate for this form of vasculitis than the designation of microscopic polyarteritis.<sup>394</sup> Microscopic polyangiitis is distinct from PAN, is mediated by ANCA, and falls under the category of pauci-immune glomerulonephritis/vasculitis.<sup>376</sup> The incidence of microscopic polyangiitis is approximately 1 per 100,000.<sup>395</sup> Males are affected slightly more than females, and although it can occur at any age, it is more frequent during the sixth decade of life. Clinical manifestations are quite varied and nonspecific. Depending upon the organ(s) affected, the most common clinical features are hematuria and proteinuria, hemoptysis, palpable purpura, abdominal pain, myalgias, and arthralgias. Hypertension may occur, but it is usually mild. About 80%–90% of the patients have renal involvement.<sup>396</sup> In contrast to PAN, however, the lungs are commonly affected in microscopic polyangiitis.<sup>397</sup> A frequent clinical presentation of microscopic polyangiitis is as pulmonary–renal syndrome. This syndrome raises the possibility of anti-GBM disease (Goodpasture syndrome); however, the demonstration of ANCA in microscopic polyangiitis or anti-GBM antibodies in anti-GBM disease will establish the correct diagnosis. Over 80% of patients have detectable ANCA, most often P-ANCA (and anti-MPO). In addition to ANCAs, a recent study suggested a pathogenic role for anti-moesin antibodies in MPO-ANCA-associated vasculitis.<sup>335</sup> In the kidney, the most frequent lesion is glomerulonephritis, and the glomerular involvement ranges from a focal and

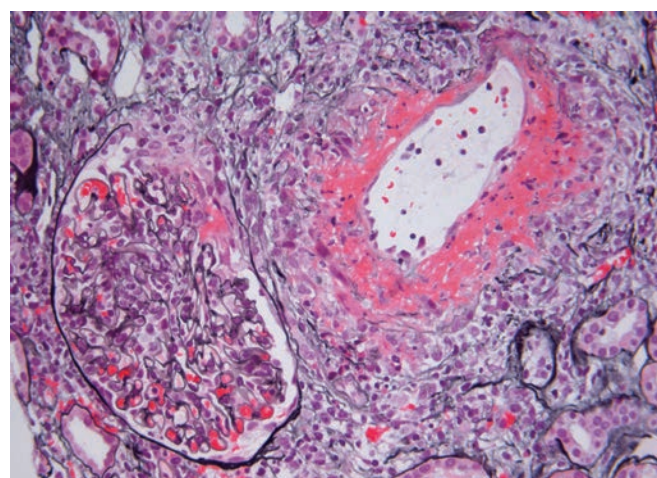


**Figure 23.55** Renal biopsy from a patient with microscopic polyangiitis showing a small vessel with necrosis and inflammatory infiltrate. The glomerulus has a segmental area of necrosis, and an early crescent (methenamine silver). (Image courtesy Megan Troxell, MD, PhD.)

segmental necrosis to a severe diffuse crescentic glomerulonephritis (see Fig. 23.55).<sup>395,396</sup> When present, necrotizing arteritis most often affects the interlobular arteries and rarely arcuate arteries.<sup>397</sup> Histologically, vasculitis in microscopic polyangiitis may be indistinguishable from that seen in PAN. However, in contrast to the lesions seen in PAN, which are usually in varying stages of evolution, those in microscopic polyangiitis almost invariably appear to be temporally uniform; glomerular involvement indicates a diagnosis of microscopic polyangiitis.<sup>398</sup> A tubulointerstitial infiltrate including eosinophils is frequently present. Immune complex deposits are not usually seen in the glomeruli, though there have been reports of sparse deposits containing IgG or IgM with C3 in various intraglomerular locations.<sup>398</sup>

### Granulomatosis With Polyangiitis

GPA (previously known as Wegener granulomatosis) is a multisystem disease of unknown etiology characterized by the triad of: (1) necrotizing granulomatous inflammation involving the upper respiratory tract (ear, nose, throat, and sinuses) and/or lungs; (2) necrotizing vasculitis affecting small- to medium-sized vessels (capillaries, venules, arterioles, and arteries) most prominently in the lungs and upper airways but also involving other sites as well; and (3) renal disease, most often manifested in the form of focal necrotizing glomerulonephritis.<sup>399</sup> Those patients who do not manifest the full triad are considered to have limited GPA. In these cases, involvement is limited to the respiratory tract and the kidneys are unaffected. The prevalence of GPA in the United States has been estimated to be 3 per 100,000,<sup>400</sup> with slight male predominance. It may occur at any age, but it is more common in the fourth and fifth decades.<sup>401</sup> The first clinical indication is usually upper respiratory symptoms which are followed by systemic phenomena related to the vasculitis.<sup>402</sup> About 80%–85% of patients present some signs of renal involvement, usually simultaneously with other clinical features,<sup>403</sup> but fewer than 20% actually present with renal functional impairment. Patients with renal involvement, if untreated, usually have a rapidly progressive and fatal disease. Therapy with cyclophosphamide, rituximab, and corticosteroids produces remission in most patients, but up to 50% of the patients may relapse.<sup>329,403</sup>

The differentiation of GPA from other types of vasculitis can be difficult clinically and morphologically. A positive ANCA test, especially C-ANCA (and/or PR3), can be extremely helpful in establishing or supporting the diagnosis of GPA. The specificity of C-ANCA in biopsy-proven GPA has been shown to be about 90%. The sensitivity depends upon the extent and activity of the disease. Although it has been shown that serum levels parallel the clinical activity of the disease<sup>404</sup> and that rising levels may be used as a predictor of relapse, there are some patients in whom C-ANCA titers do not follow disease activity.<sup>401,403</sup> The pathogenic role of ANCA with specificity to PR3 has been previously well established,<sup>399</sup> but recent studies have pointed to several pathways involving cell-mediated processes, neutrophil traps, and inflammatory mediators mediating tissue injury in GPA.<sup>405</sup>

The most common renal lesion is focal necrotizing glomerulonephritis, often with crescents.<sup>406</sup> Granulomatous glomerulonephritis occurs but it is uncommon, even in autopsy series, and is usually accompanied by necrosis of the hilar arterioles.<sup>407</sup> Necrotizing vasculitis involving the arterioles and small arteries occurs, but it is not a common finding in kidney biopsies. Interstitial inflammatory infiltrates are common, but necrotizing granulomata are rarely seen in renal biopsy specimens.<sup>403</sup>

As a rule, immune complex deposits are absent in GPA by electron microscopy, though there have been reports of the occurrence of sparse electron-dense deposits at different sites in the glomerulus.<sup>406,408</sup>

Immunofluorescence shows fibrinogen in glomeruli and the walls of involved vessels, and small amounts of IgM and/or IgG and C3 have been reported in glomeruli and vessels.

### Eosinophilic Granulomatosis With Polyangiitis

Eosinophilic granulomatosis with polyangiitis (EGPA), also known as Churg–Strauss syndrome or allergic granulomatosis, is a rare disorder characterized by asthma, eosinophilia, and systemic vasculitis affecting small- to medium-sized vessels.<sup>409,410</sup> The syndrome has no gender predilection, and while it has been reported in all ages, the mean age at diagnosis is approximately 50 years.<sup>411–414</sup> Renal involvement can be seen in 50% or more of these patients.<sup>411–413</sup> Patients with EGPA often have elevated IgE levels in their serum, and ANCA positivity (P-ANCA and anti-MPO) has been reported in 40%–80% of the cases.<sup>414–416</sup> In contrast to other vasculitides, renal involvement in EGPA rarely predominates. It is manifested by microscopic hematuria and mild proteinuria and, less frequently, by the nephrotic syndrome or rapidly progressive renal failure.<sup>411–414,417</sup> The renal prognosis in EGPA is generally better than that of other pauci-immune vasculitides, such as GPA or microscopic polyangiitis.<sup>417</sup> Patients usually respond to high dose steroids, but cyclophosphamide and rituximab are effective in refractory cases.<sup>418</sup>

The most common light microscopic abnormality on renal biopsy is that of a focal and segmental necrotizing glomerulonephritis with crescent formation similar to that found in other ANCA-associated vasculitides, with eosinophil-rich arteritis (a distinctive feature) in a minority of cases.<sup>419,420</sup> The interstitium may be affected by inflammatory cells, including eosinophils, lymphocytes, and plasma cells. Interstitial granulomas can also occur but are uncommon. Immunofluorescence studies may show positivity for IgM, C3, and fibrinogen in glomeruli in the segmental areas of necrosis. No immune complex deposits are found by electron microscopy.

### Henoch–Schönlein Purpura

HSP is a distinct systemic vasculitic syndrome that is characterized by palpable purpura (most often symmetrically distributed over the extensor-dependent surfaces of the lower extremities and buttocks), migratory arthralgias, abdominal manifestations (including pain, vomiting, and intestinal bleeding), and renal disease.<sup>421,422</sup> The clinical manifestations of the syndrome are caused by a systemic small vessel vasculitis of the leukocytoclastic type. The inflammatory reaction seen in the skin, kidney, and other organs is caused by deposition of IgA-containing immune complexes. HSP can occur at any age but is more common in young children, with over 50% of the cases under 5 years and over 75% under 10 years.<sup>423,424</sup> A male predominance has been reported in both children and adults, with a ratio of up to 2:1.<sup>422,423</sup> HSP is uncommon in blacks, and familial cases have rarely been reported.<sup>425</sup> About one-fourth of the patients have a history of allergies. Renal involvement has been reported to occur in approximately 20%–55% of children<sup>426,427</sup> and 50%–85% of adults<sup>423,428</sup> and ranges from mild hematuria and proteinuria with no reduction in renal function to the nephrotic syndrome and severe renal insufficiency. Upper respiratory tract infections often precede the onset of HSP. The disease undergoes complete, spontaneous remission in half of the patients, usually within a year of onset, but in many others, it progresses to ESRD over a period of 5–10 years. The prognosis in children is excellent with ESRD reportedly occurring in only 2% of patients. In general, there is good correlation between the severity of the lesion and the clinical manifestations, and patients with the nephrotic syndrome usually progress to renal failure.<sup>428</sup> Recurrence can occur in allografts, but it is rarely responsible for graft failure.

By light microscopy, the most characteristic feature is a mesangial proliferative glomerulonephritis with a variable degree of crescent formation. The mesangial changes, which may be focal or diffuse, include both mesangial hypercellularity and an increase in mesangial matrix. Occasional cases may show a membranoproliferative pattern. In the most severe cases, the glomerular tufts may be infiltrated by polymorphonuclear leukocytes and mononuclear cells and may exhibit areas of necrosis. Vasculitis involving glomerular arterioles and interlobular arteries can also occur, but this is rare finding on renal biopsies. Tubulointerstitial changes of atrophy and IF correlate with the degree of glomerular damage. Electron microscopy shows mesangial deposits that may extend into the subendothelial areas. Subepithelial deposits similar to those in membranous nephropathy or resembling the humps of postinfectious glomerulonephritis have been reported.<sup>429</sup> But in such instances, a recently characterized entity, IgA-dominant postinfectious glomerulonephritis, associated with co-dominant C3 staining and frequent hypocomplementemia, should be considered.<sup>239</sup> The most distinctive feature of HSP is the demonstration of dominant or co-dominant IgA by immunofluorescence. As in IgAN, the deposits may also contain IgG, IgM, C3, and properdin but not C1q or C4. The fact that the deposits consist mainly of aberrantly glycosylated polymeric IgA1 supports the notion that IgAN and HSP are spectra of the same disease.<sup>311,430</sup>

### Cryoglobulinemic Vasculitis

Cryoglobulins are immunoglobulins or complexes of immunoglobulins that precipitate at low temperatures (4°C) and redissolve when the serum is heated to 37°C. Three types of cryoglobulinemia are recognized: type I, in which the cryoglobulins are composed exclusively of a single monoclonal immunoglobulin of either IgG or IgM class, usually generated by a lymphoplasmacytic disorder, and types II and III, which are composed of "mixed" cryoglobulins, a designation based on their composition as complexes of immunoglobulins. Type II cryoglobulins consist of a complex of monoclonal immunoglobulins (typically IgM) with rheumatoid factor activity, causing it to bind to polyclonal IgG, whereas type III cryoglobulins are a mixture of polyclonal IgM and IgG. Mixed cryoglobulins (types II and III) can be found in the serum of patients with a variety of clinical conditions, including lymphoproliferative disorders, chronic infections, chronic liver disease, and autoimmune diseases, particularly SLE.<sup>431</sup> In the past, no clear cause could be found in about 30% of all mixed cryoglobulinemias (and so referred to as "essential" cryoglobulinemia), but it is now clear that majority are associated with hepatitis C virus infection.<sup>432</sup> Approximately 10%–15% of all cases of cryoglobulinemia involve type I cryoglobulins, 50%–60% type II, and 25%–40% type III.<sup>178,432</sup> Any of the three types of cryoglobulin can precipitate in the vasculature, forming thrombi in virtually any organ of the body, and may elicit an inflammatory reaction (vasculitis) in the vessel wall.<sup>433,434</sup>

A distinctive clinical syndrome characterized by a variable combination of fatigue, purpura, arthralgias, hepatosplenomegaly, lymphadenopathy, Raynaud phenomenon, and glomerulonephritis has been observed in patients with mixed cryoglobulinemia. Both sexes are affected, though it is most common in women in the fourth and fifth decades.<sup>435</sup> Purpura is almost always present and is usually distributed over the lower extremities. Renal disease occurs in about 50% of the patients and becomes apparent 1–3 years after the purpura, but it can be a presenting symptom.<sup>436</sup> Typical clinical manifestations are nephrotic-range proteinuria, microscopic hematuria, and hypertension. Acute nephritic syndrome occurs in 20%–30% of the cases, and oliguric acute renal failure in about 5% of patients with renal disease. Although rare, renal involvement can occur in type I cryoglobulinemia. In the few reported cases, the clinical manifestations

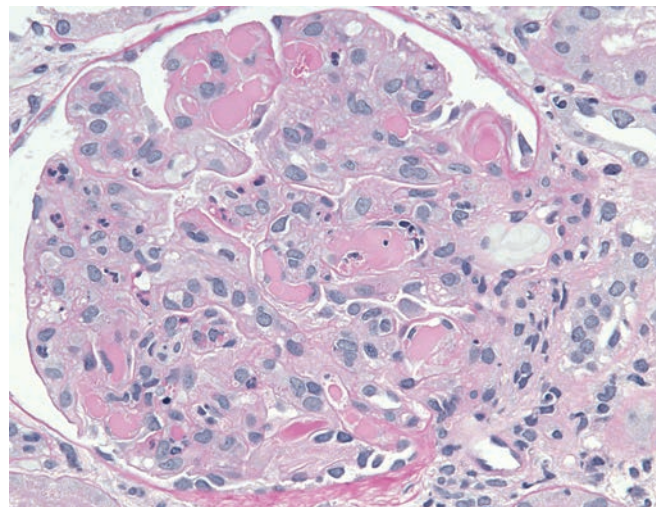


**Figure 23.56** Cryoglobulinemic glomerulonephritis with diffuse proliferation, lobular accentuation and intraluminal hyaline thrombi (deposits) (PAS).

and pathologic features of type I cryoglobulinemia are identical to those of mixed cryoglobulinemia.<sup>433</sup> Hypocomplementemia is common, especially low C4, but several cases have reduced levels of C3 as well. False negative result for serum cryoglobulins is real concern, and appropriate sample collection and transportation to maintain the serum temperature at 37°C is extremely important. Some cryoglobulins, especially type III, can take up to 7 days or more to precipitate.<sup>437</sup>

The most common renal biopsy finding in patients with all types of cryoglobulinemia is a diffuse proliferative glomerulonephritis (often with a membranoproliferative pattern). Focal and segmental glomerulonephritis and, less frequently, membranous or crescentic glomerulonephritis can also occur. Abundant glomerular intracapillary macrophages are a frequent feature. In more acute cases, the bulky deposits produce the appearance of thrombi or wire loops as can be seen in lupus nephritis (Fig. 23.56). Vasculitis is the basic pathologic lesion in every affected tissue including the kidney, where it tends to involve the interlobular arteries and afferent arterioles. Electron microscopy often demonstrates abundant subendothelial deposits and, less frequently, mesangial, intramembranous, or subepithelial deposits. In approximately half of the cases, the glomerular deposits appear as fibrillar, tubular, or annular structures or may exhibit a fingerprint-like pattern (Fig. 23.57).<sup>438</sup> In some cases, especially those associated with plasma cell dyscrasias, it is possible to find rhomboid- or needle-shaped crystals in the cytoplasm of glomerular epithelial and mesangial cells.<sup>439</sup> Immunofluorescence usually demonstrates positivity for the immunoglobulins present in the cryoglobulins in the glomeruli and vessels. C3 deposition is often found in these locations, whereas C1q and C4 occur in only about one-third of the cases. Heavy and/or light chain restriction can be observed in type I cryoglobulinemia.

### Hemolytic Uremic Syndrome and Thrombotic Thrombocytopenic Purpura

TMAs constitute a group of microvascular occlusive disorders characterized by hemolytic anemia that is caused by fragmentation of erythrocytes, thrombocytopenia due to increased platelet aggregation, and thrombus formation that produces variable signs and symptoms of organ ischemia.<sup>440</sup> In addition to schistocytes on peripheral smear, patients with TMA have elevated serum lactate dehydrogenase, low

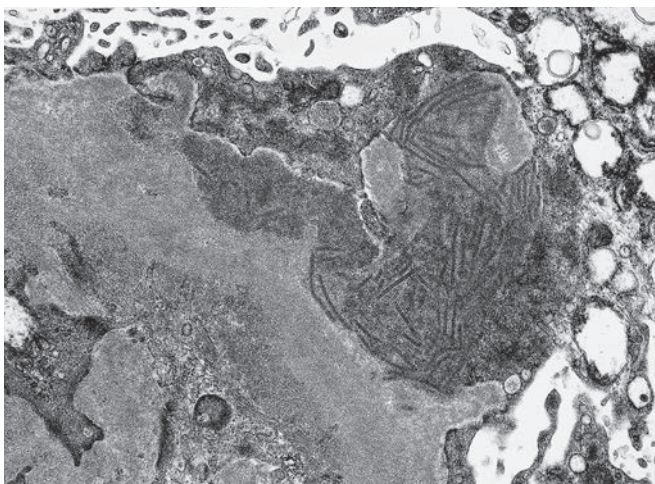


**Figure 23.57** Subepithelial deposits demonstrating fibrillary configuration in a case of cryoglobulinemic glomerulonephritis ( $\times 21,500$ ).

haptoglobin levels, and negative Coombs test. Although TMA may be a manifestation of various disease states,<sup>441</sup> the two most prominent conditions are thrombotic thrombocytopenic purpura (TTP) and HUS. Traditionally, the diagnosis of HUS was made when renal failure was the predominant feature and children were the ones primarily affected, whereas the term TTP was used for adult patients having predominantly central nervous system impairment. Because of the overlap of clinical manifestations, these two syndromes were previously considered to be a continuum of a single disease entity. However, newly identified pathophysiologic mechanisms have allowed these syndromes to be distinguished from each other on a molecular basis.<sup>442</sup> Studies have shown that patients with TTP are severely deficient in a plasma protein ADAMS13, while those with HUS have either normal or only moderately reduced levels.<sup>443,444</sup> ADAMS13 is a metalloprotease that cleaves the large von Willebrand factor (vWF) multimers produced by the endothelial cells. When ADAMS13 activity is deficient, the resulting abnormally large vWF multimers in the plasma have a greater ability to react with platelets and cause the disseminated platelet microthrombi characteristic of TTP. These microthrombi can be found in arterioles and capillaries in a variety of organs, including the brain, gastrointestinal tract, pancreas, skin, heart, adrenal glands, and kidneys.<sup>445,446</sup> The deficiency of ADAMS13 activity can be inherited, but it is more commonly caused by an acquired autoantibody (as triggered by drugs such as ticlopidine and clopidogrel) that binds and inhibits the metalloprotease.<sup>447</sup>

HUS is defined by the triad of thrombocytopenia, microangiopathic hemolysis, and acute renal failure. The underlying causes of HUS have been broadly divided into diarrhea-associated (D+ HUS), also known as classic HUS, and nondiarrheal forms (D- HUS), also known as atypical HUS.<sup>448,449</sup> The classic form occurs primarily in infants and young children, but it may appear at any age, and both sexes are equally affected. It accounts for most of the cases of HUS in North America and is characterized by sometimes occurring in small epidemics after exposure to contaminated foods, such as undercooked ground beef, unpasteurized apple juice, and dairy products, with verotoxin-producing *Escherichia coli* O157:H7 and, less commonly, with *Shigella dysenteriae* type I.<sup>450,451</sup> The verotoxin/Shiga-like toxin binds to globotriaosylceramide (Gb3) receptors that are expressed in highest concentration in microvascular endothelial cells in kidney, gut, pancreas, and brain and mediate endothelial damage. Patients usually present with prodromal diarrhea (often

bloody) followed by acute renal failure. About one-third of the patients may present symptoms of neurologic involvement, commonly manifested by seizures, altered consciousness, and focal neurologic signs. Because thrombotic changes are most often confined to the glomeruli, patients with classic HUS usually have a good prognosis and recovery occurs in about 80%–90% of the cases. About 5% of the patients, however, die of disease, usually of cerebral causes.

D- HUS is much less common than the classic type and accounts for only 5%–10% of all cases of the disease.<sup>449</sup> It may occur at any age but is more frequent in adults. The etiology of D- HUS is heterogeneous.<sup>452,453</sup> It can be associated with nonenteric infections caused by bacteria, such as *Streptococcus pneumoniae*, *Mycoplasma pneumoniae*, and *Legionella* or viruses, such as influenza A virus and HIV. Infection caused by *Streptococcus pneumoniae* accounts for 40% of D- HUS and 4.7% of all cases of HUS in children in the United States.<sup>454</sup> D- HUS can also occur in association with disorders such as SLE, systemic sclerosis, antiphospholipid antibody syndrome, malignant hypertension, or various forms of cancer, especially prostatic, gastric, breast, and pancreatic carcinomas.<sup>440,452,453</sup> This form of HUS can be induced by total body irradiation, antineoplastic agents (mitomycin, cisplatin, bleomycin, and gemcitabine), anti-vascular endothelial growth factor [VEGF] or immunosuppressive drugs (cyclosporine, tacrolimus, OKT3, sirolimus, and interferon), quinine, and oral contraceptives. A severe form occurs in association with pregnancy, especially in the postpartum period.<sup>455</sup> The overall prognosis of these patients is poor, with a high mortality rate from central nervous system disease or uncontrollable bleeding, and, if they survive, usually develop chronic renal failure.

Several forms of D- HUS are hereditary, involving complement regulatory proteins, factor H, factor B, C3, membrane cofactor protein (MCP or CD46), or factor I.<sup>453,456</sup> Defects in these proteins as a result of mutations of the corresponding genes cause excessive alternative complement pathway activation that damages endothelial cells, leading to a prothrombotic stage and local accumulation of platelet-fibrin thrombi. Certain high-risk haplotypes have also been identified and might account for variability in penetrance among family members. It has also been proposed that environmental triggers such as infection, pregnancy, transplantation, oral contraceptive pills, and drugs act as a second hit, overwhelm the delicate complement "balance" in these patients, and precipitate atypical HUS in adult life. Low serum C3 levels in HUS may indicate a genetic component.<sup>457</sup> Other genetic disorders affecting cobalamin metabolism and coagulation pathway also cause clinical features and histologic changes of TMA.<sup>441</sup>

A biopsy taken early in the disease course shows fibrinoid necrosis, intimal and subintimal fibrin deposits with entrapped fragmented red cells, thrombosis, and endothelial cell proliferation in small arteries and arterioles. The glomeruli may be affected similarly (Fig. 23.58), exhibit acute ischemic changes, or be infarcted. There is endothelial swelling with narrowing of the capillary lumina. The mesangium is expanded, and, in severe cases, mesangiolysis may occur. As the lesion progresses, there is an intense basophilic intimal thickening in the small arteries and arterioles which greatly restricts the vascular lumina. These mucoid intimal changes usually develop over several weeks, although they may be seen in very early phase of the disease. Aneurysmal dilation, accompanied by proliferation of some arterioles, particularly at the hilus of the glomerulus is a typical finding. Insidious presentation and chronic glomerular TMA lesions are characterized mainly by mesangiolysis and basement membrane irregularities and double contours (Fig. 23.59).

Electron microscopy reveals the most characteristic feature of HUS: narrowing of the capillary lumen due to marked widening of the subendothelial space that is filled with a pale, finely particulated

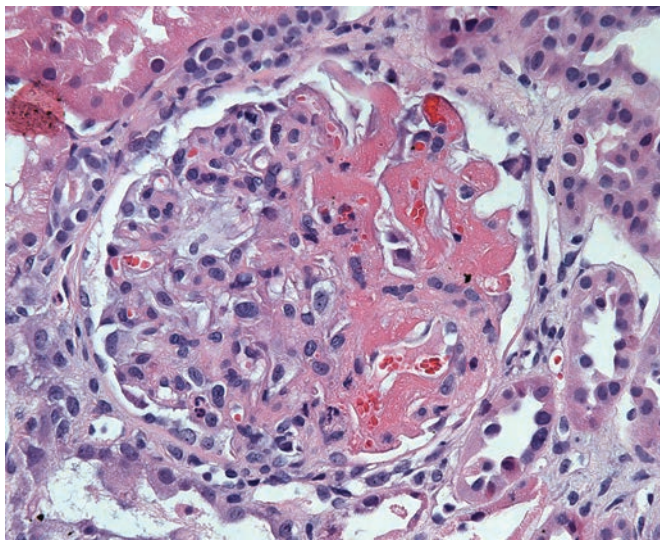


**Figure 23.58** Glomerulus with capillary fibrin thrombi, karyorrhexis and entrapped fragmented red blood cells in acute thrombotic microangiopathy.

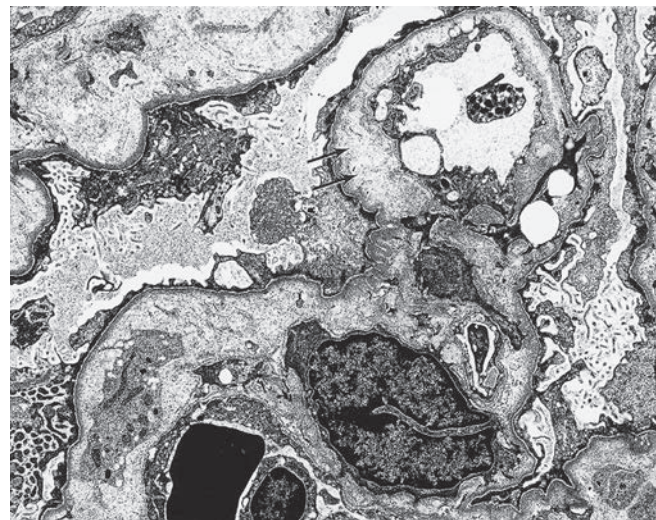


**Figure 23.60** Portion of a glomerulus showing a prominent subendothelial electron-lucent zone (arrows) and mesangiolysis in a case of acute thrombotic microangiopathy (x9000).

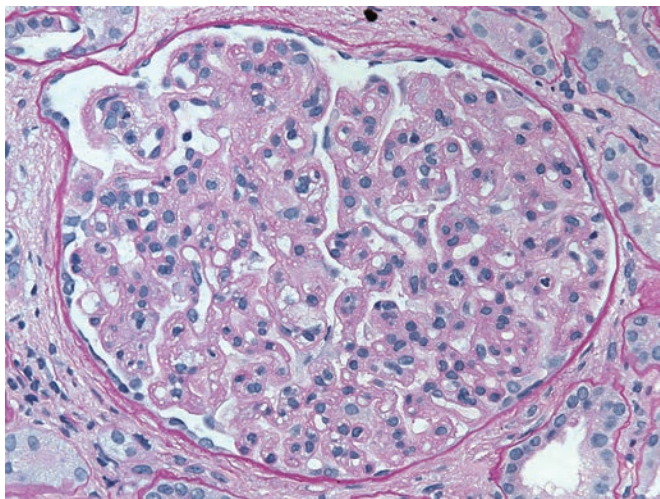


**Figure 23.59** Glomerulus From a Patient With Antiphospholipid Antibody Syndrome. Diffuse glomerular basement membrane multilayering is seen along with mesangiolysis and endothelial swelling (PAS).

or fibrillar material that stains positively for fibrinogen by immunohistochemical methods (Fig. 23.60). In the chronic phase, an irregular, thin layer of basement membrane-like substance is present between the endothelial cell cytoplasm and the electron-lucent area. Because of its argyrophilic characteristics, this material can produce a double contour on light microscopy, thus simulating a membranoproliferative pattern (see Fig. 23.59). Fibrin and platelet aggregates may occlude the capillary lumina, and the endothelium is often disrupted in these thrombosed areas. The mesangial cells are swollen and hypertrophic and contain many phagolysosomes. Extensive foot process effacement is seen in the areas of capillary wall collapse. In the later stages, interlobular arteries and arterioles are affected by a mucinous, onion-skin-like obliterating vasculopathy devoid of inflammation. The vascular lesions are identical to those seen in systemic sclerosis and malignant hypertension, so careful analysis of the clinical data is required for accurate diagnosis.

## Systemic Sclerosis

Systemic sclerosis, progressive systemic sclerosis, or systemic sclerosis are terms used to designate a connective tissue disorder of unknown etiology characterized by multiple organ system involvement. Although a rare disease, with a reported prevalence ranging from 3.1 to 20.8 per 100,000,<sup>458</sup> systemic sclerosis is associated with significant morbidity and mortality. Women are more commonly affected than men, with a ratio of approximately 3:1.<sup>459</sup> It may occur at any age but is more common between the fourth and sixth decades of life. The pathogenesis of systemic sclerosis is not fully understood but most likely involves a complex interplay of excessive fibrosis, vascular abnormalities, and abnormalities in the immune system.<sup>460,461</sup> Most patients are ANA positive, which is a rather nonspecific feature. Several other autoantibodies such as RNA polymerase III, antitopoisomerase-1, and anticentromere antibodies are specific markers of systemic sclerosis but are not clearly linked to the pathogenesis of systemic sclerosis.<sup>462</sup> The autoimmune mechanisms in these patients potentially target endothelial cells and fibroblasts. The downstream effects of this targeted injury include increased vascular permeability, endothelial apoptosis, and platelet aggregation, and increased matrix production mediated by fibroblast-derived TGF- $\beta$  and reduced matrix degradation.

The clinical features of the disease are produced by differing combinations of excessive collagen deposition and vascular disease, the former causing deformation and morbidity, and the latter being the mechanism of most systemic complications. Diffuse form of the disease with widespread cutaneous fibrosis is frequently associated with severe organ involvement while a disease limited to the distal extremities has milder organ involvement. Raynaud syndrome, skin thickening, digital pulp atrophy (sclerodactyly), and telangiectasia are the primary clinical manifestations of systemic sclerosis. Musculoskeletal involvement includes periaricular, tendon, and nerve entrapment, flexion contractures, acral osteolysis, and myopathy. In the gastrointestinal tract, the disease can cause esophageal dysmotility and malabsorption. Pulmonary hypertension and IF, cardiomyopathy, and scleroderma renal crisis are the major causes of mortality. Renal involvement occurs in 60%–70% of the patients.<sup>463,464</sup> Two clinical forms of renal involvement have been recognized: an acute and rapidly progressive form of renal failure often associated with malignant hypertension, systemic vasoconstriction,

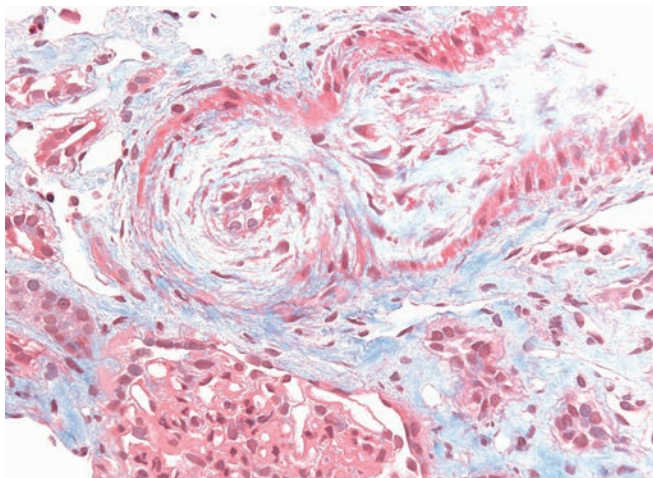


**Figure 23.61** Interlobular artery showing stenosing intimal mucoid edema in a patient with systemic sclerosis and acute renal failure (trichrome).

and microangiopathic hemolytic anemia (referred to as scleroderma renal crisis); and a more common, slowly progressive chronic form that is manifested by varying combinations of proteinuria, hypertension, and azotemia.<sup>464–466</sup> Scleroderma renal crisis in most cases can be successfully treated with angiotensin-converting enzyme (ACE) inhibitors and effective blood pressure control, but some patients do progress to end-stage kidney.<sup>465</sup>

The main morphologic changes in scleroderma renal crisis are in the interlobular arteries that show intimal thickening by loose, myxoid fibrous tissue (Fig. 23.61).<sup>440</sup> Subendothelial fibrin deposition and intimal hemorrhage may also be seen. The muscular wall of the artery is usually attenuated and stretched around the excessive intima, and periarterial fibrosis may be prominent. Arterioles frequently exhibit fibrinoid necrosis and thrombosis, which may continue uninterrupted into the glomeruli. The arcuate and interlobular arteries are minimally involved in acute systemic sclerosis renal damage, but in chronic disease, they may show nonspecific, sclerotic intimal thickening that can be difficult to distinguish from normal age-related changes. The glomeruli are typically small and show varying degrees of acute ischemic changes and, on occasion, intracapillary fibrin thrombi. Juxtaglomerular hyperplasia may be prominent, especially in patients with malignant hypertension and hyperreninemia. In the chronic form, varying degrees of glomerulosclerosis, TA, and interstitial scarring are observed.<sup>467</sup>

By electron microscopy, affected blood vessels show intimal widening by amorphous electron-lucent material corresponding to the myxoid ground substance seen by light microscopy. The glomeruli present basement membrane wrinkling with focal widening of the subendothelial area, which may contain fibrin strands. In the chronic form, the vascular lumina of the arteries are narrowed by dense concentric intimal fibroelastosis. Immunofluorescence studies often demonstrate reactivity for fibrinogen, with or without IgM and C3, in the intima of blood vessels and along the glomerular capillaries. Since the renal lesions in systemic sclerosis, HUS, and malignant hypertension can be identical, careful evaluation of the patient's clinical history and laboratory data is essential in establishing the diagnosis.

## Renal Diseases of Pregnancy

Renal disease may be initiated or exacerbated during pregnancy. Because of the extent and complexity of the topic and space limitations, only preeclampsia will be discussed here.

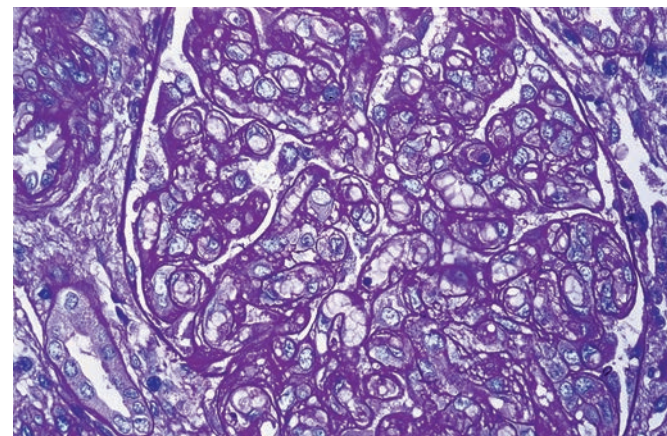


**Figure 23.62** Preeclamptic Renal Disease. The glomerular capillary lumina are obliterated by swollen endothelial cells.

## Preeclampsia

Preeclampsia is a pregnancy-induced systemic syndrome characterized by new-onset hypertension, proteinuria, and edema that usually occurs after the 20th week of gestation. When the syndrome progresses to a convulsive stage, it is termed eclampsia, and HELLP syndrome refers to a subset of preeclampsia patients with hemolysis, elevated liver enzymes, and low platelets. Preeclampsia affects approximately 3%–5% of pregnancies worldwide. Most cases occur in primigravidae, with an incidence as high as 7.5%.<sup>468,469</sup> Although the etiology of the syndrome remains unknown, recent studies have shown that a reduction of VEGF—caused by an excess circulating antiangiogenic factors, most notably soluble FMS-like tyrosinase kinase (sFlt1) and soluble endoglin, which are highly elevated during preeclampsia—plays an important role in the pathogenesis of the syndrome.<sup>468–470</sup> Derived from placenta, sFlt1 serves as a receptor for VEGF. VEGF is important not only in angiogenesis but is also a critical factor for the maintenance and health of the fenestrated and sinusoidal endothelium found in the renal glomerulus, brain, and liver.<sup>471</sup>

The changes in preeclampsia occur primarily in the glomeruli, which appear characteristically enlarged, swollen, and bloodless, with thickened capillary walls (Fig. 23.62). The bloodless pattern is produced by an intense swelling and hypertrophy of the endothelial and, to a lesser extent, the mesangial cells (endotheliosis).<sup>470</sup> Glomerular cellularity is usually normal or mildly increased. By electron microscopy, the capillary lumens appear narrow or obliterated by swollen endothelium, which often exhibits a loss of its normal fenestration. When mesangial cell hypertrophy is severe, the mesangium may become interposed between the endothelium and the basement membrane. Distinct strands of fibrin are present in translucent subendothelial zones containing loose fibrillar material.<sup>472</sup> Immunofluorescence studies have shown that the deposits in the glomeruli consist mainly of fibrinogen. Immunoglobulins, especially IgM, may on occasion be present due to nonspecific trapping in injured glomeruli. The afferent arterioles and their endothelial cells retain a normal appearance, which is striking in contrast to the swollen, vacuolated glomerular endothelial cells. Patients in whom preeclampsia nephropathy is superimposed on essential hypertension have hypertensive arterial and arteriolar changes in addition to the glomerular lesion.

Preeclampsia usually carries a good prognosis, and the changes in the glomerular capillaries disappear in a few weeks following delivery. Blood pressure falls to normal levels within a month. However, preeclampsia recurs in approximately 20% of subsequent pregnancies.

The clinical presentation of HELLP syndrome in a pregnant woman might indicate an underlying atypical HUS due to mutations in genes encoding alternative complement pathway components or circulating autoantibodies to complement factors.<sup>473</sup> It is being recognized that pregnancy-related stress may serve as a trigger for precipitating atypical HUS in a genetically predisposed individual.

## Hereditary Glomerular Diseases

### Alport Syndrome

AS (also known as hereditary nephritis) is an inherited type IV collagen disorder of the basement membranes manifested by progressive nephritis associated with deafness and ocular abnormalities.<sup>474-476</sup> In the United States, it accounts for 2.5% of children and 0.3% of adults with ESRD.<sup>140</sup> Males are more commonly affected than females. AS is a genetically heterogeneous disorder. Approximately 85% of the patients have the X-linked dominant form of the syndrome resulting from mutations in the *COL4A5* gene located at Xq22, which encodes the  $\alpha 5$  chain of type IV collagen. Most of the remaining patients have autosomal recessive AS due to mutations in either the *COL4A3* or *COL4A4* genes, while only a minority of families exhibit the autosomal dominant disease that also arises from mutations in these genes.<sup>477-481</sup> To date, over 800 different mutations have been identified in X-linked dominant AS by different groups of investigators in various parts of the world.<sup>475,480</sup>

The disorder is usually manifested in children and young adults by recurrent microscopic or gross hematuria. Although proteinuria is usually mild, in advanced stages of the disease it can be in the nephrotic range. In males, the disease is usually progressive. In X-linked disease, the risk for males progressing to ESRD before the age of 40 is 90% compared with only 12% in females,<sup>475,482</sup> and the location of the mutation appears to determine the age of onset of ESRD.<sup>483</sup> In autosomal recessive AS, females are affected as severely and as early as males with X-linked disease. While patients with autosomal dominant disease show a great variability in their clinical course, this is generally milder than in males with X-linked AS. Bilateral high-frequency sensorineural hearing loss is the most common extrarenal manifestation of AS, often occurring in childhood in males, with females being affected later in life. Hearing impairment is always accompanied by renal involvement, but there is no relationship between the severity of the hearing loss and renal disease. Ocular abnormalities occur in 15%-30% of patients and appear to be confined to juvenile kindreds.<sup>483,484</sup>

Other uncommon variant of AS includes its association with diffuse leiomyomatosis (esophagus, tracheobronchial tree, and urogenital tract), which has been reported in 2%-3% of families with the juvenile form of the disease.<sup>474,485</sup> After transplantation, 3%-5% of males with AS develop anti-GBM nephritis, presumably because tolerance for the normal GBM antigen has not been acquired at birth.<sup>475,486</sup> Most patients with X-linked AS and anti-GBM nephritis in the allograft have antibodies to the NC1 domain of the  $\alpha 5$  chain of collagen IV, but antibodies against the NC1 domain of the  $\alpha 3$  chain have also been reported.<sup>487</sup>

The light microscopic features in the kidney are nonspecific, and the diagnosis depends on the electron microscopic and immunofluorescence findings. In biopsies taken in the early stage of the disease, the glomeruli appear normal or may show mild mesangial hypercellularity with minor thickening of the capillary walls. As the disease progresses, however, the glomeruli undergo segmental and global sclerosis. Tubulointerstitial changes appear relatively early, and consist of irregular areas of nonspecific sclerosis. The presence of

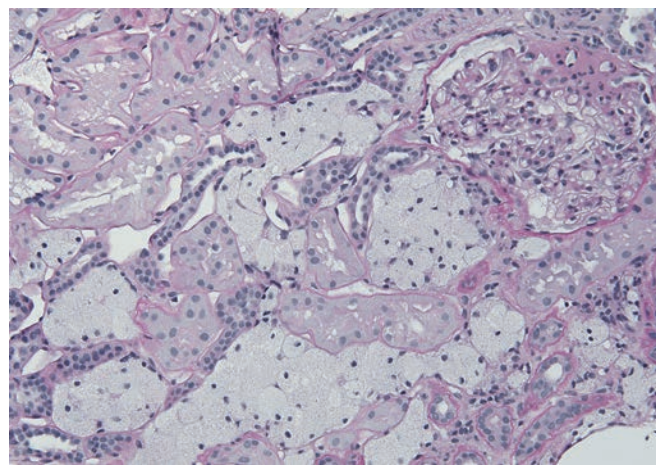


**Figure 23.63** Interstitial foam cells and focal segmental glomerulosclerosis in a patient with microscopic hematuria and ultrastructural features of Alport syndrome (PAS).

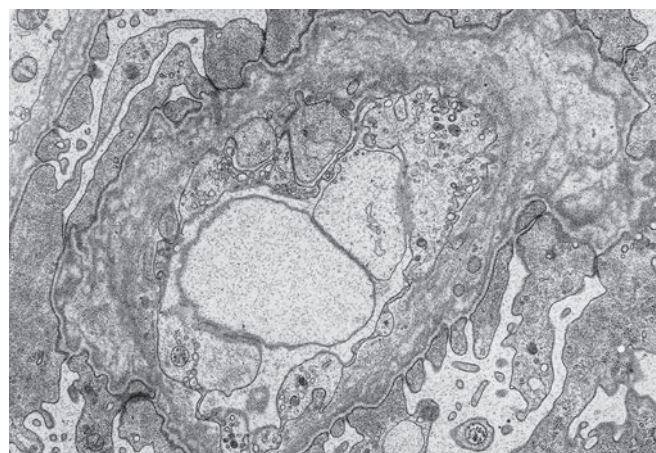


**Figure 23.64** Glomerular capillary loop showing diffuse, irregular, thickening of the glomerular basement membrane. The lamina densa is split into multiple interwoven lamellae ( $\times 11,400$ ).

interstitial foam cells in the absence of nephrotic-range proteinuria is a characteristic but nonspecific feature of AS (Fig. 23.63).

The most specific finding of AS can only be seen by electron microscopic examination of the glomeruli. The typical lesion is thickening of the GBM with transformation of the lamina densa into multiple interwoven lamellae (Fig. 23.64). The epithelial aspect of the basement membrane often has a scalloped appearance, whereas the endothelial surface is usually smooth. The typical lesion of the GBM occurs in most but not all patients with AS. Affected young males and heterozygous females of any age may only have attenuated GBM measuring as little as 100 nm or even less,<sup>488</sup> representing the earliest manifestation of disease; the extent and severity of the multilamellation increases with age. Some authors have found a correlation between the percentage of the GBM having a splitting of the lamina densa and the degree of proteinuria in patients with AS, which suggests that the increased permeability of the GBM to protein is the functional consequence of the GBM alteration.<sup>489</sup> Although multilamellation of the GBM suggests hereditary nephritis, it can also be seen in other conditions, such as in the resolving stages of MGN and in IgAN-associated GBM repair.<sup>490</sup>

The panel of antibodies used in routine immunofluorescence studies usually fails to show any reactivity, although small and

**Table 23.6** Immunohistochemical findings in the basement membranes of patients with Alport syndrome using antibodies to  $\alpha$ 3,  $\alpha$ 4, and  $\alpha$ 5 chains of type IV collagen

	GLOMERULAR BASEMENT MEMBRANE	BOWMAN'S CAPSULE	DISTAL TUBULAR BASEMENT MEMBRANE	EPIDERMAL BASEMENT MEMBRANE
<b>Normal (Both Sexes)</b>				
$\alpha$ 3 (or $\alpha$ 4)	Present	Present	Present	Absent
$\alpha$ 5	Present	Present	Present	Present
<b>X-Linked (Males)<sup>a</sup></b>				
$\alpha$ 3 (or $\alpha$ 4)	Absent	Absent	Absent	Absent
$\alpha$ 5	Absent	Absent	Absent	Absent
<b>X-Linked (Females)<sup>b</sup></b>				
$\alpha$ 3 (or $\alpha$ 4)	Mosaic	Mosaic	Mosaic	Absent
$\alpha$ 5	Mosaic	Mosaic	Mosaic	Mosaic
<b>Autosomal Recessive (Both Sexes)<sup>c</sup></b>				
$\alpha$ 3 (or $\alpha$ 4)	Absent	Absent	Absent	Absent
$\alpha$ 5	Absent	Present	Present	Present
<b>Autosomal Dominant (Both Sexes)</b>				
$\alpha$ 3 (or $\alpha$ 4)	Present	Present	Present	Absent
$\alpha$ 5	Present	Present	Present	Present
<b>Thin Basement Membrane Nephropathy (Both Sexes)</b>				
$\alpha$ 3 (or $\alpha$ 4)	Present <sup>d</sup>	Present	Present	Absent
$\alpha$ 5	Present <sup>d</sup>	Present	Present	Present

<sup>a</sup>Approximately 10% of males with X-linked AS (attributable to missense and intron mutations) exhibit positive immunostaining of the renal basement membranes for the  $\alpha$ 3,  $\alpha$ 4, and  $\alpha$ 5 chains, and the epidermal basement membranes for the  $\alpha$ 5 chain.

<sup>b</sup>Approximately 30% of females with X-linked AS exhibit positive uninterrupted immunostaining (with reduced intensity in some) of the renal basement membranes for the  $\alpha$ 3,  $\alpha$ 4, and  $\alpha$ 5 chains, and the epidermal basement membranes for the  $\alpha$ 5 chain.

<sup>c</sup>Some patients with autosomal recessive AS exhibit positive immunostaining (but reduced intensity) of the renal basement membranes for the  $\alpha$ 3,  $\alpha$ 4, and  $\alpha$ 5 chains.

<sup>d</sup>Some patients with thin basement membrane disease exhibit reduced intensity staining of the glomerular basement membranes for the  $\alpha$ 3,  $\alpha$ 4, and  $\alpha$ 5 chains. Modified from Kashtan CE. The nongenetic diagnosis of thin basement membrane nephropathy. *Semin Nephrol*. 2005;25:159–162.

scattered deposits of IgM and C3 can sometimes be seen in partially sclerosed glomeruli. Staining for specific monoclonal antibodies directed against different subunits of type IV collagen has greatly facilitated the diagnosis of AS.<sup>491,492</sup> Kidneys from individuals who are not affected by AS show strong continuous immunostaining with antibodies to the  $\alpha$ 3,  $\alpha$ 4, and  $\alpha$ 5 chains along the GBM, and the basement membrane of the Bowman capsule and the distal convoluted tubules. This reactivity is absent in male patients with X-linked AS. Skin biopsies examined by immunofluorescence can also be an important diagnostic tool since the  $\alpha$ 5 chain is expressed in the normal epidermal basement membrane but not in X-linked AS patients. Therefore, in male patients with a clinical and familial history suggestive of X-linked AS, skin examination for the  $\alpha$ 5 chain may obviate the necessity for a kidney biopsy. It should be borne in mind, however, that some affected males do retain the expression of the  $\alpha$ 5 chain in their basement membranes.<sup>493</sup> A mosaic staining pattern (interrupted or segmentally weaker staining) for the  $\alpha$ 5 chain is frequently seen in the epidermal and renal basement membranes of heterozygous females with X-linked AS, reflective of random inactivation of X chromosome in females. While this finding is

diagnostic of the carrier state, a normal result does not exclude heterozygosity. The immunofluorescence/immunohistology findings in the basement membranes of patients with AS are summarized in Table 23.6.

When the diagnosis of AS cannot be unequivocally excluded on a kidney biopsy or if a female relative of a patient with X-linked AS is suspected to be the carrier of the disease, genetic testing should be performed. The sensitivity of the linkage analysis is only 60%, but the next-generation sequencing has proven to be vastly more sensitive (90%) in detecting the mutations in AS, especially in patients with autosomal dominant AS.<sup>480</sup> Genetic testing is increasingly considered standard of care in all patients suspected of AS and thin basement membrane nephropathy (TBMN).<sup>494</sup>

### Thin Basement Membrane Nephropathy

The descriptive term TBMN is used to designate a hereditary renal disease that is characterized by the uniform thinning of the GBM and normal patient survival without deterioration of renal function. Benign familial hematuria is another designation that has also been

used for this condition; however, it is now considered inappropriate since it could embrace other pathologic entities, such as familial cases of IgAN, in which the prognosis is not always benign. Although TBMN has generally been considered an autosomal dominant hereditary condition, recent genetic studies indicate that it is a heterogeneous disease with some being related to mutations in the *COL4A3* and *COL4A4* genes with autosomal recessive inheritance.<sup>495,496</sup> It has been shown that patients with TBMN exhibiting these *COL4A3* and *COL4A4* mutations are in fact carriers of autosomal recessive AS, and thus TBMN falls within the spectrum of type IV collagen diseases.<sup>497,498</sup> These findings further emphasize the importance of genetic testing in TBMN.<sup>494</sup>

TBMN is the most common cause of persistent hematuria in children and adults, and although its true incidence is unknown, it has been estimated that it affects at least 1% of the population.<sup>499,500</sup> Both sexes are equally affected, and even though it can manifest at any age, it is seldom reported after the age of 50 years. The onset of the hematuria is usually in childhood, and it is typically microscopic and persistent; however, on occasion, it may be macroscopic and recurrent.<sup>499</sup> Mild proteinuria is not uncommon, but heavy proteinuria in the nephrotic range is rare. Severe proteinuria likely represents a manifestation of a coexistent glomerular lesion, such as MCD, IgAN, focal glomerulosclerosis, or MGN.<sup>501</sup> In contrast to patients with AS, those with TBMN have only rarely been reported to exhibit extrarenal manifestations of AS.<sup>499</sup>

Aside from finding erythrocytes in the Bowman space and renal tubules, renal biopsies appear normal by light microscopy.<sup>492,502</sup> The diagnosis is made by the ultrastructural demonstration of a uniform thinning of the lamina densa of the GBM (Fig. 23.65). The overall width of the GBM is reduced to one-third or is  $\leq 200$  nm.<sup>492,498,502</sup> Immunofluorescence studies are usually negative for immunoglobulins and complement components, but deposits of IgM and IgG, with and without C3, have occasionally been reported.<sup>502</sup> Immunohistochemical evaluation for type IV collagen may assist in distinguishing TBMN from AS. A normal distribution of type IV collagen  $\alpha$  chains is supportive of the diagnosis of TBMN.<sup>492</sup>

### Fabry Disease

Fabry disease, also known as Anderson–Fabry disease and angiokeratoma corporis diffusum universalis, is an uncommon inherited

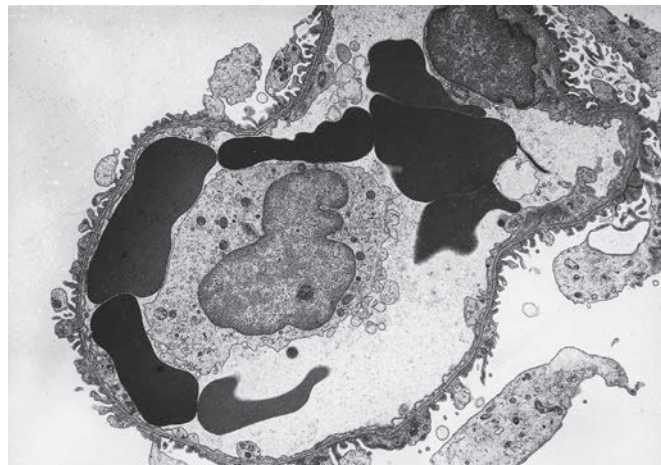


**Figure 23.65** Capillary loop showing marked uniform thinning of the glomerular basement membrane (x4200). (Reproduced from Spargo BH, Seymour AE, Ordóñez NG. *Renal Biopsy Pathology with Diagnostic and Therapeutic Implications*. New York, NY: John Wiley and Sons; 1980:398. By permission of John Wiley and Sons, Inc.)

X-linked disorder caused by a deficiency of the enzyme  $\alpha$ -galactosidase A found in lysosomes. This results in the accumulation of the neutral glycosphingolipid Gb3 in the lysosomes of many tissues, including the kidneys, heart, neurons of the dorsal root of ganglia, and blood vessels in affected males and, to less extent, in female carriers. The incidence of the disease has been estimated to range from 1 in 40,000 to 1 in 117,000 live male births. About 5% of the cases are sporadic. More than 500 mutations of the  $\alpha$ -galactosidase gene located on chromosome Xq22.1 have been described and most are family specific.<sup>503</sup> The most common presenting symptoms of the disease in children or adolescents are painful paresthesias in the lower extremities, hypohidrosis or anhidrosis, corneal opacities, and skin lesions that consist of small angiokeratomas scattered throughout the body, especially the abdomen, buttocks, lips, genitalia, and upper thighs. These patients have little or no  $\alpha$ -galactosidase A enzyme activity. In contrast, males with residual  $\alpha$ -galactosidase A enzyme present with renal failure and cardiac disease in the fourth decade of life. Female carriers, being heterozygous for the genetic abnormality, are usually only mildly affected, with rare occurrence of end-stage kidney disease.

Renal involvement is often manifested by hematuria and proteinuria in the second decade of life, followed by gradual deterioration of renal function in the third and fourth decades. Death occurs around the fifth decade from renal, cardiac, or cerebrovascular involvement. Recurrence in the transplanted kidney has been reported, but there is no indication that this event has a significant impact on long-term allograft survival in most patients.<sup>504</sup> Treatment of extrarenal disease includes enzyme replacement therapy with recombinant  $\alpha$ -galactosidase.<sup>505,506</sup>

On light microscopy, the visceral epithelial cells are enlarged and vacuolated, giving a honeycomb appearance to the glomeruli. Similar changes are seen in the parietal epithelium, and in endothelial and mesangial cells (Fig. 23.66). There is also prominent vacuolization in the distal convoluted tubules and loops of Henle, as well as in the arteries. The vacuoles in each of these locations are PAS negative. With increasing age, there is segmental and global glomerulosclerosis with interstitial scarring and nodular arteriolar hyalinosis. Electron microscopy demonstrates a massive accumulation of laminated

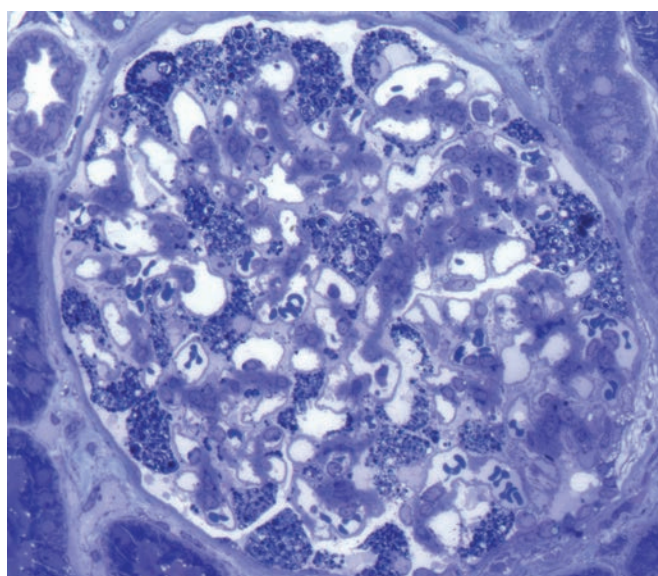


**Figure 23.66** Plastic-embedded semi-thin section of a portion of a glomerulus stained with toluidine blue showing numerous deeply stained visceral epithelial cell inclusions in a case of Fabry disease.



**Figure 23.67** Portion of a glomerulus from a patient with Fabry disease demonstrating numerous laminated inclusions in the epithelial cell cytoplasm (x7750).

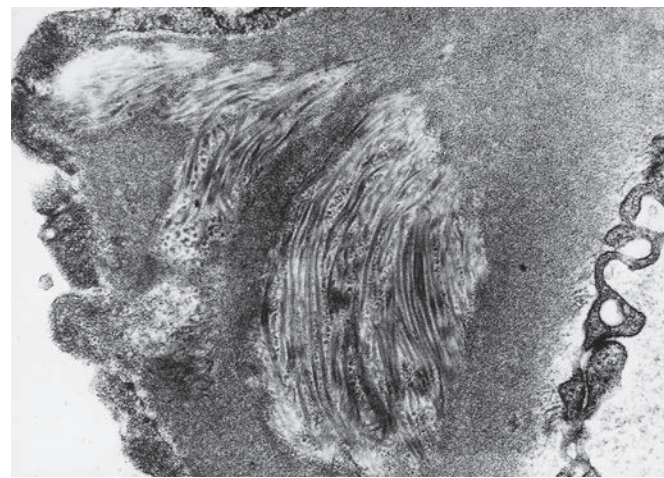


**Figure 23.68** Collagen-like fibers in the glomerular basement membrane in nail-patella syndrome (x35,000). (Reproduced from Spargo BH, Seymour AE, Ordóñez NG. *Renal Biopsy Pathology with Diagnostic and Therapeutic Implications*. New York, NY: John Wiley and Sons; 1980:400. By permission of John Wiley and Sons, Inc.)

inclusion bodies in the cytoplasm of the affected cells. Each is surrounded by a single unit membrane and measures up to 5  $\mu\text{m}$  in diameter. They are either round with a concentric myelin-like structure, or ovoid with parallel layers ("zebra" bodies) (Fig. 23.67). Similar inclusions are present outside of the glomeruli in the endothelial and smooth muscle cells of blood vessels, and in the tubular epithelium, especially those of the convoluted tubule and the loops of Henle. Although the ultrastructural pattern is almost diagnostic of the disease, similar inclusions are seen in other conditions such as chloroquine toxicity and I-cell disease<sup>507,508</sup> and, hence the importance of clinical and biochemical correlation.

### Nail-Patella Syndrome

Nail-patella syndrome (NPS; also known as hereditary onychoosteodysplasia) is an uncommon autosomal dominant disorder defined by the association of nail dysplasia, absent or hypoplastic patella, elbow dysplasia, iliac horns, open angle glaucoma, and nephropathy.<sup>509</sup> It is caused by mutations of the *LMX1B* gene located on chromosome 9q34.1. The *LMX1B* gene encodes LIM homeodomain transcription factor expressed in podocytes and is crucial in limb development. The incidence of the syndrome has been estimated to be 1 per 50,000 live births. Nail dysplasia is the most constant feature of the syndrome and can be observed at birth, but nephropathy and glaucoma are the most relevant clinical manifestations. Renal involvement occurs in about 30%–50% of patients.<sup>510,512</sup> Asymptomatic proteinuria is the most common event, but the nephrotic syndrome can occur and some patients progress to renal failure.<sup>512</sup>

Light microscopy of the kidney shows nonspecific changes such as focal thickening of the glomerular capillary walls and FSGS. By electron microscopy, the GBM appears irregularly thickened and often exhibits electron-lucent areas, giving it the so-called moth-eaten appearance. Collagen-like fibers are seen in the electron-lucent areas and in the mesangium, further enhanced by phosphotungstic acid stain (Fig. 23.68). The LIM homeodomain transcription factor regulates the transcription of type IV collagen and podocyte proteins, thus contributing to these ultrastructural changes. No recurrences of the renal changes have been reported after transplantation.<sup>513</sup>

### Collagen Type III Glomerulopathy

Collagen type III glomerulopathy (also known as collagenofibrotic glomerulopathy)<sup>514</sup> is an idiopathic glomerular disease that is characterized by the massive accumulation of atypical type III collagen fibrils within the mesangial matrix and subendothelial space and an increase in serum type III procollagen peptide levels. This type of collagen is absent in normal human kidneys. Although initially thought to be a clinical variant of NPS, it is now considered to be a separate clinicopathologic entity.<sup>515</sup> Collagen type III glomerulopathy occurs in both familial and sporadic forms, and the familial cases show an autosomal recessive pattern of inheritance.<sup>516–518</sup> The disease affects both sexes equally and manifests during childhood. Children often present with increasing proteinuria leading to the nephrotic syndrome, hypertension, and progressive renal failure.<sup>514,517</sup> An important feature in these patients is that they may develop HUS,<sup>517</sup> and associated inherited factor H deficiency has been documented in the literature.<sup>519</sup> In adults, the disease is often sporadic and has a more indolent course.

Light microscopy shows a diffuse increase in the mesangial matrix and generalized widening of the glomerular capillary walls, sometimes associated with mesangial cell interposition. By electron microscopy, there is a large accumulation of fibrils in the subendothelial aspect of the GBM and in the mesangial matrix. These curvilinear fibrils have a distinctive transverse band periodicity of approximately 60 nm, characteristic of type III collagen. Conventional immunofluorescence studies are either negative or show nonspecific deposits of immunoglobulins, especially IgM and complement components. The most important diagnostic feature is the presence of strong mesangial and capillary loop reactivity with anticollagen type III antibodies. Type III collagen deposition can also be seen in other organs, including the liver, spleen, myocardium, and thyroid gland.<sup>520,521</sup>

### Fibronectin Glomerulopathy

Fibronectin glomerulopathy is an autosomal dominant disease with age-related penetrance, characterized by massive fibronectin deposition in the glomeruli.<sup>522–524</sup> Both sexes are equally affected, and in approximately 40% of the patients, it is caused by mutations of the *FN1* gene located on chromosome 2q34.<sup>525</sup> Clinically, the disease

usually manifests as proteinuria (often within the nephrotic range), microscopic hematuria, and the slow deterioration of renal function that occurs over a period of several years.

By light microscopy, the glomeruli appear enlarged and lobulated, with a minimal degree of hypercellularity. The most characteristic feature is a marked enlargement of the mesangium and subendothelial space, resulting from the deposition of a homogeneous PAS-positive, Congo red-negative material that, by electron microscopy, has a dense granular appearance. Intermixed within the deposits are focal filamentous structures measuring 12–16 nm in diameter. Immunohistochemical or immunofluorescence studies demonstrate strong positivity for fibronectin in the areas corresponding to the deposits, but immunoglobulins and complement deposition are absent or scant at best. The disease has been reported to recur after renal transplantation, and an underlying abnormality in the metabolism of circulating fibronectin is involved in the pathogenesis of this condition.<sup>526</sup> The *FN1* mutations detected thus far affect the heparin-binding domains of the fibronectin, causing conformational changes to the protein. It has been suggested that the mutant fibronectin deposited in the glomerulus results in defective endothelial spreading and podocyte cytoskeletal organization, contributing to the proteinuria.<sup>525,527</sup>

## Renal Transplant Pathology

Renal biopsies on transplanted kidneys are performed to determine: (1) whether the failure of the graft is due to rejection, nephrotoxicity caused by immunosuppressive drugs (i.e., cyclosporine A [CsA], tacrolimus), or other causes, such as acute tubular necrosis (ATN), acute infectious pyelonephritis, obstruction of the vasculature or urinary outflow tract, or recurrent or *de novo* glomerular disease; or (2) if rejection is present, to evaluate the intensity and nature of the rejection and to predict the potential reversibility of the lesions with therapy.

### Allograft Rejection

Traditionally, rejection has been classified as hyperacute, acute, and chronic. Hyperacute rejection is antibody-mediated, while acute and chronic rejections can be either T-cell mediated (cellular rejection) or antibody mediated (humoral).

### Hyperacute Rejection

Hyperacute rejection may occur within minutes or hours after revascularization, the immediate result being the abrupt cessation of urine flow. The diagnosis may be obvious to the surgeon with mottling cyanosis and diminished turgor in the graft. The reaction is produced by the interaction of preformed circulating antibodies in the recipient with antigens on donor endothelial cells such as HLA, ABO, and other less characterized endothelial antigens.<sup>528,529</sup> These preformed antibodies are often related to previous pregnancies, blood transfusions, or previous kidney transplant.<sup>530</sup> The introduction of routine transplant screening and cross-matching techniques has made this a rare complication, with an estimated incidence of less than 0.5% of transplants.<sup>530,531</sup>

In hyperacute rejection, fibrin thrombi are present in all the renal vessels, including the glomerular and peritubular capillaries. Early features (1–12 hours after implantation) may be limited to platelet and neutrophil margination in these vascular spaces. The thrombosis is associated with infarction and cortical and medullary tubular necrosis. These histologic features resemble those of severe acute AMR. Immunofluorescence may show linear staining for IgM or IgG and C3 along the glomerular and peritubular capillaries. Positive

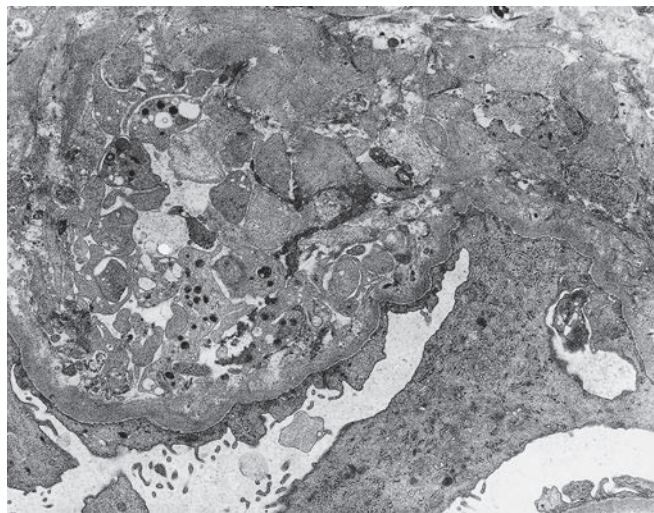


**Figure 23.69** Hyperacute Rejection. There is endothelial denudation of the glomerular basement membrane and capillary occlusion by degranulated platelets ( $\times 7980$ ).

staining for C4d in peritubular capillaries supports the diagnosis, but poor perfusion and tissue necrosis often precludes demonstration of C4d deposition. Electron microscopy shows platelets, fibrin, sludged red blood cells, and evidence of necrosis of the endothelial cells of glomerular capillaries and other vessels (Fig. 23.69).<sup>530</sup>

### Acute Rejection

Acute rejection, despite its name, can occur at any time during the post-transplantation period. It is most often seen in the months following implantation and becomes less common after the first year. Two types of acute allograft rejection are recognized: antibody mediated and T-cell mediated.

AMR is caused by anti-donor-specific antibodies (DSAs) directed against graft endothelium in glomeruli and peritubular capillaries. The target antigens are HLA class I and II molecules and in ABO-incompatible grafts, ABO antigens.<sup>530</sup> Less common endothelial cell-specific antigens, angiotensin II type I receptor, and other non-MHC antigens have also been implicated. Early on, these pathogenic DSAs are preformed in recipient circulation (resulting in positive cross match) but late post-transplant acute AMR is caused by *de novo* DSA.<sup>532</sup> The histologic features of acute AMR are mainly in glomeruli, peritubular capillaries, and arteries. The glomeruli show endothelial cell swelling, an increase in cellularity, and occasional fibrin thrombi.<sup>533</sup> The peritubular capillaries are dilated with intra-luminal cells, referred to as "peritubular capillaritis" (Fig. 23.70). Neutrophils and monocytes predominate the glomerular and peritubular capillary infiltrate.<sup>534</sup> The arteries (and arterioles) may show endothelialitis or fibrinoid necrosis.<sup>530</sup> Interstitial hemorrhage, tubular necrosis, and infarction are also seen, but interstitial inflammation and tubulitis are not predominant features unless combined with T cell-mediated rejection. On occasion, the histology of acute AMR is limited to acute tubular injury alone. Electron microscopy demonstrates endothelial cell swelling associated with separation of the endothelium from the basement membrane by fluffy fibrillar material, which occasionally contains fibrin strands and platelet fragments (Fig. 23.71). The immunofluorescence or immunohistochemical demonstration of C4d deposition in graft peritubular capillaries is a durable and reliable marker of AMR, circulating anti-donor antibodies, and poor graft survival (Fig. 23.72).<sup>11,534,535</sup> C4d is a 44.5-kDa

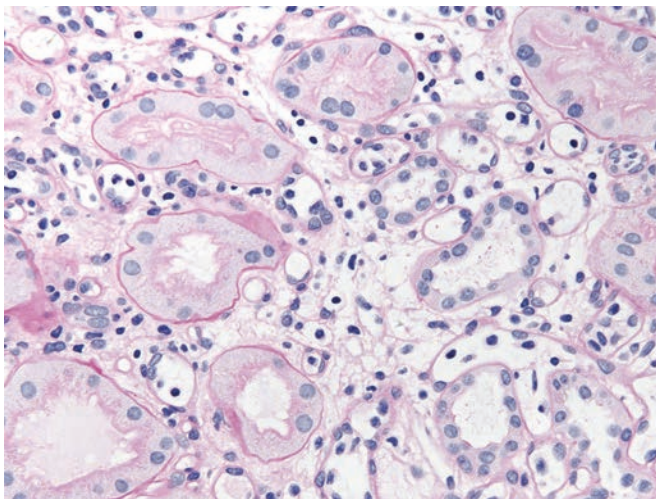


**Figure 23.70** Peritubular Capillaritis With Dilated Capillaries and Intraluminal Mononuclear Cells. Prominent interstitial edema is also seen (PAS).

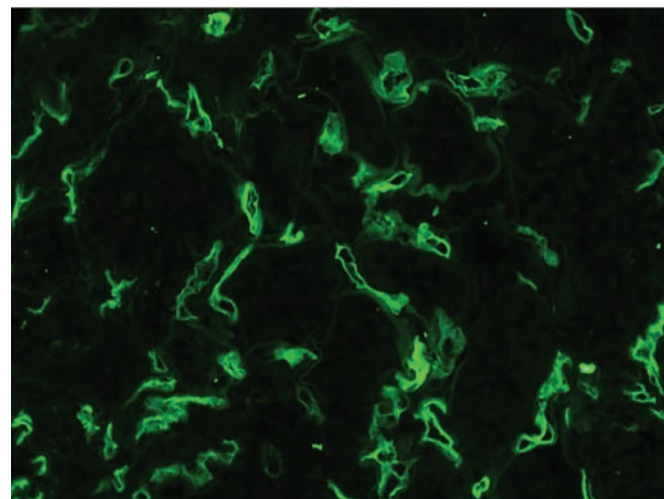


**Figure 23.72** Immunofluorescence microscopy testing with antibody to C4d shows diffuse peritubular capillary wall staining (anti-C4d).



**Figure 23.71** Endothelial Injury in Antibody-Mediated Rejection. Portion of a glomerulus showing prominent widening of the subendothelial region by electron lucent material (arrows) (x3500).

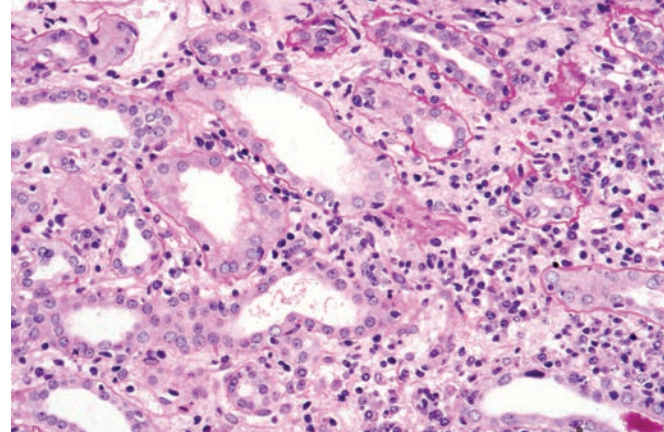


**Figure 23.73** Tubulointerstitial T cell-mediated acute rejection with interstitial edema and inflammation. Intraepithelial lymphocytes are seen in the tubules and many demonstrate acute injury with dilated lumens and brush border loss (PAS).

prompting further study of C4d-negative AMR.<sup>539,540</sup> AMR is not steroid responsive, and treatment modalities have included plasmapheresis, IV immunoglobulin, rituximab, and more recently, complement inhibition.

In the early stages of acute T cell-mediated rejection, light microscopy reveals edema and focal infiltration of the interstitium by lymphocytes (Fig. 23.73). As the rejection progresses, the inflammatory infiltrate becomes more diffuse and the lymphocytes, many of them immunoblasts, are accompanied by plasma cells, monocytes, and macrophages. Granulocytes may be present, but they are not numerous. When they are abundant, the possibility of AMR or pyelonephritis should be considered.<sup>541</sup> Eosinophils can also be present but rarely in large numbers. A characteristic finding in acute T cell-mediated rejection is invasion of the tubular epithelial cells by lymphocytes, a feature referred to as tubulitis. Tubulitis has been regarded as a reliable marker for acute rejection even though it can be seen in other forms of interstitial nephritis.<sup>541,542</sup> The intensity of the infiltrate and tubular injury are features often used to grade the rejection. The infiltrate is more concentrated in the cortex than in the renal medulla. Immunophenotyping shows that most of the

stable inactive degradation product of the complement factor C4 that is formed when the classic complement cascade is activated by binding of DSA to the endothelium of the graft.<sup>536</sup> Overall, immunofluorescence method is more sensitive than the immunohistochemical method, and it is taken into account in the scoring of positive C4d staining in peritubular capillaries.<sup>537</sup> Interestingly, diffuse peritubular capillary C4d is a constant feature in ABO-incompatible grafts, even in the absence of other histologic features of AMR, likely representing an accommodation reaction.<sup>538</sup> It is increasingly being recognized that AMR can occur in the absence of C4d deposition,

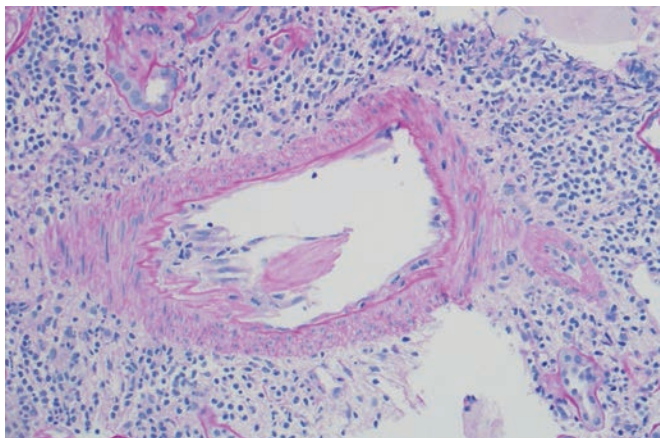


**Figure 23.74** Acute Vascular Rejection (Banff IIA). An interlobular artery with intimal arteritis (PAS).

lymphoid cells are T lymphocytes, and as many as 60%–80% are CD8-positive cells, the remainder being CD4-positive T lymphocytes, plasma cells, and monocytes/macrophages. This immunologic tissue injury mediated by T cells is directed against MHC and non-MHC donor antigens. Immunofluorescence is generally negative, except for focal fibrin in affected vessels in a few cases and immunoglobulins in inflammatory cells. C4d stain is negative in a pure T cell-mediated rejection. Electron microscopy shows tubular damage and regeneration, and many inflammatory cells in the interstitium. Glomeruli are usually spared, but mononuclear cells in glomeruli (i.e., glomerulitis) can on occasion be a feature of T cell-mediated rejection and is unclear if it represents a component of AMR. Tubulointerstitial rejection that is predominantly T-cell mediated is considered readily reversible with pulse steroid therapy.

Mononuclear cells may infiltrate beneath the endothelium of arteries or arterioles, and it signifies early vascular rejection (Fig. 23.74). The cells are typically CD3+ T cells or CD68+ monocytes/macrophages. Associated swelling and vacuolization of vascular endothelial cells are often present, and the adjacent smooth muscle cells may show vacuolization caused by dilation of the endoplasmic reticulum. The intimal changes can be accompanied by either thrombosis or intimal proliferation. Thromboses are often small and nonocclusive, but in those cases progressing to irreversible rejection, they become obliterative and widespread with transmural necrosis of the vessel walls. Milder forms of intimal arteritis are often considered T-cell mediated, while AMR likely mediates most cases of transmural arteritis. Endarteritis is usually present in the background of severe tubulointerstitial inflammation. On occasion, it is observed with little or no interstitial inflammation (isolated endarteritis), and recent data suggest these cases mimic the behavior and survival of T cell-mediated tubulointerstitial and vascular rejection.<sup>543</sup> The diagnostic criteria and scoring of cellular rejection and AMR are delineated in **Box 23.6**.

Although it is convenient for descriptive purposes to consider the two types of allograft rejection reactions separately, many cases are a combination of antibody- and T cell-mediated changes. Since the T cell-mediated component of allograft rejection is more responsive to some forms of therapy than the antibody-mediated form, it is important to identify and, as far as possible, quantitate the relative contribution of the two components. This is essential in assisting the clinician in determining the appropriate form of treatment. It is also of importance in studying follow-up biopsies after therapy, particularly when the therapeutic response has not been favorable.

## Chronic Rejection

Chronic rejection occurs anywhere from several months to several years after transplantation and, once initiated, can be progressive and irreversible. It constitutes the most common cause of graft failure after the initial 6–12 months post transplantation. Chronic rejection is not a distinct entity but rather the end stage of repeated episodes of acute antibody- and/or T cell-mediated rejection.<sup>544</sup> In addition, long-term administration of CsA or tacrolimus probably contributes to the development of some of the changes seen in chronic rejection.

Clinically, there is a gradual decrease in renal function. The deterioration may be preceded by proteinuria, sometimes nephrotic range,<sup>545</sup> and is commonly associated with hypertension. Microscopically, the changes can be seen in glomeruli, arteries, and tubulointerstitium. Nonspecific features of TA and IF may be accompanied by features of underlying T cell-mediated rejection such as interstitial inflammation and tubulitis in nonatrophic cortex. The blood vessels, especially the interlobular and arcuate arteries, show severe obliterative fibrointimal proliferation or mucoid widening of the intima, referred to as chronic transplant arteriopathy.<sup>541</sup> Fibrosis of the media and intimal foam cells may be seen, but reduplication of the elastic lamina is typically a feature of hypertensive arteriosclerosis. The distribution of the vascular lesions is irregular and some blood vessels appear normal while others present lesions of variable degrees of severity. The glomerular lesions consist of ischemic glomerular capillary collapse, and segmental and global sclerosis.<sup>546</sup> While these changes described may be present in T cell- or antibody-mediated alloimmune injury, the hallmarks of chronic AMR are transplant glomerulopathy and peritubular capillaropathy.<sup>541</sup> Reflective of repeated insults to the glomerular and peritubular capillary endothelium, this histologic evidence of chronic AMR is often accompanied by positive C4d stain in peritubular capillaries and circulating DSA.<sup>539</sup> Transplant glomerulopathy is characterized by duplication of GBMs, often accompanied by mononuclear glomerulitis and peritubular capillaritis (Fig. 23.75). The capillary walls are thickened due to marked widening of the subendothelial space or mesangial interposition, better demonstrated by silver staining or electron microscopy. Similar multilamination of peritubular capillary basement membranes is evident on electron microscopy.<sup>547</sup> No immune complexes are seen, although immunofluorescent studies occasionally show linear or granular deposition of IgM, IgG, and complement components. Peritubular capillary C4d deposition in chronic AMR may be patchy and focal, perhaps in part due to loss of peritubular capillaries with repeated endothelial insults. Of note, immunohistochemical staining of glomerular endothelium with C4d suggests chronic AMR, especially if immune complex glomerulonephritis is excluded.

## The Banff Classification

To help establish uniform therapeutic guidelines for clinical management and to provide an objective evaluation of clinical trials of new antirejection agents, several classification systems for the evaluation of the histologic appearance of renal allograft biopsies have been developed over the past several decades. The best known of these is the Banff Working Classification of Renal Allograft Pathology, which was formulated by an international group of renal pathologists, nephrologists, and transplant surgeons who met in Banff, Canada, in August, 1991, and which was first published in 1993.<sup>548</sup> Since its introduction, this classification has undergone several revisions, the latest of which was published in 2014.<sup>540</sup>

Per Banff classification, there are six diagnostic categories: normal, AMR, borderline changes, T cell-mediated rejection, IF and TA without evidence of any specific etiology, and other changes not considered

**Box 23.6** Banff diagnostic categories for renal allograft biopsies

1. Normal
2. ABMR
 

*Hyperacute rejection*  
Acute/active ABMR; all three features must be present for diagnosis

  - a. Histologic evidence of acute tissue injury, including one or more of the following:  
Microvascular inflammation ( $g > 0$  and/or  $ptc > 0$ ), intimal or transmural arteritis ( $v > 0$ ), acute thrombotic microangiopathy, in the absence of any other cause, acute tubular injury, in the absence of any other apparent cause
  - b. Evidence of current/recent antibody interaction with vascular endothelium, including at least one of the following:  
Linear C4d staining in peritubular capillaries (C4d2 or C4d3 by IF on frozen sections, or C4d > 0 by IHC on paraffin sections<sup>a</sup>), at least moderate microvascular inflammation ( $[g + ptc] \geq 2$ ), increased expression of gene transcripts in the biopsy tissue indicative of endothelial injury, if thoroughly validated
  - c. Serologic evidence of DSAs (HLA or other antigens)  
Chronic, active ABMR; all three features must be present for diagnosis
  - a. Morphologic evidence of chronic tissue injury, including one or more of the following:  
TG ( $cg > 0$ ), if no evidence of chronic thrombotic microangiopathy due to other causes, severe peritubular capillary basement membrane multilayering (requires EM), arterial intimal fibrosis of new onset, excluding other causes
  - b. Evidence of current/recent antibody interaction with vascular endothelium, including at least one of the following:  
Linear C4d staining in peritubular capillaries (C4d2 or C4d3 by IF on frozen sections, or C4d > 0 by IHC on paraffin sections), at least moderate microvascular inflammation ( $[g + ptc] \geq 2$ ), increased expression of gene transcripts in the biopsy tissue indicative of endothelial injury, if thoroughly validated
  - c. Serologic evidence of DSAs (HLA or other antigens)  
C4d staining without evidence of rejection; all three features must be present for diagnosis

Linear C4d staining in peritubular capillaries (C4d2 or C4d3 by IF on frozen sections, or C4d > 0 by IHC on paraffin sections<sup>a</sup>),  $g = 0$ ,  $ptc = 0$ ,  $cg = 0$  (by light microscopy and by EM if available),  $v = 0$ ; no thrombotic microangiopathy, no
3. Borderline changes: "Suspicious" for acute T cell-mediated rejection
 

Focal moderate tubulitis with mild interstitial inflammation or interstitial inflammation with focal mild tubulitis (not meeting criteria for type IA); no intimal arteritis
4. T cell-mediated rejection
 

Acute T cell-mediated rejection

*Type IA:* Significant interstitial infiltration (>25% of parenchyma affected) and foci of moderate tubulitis (5–10 mononuclear cells/tubular cross section)

*Type IB:* Significant interstitial infiltration (>25% of parenchyma affected) and foci of severe tubulitis (>10 mononuclear cells/tubular cross section)

*Type IIA:* Mild to moderate intimal arteritis comprising <25% of the luminal area (v1)

*Type IIB:* Severe intimal arteritis comprising >25% of the luminal area (v2)

*Type III:* "Transmural" arteritis and/or arterial fibrinoid change and necrosis of medial smooth muscle cells with accompanying lymphocytic inflammation (v3)

Chronic active T cell-mediated rejection  
"Chronic allograft arteriopathy" (arterial intimal fibrosis with mononuclear cell infiltration in fibrosis, formation of neo-intima)
5. Interstitial fibrosis and tubular atrophy, no evidence of any specific etiology
  - I. Mild interstitial fibrosis and tubular atrophy (<25% of cortical area)
  - II. Moderate interstitial fibrosis and tubular atrophy (26%–50% of cortical area)
  - III. Severe interstitial fibrosis and tubular atrophy/loss (>50% of cortical area)
6. Other
 

Changes not considered to be due to rejection—acute and/or chronic

Calcineurin inhibitor toxicity, polyomavirus infection and others

<sup>a</sup>C4d scoring in peritubular capillaries: C4d0: 0%; C4d1: 1%–9%; C4d2: 10%–50%; C4d3: >50%.

ABMR, Antibody-mediated rejection; DSAs, donor-specific antibodies; EM, electron microscopy; IF, immunofluorescence; IHC, immunohistochemistry; TG, transplant glomerulopathy.

Adapted from Haas M, Sis B, Racusen LC, et al. Banff 2013 meeting report: inclusion of C4d negative antibody-mediated rejection and antibody-associated arterial lesions. *Am J Transplant.* 2014;14(2):272–283.

to be due to rejection. The details of the current Banff classification are shown in **Box 23.6**. In this classification, an adequate core biopsy must contain a minimum of 10 glomeruli and at least two arteries; a marginal sample is that with 7–10 glomeruli and one artery; and an unsatisfactory biopsy is a core with fewer than 7 glomeruli or no arteries.

## Cyclosporine A (Cyclosporin) Toxicity

CsA is an immunosuppressant drug that belongs to the calcineurin inhibitors group which selectively targets IL-2-dependent T-cell proliferation.<sup>549</sup> It is extremely effective in controlling transplant rejection; unfortunately, however, it is nephrotoxic. Other CsA-related toxicities include hepatotoxicity, neurotoxicity, gingival hyperplasia, hypertrichosis, and malignancies, particularly lymphomas.<sup>550,551</sup> Nephrotoxicity can occur not only in patients receiving renal

transplants but also in those receiving the drug for any other reason. CsA nephrotoxicity is dose related and has been classified into functional toxicity in which there are no structural changes and morphologic forms in which the toxicity is manifested by a variety of lesions affecting tubules, vessels, and renal interstitium. Three major morphologic forms are recognized: acute nephrotoxicity, chronic nephrotoxicity, and TMA.<sup>541</sup>

## Functional Toxicity

Functional CsA toxicity probably affects every patient who receives this medication. A mild decrease in renal function and a mild elevation of serum creatinine levels are seen soon after therapy starts, but both are reversible if the dosage is reduced. Hypertension is seen in up to 50% of the patients.<sup>552</sup> Renal biopsies in these patients appear normal or at most show some dilation and congestion of

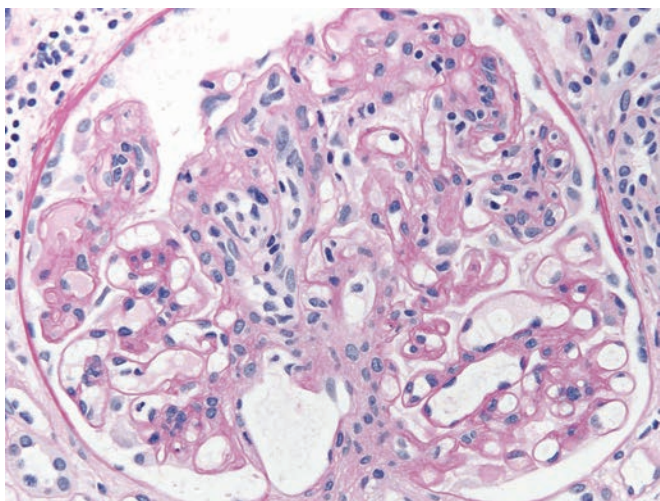


**Figure 23.75 Transplant Glomerulitis and Glomerulopathy.** The glomerulus shows increased intraluminal mononuclear inflammatory cells, consistent with transplant glomerulitis. The glomerular basement membrane double contours are a feature of chronic rejection (PAS).

peritubular capillaries. The pathogenesis is an alteration of intrarenal hemodynamics that results from the ability of CsA to induce intense renal vasoconstriction.

### Acute Toxicity

The clinical manifestations of acute CsA toxicity are similar to that seen in functional toxicity, but tend to be more severe. Genetic factors seem to account for dose-independent susceptibility to acute toxicity in an individual.<sup>553</sup> Histologically, the lesion is characterized by vacuolization of the proximal tubules, often in an isometric pattern, with giant mitochondria, large lysosomes, and microcalcifications.<sup>552</sup> Electron microscopic studies have demonstrated that the vacuolization is the result of dilation of the endoplasmic reticulum. In addition, the arterioles may show individual medial smooth-muscle cell degeneration, necrosis/apoptosis and myocyte drop-out, endothelial cell swelling, intimal thickening, and mucoid medial edema, which together may result in significant narrowing of the vascular lumina. Acute nephrotoxicity is usually dose dependent and reversible.

### Thrombotic Microangiopathy

Patients with CsA toxicity can develop symptoms of HUS a few days or weeks after transplantation. The histologic findings are those of TMA with platelet and fibrin thrombi in the glomeruli and vessels, and minimal inflammatory infiltrate.<sup>541</sup> The prognosis of these patients is generally poor, but in some instances the lesions have resolved after the drug has been withdrawn.

### Chronic Toxicity

Chronic CsA toxicity is clinically manifested by slow progression into renal failure and hypertension. Biopsies show arteriolopathy and IF with TA, features that are not entirely specific.<sup>554,555</sup> The arteriolopathy consists of nodular or diffuse hyalinosis of the vessel walls, or mucoid thickening of the intima, resulting in the narrowing or complete occlusion of the vascular lumina.<sup>541</sup> The nodular hyalinosis replaces the necrotic myocytes and typically affects the outer media with eventual circumferential involvement. The changes are

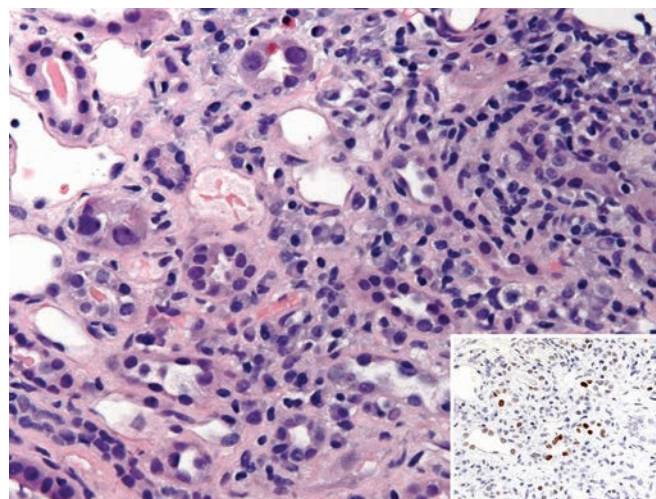


**Figure 23.76 Prominent Interstitial Lymphoplasmacytic Inflammation in Polyomavirus Nephropathy.** A few tubular nuclei are enlarged with fine chromatin. The presence of viral inclusions is confirmed on immunohistochemical stain (anti-SV40) as seen in the inset.

usually accompanied by patchy IF and TA (striped fibrosis), best seen in the cortex. The glomeruli are usually spared in the early stages, but subsequent segmental and global glomerulosclerosis ensues.<sup>554</sup> In contrast to acute nephrotoxicity, the changes in chronic nephrotoxicity are irreversible.

### Tacrolimus (FK506) Toxicity

Tacrolimus is an immunosuppressant drug that is also used in the control of transplant rejection. The morphologic changes associated with tacrolimus toxicity are identical to those of CsA toxicity.<sup>556</sup> These changes include vacuolization of the straight and convoluted portion of the proximal tubules, myocyte vacuolization, peritubular calcifications, TMA, arteriolar hyalinosis, and IF.

### Polyomavirus Nephropathy

The human polyoma virus type I has surfaced as a significant pathogen in kidney transplant recipients, causing polyomavirus nephropathy. Approximately 85% of polyomavirus nephropathy is attributed to BK virus, with the remainder caused by JC virus.<sup>557</sup> BK virus reactivation occurs in 10%–60% of renal transplants and 1%–5% of renal allografts develop BK nephropathy.<sup>558</sup> High-risk patients are monitored by serial measurements of urine and plasma polyoma viral loads. A plasma level of  $10^4$  virions/mL is considered highly specific (but significantly less sensitive) for polyomavirus nephropathy. The typical presentation is impaired renal function that is resistant to immunosuppressive therapy. The definite diagnosis of polyomavirus nephropathy requires the histologic demonstration of polyomavirus. The interstitium usually is infiltrated by mononuclear inflammatory cells, mimicking the changes seen in acute rejection.<sup>559</sup> Renal tubular epithelial cells typically show enlarged nuclei with amorphous basophilic viral inclusions.<sup>560</sup> Immunohistochemical stains can be helpful in assisting in the demonstration of the infected cells (Fig. 23.76). The immunostains can either be directed specifically to BK and JC virus or can be for SV40, another polyomavirus that has a shared large T antigen. Treatment of polyomavirus nephropathy primarily includes reduced immunosuppression. A coexistent acute rejection poses a diagnostic challenge, and the presence of endarteritis confirms the presence of acute rejection.

## Tubulointerstitial Diseases

Tubulointerstitial disease is a generic term used to designate a heterogeneous group of disorders that primarily affect the renal interstitium and tubules and only secondarily involves the other structures of the kidney. The frequency with which tubulointerstitial diseases affect the kidney is difficult to determine; however, it is believed that primary tubulointerstitial disease is the cause of renal failure in an estimated 20%–40% of all patients undergoing treatment for ESRD. The clinical presentations are usually very similar, but the etiologies are quite different and include infection, obstruction, and immune-mediated and toxic-tubulointerstitial diseases (Box 23.7). The functional manifestations include impaired concentrating ability, impaired ability to secrete acid, diminished reabsorption of sodium, hyperkalemia, and azotemia. Symptoms may be acute or chronic with corresponding morphologic changes.

### Acute Tubular Necrosis

ATN is a clinicopathologic syndrome that is characterized by the acute suppression of renal function accompanied by morphologic evidence of tubular epithelial cell injury. Two subtypes of ATN have been recognized: ischemic and toxic.

The ischemic form of ATN is the most common and results from hypoperfusion of the kidney. It is usually associated with hypotension that occurs in a wide variety of conditions such as severe traumatic lesions and burns, shock after a surgical operation, septic shock, pancreatitis, and dehydration after diarrhea, vomiting, or extensive sweating.

The less common nephrotoxic form is a chemically induced injury of the tubular epithelial cells that can be caused by a wide variety of substances, including organic solvents (e.g., carbon tetrachloride, ethylene glycol), heavy metals (e.g., mercury, lead), drugs such as antibiotics (e.g., amphotericin B, gentamicin), antivirals (tenofovir, acyclovir, indinavir), chemotherapeutic agents (e.g., methotrexate, cisplatin), nonsteroidal anti-inflammatory agents, calcineurin inhibitors, and radiographic contrast agents. Hemoglobin and myoglobin are considered endogenous toxins capable of causing ATN when present in urine in high concentrations. Hemoglobinuria can be due to incompatible blood transfusion, malaria, and paroxysmal hemoglobinuria. Myoglobinuric acute renal failure can be caused by the liberation of myoglobin from muscles caused by trauma (crush injury), myositis, ischemia, excessive exertion, or exposure to toxins (snake venom, alcohol, cocaine). It is believed that, while the toxicity of the hemoglobin and myoglobin may contribute to the pathogenesis of ATN, ischemia and microcirculatory disturbances probably play a greater role in its development.<sup>561</sup>

Clinically, ATN is manifested by rapidly increasing serum creatinine levels associated with oliguria or anuria. Less frequently, ATN induces nonoliguric renal failure. Urinalysis typically demonstrates sloughed degenerated epithelial cells and granular casts. The clinical course of ATN is highly variable, and the prognosis largely depends on the clinical setting in which it occurs.

The morphologic changes in ischemic ATN depend on the severity of the renal failure and the evolution of the lesion.<sup>561,562</sup> In early stages, the cellular changes can range from minimal cell swelling to individual cell necrosis accompanied by focal denudation of the basement membrane and desquamation of the necrotic cells into the tubular lumen (Fig. 23.77A). The proximal tubules may appear dilated and their PAS-positive brush border thinned or absent. Hyaline, granular, and pigmented casts are common, especially in the distal and collecting ducts. These casts consist mainly of Tamm-Horsfall protein mixed with cellular necrotic debris. Other findings in ischemic ATN are interstitial edema and the accumulation of mononuclear

### Box 23.7 Classification of tubulointerstitial diseases

#### Genetic

Ciliopathies  
Nephronophthisis  
ADTKD  
Mutations in UMOD, MUC1, HNF1 $\beta$   
Mitochondriopathies  
Crystal deposition and transport diseases

#### Infections

Acute pyelonephritis  
Ascending infection  
Hematogenous spread  
Bacterial, fungal, viral, other  
Chronic pyelonephritis  
Nonobstructive (reflux associated)  
Obstructive  
Xanthogranulomatous  
Malakoplakia

#### Obstructive uropathy

Hydronephrosis without infection  
Reflux-associated nephropathy

#### Metabolic

Nephrocalcinosis  
Acute phosphate nephropathy  
Urate nephropathy  
Secondary oxalosis

#### Immunologic tubulointerstitial nephritis

Drug induced (antibiotics, diuretics, nonsteriodals)  
Associated with systemic vasculitis  
Lupus associated, Sjögren syndrome-associated  
Antitubular basement membrane disease  
IgG4-related tubulointerstitial nephritis  
Tubulointerstitial nephritis with uveitis

#### Toxic tubulointerstitial nephritis

Drug induced  
Aminoglycosides  
Cyclosporine  
Lithium  
Analgesics  
Cisplatin  
Heavy metals toxicity  
Lead, mercury, and others  
Other  
Radiation  
Sarcoid  
Idiopathic

ADTKD, Autosomal dominant tubulointerstitial kidney disease; HNF1 $\beta$ , HNF1 $\beta$  mutation; MUC-1, mucin-1 related kidney disease; UMOD, uromodulin-related kidney disease.

leukocytes within the vasa recta of the outer medulla. As the disease progresses after the initial injury, evidence of tubular regeneration can be seen. Changes that are believed to represent regeneration include flattened epithelium with dilation of the tubular lumen, the presence of large nuclei with prominent nucleoli, and mitotic activity (see Fig. 23.77B).

Toxic ATN is characterized by extensive necrosis of the tubular cells along segments of the proximal tubule. Depending on the type of poisoning, several patterns of injury have been recognized.<sup>561,563</sup> For example, ethylene glycol produces marked ballooning and

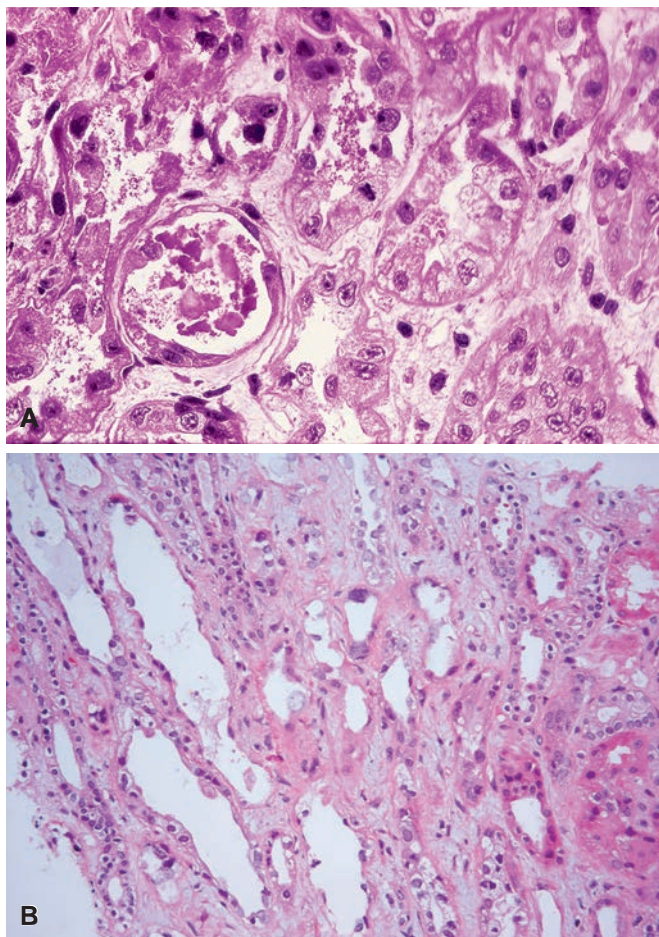


**Figure 23.77 Acute Tubular Necrosis.** **A**, There is focal necrosis and desquamation of the cells into the tubular lumen. **B**, The tubules are dilated and lined by flattened epithelium.

hydropic or vacuolar degeneration of the proximal convoluted tubules, and extensive deposition of oxalate crystals in the tubular lumina, whereas carbon tetrachloride poisoning is characterized by the accumulation of neutral lipids in the injured cells followed by necrosis.<sup>563</sup> In acute lead nephropathy, dark intranuclear eosinophilic inclusions are seen in addition to the cellular necrosis. Hemoglobinuric and myoglobinuric ATN following hemolysis or severe muscle damage shows histologic features of ischemic ATN, with numerous deeply pigmented, red-brown casts in the distal and collecting ducts. These casts stain positively with hemoglobin A and myoglobin immunohistochemical stains, respectively. Tenofovir and related antiviral drugs cause tubular nucleomegaly and pleomorphism, and sometimes megamitochondria can be visualized.

Recent studies have suggested that kidney injury molecule-1 (KIM-1) can be a useful immunohistochemical marker that can assist in the histopathologic diagnosis of tubular injury. KIM-1 is an immunoglobulin superfamily cell-surface protein that is undetectable in normal kidney but is highly overexpressed in proximal tubule cells after ischemic or nephrotoxic acute renal injury.<sup>564,565</sup> KIM-1 is a sensitive and specific early indicator of proximal tubular injury and can be detected in the urine and blood of individuals with acute renal injury.<sup>566-568</sup> Acute kidney injury can lead to chronic kidney disease and a progression to end-stage kidney disease especially in the presence of other predisposing factors or preexisting chronic kidney disease.<sup>569</sup>

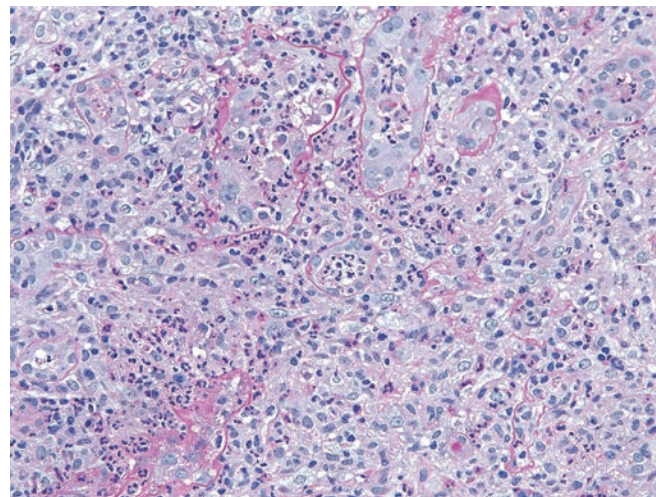


**Figure 23.78 Acute Pyelonephritis in a Patient Presenting With Fever and Elevated Serum Creatinine.** There is acute inflammatory infiltrate in the interstitium and tubular lumina.

### Acute and Chronic Pyelonephritis

Infectious TIN is generally designated as pyelonephritis, implying that the inflammatory process involves the collecting system, as well as the renal parenchyma.<sup>570</sup> There are three peaks of incidence: infancy and early childhood, women of childbearing age, and both men and women older than 60 years of age. Both acute and chronic pyelonephritis are frequently associated with congenital or acquired obstructive lesions of the lower urinary tract or are associated with conditions resulting in residual retention of urine in the bladder. Congenital lesions are often the cause of pyelonephritis in infancy and early childhood. In older adults, obstruction by nodular hyperplasia of the prostate gland in men and the development of cystoceles in women are important etiologic factors. In addition, conditions such as cancer of the cervix and nephrolithiasis are also commonly associated with renal infection.

Acute pyelonephritis is most often associated with an ascending infection and the acute inflammatory infiltrate involves the renal medulla and cortex (Fig. 23.78). The inflammatory cells are mostly polymorphonuclear leukocytes, and they are present in the interstitium and within the tubular lumina. Foci of necrosis and abscess formation can also be present in the cortex. The kidney can occasionally be infected by organisms arriving via the hematogenous route, resulting in the formation of many small cortical abscesses with little involvement of the medulla. Special stains may reveal the responsible pathogens. The ascending infections are caused by the normal gram-negative flora of the intestinal tract. By far the most common is *Escherichia coli*, followed by *Klebsiella* and *Enterobacter*. *S. aureus* or fungal organisms, including *Candida* and *Aspergillus*, may be the cause of hematogenous infections, and they are seen more often in immunosuppressed individuals.

Chronic pyelonephritis produces a coarse fibrosis of the kidney parenchyma that is distinctly focal in its distribution. Cortical and papillary scars overlie dilated, blunted, deformed calyces. The architecture of the medulla is distorted, and papillae may be flattened. Light microscopy shows tubular damage, interstitial inflammation, and fibrosis (Fig. 23.79). The tubules are atrophic or dilated and are lined by flattened epithelium and filled with hyaline casts, a pattern that has been called thyroidization. Lymphocytes, histiocytes, and plasma cells form the bulk of the inflammatory infiltrate. In chronic pyelonephritis associated with reflux or obstruction,

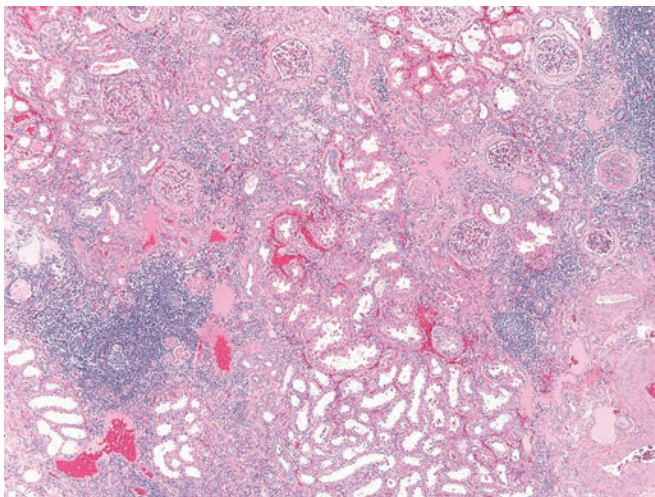


**Figure 23.79 Nephrectomy Specimen From a Patient With Obstructive Hydronephrosis.** There is interstitial scarring with intense mononuclear inflammatory cell infiltration. The tubules are atrophic, and the glomeruli are relatively spared with periglomerular fibrosis.

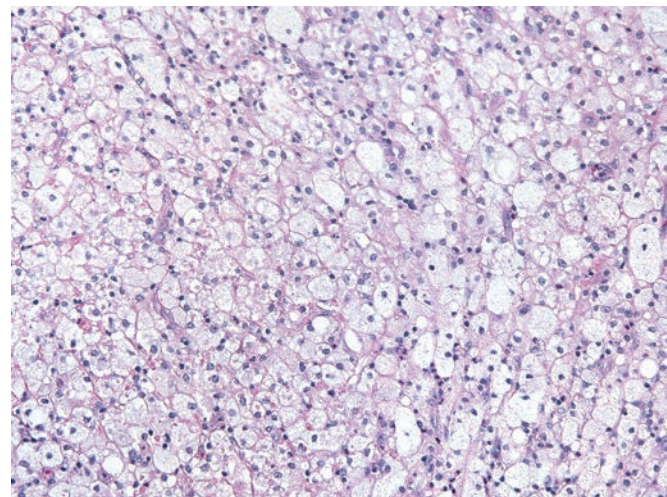


**Figure 23.80 Foamy Histiocytes in Xanthogranulomatous Pyelonephritis.** Lymphocytes and plasma cells were also present at the edges of this mass-like lesion.

Tamm–Horsfall protein can be identified in the interstitium as small bodies of amorphous fibrillary material that are strongly PAS positive and surrounded by inflammatory cells. The glomeruli are not primarily involved, but they can be initially affected by periglomerular fibrosis (see Fig. 23.79). Ischemic changes consisting of focal and segmental sclerosis and hyalinosis may also occur.

The histopathologic changes associated with chronic pyelonephritis have also been described in vesicoureteral reflux and chronic urinary obstruction.<sup>571</sup> An extreme form of localized scarring is seen in the so-called Ask–Upmark kidney, where total fibrosis of a lobule produces an appearance of segmental hypoplasia.

*Xanthogranulomatous pyelonephritis* is an uncommon and distinct type of chronic infectious pyelonephritis in which yellow, lobulated masses diffusely replace the renal architecture.<sup>572</sup> There are cases in which only a portion of the kidney, such as one pole, is involved. The condition is usually unilateral, although rare bilateral cases have been reported. This disease can occur at any age: it has been reported in patients as young as 11 months to as old as 89 years but is more common in adults in the fifth through the seventh decades.<sup>570,573</sup> It is twice as common in women as in men.<sup>574</sup> Urinary obstruction is almost invariably present and is most often caused by stones. Other causes of obstruction include postradiation strictures, congenital pelviureteric stenosis, and tumors.<sup>575</sup> The mass-occupying nature of this lesion frequently mimics that of a renal cell carcinoma and can result in unnecessary nephrectomies. A correct preoperative diagnosis is rarely made. Microscopically, there is a diffuse granulomatous inflammatory infiltrate that includes large numbers of foamy histiocytes and some multinucleated giant cells, as well as lymphocytes, plasma cells, and neutrophils (Fig. 23.80).<sup>576</sup> If renal cell carcinoma is suspected, the presence of histiocytes in xanthogranulomatous pyelonephritis can be confirmed on CD163 immunostain and the lack of infiltrating carcinoma can be demonstrated by the absence of cytokeratin expression. Electron microscopy shows that the foamy macrophages initially contain bacteria and subsequently contain numerous phagolysosomes with a myeloid configuration and amorphous material.<sup>577</sup> The lesion is destructive, tending to obliterate renal parenchyma within the affected areas. *E. coli* is the usual etiologic agent, but *Proteus mirabilis* and *S. aureus* have also been found to be responsible.<sup>570</sup>

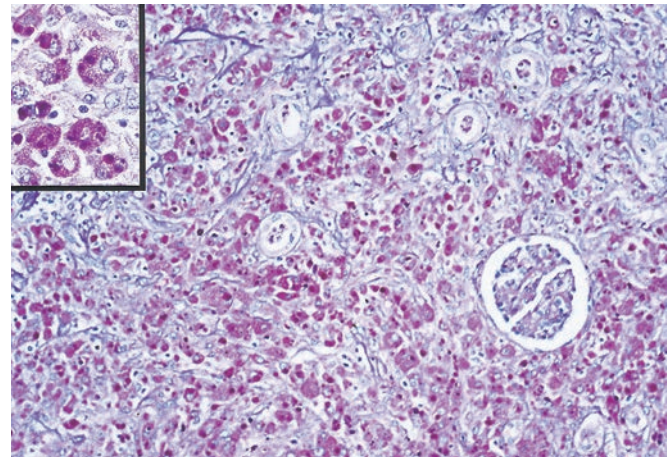


**Figure 23.81 Nephrectomy Specimen From a Patient With Malakoplakia.** The interstitium is infiltrated by numerous macrophages with granular cytoplasm. *Inset:* Several Michaelis–Gutmann bodies are seen in the cytoplasm.

*Malakoplakia* is a rare, histologically distinct, inflammatory reaction usually caused by enteric bacteria that can involve many organs but most frequently affects the urinary system.<sup>578</sup> In the kidney, the gross and microscopic appearances of this condition resemble those of xanthogranulomatous pyelonephritis. Confluent nodules of homogeneous yellow–tan tissue replace large areas of renal parenchyma. Fibrosis is also prominent. The inflammatory infiltrate consists largely of histiocytes with relatively few lymphocytes and plasma cells. The distinctive Michaelis–Gutmann bodies, composed of iron and calcium, are found both within the histiocytes and extracellularly in the stroma (Fig. 23.81). Ultrastructurally, these bodies are round with a core of concentric membranes, amorphous material or foci of calcification, and are highlighted on PAS stain (see Figs. 23.81 inset, and 23.82).<sup>579</sup> The pathogenesis of this cellular accumulation is unknown, but there is evidence that the lesions result from a defective macrophage function that compromises the lysosomal degradation of engulfed bacteria and overloads the cytoplasm with undigested cellular debris.<sup>580</sup>

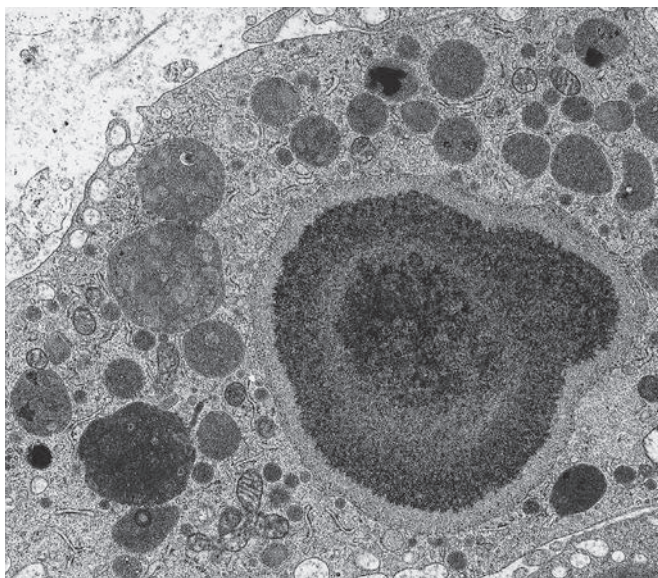


**Figure 23.82** Electron micrograph of a histiocyte showing numerous phagolysosomes and a Michaelis–Gutmann body with calcified central core (x11,400).

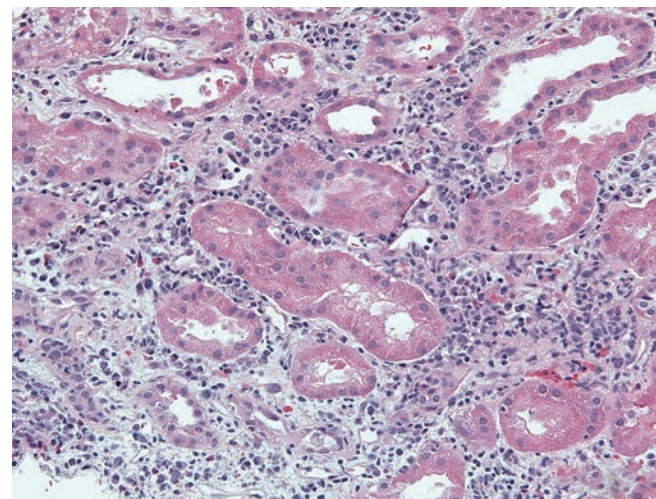


**Figure 23.83** Antibiotic therapy-related acute allergic tubulointerstitial nephritis with interstitial edema and inflammation composed of lymphocytes, monocytes, plasma cells, and eosinophils.

### Acute Allergic Tubulointerstitial Nephritis

Many drugs, including  $\beta$ -lactam antibiotics, proton pump inhibitors, nonsteroidal anti-inflammatory drugs, diuretics, and diverse other substances, can be responsible for acute TIN.<sup>581–583</sup> According to a series, omeprazole, amoxicillin, and ciprofloxacin are the most common offenders.<sup>584</sup> The clinical presentation is quite variable, but fevers and azotemia are common, and eosinophilia occurs in a majority of cases. Microscopic hematuria is not uncommon. A skin rash, usually described as maculopapular, is sometimes seen. Urinalysis reveals hematuria, sterile pyuria, and moderate proteinuria, and eosinophils may be detected in the sediment.<sup>585</sup> Acute interstitial nephritis combined with MCD producing nephrotic-range proteinuria has been described with nonsteroidal anti-inflammatory drugs.<sup>586</sup>

Light microscopy reveals generalized interstitial edema and infiltration of the interstitium by lymphocytes, macrophages, plasma cells, and eosinophils (Fig. 23.83).<sup>587</sup> Damage to tubular epithelial cells with evidence of regeneration is always found, and lymphocytes may be seen infiltrating the epithelium. The glomeruli and vessels are not usually involved. Occasionally, ill-formed granulomas with giant cells can be seen with some drugs and in that setting, the differential diagnosis includes sarcoidosis, infections, and GPA.<sup>588</sup>

Although bacterial infection and drugs are the most common causes of acute interstitial nephritis, a similar picture can be found in patients with autoimmune or immunologic disease such as SLE, Sjögren syndrome, IgG4-related TIN, TIN with uveitis, or, rarely, in association with antitubular basement membrane antibodies.<sup>589</sup> The clinical and pathologic findings are parallel to those seen in allergic TIN. Although the renal disease in SLE predominantly affects glomeruli, coexistent interstitial inflammation is common and, on rare occasion, TIN exists in isolation. Sjögren's syndrome-related TIN is characterized by lymphoplasmacytic infiltrate and associated glomerular disease is uncommon. The clinical presentation, extrarenal manifestations, and serologic studies are helpful in the diagnosis of SLE and Sjögren's syndrome. In both diseases, the tubular basement membrane and interstitial deposits, when present, stain for IgG and C3 and, in the case of SLE, can show a full-house pattern. A syndrome of acute TIN with anterior uveitis and constitutional symptoms such

as fever, weight loss, and anorexia can occur, usually in adolescent and young adult women.<sup>590</sup> Renal presentation of mild proteinuria and Fanconi syndrome is typical and the etiology is unclear. Interstitial granulomas can be present in a minority of these cases and potential etiologic factors include autoimmune, genetic, and infections such as *Mycoplasma*, *Klebsiella*, *Toxoplasma*, EBV, and herpes zoster.

### Immunoglobulin G4–Related Tubulointerstitial Nephritis

IgG4-related related disease is a systemic fibroinflammatory disease, and the kidney involvement is characterized by polyclonal plasma cell–rich interstitial inflammation.<sup>591</sup> The frequent clinical presentation of IgG4-related TIN is chronic renal insufficiency and proteinuria that is typically mild unless the patient has glomerular involvement resulting in nephrotic syndrome. The presence of hypergammaglobulinemia and elevated serum IgG and IgG4 levels supports the diagnosis and approximately 50% of the patients have hypocomplementemia. Serum ANA is occasionally positive, and peripheral eosinophilia may be present. Imaging studies can reveal low attenuation cortical mass–like lesions, corresponding to patchy fibroinflammatory process. The plasma cell–rich interstitial infiltrate frequently alternates with paucicellular fibrotic areas, especially with increasing chronicity. The dense IF has a characteristic storiform pattern. The presence of greater than 10 IgG4+ cells/40× field, although not entirely specific, meets the criteria for renal IgG4-related TIN (Fig. 23.84).<sup>592</sup> Immunofluorescence and electron microscopy reveal tubular basement membrane deposits in greater than 80% of cases and these are IgG, C3,  $\kappa$  and  $\lambda$  positive. It should be noted that plasma cell–rich and IgG4 cell–rich infiltrate can be observed in a variety of lesions such as chronic pyelonephritis and vasculitis-associated tubulointerstitial inflammation. The accurate diagnosis of IgG4-related TIN rests on evidence of systemic disease either in the form of elevated IgG4 levels or extrarenal disease.<sup>592</sup> Glomerular involvement is seen in less than 10% of IgG4-related TIN, often represented by a secondary membranous nephropathy with the deposits being PLA2R negative.<sup>593</sup>

### Analgesic Abuse Nephropathy

Analgesic abuse nephropathy is a bilateral renal disease characterized by papillary necrosis and chronic TIN that results from the

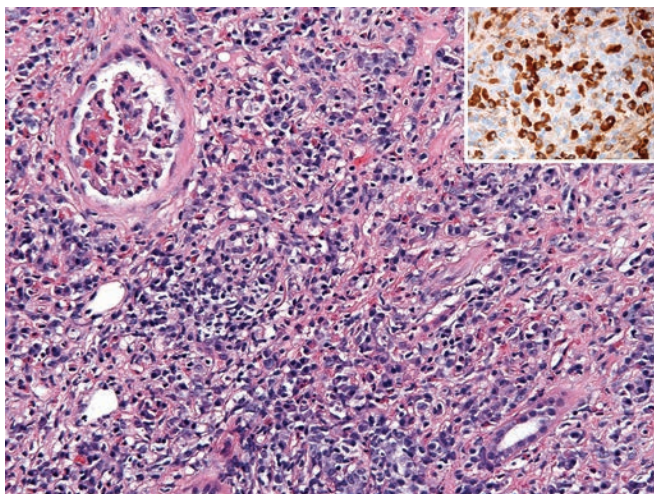


**Figure 23.84** IgG4-related tubulointerstitial nephritis with dense storiform fibrosis, tubular destruction, and intense lymphoplasmacytic infiltrate. In the appropriate clinical setting, the presence of greater than 10 IgG4+ cells/HPF supports the diagnosis.

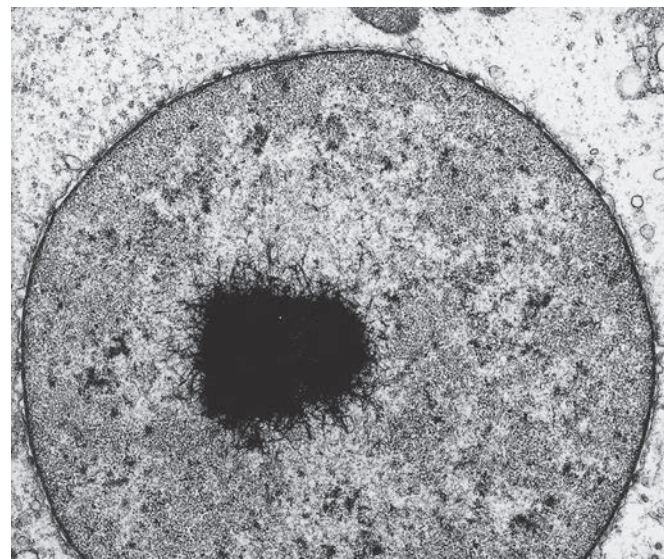


**Figure 23.85** Intranuclear lead inclusions showing dense central cores surrounded by fibrillar material (x15,600).

excessive intake of analgesic mixtures containing aspirin or antipyrine, combined with phenacetin, acetaminophen (paracetamol), or salicylamide, and caffeine or codeine.<sup>594</sup> The incidence of analgesic nephropathy varies in different countries. In the early 1990s, the reported incidence of analgesic nephropathy among patients receiving dialysis was estimated to be 0.8% in the United States, 3% in Europe, and 9% in Australia.<sup>595,596</sup> The condition is more common in women than in men. Phenacetin has been removed from the United States market more than 20 years ago and since then, the incidence of analgesic nephropathy, although not eliminated, has reduced dramatically.<sup>597,598</sup>

The most important diagnostic feature is a history of chronic pain syndromes and analgesic abuse over several years or decades. Renal function abnormalities include impaired urine concentration defects and impaired sodium conservation. Urinary infection is a complication in about 50% of the cases. On occasion, fragments of necrotic papillae are excreted. This may cause gross hematuria or renal colic due to obstruction of the ureter by the necrotic tissue. Renal imaging studies are helpful in detecting papillary necrosis and calcification. Progressive impairment of renal function may lead to chronic renal failure. An important association in analgesic nephropathy is the increased risk for developing transitional cell carcinoma.<sup>599</sup>

In the early stages of analgesic nephropathy, the cortex is normal, but the papillae are firmer and show gray streaks. Microscopically, there is interstitial homogenization, and thickening of the basement membranes of the loops of Henle and peritubular capillaries. Foci of necrotic epithelial, endothelial, and interstitial cells are associated with fine calcification. As the disease progresses, the papillae are shrunken and they have a brown coloration. Microscopically, confluent zones of necrosis within the inner medulla involve the loops of Henle, peritubular capillaries, and vasa recta, and the cortex may contain foci of TA, IF, and patches of chronic inflammation. In advanced disease, the kidneys are shrunken and the gross and microscopic changes mimic chronic pyelonephritis. Total papillary necrosis occurs and extensive calcification is usually present. Papillary necrosis is not specific for analgesic nephropathy. It can also occur in a variety of other conditions including diabetes mellitus, urinary tract obstruction, and sickle cell disease.<sup>600</sup>

## Heavy Metals Nephrotoxicity

Renal damage can result from environmental or occupational exposure to heavy metals, such as lead, cadmium, mercury, uranium, chromium, copper, and arsenic,<sup>601–604</sup> or the administration of therapeutic forms of platinum,<sup>605</sup> gold,<sup>606</sup> and bismuth.<sup>607,608</sup> Due to its rather characteristic morphologic features and clinical importance, only the changes in the kidney produced by lead exposure will be discussed.

### Lead Nephropathy

Lead poisoning may be the result of occupational or environmental exposure.<sup>609,610</sup> Workers at risk include electric storage battery makers, painters, welders, foundrymen, and jewelers. Children may be exposed by eating flaking lead paint. Inadvertent ingestion of lead can occur from drinking water contaminated by lead pipes, earthenware, or from adulterated wine or moonshine liquor. Lead is also present as an atmospheric contaminant resulting from the use of lead-containing gasoline and various industrial processes. Associated with chronic kidney disease, it can often go unrecognized in the modern era.<sup>611</sup>

The organs most commonly affected by lead exposure are the central and peripheral nervous systems, gastrointestinal tract, and kidney. The most striking morphologic changes in lead exposure occur in the tubules and consist of eosinophilic intranuclear or cytoplasmic acid-fast inclusions that stain red with Giemsa stain. These inclusions consist of a lead–protein complex that by electron microscopy appear as compact cores surrounded by a loose meshwork of fibrils (Fig. 23.85). They may be seen in tubular epithelial cells in urinary sediment during acute poisoning.<sup>612</sup> Lead-containing inclusions have also been found in the liver and neural tissue.

Renal biopsies in chronic lead nephropathy often show TA and IF with minimal inflammatory reaction. Arteriolar changes reminiscent of hypertensive nephrosclerosis may be present even in the absence of hypertension. The inclusions are often absent when the disease is longstanding or after the administration of chelating agents.

## Nephrolithiasis and Nephrocalcinosis

Nephrolithiasis is a common disorder defined as the development and accumulation of stones within the collecting system of the kidney.

The estimated incidence in the United States ranges from 7 to 21 cases per 10,000 population.<sup>613</sup> Men are affected approximately four times more frequently than women, and the predominant age at onset is in the third to fifth decades. The most characteristic symptoms of nephrolithiasis are pain and hematuria. The classic pain is that of severe, abrupt, flank pain (renal colic) that only resolves after the passage or removal of the stone. The hematuria can be gross or microscopic and most commonly occurs with large calculi during infection or colic. About 75% of the stones are composed of a combination of calcium oxalate or calcium oxalate mixed with calcium phosphate; 15% are the so-called struvite stones that are composed of magnesium ammonium phosphate and are often associated with urea-splitting bacterial infections; 6%–10% consist of uric acid; and 1%–2% of cystine. Renal stones within the pelvic calyceal system can cause gross and microscopic changes in the renal parenchyma that are identical to those seen in pyelonephritis and hydronephrosis.

The presence of calcium within the renal parenchyma is known as nephrocalcinosis.<sup>614</sup> Calcium deposition occurs on tubular basement membranes and in the interstitium. TA, IF, and periglomerular fibrosis are also present. Some of the glomeruli may be sclerosed. Several systemic disorders are associated with nephrocalcinosis and the formation of stones. Calcium phosphate and oxalate stones occur in hyperparathyroidism, sarcoidosis, milk-alkali syndrome, excessive dietary intake of vitamin D, multiple myeloma, and renal tubular acidosis. Abundant intratubular calcium phosphate deposition can occur in patients who receive oral sodium phosphate bowel purgative prior to colonoscopy. Referred to as acute phosphate nephropathy, it is often associated with inadequate hydration and concomitant use of diuretics, ACE inhibitors, or angiotensin receptor blockers. Renal insufficiency occurs weeks or months after the colonoscopy was performed.<sup>615</sup>

Uric acid stone formation takes place in an acid urine in the presence of hyperuricosuria, which may result from an inborn error of metabolism such as gout or the Lesch–Nyhan syndrome, glycogen storage disease following treatment of hematopoietic malignancies, overindulgence in dietary proteins, or the use of uricosuric drugs.<sup>616</sup> Uric acid stones are usually radiolucent, and because they are often small they may be passed, but larger ones in the renal pelvis can grow and become staghorn calculi. Uric acid crystals are also deposited within the renal parenchyma, and they can be seen within the collecting tubules as elongated or rectangular crystals or as doubly refractile crystals in the interstitium surrounded by a giant cell reaction.<sup>617,618</sup>

A clinical sign of cystinuria is calculi in the urinary tract. The stones are formed in acid urine. They are typically yellow–brown and radiopaque. Cystine crystals appear as microscopic, flat hexagons in the urine, and this feature constitutes the clue for the diagnosis. The disorder is characterized by the defective transport of cystine, lysine, arginine, and ornithine by epithelial cells of the renal tubules and the gastrointestinal tract; it is transmitted as an autosomal recessive trait with an incidence of 1 in 20,000.<sup>619,620</sup> Complications of calculi formation include urinary tract obstruction and infection, which may result in renal failure. This entity is distinct from cystinosis, a lysosomal storage disorder that presents as a severe nephropathic form in infants.<sup>621</sup>

Hyperoxaluria is characterized by recurring calcium oxalate nephrolithiasis and/or nephrocalcinosis, often terminating in chronic renal failure (Fig. 23.86). Primary hyperoxaluria is a rare autosomal recessive disorder of glyoxylate metabolism resulting in hyperoxaluria in children.<sup>622</sup> Approximately 80% of mutations detected in these patients affect gene encoding alanine glyoxylate aminotransferase.<sup>623</sup> Ethylene glycol poisoning, methoxyflurane anesthesia, pyridoxine deficiency, excess ascorbic acid ingestion, pyridoxine (vitamin B6)



**Figure 23.86** Severely distorted kidney with dilated pelvicalyceal system containing numerous stones in a case of primary oxalosis.

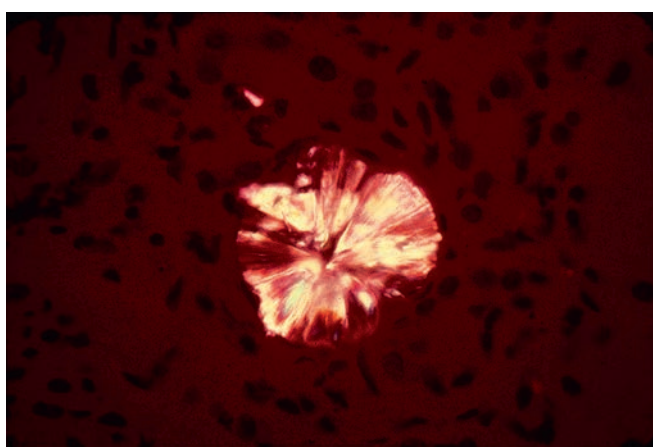


**Figure 23.87** Oxalate Crystal Under Polarized Light.

deficiency, and various chronic gastrointestinal disorders (including Crohn disease, chronic pancreatitis, celiac sprue, and status post-jejunooileal bypass procedure) have been associated with oxalosis.<sup>624,625</sup> In the kidney, oxalate crystals are deposited in the interstitium, tubules, and, rarely, the glomeruli. They have radial striations that show up particularly well with polarized light (Fig. 23.87). TA, IF and inflammation, and glomerulosclerosis are the end results.

Xanthinuria is a rare hereditary condition transmitted as an autosomal recessive trait. The enzyme xanthine oxidase, which is responsible for the conversion of xanthine and hypoxanthine to uric acid, is deficient. Xanthine stone formation occurs in one-third of patients with this disorder. Similar stones are seen as a complication of allopurinol therapy since this drug blocks xanthine oxidase activity.<sup>626</sup>

## Light Chain Cast Nephropathy

Light chain cast nephropathy, also known as Bence Jones cast nephropathy, myeloma cast nephropathy, or myeloma kidney, is the most common form of renal disease associated with multiple myeloma.<sup>627</sup> Clinically, it may present as progressive renal insufficiency or acute renal failure, often precipitated by dehydration, hypercalcemia, IV infusion of contrast media, nonsteroidal anti-inflammatory drugs, hyperuricemia, nephrotoxic infections, or loop diuretics, such

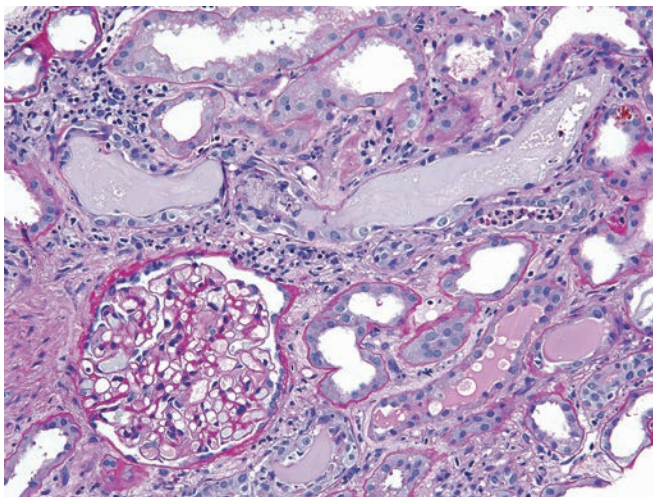


**Figure 23.88 Light Chain Cast Nephropathy.** Large, dense PAS-negative tubular casts associated with tubular injury and intratubular neutrophils (PAS).

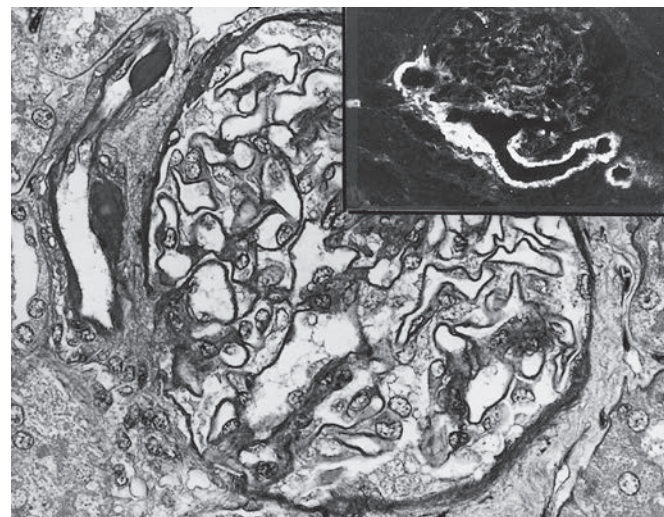


**Figure 23.89 Afferent Arteriole With Subintimal Homogeneous Hyaline Material.** Inset: Immunofluorescence preparation showing reaction for C3. (Reproduced from Spargo BH, Seymour AE, Ordóñez NG. *Renal Biopsy Pathology with Diagnostic and Therapeutic Implications*. New York, NY: John Wiley and Sons; 1980:297. By permission of John Wiley and Sons, Inc.)

as furosemide. Proteinuria is found, although not usually in the nephrotic range, and it most often consists predominantly of immunoglobulin light chains (Bence Jones protein). Circulating monoclonal light chains can be confirmed by serum protein electrophoresis or free light chain assay. The light chains are normally filtered by the glomeruli and reabsorbed and metabolized by proximal tubular cells. In patients with multiple myeloma, the excess monoclonal light chains overwhelm the catabolic capacity of the proximal tubules, thus allowing them to reach the distal nephron where the presence of Tamm-Horsfall protein may facilitate their precipitation in the form of voluminous casts. These monoclonal free light chains can also cause proximal tubular cell cytotoxicity, TIN, and ultimately damage the entire nephron, resulting in renal failure.<sup>628</sup>

By light microscopy, the distal and collecting tubules appear occluded by numerous dense, markedly eosinophilic, lamellated and fractured casts, sometimes surrounded by multinucleated giant cells derived from interstitial macrophages that invade the tubules through breaks in the basement membrane (Fig. 23.88).<sup>629,630</sup> Some casts may exhibit Congo red and thioflavin T positivity, but this alone is not indicative of amyloidosis. The tubular cells may appear flattened or can show varying degrees of degeneration with necrosis and denudation of the tubular basement membranes. Depending on the stage of the disease, there is a variable degree of IF usually associated with acute and/or chronic inflammatory cell infiltrates. Prominent intratubular collections of neutrophils may be seen, mimicking acute pyelonephritis. Sometimes the casts may contain rhomboid or needle-shaped crystalline structures that may also be found in the tubular epithelium and, on rare occasions, in the glomeruli.<sup>631</sup> Immunofluorescence studies demonstrate that the casts are largely made of the pathogenic light chain, either kappa or lambda (although kappa tends to be more frequent).

## Renal Vascular Disease

### Renal Arteriolar Disease

The kidney plays an essential role in hypertension, and the vessels of the kidney are susceptible to a variety of pathologic changes directly related to increased pressure.<sup>632</sup> The vessels most susceptible are small arteries and arterioles, with preglomerular vessels being more prominently affected. Vascular narrowing of these intrarenal

vessels eventually leads to glomerular sclerosis, TA, and IF (nephrosclerosis). The hypertensive vascular changes of the small vessels of the kidney fall into three general categories: hyaline arteriolosclerosis, myointimal hypertrophy and hyperplasia, and fibrinoid necrosis.<sup>633</sup>

In **hyaline arteriolosclerosis**, the outer part of the wall of affected vessels is thickened by deposition of a homogeneous, eosinophilic, PAS-positive material (Fig. 23.89). Associated changes are atrophy of the smooth muscle cells in the vessel walls and a uniform thickening of the basement membrane. Hyaline arteriolosclerosis is most marked in the afferent arteriole and in smaller vessels lacking an internal elastic lamina. Mild hyaline arteriolosclerosis is often seen with increasing age, but it is more prominent in patients with hypertension or diabetes. The effects are more marked in hypertension where the arteriolar lumens become severely narrowed, causing diffuse renal ischemia and symmetric shrinking of the kidneys. It is believed that the hyaline deposition results from leakage of plasma components across the vascular endothelium, triggering extracellular matrix production by smooth muscle cells. The hyalinized arterioles usually immunoreact for IgM and complement components, especially C3 (see Fig. 23.89 inset). Hyaline arteriolosclerosis is a major morphologic feature in benign nephrosclerosis, in which the interlobular and arcuate arteries may also exhibit medial hypertrophy and reduplication of the elastic lamina.

The second type of vascular abnormality seen in hypertension is that hyperplasia involving the smooth muscle and intima of small arteries and arterioles (**myointimal hypertrophy and hyperplasia**). Hyperplastic arteriolosclerosis is generally associated with acute or persistent severe high blood pressure and, therefore, is seen more often in accelerated/malignant than benign hypertension. In the early stages, the lesions are characterized by profuse intimal thickening by myxoid and sparse cellular connective tissue that drastically reduces the vascular lumen. Over time, this acute change shows progressive intimal scarring and uniform concentric thickening of the vessel wall by a proliferation of myointimal cells, and deposition of basement membrane-like material. The microscopic appearance of this lesion has led to the descriptive term of "onion skinning" (Fig. 23.90). These changes are more pronounced in arcuate and

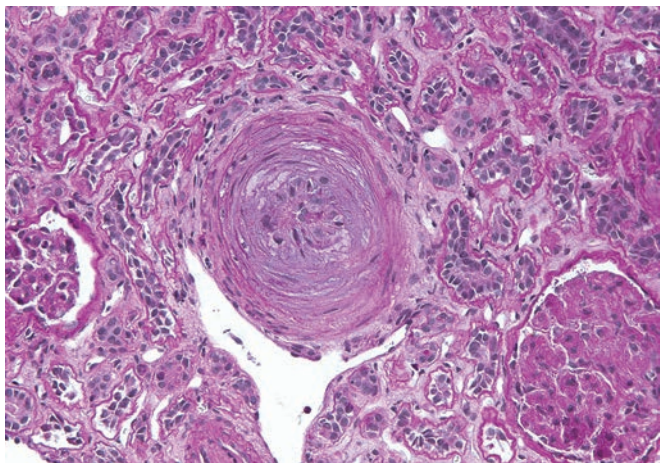


**Figure 23.90** Malignant Hypertension. Interlobular artery with thinning of the media and marked intimal edema and early fibrosis. The cortex shows glomerular ischemic changes and extensive tubular atrophy (PAS).

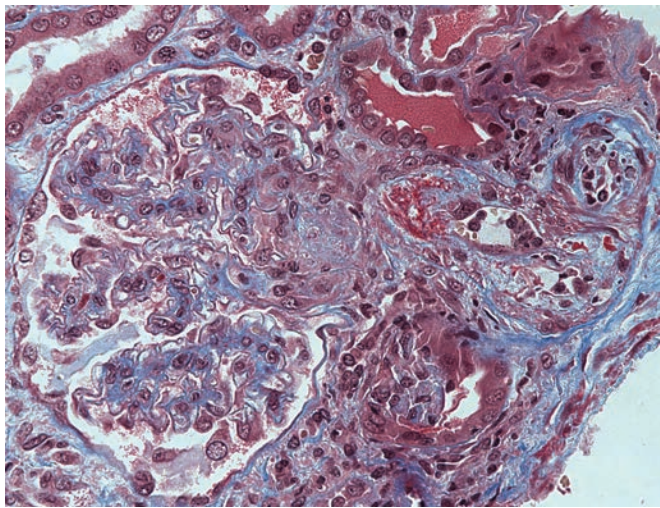


**Figure 23.91** Malignant Hypertension. Fibrinoid necrosis and intimal edema of the afferent arteriole with ischemic shrinkage of the glomerular capillary tuft (trichrome).

interlobular arteries but extend into the arterioles where they may coexist with hyalinosis from longstanding hypertension.

**Fibrinoid necrosis** of the afferent arteriole has been regarded as the hallmark of accelerated (malignant) hypertension. The necrosis is usually superimposed on a preexisting hyperplastic or hyaline lesion, but it can be the initial event in young patients with severe acute malignant hypertension. The architecture of the media of affected vessels is obliterated by the necrotizing process and further obscured by deposition of deeply eosinophilic, fibrillar material which, by histochemical and immunofluorescent techniques, has been demonstrated to be fibrin and fibrinogen.<sup>634</sup> The arteriolar lumen may be reduced in size as a result of wall thickening, extravasation of red blood cells, and intraluminal thrombosis.

In malignant hypertension, the glomeruli often show variable degrees of ischemic change, characterized by wrinkling and collapse of the capillary walls (Fig. 23.91). In addition to this diffuse pattern of ischemic damage, segmental lesions such as apparent necrosis in direct continuity with arteriolar lesions may be seen. By electron microscopy, the endothelium often appears swollen and sometimes

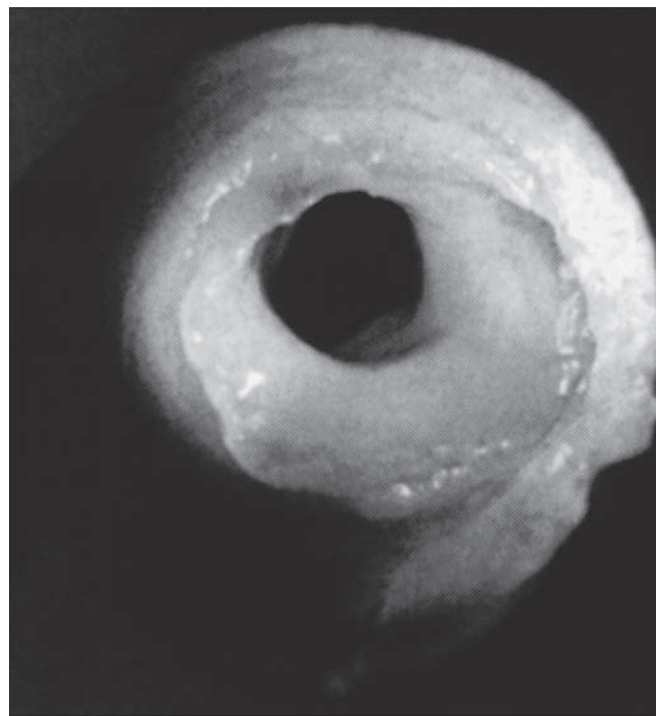


**Figure 23.92** Eccentric arteriosclerotic plaque in renal artery causing almost complete obstruction and hypertension. This was resected and arterial continuity reestablished.

focally disrupted or separated from the GBM by the accumulation of electron-lucent material. On occasion, subendothelial or intracapillary strands of fibrin may be seen. Immunofluorescence microscopy may reveal fibrin, fibrinogen, IgM, and complement components in a segmental distribution.

### Renal Arterial Disease

The larger arteries in the kidney can also be the site of renal vascular disease. Atheromatous involvement is accelerated in patients with hypertension and may be a source of atheromatous emboli and give rise to renal parenchymal infarcts. Arteries down to the arcuate size can show arteriosclerotic changes, but smaller vessels are more commonly involved by intimal thickening of the hyperplastic type, similar to that seen in the small arteries. Disease of the major arteries becomes particularly important when it involves a main renal artery and causes significant stenosis, resulting in secondary hypertension (Fig. 23.92).<sup>635</sup> The lesions involving the main renal artery can be broken down into three categories: atherosclerosis, dysplastic diseases of the fibromuscular vessels, and a miscellaneous group that includes congenital anomalies, Takayasu aortitis, and radiation injury.

The most common cause of renal artery stenosis is obstruction of the lumen by an **atheromatous plaque** at the orifice of the main renal artery.<sup>635</sup> It is usually associated with severe atheromatous disease of the aorta and is seen more often in males and in patients with diabetes mellitus. Major complications of the lesions include saccular or dissecting aneurysm formation and the occurrence of cholesterol emboli. Microscopically, these emboli appear as needle-like spaces representing cholesterol crystals embedded in amorphous debris frequently surrounded by multinucleated giant cells. Although symptomatic presentation is rare, cholesterol emboli occur immediately after or with a few months of angiographic or surgical procedures involving vessels.

**Table 23.7** Dysplastic lesions of the renal artery

DIAGNOSIS	AGE INCIDENCE	SEX INCIDENCE	RELATIVE FREQUENCY (%)	LESION
Intimal fibroplasia	1–50	M = F	1–2	Narrowing by intimal proliferation without lipid
Medial fibroplasia with aneurysms	30–60	F > M	60–70	“String of beads,” alternating stenosis and mural thinning
Medial hyperplasia	30–60	F > M	5–15	Smooth muscle hyperplasia and thickening
Perimedial fibroplasia	30–60	F > M	15–24	Fibrosis of outer media, occasionally aneurysms
Medial dissection	30–60	F > M	5–15	Fibrosis of media with dissecting aneurysms
Periarterial fibroplasia	15–50	F > M	1	Perivascular fibrosis and inflammation

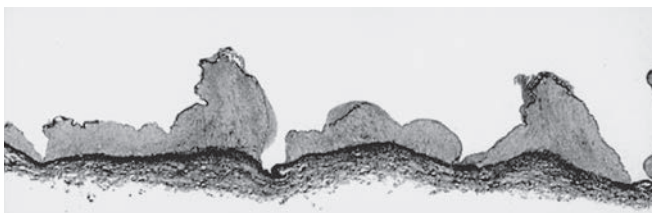


**Figure 23.93 Fibromuscular Dysplasia in a Young Woman With Hypertension.** Note aneurysmal formations in this longitudinally sectioned artery demonstrating medial fibrodysplasia with mural aneurysms.

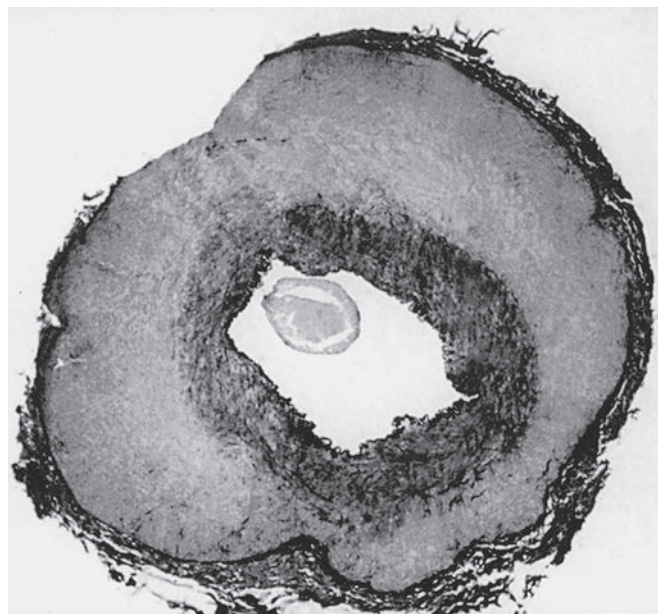


**Figure 23.94 Fibromuscular Dysplasia in a 23-Year-Old Woman With Hypertension.** Segmental resection revealed an artery with the perimedial variety of fibrodysplasia.

The second group of conditions that leads to stenosis are **dysplastic lesions of the renal artery**, currently termed **fibromuscular dysplasia**, which account for less than 10% of the cases of renal artery stenosis.<sup>636–638</sup> These lesions can involve other systemic vessels, suggesting that there may be an underlying defect in vessel structure, and can become clinically important when they cause obstruction of a major renal artery, thereby leading to severe hypertension unresponsive to antihypertensive drugs. Typically, these lesions occur in the distal two-thirds of the artery and are bilateral in 50% of the cases. Fibromuscular dysplasia can be divided into three types: intimal, medial, and periarterial/adventitial. The medial category in turn consists of three subtypes: medial fibroplasia, medial hyperplasia, and perimedial fibroplasia. As the terms indicate, differences are somewhat subtle, but given that different patient populations may be affected in each subgroup, this categorization is clinically useful (Table 23.7).

The lesion in *intimal fibromuscular dysplasia* is hyperplasia of the intima, and microscopically it is virtually indistinguishable from the proliferative stage of atherosclerosis, although it is not associated with an increased deposition of lipids. The architecture of the elastica and media are preserved so the only abnormality in the vessel wall is the intimal hyperplasia. Individuals as young as 1 year of age have been affected, but it is seen more often in the third and fourth decades. The most common of the dysplastic lesions is *medial fibroplasia*. In this condition, multiple foci of stenosis alternating with microaneurysms produce a “string of beads” appearance (Fig. 23.93).<sup>637</sup> Microscopically, atrophy of the muscle coat and fibrosis of the media near small aneurysms alternate with foci of muscular hypertrophy and fibrosis in the stenotic areas. Second in frequency is *perimedial fibroplasia* (Fig. 23.94). In this variant, segmental aneurysmal dilation does not occur, and the outer half of the media, elastica, and intima maintain their normal architecture. *Medial hyperplasia* is seen less frequently. Hyperplasia of the muscle produces

a uniform circumferential thickening of the vessel wall with narrowing of the lumen. *Periarterial fibromuscular dysplasia* is a rare lesion in which fibrosis of the adventitia extends into the surrounding adipose and connective tissue, causing extrinsic constriction of the vessel (rather than thickening from within the wall).

Among the **miscellaneous causes** of renal artery stenosis, **radiation injury** is of particular interest.<sup>639</sup> The lesion is characterized by a loss of muscle and an intense fibrosis in all layers of the vessel wall. It is usually a distant event that follows radiation therapy for a malignant tumor where the renal artery was included in the irradiated area. *Takayasu aortitis* or pulseless disease is a chronic sclerosing aortitis of unknown etiology that can cause renal artery stenosis from narrowing of the ostium.<sup>640</sup> An inflammatory infiltrate with giant cells is frequently present, suggesting an immunologic mechanism.

An ischemic kidney is smaller than the contralateral kidney, irrespective of the etiology. Glomeruli are small with ischemic wrinkling of the basement membranes, and the tubules are atrophic. The atrophic tubules have simplified epithelium with inconspicuous lumina mimicking parathyroid, often referred to as “endocrine

change." IF is present, and the hyperplastic juxtaglomerular apparatus shows increased granularity with special stains. The small vessels are protected from the hypertension, in contrast to the contralateral kidney, where biopsy may show hypertensive microvascular disease.

## Radiation Nephropathy

Radiation nephropathy is the term used to designate the renal disease that occurs with irradiation of the abdomen (or total body) during the treatment of malignant tumors. More recently, this has also been noted in association with use of radiolabeled substances such as monoclonal antibodies, antibody fragments, and low-molecular-weight onconophilic peptides.<sup>440</sup> Although the term acute radiation nephritis has also been used for this disease, since no inflammation occurs immediately after kidney irradiation and histologic examination of the radiation-damaged kidneys usually reveals only minimal proliferation and inflammatory changes, the terms acute and chronic radiation nephropathy, rather than nephritis, are preferred.<sup>440,441</sup> The severity of the pathologic changes in the damaged kidney depends upon multiple factors, including radiation dosage, method of irradiation, age of the patient, amount of perirenal fat, preexistence of renal disease, and the concomitant use of chemotherapeutic agents, as well as individual susceptibility. In general, a radiation dose of 9.8 Gy in the absence of exposure to nephrotoxic drugs and other predisposing factors is associated with 5% incidence of kidney toxicity.<sup>642</sup>

*Acute radiation nephropathy* usually occurs 6–12 months after radiation exposure.<sup>440</sup> However, the period of latency can be shorter, especially in children. Clinically, the disease is manifested by the gradual onset of edema, hypertension, dyspnea on exercise, pleural and peritoneal serous effusions, anemia, headaches, and urinary changes, which include proteinuria and the presence of casts. Rare cases of radiation nephropathy causing nephrotic syndrome have been reported.<sup>643</sup> The glomerular filtration rate decreases and over half of the patients progress to renal failure. Those who recover from the acute episode usually have persistent proteinuria and renal impairment. On occasion, malignant hypertension may develop during the acute radiation syndrome. The mortality of patients with this complication is high.

*Chronic radiation nephropathy* either follows the acute phase or develops insidiously over a period of years. Although no specific threshold has been established for total cumulative radiation exposure that leads to this form of injury, it appears that relatively small doses of radiation (500–1000 rad) may, in susceptible individuals, cause renal damage. In most patients, the findings of mild proteinuria and moderate hypertension are not detected until many years after radiation exposure.

Depending on the severity and the stage of the disease, kidney biopsies from patients with radiation nephropathy will show a wide range of glomerular changes.<sup>440</sup> Some glomeruli may appear segmentally or completely scarred, while others may show no significant changes. Segmental areas of fibrinoid necrosis of the tuft in continuity with similar changes in the arterioles may be seen. The glomerular capillary walls may be thickened, and a double contour may be demonstrated by silver impregnation techniques.<sup>644</sup> The mesangium may be prominent as a result of an increase in mesangial matrix. Mesangiolysis and adhesions to the Bowman capsule may be seen. Vascular injury is manifested by fibrinoid necrosis of the arterioles and small arteries, sometimes accompanied by thrombosis. A loose myxoid intimal thickening involving arterioles and interlobular arteries is a frequent feature. The glomerular and vascular changes are within the spectrum of pathology seen in TMA. Swelling of the tubular epithelium with desquamation of the cells, and basement membrane thickening and splitting followed by tubular loss and

atrophy are common findings and may be severe. Regeneration is often abnormal so that the cells may have poorly formed cytoplasm and abnormal nuclei. The interstitium is focally scarred and has no significant inflammation.

Electron microscopic examination of the glomeruli shows a widening of the subendothelial zone that may contain flocculent material or strands of fibrin. Focal extension of the mesangium into the subendothelial space may also be seen, sometimes associated with GBM duplication. The endothelial cells may appear swollen or focally detached from the endothelial aspect of the GBM. Immunofluorescence may show focal deposition of IgM and fibrinogen in glomeruli and blood vessels.

## Hematopoietic Stem Cell Transplantation-Associated Thrombotic Microangiopathy

Hematopoietic stem cell transplantation (HSCT)-associated TMA is the term used to designate a syndrome of late-onset renal insufficiency that has been reported to occur in up to 20% of patients who have received a bone marrow transplant and was previously referred to as bone marrow transplant nephropathy.<sup>440,645</sup> Although hematopoietic stem cells can be derived from bone marrow, peripheral blood is the most common source now.<sup>36</sup> Total body irradiation is an important component of the treatment in these patients and appears to be the main factor in the development of HSCT-associated TMA. However, other factors, such as drug therapy and infections also contribute to this syndrome.<sup>440,645</sup> It is also known that HSCT-associated TMA can occur in autologous or allogeneic HSCT, in the absence of graft versus host disease, total body irradiation, cyclosporine use, or infections. Individual susceptibility may also be an important factor, as a few pediatric patients with HSCT-associated TMA were found to have mutations in complement genes or develop autoantibodies against complement factors posttransplantation.<sup>646</sup>

The renal insufficiency usually manifests 9–12 months after the transplant but can be variable given the wide variety of treatment protocols and associated comorbidities.<sup>36</sup> In some patients, the clinical picture can be similar to that of HUS with a rapid decline of renal function, while in others there may be a slow decline in renal function without apparent ongoing hemolysis.<sup>647–649</sup> The renal lesions, regardless of whether or not the patient has clinical evidence of systemic HUS, typically affect the glomeruli, small arteries, and arterioles and are histologically similar to those reported in radiation nephropathy and HUS.<sup>440</sup>

## Cystic Diseases of the Kidney

Renal cystic diseases are a large family of hereditary, sporadic, developmental, and acquired disorders characterized by the presence of cysts in one or both kidneys.<sup>650–653</sup> Only the most common cystic renal diseases will be discussed in this section. A subset of hereditary cystic diseases with gene mutations involving primary (nonmotile) cilia is now being reclassified as "ciliopathies." This category of disease includes autosomal dominant polycystic kidney disease (ADPKD), autosomal recessive polycystic kidney disease (ARPKD), and nephronophthisis (NPHP), and other related ciliopathies. Primary cilia are antenna-like projections on the apical surfaces of almost all cells and consist of a basal body and an axoneme with nine peripheral doublets. Primary cilia detect flow as well as a variety of stimuli and participate in transmembrane transport of proteins.

## Multicystic Renal Dysplasia

In this disorder, the development of the kidney is disorganized because of anomalous differentiation of the metanephros (Fig. 23.95).



**Figure 23.95** Dysplastic Kidney of an Infant. Opposite kidney appeared normal by pyelogram.

Multicystic renal dysplasia is the most common form of cystic renal disease in children and the most common cause of abdominal masses in newborns. The dysplasia is usually unilateral but can be bilateral, segmental, or focal. Abnormalities of the collecting system are common and include obstruction of the uretero-pelvic junction, ureteral atresia, and urethral obstruction. Malformations of other organs, especially of the heart, can occur in conjunction with renal dysplasia. The clinical presentation largely depends on the extent of the dysplastic involvement and the degree of associated urinary obstruction. Most dysplastic kidneys arise sporadically but a few are familial or occur in syndromes of multiple malformations.<sup>654,655</sup> A large reniform mass of cysts of various sizes obscures any renal parenchyma that may be present. In focal and segmental dysplasia, only part of the kidney is involved by the dysplasia and cyst formation. Microscopically, the findings are quite characteristic.<sup>656,657</sup> The cysts are lined by cuboidal epithelial cells and surrounded by immature stromal elements. Primitive tubules and glomerular structures may be present, as may islands of dysplastic mesenchyme including cartilage and fibromuscular tissue (Fig. 23.96).

### Autosomal Dominant Polycystic Kidney Disease

ADPKD is a hereditary condition characterized by expanding cysts that progressively destroy the renal parenchyma of both kidneys, ultimately causing renal failure. It is one of the most common hereditary human disorders, occurring in about 1 or 2 per 1000 live births and accounting for approximately 10% of cases requiring dialysis or renal transplantation.<sup>658</sup> The pattern of inheritance is autosomal dominant with complete penetrance, and each offspring of an affected individual has a 50% chance of inheriting the disease. The disease is genetically heterogeneous and is caused by a mutation in two genes, *PKD1* and *PKD2*, that are located on chromosomes 16p13.3 and 4q13–23, respectively.<sup>659,660</sup> The protein products of the PKD genes, polycystin-1 and polycystin-2, have similar cellular distribution resulting in phenotypic similarities between *PKD1*- and *PKD2*-mutated ADPKD.<sup>661,662</sup> Polycystin-1 is an epithelial cell membrane receptor involved in signaling of renal tubular epithelial cell proliferation and differentiation. Polycystin-2 has similarities to a sodium/calcium channel and likely modulates intracellular calcium levels; this ion channel function is enabled by heterodimerization of polycystin 1 and 2. The polycystin complex is implicated in the regulation of the cell cycle via multiple transduction pathways, as well as in the mechanosensory function of the renal primary

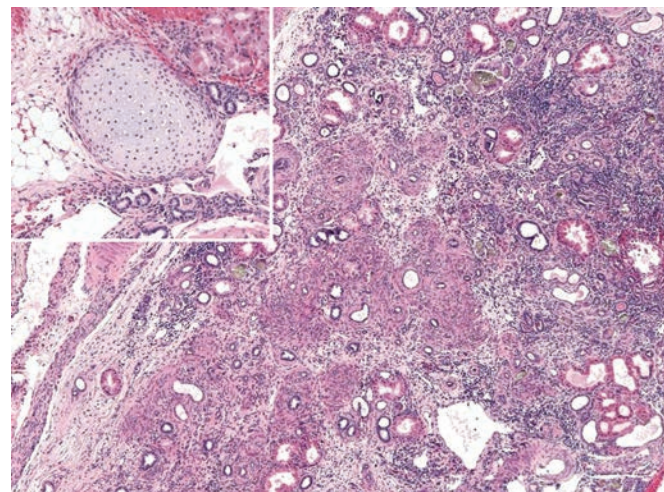


**Figure 23.96** Dysplastic kidney showing embryonic-like connective tissue and primitive tubules. Immature cartilage is also seen focally (inset).

cilium.<sup>663</sup> Abnormalities in tubular cell proliferation, apoptosis, cell polarity, and secretions have been detected within the cysts. Mutations in the *PKD1* gene are responsible for about 85%–90% of all cases of ADPKD, while mutations in *PKD2* cause the disease in majority of the remaining patients. A small number of families with ADPKD do not demonstrate linkage to either *PKD1* or *PKD2*, which suggests the potential presence of an as yet unidentified *PKD3* gene.<sup>664</sup> Males and females are affected equally, and there is no racial predilection. Although it can present at any time during life, it most frequently becomes symptomatic during the fourth and fifth decades with a gradual onset of renal failure. Early-onset ADPKD can occur rarely in children, causing a diagnostic challenge, and the presence of glomerular cysts should favor ADPKD.<sup>665</sup>

Clinical manifestations of ADPKD include flank pain, flank masses, hematuria, hypertension, and renal failure. Approximately 20% of patients with ADPKD develop nephrolithiasis, and uric acid stones are more common than calcium oxalate stones.<sup>666</sup> Although individuals with *PKD1* are clinically indistinguishable from those with *PKD2*, the latter patients have a less severe disease course with a later mean age at diagnosis, onset of hypertension, and ESRD.<sup>667</sup> Radiographic findings are usually diagnostic, and sonography and computed tomography are reliable procedures for the demonstration of early involvement. Gene linkage analysis allows prenatal diagnosis but requires at least four affected family members.<sup>658</sup> Although direct sequencing is more sensitive, even by this method, only 70% of ADPKD mutations are detected.

ADPKD is bilateral, but significant asynchrony of involvement of the kidneys may be noted on occasion. The kidneys are markedly enlarged and have a bosselated outer cortical surface produced by multiple cysts of varying sizes (Fig. 23.97). When the disease is severe, normal renal parenchyma is apparent only microscopically. The cysts develop in all segments of the renal tubule and glomerular capsule as saccular expansions or diverticula. In the early stages, the fluid of the cysts is derived from glomerular filtrate. As the cysts enlarge, however, they commonly become disconnected from the tubule of origin, thereafter filling with fluid exclusively by transepithelial secretion.<sup>668</sup> On light microscopy, the cysts are lined by cuboidal, flattened epithelium, and hyperplastic polypoid foci are often found. Intervening renal parenchyma appears relatively normal, although foci of interstitial scarring, TA, and IF are common. The development of renal adenomas has been reported to occur in about 20% of patients with ADPKD.<sup>669</sup> ADPKD is considered

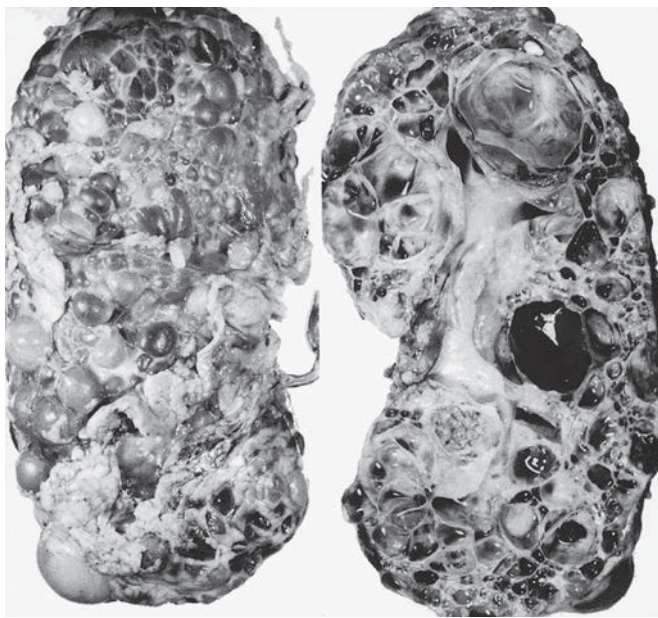


**Figure 23.97** External and cut surface of a nephrectomy specimen from a patient with autosomal dominant polycystic kidney disease.

a systemic condition since over half of the patients develop cysts in other organs including the liver, pancreas, spleen, pineal gland, seminal vesicles, and lungs.<sup>670</sup> Other abnormalities include the presence of cerebral and coronary artery aneurysms, mitral valve prolapse, abnormal aortic valves, colonic diverticula, and skeletal malformations.<sup>658,671,672</sup>

### Autosomal Recessive Polycystic Kidney Disease

ARPKD is a rare hereditary disorder with an estimated incidence of 1 per 20,000 live births.<sup>673</sup> ARPKD is caused by mutations of a gene located on chromosome 6p21.1-p12 named polycystic kidney hepatic disease gene (*PKHD1*)<sup>674,675</sup> whose related protein polyductin,<sup>676</sup> also known as fibrocystin,<sup>677</sup> is highly expressed in the epithelial cells of the collecting ducts and thick ascending loops of Henle and, to a lesser extent, in the biliary and pancreatic duct epithelia.<sup>678</sup> Of date, more than 300 *PKHD1* mutations have been identified and the majority of patients are compound heterozygotes.<sup>679</sup> As in other polycystic kidney diseases, polyductin localizes to the primary cilia of the renal epithelial cells.<sup>678</sup> Although the liver and both kidneys are invariably affected, the severity of involvement varies, thus creating a spectrum of clinical presentation.<sup>680</sup> In the neonatal period, the renal symptoms usually predominate.<sup>681</sup> Truncating *PKHD1* mutations are associated with severe neonatal disease.<sup>682</sup> Later in life, patients seek medical attention because of hepatic disease, which consists of congenital hepatic fibrosis with a variable degree of biliary dysgenesis and bile duct ectasia. These patients may also develop portal hypertension with hepatosplenomegaly and esophageal varices. Occasional patients may present with liver cysts, but cysts in other viscera aside from the kidneys and liver are rare and their presence should suggest an alternate diagnosis.

Majority of patients with ARPKD present with large abdominal masses at birth. They may also have the "Potter" phenotype with its characteristic facies secondary to oligohydramnios, joint deformities, and pulmonary hypoplasia. Newborns that have the severe form of the disease die shortly after birth, usually due to respiratory failure. Patients who survive the perinatal period

develop renal failure, hypertension, and portal hypertension. The estimated perinatal mortality is 30%–50%; for those who survive the first month of life, the reported mean 5-year survival rate is 80%–95%.<sup>676,683</sup>

The kidneys are markedly enlarged bilaterally but retain their reniform configuration. The cysts tend to be linear and radiate from the medulla to the outer cortex. They develop in the collecting ducts, which expand to a large size due to fluid accumulation within the cyst cavity. Microscopically, the cysts appear as dilated tubular structures lined by cuboidal or flattened epithelium. The intervening tissue may contain unininvolved nephrons, but this depends on the severity of the disorder.

### Nephronophthisis

Although NPHP has traditionally been grouped with medullary cystic kidney disease based on similarities in their clinical and pathologic features, these conditions are now regarded as two distinct entities.<sup>684</sup> NPHP is an autosomal *recessive* cystic disease characterized by tubular basement membrane disruption, IF, and cyst formation. It is the most frequent genetic cause of ESRD in children and adolescents, accounting for 10%–20% of cases of renal failure in this age group.<sup>685</sup> Three clinical forms, referred to as juvenile,<sup>686</sup> infantile,<sup>687</sup> and adolescent,<sup>688</sup> with a median age at onset of ESRD of 13 years, 1–3 years, and 19 years, respectively, have been recognized. NPHP is genetically heterogeneous, and mutations have been detected in increasing number of genes.<sup>689</sup> The mutations are in genes encoding primary cilia proteins (*NPHP1*–*NPHP18*, *NPHP1*, *NPHP2L*, *AHI1*, *CC2D2A*, *MSK1*, *ATXN10*, *B9D2*), and patients often have associated renal disease of NPHP, which is now considered a form of "ciliopathy."<sup>690,691</sup> Majority of proteins encoded by the NPHP genes are known as nephrocystins, and it has been proposed that mutated proteins alter the function of primary cilia, causing renal cystic disease and, in some, extrarenal manifestations.<sup>684,691</sup>

Typical signs and symptoms of NPHP include the inability to concentrate urine, polydipsia, anuresis, severe anemia, and growth retardation. The disease occurs in a pure renal form in approximately 85% of the patients. About 12% of the cases are associated with retinitis pigmentosa (Senior–Løken syndrome).<sup>692–694</sup> Other less common associations that have been described include hepatic fibrosis, skeletal malformations, and various defects in the central nervous system. Clinical syndromes described with NPHP and extrarenal manifestations include Bardet–Biedl syndrome, Joubert syndrome, and Meckel–Gruber syndrome.<sup>690,691</sup>

All types of NPHP have similar macroscopic and histopathologic features. Renal involvement is always bilateral. Both kidneys are moderately reduced in size and exhibit a granular surface. On cut sections, the cortex and medulla are both thinned. The cortico-medullary junction is indistinct and typically the site of a variable number of thin-walled, fluid-filled cysts, ranging in size from barely visible up to 2.0 cm in diameter. The cysts may also occur deeper in the renal medulla and occasionally in the papillae. Microdissection studies have shown that the cysts arise from the loop of Henle, distal convoluted tubules, and collecting ducts. Histologic findings are nonspecific and depend on the severity of the disease. Tubulointerstitial fibrosis with lymphocytic inflammatory infiltrate, TA, and cyst formation is seen. The TA is often accompanied by a marked thickening of the tubular basement membrane and is better seen in PAS-stained sections. Pools of Tamm–Horsfall protein without clinical evidence of obstructive or reflux nephropathy in a young patient should prompt genetic evaluation for NPHP. By electron microscopy, these basement membranes can appear homogeneously thickened, split into thin lamellae, reticulated, or completely disintegrated.<sup>695</sup>

## Autosomal Dominant Tubulointerstitial Kidney Disease

Autosomal dominant tubulointerstitial kidney disease (ADTKD) represents a new terminology for a group of disorders that are characterized by TA, IF, thickening and lamellation of tubular basement membranes, and in some cases, tubular microcysts. This entity encompasses mucin-1-related kidney disease (MUC-1), uromodulin-related kidney disease (UMOD), renin mutation with tubulointerstitial nephritis (*REN*), and kidney disease due to *HNF1 $\beta$*  mutation (HNF1B), with two former diseases being most frequently encountered.<sup>696,697</sup> ADTKD-MUC1 was previously referred to as medullary cystic kidney disease type I (MCKD1), and the previous terminology for ADTKD-UMOD was medullary cystic kidney disease type 2 (MCKD2). These disorders share clinical and morphologic similarities with NPHP, but cysts are not uniformly observed.<sup>650,696</sup>

Patients with ADTKD-MUC1 develop progressive renal failure in adulthood. The median age at end-stage kidney disease is 62 years, although it varies within families.<sup>698</sup> The disease is caused by mutations in *MUC1* gene that maps to chromosome 1q21.<sup>696,699</sup> The protein, mucin-1, is expressed in distal tubules and collecting ducts and presumably protects the epithelial surfaces from bacteria. ADTKD-UMOD is caused by mutations in *UMOD* gene located on chromosome 16p12.<sup>700,701</sup> The mutant uromodulin (Tamm-Horsfall protein) is misfolded, leading to accumulation within the endoplasmic reticulum of the thick ascending loop of Henle and distal tubules. The end-stage renal failure occurs from 20–70 years, with a median age being 54 years.<sup>700,701</sup>

Both MUC-1 and UMOD-associated ADTKD patients have minimal proteinuria accompanying chronic renal failure and usually lack extrarenal disease.<sup>696,697</sup> There is an association with hyperuricemia and gout, especially in ADTKD-UMOD patients.<sup>700,701</sup> The kidneys are normal or moderately reduced in size. Small corticomedullary cysts may be seen in both diseases and in ADTKD-UMOD, cysts can also be detected in cortex and medulla. Microscopically, there is diffuse interstitial inflammation with fibrosis and TA interspersed with hypertrophied and dilated tubules. Ultrastructural similarities with NPHP include tubular basement membrane lamellation. Patients with UMOD mutations have characteristic intracytoplasmic fibrillar inclusions composed of uromodulin in the thick ascending loops of Henle and on rare occasion, glomerular cysts.<sup>702</sup>

Interstitial nephritis attributable to mutated *REN*, a gene encoding renin, is rare, and renal cysts are not a typical feature in these patients. Anemia and hyperuricemia are common presenting features along with chronic renal failure.<sup>696</sup> Heterozygous mutations in *REN* result in reduced production of renin in juxtaglomerular cells and intracellular accumulation of unfolded precursor protein causes accelerated apoptosis and nephron loss.<sup>703,704</sup> Up to a third of patients with *HNF1 $\beta$*  mutations have congenital abnormalities of the kidney and urinary tract, and the age at presentation in such instances is typically in utero and in young children.<sup>705</sup> The renal cysts can be either widespread or limited to glomeruli and adjacent parenchyma often shows features of dysplasia. Adults with these mutations come to attention due to unexplained chronic renal failure, minimal proteinuria, and tubulointerstitial disease.<sup>706</sup> The transcription factor *HNF1 $\beta$*  is also expressed in pancreas and hence the association with maturity onset diabetes mellitus.

## Medullary Sponge Kidney

Medullary sponge kidney (MSK) is a renal cystic disorder characterized by tubular ectasia of the collecting ducts and cyst formation confined to the medullary pyramids.<sup>707</sup> It typically affects both kidneys and represents developmental malformation of the collecting system.

The true incidence of MSK is unknown, although it has been estimated at 1 per 5000 population.<sup>708</sup> The disease is asymptomatic unless complicated by nephrolithiasis, hematuria, or infections. In these instances, the diagnosis is established when the patient undergoes radiographic examination.<sup>709</sup> Typically, symptoms start in adulthood, but presentation in adolescence and childhood has been reported.<sup>710</sup> In patients with recurrent nephrolithiasis, the stones are composed of calcium oxalate and/or calcium phosphate and a third of the patients have distal renal tubular acidosis. Both sexes are equally affected. Most cases appear sporadically, but a few familial clusters have been documented.<sup>710</sup> MSK has been reported in association with various conditions such as hemihypertrophy, Wilms tumor, congenital hepatic fibrosis, multiple endocrine neoplasia type 2 (MEN2), Marfan syndrome, and Ehlers-Danlos syndrome. Mutations or polymorphisms of glial cell line-derived neurotrophic factor (GDNF) and receptor tyrosine kinase (RET) genes (previously known to be involved in genitourinary development) have been recently reported in MSK, confirming a genetic component in a minority of patients.<sup>711</sup>

The involved kidneys are usually normal in size, but they can be slightly enlarged in those cases with pronounced sponge-like changes. The cysts are multiple, small, and limited to the medullary pyramids and papillae. They usually affect all pyramids in both kidneys; however, on occasion, only one or two pyramids or only one kidney may be affected. The cysts are lined by collecting duct epithelium and usually communicate with collecting tubules. Concrections adherent to the walls of the cysts and the dilated collecting ducts may be seen. The interstitium often shows severe inflammation and scarring, frequently accompanied by TA, especially near the papillary tips. In instances where there is nephrolithiasis and pyelonephritis, the cortex may show significant cortical scarring.

## Acquired Renal Cystic Disease

Although acquired renal cystic disease (ARCD) was initially reported in patients undergoing long-term dialysis, similar changes can also occur in uremic nondialyzed patients.<sup>712</sup> ARCD has been reported to occur in 7%–22% of patients with renal failure who are not on dialysis, 40% of patients who have been on dialysis for 3 years, and 80%–90% of patients who have been on dialysis for 10 years or more.<sup>713</sup> The etiology of ARCD has not yet been well established, and it has been suggested that the cysts found in this condition result from obstruction of the renal tubules by local fibrosis, oxalate deposition, or epithelial hyperplasia. The cysts often regress after transplantation. Men are more affected than women. In most cases, the disease is asymptomatic, but sometimes the cysts bleed, rupture, or become infected, causing fever, hematuria, and flank pain. The most serious complication, however, is the development of renal carcinomas in the walls of the cysts. It has been estimated that renal cell carcinoma is found 50 times more frequently in dialysis patients with ARCD than in the general population.

The cysts in ARCD are usually bilateral and occur in both the renal cortex and medulla.<sup>714</sup> Their number can vary from a few subcapsular cysts to diffuse involvement of almost the entire renal parenchyma. A diagnosis of ARCD requires five or more cysts are found on imaging studies and absence of known cystic renal disease as the cause of renal failure. The cysts are filled with straw-colored or hemorrhagic fluid and often contain calcium oxalate crystals. Most cysts are less than 0.5 cm, but they can measure up to 2–3 cm in diameter. Microscopically, cysts are lined by flattened epithelium or by hyperplastic cuboidal or columnar cells with prominent eosinophilic cytoplasm, sometimes forming papillary projections. Renal neoplasms arising in this setting are fully discussed in Chapter 24.<sup>715</sup>

## Simple Cysts

Simple cysts are the most common cystic abnormality encountered in the kidneys.<sup>716</sup> They are found in about 5%–12% of the general population undergoing abdominal ultrasound examination for various reasons.<sup>717,718</sup> Their occurrence increases with age, with an incidence of less than 0.1% in children and up to 20% in individuals over 50 years of age.<sup>713</sup> They are usually asymptomatic and are often detected at autopsy or as an incidental finding in the radiologic evaluation for other diseases. On occasion, however, when complicated by hemorrhage or infection, they can cause

pain. Simple cysts can be solitary or multiple and bilateral. They occur more commonly in the renal cortex, and although their etiology has not been well established, it is believed that they originate from diverticula of cortical tubules.<sup>719</sup> Most are under 5 cm in diameter, but larger cysts have been documented.<sup>718</sup> Usually unilocular, on occasion they can be bilocular or multilocular. The cysts are normally translucent, filled with clear serous fluid, and lined by a single layer of cuboidal or flattened epithelium. Cases complicated by hemorrhage or infection can have thick capsular walls with hemosiderin-laden macrophages and atrophic lining epithelium.

## References

1. Israni A, Kasiske BL. Laboratory assessment of kidney disease: clearance, urinalysis, and kidney biopsy. In: Brenner BM, ed. *Brenner and Rector's the Kidney*. 8th ed. Philadelphia, PA: WB Saunders; 2008:724-756.
2. Piotto GH, Moraes MC, Malheiros DM, et al. Percutaneous ultrasound-guided renal biopsy in children—safety, efficacy, indications and renal pathology findings: 14-year Brazilian university hospital experience. *Clin Nephrol*. 2008;69:417-424.
3. Rivera F, Lopez-Gomez JM, Perez-Garcia R. Clinicopathologic correlations of renal pathology in Spain. *Kidney Int*. 2004;66:898-904.
4. Richards NT, Darby S, Howie AJ, et al. Knowledge of renal histology alters patient management in over 40% of cases. *Nephrol Dial Transplant*. 1994;9:1255-1259.
5. Shah RP, Vathsala A, Chiang GS, et al. The impact of percutaneous renal biopsies on clinical management. *Ann Acad Med Singapore*. 1993;22:908-911.
6. Turner MW, Hutchinson TA, Barre PE, et al. A prospective study on the impact of the renal biopsy in clinical management. *Clin Nephrol*. 1986;26:217-221.
7. Messias NC, Walker PD, Larsen CP. Paraffin immunofluorescence in the renal pathology laboratory: more than a salvage technique. *Mod Pathol*. 2015;28:854-860.
8. Nasr SH, Galgano SJ, Markowitz GS, et al. Immunofluorescence on pronase-digested paraffin sections: a valuable salvage technique for renal biopsies. *Kidney Int*. 2006;70:2148-2151.
9. Johannessen JV. Rapid processing of kidney biopsies for electron microscopy. *Kidney Int*. 1973;3:46-50.
10. Hoffmann EO, Flores TR. High resolution light microscopy in renal pathology. *Am J Clin Pathol*. 1981;76:636-643.
11. Colvin RB. Antibody-mediated renal allograft rejection: diagnosis and pathogenesis. *J Am Soc Nephrol*. 2007;18:1046-1056.
12. Truong LD, Barrios R, Adrogue HE, Gaber LW. Acute antibody-mediated rejection of renal transplant: pathogenetic and diagnostic considerations. *Arch Pathol Lab Med*. 2007;131:1200-1208.
13. Boldorini R, Veggiani C, Barco D, Monga G. Kidney and urinary tract polyomavirus infection and distribution: molecular biology investigation of 10 consecutive autopsies. *Arch Pathol Lab Med*. 2005;129:69-73.
14. Eyzaguirre E, Haque AK. Application of immunohistochemistry to infections. *Arch Pathol Lab Med*. 2008;132:424-431.
15. Weber M. Basement membrane proteins. *Kidney Int*. 1992;41:620-628.
16. Clapp WL, Croker BP. Adult kidney. In: Mills SE, ed. *Histology for Pathologists*. 3rd ed. Philadelphia, PA: Lippincott Williams & Wilkins; 2007:839-907.
17. Sraer JD, Adida C, Peraldi MN, et al. Species-specific properties of the glomerular mesangium. *J Am Soc Nephrol*. 1993;3:1342-1350.
18. Drenckhahn D, Schnittler H, Nobiling R, Kriz W. Ultrastructural organization of contractile proteins in rat glomerular mesangial cells. *Am J Pathol*. 1990;137:1343-1351.
19. Johnson RJ, Floege J, Yoshimura A, et al. The activated mesangial cell: a glomerular "myofibroblast"? *J Am Soc Nephrol*. 1992;2:S190-S197.
20. Mene P, Simonson MS, Dunn MJ. Physiology of the mesangial cell. *Physiol Rev*. 1989;69:1347-1424.
21. Michael AE, Keane WF, Raij L, et al. The glomerular mesangium. *Kidney Int*. 1980;17:141-154.
22. Mathieson PW. Update on the podocyte. *Curr Opin Nephrol Hypertens*. 2009;18:206-211.
23. Stamenkovic I, Skalli O, Gabbiani G. Distribution of intermediate filament proteins in normal and diseased human glomeruli. *Am J Pathol*. 1986;125:465-475.
24. Shankland SJ, Smeets B, Pippin JW, Moeller MJ. The emergence of the glomerular parietal epithelial cell. *Nat Rev Nephrol*. 2014;10:158-173.
25. Winyard PJ, Price KL. Experimental renal progenitor cells: repairing and recreating kidneys? *Pediatr Nephrol*. 2014;29:665-672.
26. Habib R, Kleinknecht C. The primary nephrotic syndrome in children. Classification and clinicopathologic study of 406 cases. In: Sommers SC, ed. *Kidney Pathology Decennial, 1966-1975*. New York, NY: Appleton-Century-Crofts; 1975:165-224.
27. Primary nephrotic syndrome in children: clinical significance of histopathologic variants of minimal change and of diffuse mesangial hypercellularity. A Report of the International Study of Kidney Disease in Children. *Kidney Int*. 1981;20:765-771.
28. Cameron JS. Nephrotic syndrome in the elderly. *Semin Nephrol*. 1996;16:319-329.
29. Waldman M, Crew RJ, Valeri A, et al. Adult minimal-change disease: clinical characteristics, treatment, and outcomes. *Clin J Am Soc Nephrol*. 2007;2:445-453.
30. Wyatt RJ, Marx MB, Kazee M, Holland NH. Current estimates of the incidence of steroid responsive idiopathic nephrosis in Kentucky children 1–9 years of age. *Int J Pediatr Nephrol*. 1982;3:63-65.
31. van den Berg JG, Weening JJ. Role of the immune system in the pathogenesis of idiopathic nephrotic syndrome. *Clin Sci*. 2004;107:125-136.
32. Artinano M, Etheridge WB, Stroehlein KB, Barcenas CG. Progression of minimal-change glomerulopathy to focal glomerulosclerosis in a patient with fenoprofen nephropathy. *Am J Nephrol*. 1986;6:353-357.
33. Warren GV, Korbet SM, Schwartz MM, Lewis EJ. Minimal change glomerulopathy associated with nonsteroidal antiinflammatory drugs. *Am J Kidney Dis*. 1989;13:127-130.
34. Audard V, Larousserie F, Grimbart P, et al. Minimal change nephrotic syndrome and classical Hodgkin's lymphoma: report of 21 cases and review of the literature. *Kidney Int*. 2006;69:2251-2260.
35. Kraft SW, Schwartz MM, Korbet SM, Lewis EJ. Glomerular podocytopathy in patients with systemic lupus erythematosus. *J Am Soc Nephrol*. 2005;16:175-179.
36. Troxell ML, Higgins JP, Kambham N. Renal pathology associated with hematopoietic stem cell transplantation. *Adv Anat Pathol*. 2014;21:330-340.
37. Zafarmand AA, Baranowska-Daca E, Ly PD, et al. De novo minimal change disease associated with reversible post-transplant nephrotic syndrome. A report of five cases and review of literature. *Clin Transplant*. 2002;16:350-361.
38. Grimbart P, Audard V, Remy P, et al. Recent approaches to the pathogenesis of minimal-change nephrotic syndrome. *Nephrol Dial Transplant*. 2003;18:245-248.
39. Tesar V, Zima T. Recent progress in the pathogenesis of nephrotic proteinuria. *Crit Rev Clin Lab Sci*. 2008;45:139-220.
40. Ishimoto T, Shimada M, Araya CE, et al. Minimal change disease: a CD80 podocytopathy? *Semin Nephrol*. 2011;31:320-325.
41. Ling C, Liu X, Shen Y, et al. Urinary CD80 levels as a diagnostic biomarker of minimal change disease. *Pediatr Nephrol*. 2015;30:309-316.
42. White RH, Glasgow EF, Mills RJ. Clinicopathological study of nephrotic syndrome in childhood. *Lancet*. 1970;1:1353-1359.
43. Olson JL. The nephrotic syndrome and minimal change disease. In: Jennette JC, Olson JL, Silva FG, A'gati VD, eds. *Heptinstall's Pathology of the Kidney*. 7th ed. Philadelphia, PA: Wolters Kluwer; 2015:173-206.
44. Munyentwali H, Bouachi K, Audard V, et al. Rituximab is an efficient and safe treatment in adults with steroid-dependent minimal change disease. *Kidney Int*. 2013;83:511-516.
45. Garin EH, Reiser J, Cara-Fuentes G, et al. Case series: CTLA4-IgG1 therapy in minimal change disease and focal segmental glomerulosclerosis. *Pediatr Nephrol*. 2015;30:469-477.
46. Munk F. Klinische Diagnostik der degenerativen Nierenerkrankungen. *Z Klin Med*. 1913;78:1-52.
47. Patrakka J, Lahdenkari AT, Koskimies O, et al. The number of podocyte slit diaphragms is decreased in minimal change nephrotic syndrome. *Pediatr Res*. 2002;52:349-355.

48. Fatima H, Moeller MJ, Smeets B, et al. Parietal epithelial cell activation marker in early recurrence of FSGS in the transplant. *Clin J Am Soc Nephrol*. 2012;7:1852-1858.
49. Giannico G, Yang H, Neilson EG, Fogo AB. Dystroglycan in the diagnosis of FSGS. *Clin J Am Soc Nephrol*. 2009;4:1747-1753.
50. D'Agati VD, Fogo AB, Bruijn JA, Jennette JC. Pathologic classification of focal segmental glomerulosclerosis: a working proposal. *Am J Kidney Dis*. 2004;43:368-382.
51. D'Agati VD. The spectrum of focal segmental glomerulosclerosis: new insights. *Curr Opin Nephrol Hypertens*. 2008;17:271-281.
52. Fogo AB. Causes and pathogenesis of focal segmental glomerulosclerosis. *Nat Rev Nephrol*. 2015;11:76-87.
53. Stokes MB, D'Agati VD. Morphologic variants of focal segmental glomerulosclerosis and their significance. *Adv Chronic Kidney Dis*. 2014;21:400-407.
54. D'Agati VD, Alster JM, Jennette JC, et al. Association of histologic variants in FSGS clinical trial with presenting features and outcomes. *Clin J Am Soc Nephrol*. 2013;8:399-406.
55. Savin VJ, Sharma R, Sharma M, et al. Circulating factor associated with increased glomerular permeability to albumin in recurrent focal segmental glomerulosclerosis. *N Engl J Med*. 1996;334:878-883.
56. Wei C, El Hindi S, Li J, et al. Circulating urokinase receptor as a cause of focal segmental glomerulosclerosis. *Nat Med*. 2011;17:952-960.
57. Barisoni L, Schnaper HW, Kopp JB. Advances in the biology and genetics of the podocytopathies: implications for diagnosis and therapy. *Arch Pathol Lab Med*. 2009;133:201-216.
58. D'Agati VD, Kaskel FJ, Falk RJ. Focal segmental glomerulosclerosis. *N Engl J Med*. 2011;365:2398-2411.
59. Sadowski CE, Lovric S, Ashraf S, et al. A single-gene cause in 29.5% of cases of steroid-resistant nephrotic syndrome. *J Am Soc Nephrol*. 2015;26:1279-1289.
60. Genovese G, Friedman DJ, Ross MD, et al. Association of trypanolytic ApoL1 variants with kidney disease in African Americans. *Science*. 2010;329:841-845.
61. Parsa A, Kao WH, Xie D, et al. APOL1 risk variants, race, and progression of chronic kidney disease. *N Engl J Med*. 2013;369:2183-2196.
62. Deegens JK, Steenbergen EJ, Wetzels JF. Review on diagnosis and treatment of focal segmental glomerulosclerosis. *Neth J Med*. 2008;66:3-12.
63. Del Rio M, Kaskel F. Evaluation and management of steroid-unresponsive nephrotic syndrome. *Curr Opin Pediatr*. 2008;20:151-156.
64. Korbet SM. Clinical picture and outcome of primary focal segmental glomerulosclerosis. *Nephrol Dial Transplant*. 1999;14(suppl 3):68-73.
65. Braden GL, Mulhern JG, O'Shea MH, et al. Changing incidence of glomerular diseases in adults. *Am J Kidney Dis*. 2000;35:878-883.
66. Beaufils H, Alphonse JC, Guedon J, Legrain M. Focal glomerulosclerosis: natural history and treatment. A report of 70 cases. *Nephron*. 1978;21:75-85.
67. Mongeau JG, Robitaille PO, Clermont MJ, et al. Focal segmental glomerulosclerosis (FSG) 20 years later. From toddler to grown up. *Clin Nephrol*. 1993;40:1-6.
68. Artero M, Biava C, Amend W, et al. Recurrent focal glomerulosclerosis: natural history and response to therapy. *Am J Med*. 1992;92:375-383.
69. Crosson JT. Focal segmental glomerulosclerosis and renal transplantation. *Transplant Proc*. 2007;39:737-743.
70. Fine RN. Recurrence of nephrotic syndrome/focal segmental glomerulosclerosis following renal transplantation in children. *Pediatr Nephrol*. 2007;22:496-502.
71. Stephanian E, Matas AJ, Mauer SM, et al. Recurrence of disease in patients retransplanted for focal segmental glomerulosclerosis. *Transplantation*. 1992;53:755-757.
72. Cameron JS, Senguttuvan P, Hartley B, et al. Focal segmental glomerulosclerosis in fifty-nine renal allografts from a single centre: analysis of risk factors for recurrence. *Transplant Proc*. 1989;21:2117-2118.
73. Schonholzer KW, Waldron M, Magil AB. Intraglomerular foam cells and human focal glomerulosclerosis. *Nephron*. 1992;62:130-136.
74. Howie AJ, Brewer DB. Further studies on the glomerular tip lesion: early and late stages and life table analysis. *J Pathol*. 1985;147:245-255.
75. Magil AB. Focal and segmental glomerulosclerosis. *Mod Pathol*. 1991;4:383-391.
76. Schwartz MM, Korbet SM, Rydell J, et al. Primary focal segmental glomerular sclerosis in adults: prognostic value of histologic variants. *Am J Kidney Dis*. 1995;25:845-852.
77. Wehrmann M, Bohle A, Held H, et al. Long-term prognosis of focal sclerosing glomerulonephritis. An analysis of 250 cases with particular regard to tubulointerstitial changes. *Clin Nephrol*. 1990;33:115-122.
78. Deegens JK, Dijkman HB, Borm GE, et al. Podocyte foot process effacement as a diagnostic tool in focal segmental glomerulosclerosis. *Kidney Int*. 2008;74:1568-1576.
79. Stokes MB, Valeri AM, Markowitz GS, D'Agati VD. Cellular focal segmental glomerulosclerosis: clinical and pathologic features. *Kidney Int*. 2006;70:1783-1792.
80. Kopp JB, Nelson GW, Sampath K, et al. APOL1 genetic variants in focal segmental glomerulosclerosis and HIV-associated nephropathy. *J Am Soc Nephrol*. 2011;22:2129-2137.
81. Detwiler RK, Falk RJ, Hogan SL, Jennette JC. Collapsing glomerulopathy: a clinically and pathologically distinct variant of focal segmental glomerulosclerosis. *Kidney Int*. 1994;45:1416-1424.
82. Singh HK, Baldre LA, McKenney DW, et al. Idiopathic collapsing glomerulopathy in children. *Pediatr Nephrol*. 2000;14:132-137.
83. El-Refaey AM, Kapur G, Jain A, et al. Idiopathic collapsing focal segmental glomerulosclerosis in pediatric patients. *Pediatr Nephrol*. 2007;22:396-402.
84. Clarkson MR, O'Meara YM, Murphy B, et al. Collapsing glomerulopathy—recurrence in a renal allograft. *Nephrol Dial Transplant*. 1998;13:503-506.
85. Albaqumi M, Barisoni L. Current views on collapsing glomerulopathy. *J Am Soc Nephrol*. 2008;19:1276-1281.
86. D'Agati V, Appel GB. Renal pathology of human immunodeficiency virus infection. *Semin Nephrol*. 1998;18:378-395.
87. Ross MJ, Klotman PE. HIV-associated nephropathy. *AIDS*. 2004;18:1089-1099.
88. Nochy D, Glotz D, Dosquet P, et al. Renal lesions associated with human immunodeficiency virus infection: North American vs. European experience. *Adv Nephrol Necker Hosp*. 1993;22:269-286.
89. Markowitz GS, Appel GB, Fine PL, et al. Collapsing focal segmental glomerulosclerosis following treatment with high-dose pamidronate. *J Am Soc Nephrol*. 2001;12:1164-1172.
90. Moudgil A, Nast CC, Bagga A, et al. Association of parvovirus B19 infection with idiopathic collapsing glomerulopathy. *Kidney Int*. 2001;59:2126-2133.
91. Kriz W, Lemley KV. The role of the podocyte in glomerulosclerosis. *Curr Opin Nephrol Hypertens*. 1999;8:489-497.
92. Sakamoto K, Ueno T, Kobayashi N, et al. The direction and role of phenotypic transition between podocytes and parietal epithelial cells in focal segmental glomerulosclerosis. *Am J Physiol Renal Physiol*. 2014;306:F98-F104.
93. Hakroush S, Cebulla A, Schaldecker T, et al. Extensive podocyte loss triggers a rapid parietal epithelial cell response. *J Am Soc Nephrol*. 2014;25:927-938.
94. Barisoni L, Kriz W, Mundel P, D'Agati V. The dysregulated podocyte phenotype: a novel concept in the pathogenesis of collapsing idiopathic focal segmental glomerulosclerosis and HIV-associated nephropathy. *J Am Soc Nephrol*. 1999;10:51-61.
95. Chander P, Soni A, Suri A, et al. Renal ultrastructural markers in AIDS-associated nephropathy. *Am J Pathol*. 1987;126:513-526.
96. Laurinavicius A, Hurwitz S, Rennke HG. Collapsing glomerulopathy in HIV and non-HIV patients: a clinicopathological and follow-up study. *Kidney Int*. 1999;56:2203-2213.
97. Fukuma Y, Hisano S, Segawa Y, et al. Clinicopathologic correlation of C1q nephropathy in children. *Am J Kidney Dis*. 2006;47:412-418.
98. Iskandar SS, Browning MC, Lorentz WB. C1q nephropathy: a pediatric clinicopathological study. *Am J Kidney Dis*. 1991;18:459-465.
99. Jennette JC, Hipp CG. C1q nephropathy: a distinct pathologic entity usually causing nephrotic syndrome. *Am J Kidney Dis*. 1985;6:103-110.
100. Kersnik Levart T, Kenda RB, Avgustin Cavic M, et al. C1q nephropathy in children. *Pediatr Nephrol*. 2005;20:1756-1761.
101. Lau KK, Gaber LW, Delos Santos NM, Wyatt RJ. C1q nephropathy: features at presentation and outcome. *Pediatr Nephrol*. 2005;20:744-749.
102. Markowitz GS, Schwimmer JA, Stokes MB, et al. C1q nephropathy: a variant of focal segmental glomerulosclerosis. *Kidney Int*. 2003;64:1232-1240.
103. Wenderfer SE, Swinford RD, Braun MC. C1q nephropathy in the pediatric population: pathology and pathogenesis. *Pediatr Nephrol*. 2010;25:1385-1396.
104. Gunasekara VN, Sebire NJ, Tullus K. C1q nephropathy in children: clinical characteristics and outcome. *Pediatr Nephrol*. 2014;29:407-413.
105. Hayslett JP, Kashgarian M, Bensch KG, et al. Clinicopathological correlations in the nephrotic syndrome due to primary renal disease. *Medicine (Baltimore)*. 1973;52:93-120.
106. Ramirez F, Brouhard BH, Travis LB, Ellis EN. Idiopathic membranous nephropathy in children. *J Pediatr*. 1982;101:677-681.
107. Wasserstein AG. Membranous glomerulonephritis. *J Am Soc Nephrol*. 1997;8:664-674.
108. Scolari F, Amoroso A, Savoldi S, et al. Familial membranous nephropathy. *J Nephrol*. 1998;11:35-39.
109. Couser WG, Nangaku M. Cellular and molecular biology of membranous nephropathy. *J Nephrol*. 2006;19:699-705.
110. Beck LH Jr, Bonegio RG, Lambeau G, et al. M-type phospholipase A2 receptor as target antigen in idiopathic membranous nephropathy. *N Engl J Med*. 2009;361:11-21.
111. Ronco P, Debiec H, Imai H. Circulating antipodocyte antibodies in membranous nephropathy: pathophysiologic and clinical relevance. *Am J Kidney Dis*. 2013;62:16-19.
112. Hofstra JM, Beck LH Jr, Beck DM, et al. Anti-phospholipase A(2) receptor antibodies correlate with clinical status in idiopathic

- membranous nephropathy. *Clin J Am Soc Nephrol*. 2011;6:1286-1291.
113. Kattah A, Ayalon R, Beck LH Jr, et al. Anti-phospholipase A(2) receptor antibodies in recurrent membranous nephropathy. *Am J Transplant*. 2015;15:1349-1359.
114. Debiec H, Ronco P. Immunopathogenesis of membranous nephropathy: an update. *Semin Immunopathol*. 2014;36:381-397.
115. Tomas NM, Hoxha E, Reinicke AT, et al. Autoantibodies against thrombospondin type 1 domain-containing 7A induce membranous nephropathy. *J Clin Invest*. 2016;126:2519-2532.
116. Tomas NM, Beck LH Jr, Meyer-Schweinger C, et al. Thrombospondin type-1 domain-containing 7A in idiopathic membranous nephropathy. *N Engl J Med*. 2014;371:2277-2287.
117. Debiec H, Guigonis V, Mougenot B, et al. Antenatal membranous glomerulonephritis due to anti-neutral endopeptidase antibodies. *N Engl J Med*. 2002;346:2053-2060.
118. Ronco P, Debiec H. New insights into the pathogenesis of membranous glomerulonephritis. *Curr Opin Nephrol Hypertens*. 2006;15:258-263.
119. Horl WH, Kerjaschki D. Membranous glomerulonephritis (MGN). *J Nephrol*. 2000;13:291-316.
120. Debiec H, Lefeu F, Kemper MJ, et al. Early-childhood membranous nephropathy due to cationic bovine serum albumin. *N Engl J Med*. 2011;364:2101-2110.
121. Takekoshi Y, Tanaka M, Shida N, et al. Strong association between membranous nephropathy and hepatitis-B surface antigenaemia in Japanese children. *Lancet*. 1978;2:1065-1068.
122. Seggie J, Nathoo K, Davies PG. Association of hepatitis B (HBs) antigenaemia and membranous glomerulonephritis in Zimbabwean children. *Nephron*. 1984;38:115-119.
123. Wing AJ, Hutt MS, Kibukamusoke JW. Progression and remission in the nephrotic syndrome associated with quartan malaria in Uganda. *Q J Med*. 1972;41:273-289.
124. Coggins CH, Frommer JP, Glasscock RJ. Membranous nephropathy. *Sem Nephrol*. 1982;2:264-273.
125. Markowitz GS, D'Agati VD. Membranous glomerulonephritis. In: Jennette JC, Olson JL, Silva FG, A'gati VD, eds. *Heptinstall's Pathology of the Kidney*. 7th ed. Philadelphia, PA: Wolters Kluwer; 2015:255-300.
126. Schwartz MM. Membranous glomerulonephritis. In: Jennette JC, Olson JL, Schwartz MM, Silva FG, eds. *Heptinstall's Pathology of the Kidney*. 6th ed. Philadelphia, PA: Lippincott Williams & Wilkins; 2007:205-251.
127. Schieppati A, Mosconi L, Perna A, et al. Prognosis of untreated patients with idiopathic membranous nephropathy. *N Engl J Med*. 1993;329:85-89.
128. Donadio JV Jr, Torres VE, Velosa JA, et al. Idiopathic membranous nephropathy: the natural history of untreated patients. *Kidney Int*. 1988;33:708-715.
129. Noel LH, Zanetti M, Droz D, Barbanell C. Long-term prognosis of idiopathic membranous glomerulonephritis. Study of 116 untreated patients. *Am J Med*. 1979;66:82-90.
130. Poduval RD, Josephson MA, Javaid B. Treatment of de novo and recurrent membranous nephropathy in renal transplant patients. *Semin Nephrol*. 2003;23:392-399.
131. Ehrenreich T, Churg J. Pathology of membranous nephropathy. *Pathol Annu*. 1968;3:145-186.
132. Jennette JC, Iskandar SS, Dalldorf FG. Pathologic differentiation between lupus and nonlupus membranous glomerulopathy. *Kidney Int*. 1983;24:377-385.
133. Svbodova B, Honsova E, Ronco P, et al. Kidney biopsy is a sensitive tool for retrospective diagnosis of PLA2R-related membranous nephropathy. *Nephrol Dial Transplant*. 2013;28:1839-1844.
134. Larsen CP, Messias NC, Silva FG, et al. Determination of primary versus secondary membranous glomerulopathy utilizing phospholipase A2 receptor staining in renal biopsies. *Mod Pathol*. 2013;26:709-715.
135. Larsen CP, Walker PD. Phospholipase A2 receptor (PLA2R) staining is useful in the determination of de novo versus recurrent membranous glomerulopathy. *Transplantation*. 2013;95:1259-1262.
136. Kearney N, Podolak J, Matsumura L, et al. Patterns of IgG subclass deposits in membranous glomerulonephritis in renal allografts. *Transplant Proc*. 2011;43:3743-3746.
137. Comparison of idiopathic and systemic lupus erythematosus-associated membranous glomerulonephropathy in children. The Southwest Pediatric Nephrology Study Group. *Am J Kidney Dis*. 1986;7:115-124.
138. Llach F, Arieff AI, Massry SG. Renal vein thrombosis and nephrotic syndrome. A prospective study of 36 adult patients. *Ann Intern Med*. 1975;83:8-14.
139. Katz A, Fish AJ, Santamaria P, et al. Role of antibodies to tubulointerstitial nephritis antigen in human anti-tubular basement membrane nephritis associated with membranous nephropathy. *Am J Med*. 1992;93:691-698.
140. Incidence of reported ESRD by primary diagnosis. USRDS. United States Renal Data System annual data report. 2015 [https://wwwUSRDS.org/2015/download/vol2USRDS\\_ESRD\\_15.pdf](https://wwwUSRDS.org/2015/download/vol2USRDS_ESRD_15.pdf).
141. Dronavalli S, Duka I, Bakris GL. The pathogenesis of diabetic nephropathy. *Nat Clin Pract Endocrinol Metab*. 2008;4:444-452.
142. Vora JP, Ibrahim H. Clinical manifestations and natural history of diabetic nephropathy. In: Johnson RJ, Feehally J, eds. *Comprehensive Clinical Nephrology*. 2nd ed. Edinberg, NY: Mosby; 2003:425.
143. Rajashekhar A, Perazella MA, Crowley S. Systemic diseases with renal manifestations. *Prim Care*. 2008;35:297-328, vi-vii.
144. D'Agati V, Schmidt AM. RAGE and the pathogenesis of chronic kidney disease. *Nat Rev Nephrol*. 2010;6:352-360.
145. Ritz E, Stefanski A. Diabetic nephropathy in type II diabetes. *Am J Kidney Dis*. 1996;27:167-194.
146. Fioretto P, Mauer M. Histopathology of diabetic nephropathy. *Semin Nephrol*. 2007;27:195-207.
147. Mauer SM, Steffes MW, Ellis EN, et al. Structural-functional relationships in diabetic nephropathy. *J Clin Invest*. 1984;74:1143-1155.
148. Mauer SM, Steffes MW, Connell J, et al. The development of lesions in the glomerular basement membrane and mesangium after transplantation of normal kidneys to diabetic patients. *Diabetes*. 1983;32:948-952.
149. Tervaert TW, Mooyaart AL, Amann K, et al. Pathologic classification of diabetic nephropathy. *J Am Soc Nephrol*. 2010;21:556-563.
150. Markowitz GS, Lin J, Valeri AM, et al. Idiopathic nodular glomerulosclerosis is a distinct clinicopathologic entity linked to hypertension and smoking. *Hum Pathol*. 2002;33:826-835.
151. Najafian B, Alpers CE, Fogo AB. Pathology of human diabetic nephropathy. *Contrib Nephrol*. 2011;170:36-47.
152. Sharma SG, Bomback AS, Radhakrishnan J, et al. The modern spectrum of renal biopsy findings in patients with diabetes. *Clin J Am Soc Nephrol*. 2013;8:1718-1724.
153. Nasr SH, D'Agati VD, Said SM, et al. Pauci-immune crescentic glomerulonephritis superimposed on diabetic glomerulosclerosis. *Clin J Am Soc Nephrol*. 2008;3:1282-1288.
154. Elfenbein IB, Reyes JW. Crescents in diabetic glomerulopathy. Incidence and clinical significance. *Lab Invest*. 1975;33:687-695.
155. Westermark P, Benson MD, Buxbaum JN, et al. A primer of amyloid nomenclature. *Amyloid*. 2007;14:179-183.
156. Sethi S, Vrana JA, Theis JD, et al. Laser microdissection and mass spectrometry-based proteomics aids the diagnosis and typing of renal amyloidosis. *Kidney Int*. 2012;82:226-234.
157. Said SM, Sethi S, Valeri AM, et al. Renal amyloidosis: origin and clinicopathologic correlations of 474 recent cases. *Clin J Am Soc Nephrol*. 2013;8:151-1523.
158. Pepys MB. Amyloidosis. *Annu Rev Med*. 2006;57:223-241.
159. Sayed RH, Hawkins PN, Lachmann HJ. Emerging treatments for amyloidosis. *Kidney Int*. 2015;87:516-526.
160. Falk RH, Comenzo RL, Skinner M. The systemic amyloidoses. *N Engl J Med*. 1997;337:898-909.
161. Buxbaum JN. The systemic amyloidoses. *Curr Opin Rheumatol*. 2004;16:67-75.
162. Obici L, Perfetti V, Palladini G, et al. Clinical aspects of systemic amyloid diseases. *Biochim Biophys Acta*. 2005;1753:11-22.
163. Westermark GT, Fandrich M, Westermark P. AA amyloidosis: pathogenesis and targeted therapy. *Annu Rev Pathol*. 2015;10:321-344.
164. Husby G, Marhaug G, Dowton B, et al. Serum amyloid A (SAA): biochemistry, genetics and the pathogenesis of AA amyloidosis. *Amyloid*. 1994;1:119-137.
165. Uhlar CM, Whitehead AS. Serum amyloid A, the major vertebrate acute-phase reactant. *Eur J Biochem*. 1999;265:501-523.
166. Benson MD. The hereditary amyloidoses. *Best Pract Res Clin Rheumatol*. 2003;17:909-927.
167. Padeh S. Periodic fever syndromes. *Pediatr Clin North Am*. 2005;52:577-609, vii.
168. Said SM, Sethi S, Valeri AM, et al. Characterization and outcomes of renal leukocyte chemotactic factor 2-associated amyloidosis. *Kidney Int*. 2014;86:370-377.
169. Larsen CP, Kossmann RJ, Beggs ML, et al. Clinical, morphologic, and genetic features of renal leukocyte chemotactic factor 2 amyloidosis. *Kidney Int*. 2014;86:378-382.
170. Gejyo F, Narita I. Current clinical and pathogenetic understanding of beta2-m amyloidosis in long-term haemodialysis patients. *Nephrology (Carlton)*. 2003;8(suppl):S 45-S49.
171. Kyle RA, Gertz MA. Primary systemic amyloidosis: clinical and laboratory features in 474 cases. *Semin Hematol*. 1995;32:45-59.
172. Bohle A, Wehrmann M, Eissele R, et al. The long-term prognosis of AA and AL renal amyloidosis and the pathogenesis of chronic renal failure in renal amyloidosis. *Pathol Res Pract*. 1993;189:316-331.
173. Demer LM. Amyloidosis-associated kidney disease. *J Am Soc Nephrol*. 2006;17:3458-3471.
174. Herrera GA, Picken MM. Renal diseases associated with plasma cell dyscrasias, amyloidoses, and Waldenström macroglobulinemia. In: Jennette JC, Olson JL, Silva FG, A'gati VD, eds. *Heptinstall's Pathology of the Kidney*. 7th ed. Philadelphia, PA: Wolters Kluwer; 2015:951-1014.
175. Satoskar AA, Burdge K, Cowden DJ, et al. Typing of amyloidosis in renal biopsies: diagnostic pitfalls. *Arch Pathol Lab Med*. 2007;131:917-922.
176. Yang GC, Nieto R, Stachura I, Gallo GR. Ultrastructural immunohistochemical localization of polyclonal IgG, C3, and amyloid P component on the congo

- red-negative amyloid-like fibrils of fibrillary glomerulopathy. *Am J Pathol*. 1992;141:409-419.
177. Dyck RF, Lockwood CM, Kershaw M, et al. Amyloid P-component is a constituent of normal human glomerular basement membrane. *J Exp Med*. 1980;152:1162-1174.
178. Alpers CE, Kowalewska J. Fibrillary glomerulonephritis and immunotactoid glomerulopathy. *J Am Soc Nephrol*. 2008;19:34-37.
179. Brady HR. Fibrillary glomerulopathy. *Kidney Int*. 1998;53:1421-1429.
180. Fogo A, Qureshi N, Horn RG. Morphologic and clinical features of fibrillary glomerulonephritis versus immunotactoid glomerulopathy. *Am J Kidney Dis*. 1993;22:367-377.
181. Iskandar SS, Falk RJ, Jennette JC. Clinical and pathologic features of fibrillary glomerulonephritis. *Kidney Int*. 1992;42:1401-1407.
182. Rosenstock JL, Markowitz GS, Valeri AM, et al. Fibrillary and immunotactoid glomerulonephritis: distinct entities with different clinical and pathologic features. *Kidney Int*. 2003;63:1450-1461.
183. Devaney K, Sabnis SG, Antonovich TT. Nonamyloidotic fibrillary glomerulopathy, immunotactoid glomerulopathy, and the differential diagnosis of filamentous glomerulopathies. *Mod Pathol*. 1991;4:36-45.
184. Nasr SH, Valeri AM, Cornell LD, et al. Fibrillary glomerulonephritis: a report of 66 cases from a single institution. *Clin J Am Soc Nephrol*. 2011;6:775-784.
185. Pronovost PH, Brady HR, Gunning ME, et al. Clinical features, predictors of disease progression and results of renal transplantation in fibrillary/immunotactoid glomerulopathy. *Nephrol Dial Transplant*. 1996;11:837-842.
186. Samaniego M, Nadasy GM, Laszik Z, Nadasy T. Outcome of renal transplantation in fibrillary glomerulonephritis. *Clin Nephrol*. 2001;55:159-166.
187. Churg J, Venkateshwaran VS. Fibrillary glomerulonephritis without immunoglobulin deposits in the kidney. *Kidney Int*. 1993;44:837-842.
188. Duffy JL, Khurana E, Susin M, et al. Fibrillary renal deposits and nephritis. *Am J Pathol*. 1983;113:279-290.
189. Lin J, Markowitz GS, Valeri AM, et al. Renal monoclonal immunoglobulin deposition disease: the disease spectrum. *J Am Soc Nephrol*. 2001;12:1482-1492.
190. Herrera GA, Turbat-Herrera EA. Renal diseases with organized deposits: an algorithmic approach to classification and clinicopathologic diagnosis. *Arch Pathol Lab Med*. 2010;134:512-531.
191. Nasr SH, Valeri AM, Cornell LD, et al. Renal monoclonal immunoglobulin deposition disease: a report of 64 patients from a single institution. *Clin J Am Soc Nephrol*. 2012;7:231-239.
192. Buxbaum J, Gallo G. Nonamyloidotic monoclonal immunoglobulin deposition disease. Light-chain, heavy-chain, and light- and heavy-chain deposition diseases. *Hematol Oncol Clin North Am*. 1999;13:1235-1248.
193. Preud'homme JL, Aucouturier P, Touchard G, et al. Monoclonal immunoglobulin deposition disease (Randall type). Relationship with structural abnormalities of immunoglobulin chains. *Kidney Int*. 1994;46:965-972.
194. Sanders PW, Herrera GA. Monoclonal immunoglobulin light chain-related renal diseases. *Semin Nephrol*. 1993;13:324-341.
195. Ronco P, Plaisier E, Mougenot B, Aucouturier P. Immunoglobulin light (heavy)-chain deposition disease: from molecular medicine to pathophysiology-driven therapy. *Clin J Am Soc Nephrol*. 2006;1:1342-1350.
196. Pozzi C, D'Amico M, Fogazzi GB, et al. Light chain deposition disease with renal involvement: clinical characteristics and prognostic factors. *Am J Kidney Dis*. 2003;42:1154-1163.
197. Shimamura T, Weiss LS, Walker JA, et al. Light chain nephropathy in a 19-month-old boy with AIDS. *Acta Pathol Jpn*. 1992;42:500-503.
198. Leung N, Lager DJ, Gertz MA, et al. Long-term outcome of renal transplantation in light-chain deposition disease. *Am J Kidney Dis*. 2004;43:147-153.
199. Pozzi C, Fogazzi GB, Banfi G, et al. Renal disease and patient survival in light chain deposition disease. *Clin Nephrol*. 1995;43:281-287.
200. Herrera GA, Russell WJ, Isaac J, et al. Glomerulopathic light chain-mesangial cell interactions modulate in vitro extracellular matrix remodeling and reproduce mesangiopathic findings documented in vivo. *Ultrastruct Pathol*. 1999;23:107-126.
201. Zhu L, Herrera GA, Murphy-Ullrich JE, et al. Pathogenesis of glomerulosclerosis in light chain deposition disease. Role for transforming growth factor-beta. *Am J Pathol*. 1995;147:375-385.
202. Aucouturier P, Khamliche AA, Touchard G, et al. Brief report: heavy-chain deposition disease. *N Engl J Med*. 1993;329:1389-1393.
203. Kambham N, Markowitz GS, Appel GB, et al. Heavy chain deposition disease: the disease spectrum. *Am J Kidney Dis*. 1999;33:954-962.
204. Nasr SH, Satoskar A, Markowitz GS, et al. Proliferative glomerulonephritis with monoclonal IgG deposits. *J Am Soc Nephrol*. 2009;20:2055-2064.
205. Nasr SH, Sethi S, Cornell LD, et al. Proliferative glomerulonephritis with monoclonal IgG deposits recurs in the allograft. *Clin J Am Soc Nephrol*. 2011;6:122-132.
206. Larsen CP, Ambuzs JM, Bonsib SM, et al. Membranous-like glomerulopathy with masked IgG kappa deposits. *Kidney Int*. 2014;86:154-161.
207. Habib R. Nephrotic syndrome in the 1st year of life. *Pediatr Nephrol*. 1993;7:347-353.
208. Hinkes BG, Mucha B, Vlangos CN, et al. Nephrotic syndrome in the first year of life: two thirds of cases are caused by mutations in 4 genes (NPHS1, NPHS2, WT1, and LAMB2). *Pediatrics*. 2007;119:e907-e919.
209. Besbas N, Bayrakci US, Kale G, et al. Cytomegalovirus-related congenital nephrotic syndrome with diffuse mesangial sclerosis. *Pediatr Nephrol*. 2006;21:740-742.
210. Ramirez-Seijas F, Granado-Villar D, Cepeiro-Akselrad A, et al. Congenital nephrotic syndrome. *Int Pediatr*. 2000;15:121-122.
211. Kari JA, Montini G, Bockenhauer D, et al. Clinico-pathological correlations of congenital and infantile nephrotic syndrome over twenty years. *Pediatr Nephrol*. 2014;29:2173-2180.
212. Liapis H. Molecular pathology of nephrotic syndrome in childhood: a contemporary approach to diagnosis. *Pediatr Dev Pathol*. 2008;11:154-163.
213. Frishberg Y, Ben-Neriah Z, Suvanto M, et al. Misleading findings of homozygosity mapping resulting from three novel mutations in NPHS1 encoding nephrin in a highly inbred community. *Genet Med*. 2007;9:180-184.
214. Kestila M, Lenkkari U, Mannikko M, et al. Positionally cloned gene for a novel glomerular protein—nephrin—is mutated in congenital nephrotic syndrome. *Mol Cell*. 1998;1:575-582.
215. Kestila M, Mannikko M, Holmberg C, et al. Congenital nephrotic syndrome of the Finnish type maps to the long arm of chromosome 19. *Am J Hum Genet*. 1994;54:757-764.
216. Ruotsalainen V, Ljungberg P, Wartiovaara J, et al. Nephrin is specifically located at the slit diaphragm of glomerular podocytes. *Proc Natl Acad Sci USA*. 1999;96:7962-7967.
217. Jackson LW. Congenital nephrotic syndrome. *Neonatal Netw*. 2007;26:47-55.
218. Patrakka J, Ruotsalainen V, Reponen P, et al. Recurrence of nephrotic syndrome in kidney grafts of patients with congenital nephrotic syndrome of the Finnish type: role of nephrin. *Transplantation*. 2002;73:394-403.
219. Holmberg C, Jalanko H. Congenital nephrotic syndrome and recurrence of proteinuria after renal transplantation. *Pediatr Nephrol*. 2014;29:2309-2317.
220. Habib R, Gubler MC, Antignac C, Gagnadoux MF. Diffuse mesangial sclerosis: a congenital glomerulopathy with nephrotic syndrome. *Adv Nephrol Necker Hosp*. 1993;22:43-57.
221. Yang Y, Jeanpierre C, Dressler GR, et al. WT1 and PAX-2 podocyte expression in Denys-Drash syndrome and isolated diffuse mesangial sclerosis. *Am J Pathol*. 1999;154:181-192.
222. Lipska BS, Ranchor B, Iatropoulos P, et al. Genotype-phenotype associations in WT1 glomerulopathy. *Kidney Int*. 2014;85:1169-1178.
223. Gbadegesin R, Hinkes BG, Hoskins BE, et al. Mutations in PLCE1 are a major cause of isolated diffuse mesangial sclerosis (IDMS). *Nephrol Dial Transplant*. 2008;23:1291-1297.
224. Montseny JJ, Meyrier A, Kleinknecht D, Callard P. The current spectrum of infectious glomerulonephritis. Experience with 76 patients and review of the literature. *Medicine (Baltimore)*. 1995;74:63-73.
225. Rodriguez-Iturbe B. Acute poststreptococcal glomerulonephritis. In: Schrier RW, Gottschalk CW, eds. *Diseases of the Kidney*. 5th ed. Boston, MA: Little, Brown & Co; 1993:1715-1730.
226. Satoskar AA, Nadasy T, Silva FG. Acute postinfectious glomerulonephritis and glomerulonephritis caused by persistent bacterial infection. In: Jennette JC, Olson JL, Silva FG, Agati VD, eds. *Heptinstall's Pathology of the Kidney*. 7th ed. Philadelphia, PA: Lippincott Williams & Wilkins; 2015:367-436.
227. Nasr SH, Fidler ME, Valeri AM, et al. Postinfectious glomerulonephritis in the elderly. *J Am Soc Nephrol*. 2011;22:187-195.
228. Kambham N. Postinfectious glomerulonephritis. *Adv Anat Pathol*. 2012;19:338-347.
229. Yoshizawa N. Acute glomerulonephritis. *Intern Med*. 2000;39:687-694.
230. Rodriguez-Iturbe B, Musser JM. The current state of poststreptococcal glomerulonephritis. *J Am Soc Nephrol*. 2008;19:1855-1864.
231. Ferrario F, Kourilsky O, Morel-Maroger L. Acute endocapillary glomerulonephritis in adults: a histologic and clinical comparison between patients with and without initial acute renal failure. *Clin Nephrol*. 1983;19:17-23.
232. Melby PC, Musick WD, Luger AM, Khanna R. Poststreptococcal glomerulonephritis in the elderly. Report of a case and review of the literature. *Am J Nephrol*. 1987;7:235-240.
233. Dodge WF, Spargo BH, Bass JA, Travis LB. The relationship between the clinical and pathologic features of poststreptococcal glomerulonephritis. A study of the early natural history. *Medicine (Baltimore)*. 1986;47:227-267.
234. Sethi S, Fervenza FC, Zhang Y, et al. Atypical postinfectious glomerulonephritis is associated with abnormalities in the alternative pathway of complement. *Kidney Int*. 2013;83:293-299.
235. Prasto J, Kaplan BS, Russo P, et al. Streptococcal infection as possible trigger for

- dense deposit disease (C3 glomerulopathy). *Eur J Pediatr.* 2014;173:767-772.
236. Vernon KA, Goicoechea de Jorge E, Hall AE, et al. Acute presentation and persistent glomerulonephritis following streptococcal infection in a patient with heterozygous complement factor H-related protein 5 deficiency. *Am J Kidney Dis.* 2012;60:121-125.
237. Stratta P, Musetti C, Barreca A, Mazzucco G. New trends of an old disease: the acute post infectious glomerulonephritis at the beginning of the new millennium. *J Nephrol.* 2014;27:229-239.
238. Nast CC. Infection-related glomerulonephritis: changing demographics and outcomes. *Adv Chronic Kidney Dis.* 2012;19:68-75.
239. Nasr SH, D'Agati VD. IgA-dominant postinfectious glomerulonephritis: a new twist on an old disease. *Nephron Clin Pract.* 2011;119:c18-c25, discussion c26.
240. Haas M, Racusen LC, Bagnasco SM. IgA-dominant postinfectious glomerulonephritis: a report of 13 cases with common ultrastructural features. *Hum Pathol.* 2008;39:1309-1316.
241. Koyama A, Kobayashi M, Yamaguchi N, et al. Glomerulonephritis associated with MRSA infection: a possible role of bacterial superantigen. *Kidney Int.* 1995;47:207-216.
242. Koyama A, Sharmin S, Sakurai H, et al. *Staphylococcus aureus* cell envelope antigen is a new candidate for the induction of IgA nephropathy. *Kidney Int.* 2004;66:121-132.
243. Nasr SH, Markowitz GS, Stokes MB, et al. Acute postinfectious glomerulonephritis in the modern era: experience with 86 adults and review of the literature. *Medicine (Baltimore).* 2008;87:21-32.
244. Satoskar AA, Molenda M, Scipio P, et al. Henoch-Schonlein purpura-like presentation in IgA-dominant *Staphylococcus* infection—associated glomerulonephritis—a diagnostic pitfall. *Clin Nephrol.* 2013;79:302-312.
245. Haas M. Postinfectious glomerulonephritis complicating diabetic nephropathy: a frequent association, but how clinically important? *Hum Pathol.* 2003;34:1225-1227.
246. Wen YK, Chen ML. Discrimination between postinfectious IgA-dominant glomerulonephritis and idiopathic IgA nephropathy. *Ren Fail.* 2010;32:572-577.
247. Walker PD, Ferrario F, Joh K, Bonsib SM. Dense deposit disease is not a membranoproliferative glomerulonephritis. *Mod Pathol.* 2007;20:605-616.
248. Anders D, Agricola B, Sippel M, Thoenes W. Basement membrane changes in membranoproliferative glomerulonephritis. II. Characterization of a third type by silver impregnation of ultra thin sections. *Virchows Arch A Pathol Anat Histol.* 1977;376:1-19.
249. Burkholder PM, Marchand A, Krueger RP. Mixed membranous and proliferative glomerulonephritis. A correlative light, immunofluorescence, and electron microscopic study. *Lab Invest.* 1970;23:459-479.
250. Strife CF, Jackson EC, McAdams AJ. Type III membranoproliferative glomerulonephritis: long-term clinical and morphologic evaluation. *Clin Nephrol.* 1984;21:323-334.
251. Fakhouri F, Fremeaux-Bacchi V, Noel LH, et al. C3 glomerulopathy: a new classification. *Nat Rev Nephrol.* 2010;6:494-499.
252. Servais A, Fremeaux-Bacchi V, Lequintrec M, et al. Primary glomerulonephritis with isolated C3 deposits: a new entity which shares common genetic risk factors with haemolytic uraemic syndrome. *J Med Genet.* 2007;44:193-199.
253. Bomba AS, Appel GB. Pathogenesis of the C3 glomerulopathies and reclassification of MPGN. *Nat Rev Nephrol.* 2012;8:634-642.
254. Pickering MC, D'Agati VD, Nester CM, et al. C3 glomerulopathy: consensus report. *Kidney Int.* 2013;84:1079-1089.
255. Hou J, Markowitz GS, Bomba AS, et al. Toward a working definition of C3 glomerulopathy by immunofluorescence. *Kidney Int.* 2014;85:450-456.
256. Cook HT, Pickering MC. Histopathology of MPGN and C3 glomerulopathies. *Nat Rev Nephrol.* 2015;11:14-22.
257. Servais A, Noel LH, Roumenina LT, et al. Acquired and genetic complement abnormalities play a critical role in dense deposit disease and other C3 glomerulopathies. *Kidney Int.* 2012;82:454-464.
258. Barbour TD, Pickering MC, Terence Cook H. Dense deposit disease and C3 glomerulopathy. *Semin Nephrol.* 2013;33:493-507.
259. Gale DP, de Jorge EG, Cook HT, et al. Identification of a mutation in complement factor H-related protein 5 in patients of Cypriot origin with glomerulonephritis. *Lancet.* 2010;376:794-801.
260. Bomba AS, Smith RJ, Barile GR, et al. Eculizumab for dense deposit disease and C3 glomerulonephritis. *Clin J Am Soc Nephrol.* 2012;7:748-756.
261. Smith RJ, Alexander J, Barlow PN, et al. New approaches to the treatment of dense deposit disease. *J Am Soc Nephrol.* 2007;18:2447-2456.
262. Xiao X, Pickering MC, Smith RJ. C3 glomerulopathy: the genetic and clinical findings in dense deposit disease and C3 glomerulonephritis. *Semin Thromb Hemost.* 2014;40:465-471.
263. Appel GB, Cook HT, Hageman G, et al. Membranoproliferative glomerulonephritis type II (dense deposit disease): an update. *J Am Soc Nephrol.* 2005;16:1392-1403.
264. Walker PD. Dense deposit disease: new insights. *Curr Opin Nephrol Hypertens.* 2007;16:204-212.
265. Abrera-Abeleda MA, Nishimura C, Smith JL, et al. Variations in the complement regulatory genes factor H (CFH) and factor H related 5 (CFHR5) are associated with membranoproliferative glomerulonephritis type II (dense deposit disease). *J Med Genet.* 2006;43:582-589.
266. Gold B, Merriam JE, Zernant J, et al. Variation in factor B (BF) and complement component 2 (C2) genes is associated with age-related macular degeneration. *Nat Genet.* 2006;38:458-462.
267. Mathieson PW, Peters DK. Lipodystrophy in MCGN type II: the clue to links between the adipocyte and the complement system. *Nephrol Dial Transplant.* 1997;12:1804-1806.
268. Misra A, Peethambaran A, Garg A. Clinical features and metabolic and autoimmune derangements in acquired partial lipodystrophy: report of 35 cases and review of the literature. *Medicine (Baltimore).* 2004;83:18-34.
269. Zipfel PF, Heinen S, Jozsi M, Skerka C. Complement and diseases: defective alternative pathway control results in kidney and eye diseases. *Mol Immunol.* 2006;43:97-106.
270. Kher KK, Makker SP, Aikawa M, Kirson JJ. Regression of dense deposits in type II membranoproliferative glomerulonephritis: case report of clinical course in a child. *Clin Nephrol.* 1982;17:100-103.
271. McEnery PT, McAdams AJ. Regression of membranoproliferative glomerulonephritis type II (dense deposit disease): observations in six children. *Am J Kidney Dis.* 1988;12:138-146.
272. Figueiras ML, Fremeaux-Bacchi V, Rabant M, et al. Heterogeneous histologic and clinical evolution in 3 cases of dense deposit disease with long-term follow-up. *Hum Pathol.* 2014;45:2326-2333.
273. Hariharan S. Recurrent and de novo diseases after renal transplantation. *Semin Dial.* 2000;13:195-199.
274. Sethi S, Sukov WR, Zhang Y, et al. Dense deposit disease associated with monoclonal gammopathy of undetermined significance. *Am J Kidney Dis.* 2010;56:977-982.
275. Habib R, Kleinknecht C, Gubler MC, Levy M. Idiopathic membranoproliferative glomerulonephritis in children. Report of 105 cases. *Clin Nephrol.* 1973;1:194-214.
276. Sethi S, Gamez JD, Vrana JA, et al. Glomeruli of Dense Deposit Disease contain components of the alternative and terminal complement pathway. *Kidney Int.* 2009;75:952-960.
277. Sethi S, Fervenza FC, Zhang Y, et al. C3 glomerulonephritis: clinicopathological findings, complement abnormalities, glomerular proteomic profile, treatment, and follow-up. *Kidney Int.* 2012;82:465-473.
278. Zhang Y, Nester CM, Martin B, et al. Defining the complement biomarker profile of C3 glomerulopathy. *Clin J Am Soc Nephrol.* 2014;9:1876-1882.
279. Sethi S, Fervenza FC. Membranoproliferative glomerulonephritis—a new look at an old entity. *N Engl J Med.* 2012;366:1119-1131.
280. Smith KD, Alpers CE. Pathogenic mechanisms in membranoproliferative glomerulonephritis. *Curr Opin Nephrol Hypertens.* 2005;14:396-403.
281. Fervenza FC, Sethi S, Glasscock RJ. Idiopathic membranoproliferative glomerulonephritis: does it exist? *Nephrol Dial Transplant.* 2012;27:4288-4294.
282. West CD. Idiopathic membranoproliferative glomerulonephritis in childhood. *Pediatr Nephrol.* 1992;6:96-103.
283. D'Amico G, Ferrario F. Mesangiocapillary glomerulonephritis. *J Am Soc Nephrol.* 1992;2:S159-S166.
284. Zhou XJ, Silva FG. Membranoproliferative glomerulonephritis. In: Jennette JC, Olson JL, Silva FG, D'Amico G, eds. *Heptinstall's Pathology of the Kidney.* 7th ed. Philadelphia, PA: Wolters Kluwer; 2015:301-340.
285. Schmitt H, Bohle A, Reineke T, et al. Long-term prognosis of membranoproliferative glomerulonephritis type I. Significance of clinical and morphological parameters: an investigation of 220 cases. *Nephron.* 1990;55:242-250.
286. Lien YH, Scott K. Long-term cyclophosphamide treatment for recurrent type I membranoproliferative glomerulonephritis after transplantation. *Am J Kidney Dis.* 2000;35:539-543.
287. Lorenz EC, Sethi S, Leung N, et al. Recurrent membranoproliferative glomerulonephritis after kidney transplantation. *Kidney Int.* 2010;77:721-728.
288. Strife CF, McEnery PT, McAdams AJ, West CD. Membranoproliferative glomerulonephritis with disruption of the glomerular basement membrane. *Clin Nephrol.* 1977;7:65-72.
289. Haas M. Histology and immunohistology of IgA nephropathy. *J Nephrol.* 2005;18:676-680.
290. Tumlin JA, Madaio MP, Hennigar R. Idiopathic IgA nephropathy: pathogenesis, histopathology, and therapeutic options. *Clin J Am Soc Nephrol.* 2007;2:1054-1061.
291. Beerman I, Novak J, Wyatt RJ, et al. The genetics of IgA nephropathy. *Nat Clin Pract Nephrol.* 2007;3:325-338.
292. Hsu SI, Ramirez SB, Winn MP, et al. Evidence for genetic factors in the development and progression of IgA nephropathy. *Kidney Int.* 2000;57:1818-1835.
293. Scilaro F. Familial IgA nephropathy. *J Nephrol.* 1999;12:213-219.
294. Gharavi AG, Kiryluk K, Choi M, et al. Genome-wide association study identifies

- susceptibility loci for IgA nephropathy. *Nat Genet*. 2011;43:321-327.
295. Kiryluk K, Novak J. The genetics and immunobiology of IgA nephropathy. *J Clin Invest*. 2014;124:2325-2332.
296. Davin JC, Ten Berge IJ, Weening JJ. What is the difference between IgA nephropathy and Henoch-Schönlein purpura nephritis? *Kidney Int*. 2001;59:823-834.
297. Haas M. IgA nephropathy and IgA vasculitis (Henoch-Schönlein purpura nephritis). In: Jennette JC, Olson JL, Silva FG, Agati VD, eds. *Heptinstall's Pathology of the Kidney*. 7th ed. Philadelphia, PA: Wolters Kluwer; 2015:463-524.
298. Barratt J, Smith AC, Molyneux K, Feehally J. Immunopathogenesis of IgAN. *Semin Immunopathol*. 2007;29:427-443.
299. Novak J, Julian BA, Tomana M, Mestecky J. IgA glycosylation and IgA immune complexes in the pathogenesis of IgA nephropathy. *Semin Nephrol*. 2008;28:78-87.
300. Zhao N, Hou P, Lv J, et al. The level of galactose-deficient IgA1 in the sera of patients with IgA nephropathy is associated with disease progression. *Kidney Int*. 2012;82:790-796.
301. D'Amico G. Natural history of idiopathic IgA nephropathy: role of clinical and histological prognostic factors. *Am J Kidney Dis*. 2000;36:227-237.
302. Niaudet P, Murcia I, Beaufils H, et al. Primary IgA nephropathies in children: prognosis and treatment. *Adv Nephrol Necker Hosp*. 1993;22:121-140.
303. Donadio JV Jr, Grande JP. Immunoglobulin A nephropathy: a clinical perspective. *J Am Soc Nephrol*. 1997;8:1324-1332.
304. Floege J. Recurrent IgA nephropathy after renal transplantation. *Semin Nephrol*. 2004;24:287-291.
305. Roberts IS. Pathology of IgA nephropathy. *Nat Rev Nephrol*. 2014;10:445-454.
306. Haas M. Histologic subclassification of IgA nephropathy: a clinicopathologic study of 244 cases. *Am J Kidney Dis*. 1997;29:829-842.
307. Working Group of the International IgA ANN, the Renal Pathology Society, Catrnan DC, Coppo R, et al. The Oxford classification of IgA nephropathy: rationale, clinicopathological correlations, and classification. *Kidney Int*. 2009;76:534-545.
308. Haas M, Rastaldi MP, Fervenza FC. Histologic classification of glomerular diseases: clinicopathologic correlations, limitations exposed by validation studies, and suggestions for modification. *Kidney Int*. 2014;85:779-793.
309. Faile-Kuyper EH, Kater L, Kuijten RH, et al. Occurrence of vascular IgA deposits in clinically normal skin of patients with renal disease. *Kidney Int*. 1976;9:424-429.
310. Thompson AJ, Chan YL, Woodroffe AJ, et al. Vascular IgA deposits in clinically normal skin of patients with renal disease. *Pathology*. 1980;12:407-413.
311. Sanders JT, Wyatt RJ. IgA nephropathy and Henoch-Schönlein purpura nephritis. *Curr Opin Pediatr*. 2008;20:163-170.
312. Waldo FB. Is Henoch-Schönlein purpura the systemic form of IgA nephropathy? *Am J Kidney Dis*. 1988;12:373-377.
313. Jennette JC, Nickeleit V. Anti-glomerular basement membrane glomerulonephritis and Goodpasture's syndrome. In: Jennette JC, Olson JL, Silva FG, Agati VD, eds. *Heptinstall's Pathology of the Kidney*. 7th ed. Philadelphia, PA: Wolters Kluwer; 2015:657-684.
314. Nachman PH, Jennette JC, Falk RJ. Rapidly progressive glomerulonephritis and crescentic glomerulonephritis. In: Brenner M, ed. *Brenner and Rector's the Kidney*. 8th ed. Philadelphia, PA: WB Saunders; 2006:1034-1046.
315. Fischer EG, Lager DJ. Anti-glomerular basement membrane glomerulonephritis: a morphologic study of 80 cases. *Am J Clin Pathol*. 2006;125:445-450.
316. Hudson BG, Kalluri R, Gunwar S, et al. Molecular characteristics of the Goodpasture autoantigen. *Kidney Int*. 1993;43:135-139.
317. Kalluri R, Wilson CB, Weber M, et al. Identification of the alpha 3 chain of type IV collagen as the common autoantigen in ant basement membrane disease and Goodpasture syndrome. *J Am Soc Nephrol*. 1995;6:1178-1185.
318. Pedchenko V, Bondar O, Fogo AB, et al. Molecular architecture of the Goodpasture autoantigen in anti-GBM nephritis. *N Engl J Med*. 2010;363:343-354.
319. Cui Z, Zhao MH. Advances in human anti-glomerular basement membrane disease. *Nat Rev Nephrol*. 2011;7:697-705.
320. Goldman M, Depierreux M, De Pauw L, et al. Failure of two subsequent renal grafts by anti-GBM glomerulonephritis in Alport's syndrome: case report and review of the literature. *Transpl Int*. 1990;3:82-85.
321. Oliver TB, Goudeborough DR, Swainson CP. Acute crescentic glomerulonephritis associated with anti-glomerular basement membrane antibody in Alport's syndrome after second transplantation. *Nephrol Dial Transplant*. 1991;6:893-895.
322. Hecht N, Mololoja A, Witte D, Canessa L. Evolution of anti-glomerular basement membrane glomerulonephritis into membranous glomerulonephritis. *Pediatr Nephrol*. 2008;23:477-480.
323. Troxell ML, Saxena AB, Kambham N. Concurrent anti-glomerular basement membrane disease and membranous glomerulonephritis: a case report and literature review. *Clin Nephrol*. 2006;66:120-127.
324. Bonsib SM, Goeken JA, Kemp JD, et al. Coexistent anti-neutrophil cytoplasmic antibody and anti-glomerular basement membrane antibody associated disease = report of six cases. *Mod Pathol*. 1993;6:526-530.
325. Levy JB, Hammad T, Coulthart A, et al. Clinical features and outcome of patients with both ANCA and anti-GBM antibodies. *Kidney Int*. 2004;66:1535-1540.
326. Rutgers A, Slot M, van Paassen P, et al. Coexistence of anti-glomerular basement membrane antibodies and myeloperoxidase-ANCA in crescentic glomerulonephritis. *Am J Kidney Dis*. 2005;46:253-262.
327. Lionaki S, Jennette JC, Falk RJ. Anti-neutrophil cytoplasmic (ANCA) and anti-glomerular basement membrane (GBM) autoantibodies in necrotizing and crescentic glomerulonephritis. *Semin Immunopathol*. 2007;29:459-474.
328. Jennette JC, Thomas DB. Pauci-immune and anti-neutrophil cytoplasmic autoantibody-mediated crescentic glomerulonephritis and vasculitis. In: Jennette JC, Olson JL, Silva FG, Agati VD, eds. *Heptinstall's Pathology of the Kidney*. 7th ed. Philadelphia, PA: Wolters Kluwer; 2015:685-714.
329. Stone JH, Merkel PA, Spiera R, et al. Rituximab versus cyclophosphamide for ANCA-associated vasculitis. *N Engl J Med*. 2010;363:221-232.
330. Jones RB, Tervaert JW, Hauser T, et al. Rituximab versus cyclophosphamide in ANCA-associated renal vasculitis. *N Engl J Med*. 2010;363:211-220.
331. Falk RJ, Hogan S, Carey TS, Jennette JC. Clinical course of anti-neutrophil cytoplasmic autoantibody-associated glomerulonephritis and systemic vasculitis. The Glomerular Disease Collaborative Network. *Ann Intern Med*. 1990;113:656-663.
332. Falk RJ, Jennette JC. Proceedings of the Third International Workshop on ANCA. *Am J Kidney Dis*. 1991;18:145-193.
333. Jennette JC, Falk RJ. Pathogenesis of anti-neutrophil cytoplasmic autoantibody-mediated disease. *Nat Rev Rheumatol*. 2014;10:463-473.
334. Furuta S, Jayne DR. Anti-neutrophil cytoplasmic antibody-associated vasculitis: recent developments. *Kidney Int*. 2013;84:244-249.
335. Suzuki K, Nagao T, Itabashi M, et al. A novel autoantibody against moesin in the serum of patients with MPO-ANCA-associated vasculitis. *Nephrol Dial Transplant*. 2014;29:1168-1177.
336. Charles Jennette J, Xiao H, Hu P. Complement in ANCA-associated vasculitis. *Semin Nephrol*. 2013;33:557-564.
337. Hochberg MC. Updating the American College of Rheumatology revised criteria for the classification of systemic lupus erythematosus. *Arthritis Rheum*. 1997;40:1725.
338. Gloor JM. Lupus nephritis in children. *Lupus*. 1998;7:639-643.
339. Perfumo F, Martini A. Lupus nephritis in children. *Lupus*. 2005;14:83-88.
340. Hess E. Drug-related lupus. *N Engl J Med*. 1988;318:1460-1462.
341. Yung RL, Richardson BC. Drug-induced lupus. *Rheum Dis Clin North Am*. 1994;20:61-86.
342. D'Agati VD, Stokes MB. Renal disease in systemic lupus erythematosus, mixed connective tissue disease, Sjögren's syndrome, and rheumatoid arthritis. In: Jennette JC, Olson JL, Silva FG, Agati VD, eds. *Heptinstall's Pathology of the Kidney*. Philadelphia, PA: Wolters Kluwer; 2015:559-656.
343. Armstrong DL, Zidovetzki R, Alarcon-Riquelme ME, et al. GWAS identifies novel SLE susceptibility genes and explains the association of the HLA region. *Genes Immun*. 2014;15:347-354.
344. Harley IT, Kaufman KM, Langefeld CD, et al. Genetic susceptibility to SLE: new insights from fine mapping and genome-wide association studies. *Nat Rev Genet*. 2009;10:285-290.
345. Weening JJ, D'Agati VD, Schwartz MM, et al. The classification of glomerulonephritis in systemic lupus erythematosus revisited. *J Am Soc Nephrol*. 2004;15:241-250.
346. McCluskey RT. Lupus nephritis. In: Sommers SC, ed. *Kidney Pathology Decennial*. East Norwalk, CT: Appleton-Century-Crofts; 1975:435-450.
347. Churg J, Sobin LH. *Lupus Nephritis*. 2nd ed. New York, NY: Igaku-Shoin; 1982.
348. Churg J, Bernstein J, Glasscock RJ. *Renal Disease: Classification and Atlas of Glomerular Diseases*. 2nd ed. New York, NY: Igaku-Shoin; 1995.
349. Furness PN, Taub N. Interobserver reproducibility and application of the ISN/RPS classification of lupus nephritis—a UK-wide study. *Am J Surg Pathol*. 2006;30:1030-1035.
350. Hiramatsu N, Kuroiwa T, Ikeuchi H, et al. Revised classification of lupus nephritis is valuable in predicting renal outcome with an indication of the proportion of glomeruli affected by chronic lesions. *Rheumatology (Oxford)*. 2008;47:702-707.
351. Markowitz GS, D'Agati VD. The ISN/RPS 2003 classification of lupus nephritis: an assessment at 3 years. *Kidney Int*. 2007;71:491-495.
352. Yokoyama H, Wada T, Hara A, et al. The outcome and a new ISN/RPS 2003 classification of lupus nephritis in Japanese. *Kidney Int*. 2004;66:2382-2388.
353. Dube GK, Markowitz GS, Radhakrishnan J, et al. Minimal change disease in systemic lupus erythematosus. *Clin Nephrol*. 2002;57:120-126.

354. Watanabe T. Nephrotic syndrome in mesangial proliferative lupus nephritis. *Pediatr Int.* 2007;49:1009-1011.
355. Ordóñez NG, Gomez LG. The ultrastructure of glomerular haematoxylin bodies. *J Pathol.* 1981;135:259-265.
356. Herrera GA. The value of electron microscopy in the diagnosis and clinical management of lupus nephritis. *Ultrastruct Pathol.* 1999;23:63-77.
357. Su CF, Chen HH, Yeh JC, et al. Ultrastructural 'fingerprint' in cryoprecipitates and glomerular deposits: a clinicopathologic analysis of fingerprint deposits. *Nephron.* 2002;90:37-42.
358. Rich SA. Human lupus inclusions and interferon. *Science.* 1981;213:772-775.
359. Haring CM, Rietveld A, van den Brand JA, Berden JH. Segmental and global subclasses of class IV lupus nephritis have similar renal outcomes. *J Am Soc Nephrol.* 2012;23:149-154.
360. Le Thi Huong D, Papo T, Beaufils H, et al. Renal involvement in systemic lupus erythematosus: a study of 180 patients from a single center. *Medicine (Baltimore).* 1999;78:148-166.
361. Mahajan SK, Ordóñez NG, Spargo BH, Katz AI. Changing histopathology patterns in lupus nephropathy. *Clin Nephrol.* 1978;10:1-8.
362. Zimmerman SW, Jenkins PG, Shelf WD, et al. Progression from minimal or focal to diffuse proliferative lupus nephritis. *Lab Invest.* 1975;32:665-672.
363. Hecht B, Siegel N, Adler M, et al. Prognostic indices in lupus nephritis. *Medicine (Baltimore).* 1976;55:163-181.
364. Appel GB, Silva FG, Pirani CL, et al. Renal involvement in systemic lupus erythematosus (SLE): a study of 56 patients emphasizing histologic classification. *Medicine (Baltimore).* 1978;57:371-410.
365. Schwartz MM, Kawala K, Roberts JL, et al. Clinical and pathological features of membranous glomerulonephritis of systemic lupus erythematosus. *Am J Nephrol.* 1984;4:301-311.
366. Chang A, Henderson SG, Brandt D, et al. In situ B cell-mediated immune responses and tubulointerstitial inflammation in human lupus nephritis. *J Immunol.* 2011;186:1849-1860.
367. Alsuwaide AO. Interstitial inflammation and long-term renal outcomes in lupus nephritis. *Lupus.* 2013;22:1446-1454.
368. Michail S, Stathakis C, Marinakis S, et al. Relapse of predominant tubulointerstitial lupus nephritis. *Lupus.* 2003;12:728-729.
369. Mori Y, Kishimoto N, Yamahara H, et al. Predominant tubulointerstitial nephritis in a patient with systemic lupus nephritis. *Clin Exp Nephrol.* 2005;9:79-84.
370. Wu LH, Yu F, Tan Y, et al. Inclusion of renal vascular lesions in the 2003 ISN/RPS system for classifying lupus nephritis improves renal outcome predictions. *Kidney Int.* 2013;83:715-723.
371. Austin HA 3rd, Muenz LR, Joyce KM, et al. Prognostic factors in lupus nephritis. Contribution of renal histologic data. *Am J Med.* 1983;75:382-391.
372. Schwartz MM, Lan SP, Bernstein J, et al. Irreproducibility of the activity and chronicity indices limits their utility in the management of lupus nephritis. *Lupus Nephritis Collaborative Study Group. Am J Kidney Dis.* 1993;21:374-377.
373. Azevedo LS, Romao JE Jr, Malheiros D, et al. Renal transplantation in systemic lupus erythematosus. A case control study of 45 patients. *Nephrol Dial Transplant.* 1998;13:2894-2898.
374. Ponticelli C, Moroni G. Renal transplantation in lupus nephritis. *Lupus.* 2005;14:95-98.
375. Stone JH, Millward CL, Olson JL, et al. Frequency of recurrent lupus nephritis among ninety-seven renal transplant patients during the cyclosporine era. *Arthritis Rheum.* 1998;41:678-686.
376. Jennette JC, Falk RJ, Bacon PA, et al. 2012 revised International Chapel Hill Consensus Conference Nomenclature of Vasculitides. *Arthritis Rheum.* 2013;65:1-11.
377. Weyand CM, Goronzy JJ. Medium- and large-vessel vasculitis. *N Engl J Med.* 2003;349:160-169.
378. Puechal X. Antineutrophil cytoplasmic antibody-associated vasculitides. *Joint Bone Spine.* 2007;74:427-435.
379. Radice A, Sinico RA. Antineutrophil cytoplasmic antibodies (ANCA). *Autoimmunity.* 2005;38:93-103.
380. Kallenberg CG. Antineutrophil cytoplasmic autoantibody-associated small-vessel vasculitis. *Curr Opin Rheumatol.* 2007;19:17-24.
381. Kallenberg CG. Pathogenesis of PR3-ANCA associated vasculitis. *J Autoimmun.* 2008;30:29-36.
382. Pagnoux C, Seror R, Henegar C, et al. Clinical features and outcomes in 348 patients with polyarteritis nodosa: a systematic retrospective study of patients diagnosed between 1963 and 2005 and entered into the French Vasculitis Study Group Database. *Arthritis Rheum.* 2010;62:616-626.
383. Agard C, Mouthon L, Mahr A, Guillevin L. Microscopic polyangiitis and polyarteritis nodosa: how and when do they start? *Arthritis Rheum.* 2003;49:709-715.
384. Bonsib SM. Polyarteritis nodosa. *Semin Diagn Pathol.* 2001;18:14-23.
385. Hernandez-Rodriguez J, Alba MA, Prieto-Gonzalez S, Cid MC. Diagnosis and classification of polyarteritis nodosa. *J Autoimmun.* 2014;48-49:84-89.
386. Druet T, Barbanel C, Jungers P, et al. Hepatitis B antigen-associated periarteritis nodosa in patients undergoing long-term hemodialysis. *Am J Med.* 1980;68:86-90.
387. Guillevin L, Lhote F, Cohen P, et al. Polyarteritis nodosa related to hepatitis B virus. A prospective study with long-term observation of 41 patients. *Medicine (Baltimore).* 1995;74:238-253.
388. Saadoun D, Terrier B, Semoun O, et al. Hepatitis C virus-associated polyarteritis nodosa. *Arthritis Care Res (Hoboken).* 2011;63:427-435.
389. Navon Elkan P, Pierce SB, Segel R, et al. Mutant adenosine deaminase 2 in a polyarteritis nodosa vasculopathy. *N Engl J Med.* 2014;370:921-931.
390. Minardi D, Densi-Fulgheri P, Sarzani R, et al. Massive spontaneous perirenal hematoma and accelerated hypertension in a patient with polyarteritis nodosa. *Urol Int.* 2003;70:227-231.
391. Jennette JC, Singh HK. Renal involvement in polyarteritis nodosa, Kawasaki disease, Takayasu arteritis, and giant cell arteritis. In: Jennette JC, Olson JL, Silva FG, A'gati VD, eds. *Heptinstall's Pathology of the Kidney.* 7th ed. Philadelphia, PA: Wolters Kluwer; 2015:715-738.
392. Masuda M, Kai K, Takase Y, Tokunaga O. Pathological features of classical polyarteritis nodosa: analysis of 19 autopsy cases. *Pathol Res Pract.* 2013;209:161-166.
393. Kallenberg CG. The diagnosis and classification of microscopic polyangiitis. *J Autoimmun.* 2014;48-49:90-93.
394. Jennette JC, Falk RJ. Small-vessel vasculitis. *N Engl J Med.* 1997;337:1512-1522.
395. Jennette JC, Thomas DB, Falk RJ. Microscopic polyangiitis (microscopic polyarteritis). *Semin Diagn Pathol.* 2001;18:3-13.
396. Guillevin L, Durand-Gasselin B, Cevallos R, et al. Microscopic polyangiitis: clinical and laboratory findings in eighty-five patients. *Arthritis Rheum.* 1999;42:421-430.
397. Lhote F, Cohen P, Guillevin L. Polyarteritis nodosa, microscopic polyangiitis and Churg-Strauss syndrome. *Lupus.* 1998;7:238-258.
398. D'Agati V, Chander P, Nash M, Mancilla-Jimenez R. Idiopathic microscopic polyarteritis nodosa: ultrastructural observations on the renal vascular and glomerular lesions. *Am J Kidney Dis.* 1986;7:95-110.
399. Lutalo PM, D'Cruz DP. Diagnosis and classification of granulomatosis with polyangiitis (aka Wegener's granulomatosis). *J Autoimmun.* 2014;48-49:94-98.
400. Coth MF, Hoffman GS, Yerg DE, et al. The epidemiology of Wegener's granulomatosis. Estimates of the five-year period prevalence, annual mortality, and geographic disease distribution from population-based data sources. *Arthritis Rheum.* 1996;39:87-92.
401. Hoffman GS. Wegener's granulomatosis. *Curr Opin Rheumatol.* 1993;5:11-17.
402. Yi ES, Colby TV. Wegener's granulomatosis. *Semin Diagn Pathol.* 2001;18:34-46.
403. Hoffman GS, Kerr GS, Leavitt RY, et al. Wegener granulomatosis: an analysis of 158 patients. *Ann Intern Med.* 1992;116:488-498.
404. Cohen Tervaert JW, Huittem MG, Hene RJ, Sluiter WJ. Prevention of relapses in Wegener's granulomatosis by treatment based on anti-neutrophil cytoplasmic antibody titer. *Lancet.* 1990;336:709-711.
405. Csernok E, Gross WL. Current understanding of the pathogenesis of granulomatosis with polyangiitis (Wegener's). *Expert Rev Clin Immunol.* 2013;9:641-648.
406. Weiss MA, Crissman JD. Renal biopsy findings in Wegener's granulomatosis: segmental necrotizing glomerulonephritis with glomerular thrombosis. *Hum Pathol.* 1984;15:943-956.
407. Yoshikawa Y, Watanabe T. Granulomatous glomerulonephritis in Wegener's granulomatosis. *Virchows Arch A Pathol Anat Histopathol.* 1984;402:361-372.
408. Gaber LW, Wall BM, Cooke CR. Coexistence of anti-neutrophil cytoplasmic antibody-associated glomerulonephritis and membranous glomerulopathy. *Am J Clin Pathol.* 1993;99:211-215.
409. Greco A, Rizzo MI, De Virgilio A, et al. Churg-Strauss syndrome. *Autoimmun Rev.* 2015;14:341-348.
410. Comarmond C, Pagnoux C, Khellaf M, et al. Eosinophilic granulomatosis with polyangiitis (Churg-Strauss): clinical characteristics and long-term followup of the 383 patients enrolled in the French Vasculitis Study Group cohort. *Arthritis Rheum.* 2013;65:270-281.
411. Abril A, Calamia KT, Cohen MD. The Churg-Strauss syndrome (allergic granulomatous angiitis): review and update. *Semin Arthritis Rheum.* 2003;33:106-114.
412. Guillevin L, Cohen P, Gayraud M, et al. Churg-Strauss syndrome. Clinical study and long-term follow-up of 96 patients. *Medicine (Baltimore).* 1999;78:26-37.
413. Hellmich B, Ehlers S, Csernok E, Gross WL. Update on the pathogenesis of Churg-Strauss syndrome. *Clin Exp Rheumatol.* 2003;21:S69-S77.
414. Sinico RA, Di Toma L, Maggiore U, et al. Renal involvement in Churg-Strauss syndrome. *Am J Kidney Dis.* 2006;47:770-779.
415. Hellmich B, Gross WL. Recent progress in the pharmacotherapy of Churg-Strauss syndrome. *Expert Opin Pharmacother.* 2004;5:25-35.
416. Mouthon L, Dunoguie B, Guillevin L. Diagnosis and classification of eosinophilic granulomatosis with polyangiitis (formerly named Churg-Strauss syndrome). *J Autoimmun.* 2014;48-49:99-103.
417. Samarkos M, Loizou S, Vaiopoulos G, Davies KA. The clinical spectrum of primary renal

- vasculitis. *Semin Arthritis Rheum.* 2005;35:95-111.
418. Thiel J, Hassler F, Salzer U, et al. Rituximab in the treatment of refractory or relapsing eosinophilic granulomatosis with polyangiitis (Churg-Strauss syndrome). *Arthritis Res Ther.* 2013;15:R133.
419. Kikuchi Y, Ikehata N, Tajima O, et al. Glomerular lesions in patients with Churg-Strauss syndrome and the anti-myeloperoxidase antibody. *Clin Nephrol.* 2001;55:429-435.
420. Sinico RA, Di Toma L, Maggiore U, et al. Prevalence and clinical significance of antineutrophil cytoplasmic antibodies in Churg-Strauss syndrome. *Arthritis Rheum.* 2005;52:2926-2935.
421. Roberto PF, Waller TA, Brinker TM, et al. Henoch-Schönlein purpura: a review article. *South Med J.* 2007;100:821-824.
422. Davin JC, Coppo R. Henoch-Schönlein purpura nephritis in children. *Nat Rev Nephrol.* 2014;10:563-573.
423. Blanco R, Martínez-Taboada VM, Rodriguez-Valverde V, et al. Henoch-Schönlein purpura in adulthood and childhood: two different expressions of the same syndrome. *Arthritis Rheum.* 1997;40:859-864.
424. Gedalia A. Henoch-Schönlein purpura. *Curr Rheumatol Rep.* 2004;6:195-202.
425. Cakir N, Pamuk ON, Donmez S. Henoch-Schönlein purpura in two brothers imprisoned in the same jail: presentation two months apart. *Clin Exp Rheumatol.* 2004;22:235-237.
426. Chang WL, Yang YH, Wang LC, et al. Renal manifestations in Henoch-Schönlein purpura: a 10-year clinical study. *Pediatr Nephrol.* 2005;20:1269-1272.
427. Garcia-Porrúa C, Calvino MC, Llorca J, et al. Henoch-Schönlein purpura in children and adults: clinical differences in a defined population. *Semin Arthritis Rheum.* 2002;32:149-156.
428. Saulsbury FT. Henoch-Schönlein purpura. *Curr Opin Rheumatol.* 2001;13:35-40.
429. Urizar RE, Singh JK, Muhammad T, Hines O. Henoch-Schönlein anaphylactoid purpura nephropathy: electron microscopic lesions mimicking acute poststreptococcal nephritis. *Hum Pathol.* 1978;9:223-229.
430. Lau KK, Suzuki H, Novak J, Wyatt RJ. Pathogenesis of Henoch-Schönlein purpura nephritis. *Pediatr Nephrol.* 2010;25:19-26.
431. Dispensieri A, Gorevic PD. Cryoglobulinemia. *Hematol Oncol Clin North Am.* 1999;13:1315-1349.
432. Alpers CE, Smith KD. Cryoglobulinemia and renal disease. *Curr Opin Nephrol Hypertens.* 2008;17:243-249.
433. Karras A, Noel LH, Droz D, et al. Renal involvement in monoclonal (type I) cryoglobulinemia: two cases associated with IgG3 kappa cryoglobulin. *Am J Kidney Dis.* 2002;40:1091-1096.
434. Cacoub P, Comarmond C, Domont F, et al. Cryoglobulinemia vasculitis. *Am J Med.* 2015;128:950-955.
435. D'Amico G, Colasanti G, Ferrario F, Sinico RA. Renal involvement in essential mixed cryoglobulinemia. *Kidney Int.* 1989;35:1004-1014.
436. Gorevic PD, Kassab HJ, Levo Y, et al. Mixed cryoglobulinemia: clinical aspects and long-term follow-up of 40 patients. *Am J Med.* 1980;69:287-308.
437. Ramos-Casals M, Stone JH, Cid MC, Bosch X. The cryoglobulinaemias. *Lancet.* 2012;379:348-360.
438. Iskandar SS, Herrera GA. Glomerulopathies with organized deposits. *Semin Diagn Pathol.* 2002;19:116-132.
439. Rossmann P, Hornych A, Englis M. Histology and ultrastructure of crystalloid inclusions in the podocytes in a case of paraproteinemia. *Virchows Arch Pathol Anat Physiol Klin Med.* 1968;344:151-158.
440. Laszik Z, Kambham N, Silva FG. Thrombotic Microangiopathies. In: Jennette JC, Olson JL, Silva FG, A'gati VD, eds. *Heptinstall's Pathology of the Kidney.* 7th ed. Philadelphia, PA: Wolters Kluwer; 2015:739-814.
441. George JN, Nester CM. Syndromes of thrombotic microangiopathy. *N Engl J Med.* 2014;371:654-666.
442. Tsai HM. The molecular biology of thrombotic microangiopathy. *Kidney Int.* 2006;70:16-23.
443. Furlan M, Robles R, Galbusera M, et al. von Willebrand factor-cleaving protease in thrombotic thrombocytopenic purpura and the hemolytic-uremic syndrome. *N Engl J Med.* 1998;339:1578-1584.
444. Tsai HM, Lian EC. Antibodies to von Willebrand factor-cleaving protease in acute thrombotic thrombocytopenic purpura. *N Engl J Med.* 1998;339:1585-1594.
445. Moake JL. Thrombotic microangiopathies. *N Engl J Med.* 2002;347:589-600.
446. Zheng XL, Sadler JE. Pathogenesis of thrombotic microangiopathies. *Annu Rev Pathol.* 2008;3:249-277.
447. Zakaria A, Bennett C. Drug-induced thrombotic microangiopathy. *Semin Thromb Hemost.* 2005;31:681-690.
448. Kavanagh D, Goodship TH, Richards A. Atypical haemolytic ureamic syndrome. *Br Med Bull.* 2006;77-78:5-22.
449. Noris M, Remuzzi G. Hemolytic uremic syndrome. *J Am Soc Nephrol.* 2005;16:1035-1050.
450. Gordjani N, Sutor AH, Zimmerhackl LB, Brandis M. Hemolytic uremic syndromes in childhood. *Semin Thromb Hemost.* 1997;23:281-293.
451. Keusch GT, Acheson DW. Thrombotic thrombocytopenic purpura associated with Shiga toxins. *Semin Hematol.* 1997;34:106-116.
452. Noris M, Remuzzi G. Atypical hemolytic-uremic syndrome. *N Engl J Med.* 2009;361:1676-1687.
453. Kavanagh D, Goodship TH, Richards A. Atypical hemolytic uremic syndrome. *Semin Nephrol.* 2013;33:508-530.
454. Constantinescu AR, Bitzan M, Weiss LS, et al. Non-enteropathic hemolytic uremic syndrome: causes and short-term course. *Am J Kidney Dis.* 2004;43:976-982.
455. George JN. The association of pregnancy with thrombotic thrombocytopenic purpura-hemolytic uremic syndrome. *Curr Opin Hematol.* 2003;10:339-344.
456. Niaudet P, Gagnadoux MF, Broyer M, Salomon R. Hemolytic-uremic syndrome: hereditary forms and forms associated with hereditary diseases. *Adv Nephrol Necker Hosp.* 2000;30:261-280.
457. Rodriguez de Cordoba S, Hidalgo MS, Pinto S, Tortajada A. Genetics of atypical hemolytic uremic syndrome (aHUS). *Semin Thromb Hemost.* 2014;40:422-430.
458. Agarwal SK, Tan FK, Arnett FC. Genetics and genomic studies in scleroderma (systemic sclerosis). *Rheum Dis Clin North Am.* 2008;34:17-40, v.
459. Rocco VK, Hurd ER. Scleroderma and scleroderma-like disorders. *Semin Arthritis Rheum.* 1986;16:22-69.
460. Kahaleh B. Vascular disease in scleroderma: mechanisms of vascular injury. *Rheum Dis Clin North Am.* 2008;34:57-71, vi.
461. Yazawa N, Fujimoto M, Tamaki K. Recent advances on pathogenesis and therapies in systemic sclerosis. *Clin Rev Allergy Immunol.* 2007;33:107-112.
462. Kayser C, Fritzler MJ. Autoantibodies in systemic sclerosis: unanswered questions. *Front Immunol.* 2015;6:167.
463. Eknayan G, Suki WN. Renal vascular phenomena in systemic sclerosis (scleroderma). *Semin Nephrol.* 1985;5:34-45.
464. Woodworth TG, Suliman YA, Furst DE, Clements P. Scleroderma renal crisis and renal involvement in systemic sclerosis. *Nat Rev Nephrol.* 2016;12:678-691.
465. Bose N, Chiesa-Vottero A, Chatterjee S. Scleroderma renal crisis. *Semin Arthritis Rheum.* 2015;44:687-694.
466. Steen VD. Kidney involvement in systemic sclerosis. *Presse Med.* 2014;43:e305-e314.
467. Stone RA, Tisher CC, Hawkins HK, Robinson RR. Juxtaglomerular hyperplasia and hyperreninemia in progressive systemic sclerosis complicated acute renal failure. *Am J Med.* 1974;56:119-123.
468. Baumwell S, Karumanchi SA. Pre-eclampsia: clinical manifestations and molecular mechanisms. *Nephron Clin Pract.* 2007;106:c7-c81.
469. Maynard S, Epstein FH, Karumanchi SA. Preeclampsia and angiogenic imbalance. *Annu Rev Med.* 2008;59:61-78.
470. Stillman IE, Karumanchi SA. The glomerular injury of preeclampsia. *J Am Soc Nephrol.* 2007;18:2281-2284.
471. Esser S, Wolburg K, Wolburg H, et al. Vascular endothelial growth factor induces endothelial fenestrations in vitro. *J Cell Biol.* 1998;140:947-959.
472. Sheehan HL. Renal morphology in preeclampsia. *Kidney Int.* 1980;18:241-252.
473. Fakhouri F, Jablonski M, Lepercq J, et al. Factor H, membrane cofactor protein, and factor I mutations in patients with hemolysis, elevated liver enzymes, and low platelet count syndrome. *Blood.* 2008;112:4542-4545.
474. Cubler MC. Inherited diseases of the glomerular basement membrane. *Nat Clin Pract Nephrol.* 2008;4:24-37.
475. Jais JP, Knebelmann B, Giatras I, et al. X-linked Alport syndrome: natural history in 195 families and genotype-phenotype correlations in males. *J Am Soc Nephrol.* 2000;11:649-657.
476. Kashtan CE. Alport syndromes: phenotypic heterogeneity of progressive hereditary nephritis. *Pediatr Nephrol.* 2000;14:502-512.
477. Jefferson JA, Lemmink HH, Hughes AE, et al. Autosomal dominant Alport syndrome linked to the type IV collagen alpha 3 and alpha 4 genes (COL4A3 and COL4A4). *Nephrol Dial Transplant.* 1997;12:1595-1599.
478. Longo I, Porcedda P, Mari F, et al. COL4A3/COL4A4 mutations: from familial hematuria to autosomal-dominant or recessive Alport syndrome. *Kidney Int.* 2002;61:1947-1956.
479. Pescucci C, Mari F, Longo I, et al. Autosomal-dominant Alport syndrome: natural history of a disease due to COL4A3 or COL4A4 gene. *Kidney Int.* 2004;65:1598-1603.
480. Moriniere V, Dahan K, Hilbert P, et al. Improving mutation screening in familial hematuric nephropathies through next generation sequencing. *J Am Soc Nephrol.* 2014;25:2740-2751.
481. Storey H, Savage J, Sivakumar V, et al. COL4A3/COL4A4 mutations and features in individuals with autosomal recessive Alport syndrome. *J Am Soc Nephrol.* 2013;24:1945-1954.
482. Jais JP, Knebelmann B, Giatras I, et al. X-linked Alport syndrome: natural history and genotype-phenotype correlations in girls and women belonging to 195 families: a "European Community Alport Syndrome Concerted Action" study. *J Am Soc Nephrol.* 2003;14:2603-2610.
483. Bekhemia MR, Reed B, Gregory MC, et al. Genotype-phenotype correlation in X-linked Alport syndrome. *J Am Soc Nephrol.* 2010;21:876-883.

484. Colville DJ, Savage J. Alport syndrome. A review of the ocular manifestations. *Ophthalmic Genet.* 1997;18:161-173.
485. Antignac C, Heidet L. Mutations in Alport syndrome associated with diffuse esophageal leiomyomatosis. *Contrib Nephrol.* 1996;117:172-182.
486. Kashtan CE. Renal transplantation in patients with Alport syndrome. *Pediatr Transplant.* 2006;10:651-657.
487. Brainwood D, Kashtan C, Gubler MC, Turner AN. Targets of alloantibodies in Alport anti-glomerular basement membrane disease after renal transplantation. *Kidney Int.* 1998;53:762-766.
488. Kashtan CE. Alport syndrome. An inherited disorder of renal, ocular, and cochlear basement membranes. *Medicine (Baltimore).* 1999;78:338-360.
489. Rumpelt HJ. Alport's syndrome: specificity and pathogenesis of glomerular basement membrane alterations. *Pediatr Nephrol.* 1987;1:422-427.
490. Hill GS, Jenis EH, Goodloe S Jr. The nonspecificity of the ultrastructural alterations in hereditary nephritis with additional observations on benign familial hematuria. *Lab Invest.* 1974;31:516-532.
491. Kashtan CE. The nongenetic diagnosis of thin basement membrane nephropathy. *Semin Nephrol.* 2005;25:159-162.
492. Haas M. Alport syndrome and thin glomerular basement membrane nephropathy: a practical approach to diagnosis. *Arch Pathol Lab Med.* 2009;133:224-232.
493. Kashtan CE, Michael AF. Alport syndrome. *Kidney Int.* 1996;50:1445-1463.
494. Savage J, Gregory M, Gross O, et al. Expert guidelines for the management of Alport syndrome and thin basement membrane nephropathy. *J Am Soc Nephrol.* 2013;24:364-375.
495. Rana K, Wang YY, Buzzetta M, et al. The genetics of thin basement membrane nephropathy. *Semin Nephrol.* 2005;25:163-170.
496. Kashtan CE, Segal Y. Genetic disorders of glomerular basement membranes. *Nephron Clin Pract.* 2011;118:c9-c18.
497. Frasca GM, Onetti-Muda A, Renieri A. Thin glomerular basement membrane disease. *J Nephrol.* 2000;13:15-19.
498. Tryggvason K, Patrakka J. Thin basement membrane nephropathy. *J Am Soc Nephrol.* 2006;17:813-822.
499. Gregory MC. The clinical features of thin basement membrane nephropathy. *Semin Nephrol.* 2005;25:140-145.
500. Wang YY, Savage J. The epidemiology of thin basement membrane nephropathy. *Semin Nephrol.* 2005;25:136-139.
501. Norby SM, Cosio FG. Thin basement membrane nephropathy associated with other glomerular diseases. *Semin Nephrol.* 2005;25:176-179.
502. Foster K, Markowitz GS, D'Agati VD. Pathology of thin basement membrane nephropathy. *Semin Nephrol.* 2005;25:149-158.
503. Stenson PD, Ball EV, Mort M, et al. Human Gene Mutation Database (HGMD): 2003 update. *Hum Mutat.* 2003;21:577-581.
504. Ojo A, Meier-Kriesche HU, Friedman G, et al. Excellent outcome of renal transplantation in patients with Fabry's disease. *Transplantation.* 2000;69:2337-2339.
505. Rohrbach M, Clarke JT. Treatment of lysosomal storage disorders: progress with enzyme replacement therapy. *Drugs.* 2007;67:2697-2716.
506. Rombach SM, Smid BE, Bouwman MG, et al. Long term enzyme replacement therapy for Fabry disease: effectiveness on kidney, heart and brain. *Orphanet J Rare Dis.* 2013;8:47.
507. Bracamonte ER, Kowalewska J, Starr J, et al. Iatrogenic phospholipidosis mimicking Fabry disease. *Am J Kidney Dis.* 2006;48:844-850.
508. van der Tol L, Svarstad E, Ortiz A, et al. Chronic kidney disease and an uncertain diagnosis of Fabry disease: approach to a correct diagnosis. *Mol Genet Metab.* 2015;114:242-247.
509. McIntosh I, Dunston JA, Liu L, et al. Nail patella syndrome revisited: 50 years after linkage. *Ann Hum Genet.* 2005;69:349-363.
510. Bongers EM, Huysmans FT, Levchenko E, et al. Genotype-phenotype studies in nail-patella syndrome show that LMX1B mutation location is involved in the risk of developing nephropathy. *Eur J Hum Genet.* 2005;13:935-946.
511. Bongers EM, Gubler MC, Knoers NV. Nail-patella syndrome. Overview on clinical and molecular findings. *Pediatr Nephrol.* 2002;17:703-712.
512. Meyrier A, Rizzo R, Gubler MC. The nail-patella syndrome. A review. *J Nephrol.* 1990;2:133-140.
513. Chan PC, Chan KW, Cheng IK, Chan MK. Living-related renal transplantation in a patient with nail-patella syndrome. *Nephron.* 1988;50:164-166.
514. Alchi B, Nishi S, Narita I, Gejyo F. Collagenofibrotic glomerulopathy: clinicopathologic overview of a rare glomerular disease. *Am J Kidney Dis.* 2007;49:499-506.
515. Cohen AH. Collagen type III glomerulopathies. *Adv Chronic Kidney Dis.* 2012;19:101-106.
516. Chen N, Pan X, Xu Y, et al. Two brothers in one Chinese family with collagen type III glomerulopathy. *Am J Kidney Dis.* 2007;50:1037-1042.
517. Gubler MC, Dommergues JP, Foulard M, et al. Collagen type III glomerulopathy: a new type of hereditary nephropathy. *Pediatr Nephrol.* 1993;7:354-360.
518. Tamura H, Matsuda A, Kidoguchi N, et al. A family with two sisters with collagenofibrotic glomerulonephropathy. *Am J Kidney Dis.* 1996;27:588-595.
519. Vogt BA, Wyatt RJ, Burke BA, et al. Inherited factor H deficiency and collagen type III glomerulopathy. *Pediatr Nephrol.* 1995;9:11-15.
520. Mizuiri S, Hasegawa A, Kikuchi A, et al. A case of collagenofibrotic glomerulopathy associated with hepatic perisinusoidal fibrosis. *Nephron.* 1993;63:183-187.
521. Yasuda T, Imai H, Nakamoto Y, et al. Collagenofibrotic glomerulopathy: a systemic disease. *Am J Kidney Dis.* 1999;33:123-127.
522. Assmann KJ, Koene RA, Wetzels JF. Familial glomerulonephritis characterized by massive deposits of fibronectin. *Am J Kidney Dis.* 1995;25:781-791.
523. Mazzucco G, Maran E, Rollino C, Monga G. Glomerulonephritis with organized deposits: a mesangiopathic, not immune complex-mediated disease? A pathologic study of two cases in the same family. *Hum Pathol.* 1992;23:63-68.
524. Strom EH, Hurwitz N, Mayr AC, et al. Immunotactoid-like glomerulopathy with massive fibrillary deposits in liver and bone marrow in monoclonal gammopathy. *Am J Nephrol.* 1996;16:523-528.
525. Castelletti F, Donadelli R, Banterla F, et al. Mutations in FN1 cause glomerulopathy with fibronectin deposits. *Proc Natl Acad Sci USA.* 2008;105:2538-2543.
526. Strom EH, Banfi G, Krapf R, et al. Glomerulopathy associated with predominant fibronectin deposits: a newly recognized hereditary disease. *Kidney Int.* 1995;48:163-170.
527. Nadamuni M, Piras R, Mazbar S, et al. Fibronectin glomerulopathy: an unusual cause of adult-onset nephrotic syndrome. *Am J Kidney Dis.* 2012;60:839-842.
528. Jackson AM, Kuperman MB, Montgomery RA. Multiple hyperacute rejections in the absence of detectable complement activation in a patient with endothelial cell reactive antibody. *Am J Transplant.* 2012;12:1643-1649.
529. Jackson AM, Sigdel TK, Delville M, et al. Endothelial cell antibodies associated with novel targets and increased rejection. *J Am Soc Nephrol.* 2015;26:1161-1171.
530. Racusen LC, Haas M. Antibody-mediated rejection in renal allografts: lessons from pathology. *Clin J Am Soc Nephrol.* 2006;1:415-420.
531. Iwaki Y, Terasaki PI. Primary nonfunction in human cadaver kidney transplantation: evidence for hidden hyperacute rejection. *Clin Transplant.* 1987;1:125-131.
532. Burns JM, Cornell LD, Perry DK, et al. Alloantibody levels and acute humoral rejection early after positive crossmatch kidney transplantation. *Am J Transplant.* 2008;8:2684-2694.
533. Verani RR, Bergman D, Kerman RH. Glomerulopathy in acute and chronic rejection: relationship of ultrastructure to graft survival. *Am J Nephrol.* 1983;3:253-263.
534. Mauiyedi S, Crespo M, Collins AB, et al. Acute humoral rejection in kidney transplantation: II. Morphology, immunopathology, and pathologic classification. *J Am Soc Nephrol.* 2002;13:779-787.
535. Collins AB, Schneeberger EE, Pascual MA, et al. Complement activation in acute humoral renal allograft rejection: diagnostic significance of C4d deposits in peritubular capillaries. *J Am Soc Nephrol.* 1999;10:2208-2214.
536. Nickleit V, Zeiler M, Gudat F, et al. Detection of the complement degradation product C4d in renal allografts: diagnostic and therapeutic implications. *J Am Soc Nephrol.* 2002;13:242-251.
537. Solez K, Colvin RB, Racusen LC, et al. Banff 07 classification of renal allograft pathology: updates and future directions. *Am J Transplant.* 2008;8:753-760.
538. Haas M, Segev DL, Racusen LC, et al. C4d deposition without rejection correlates with reduced early scarring in ABO-incompatible renal allografts. *J Am Soc Nephrol.* 2009;20:197-204.
539. Mengel M, Sis B, Haas M, et al. Banff 2011 Meeting report: new concepts in antibody-mediated rejection. *Am J Transplant.* 2012;12:563-570.
540. Haas M, Sis B, Racusen LC, et al. Banff 2013 meeting report: inclusion of C4d-negative antibody-mediated rejection and antibody-associated arterial lesions. *Am J Transplant.* 2014;14:272-283.
541. Nickleit V, Mengel M, Colvin RB. Renal transplant pathology. In: Jennette JC, Olson JL, Silva FG, A'gati VD, eds. *Heptinstall's Pathology of the Kidney.* 6th ed. Philadelphia, PA: Wolters Kluwer; 2015:1321-1459.
542. Colvin RB. The renal allograft biopsy. *Kidney Int.* 1996;50:1069-1082.
543. Sis B, Bagnasco SM, Cornell LD, et al. Isolated endarteritis and kidney transplant survival: a multicenter collaborative study. *J Am Soc Nephrol.* 2015;26:1216-1227.
544. Gago M, Cornell LD, Kremers WK, et al. Kidney allograft inflammation and fibrosis, causes and consequences. *Am J Transplant.* 2012;12:1199-1207.
545. Petersen VP, Olsen TS, Kissmeyer-Nielsen F, et al. Late failure of human renal transplants. An analysis of transplant disease and graft failure among 125 recipients surviving for one to eight years. *Medicine (Baltimore).* 1975;54:45-71.

546. Maryniak RK, First MR, Weiss MA. Transplant glomerulopathy: evolution of morphologically distinct changes. *Kidney Int*. 1985;27:799-806.
547. Regele H, Bohmig GA, Habicht A, et al. Capillary deposition of complement split product C4d in renal allografts is associated with basement membrane injury in peritubular and glomerular capillaries: a contribution of humoral immunity to chronic allograft rejection. *J Am Soc Nephrol*. 2002;13:2371-2380.
548. Solez K, Axelsen RA, Benedictsson H, et al. International standardization of criteria for the histologic diagnosis of renal allograft rejection: the Banff working classification of kidney transplant pathology. *Kidney Int*. 1993;44:411-422.
549. Kahan BD. Cyclosporine. *N Engl J Med*. 1989;321:1725-1738.
550. Atkinson A, Biggs J, Dodds A, Concannon A. Cyclosporine-associated hepatotoxicity after allogeneic marrow transplantation in man: differentiation from other causes of posttransplant liver disease. *Transplant Proc*. 1983;15:2761-2767.
551. Graham RM. Cyclosporine: mechanisms of action and toxicity. *Cleve Clin J Med*. 1994;61:308-313.
552. Mihatsch MJ, Thiel G, Ryffel B. Morphologic diagnosis of cyclosporine nephrotoxicity. *Semin Diagn Pathol*. 1988;5:104-121.
553. Jacobson PA, Schladt D, Israni A, et al. Genetic and clinical determinants of early, acute calcineurin inhibitor-related nephrotoxicity: results from a kidney transplant consortium. *Transplantation*. 2012;93:624-631.
554. Morozumi K, Takeda A, Uchida K, Mihatsch MJ. Cyclosporine nephrotoxicity: how does it affect renal allograft function and transplant morphology? *Transplant Proc*. 2004;36:251s-256s.
555. Snanoudj R, Royal V, Elie C, et al. Specificity of histological markers of long-term CNI nephrotoxicity in kidney-transplant recipients under low-dose cyclosporine therapy. *Am J Transplant*. 2011;11:2635-2646.
556. Morozumi K, Sugito K, Oda A, et al. A comparative study of morphological characteristics of renal injuries of tacrolimus (FK506) and cyclosporin (CyA) in renal allografts: are the morphologic characteristics of FK506 and CyA nephrotoxicity similar? *Transplant Proc*. 1996;28:1076-1078.
557. Hirsch HH. BK virus: opportunity makes a pathogen. *Clin Infect Dis*. 2005;41:354-360.
558. Hirsch HH, Knowles W, Dickenmann M, et al. Prospective study of polyomavirus type BK replication and nephropathy in renal-transplant recipients. *N Engl J Med*. 2002;347:488-496.
559. Nickleit V, Singh HK, Mihatsch MJ. Polyomavirus nephropathy: morphology, pathophysiology, and clinical management. *Curr Opin Nephrol Hypertens*. 2003;12:599-605.
560. Randhawa PS, Finkelstein S, Scantlebury V, et al. Human polyoma virus-associated interstitial nephritis in the allograft kidney. *Transplantation*. 1999;67:103-109.
561. Moeckel GW, Kashgarian M, Racusen LC. Ischemic and toxic acute tubular injury and other ischemic renal injury. In: Jennette JC, Olson JL, Silva FG, Agati VD, eds. *Heptinstall's Pathology of the Kidney*. 7th ed. Philadelphia, PA: Wolters Kluwer; 2015:1167-1222.
562. Rosen S, Stillman IE. Acute tubular necrosis is a syndrome of physiologic and pathologic dissociation. *J Am Soc Nephrol*. 2008;19:871-875.
563. Seshan SV, D'Agati VD, Appel GA, Churg J. *Acute Vasomotor Injury/Toxic Tubular Necrosis*. Baltimore, MD: Williams & Wilkins; 1999.
564. Han WK, Baily V, Abichandani R, et al. Kidney Injury Molecule-1 (KIM-1): a novel biomarker for human renal proximal tubule injury. *Kidney Int*. 2002;62:237-244.
565. Ichimura T, Hung CC, Yang SA, et al. Kidney injury molecule-1: a tissue and urinary biomarker for nephrotoxicant-induced renal injury. *Am J Physiol Renal Physiol*. 2004;286:F552-F563.
566. Han WK, Alinan A, Wu CL, et al. Human kidney injury molecule-1 is a tissue and urinary tumor marker of renal cell carcinoma. *J Am Soc Nephrol*. 2005;16:1126-1134.
567. Vaidya VS, Ramirez V, Ichimura T, et al. Urinary kidney injury molecule-1: a sensitive quantitative biomarker for early detection of kidney tubular injury. *Am J Physiol Renal Physiol*. 2006;290:F517-F529.
568. Sabbisetti VS, Waikar SS, Antoine DJ, et al. Blood kidney injury molecule-1 is a biomarker of acute and chronic kidney injury and predicts progression to ESRD in type 1 diabetes. *J Am Soc Nephrol*. 2014;25:2177-2186.
569. Sharfuddin AA, Molitoris BA. Pathophysiology of ischemic acute kidney injury. *Nat Rev Nephrol*. 2011;7:189-200.
570. Tolkkoff-Rubin NE, Cotran RS, Rubin RH. Urinary tract infection, pyelonephritis and reflux nephropathy. In: Brenner BM, ed. *Brenner's and Rector's the Kidney*. 8th ed. Philadelphia, PA: WB Saunders; 2008:1239-1264.
571. Becker GJ, Kincard-Smith P. Reflux nephropathy: the glomerular lesion and progression of renal failure. *Pediatr Nephrol*. 1993;7:365-369.
572. Goodman M, Curry T, Russell T. Xanthogranulomatous pyelonephritis (XGP): a local disease with systemic manifestations. Report of 23 patients and review of the literature. *Medicine (Baltimore)*. 1979;58:171-181.
573. Hammadah MY, Nicholls CJ, Calder JC, et al. Xanthomatous pyelonephritis in childhood: pre-operative diagnosis is possible. *Br J Urol*. 1994;73:83-86.
574. Kim SW, Yoon BI, Ha US, et al. Xanthogranulomatous pyelonephritis: clinical experience with 21 cases. *J Infect Chemother*. 2013;19:1221-1224.
575. Huisman TK, Sands JP. Focal xanthogranulomatous pyelonephritis associated with renal cell carcinoma. *Urology*. 1992;39:281-284.
576. Li L, Parwani AV. Xanthogranulomatous pyelonephritis. *Arch Pathol Lab Med*. 2011;135:671-674.
577. Khalyl-Mawad J, Greco MA, Schinella RA. Ultrastructural demonstration of intracellular bacteria in xanthogranulomatous pyelonephritis. *Hum Pathol*. 1982;13:41-47.
578. Kobayashi A, Utsunomiya Y, Kono M, et al. Malakoplakia of the kidney. *Am J Kidney Dis*. 2008;51:326-330.
579. Esparza AR, McKay DB, Cronan JJ, Chazan JA. Renal parenchymal malakoplakia. Histologic spectrum and its relationship to megalocytic interstitial nephritis and xanthogranulomatous pyelonephritis. *Am J Surg Pathol*. 1989;13:225-236.
580. Abdou NI, NaPombejara C, Sagawa A, et al. Malakoplakia: evidence for monocyte lysosomal abnormality correctable by cholinergic agonist in vitro and in vivo. *N Engl J Med*. 1977;297:1413-1419.
581. Murray KM, Keane WR. Review of drug-induced acute interstitial nephritis. *Pharmacotherapy*. 1992;12:462-467.
582. Remuzzi G, Ruggenenti P. The hemolytic uremic syndrome. *Kidney Int Suppl*. 1998;66:S54-S57.
583. Rossert J. Drug-induced acute interstitial nephritis. *Kidney Int*. 2001;60:804-817.
584. Muriithi AK, Leung N, Valeri AM, et al. Biopsy-proven acute interstitial nephritis, 1993-2011: a case series. *Am J Kidney Dis*. 2014;64:558-566.
585. Corwin HL, Korbet SM, Schwartz MM. Clinical correlates of eosinophiluria. *Arch Intern Med*. 1985;145:1097-1099.
586. Kleinknecht D. Interstitial nephritis, the nephrotic syndrome, and chronic renal failure secondary to nonsteroidal anti-inflammatory drugs. *Semin Nephrol*. 1995;15:228-235.
587. Brodsky SV, Nadasdy T. Acute and chronic tubulointerstitial nephritis. In: Jennette JC, Olson JL, Silva FG, Agati VD, eds. *Heptinstall's Pathology of the Kidney*. 7th ed. Philadelphia, PA: Wolters Kluwer; 2015:1111-1166.
588. Magil AB. Drug-induced acute interstitial nephritis with granulomas. *Hum Pathol*. 1983;14:36-41.
589. Praga M, Sevillano A, Aunon P, Gonzalez E. Changes in the aetiology, clinical presentation and management of acute interstitial nephritis, an increasingly common cause of acute kidney injury. *Nephrol Dial Transplant*. 2015;30:1472-1479.
590. Okada K, Okamoto Y, Kagami S, et al. Acute interstitial nephritis and uveitis with bone marrow granulomas and anti-neutrophil cytoplasmic antibodies. *Am J Nephrol*. 1995;15:337-342.
591. Saeki T, Nishi S, Imai N, et al. Clinicopathological characteristics of patients with IgG4-related tubulointerstitial nephritis. *Kidney Int*. 2010;78:1016-1023.
592. Cornell LD. IgG4-related kidney disease. *Curr Opin Nephrol Hypertens*. 2012;21:279-288.
593. Alexander MP, Larsen CP, Gibson IW, et al. Membranous glomerulonephritis is a manifestation of IgG4-related disease. *Kidney Int*. 2013;83:455-462.
594. Gaul MH, Barrett BJ. Analgesic nephropathy. *Am J Kidney Dis*. 1998;32:351-360.
595. De Broe ME, Elseviers MM. Analgesic nephropathy. *N Engl J Med*. 1998;338:446-452.
596. United States Renal Data System. 1996 Annual Data Report. Bethesda, MD, 1996.
597. Mihatsch MJ, Khanlari B, Brunner FP. Obituary to analgesic nephropathy—an autopsy study. *Nephrol Dial Transplant*. 2006;21:3139-3145.
598. De Broe ME, Elseviers MM. Over-the-counter analgesic use. *J Am Soc Nephrol*. 2009;20:2098-2103.
599. Bokemeyer C, Thon WF, Brunkhorst T, et al. High frequency of urothelial cancers in patients with kidney transplants for end-stage analgesic nephropathy. *Eur J Cancer*. 1996;32a:175-176.
600. Griffin MD, Bergstrahl EJ, Larson TS. Renal papillary necrosis: a 16-year clinical experience. *J Am Soc Nephrol*. 1995;6:248-256.
601. Fowler BA. Mechanisms of kidney cell injury from metals. *Environ Health Perspect*. 1993;100:57-63.
602. Prasad GV, Rossi NF. Arsenic intoxication associated with tubulointerstitial nephritis. *Am J Kidney Dis*. 1995;26:373-376.
603. Yasuda M, Miwa A, Kitagawa M. Morphometric studies of renal lesions in Itai-itai disease: chronic cadmium nephropathy. *Nephron*. 1995;69:14-19.
604. Li SJ, Zhang SH, Chen HP, et al. Mercury-induced membranous nephropathy: clinical and pathological features. *Clin J Am Soc Nephrol*. 2010;5:439-444.
605. Friedman AC, Lautin EM. Cis-platinum (II) diaminodichloride: another cause of bilateral small kidneys. *Urology*. 1980;16:584-586.
606. Hall CL, Fothergill NJ, Blackwell MM, et al. The natural course of gold nephropathy: long term study of 21 patients. *Br Med J (Clin Res Ed)*. 1987;295:745-748.
607. Randall RE Jr, Osherson RJ, Bakerman S, Setter JG. Bismuth nephrotoxicity. *Ann Intern Med*. 1972;77:481-482.

608. Sabath E, Robles-Osorio ML. Renal health and the environment: heavy metal nephrotoxicity. *Nefrologia*. 2012;32:279-286.
609. Lockitch G. Perspectives on lead toxicity. *Clin Biochem*. 1993;26:371-381.
610. Newman LS. Occupational illness. *N Engl J Med*. 1995;333:1128-1134.
611. Brewster UC, Perazella MA. A review of chronic lead intoxication: an unrecognized cause of chronic kidney disease. *Am J Med Sci*. 2004;327:341-347.
612. Schumann GB, Lerner SI, Weiss MA, et al. Inclusion-bearing cells in industrial workers exposed to lead. *Am J Clin Pathol*. 1980;74:192-196.
613. Bushinsky DA. Nephrolithiasis. *J Am Soc Nephrol*. 1998;9:917-924.
614. Vervaet BA, Verhulst A, D'Haese PC, De Broe ME. Nephrocalcinosis: new insights into mechanisms and consequences. *Nephrol Dial Transplant*. 2009;24:2030-2035.
615. Markowitz GS, Perazella MA. Acute phosphate nephropathy. *Kidney Int*. 2009;76:1027-1034.
616. Gutman AB, Yu TF. Uric acid nephrolithiasis. *Am J Med*. 1968;45:756-779.
617. Johnson RJ, Kivlighn SD, Kim YG, et al. Reappraisal of the pathogenesis and consequences of hyperuricemia in hypertension, cardiovascular disease, and renal disease. *Am J Kidney Dis*. 1999;33:225-234.
618. Nickeleit V, Mihatsch MJ. Uric acid nephropathy and end-stage renal disease—review of a non-disease. *Nephrol Dial Transplant*. 1997;12:1832-1838.
619. Crawhall JC, Purkiss P, Watts RW, Young EP. The excretion of amino acids by cystinuric patients and their relatives. *Ann Hum Genet*. 1969;33:149-169.
620. Sakhaei K. Pathogenesis and medical management of cystinuria. *Semin Nephrol*. 1996;16:435-447.
621. Emma F, Nesterova G, Langman C, et al. Nephropathic cystinosis: an international consensus document. *Nephrol Dial Transplant*. 2014;29(suppl 4):iv87-iv94.
622. Lieske JC, Toback FG. Renal cell-urinary crystal interactions. *Curr Opin Nephrol Hypertens*. 2000;9:349-355.
623. Rumsby G, Cochat P. Primary hyperoxaluria. *N Engl J Med*. 2013;369:2163.
624. Asplin JR. Hyperoxaluric calcium nephrolithiasis. *Endocrinol Metab Clin North Am*. 2002;31:927-949.
625. Nasr SH, D'Agati VD, Said SM, et al. Oxalate nephropathy complicating Roux-en-Y Gastric Bypass: an underrecognized cause of irreversible renal failure. *Clin J Am Soc Nephrol*. 2008;3:1676-1683.
626. Smith LH. The pathophysiology and medical treatment of urolithiasis. *Semin Nephrol*. 1990;10:31-52.
627. Leung N, Nasr SH. Myeloma-related kidney disease. *Adv Chronic Kidney Dis*. 2014;21:36-47.
628. Hutchison CA, Batuman V, Behrens J, et al. The pathogenesis and diagnosis of acute kidney injury in multiple myeloma. *Nat Rev Nephrol*. 2011;8:43-51.
629. Sedmak DD, Tubbs RR. The macrophagic origin of multinucleated giant cells in myeloma kidney: an immunohistologic study. *Hum Pathol*. 1987;18:304-306.
630. Start DA, Silva FG, Davis LD, et al. Myeloma cast nephropathy: immunohistochemical and lectin studies. *Mod Pathol*. 1988;1:336-347.
631. Carstens PH, Woo D. Crystalline glomerular inclusions in multiple myeloma. *Am J Kidney Dis*. 1989;14:56-60.
632. Bohle A, Ratschek M. The compensated and the decompensated form of benign nephrosclerosis. *Pathol Res Pract*. 1982;174:357-367.
633. Kashgarian M. Pathology of the kidney in hypertension. In: Kaplan NM, Brenner BM, Laragh JH, eds. *The Kidney in Hypertension*. New York, NY: Raven Press; 1987:77-89.
634. Valenzuela R, Gogate PA, Deodhar SD, Gifford RW. Hyaline arteriolonephrosclerosis. Immunofluorescent findings in vascular lesions. *Lab Invest*. 1980;43:530-534.
635. Ram CV. Current concepts in renovascular hypertension. *Am J Med Sci*. 1992;304:53-71.
636. Harrison EG Jr, McCormack LJ. Pathologic classification of renal arterial disease in renovascular hypertension. *Mayo Clin Proc*. 1971;46:161-167.
637. Plouin PF, Perdu J, La Batide-Alanore A, et al. Fibromuscular dysplasia. *Orphanet J Rare Dis*. 2007;2:28.
638. Slovut DP, Olin JW. Fibromuscular dysplasia. *N Engl J Med*. 2004;350:1862-1871.
639. Gerlock AJ Jr, Goncharenko VA, Ekelund L. Radiation-induced stenosis of the renal artery causing hypertension: case report. *J Urol*. 1977;118:1064-1065.
640. Chugh KS, Jain S, Sakhija V, et al. Renovascular hypertension due to Takayasu's arteritis among Indian patients. *Q J Med*. 1992;85:833-843.
641. Crosson JT, Keane WF, Anderson WR. Radiation nephropathy. In: Tisher CC, Brenner BM, eds. *Renal Pathology: with Clinical and Functional Correlations*. 2nd ed. Philadelphia, PA: JB Lippincott Co; 1994:937-947.
642. Cheng JC, Schultheiss TE, Wong JY. Impact of drug therapy, radiation dose, and dose rate on renal toxicity following bone marrow transplantation. *Int J Radiat Oncol Biol Phys*. 2008;71:1436-1443.
643. Jennette JC, Ordonez NG. Radiation nephritis causing nephrotic syndrome. *Urology*. 1983;22:631-634.
644. Keane WF, Crosson JT, Staley NA, et al. Radiation-induced renal disease. A clinicopathologic study. *Am J Med*. 1976;60:127-137.
645. Cohen EP, Lawton CA, Moulder JE. Bone marrow transplant nephropathy: radiation nephritis revisited. *Nephron*. 1995;70:217-222.
646. Jodele S, Licht C, Goebel J, et al. Abnormalities in the alternative pathway of complement in children with hematopoietic stem cell transplant-associated thrombotic microangiopathy. *Blood*. 2013;122:2003-2007.
647. Cohen EP, Lawton CA, Moulder JE, et al. Clinical course of late-onset bone marrow transplant nephropathy. *Nephron*. 1993;64:626-635.
648. George JN, Li X, McMinn JR, et al. Thrombotic thrombocytopenic purpura-hemolytic uremic syndrome following allogeneic HPC transplantation: a diagnostic dilemma. *Transfusion*. 2004;44:294-304.
649. Ho VT, Cutler C, Carter S, et al. Blood and marrow transplant clinical trials network toxicity committee consensus summary: thrombotic microangiopathy after hematopoietic stem cell transplantation. *Biol Blood Marrow Transplant*. 2005;11:571-575.
650. Bisceglia M, Galliani CA, Senger C, et al. Renal cystic diseases: a review. *Adv Anat Pathol*. 2006;13:26-56.
651. Rohatgi R. Clinical manifestations of hereditary cystic kidney disease. *Front Biosci*. 2008;13:4175-4197.
652. Torres VE, Grantham JJ. Cystic diseases of the kidney. In: Brenner BM, ed. *Brenner's and Rector's the Kidney*. 8th ed. Philadelphia, PA: WB Saunders; 2008:1428-1462.
653. Liapis H, Winyard PJD. Cystic diseases and developmental kidney defects. In: Jennette JC, Olson JL, Silva FG, Agati VD, eds. *Heptinstall's Pathology of the Kidney*. 7th ed. Philadelphia, PA: Wolters Kluwer; 2015:119-172.
654. Deeb A, Robertson A, MacColl G, et al. Multicystic dysplastic kidney and Kallmann's syndrome: a new association? *Nephrol Dial Transplant*. 2001;16:1170-1175.
655. Weber S, Moriniere V, Knuppel T, et al. Prevalence of mutations in renal developmental genes in children with renal hypodysplasia: results of the ESCAPE study. *J Am Soc Nephrol*. 2006;17:2864-2870.
656. Okayasu I, Kajita A. Histopathological study of congenital cystic kidneys with special reference to the multicystic, dysplastic type. *Acta Pathol Jpn*. 1978;28:427-434.
657. Risdon RA. Renal dysplasia. Part I. A clinical pathologic study of 76 cases. Part II. A necropsy study of 41 cases. *J Clin Pathol*. 1971;24:57-71.
658. Turco AE, Padovani EM, Chiaffoni GP, et al. Molecular genetic diagnosis of autosomal dominant polycystic kidney disease in a newborn with bilateral cystic kidneys detected prenatally and multiple skeletal malformations. *J Med Genet*. 1993;30:419-422.
659. Kimberling WJ, Kumar S, Gabow PA, et al. Autosomal dominant polycystic kidney disease: localization of the second gene to chromosome 4q13-q23. *Genomics*. 1993;18:467-472.
660. Reeder ST, Breuning MH, Davies KE, et al. A highly polymorphic DNA marker linked to adult polycystic kidney disease on chromosome 16. *Nature*. 1985;317:542-544.
661. Rossetti S, Harris PC. Genotype-phenotype correlations in autosomal dominant and autosomal recessive polycystic kidney disease. *J Am Soc Nephrol*. 2007;18:1374-1380.
662. Yoder BK, Mulroy S, Eustace H, et al. Molecular pathogenesis of autosomal dominant polycystic kidney disease. *Expert Rev Mol Med*. 2006;8:1-22.
663. Yoder BK, Hou X, Guay-Woodford LM. The polycystic kidney disease proteins, polycystin-1, polycystin-2, polaris, and cystin, are co-localized in renal cilia. *J Am Soc Nephrol*. 2002;13:2508-2516.
664. Rizk D, Chapman A. Treatment of autosomal dominant polycystic kidney disease (ADPKD): the new horizon for children with ADPKD. *Pediatr Nephrol*. 2008;23:1029-1036.
665. Rapola J, Kaariainen H. Polycystic kidney disease. Morphological diagnosis of recessive and dominant polycystic kidney disease in infancy and childhood. *APMIS*. 1988;96:68-76.
666. Grantham JJ. Clinical practice. Autosomal dominant polycystic kidney disease. *N Engl J Med*. 2008;359:1477-1485.
667. Chapman AB. Autosomal dominant polycystic kidney disease: time for a change? *J Am Soc Nephrol*. 2007;18:1399-1407.
668. Grantham JJ. Polycystic kidney disease: hereditary and acquired. *Adv Intern Med*. 1993;38:409-420.
669. Gregoire JR, Torres VE, Holley KE, Farrow GM. Renal epithelial hyperplastic and neoplastic proliferation in autosomal dominant polycystic kidney disease. *Am J Kidney Dis*. 1987;9:27-38.
670. Gabow PA, Johnson AM, Kaehny WD, et al. Risk factors for the development of hepatic cysts in autosomal dominant polycystic kidney disease. *Hepatology*. 1990;11:1033-1037.
671. Gabow PA. Autosomal dominant polycystic kidney disease—more than a renal disease. *Am J Kidney Dis*. 1990;16:403-413.
672. Hossack KF, Leddy CL, Johnson AM, et al. Echocardiographic findings in autosomal dominant polycystic kidney disease. *N Engl J Med*. 1988;319:907-912.
673. Guay-Woodford LM, Desmond RA. Autosomal recessive polycystic kidney disease: the clinical experience in North America. *Pediatrics*. 2003;111:1072-1080.
674. Guay-Woodford LM, Muecher G, Hopkins SD, et al. The severe perinatal form of autosomal recessive polycystic kidney disease maps to chromosome 6p21.1-p12: implications for

- genetic counseling. *Am J Hum Genet*. 1995;56:1101-1107.
675. Zerres K, Mucher G, Bachner L, et al. Mapping of the gene for autosomal recessive polycystic kidney disease (ARPKD) to chromosome 6p21-cen. *Nat Genet*. 1994;7:429-432.
676. Onuchic LF, Furukawa L, Nagasawa Y, et al. PKHD1, the polycystic kidney and hepatic disease 1 gene, encodes a novel large protein containing multiple immunoglobulin-like plexin-transcription-factor domains and parallel beta-helix 1 repeats. *Am J Hum Genet*. 2002;70:1305-1317.
677. Ward CJ, Hogan MC, Rossetti S, et al. The gene mutated in autosomal recessive polycystic kidney disease encodes a large, receptor-like protein. *Nat Genet*. 2002;30:259-269.
678. Menezes LF, Cai Y, Nagasawa Y, et al. Polyductin, the PKHD1 gene product, comprises isoforms expressed in plasma membrane, primary cilium, and cytoplasm. *Kidney Int*. 2004;66:1345-1355.
679. Gunay-Aygun M, Tuchman M, Font-Montgomery E, et al. PKHD1 sequence variations in 78 children and adults with autosomal recessive polycystic kidney disease and congenital hepatic fibrosis. *Mol Genet Metab*. 2010;99:160-173.
680. Buscher R, Buscher AK, Weber S, et al. Clinical manifestations of autosomal recessive polycystic kidney disease (ARPKD): kidney-related and non-kidney-related phenotypes. *Pediatr Nephrol*. 2014;29:1915-1925.
681. Gunay-Aygun M, Font-Montgomery E, Lukose L, et al. Correlation of kidney function, volume and imaging findings, and PKHD1 mutations in 73 patients with autosomal recessive polycystic kidney disease. *Clin J Am Soc Nephrol*. 2010;5:972-984.
682. Denamur E, Delezoide AL, Alberti C, et al. Genotype-phenotype correlations in fetuses and neonates with autosomal recessive polycystic kidney disease. *Kidney Int*. 2010;77:350-358.
683. Zerres K, Rudnik-Schoneborn S, Deget F, et al. Autosomal recessive polycystic kidney disease in 115 children: clinical presentation, course and influence of gender. Arbeitsgemeinschaft für Padiatrische, Nephrologie. *Acta Paediatr*. 1996;85:437-445.
684. Hildebrandt F, Zhou W. Nephronophthisis-associated ciliopathies. *J Am Soc Nephrol*. 2007;18:1855-1871.
685. Liapin H, Gau JP, Tomaszewski JE, Arend LJ. Pyelonephritis and other direct renal infections, reflux nephropathy, hydronephrosis, hypercalcemia and nephrolithiasis. In: Jennette JC, Olson JL, Silva FG, Agati VD, eds. *Heptinstall's Pathology of the Kidney*. 7th ed. Philadelphia, PA: Wolters Kluwer; 2015:1039-1110.
686. Fanconi G, Hanhart E, Albertini A. Die familiare juvenile Nephronophthise. *Helv Pediatr Acta*. 1951;6:1-49.
687. Gagnadoux MF, Bacri JL, Broyer M, Habib R. Infantile chronic tubulo-interstitial nephritis with cortical microcysts: variant of nephronophthisis or new disease entity? *Pediatr Nephrol*. 1989;3:50-55.
688. Omran H, Fernandez C, Jung M, et al. Identification of a new gene locus for adolescent nephronophthisis, on chromosome 3q22 in a large Venezuelan pedigree. *Am J Hum Genet*. 2000;66:118-127.
689. Halbritter J, Porath JD, Diaz KA, et al. Identification of 99 novel mutations in a worldwide cohort of 1,056 patients with a nephronophthisis-related ciliopathy. *Hum Genet*. 2013;132:865-884.
690. Chaki M, Hoefele J, Allen SJ, et al. Genotype-phenotype correlation in 440 patients with NPHP-related ciliopathies. *Kidney Int*. 2011;80:1239-1245.
691. Wolf MT. Nephronophthisis and related syndromes. *Curr Opin Pediatr*. 2015;27:201-211.
692. Loken AC, Hanssen O, Halvorsen S, Jolster NJ. Hereditary renal dysplasia and blindness. *Acta Paediatr*. 1961;50:177-184.
693. Senior B, Friedmann AI, Braudo JL. Juvenile familial nephropathy with tapetoretinal degeneration. A new oculorenal dystrophy. *Am J Ophthalmol*. 1961;52:625-633.
694. Ronquillo CC, Bernstein PS, Baehr W. Senior-Loken syndrome: a syndromic form of retinal dystrophy associated with nephronophthisis. *Vision Res*. 2012;75:88-97.
695. Cohen AH, Hoyer JR. Nephronophthisis. A primary tubular basement membrane defect. *Lab Invest*. 1986;55:564-572.
696. Eckardt KU, Alper SL, Antignac C, et al. Autosomal dominant tubulointerstitial kidney disease: diagnosis, classification, and management—a KDIGO consensus report. *Kidney Int*. 2015;88:676-683.
697. Ekici AB, Hackenbeck T, Moriniere V, et al. Renal fibrosis is the common feature of autosomal dominant tubulointerstitial kidney diseases caused by mutations in mucin 1 or urmodulin. *Kidney Int*. 2014;86:589-599.
698. Bleyer AJ, Kmoch S, Antignac C, et al. Variable clinical presentation of an MUC1 mutation causing medullary cystic kidney disease type 1. *Clin J Am Soc Nephrol*. 2014;9:527-535.
699. Kirby A, Gnrke A, Jaffe DB, et al. Mutations causing medullary cystic kidney disease type 1 lie in a large VNTR in MUC1 missed by massively parallel sequencing. *Nat Genet*. 2013;45:299-303.
700. Bollee G, Dahan K, Flamant M, et al. Phenotype and outcome in hereditary tubulointerstitial nephritis secondary to UMOD mutations. *Clin J Am Soc Nephrol*. 2011;6:2429-2438.
701. Dahan K, Devuyst O, Smaers M, et al. A cluster of mutations in the UMOD gene causes familial juvenile hyperuricemic nephropathy with abnormal expression of urmodulin. *J Am Soc Nephrol*. 2003;14:2883-2893.
702. Nasr SH, Lucia JP, Galgano SJ, et al. Urmodulin storage disease. *Kidney Int*. 2008;73:971-976.
703. Bleyer AJ, Zivna M, Hulkova H, et al. Clinical and molecular characterization of a family with a dominant renin gene mutation and response to treatment with fludrocortisone. *Clin Nephrol*. 2010;74:411-422.
704. Zivna M, Hulkova H, Matignon M, et al. Dominant renin gene mutations associated with early-onset hyperuricemia, anemia, and chronic kidney failure. *Am J Hum Genet*. 2009;85:204-213.
705. Clissold RL, Hamilton AJ, Hattersley AT, et al. HNF1B-associated renal and extra-renal disease—an expanding clinical spectrum. *Nat Rev Nephrol*. 2015;11:102-112.
706. Musetti C, Quaglia M, Mellone S, et al. Chronic renal failure of unknown origin is caused by HNF1B mutations in 9% of adult patients: a single centre cohort analysis. *Nephrology (Carlton)*. 2014;19:202-209.
707. Gambaro G, Feltrin GP, Lupo A, et al. Medullary sponge kidney (Lenarduzzi-Cacciari-Ricci disease): a Padua Medical School discovery in the 1930s. *Kidney Int*. 2006;69:663-670.
708. Kuiper JJ. Medullary sponge kidney. In: Gardner KD, ed. *Cystic Disease of the Kidney*. New York, NY: John Wiley and Sons, Inc; 1976:151-172.
709. Yendt ER. Medullary sponge kidney and nephrolithiasis. *N Engl J Med*. 1982;306:1106-1107.
710. Fabris A, Anglani F, Lupo A, Gambaro G. Medullary sponge kidney: state of the art. *Nephrol Dial Transplant*. 2013;28:1111-1119.
711. Fabris A, Lupo A, Ferraro PM, et al. Familial clustering of medullary sponge kidney is autosomal dominant with reduced penetrance and variable expressivity. *Kidney Int*. 2013;83:272-277.
712. Levine E. Acquired cystic kidney disease. *Radiol Clin North Am*. 1996;34:947-964.
713. Gabow PA. Polycystic and acquired cystic diseases. In: Greenberg A, ed. *Primer on Kidney Diseases*. 2nd ed. San Diego, CA: Academic Press; 1998:313-318.
714. Kuroda N, Ohe C, Mikami S, et al. Review of acquired cystic disease-associated renal cell carcinoma with focus on pathobiological aspects. *Histol Histopathol*. 2011;26:1215-1218.
715. Zhou XJ, Fenves AZ, Vaziri ND, Saxena R. Renal changes with aging and end-stage renal disease. In: Jennette JC, Olson JL, Silva FG, Agati VD, eds. *Heptinstall's Pathology of the Kidney*. 7th ed. Philadelphia, PA: Wolters Kluwer; 2015:1281-1320.
716. Nahm AM, Ritz E. The simple renal cyst. *Nephrol Dial Transplant*. 2000;15:1702-1704.
717. Murshidi MM, Suwan ZA. Simple renal cysts. *Arch Esp Urol*. 1997;50:928-931.
718. Terada N, Ichioka K, Matsuta Y, et al. The natural history of simple renal cysts. *J Urol*. 2002;167:21-23.
719. Baert L, Steg A. Is the diverticulum of the distal and collecting tubules a preliminary stage of the simple cyst in the adult? *J Urol*. 1977;118:707-710.

Jesse K. McKenney

## CHAPTER CONTENTS

### Pediatric tumors and tumorlike conditions, 1014

- Nephroblastic tumors, 1014
- Congenital mesoblastic nephroma, 1019
- Clear cell sarcoma, 1020
- Rhabdoid tumor, 1022
- Pediatric-type cystic nephroma and DICER1 renal sarcoma, 1023
- Intrarenal neuroblastoma, 1023
- Intrarenal Ewing sarcoma, 1024
- Intrarenal synovial sarcoma, 1024
- Metanephric tumors, 1024
- Renal cell carcinoma, 1025
- Other pediatric tumor types, 1025

### Adult tumors and tumorlike conditions, 1025

- Renal cell carcinoma, 1025

### Adenomas, 1040

- Oncocytoma, "difficult to classify" oncocytic tumors, and oncocytosis, 1040
- Neuroendocrine tumors, 1042
- Other epithelial tumors, 1042
- Angiomyolipoma, 1043
- Juxtaglomerular cell tumor, 1044
- Other benign tumors and tumorlike conditions, 1045
- Sarcomas, 1047
- Malignant lymphoma and related lymphoid lesions, 1047
- Metastatic tumors, 1047
- Tumors of renal pelvis and ureter, 1047

## Pediatric Tumors and Tumorlike Conditions

### Nephroblastic Tumors

#### Wilms Tumor (Nephroblastoma)

##### General Features

Wilms tumor is also known as nephroblastoma (currently the preferred term).<sup>1,2</sup> It constitutes the prototypical example of a neoplastic process that faithfully recapitulates embryogenesis at the morphologic and molecular levels.<sup>3-5</sup> It is seen primarily in infants, 50% of the cases occurring before the age of 3 years and 90% before the age of 6 years.<sup>6-8</sup> However, Wilms tumor is only exceptionally seen as a congenital neoplasm, a point of great importance in the differential diagnosis with mesoblastic nephroma.<sup>9</sup> There are also well-documented cases of Wilms tumors in adolescents<sup>10</sup> and adults, but this may represent a somewhat different disease with distinct genetic features and significantly worse clinical outcomes.<sup>11-15</sup> There is no appreciable sex predilection. The risk in Caucasians is lower than in Asians, but higher than in patients of African descent.

The classic location for Wilms tumor is the kidney. Both kidneys are equally affected, the incidence of synchronous or metachronous bilateral involvement being 5%–10%.<sup>16,17</sup> Cases with the typical morphologic features of Wilms tumor have rarely been recorded in extrarenal sites, including retroperitoneum, sacrococcygeal region, testis, uterus (sometimes presenting as a cervical polyp), inguinal canal, and mediastinum.<sup>18-24</sup> Some of them have arisen within a teratoma, and even those in which this feature was not evident have been viewed by some authors as teratomas with a predominant or exclusive nephroblastic component.

Wilms tumor has been reported in monozygous twins and other familial settings.<sup>7</sup> Conditions associated with the highest risk of Wilms tumor are Wilms-aniridia genital anomaly–retardation (WAGR) syndrome, omphalocele–macroglossia (Beckwith-Wiedemann syndrome), hemihypertrophy, Denys–Drash syndrome, and familial nephroblastoma.<sup>25-28</sup> Other conditions associated with Wilms tumor are renal and genital malformations, cutaneous nevi and angiomas, trisomy 18, Klippel–Trénaunay syndrome, neurofibromatosis, Bloom syndrome, Frasier syndrome, Simpson–Golabi–Behmel syndrome, Perlman syndrome, and cerebral gigantism (Sotos syndrome).<sup>28-32</sup> The incidence of congenital abnormalities of the urogenital tract is particularly high for Wilms tumors occurring during the first

## Abstract

This chapter covers the entire spectrum of neoplasms and non-neoplastic tumoral lesions that may involve the kidney. Pediatric tumors are detailed and include Wilms tumor (nephroblastoma), clear cell sarcoma of kidney, congenital mesoblastic nephroma, rhabdoid tumor, and cystic nephroma. The metanephric family of tumors is also addressed. An update on specific subtypes of renal cell carcinoma is provided, based on the 2016 WHO classification, and newer emerging entities are also covered. Other less common intrarenal neoplasms are also highlighted. Finally, lesions of the upper urinary tract (i.e. renal pelvis and ureter) are discussed.

## Keywords

Wilms tumor  
clear cell sarcoma of kidney  
renal rhabdoid tumor  
congenital mesoblastic nephroma  
metanephric adenoma  
renal cell carcinoma  
oncocytoma  
papillary adenoma  
angiomyolipoma  
urothelial carcinoma  
ureter  
renal pelvis

year of life and/or involving both kidneys. Wilms tumor has also been encountered in association with other malignancies, such as osteosarcoma, botryoid variant of embryonal rhabdomyosarcoma, retinoblastoma, hepatocellular carcinoma, and neuroblastoma.<sup>33-36</sup>

### Clinical Features

The classic clinical presentation of Wilms tumor is in the form of an abdominal mass felt by the mother when handling the child. Hematuria and pain are rare. Hypertension, present in a minority of the cases, has been shown to be caused by renin secretion by the tumor.<sup>37</sup> Proteinuria may be the result of tumor-associated glomerular disease in the non-neoplastic kidney.<sup>38</sup> Sometimes the first symptoms are related to traumatic rupture. Cases have been reported presenting as sudden death resulting from tumor embolism.<sup>39</sup>

Imaging studies show a solid intrarenal mass that often displaces and distorts the collecting system. Foci of calcification may be identified.<sup>40</sup>

### Morphologic Features

Grossly, most Wilms tumors are solitary, well circumscribed, rounded, and of soft consistency. Their size is extremely variable, and their median weight is 550 g. The cut section is predominantly solid and pale gray or tan and often exhibits areas of cystic change, necrosis, and hemorrhage (Fig. 24.1). A lobular pattern resulting from fibrous septation is common. Multicentric tumor foci are found in 7% of the cases.

Microscopically, three major components are identified: undifferentiated blastema, mesenchymal (stromal) tissue, and epithelial tissue.<sup>41-43</sup> Most Wilms tumors show a representation of all three components, but the proportions vary widely from case to case and sometimes from region to region in the same tumor. Some tumors are biphasic, and still others are monophasic (monomorphic). The *blastomatous* areas are extremely cellular and composed of small round-to-oval primitive cells; the cytoplasm is usually very scant, but sometimes is more abundant and exhibits an oncocyoid appearance. Adjacent nuclei commonly appear to overlap. The pattern of growth may be diffuse, nodular, cordlike (serpentine), or basaloid (with peripheral palisading). Particularly on biopsy, Wilms tumors in which the blastomatous component predominates can be confused with any of the small round cell tumors (including neuroblastoma), rhabdoid tumor, or clear cell sarcoma of kidney. The *mesenchymal* elements usually have spindle cells with

fibroblastic or smooth muscle features, but may also exhibit differentiation toward various heterologous cell types, particularly skeletal muscle.<sup>44</sup>

The *epithelial* component is characterized by the formation of embryonic tubular (and sometimes glomerular) structures that closely recapitulate the appearance of normal developing metanephric tubules (and glomeruli) at the light microscopic, ultrastructural, and lectin histochemistry levels (Fig. 24.2).<sup>45-48</sup> The differentiation can be so pronounced that tumor analogues of nearly all segments of the normal nephron can be formed.<sup>49</sup> These tubular structures can be small and round, thus simulating the rosettes of neuroblastoma. Features favoring tubules over rosettes are presence of a lumen, single cell layer, distinct basal lamina, and surrounding fibromyxoid stroma.<sup>41</sup> The differential diagnosis of predominantly epithelial Wilms tumors also includes cystic nephroma, renal cell carcinoma (RCC), and metanephric adenoma.<sup>41,50</sup> Exceptionally, marked hydropic changes are seen in the tubular epithelial component.<sup>51</sup> Heterologous epithelium may include ciliated, mucinous, squamous, or transitional epithelium (Fig. 24.3).<sup>41,52</sup>

In the type known as *papillonodular*, grossly evident projections are seen extending from the septa into the cyst lumina, resulting in a fibroadenoma-like appearance on low-power microscopic examination.<sup>53,54</sup>

Other heterologous tissues described in Wilms tumor are endocrine cells of various types<sup>52</sup>; renin-producing cells<sup>55</sup>; neuroepithelium, neuroblasts, and mature ganglion cells<sup>56,57</sup>; neuroglia<sup>58</sup>; adipose tissue; and cartilage, bone, and hematopoietic cells.<sup>41</sup> Sometimes the variety of tissues present is such that the distinction between Wilms tumor and teratoma becomes blurred<sup>41</sup>; the term *teratoid Wilms tumor* has been used to describe these cases.<sup>59,60</sup>

The distinct cystic partially differentiated Wilms tumor is discussed separately later.

Anaplastic features may be present focally or extensively in Wilms tumors (approximately 5%–8% of cases); they are discussed fully in the section on prognosis.

### Immunohistochemical Features

The immunohistochemical profile of the various components of Wilms tumor mirrors that of their counterparts in the developing kidney.<sup>61-63</sup>

The epithelial elements react for keratin and epithelial membrane antigen (EMA)<sup>61,64</sup>; the mesenchymal elements show a reactivity pattern consonant with their morphologic appearance (such as

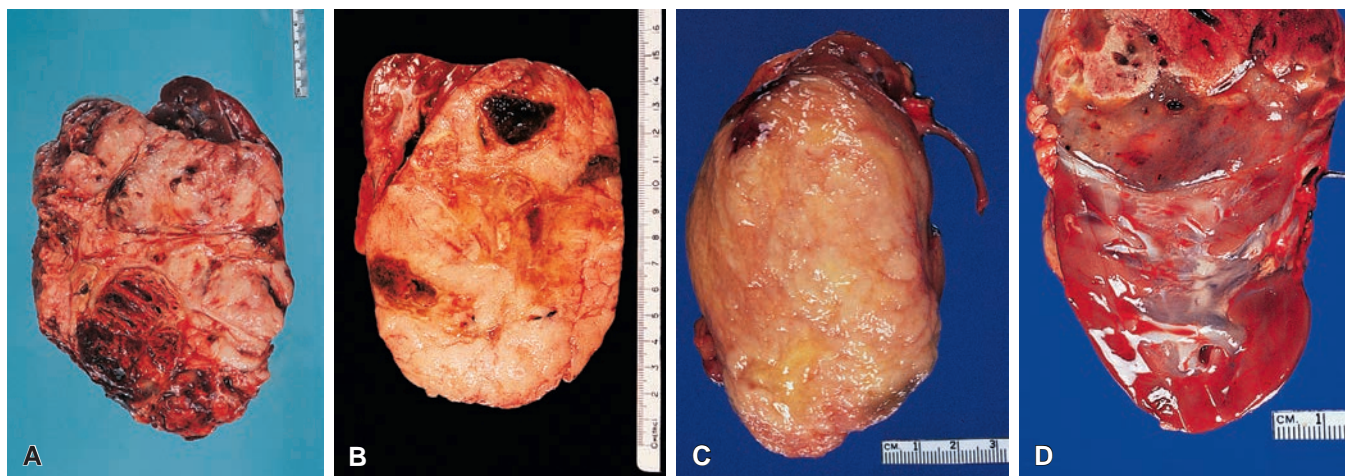


**Figure 24.1** Various Gross Appearances of Wilms Tumor. **A** and **B**, Variegated appearance. **C**, More homogeneous and nodular. **D**, Extensive areas of infarct-like necrosis.

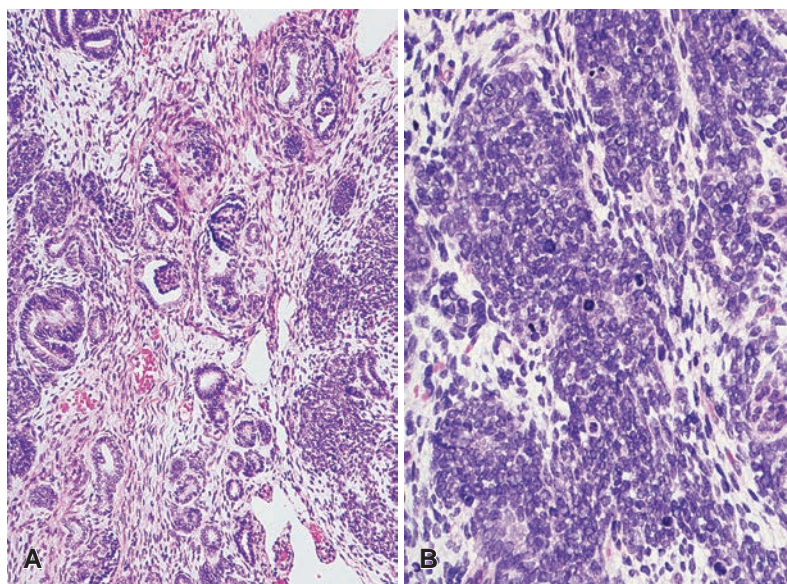


**Figure 24.2** Microscopic Appearance of Wilms Tumor. **A**, Low-power microscopic view showing a combination of blastema, stroma, epithelial tubular formations, and immature glomeruli. **B**, High-power view showing blastema, stroma, and immature tubular formations.

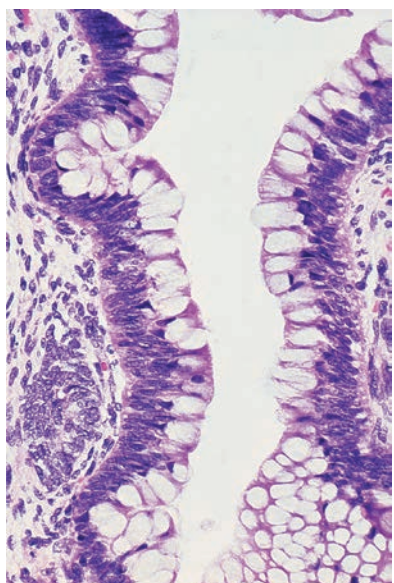


**Figure 24.3** Mucinous epithelium in Wilms tumor.

positivity for myogenin and desmin in the rhabdomyomatous foci<sup>65</sup>; and the neural elements—when present—exhibit reactivity for neuron-specific enolase, glial fibrillary acidic protein, and S-100 protein.<sup>64</sup> Additional immunoreactivities of Wilms tumor include nuclear WT1 (80%, typically in epithelial and blastemal components), nuclear PAX8, CD56 (96%), and (unexpectedly) TTF-1; the latter, which is found in 17% of cases, represents a potential source of misdiagnosis.<sup>66,67</sup>

#### Molecular Genetic Features

The genetic loci predisposing to Wilms tumor are *WT1* and *WT2*. The former is located in 11p13 and encodes a zinc finger transcription factor that is expressed in the early development of the urogenital system, with its germline point mutation and deletion being the

underlying genetic alteration in Denys–Drash syndrome and WAGR syndrome, respectively.<sup>68–70</sup> *WT2* is located in 11p15.5, which contains the gene for insulin growth factor II, and is implicated in tumors associated with Beckwith–Wiedemann syndrome.<sup>71–74</sup> Alterations of these genes may also be identified in sporadic tumors. A relationship has been shown between the level of expression of these genes and the microscopic features of the tumor.<sup>68,75–79</sup>

Inactivation of the *WTX* gene located on the X chromosome is found in 6%–30% of cases of sporadic Wilms tumor.<sup>79,80</sup> This results from somatic deletion or, less commonly, inactivating mutation of the gene on the single X chromosome in tumors of males or the active X chromosome in tumors of females.<sup>81–83</sup> The pathogenetic role of *WTX* alteration in Wilms tumor is not fully elucidated, but downregulation of *WTX* leads to increased signaling in the Wnt pathway.<sup>83</sup>

Activating mutation of the  $\beta$ -catenin gene *CTNNB1* is found in 14%–20% of Wilms tumors, resulting in disturbance of the Wnt signaling pathway. It may be found in tumors with *WT1* mutation, but not with *WT1* wild-type.<sup>84–86</sup>

Abnormalities in other chromosomes—1, 7q, 8, 12, and 16—have also been encountered.<sup>14,87,88</sup> These genetic changes are identical in the various histologic components of the tumor, and 1p and 16q loss of heterozygosity (LOH) are discussed further under prognosis.<sup>89</sup> Mutations of *TP53* and/or overexpression of the protein are found in only 5% of the cases of Wilms tumor. They are largely restricted to the anaplastic foci and carry an unfavorable prognostic connotation.<sup>90,91</sup> Similarly, *MYCN* amplification is seen in rare cases with aggressive behavior, most commonly with diffuse anaplasia. More recently, mutations in the *SIX/2* pathway and the *DROSHA/DGCR8* miRNA microprocessor complex have been described in high-risk blastemal Wilms tumors.<sup>92</sup>

#### Spread and Metastases

In advanced cases, local spread occurs in the perirenal soft tissues. From here, the tumor may directly involve the adrenal glands, bowel, liver, vertebrae, and paraspinal region; the latter may result in spinal cord compression.<sup>93</sup> Invasion of the renal vein is common, but extension into the renal pelvis or ureter is a rare and late event.

**Table 24.1** Staging of nephroblastoma, rhabdoid tumor of the kidney, clear cell sarcoma of the kidney (Children's Oncology Group)

STAGE	DESCRIPTION
Stage I	Completely resected tumor limited to the kidney. No intraoperative rupture or biopsy of the tumor prior to removal. No involvement of the vessels of the renal sinus. No evidence of tumor beyond the margins of resection. Regional lymph nodes confirmed negative microscopically.
Stage II	Completely resected tumor with no evidence of tumor at or beyond margins of resection. Tumor extends beyond the kidney as evidenced by regional extension of the tumor (through renal capsule, extensive invasion of the soft tissue of the renal sinus) or tumor in blood vessels within the nephrectomy specimen, but outside renal parenchyma. This includes blood vessels of the renal sinus.
Stage III	Residual tumor present after surgery, confined to abdomen. This includes the following: <ul style="list-style-type: none"> <li>• Lymph nodes within the abdomen/pelvis are involved by tumor.</li> <li>• Tumor has penetrated through the peritoneal surface.</li> <li>• Tumor implants are on the peritoneal surface.</li> <li>• Gross or microscopic tumor remains postoperatively (positive surgical margins on microscopic exam).</li> <li>• Involvement of vital structures precludes complete resection.</li> <li>• Tumor spillage before or during surgery.</li> <li>• Tumor is treated with preoperative chemotherapy (with or without any prior biopsy, including fine-needle aspiration).</li> <li>• Tumor is removed in more than one piece (e.g. tumor is found in tissues separate from nephrectomy specimen, such as separately excised adrenal, or separately removed thrombus from renal vein).</li> <li>• Extension of primary tumor into thoracic vena cava and/or heart.</li> </ul>
Stage IV	Hematogenous metastases or lymph node metastases outside the abdominopelvic region
Stage V	Bilateral renal involvement present at diagnosis. Each kidney should be substaged separately by above criteria.

Metastases in regional lymph nodes are found in 15% of the cases. The most common sites of distant metastases are lungs, liver, and peritoneum.<sup>94</sup> The presence of lung metastases in a child with a retroperitoneal neoplasm strongly favors a diagnosis of Wilms tumor over that of neuroblastoma. Conversely, the presence of bone metastases suggests a diagnosis other than Wilms tumor, since they occur in only 1% of the cases.

### Therapy

The therapy for Wilms tumor has been relatively standardized and is based largely on protocols from either the International Society of Paediatric Oncology (SIOP) or the Children's Oncology Group (COG).<sup>2,95-98</sup> The specifics of these protocols are being continuously updated.<sup>99</sup> The main differences between the two approaches are based on the use of presurgical therapy. The SIOP typically espouses preoperative chemotherapy followed by surgical resection. In this model, some regions require biopsies to confirm diagnosis prior to chemotherapy, while others do not. Further therapy is based on the initial response as measured by a post-therapy classification.<sup>100</sup> Advocates of the SIOP approach cite fewer intraoperative tumor ruptures (due to therapy-related tumor shrinkage) and less upstaging. The COG typically advocates for initial surgical resection with subsequent therapy determined by tumor histology and stage. Its advocates cite prognostic stratification that allows for more tailored therapy. Despite these differences, the clinical outcomes for both the SIOP and COG approaches are very similar.<sup>99,101</sup>

### Prognosis

The overall cure rate for unilateral Wilms tumor is 80%–90%.<sup>102</sup> A small percentage of long-term survivors of Wilms tumor develop a second malignant neoplasm, either because of a genetic predisposition to neoplasia or secondary to therapy.<sup>103</sup>

The prognostic connotations of various clinical and morphologic parameters are as follows:

1. **Age.** Patients under 2 years of age have significantly fewer metastases and a better 5-year survival rate than those over 2 years.<sup>104,105</sup>

2. **Stage.** Clinicopathologic staging of Wilms tumor is the most important prognostic determinant, based on either the SIOP or the COG systems (Table 24.1). Capsular invasion, rupture at surgery, extrarenal vein invasion, tumor implants, lymph node metastases, distant metastases, and bilaterality are the main criteria used.<sup>106</sup> Unfortunately, staging of Wilms tumor by the pathologist is fraught with pitfalls. The tumor “capsule” (or pseudocapsule) can be confused with the renal capsule; the renal sinus and surgical margins may be difficult to evaluate; and the renal vein may retract considerably, giving a false impression—when invaded—that tumor is present at the margin. It is important for sections to be taken from the renal sinus, the junction between tumor and normal kidney, the tumor capsule, and the uninvolved renal parenchyma. In a study of stage I cases, the following four features were found to be associated with increased rate of relapse: presence of an inflammatory pseudocapsule, invasion of the renal sinus, extensive infiltration of the renal capsule, and tumor infiltration of intrarenal vessels.<sup>107</sup>
3. **Size.** Tumor mass, as measured by the weight of the excised specimen, is an important determinant of outcome, especially in stage I tumors.<sup>108</sup>
4. **Anaplasia.** For a case of Wilms tumor to be placed into the anaplastic category, it should meet the following three criteria: (1) marked enlargement of nuclei within the blastemal, epithelial, or stromal cell lines (excepting skeletal muscle cells) to at least three times the diameter of adjacent nuclei of the same cell type; (2) obvious hyperchromasia of the enlarged nuclei; and (3) multipolar mitotic figures (Fig. 24.4).<sup>109</sup>

Anaplasia thus defined is present in about 4% of the cases, the incidence being higher in patients of African descent and in older patients.<sup>110</sup> It is very uncommon in tumors from patients under 2 years of age; this is probably the reason for the better prognosis exhibited by this age group. Sometimes it is found in the metastases and not in the primary tumor.

Currently, *focal* anaplasia applies only to cases in which the previously defined changes are restricted to *one or a few discrete*

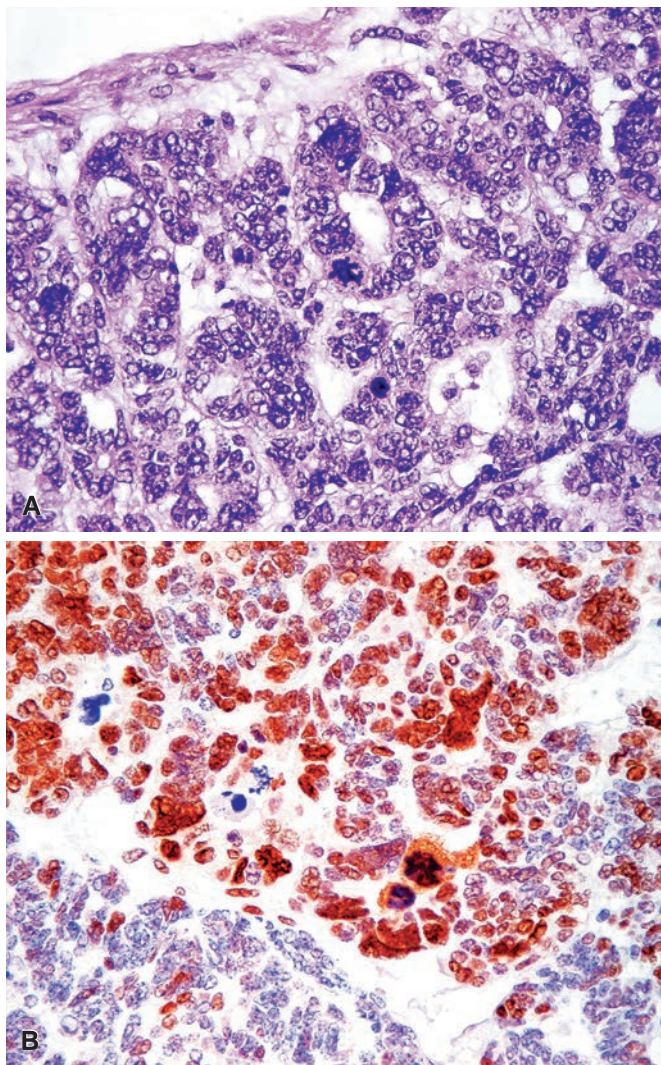


**Figure 24.4 Anaplastic ("Unfavorable Histology") Wilms Tumor.** **A**, Marked pleomorphism with giant hyperchromatic nuclei and atypical mitoses. **B**, Strong nuclear immunoreactivity for p53.

- loci within the primary tumor, with no anaplasia or marked nuclear atypia elsewhere.<sup>11</sup> Specifically, focal anaplasia cannot be present in tumor infiltrating outside the kidney (e.g. renal sinus) or in intravascular tumor. Thorough tumor sampling (one section for each centimeter of tumor diameter) and careful mapping of where sections were taken is obviously needed to evaluate this feature properly.<sup>12</sup> Cases with localized anaplasia in which the background tumor shows a degree of "marked" atypia (i.e. bordering on anaplasia, but falling short of the minimal threshold, typically due to nuclear pleomorphism without other features) have been referred to as showing "nuclear unrest" and are classified as diffuse anaplasia. Wilms tumors with anaplasia are referred to as having "unfavorable histology" in the sense of exhibiting a lesser response to chemotherapy. This predictive connotation is greater when the anaplasia is diffuse rather than focal, and since anaplasia predicts response to therapy, its significance in stage I tumors is debated.<sup>113</sup>
5. **Extensive tubular differentiation.** This is said to be a good prognostic sign. According to some authors, this is also true for cases with extensive glomerular differentiation.<sup>114-116</sup> This finding does not currently direct initial therapy.

6. **Skeletal muscle differentiation.** This feature does not seem to have a significant effect on prognosis, except when present in massive amounts. In the latter instance it is said to be associated with a better prognosis.<sup>116-118</sup> This finding does not currently direct initial therapy.
7. **Post-chemotherapy morphology.** The SIOP classification is based largely on response to chemotherapy with three simple categories: completely necrotic (low risk), blastemal predominant (high risk), and "others" (intermediate risk).<sup>100</sup> The incidence of anaplasia does not seem to be affected by this treatment modality (i.e. there is no evidence that therapy induces cytologic changes mimicking anaplasia).<sup>119</sup>
8. **TP53 mutation.** Mutations of the TP53 gene, evaluated indirectly through the immunohistochemical detection of P53 protein overexpression, correlate with the presence of anaplasia at the histologic level and therefore with an unfavorable outcome.<sup>120,121</sup>
9. **LOH at 1p and 16q.** Some studies have suggested that LOH at 1p and 16q is an adverse prognostic factor in favorable histology Wilms tumors.<sup>122-125</sup> Future COG and/or SIOP trials will likely attempt to further validate this finding.

Many of these prognostic parameters are used in the revised SIOP working classification for nephroblastoma (Table 24.2).

### Cystic Partially Differentiated Wilms Tumor (Nephroblastoma)

Cystic partially differentiated Wilms tumor typically occurs in very young children, most less than 24 months old.<sup>126</sup> By definition, this tumor should have an exclusively cystic gross appearance with thin septa and no solid nodules. It is typically large (mean of 10 cm), but well circumscribed. Histologically, the thin septa contain an admixture of different tissues, including fibrous tissue, skeletal muscle, fat, cartilage, blastema, and nephroblastomatous epithelium. Cysts may show papillary infolding, but no microscopic nodular masses should protrude from the cyst wall, as their presence suggests a cystic Wilms tumor. Hemorrhage, necrosis, and calcification are not features of cystic partially differentiated Wilms tumor. Surgical resection is typically curative and adjuvant therapy is not recommended for this clinically benign neoplasm. The main differential diagnosis is pediatric cystic nephroma, which (by definition) does not contain nephroblastomatous elements.

### Nephroblastomatosis and Nephrogenic Rests

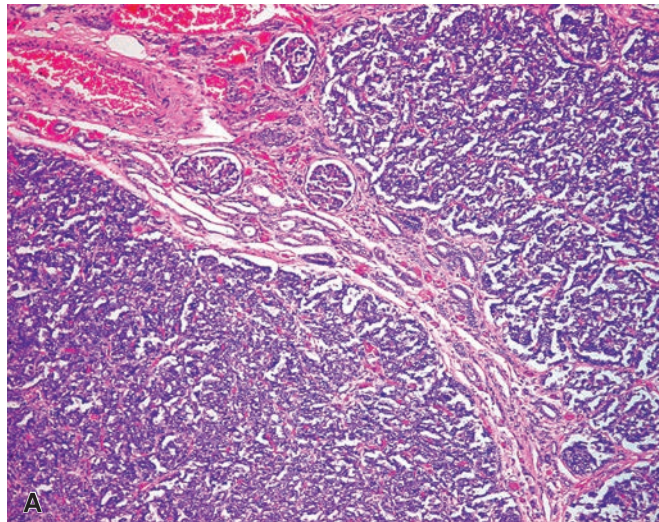
*Nephroblastomatosis* and *nephrogenic rests* are defined as persistent foci of embryonal cells (after 36 weeks gestation), but they are discussed here because of their frequent confusion and histogenetic relationship with Wilms tumor.<sup>2,127-129</sup> Nephrogenic rests are seen in up to 40% of patients with Wilms tumor and approximately 1% of neonates.<sup>127</sup> The term nephroblastomatosis refers to diffuse or multifocal nephrogenic rests. In its most florid form, the process is often associated with a variety of congenital anomalies and with hypertension.<sup>130</sup>

Nephrogenic rests have been divided into *perilobular* and *intralobular* forms (Fig. 24.5). The former, which is more common, is located peripherally, has sharply demarcated margins, is composed predominantly of blastema and tubules with scanty (or sclerotic) stroma, and is often multifocal. The intralobular form is randomly distributed in the cortex and medulla and has irregular margins. It shows a predominance of stroma over blastema and tubules and is usually solitary.<sup>131-133</sup> Further methods of nephrogenic rest subclassification have also been proposed.<sup>132</sup>

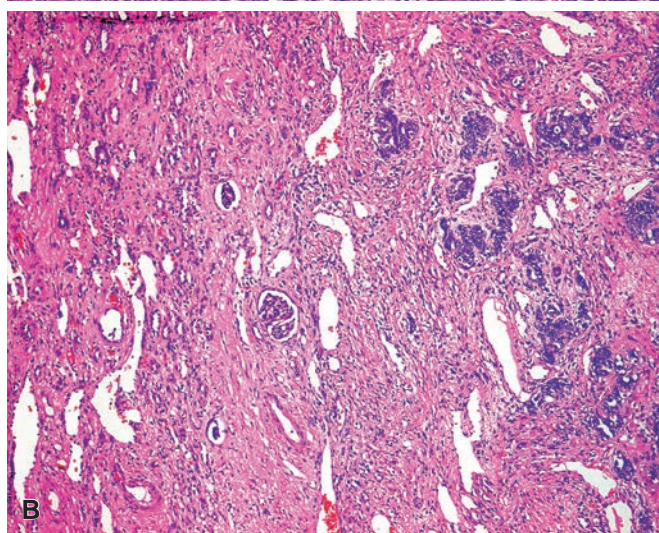
Nephroblastomatosis can be diagnosed by computed tomography (CT) scan, magnetic resonance imaging (MRI), or ultrasound.<sup>134</sup> Grossly, the most exuberant examples of this disease can be

**Table 24.2** Staging of pediatric renal tumors (International Society of Paediatric Oncology) (post-chemotherapy)

Stage I	Viable tumor limited to the kidney, or surrounded by an intact fibrous pseudocapsule and completely resected. No renal sinus invasion of soft tissue or vessels. Necrotic tumor or chemotherapy induced changes may be present in renal sinus or soft tissue outside of kidney without upstaging, as long as these changes do not extend to resection margins. Prior percutaneous core needle (Tru-cut) biopsy or fine-needle aspiration does not upstage the tumor. Tumor may infiltrate adrenal gland if adrenal capsule is intact. Tumor may be adherent to liver capsule but may not infiltrate liver parenchyma.
Stage II	Completely resected viable tumor extends beyond kidney or penetrates through the renal capsule or fibrous tumor pseudocapsule into perirenal fat. Tumor may infiltrate the renal sinus and/or invade blood vessels, but resection margins are clear. Tumor may infiltrate adjacent organs or vena cava, if completely resected with clear margins.
Stage III	Incomplete excision. Gross residual tumor remains in the patient, or tumor extends to resection margins on microscopic exam, including necrotic tumor or chemotherapy induced changes at resection margin. <ul style="list-style-type: none"> <li>• Tumor in any abdominal lymph node, including necrotic tumor or tumor with chemotherapy effect.</li> <li>• Tumor rupture before or during resection surgery</li> <li>• Tumor penetrates peritoneal surface.</li> <li>• Tumor thrombi present at resection margins of vessels or ureter, transected or removed piecemeal.</li> <li>• Wedge biopsy of the tumor prior to preoperative chemotherapy or surgery.</li> </ul>
Stage IV	Hematogenous metastases or spread of tumor beyond the abdomen and pelvis.
Stage V	Bilateral renal tumors. Each side should be substaged by above criteria.



A



B

**Figure 24.5** Nephrogenic rests. Perilobar (A) and intralobar (B) types.

distinguished from Wilms tumor because of the diffuse or multifocal nature of the process and the involvement of the entire subcapsular region. Microscopically, the mass is typically unencapsulated and composed of tightly packed nephrogenic epithelial cells that have a primitive but not anaplastic appearance. Stromal tissue is scanty; cartilage, striated cells, and primitive mesenchyme are absent. However, hyperplastic rests may have some foci that are cytologically indistinguishable from Wilms tumor, but have the distribution of a rest and no capsule. Other histologic mimics of nephrogenic rests include dysplastic medullary ray nodules (most commonly in Beckwith-Wiedemann syndrome) and embryonal hyperplasia (often in multicystic dysplasia and end-stage kidneys).<sup>135,136</sup>

In cases associated with Wilms tumor, they have been found to share similar mutations.<sup>137</sup> Perilobar rests often have 11p15 alterations and are commonly associated with hemihypertrophy and/or Beckwith-Wiedemann syndrome, while intralobar rests commonly have *WT1* mutations and may be associated with Denys-Drash syndrome.<sup>138</sup> *CTNNB1* mutations are seen in intralobar rests, even in the absence of *WT1* mutation.<sup>139</sup>

A conservative therapeutic approach is indicated in cases of nephrogenic rests and nephroblastomatosis<sup>140</sup>; however, nephrogenic rests in patients less than 1 year of age (particularly if perilobar) and especially diffuse hyperplastic nephroblastomatosis are associated with the highest risk of contralateral Wilms tumor.<sup>141</sup>

### Congenital Mesoblastic Nephroma

Congenital mesoblastic nephroma represents the most common renal tumor of newborns and is usually discovered before 6 months of age.<sup>142</sup> Extraordinary examples in adults have been reported, but the diagnosis is rare after 2 years of age and should be carefully scrutinized outside that setting.<sup>143,144</sup> Grossly, the tumor is solid, yellow-gray to tan, with a whorled configuration reminiscent of uterine leiomyoma (Fig. 24.6). Most are centered near the hilus of the kidney. The tumor often appears well circumscribed, but it may infiltrate the renal parenchyma and even the perirenal fat microscopically. Areas of hemorrhage and necrosis are usually absent. A cystic variant of this tumor has been described.<sup>145,146</sup>

Microscopically, two distinct patterns are seen. "Classic" congenital mesoblastic nephroma resembles "infantile fibromatosis" of the renal sinus with long sweeping and intersecting fascicles composed

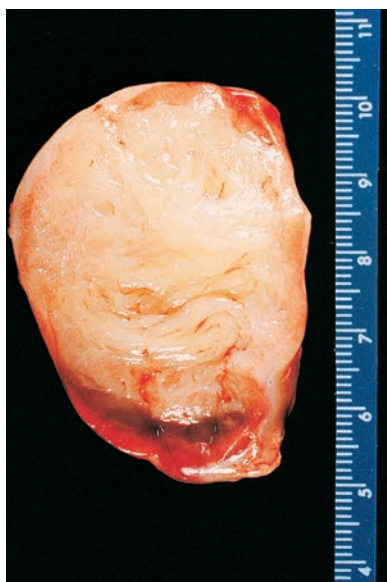


**Figure 24.6** Congenital Mesoblastic Nephroma. Gross appearance of the well-circumscribed character of this tumor and its white fibrous cut surface are well illustrated.

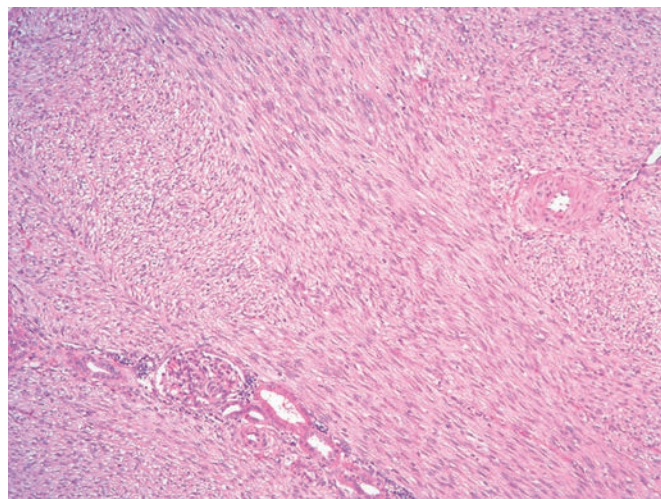


**Figure 24.7** Congenital Mesoblastic Nephroma, Classic Type. Microscopic appearance showing a monotonous proliferation of spindle cells with bland nuclei, resembling fibromatosis.

of cytologically bland, elongated spindle cells (Fig. 24.7).<sup>147</sup> There is typically fine intracellular collagen imparting a light eosinophilic appearance. Tubules and glomeruli (sometimes exhibiting hyperplastic or metaplastic changes) may be entrapped by the spindle tumor cells. Small islands of hyaline cartilage and foci of extramedullary hematopoiesis may be present. There is no capsule separating the tumor from the uninvolving renal parenchyma.

Cellular congenital mesoblastic nephroma is comprised of more densely cellular plump spindle cells with larger nuclei, resembling infantile fibrosarcoma (Fig. 24.8).<sup>148,149</sup> They are mitotically active, have a tendency to infiltrate the renal pelvis or perirenal tissue, and may contain areas of hemorrhage and necrosis.<sup>150</sup> When classic and cellular patterns coexist, the tumors are designated as mixed.

Immunohistochemically, the neoplastic cells often show expression of smooth muscle actin, while desmin staining is rare. CD34 is typically negative.

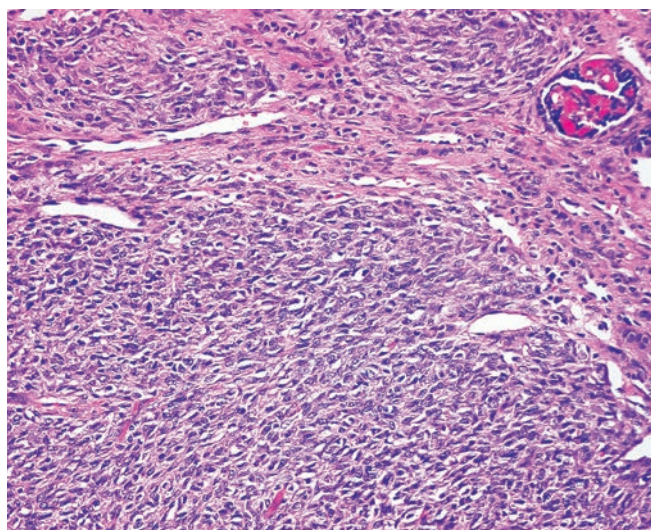


**Figure 24.8** Congenital Mesoblastic Nephroma, Cellular Type, Accompanied by Mitotic Activity. An entrapped glomerulus is present in a corner. Some of these tumors behave in an aggressive fashion.

Congenital mesoblastic nephromas lack the abnormalities in chromosome 11 that characterize Wilms tumor and are associated instead with polysomes for chromosomes 8, 11, 17, and 20.<sup>151-153</sup> Cellular congenital mesoblastic nephroma contains the t(12;15) (p13;q25) translocation, which results in the *ETV6-NTRK3* gene fusion, the latter being detectable in paraffin-embedded material.<sup>154</sup> This gene fusion is not found in classic mesoblastic nephroma.<sup>155,156</sup> It appears that the occurrence of gene fusion antedates acquisition of chromosomal polysomes.<sup>152</sup> The sharing of the same genetic abnormality between cellular congenital mesoblastic nephroma and infantile fibrosarcoma supports the notion that these two tumors represent a single neoplastic entity.<sup>152</sup> Most mixed congenital mesoblastic nephromas lack the *ETV6* fusion.<sup>156</sup>

The large majority of congenital mesoblastic nephromas are cured following nephrectomy.<sup>157</sup> Therefore, radiation therapy or chemotherapy is not indicated. In up to 7% of the cases, recurrence with local invasion of retroperitoneum will occur and may prove fatal.<sup>148,158</sup> Cases associated with distant metastases to lung and brain have rarely been reported<sup>159,160</sup>; most of these aggressive tumors have had atypical morphologic features.<sup>148,161</sup> Beckwith and Weeks<sup>162</sup> have pointed out that in all but one of the recurrent congenital mesoblastic nephromas the patients were over 3 months of age at the time of the original nephrectomy; they believe that age at diagnosis and adequacy of excision may be more important prognostic factors than the morphologic features of the tumor. In a recent series, stage III cellular congenital mesoblastic nephromas in patients aged 3 months or older were particularly prone to develop local recurrences.<sup>163</sup>

### Clear Cell Sarcoma

Clear cell sarcoma, formerly known as bone-metastasizing renal tumor and not to be confused with clear cell sarcoma of soft tissue, is a distinctive renal malignancy.<sup>142,164-166</sup> It comprises approximately 4% of childhood renal tumors; its incidence peaks during the second year of life. Isolated cases have been described in adults<sup>167,168</sup> and in association with familial colonic polyposis.<sup>169</sup> Grossly, the tumor tends to be large, sharply outlined, and centered in the medullary or mid region of the kidney. They have a homogeneous cut surface of light brown-to-gray color and myxoid appearance

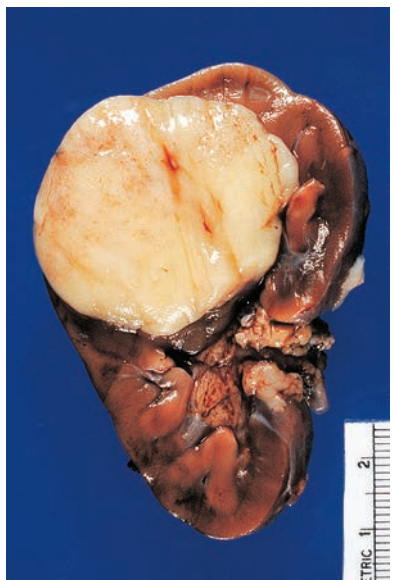


**Figure 24.9** Gross Appearance of Clear Cell Sarcoma of Kidney. The tumor is well circumscribed and whitish, and it bulges on the cut surface.

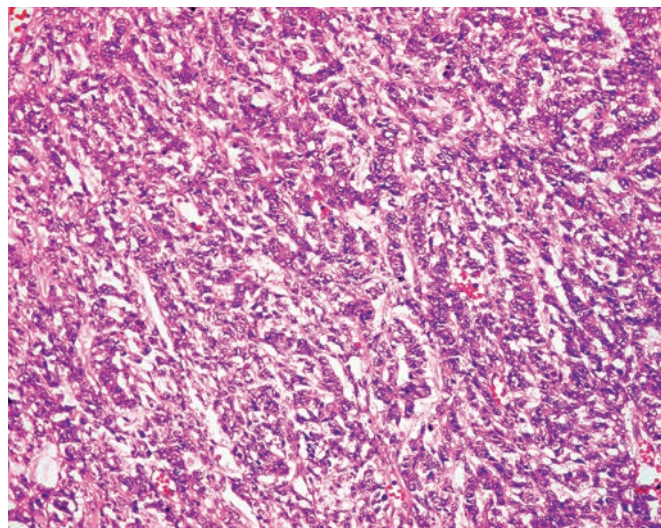


**Figure 24.11** Clear cell sarcoma of kidney, trabecular pattern of growth.

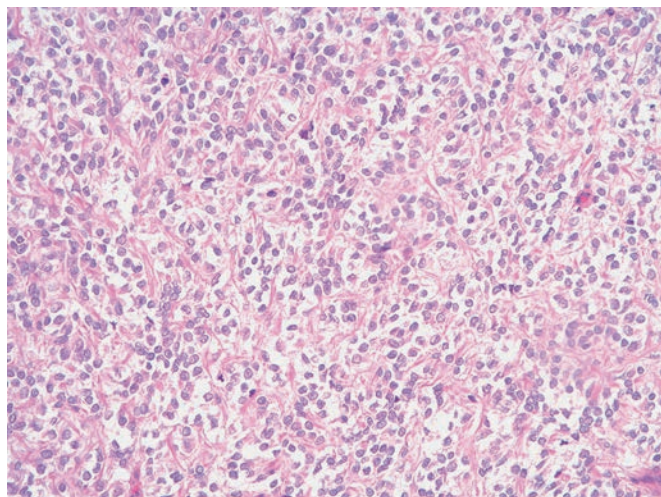


**Figure 24.10** Clear cell sarcoma of kidney, prototypical appearance.

(Fig. 24.9). The consistency is usually hard, and cystic formations are common.

Microscopically, the most common pattern is that of a diffuse growth of relatively small cells with round normochromatic nuclei, inconspicuous nucleoli, light-staining (sometimes vacuolated) cytoplasm, and indistinct cell margins (Fig. 24.10); however, the morphology is very heterogeneous. Despite the tumor name, clear cytoplasm is a prominent feature in only 20% of the cases. Nuclear grooves are common, and mitoses are infrequent. The fibrovascular stroma may result in arrangements of the tumor cells in nests, palisades, cords, or trabeculae (Fig. 24.11). The latter should not be confused with the tubules or the serpentine arrangement of Wilms tumor. Myxoid changes, fibrosis, and hyalinization may be present, the appearance of the hyalinized tissue sometimes simulating osteoid (Fig. 24.12). Cysts may result from dilation of entrapped tubules or from stromal degeneration. It has been remarked that the distinctive alveolar and arborizing vascular stroma is a more reliable diagnostic

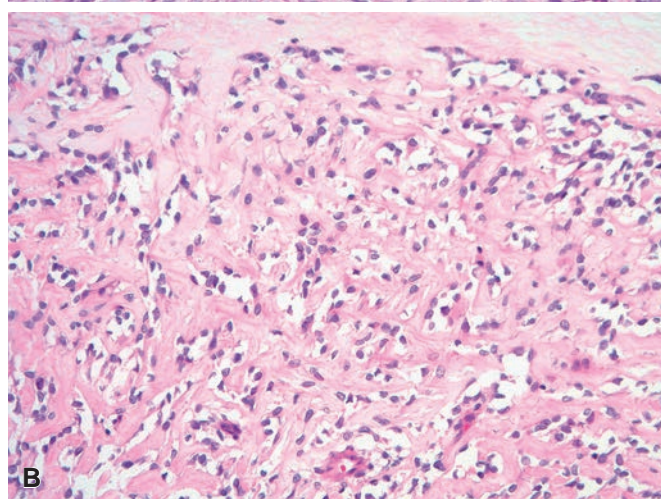
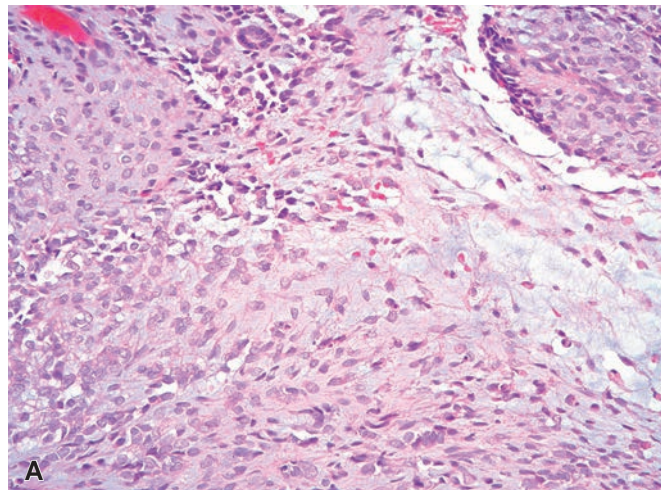


**Figure 24.12** Clear Cell Sarcoma of Kidney. **A**, Myxoid pattern. **B**, Sclerotic pattern.

feature than the clear cells or the sclerosis.<sup>170</sup> As many as nine histologic patterns of this tumor have been described, that is, classic, myxoid, sclerosing, cellular, epithelioid, palisading, spindle, storiform, and anaplastic.<sup>171</sup>

Clear cell sarcoma of kidney has recently been shown to harbor two main, and mutually exclusive, genetic events: somatic internal tandem duplication within the *BCOR* gene sequence (approximately 85%) and *YWHAE-NUTM2* fusion (approximately 10%).<sup>172-175</sup> A small subset of cases harbor neither event.<sup>172</sup> These genetic features, as well as typical patient age and histology, are shared by a subset of extrarenal undifferentiated round cell sarcomas of infancy,<sup>176</sup> suggesting a close relationship that was first noted histologically and ultrastructurally in 1991.<sup>177</sup> Immunohistochemistry has historically not been helpful in confirming the diagnosis of clear cell sarcoma of kidney, but they are usually *PAX8* negative.<sup>67</sup> A new commercially available *BCOR* antibody has high sensitivity and specificity for clear cell sarcoma of kidney (and the other tumors harboring these same genetic events).<sup>178</sup> One caveat is that a rare subset of synovial sarcomas may show *BCOR* overexpression.<sup>179</sup>

Untreated clear cell sarcoma is a very malignant tumor, with a high tendency for relapse and a propensity for skeletal metastases, particularly skull.<sup>166</sup> In this regard, it should be noted that skeletal metastases are extraordinarily rare in conventional Wilms tumors. Metastases of clear cell sarcoma also occur to regional lymph nodes, brain, lung, and liver. In contrast to Wilms tumor, these metastases tend to develop after long intervals following the removal of the primary tumor (5 years or more).

The overall survival rate in a series of 351 cases entered in a National Wilms Tumor Study (NWTS) trial was 69%. Multivariate analysis showed that treatment with doxorubicin, stage, age at diagnosis, and tumor necrosis were independent prognostic factors. Of note, stage I patients had a 98% survival rate.<sup>171</sup>

## Rhabdoid Tumor

Rhabdoid tumor of kidney is a distinct aggressive malignancy that is part of a larger family of *SMARCB1*-associated neoplasms.<sup>142,180</sup> Most cases occur in young infants, the median age at diagnosis being 18 months; 80% occur before 2 years of age.<sup>181</sup> Some of the cases have resulted in hypercalcemia.<sup>182,183</sup>

Grossly, rhabdoid tumor is solid, soft, and relatively well circumscribed. Microscopically, it is a monomorphic neoplasm that always involves the medullary region and has a generally diffuse but sometimes alveolar or trabecular pattern of growth. The tumor cells are medium sized and generally round or oval with vesicular nuclei and prominent nucleoli and indistinct cell borders (Fig. 24.13). However, they can also be spindled, prompting the possibility of confusion with mesoblastic nephroma or clear cell sarcoma. The most characteristic feature is the presence of a large cytoplasmic eosinophilic hyaline globule that displaces the nucleus laterally to result in a plasmacytoid or rhabdomyosarcomatous appearance (Fig. 24.14). Ultrastructurally, this globule is made up of a tangle of intermediate filaments.<sup>184</sup> Immunohistochemically, there is strong reactivity for vimentin and usually also for keratin, but generally not muscle (i.e. myogenin) or neural markers. It should be remarked that focal rhabdoid features resulting from accumulation of cytoplasmic filaments can be seen in many other renal tumors, including Wilms tumor, mesoblastic nephroma, and RCC.<sup>185</sup> Loss of immunohistochemical expression of *SMARCB1* (INI1/hSNF5/BAF47) is a feature of great help in the differential diagnosis with other pediatric small cell tumors.<sup>186,187</sup> This results from biallelic alteration (deletion or mutation) of the *hSNF5/INI1* locus at chromosome 22q11.2.<sup>188</sup> Rare tumors retain *SMARCB1* expression due to an alternative mutation in *SMARCA4/BRG1*. In about 15% of the cases, renal rhabdoid

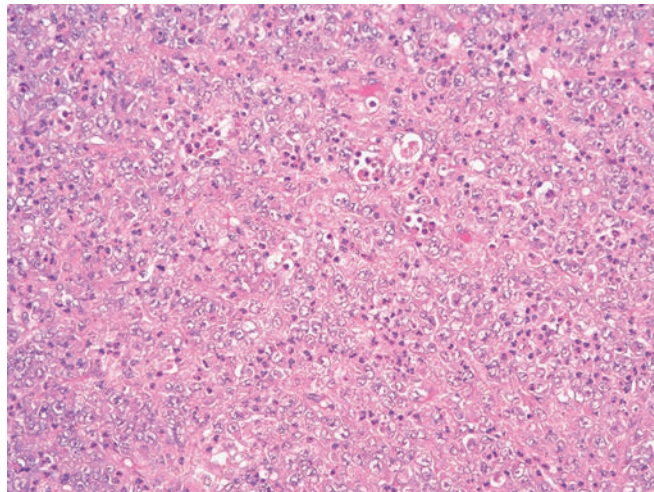


**Figure 24.13** Rhabdoid Tumor of Kidney. Syncytial sheets of highly atypical cells, often with admixed inflammation.

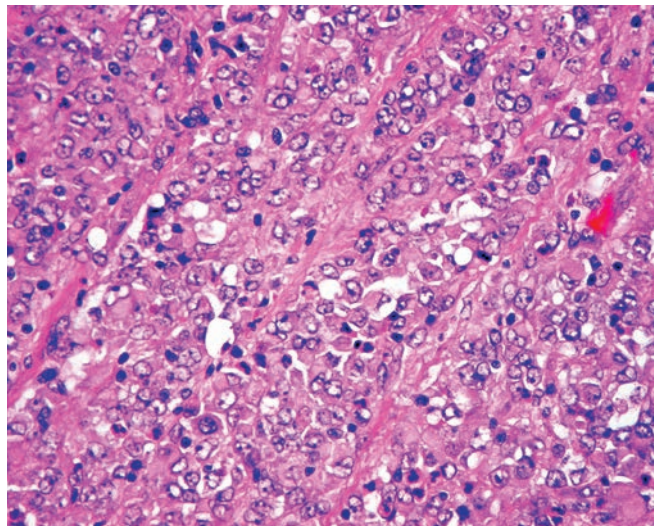


**Figure 24.14** Rhabdoid Tumor of Kidney. The nuclear grade is high. An eosinophilic amorphous ("hyaline") material fills the scanty cytoplasm and pushes the nucleus aside.

tumor is associated with primary atypical teratoid/rhabdoid tumors in the posterior fossa, and those patients typically harbor germline mutations in *SMARCB1*.

The behavior is extremely aggressive, even when occurring in young infants. The death rate is over 75%. High tumor stage and male sex are unfavorable prognostic signs.<sup>185</sup>

Tumors morphologically, immunophenotypically, and genetically indistinguishable from rhabdoid tumor of kidney have been reported in many other anatomic sites.<sup>189-191</sup>

Rhabdoid tumor of infantile kidney should not be equated to RCC with rhabdoid features (see later). Medullary carcinoma of the kidney may have significant histologic overlap with rhabdoid tumor, including loss of *SMARCB1/INI-1* nuclear expression; however, patients with medullary carcinoma present at an older age and often have sickle cell trait. Many reported examples of rhabdoid tumor in patients over 5 years of age likely represent renal medullary carcinoma.<sup>181</sup>



**Figure 24.15** Gross appearance of pediatric cystic nephroma involving most of the kidney.

### Pediatric-Type Cystic Nephroma and DICER1 Renal Sarcoma

Pediatric cystic nephroma (multilocular cystic nephroma, multilocular cyst) is an uncommon but distinctive lesion that arises in early infancy.<sup>192</sup> While this diagnostic term has previously been applied to tumors in all age groups, the World Health Organization (WHO) recommends that the term be restricted to infants, given that those tumors are genetically distinct and may be associated with a tumor predisposition syndrome (i.e. germline mutation in DICER1).<sup>193-195</sup> Clinical manifestations result from the presence of a mass or, not uncommonly, from ureteral obstruction by one of the daughter locules.

Grossly, the lesion is usually solitary, unilateral, and sharply delineated from the uninvolved renal parenchyma.<sup>196</sup> The usual size range is between 5 and 15 cm, and the outer surface is coarsely nodular. The cut surface shows a multilocular appearance, the individual cysts measuring from 1 mm to 3 cm or more (Fig. 24.15). The wall of these cysts is thin and sometimes translucent and lacks papillary projections. The fluid within the cavity is usually serous. The cysts do not communicate with each other or with the pelvis. The remaining renal parenchyma is normal. Extension of the lesion beyond the renal capsule may occur.

Microscopically, there are cysts of varying caliber separated by a spindled stroma (Fig. 24.16). The cysts are lined by epithelium that ranges in height from columnar to extremely flat, resembling endothelium and simulating the appearance of lymphangioma. A "hobnail" pattern is common (Fig. 24.17). The stroma between the cysts usually has a fibroblastic, nondescript nature (sometimes immunoreactive for hormone receptors), with variable stromal condensation adjacent to the cyst lining (Fig. 24.18).<sup>197</sup> Small well-differentiated tubules may be seen, but the presence of nephroblastomatous elements would preclude the diagnosis of cystic nephroma. As noted, many pediatric cystic nephromas have underlying *DICER1* mutations,<sup>192</sup> explaining their reported association with pleuropulmonary blastoma.

Rarely, intrarenal spindle cell sarcomas are identified in pediatric patients and have been described under various names, including embryonal sarcoma and anaplastic sarcoma.<sup>198-200</sup> The location may be parenchymal or pelvicalceal. Microscopically, the common denominator is a spindle cell component containing (either in a diffuse fashion or as multiple foci) varying levels of pleomorphism with some examples showing bizarre pleiomorphic cells and atypical mitotic figures. Chondromatous and osteoid foci are sometimes

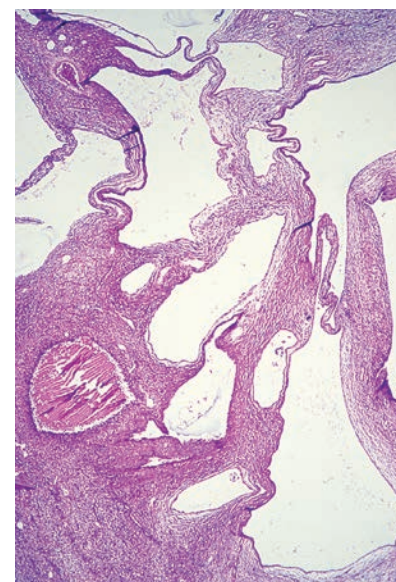


**Figure 24.16** Low-power microscopic appearance of pediatric cystic nephroma showing multiple cysts lined by flattened epithelium and separated by a cellular spindle cell stroma.

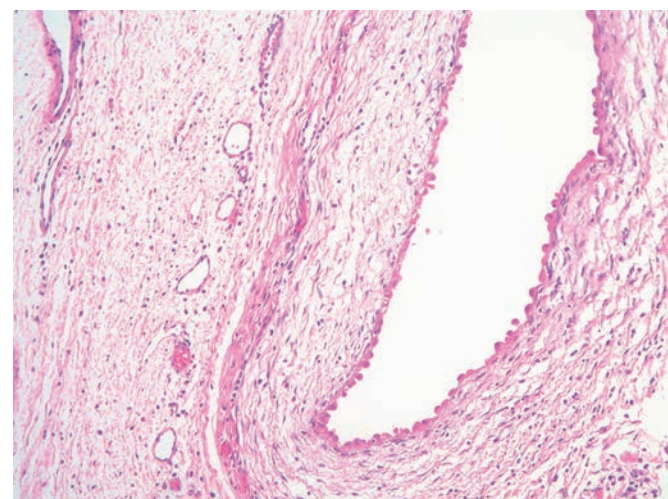


**Figure 24.17** Pediatric Cystic Nephroma. The epithelial lining of the cyst has a hobnail quality and the stroma is loose and hypocellular.

present. Immunohistochemically, a haphazard pattern of reactivity is recorded; however, keratin stains are negative. An associated cystic component, sometimes with features of cystic nephroma, has been described.<sup>201</sup> The behavior has been very aggressive.<sup>198</sup> The overall appearance of this tumor resembles pleuropulmonary blastoma of childhood, of which it may represent the renal counterpart. Recent studies have supported this histologic impression, showing frequent *DICER1* mutations and proposing a genetic pathogenesis of cystic nephroma and *DICER1*-renal sarcoma that parallels type 1 to type II/III malignant progression in pleuropulmonary blastoma.<sup>202</sup>

### Intrarenal Neuroblastoma

Neuroblastoma can invade the kidney secondarily from the adrenal or other retroperitoneal site, or it may initially present as a primary intrarenal tumor, and should be classified as outlined in the chapter

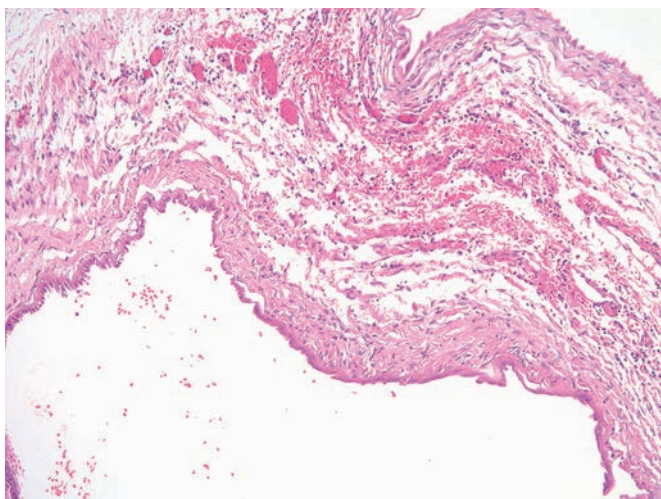


**Figure 24.18** Pediatric Cystic Nephroma. The stroma shows subtle cellularity adjacent to the epithelium, which is more atrophic.

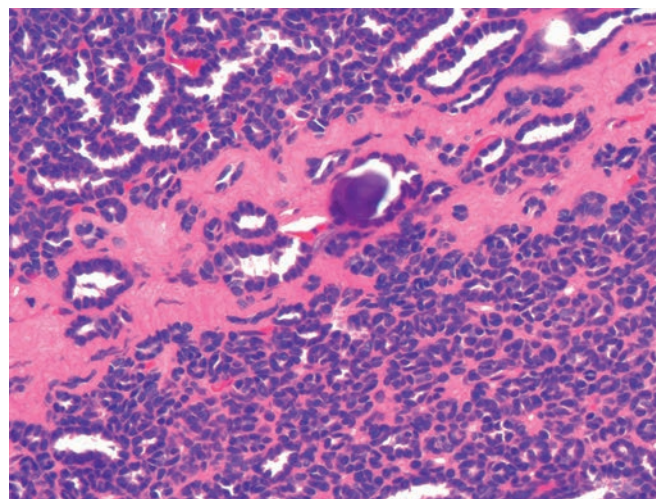


**Figure 24.20** Metanephric Adenoma. The lesion is extremely cellular with a small tubular pattern.

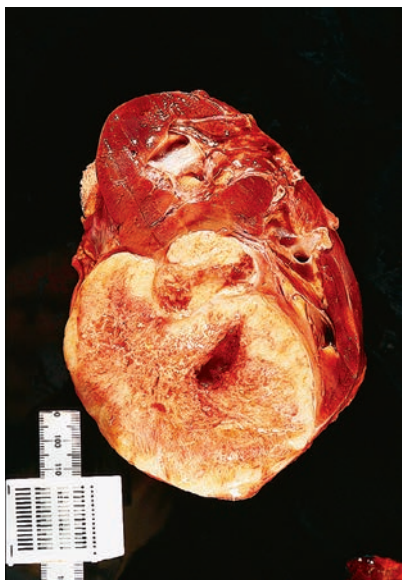


**Figure 24.19** Gross appearance of Ewing sarcoma, primary in the kidney.

on adrenal pathology.<sup>203</sup> When intrarenal, a misdiagnosis of Wilms tumor is likely. This issue is further complicated by the fact that the embryonal tubules of Wilms tumor can simulate rosettes and that true neuroblastic elements can occur in Wilms tumor. Immunohistochemical and molecular genetic evaluation are of help in this differential diagnosis.<sup>41,204</sup>

### Intrarenal Ewing Sarcoma

Ewing sarcoma can also occur as a primary renal mass.<sup>205,206</sup> Its morphologic, immunohistochemical, and molecular genetic features are analogous to those at other sites. Most patients are young adults, and the clinical course is very aggressive.<sup>207</sup> Many of the cases are centered in the medullary/pelvic region (Fig. 24.19). The main differential diagnosis is with blastema-predominant Wilms tumor, from which it is distinguished by its positivity for CD99 and its (usual) negativity for WT1.<sup>205</sup> Ideally, the diagnosis should be confirmed by the demonstration by cytogenetics, fluorescence in

situ hybridization (FISH), or reverse transcriptase-polymerase chain reaction (RT-PCR) of the t(11;22) translocation involving EWSR1.<sup>208,209</sup>

The initial analysis of 146 cases of primary malignant "neuroepithelial" tumors of the kidney from the NWTS Pathology Center files<sup>210</sup> and a subsequent review of additional cases<sup>205</sup> led the authors to the frustrating conclusion that these represent a diverse group of high-grade tumors which are not always easy to place in a specific category, even after their evaluation with immunohistochemical and molecular genetic tools. We would recommend keeping the diagnosis of Ewing sarcoma pure by requiring molecular confirmation. In our opinion, unusual tumors that do not fit into the Ewing sarcoma family, and for which other specific diagnostic categories are excluded (e.g. Wilms tumor), are best reported descriptively under terms such as "malignant neoplasm with neuroectodermal (or neuroepithelial) differentiation."

Rarely, other undifferentiated round cell sarcomas have been reported in the kidney, such as those associated with CIC-DUX4 fusion.<sup>211,212</sup>

### Intrarenal Synovial Sarcoma

Synovial sarcoma, which is histologically and genetically identical to its soft tissue counterpart, may rarely occur in the kidney.<sup>213,214</sup> It is important to note that there are variable reports of PAX-8 expression in synovial sarcoma, some reporting reactivity in the spindle cells and some in glands (which may simply represent entrapped renal tubules).<sup>67,215,216</sup>

### Metanephric Tumors

Metanephric adenoma tends to occur in young or middle-aged female patients. While more common in adults, metanephric adenoma is described here to include the related forms with a stromal component, which are more common in children. Grossly, they are solid and tan to gray in color. Microscopically, they are mostly composed of tightly packed small back-to-back tubules with minute lumina accompanied by very scanty stroma (Figs. 24.20 and 24.21).<sup>217-219</sup> More elongated branching tubules and areas with papillary architecture are not uncommon. The neoplastic cells are small and basophilic with almost no cytoplasm; nuclear features are bland. The overall appearance is very reminiscent of developing metanephric tubular epithelium.<sup>220</sup> Psammoma bodies are very common and

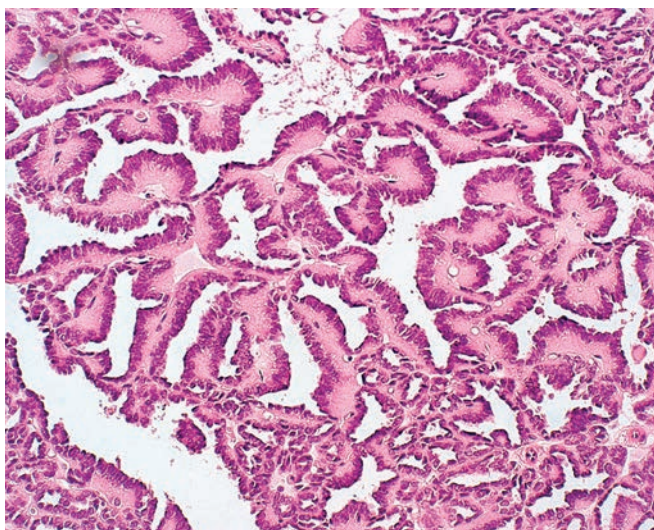


**Figure 24.21** Papillary pattern of growth of metanephric adenoma.

may be numerous. Secondary changes such as hemorrhage or cyst formation are common. Some of these features are also apparent on cytologic examination.<sup>221</sup>

Immunophenotypically, metanephric adenomas express both nuclear PAX8 and WT1, and cytoplasmic CD57 staining is common.<sup>222</sup> CK7 is negative or only focally positive. Genetically, approximately 90% have BRAF V600E mutations,<sup>223</sup> and BRAF immunohistochemistry (diffuse cytoplasmic staining) may serve as a surrogate marker.<sup>224,225</sup> The genetic features indicative of Wilms tumor and papillary RCC are absent.

The behavior of metanephric adenoma is benign.

**Metanephric stromal tumor** is a recently described pediatric renal neoplasm, occurring primarily in early childhood. It typically presents grossly as a fibrous lesion centered in the renal medulla that contains smooth-walled cysts. Microscopically, the neoplastic cells are spindle shaped, but admixed epithelioid features occur. The tumor entraps native renal tubules and blood vessels with onion-skin cuffing and myxoid change around each of the structures. Juxtaglomerular cell hyperplasia may also be seen within entrapped glomeruli (which may be associated with hypertension). There may be heterologous differentiation in the form of glia or cartilage and various types of associated vascular alterations (i.e. angiomyxoma). Immunohistochemically, most cases are reactive for CD34. Surgical excision is curative.<sup>226</sup>

**Metanephric adenofibroma** is a biphasic tumor in which an epithelial component similar to that of metanephric adenoma is intimately admixed with a bland spindle cell stroma similar to that of metanephric stromal tumor (Fig. 24.22).<sup>227,228</sup> Ages range from 1 to 36 years, but the mean is 7 years. The spindle cell component commonly expresses CD34 and entraps normal renal structures. The epithelial component has similar morphology and immunophenotype to metanephric adenoma. In some reported cases, part of the epithelial component was indistinguishable from that of Wilms tumor and in others it closely resembled papillary RCC.<sup>227</sup> The behavior of typical metanephric adenofibroma is benign.

### Renal Cell Carcinoma

While MiT family translocation RCCs represent the most common RCC subtype in children, they are fully described in the adult renal neoplasia section since they are more commonly seen in that setting (due to much higher incidence of RCC in adults). Most other subtypes

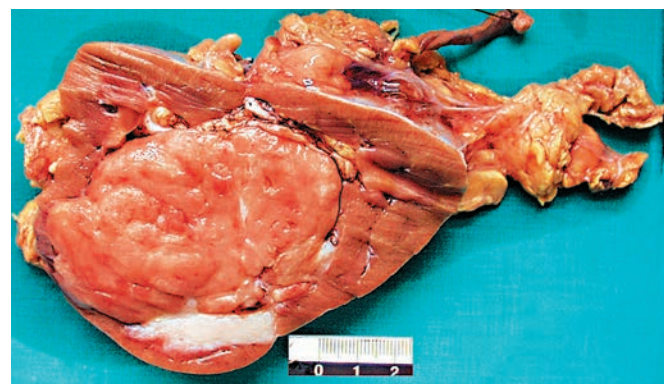


**Figure 24.22** Gross Appearance of Metanephric Adenofibroma. The tumor is solid and vaguely nodular.

of renal cell carcinoma have also been reported in children and young adults.

## Other Pediatric Tumor Types

Isolated examples of pediatric neoplasms not clearly belonging to any of the previous categories have been described. They include *ossifying renal tumor of infancy* (presenting as a calcified mass in the renal pelvis and composed of spindle cells in a partially calcified osteoid matrix),<sup>229</sup> *intrarenal teratoma* (to be distinguished from teratoid Wilms tumor),<sup>230</sup> *intrarenal pure yolk sac tumor*,<sup>231</sup> and *desmoplastic small round cell tumor*.<sup>232-234</sup>

## Adult Tumors and Tumorlike Conditions

### Renal Cell Carcinoma

#### General Features

RCC is generally a tumor of adults (average age at diagnosis: 55–60 years).<sup>235</sup> Many of the RCCs occurring in children have an appearance and behavior equivalent to those developing in adults,<sup>236-239</sup> but a high percentage belong to the MiT family translocation types.<sup>240,241</sup> The male to female ratio of adult RCC is about 2:1, and the incidence of bilaterality is 1%. Cigarette smoking and high blood pressure are said to increase the risk for development of the disease.<sup>242</sup> The list of diseases, hereditary and non-hereditary, that are associated with increased risk of RCC (including disease specific subtypes) continues to expand.<sup>243</sup>

Conditions that may be complicated by RCC are the following:

1. *von Hippel-Lindau (VHL) disease.* RCC occurs in 50% or more of individuals with this autosomal dominant syndrome, which is also characterized by the presence of CNS (usually cerebellar) and retinal hemangioblastomas; cysts of kidney, liver, and pancreas; clear cell tumors in a variety of sites (including inner ear and paratestis); and pheochromocytomas.<sup>244,245</sup> RCCs (of the clear cell subtype) in these patients tend to be multiple and associated with cysts, some of which show atypical changes in the lining epithelium.<sup>246-248</sup> The cysts, atypical cysts, and renal tumors of these patients have a similar immunohistochemical profile.<sup>249</sup> The VHL disease gene, called *VHL*, has been identified at chromosome 3p25.5. This tumor-suppressor gene is mutated in the germline of affected individuals, and in VHL-associated RCCs it is associated with a subsequent deletion of *VHL* in the wild-type allele. The marked degree of vascularization that often accompanies RCC (and other VHL-defective tumors, such as



**Figure 24.23** Renal Cell Carcinoma Developing in the Adult Form of Polycystic Kidney Disease. The tumor was multicentric.

cerebellar hemangioblastoma) is probably explained by the tumor's overproduction of hypoxia-inducible factor and its targets, such as vascular endothelial growth factor (VEGF), platelet-derived growth factor (PDGF), transforming growth factor alpha (TGF- $\alpha$ ), and erythropoietin.<sup>250</sup> Microscopically, a small subset of clear cell RCCs associated with VHL disease have some features reminiscent of clear cell-papillary RCC.<sup>251</sup> Additionally, the background kidney parenchyma may contain multiple microscopic clear cell "tumorlets."

2. *Acquired cystic disease of the kidney.* Approximately 30%–40% of patients on long-term dialysis develop an acquired form of polycystic renal disease,<sup>252</sup> and 3%–7% of these are complicated by the appearance of RCC.<sup>253</sup> Atypical cysts with papillary hyperplasia of the lining epithelium is a consistent feature in these cases and the likely pathogenetic basis for tumor development.<sup>253</sup> While any subtype may be seen in this setting, a subset has unique morphologic, immunohistochemical, and molecular genetic features described later (see section "*Acquired Cystic Kidney Disease Associated Renal Cell Carcinoma*").<sup>254</sup>
3. *Adult form of polycystic kidney disease* (Fig. 24.23). As with the preceding entity, the carcinoma in these cases is accompanied and probably preceded by atypical cysts that begin as foci of papillary epithelial hyperplasia.<sup>255</sup> The tumors are frequently multifocal/bilateral and often have papillary or clear cell morphology.<sup>256</sup>
4. *Birt-Hogg-Dubé syndrome* (*germline folliculin mutation*) is characterized by a constellation of findings that include skin adnexal tumors (fibrofolliculoma), basilar pulmonary cysts with frequent spontaneous pneumothorax, and renal neoplasia.<sup>257</sup> The renal tumors are often oncocytic and include oncocytoma, chromophobe RCC, and hybrid oncocytic tumors.<sup>258</sup> The hybrid tumors may have a unique appearance with a so-called checkerboard pattern characterized by alternating eosinophilic and clear cells; however, unlike chromophobe RCC, the nuclei are small and almost pyknotic while the cytoplasm is somewhat vacuolated. The background kidney parenchyma may also show renal oncocyrosis.<sup>259</sup>
5. *Hereditary leiomyomatosis and RCC syndrome* (*germline fumarate hydratase mutation*) is autosomal dominant and characterized by the presence of cutaneous and uterine leiomyomas and RCCs.

These renal tumors are now regarded as a specific subtype of RCC (i.e. HLRCC associated [or fumarate hydratase deficient] RCC).<sup>260,261</sup>

6. *Heredity paraganglioma syndrome* (*germline succinate dehydrogenase mutation*). Patients are predisposed to paragangliomas, renal neoplasms, pituitary adenomas, and a unique type of gastrointestinal stromal tumor (GIST). Recent studies have shown that the renal tumors represent a distinct subtype, described later as "SDH-deficient RCC."<sup>262-264</sup>
7. *Tuberous sclerosis.* Although the classic renal tumor associated with this neurocutaneous syndrome is angiomyolipoma (AML), RCCs may be encountered, sometimes seen in intimate connection with the former.<sup>265,266</sup> While cases of oncocytoma have been described in this setting, the main RCC subtypes seem identical to sporadic tumors classified as "eosinophilic solid and cystic (ESC)," "RCC with angioleiomyomatous stroma," and a heterogeneous spectrum of oncocytic tumors resembling either chromophobe RCC or hybrid oncocytic tumors (further described under individual RCC subtypes later).<sup>265-267</sup>
8. *Neuroblastoma.* Several cases of RCC developing in children previously treated for neuroblastoma have been reported; however, this seems to be a heterogeneous group of tumors that include post-therapy-related MIT family translocation carcinomas, sporadic type RCCs, and a unique renal neoplasm with "oncocytoid" features that, in our opinion, shares some features with the recently described "ESC" RCC.<sup>268,269</sup>
9. *PTEN Hamartoma Tumor Syndrome* (*germline PTEN mutation*) is the molecular diagnostic term used for the disorders that include Cowden syndrome, Bannayan-Riley-Ruvalcaba syndrome, and a spectrum of other clinical presentations. This syndrome is rarely associated with RCCs with a papillary, clear cell, or chromophobe morphology.<sup>270,271</sup>
10. *Heredity papillary RCC syndrome* is associated with a germline mutation in the *MET* gene. It predisposes to type 1 papillary RCCs, which may number in the hundreds.
11. *Hemoglobinopathy* (most commonly sickle cell trait) is associated with two types of RCC that occur a young age, renal medullary carcinoma and the extremely rare *VCL-ALK* fusion associated renal neoplasm.
12. Other rare syndromes with an increased risk of renal neoplasia are described, such as *BAP1* tumor predisposition syndrome and *MiTF*-associated cancer syndrome.

## Clinical Features

RCC usually presents with hematuria (59%), flank pain (41%), or as an abdominal mass (45%). However, the combination of these three features, classically regarded as the diagnostic triad of RCC, occurs in only 9% of the patients.<sup>272</sup> Other manifestations are weight loss (28%), anemia (21%), fever (7%), and symptoms caused by a metastatic deposit (10%). Rare systemic/paraneoplastic manifestations include leukemoid reaction, systemic amyloidosis, polyneuromyopathy, gastrointestinal disturbances, hepatosplenomegaly, hypercalcemia, polycythemia, and hepatic dysfunction.<sup>273-282</sup>

In general, the investigation of a suspected renal mass begins with CT scan or MRI.<sup>283</sup> With the increasing use of these modalities, the number of incidentally detected RCCs has increased substantially.<sup>284,285</sup> In expert hands, core needle biopsy has been shown to provide adequate diagnostic material in about 80% of the cases.<sup>286</sup> Many centers proceed directly to partial nephrectomy without biopsy in surgical candidates; however, as active surveillance of renal mass lesions and local ablation techniques gain acceptance, biopsy rates will likely increase.<sup>287</sup>

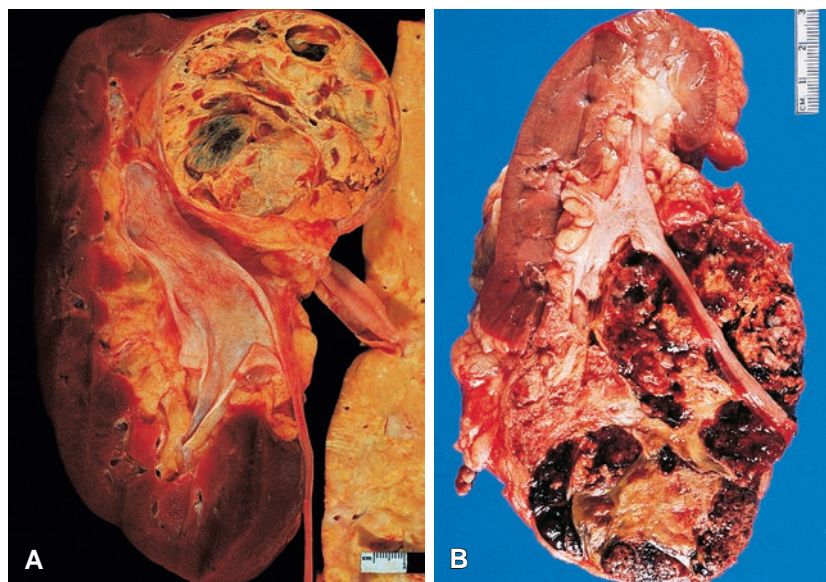


**Figure 24.24** Gross Appearances of Renal Cell Carcinoma. Both tumors are relatively well circumscribed and variegated, with a combination of cystic, solid, and hemorrhagic areas. The tumor shown in **A** has a bright yellow color, whereas that portrayed in **B** has extensive areas of hemorrhage.

### Subtypes of Renal Cell Carcinoma

Subtyping of RCC has become increasingly complicated since the modern classification was proposed in 1997.<sup>288,289</sup> Diagnosing specific subtypes is important because each has distinct underlying molecular correlates, unique immunophenotypes, varying biologic potential for aggressive behavior, emerging therapeutic implications, and in some cases important predisposition information for family members.<sup>290,291</sup> Therefore, each of the specific RCC subtypes is discussed separately to include histology, immunohistochemistry, and any known genetic features.

#### Clear Cell Renal Cell Carcinoma

Clear cell RCC is the most common type of RCC, accounting for 65%–70% of all renal cancers. Grossly, most clear cell RCCs are well delineated and centered on the cortex (Fig. 24.24). On occasion, only a small portion is connected with the cortex, the bulk of the tumor appearing as an extrarenal mass. Extension to the renal pelvis occurs only late in the course of the disease. In approximately 5% of the cases, multiple tumor nodules are seen scattered throughout the organ, but in some cases this may represent retrograde venous extension from the dominant tumor.<sup>292,293</sup>

In a typical case of clear cell RCC, the cut surface shows a solid, golden-yellow tumor, sharply separated from the surrounding tissues by a fibrous pseudocapsule. The common occurrences of hemorrhage, necrosis, calcification, and cystic change result in the variegated appearance that is so characteristic of this neoplasm (Fig. 24.25). On occasion, the cystic degeneration is so advanced that a mural nodule remains as the only evidence of the real nature of the lesion. Sometimes even this disappears, and the diagnosis is made only on microscopic examination.<sup>294</sup>

Microscopically, the tumor cells of clear cell RCC are relatively large, the appearance of the cytoplasm ranging from optically clear to deeply granular, with many transitional forms (Fig. 24.26).<sup>295-298</sup> The clear cell appearance of the tumor cells results from the accumulation of glycogen (because of abnormalities of carbohydrate metabolism)<sup>299</sup> and lipids. The nuclei are generally centrally located; their size, chromatin pattern, and nucleolar appearance vary notably from case to case, this constituting the main basis for microscopic

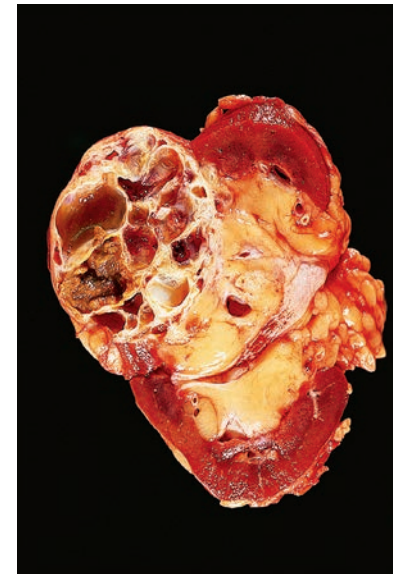


**Figure 24.25** Renal cell carcinoma with multilocular gross appearance.

grading (Table 24.3). In the usual case, the pattern of growth is predominantly solid, with formation of alveolar and acinar patterns of tumor cells separated by a stroma that is characteristically endowed with a prominent network of small, thin-walled blood vessels. This vascular pattern is an important diagnostic criterion, especially for cases with granular eosinophilic cytoplasm. Other patterns include tubular formation, microscopic and/or macroscopic cysts, associated intraluminal erythrocytes, and regression. Rarely, pseudopapillary architecture may be present. Tumors with extensive regression show large areas of edematous or collagenized stroma that contain a well-formed arborizing vasculature; in difficult cases, low-molecular-weight cytokeratin or EMA immunostains can highlight the subtle population of residual neoplastic cells that mimic histiocytes. Multiple sections usually show diverse patterns within

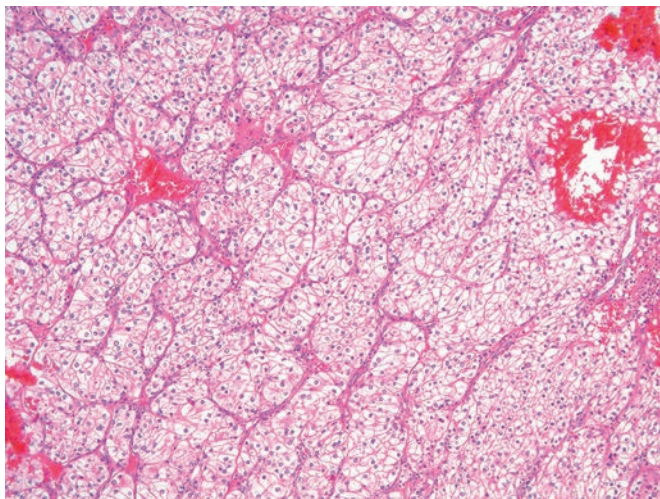


**Figure 24.26** Renal cell carcinoma, clear cell type.

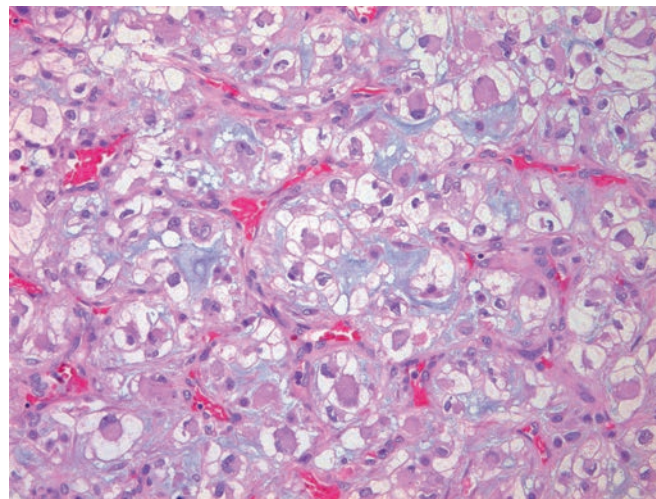


**Figure 24.27** Renal cell carcinoma, clear cell type, with rhabdoid differentiation.

**Table 24.3** World Health Organization/International Society of Urological Pathology Grading System for clear cell renal cell carcinoma and papillary renal cell carcinoma

GRADE	CRITERIA
1	Nucleoli are absent or inconspicuous and basophilic at $\times 400$ magnification
2	Nucleoli are conspicuous and eosinophilic at $\times 400$ magnification and visible but not prominent at $\times 100$ magnification
3	Nucleoli are conspicuous and eosinophilic at $\times 100$ magnification
4	Extreme nuclear pleomorphism and/or rhabdoid differentiation and/or sarcomatoid differentiation

the same tumor. High-grade progression may lead to sarcomatoid and/or rhabdoid histologic patterns. Rhabdoid differentiation is characterized by abundant homogeneous eosinophilic cytoplasm and an eccentric nucleus; the background architecture may retain a nested pattern with associated blood vessels (Fig. 24.27) or undifferentiated sheet-like growth. The stroma of RCC is nondescript and, in general, not desmoplastic as typical of collecting duct carcinoma or urothelial carcinoma. A lymphocytic infiltrate of variable degree is often present.

Immunohistochemically, clear cell RCC shows reactivity for epithelial markers such as keratin and EMA. Coexpression of keratins and vimentin is the rule, a feature not present in normal tubular cells.<sup>300,301</sup> Other antigens detected in the cells of clear cell RCC are CD10,<sup>302</sup> carbonic anhydrase IX,<sup>303,304</sup> RCC marker, PAX-2<sup>305</sup> and PAX-8. With current antibodies, PAX-8 has higher sensitivity. Cytokeratin 7 expression, which may be used in the differential diagnosis of other renal neoplasms with clear cytoplasm, is typically rare in clear cell RCC and limited to a focal or patchy pattern of reactivity. It should be recognized that any epithelial cyst lining in the kidney may stain strongly for cytokeratin 7.

From the standpoint of differential diagnosis, the choice of the markers to use depends on the specific situation at hand (i.e. whether one is trying to decide to which subtype a given RCC belongs [to be discussed later] or whether a given clear cell carcinoma in an

extrarenal site represents a metastasis of a RCC or not).<sup>306</sup> In regard to the latter, the most useful *positive* markers are the coexpression of keratin and PAX-8. It is, however, the *negative* markers that are of greatest use depending on the circumstance, to wit: (1) in the differential diagnosis with adrenal cortical carcinoma, the fact that clear cell RCC is negative for inhibin, MelanA, and SF-1<sup>307,308</sup>; (2) in the differential diagnosis with clear cell carcinoma of the ovary, the fact that clear cell RCC is usually negative for keratin 34 $\beta$ E12 and CK7<sup>309-311</sup>; (3) in the differential diagnosis with clear cell carcinoma of the thyroid, the fact that RCC is negative for thyroglobulin and TTF-1; (4) in the differential diagnosis with mesothelioma the fact that RCC is negative for calretinin, mesothelin, and CK 5/6,<sup>312</sup> and so forth.<sup>313-317</sup> While we generally find PAX-8 to be the most useful renal epithelial marker based on sensitivity and specificity, the number of tumors that may express PAX-8 must be carefully considered.<sup>318</sup> In addition, one must be aware of the possibility of cross-reactivity with other PAX epitopes when using a polyclonal antibody (e.g. cross-reactivity with PAX5 in B-cell lymphoma).

The notable feature of the genetic aspects of RCC is that there is a very close relationship with the various morphologic subtypes,<sup>319,320</sup> which can be investigated by conventional cytogenetics, PCR, FISH, microsatellite analysis, single nucleotide polymorphism (SNP) microarray, or sequencing techniques.<sup>321-324</sup> A distinctive abnormality found in most cases of clear cell RCC is alteration of the *VHL* tumor suppressor, either by a terminal deletion of the short arm of chromosome 3, beginning at 3p13,<sup>325-334</sup> silencing through promoter methylation, and somatic mutation. Since this abnormality does not characterize other types of RCC, its detection could be utilized to aid in differential diagnosis; however, this is rarely done in routine practice due to the different possible modes of *VHL* alteration. While the *VHL* gene on 3p25-26 is typically implicated (with inactivation of both copies), other tumor suppressor genes on 3p may also play a role, such as *KD-M6A*, *KMM5C*, *SETD2*, and *PBRM1*.<sup>325,328,330,332,333,335-338</sup> Mutations in *BAP1* have been associated with high-grade tumors and poor outcome. The molecular changes have shed light on the pathogenesis of some clinical and morphologic features of clear cell RCC, as well as provided the basis for the design of various targeted therapies. The *VHL* gene product is required for degradation of HIF-1 $\alpha$  (hypoxia inducible factor  $\alpha$ ). With loss of *VHL* protein in clear cell RCC, HIF-1 $\alpha$  accumulates, resulting in activation of a variety of

hypoxia-inducible genes and hence increased production of their products. These include VEGF, platelet-derived growth factor-B (PDGF-B), TGF- $\alpha$ , GLUT-1, metalloproteinases, and erythropoietin.<sup>322,339,340</sup> Furthermore, the AKT-mTOR pathway can also affect HIF-1 $\alpha$ , since mTOR normally promotes translation of HIF-1 $\alpha$ .<sup>339</sup> Targeted therapy may therefore utilize tyrosine kinase inhibitors for VEGF receptor and PDGF receptor (such as sunitinib and sorafenib), inhibitors for mTOR (such as temsirolimus), and/or antibodies targeting VEGF (bevacizumab).<sup>322,339</sup>

Clear cell RCC has a high rate of metastatic disease, sometimes years after initial diagnosis. Prognostic factors are discussed later in a separate section.

#### Papillary Renal Cell Carcinoma

Papillary RCC is the second most common subtype with series typically reporting that it accounts for 15% to 18% of all RCCs. Classification within this category continues to rapidly evolve. It has been proposed that papillary RCC can be further subdivided into two types: *type 1*, in which the papillae are lined by a single layer of cells with scanty pale cytoplasm; and *type 2*, in which the papillae are lined by a pseudostratified epithelium composed of cells with abundant eosinophilic cytoplasm, typically of higher nuclear grade.<sup>341,342</sup> Molecular studies have confirmed the type II category to be a very heterogeneous group of tumors, and one could argue that these should not be combined with type 1 in the classification scheme.<sup>343</sup>

**Type 1 papillary RCC** represents the prototypical papillary RCC. They are more likely than clear cell RCC to be localized to the kidney, but also more likely to be multicentric or bilateral.<sup>344-346</sup> Grossly, the tumors are often encapsulated and the cut surface has a tan-brown appearance; the intracystic papillary growth may mimic extensive necrosis. Microscopically, a thick fibrous capsule is typical, and the individual neoplastic cells line the inner layer of the capsule. Complex papillary formations fill the intracystic space (Fig. 24.28A), often accompanied by prominent stromal infiltration by neutrophils or foamy macrophages.<sup>347,348</sup> The neoplastic cells lining the papillae consist of a single layer of low cuboidal epithelium, often with little cytoplasm (see Fig. 24.28B). Psammoma bodies may be numerous and the nuclear grade is variable.<sup>349,350</sup> Other, histologic patterns of type 1 papillary RCC include solid growth, in which papillae are collapsed together (Fig. 24.29), and the “biphasic squamoid alveolar” pattern (Fig. 24.30). Papillary RCCs may undergo intratumoral hemorrhage and necrosis; intracytoplasmic hemosiderin deposition and cytoplasmic clearing are not uncommon in such foci. In fact, type 1 papillary RCC may undergo near complete infarction leaving only a thick fibrous capsule filled with necrosis and cholesterol granulomas. Numerous sections of the capsule will often reveal foci of residual viable tumor.

Immunohistochemically (and in contrast with clear cell RCC) there is strong expression of keratin 7 and AMACR in type 1 tumors.<sup>351</sup> According to this classification scheme, it is the type 1 tumors that have the underlying chromosome 7, 17, and Y abnormalities.<sup>352-354</sup> In contrast to clear cell RCC, there is no loss of 3p. Type 1 papillary RCC has a better prognosis than clear cell RCC.<sup>344,355</sup> In rare instances, type I papillary RCC is hereditary, associated with germline mutations of the *c-MET* oncogene, often presenting with hundreds of small tumors.<sup>356</sup>

**Type 2 papillary RCC** represents a heterogeneous collection of high-grade RCCs with papillary architecture (Fig. 24.31). Recent molecular studies have shown that MiT family translocation RCCs and RCCs associated with hereditary leiomyomatosis are frequently misclassified as “type 2” papillary RCC. Of the remaining type 2 tumors, different genetic subgroups include sporadic fumarate

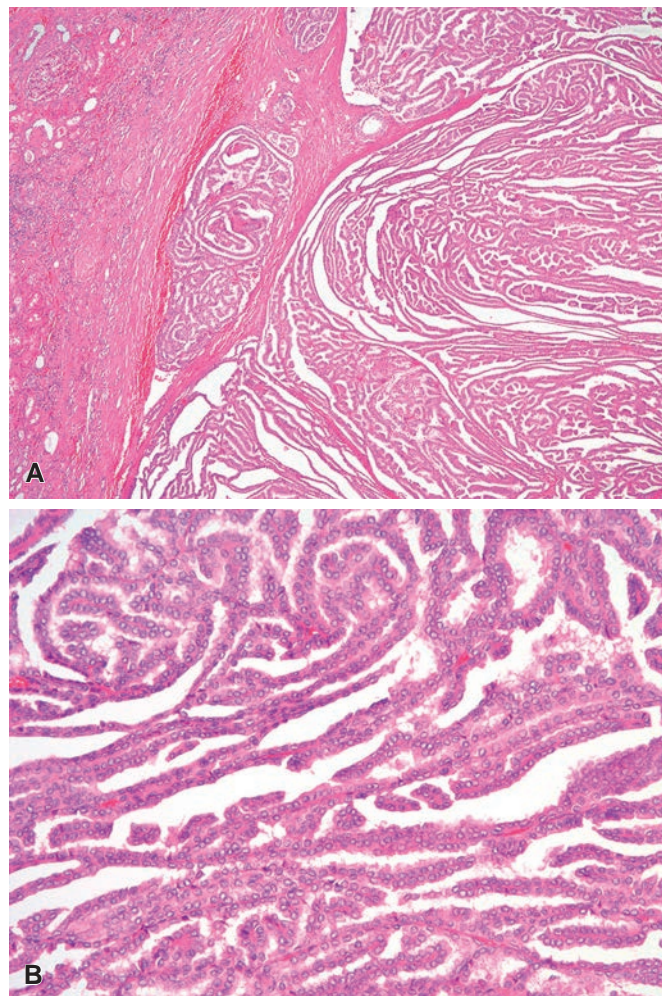


**Figure 24.28** Renal Cell Carcinoma, Papillary Type 1. **A**, Typical thick fibrous capsule with papillary tumor filling a cystic space. **B**, Single cuboidal layer of cytologically bland cells.

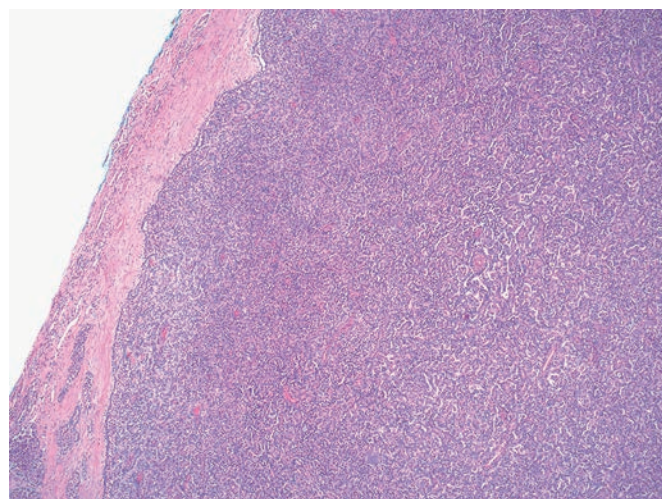


**Figure 24.29** Renal cell carcinoma, papillary type 1, with solid growth.

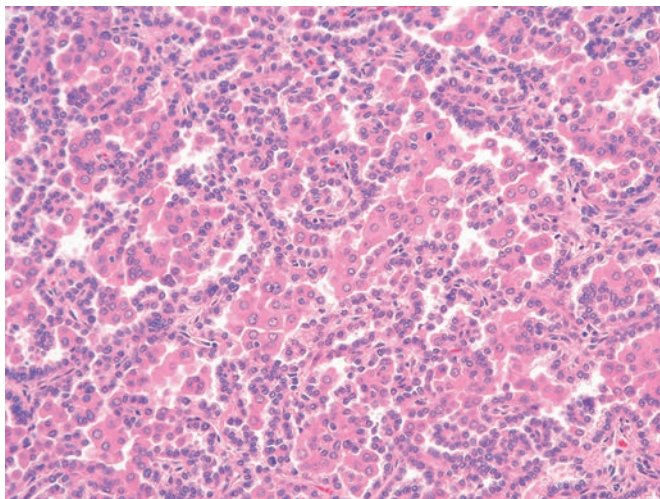


**Figure 24.30** Renal cell carcinoma, papillary type 1, with so-called squamo-alveolar pattern.

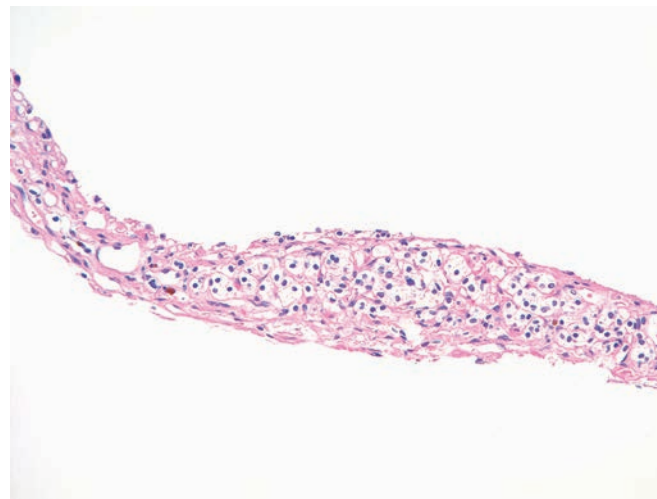


**Figure 24.32** Multilocular cystic renal neoplasm of low malignant potential.

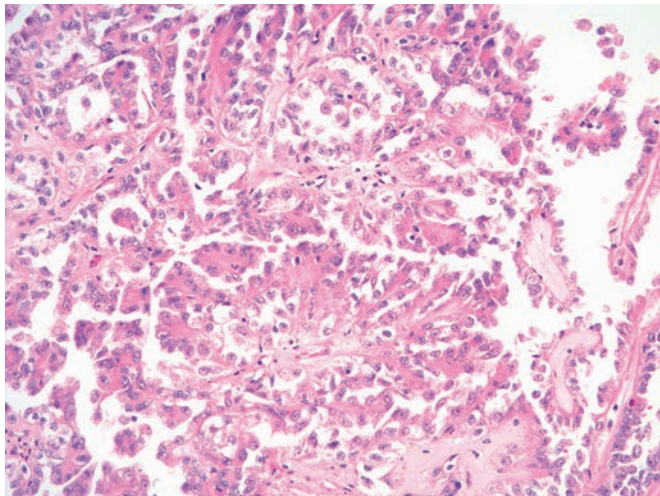


**Figure 24.31** Renal cell carcinoma, papillary type 2.

hydratase mutation (i.e. not associated with hereditary leiomyomatosis), *CDKN2A* silencing mutation, *SETD2* mutation, *NF2* mutation (Hippo pathway tumor suppressor), and *NRF2-ARE*.<sup>343</sup> It is provocative that a subset of the studied carcinomas share alterations in the Hippo pathway with the “mucinous, tubular, and spindle cell carcinoma” of the kidney (which has known histologic and immunophenotypic overlap with papillary RCC), suggesting a close relationship in that subgroup. It is likely that the type 2 category will undergo changes as distinct molecular, and possibly morphologic, subtypes emerge.

Some papillary RCCs have mixed histologic features that are difficult to classify as either type 1 or type 2, but genetic and clinical outcome studies suggest a closer relationship to type 1 papillary RCC in many of these tumors<sup>357,358</sup>; grading and staging should be emphasized in such cases.

Another morphologic subset of cases is “oncocytic papillary carcinoma.” These are not fully characterized, but often have a single layer of lower-grade round nuclei, and some show elevation of the nuclei off the basement membrane (i.e. reverse polarity).<sup>359-361</sup>

It should also be realized that papillary RCC (like all other types) can undergo anaplastic or sarcomatoid changes, but rhabdoid differentiation is uncommon.<sup>362-364</sup>

#### *Multilocular Cystic Renal Neoplasm of Low Malignant Potential*

These are rare macrocystic renal tumors, representing less than 1% of renal neoplasms, that are composed of thin septa without any macroscopic tumor nodules or expansile growth. Microscopically, the cysts are lined by a layer of clear epithelial cells, but the key diagnostic feature is the presence of small clusters of clear neoplastic cells in the thin walls of the septa (Fig. 24.32).<sup>365</sup> The presence of any solid nodules of tumor cells would warrant a diagnosis of clear cell RCC. Genetically, these tumors have 3p alterations similar to clear cell RCC, so they may simply represent an early phase of clear cell. When solid foci of tumor regression are present, the tumors are probably best diagnosed as clear cell RCC.<sup>366</sup> If diagnosed using strict histologic criteria with very close gross correlation, multilocular cystic renal neoplasm of low malignant potential follows a benign clinical course.<sup>365</sup> It is likely that staging has little prognostic value in these tumors.<sup>367</sup> The main differential diagnostic considerations are clear cell RCC, clear cell-papillary RCC, benign renal cortical cysts, and cystic nephroma (mixed epithelial and stromal tumor [MEST]).

#### *Chromophobe Renal Cell Carcinoma*

Chromophobe RCC comprises about 5% of all cases of RCC. It is grossly well circumscribed, solitary, with a homogeneous gray to brown cut surface, typically devoid of hemorrhage or necrosis (Fig. 24.33).<sup>368</sup> Microscopically, there is a characteristic broad “alveolar” arrangement of the tumor at low power, but some cases have smaller nests. There are two main histologies: classic (or “plant-cell”) type and eosinophilic variant. In the classic type, the neoplastic cells have sharply defined borders and abundant cytoplasm with very prominent cell membranes (Fig. 24.34).<sup>369</sup> The cytoplasm has a pale, acidophilic quality, and there is often a vague clear perinuclear region.<sup>370</sup> The eosinophilic variant has more pronounced perinuclear clearing, but less prominent cell membranes (Fig. 24.35). Some cases have mixed features. Calcification is present in nearly half of the cases. The nuclear features, which are critical to diagnosis, are characterized by irregular nuclear membranes, hyperchromasia, and frequent binucleation. In our opinion, these specific nuclear features are both necessary and sufficient for classification as chromophobe RCC. Rare cases are associated with multicystic, microcystic, and adenomatous patterns of growth or neuroendocrine-like features (Fig. 24.36).<sup>371-373</sup> The characteristic cytoplasmic and nuclear features of

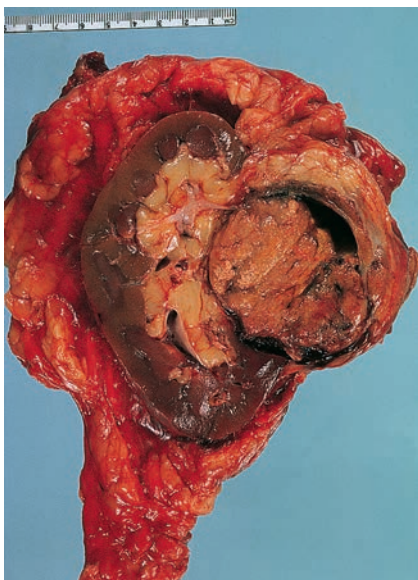


**Figure 24.33** Gross Appearance of Renal Chromophobe Cell Carcinoma. The tumor is well circumscribed and has a light brown color.

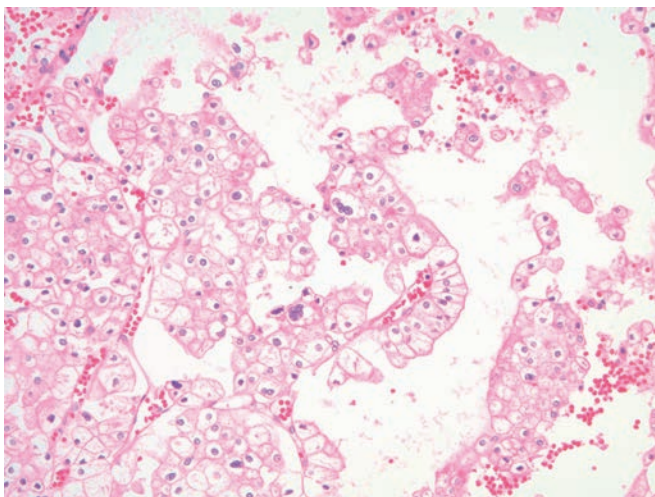


**Figure 24.34** Chromophobe renal cell carcinoma, classic type, with thick cell membranes.

the tumor can be recognized in fine-needle aspiration specimens and biopsies.<sup>374,375</sup>

This cytoplasmic appearance is due to the presence of numerous cytoplasmic microvesicles that are well appreciated by electron microscopy, but this is no longer employed for routine diagnosis.<sup>376</sup> These microvesicles stain for Hale colloidal iron; however, the stain is technically difficult to perform and we do not require its use.<sup>368,377-379</sup> The number of publications promoting the use of adjunctive immunohistochemistry in the distinction between chromophobe RCC and oncocytoma is overwhelming, to say the least. In our experience, the immunophenotype of cases with prototypical histologic features of chromophobe RCC can be much more heterogeneous than would be suggested by the literature. Therefore, we rely almost exclusively on H&E morphology for this distinction (see section on renal oncocytoma for full discussion on the handling of "difficult to classify" cases). Based on a recent publication, even expert pathologists' use of immunohistochemistry and special stains in this setting varies quite dramatically.<sup>380</sup> With that caveat, chromophobe RCC is

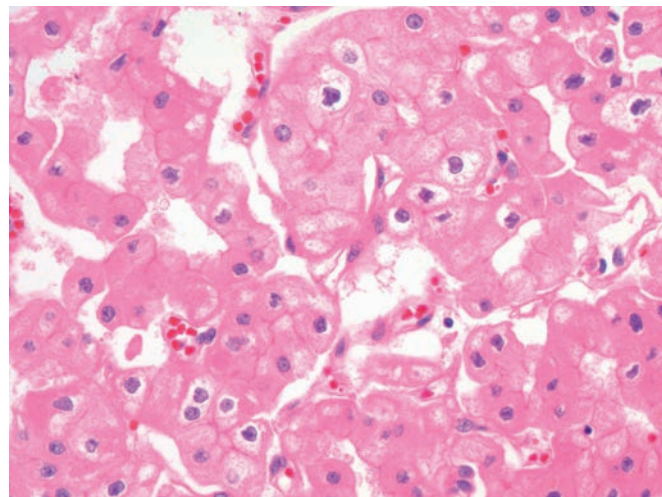


**Figure 24.35** Chromophobe renal cell carcinoma, eosinophilic type, with prominent perinuclear halos.

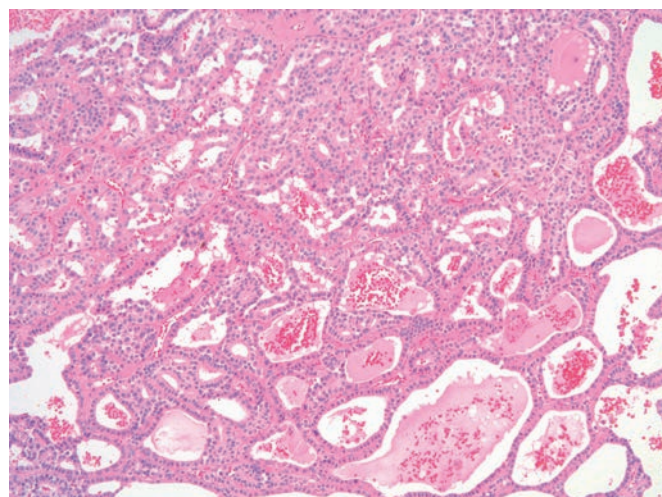


**Figure 24.36** Chromophobe renal cell carcinoma, microcystic pattern.

reported to commonly express EMA, CD117, keratin 7, CD9, CD82,<sup>381</sup> paxillin, parvalbumin,<sup>382</sup> claudin-7 and -8,<sup>383,384</sup> Ep-Cam (an epithelial adhesion molecule),<sup>385</sup> and E-cadherin, but not N-cadherin or vimentin.<sup>386-389</sup> A high percentage of chromophobe RCCs have been found to be immunoreactive for CD10 at least focally.<sup>390</sup> It should also be highlighted that, in contrast to most RCC subtypes, at least 20% of chromophobe RCCs are negative for PAX-8.<sup>391,392</sup>

Frequent loss of chromosomes 1, 2, 6, 10, 13, 17, and 21 has been found by comparative genomic hybridization<sup>393</sup> and microsatellite markers.<sup>394,395</sup> Other reported losses include chromosomes 3, 5, 8, 9, 11, 18, and Y. While the important work reported by The Cancer Genome Atlas (TCGA) revealed fascinating insights into the biology of chromophobe RCC, the molecular events were very heterogeneous, and a practical diagnostic marker was not identified.<sup>396</sup>

Chromophobe RCC can undergo sarcomatoid transformation; as a matter of fact, it may have a greater tendency to this event than many other types.<sup>395,397</sup> As a whole, the prognosis of chromophobe RCC is much more favorable than that of clear cell RCC, but distant metastases can develop (particularly liver), especially when the tumors are high stage at presentation.<sup>398,399</sup> The current consensus is that grade does not provide additional prognostic information for

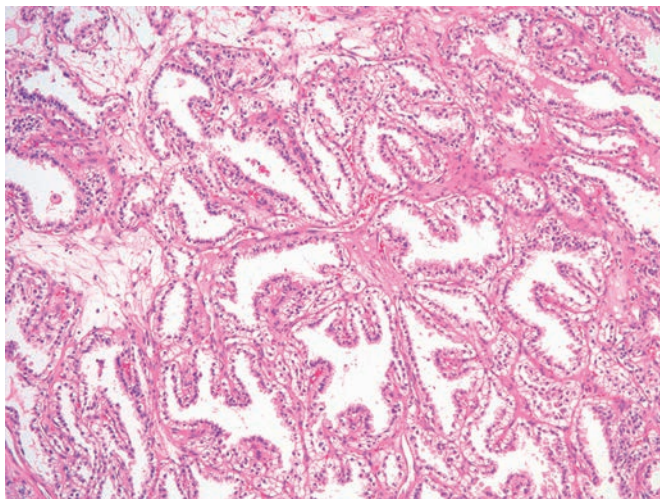


**Figure 24.37** Clear cell-papillary renal cell carcinoma with predominant papillary architecture. The linear nuclear alignment and sub-nuclear cytoplasm are also evident.

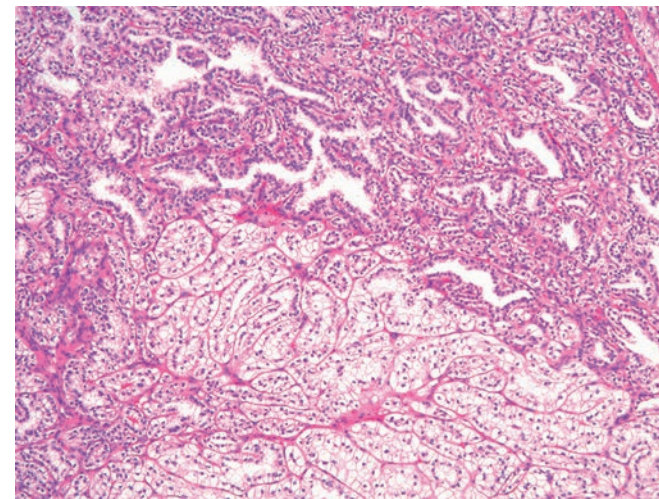


**Figure 24.38** Clear cell-papillary renal cell carcinoma with mixed branching tubules and more solid clear cell pattern.

chromophobe RCC<sup>400</sup>; however, if sarcomatoid transformation has developed, the prognosis becomes very poor.

#### *Clear Cell-Papillary Renal Cell Carcinoma*

Clear cell-papillary RCC was first described by Tickoo et al. within a series of RCCs arising in end-stage kidney disease, but it is now recognized as more common in a sporadic setting.<sup>401-403</sup> In fact, two large studies have similarly shown that it represents the fourth most common RCC after clear cell, papillary, and chromophobe.<sup>404,405</sup> Grossly, clear cell-papillary RCC is circumscribed and often encapsulated. It may be solid, but is often cystic. Microscopically, cystic areas are lined by a single low cuboidal layer of clear cells with areas of papillary tufts lined by similar cells. More solid areas have an admixture of architectural patterns, including tubular, acinar, and nested. The clear cells are cytologically low grade (International Society of Urological Pathology [ISUP] nuclear grade 1–2), and there is frequently reverse polarity with subnuclear clearing and a linear arrangement of the nuclei (Fig. 24.37). The tubular pattern almost always shows branching. Solid and nested areas may have significant overlap with clear cell carcinoma, but the absence of the dense fibrovascular septa, the linear nuclear arrangement, and the presence of other architectural patterns aid in diagnosis as clear cell-papillary RCC (Fig. 24.38). Tumor cell necrosis and invasion of renal sinus vessels should be absent.

The capsule of the tumor may show smooth muscle metaplasia, but this should not change the classification as clear cell-papillary RCC if other features are typical. Such tumors were originally described as part of the spectrum of “renal angiomyoadenomatous tumor,”<sup>402,406</sup> but clear cell-papillary RCC is now considered distinct from “RCC with (angio)leiomyomatous stroma.”

Immunophenotypically, these tumors show strong and diffuse immunoreactivity for cytokeratin 7. CD10 and racemase are typically negative, while CA-IX (“cup-like” pattern), PAX-8, and high-molecular-weight keratin are often positive. Nuclear GATA-3 expression has been recently reported.<sup>407,408</sup> When immunohistochemistry is needed, cytokeratin 7 often provides sufficient support to exclude clear cell subtype (which is negative or shows only focal staining); in fact, the absence of cytokeratin 7 staining should prompt careful reconsideration of a clear cell-papillary diagnosis. Cytokeratin 7 stains should be evaluated in solid foci because cyst-lining epithelial cells of many tumor types show strong immunoreactivity. Genetically,

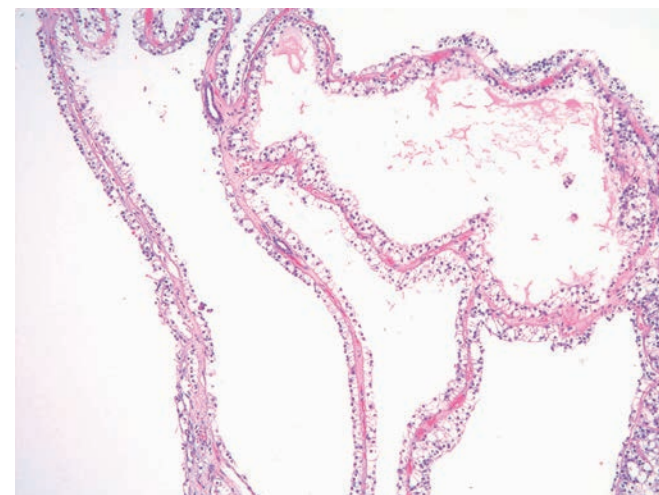


**Figure 24.39** MiT Family Translocation Renal Cell Carcinoma. Rare cases may mimic clear cell-papillary or multilocular cystic renal neoplasm.

there is no specific finding in clear cell-papillary RCC, but they do not have the changes characteristic of either clear cell RCC or papillary RCC.<sup>409-411</sup>

When diagnosed by strict criteria, no recurrence or metastasis has been reported in clear cell-papillary RCC<sup>402,412,413</sup>; therefore, the differential diagnostic distinction from clear cell RCC and a subset of MiT family translocation RCC is critical. Other less critical distinctions, such as multilocular cystic renal neoplasm of low malignant potential and atypical renal cysts, may be difficult and somewhat subjective.<sup>414,415</sup> In our experience, papillary RCC rarely enters into consideration. It is important to note that some low-grade clear cell RCCs have foci reminiscent of clear-cell papillary RCC, often due to linear alignment of nuclei. Studies have shown that tumors with such mixed features have genetic features and a clinical outcome supporting clear cell subtype.<sup>416,417</sup> Rare subsets of MiT family translocation carcinomas (specifically fusion types SFPQ-TFE3 and NONO-TFE3) may also mimic clear cell-papillary RCC (or possibly multilocular cystic renal neoplasm) based on suprabasal nuclear palisading and subnuclear vacuoles (Fig. 24.39).<sup>418,419</sup> In our practice, we would generally regard the presence of intracystic

papillary excrescences as favoring clear cell-papillary RCC over multilocular cystic renal neoplasm of low malignant potential. The distinction of an atypical renal cyst (with focal papillary excrescences lined by clear cells) from a macrocystic clear cell-papillary may be very subjective.<sup>414</sup> In the presence of papillary tufts within multiple cystic locules of the same lesion, we would favor clear cell-papillary RCC.

Finally, some patients with VHL disease have tumors with morphologic features similar to clear cell-papillary RCC; these are controversial, but in our opinion they are best interpreted as clear cell RCC, given their association with 3p abnormality.<sup>251</sup>

#### *MiT Family Translocation Renal Cell Carcinomas*

An exciting new chapter of renal tumor pathology opened with the discovery that some tumors are associated with nonrandom chromosomal alterations involving members of the microphthalmia transcription factor subfamily.<sup>420-422</sup> The better studied of these are those involving region Xp11.2, resulting in fusion of the *TFE3* gene.<sup>423</sup> Most of the initial cases were reported in young people; while they represent approximately 40% of pediatric RCCs, they can also develop in adults.<sup>424,425</sup> Microscopically, the overall features are typically those of an RCC but are very heterogeneous. Papillary structures may be prominent, and the tumor cells can be either clear or have a markedly granular eosinophilic cytoplasm; however, some cases are more solid and clear cell predominant, closely mimicking clear cell RCC (Fig. 24.40). Admixed psammoma bodies may be abundant. There are numerous fusion partners reported, some correlations having been found between the type of gene fusion and the tumor morphology.<sup>419</sup> Aberrant increased nuclear immunoreactivity for *TFE3* is consistently detected in these cases, but many labs find the antibody technically challenging to use and prefer FISH testing (as do we).<sup>426</sup> These tumors usually express PAX2 and PAX8, but do not usually express MiTF.<sup>427</sup> One specific fusion (RBM10-TFE3) may be difficult to detect by FISH due to cryptic inversion.<sup>428,429</sup>

Another, even less common translocation-associated RCC involves t(6;11), the resulting fusion affecting the *TFEB* gene at 6p21.<sup>430</sup> Microscopically, these tumors show nested and acinar-like areas of cells with clear or granular acidophilic cytoplasm with round nuclei. Some cases show a biphasic pattern with a population of smaller cells surrounding eosinophilic basement membrane-like material (Fig. 24.41). They may be difficult to morphologically distinguish from Xp11.2-related tumors, and they may express HMB45 or Melan-A. It is clear that the subject is rapidly evolving and that additional variations, both at the morphologic and the molecular genetic level, are being described.<sup>431</sup> Case in point, aggressive RCCs with *TFEB* amplification are recently described.<sup>432-434</sup>

Rare hybrid melanotic tumors showing mixed features of MiT family translocation carcinoma and AML are also described.<sup>435</sup>

#### *Collecting Duct Carcinoma*

Collecting duct carcinoma constitutes less than 1% of all RCCs under current criteria. These tumors are centered in the medulla, have destructive infiltrative growth often with surrounding desmoplastic reaction, and are almost always high stage at diagnosis.<sup>436-438</sup> Common histologic patterns include tubulopapillary, solid sheets, nests, cords, cribriform, and infiltrating glands or elongated tubules (Fig. 24.42).<sup>438</sup> Sarcomatoid differentiation may also be present. Atypical changes in the adjacent ducts (i.e. dysplasia) may be seen, but distinction from reactive tubular changes is often subjective.

Genetic profile information is limited for collecting duct carcinoma because of its rarity and the evolving diagnostic criteria that now further restricts its diagnosis.<sup>439,440</sup> Likewise, immunophenotypic data

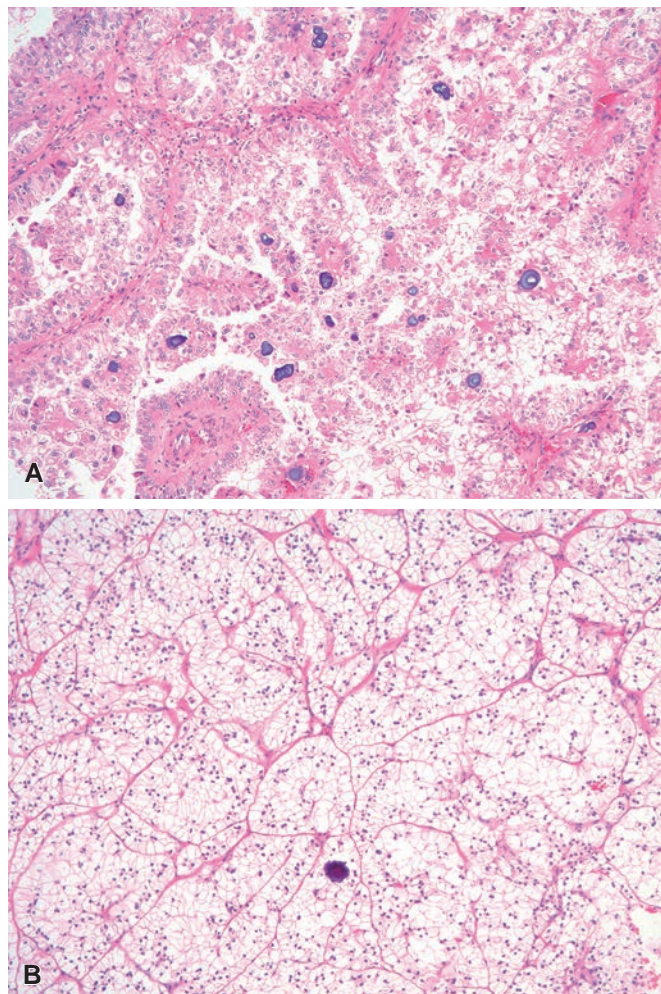


**Figure 24.40** MiT Family Translocation Renal Cell Carcinoma, TFE3 Type, With Psammoma Bodies. **A**, Papillary pattern. **B**, Nested pattern mimicking clear cell RCC.

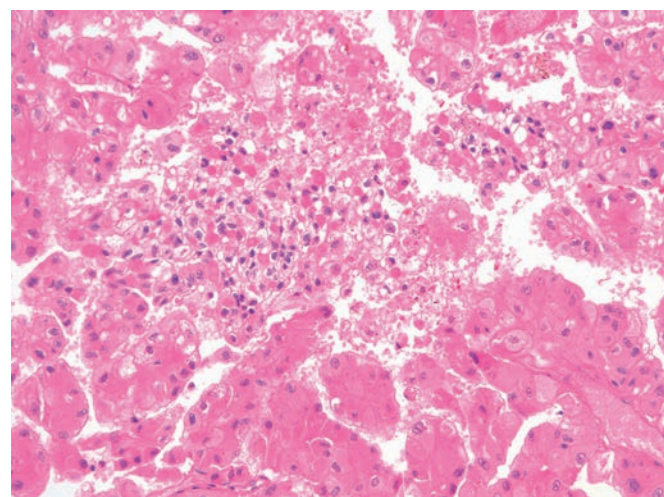


**Figure 24.41** MiT family translocation renal cell carcinoma, TFEB type, with classic biphasic pattern.

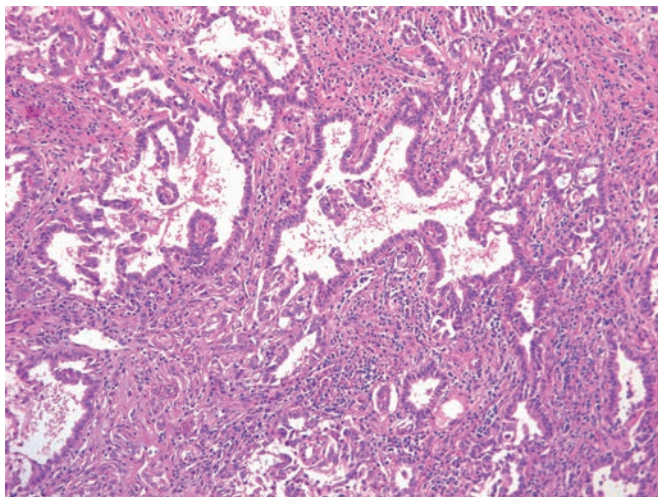


**Figure 24.42** Collecting duct carcinoma.

have historically varied, likely due to inclusion of a broad spectrum of tumors in the past.

The behavior of collecting duct carcinoma is generally very aggressive, many of the patients having distant metastases at the time of presentation.<sup>441,442</sup> Most importantly, collecting duct carcinoma should be a diagnosis of exclusion. Urothelial carcinoma (with or without glandular differentiation), metastatic carcinoma from a distant site, renal medullary carcinoma, and RCC with fumarate hydratase mutation should be carefully considered because each is more common. Additional sections from the collecting system may be most helpful in distinction from urothelial carcinoma, but immunohistochemistry may be needed if no definitive urothelial precursor lesion is identified. We would generally require at least a PAX8-positive/p63-negative phenotype for this diagnosis. Unfortunately, at least 25% of upper tract urothelial carcinoma express PAX8, so even immunohistochemical distinction may be difficult in some cases. Nuclear SMARCB1 should be retained, which is a distinguishing feature from medullary carcinoma.<sup>443-445</sup> Fumarate hydratase (FH) loss by immunohistochemistry and/or genetic counseling/testing may be needed to exclude fumarate hydratase-deficient RCC (hereditary leiomyomatosis and RCC syndrome).<sup>446</sup>

#### *Fumarate Hydratase-Deficient Renal Cell Carcinoma (Hereditary Leiomyomatosis and Renal Cell Carcinoma-Associated Renal Cell Carcinoma)*

These aggressive RCCs are associated with mutations in *FH* (the gene encoding fumarate hydratase), most of which are germline and associated with hereditary leiomyomatosis and RCC syndrome.<sup>261,446,447</sup> Many of these patients have cutaneous leiomyomas, and women may have a personal or family history of early hysterectomy for uterine leiomyomas. The renal tumors have significant morphologic overlap with collecting duct carcinoma and type II papillary RCC; however, it is no longer appropriate to diagnose or refer to these tumors as the latter. Unlike other hereditary renal neoplasia syndromes, patients may present with only a single unilateral mass due to low penetrance. Macroscopically, tumors are very heterogeneous with variable cystic and solid appearance; in some cases background renal cortical cysts can be seen. Microscopically, the classic pattern is papillary with abundant eosinophilic cytoplasm and large nucleoli with surrounding peri-nucleolar halos (Fig. 24.43).<sup>261</sup> Other patterns include tubular, tubulocystic, solid, and cribriform, with admixtures being common (Fig. 24.44).<sup>261,446,448</sup> The characteristic peri-nucleolar

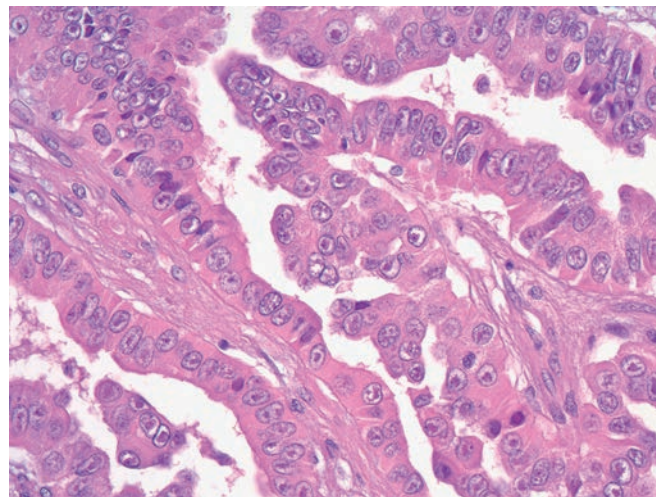


**Figure 24.43** Fumarate hydratase-deficient renal cell carcinoma with prototypical peri-nucleolar halos.

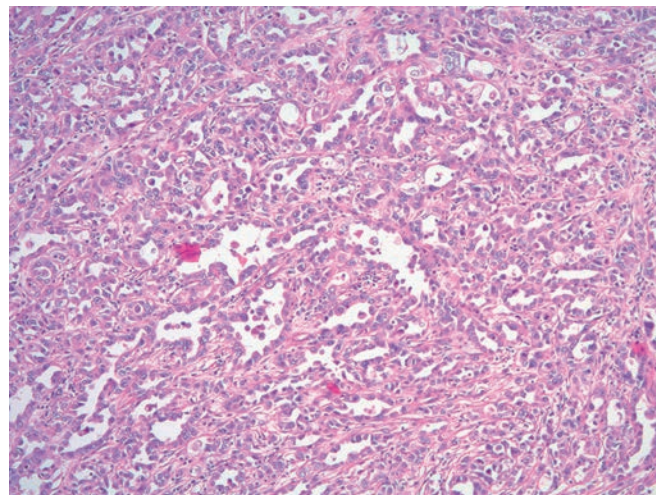


**Figure 24.44** Fumarate hydratase-deficient renal cell carcinoma with infiltrating glandular pattern.

clearing may be present only focally. Many tumors previously regarded as "de-differentiated tubulocystic carcinoma" represent FH-deficient RCC (Fig. 24.45).<sup>449</sup> Finally, rare cases, especially in younger patients, may not have fully developed features and can overlap with lower-grade oncocytic tumors (Fig. 24.46).<sup>450</sup> Immunohistochemistry can play an important role in this diagnosis, as tumors typically lose cytoplasmic expression for FH (but not in all cases). Overexpression of modified cysteine (S-(2-succino)cysteine) may also be helpful, but the antibody is not currently available from a commercial source.<sup>446</sup> A recent study from the TCGA reported that a subset of tumors with papillary morphology have somatic mutations in *FH*, suggesting a sporadic counterpart.<sup>451</sup> FH-deficient RCC often presents at high stage with distant metastases, and aggressive behavior may be seen even with small tumors.

#### *Renal Medullary Carcinoma*

Medullary carcinoma is a rare malignant renal neoplasm occurring most commonly in young patients of African descent (typically 20–30 years of age) with sickle cell trait, but it is rarely seen with other hemoglobinopathies.<sup>452,453</sup> It is centered in the medulla, and is microscopically heterogeneous with mixed morphologic patterns

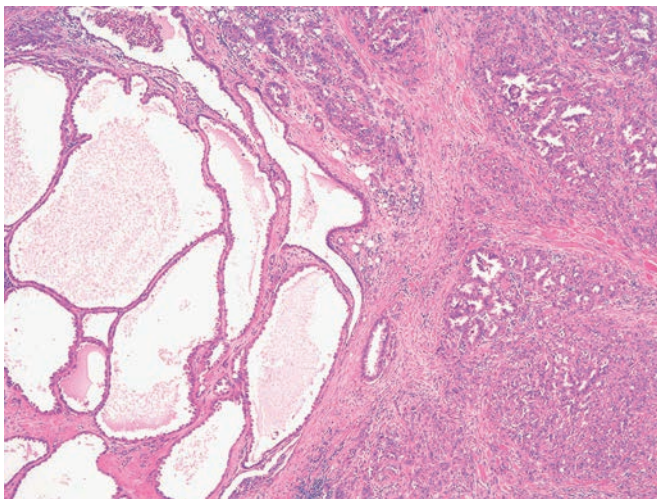


**Figure 24.45** Fumarate hydratase-deficient renal cell carcinoma with mixed tubulocystic and solid pattern.

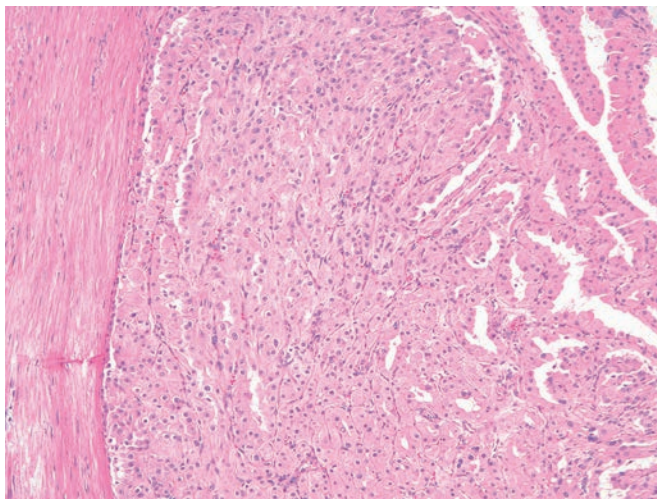


**Figure 24.46** Fumarate hydratase-deficient renal cell carcinoma with deceptive "low-grade" appearance.

that include reticular (reminiscent of yolk sac tumor), rhabdoid, cribriform, tubulopapillary, and poorly differentiated solid areas, often in a background of desmoplastic stroma admixed with neutrophils and usually marginated by lymphocytes (Fig. 24.47).<sup>454,455</sup> Associated myxoid stroma is also common. Immunohistochemically, demonstration of nuclear SMARCB1 (INI-1) loss has become required for diagnosis.<sup>456</sup> Patchy nuclear expression of OCT3/4 is also characteristic. Metastases are usually present at the time of the diagnosis, and a rapidly fatal course is typical.<sup>457,458</sup>

A separate but seemingly very rare renal neoplasm with a *VCL-ALK* fusion has recently been described in children with sickle cell trait. This *VCL-ALK* fusion-associated RCC is distinct from renal medullary carcinoma with a unique spindled to polygonal eosinophilic cell population containing conspicuous intracytoplasmic vacuoles. Unlike renal medullary carcinoma, these have followed an indolent clinical course.<sup>459-461</sup>

#### Tubulocystic Carcinoma

Tubulocystic carcinoma is a rare subtype of RCC with unique pathologic features that constitutes less than 1% of renal neoplasms.

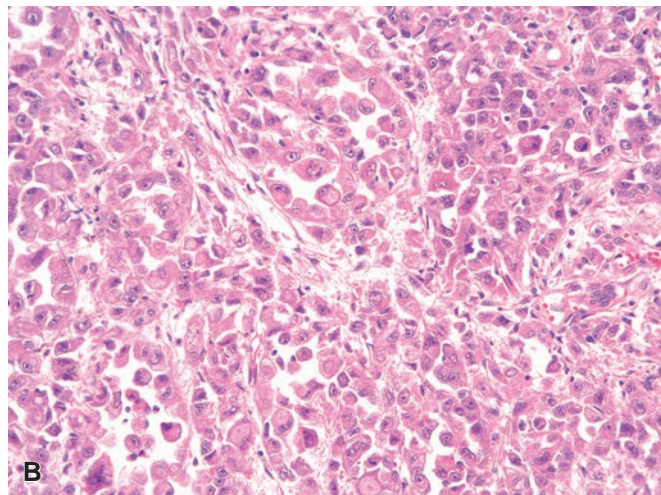
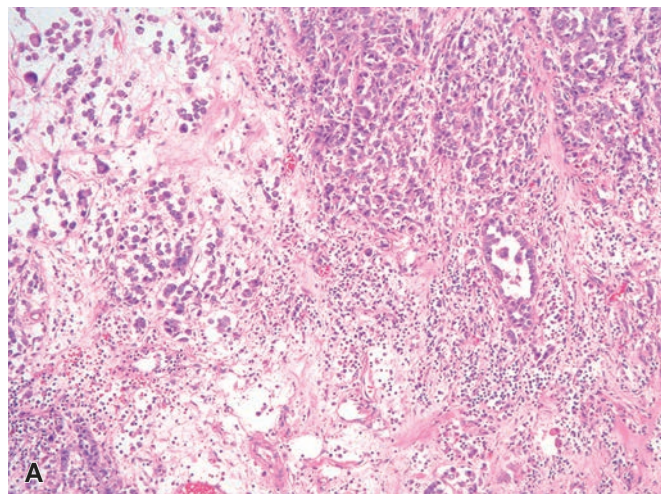


**Figure 24.47** Renal Medullary Carcinoma. **A**, Admixture of glands, single cells, and cords. **B**, Rhabdoid features.

Grossly, its appearance has been described as spongy and "bubble wrap."<sup>462</sup> Microscopically, there are variably sized cystically dilated tubules lined by a single layer of eosinophilic epithelium with a cuboidal, flat, or hobnail appearance (Fig. 24.48).<sup>462,463</sup> The nuclei are often enlarged with prominent nucleoli. The individual cysts are separated by a scant fibrous stroma. The prognosis tends to be favorable.<sup>462</sup> While a subset of cases with high-grade areas showing solid or destructive growth are described under the term "de-differentiated tubulocystic carcinoma," many of these represent fumarate hydratase-deficient RCC.<sup>449,464,465</sup> While there has been suggestion of a genetic relationship to papillary RCC, this remains controversial and no distinct genetic signature has been reported for tubulocystic carcinoma.<sup>466,467</sup>

#### Mucinous Tubular and Spindle Cell Carcinoma

Mucinous tubular and spindle cell carcinoma (MTSCC) is a unique type of low-grade RCC. Microscopically, the tumor is composed of an admixture of spindle cells and elongated tubules lined by bland cuboidal cells with variable amounts of myxoid/mucinous stroma (Fig. 24.49).<sup>468-470</sup> Cases containing scanty mucin ("mucin-poor") can be easily misdiagnosed, the presence of a spindle cell component being an important clue for their correct identification.<sup>471</sup> Focal neuroendocrine features have been occasionally found.<sup>472</sup> The immunohistochemical profile of MTSCC is similar to that of papillary

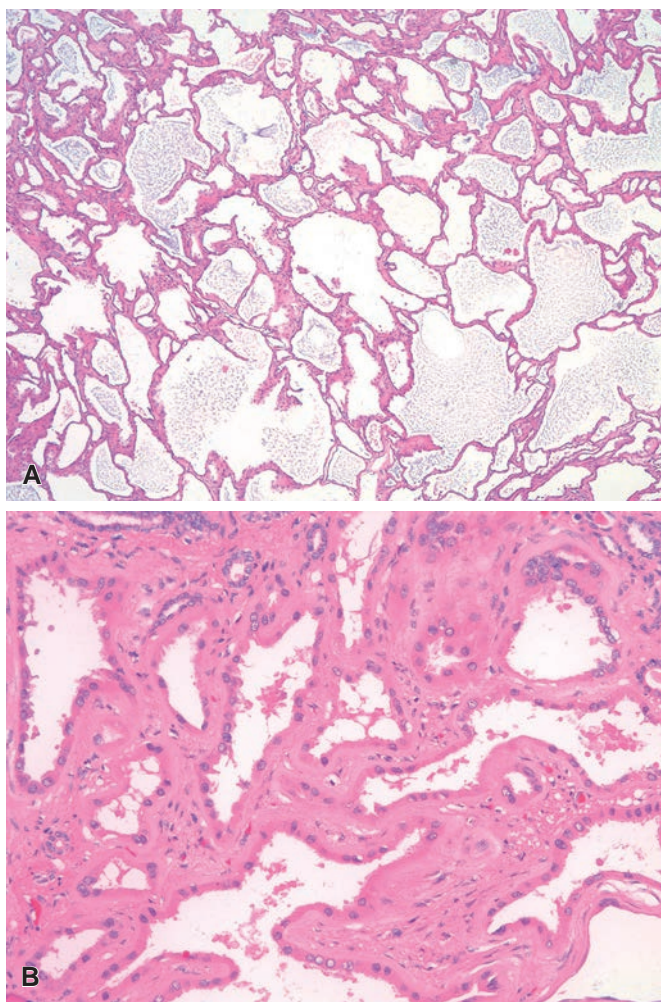


**Figure 24.48** Tubulocystic Carcinoma. **A**, Prototypical low-power architecture. **B**, Lining cells are eosinophilic and atypical.

RCC,<sup>473</sup> but their cytogenetic profile is different.<sup>474</sup> Whether MTSCC is a variant of papillary RCC or a distinct tumor subtype has been debated; however, the recent finding of recurring alterations in the Hippo pathway in MTSCC provides strong evidence for the latter.<sup>475-477</sup> The prognosis is generally favorable, unless the tumor is accompanied by a high grade sarcomatoid component, an exceedingly rare event.<sup>478</sup>

#### Acquired Cystic Kidney Disease–Associated Renal Cell Carcinoma

This neoplasm is seen only in patients with acquired cystic kidney disease related to dialysis. Patients with acquired cystic kidney disease are at a high risk for developing RCC of any subtype.<sup>253,401,479</sup> The diagnosis of “acquired cystic kidney disease–associated RCC” should be reserved for cases with unique and specific histologic features.<sup>401,480,481</sup> The tumors often have macrocystic growth, but solid and papillary architecture is also frequent. The cytoplasm of the neoplastic cells is typically eosinophilic, and prominent nucleoli are common. Two characteristic features include intratumoral oxalate crystals and a unique sieve-like architecture characterized by inter- and intracellular “lumina” separated by very thin strands of cytoplasm (Fig. 24.50). The background kidney, in addition to acquired cystic disease, may contain cysts with atypical papillary proliferations. Immunophenotypically, these RCCs are often negative (or only focally positive) for cytokeratin 7, but they often express AMACR. While

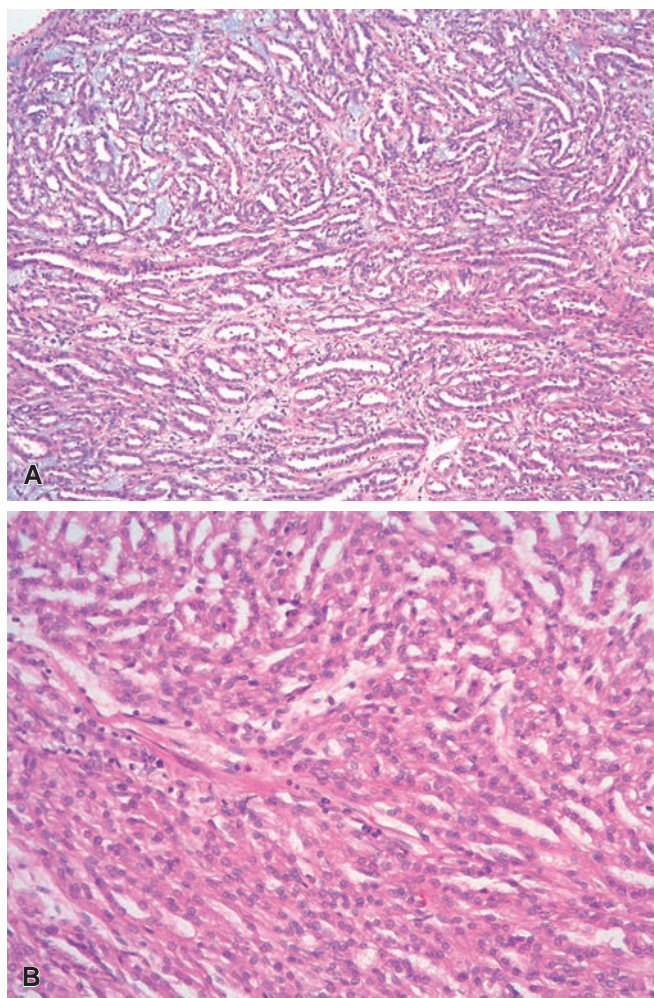


**Figure 24.49** Mucinous, Tubular, and Spindle Cell Carcinoma. **A**, Classic tubular architecture with interspersed mucin. **B**, Spindled morphology with bland cytologic features.

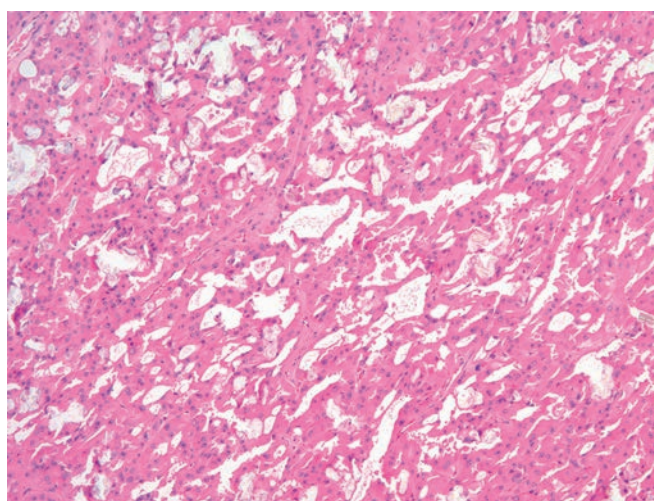


**Figure 24.50** Acquired cystic kidney disease–associated renal cell carcinoma.

studies have shown no 3p loss and no chromosome 7 or 17 trisomies, a specific genetic signature has not been identified. Acquired cystic kidney disease–associated RCC generally presents at low stage (possibly due to radiographic surveillance for known cystic disease) and follows an indolent clinical course. However, rare cases may have sarcomatoid or rhabdoid differentiation and are associated with an aggressive behavior.<sup>482</sup>

#### Succinate Dehydrogenase–Deficient Renal Cell Carcinoma

This recently described subtype of RCC has distinct morphologic features, but is defined by loss of cytoplasmic SDHB expression by immunohistochemistry.<sup>262–264</sup> It is almost always associated with germline mutations in an *SDH* gene (most commonly *SDHB*) and occurs in a younger age range (mean, 38 years). Because of the syndromic association, patients may have a history of paraganglioma, SDH-deficient GIST, or pituitary adenoma. Grossly, the tumors are well circumscribed with tan-brown or red color; cystic areas may be seen. Morphologically, the neoplastic cells of SDH-deficient RCC have eosinophilic cytoplasm and are arranged in solid, nested, or tubular architecture, and cystic areas are common. The individual cells are monomorphic with round, cytologically bland nuclei. The most helpful diagnostic feature is the presence of an intracytoplasmic vacuole or inclusion that contains eosinophilic material, the consistency of which varies from pale and wispy to densely eosinophilic (Fig. 24.51). The tumor has a rounded, well-delineated border but commonly entraps normal renal tubules. While these typical morphologic patterns are most common, rare tumors show high-grade transformation in which the inclusions are focal and more difficult to appreciate. These cases show more cytologic atypia, denser cytoplasm, and increased mitotic activity and may invade the renal sinus (Fig. 24.52). Frank sarcomatoid change is also reported. Immunophenotypically, reactivity for CD117 and cytokeratin 7 is very rare, but PAX8 and kidney-specific cadherin are consistently positive. By definition, SDHB immunostains show loss of cytoplasmic reactivity in the neoplastic cells, while internal intratumoral blood vessels or entrapped renal tubules are positive (Fig. 24.53). SDH-deficient RCCs with typical morphologic features most commonly follow an indolent course, but metastases may occur many years after initial diagnosis (~11% of patients). Cases with high-grade transformation have an aggressive clinical course.

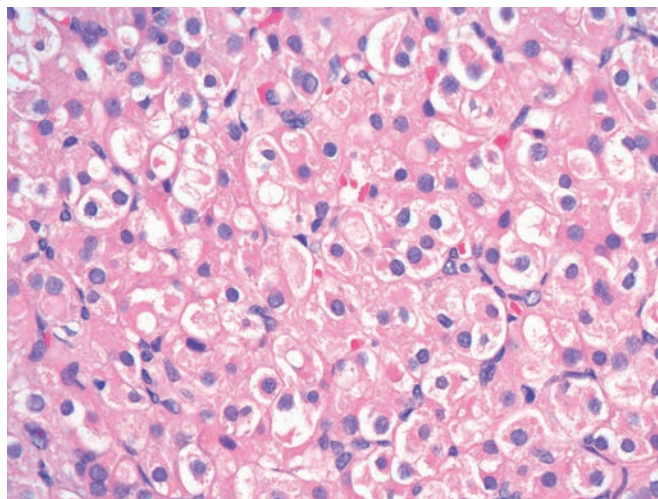


**Figure 24.51** SDH-deficient renal cell carcinoma.

#### Eosinophilic Solid and Cystic Renal Cell Carcinoma

ESC RCC is an emerging subtype of renal neoplasia that was formally described in a series of tuberous sclerosis–associated RCCs<sup>265</sup>; however, it is now recognized to occur more frequently in a sporadic setting.<sup>483,484</sup> The sporadic tumors appear to occur exclusively in women with a wide age range. Grossly, these tumors are often tan with mixed solid and macrocystic appearance (Fig. 24.54). Histologically, the neoplastic cells are characterized by abundant eosinophilic cytoplasm, prominent granular cytoplasmic stippling (said to resemble leishmaniasis), and large round to oval nuclei with prominent nucleoli (Fig. 24.55). In cystic areas, thin septa are lined by these large eosinophilic cells, often with a hobnail arrangement. Immunohistochemically, the cells most commonly have an unusual CK20-positive/CK7-negative phenotype. Common molecular karyotype alterations, distinct from other subtypes of RCC, are described.<sup>483,484</sup>

While these tumors seem to have a more indolent behavior than their nuclear grade would predict, we have seen one metastasis to a regional lymph node and are aware of one liver metastasis (personal communication, Dr. Peter Argani, Johns Hopkins University). As

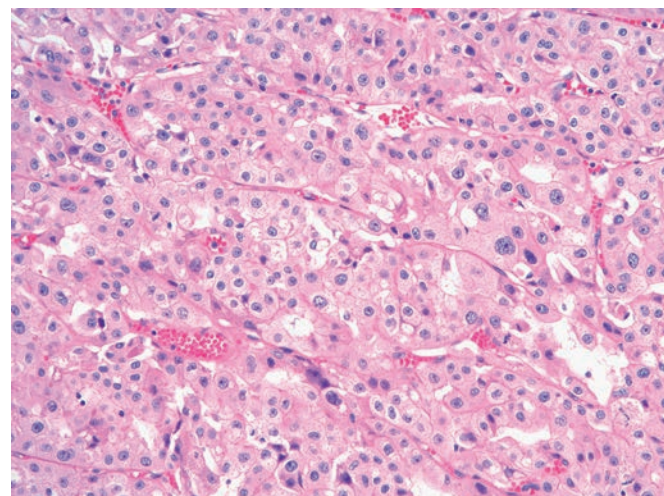


**Figure 24.52** SDH-deficient renal cell carcinoma with nuclear pleomorphism and mitotic activity, clinically malignant.

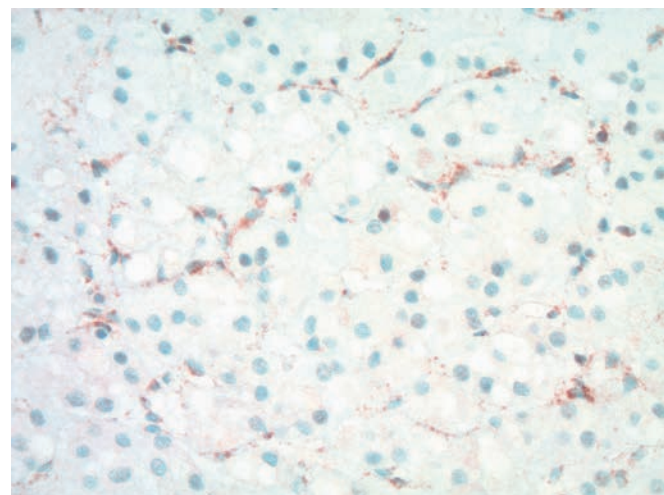


**Figure 24.53** SDH-Deficient Renal Cell Carcinoma (SDHB Immunostain). Cytoplasmic loss in neoplastic cells, but retained in endothelial cells.

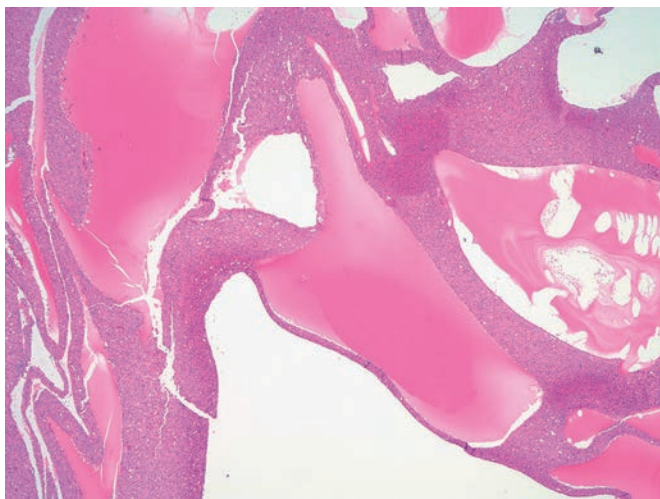


**Figure 24.54** Eosinophilic, solid, and cystic (ESC) renal cell carcinoma, low-power magnification.

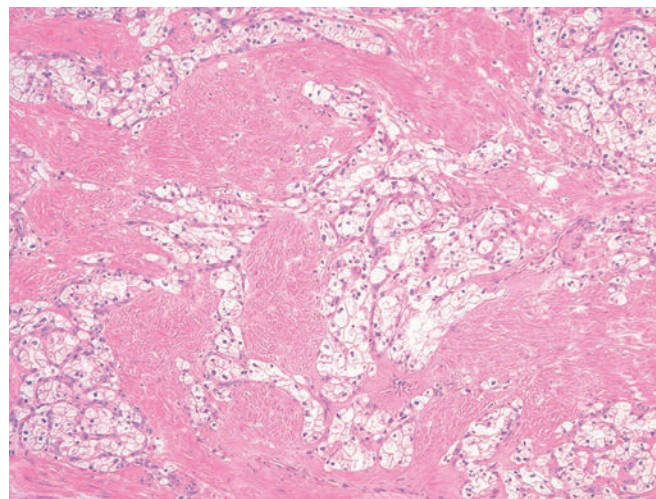
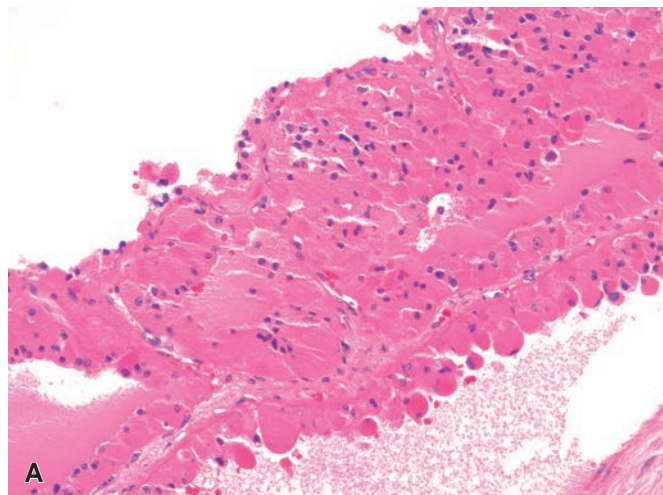
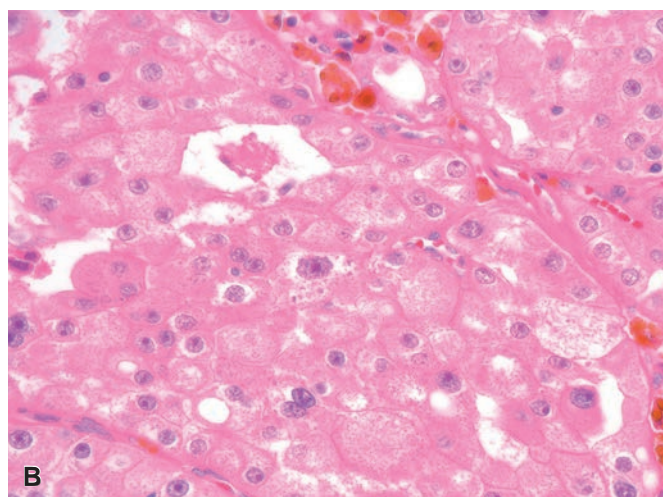


**Figure 24.56** Renal cell carcinoma with (angio)leiomyomatous stroma.



A



B

**Figure 24.55** Eosinophilic, Solid, and Cystic (ESC) Renal Cell Carcinoma. **A**, Eosinophilic cells lining septa have a hobnail appearance. **B**, Nuclei are large with variable nucleoli and coarse cytoplasmic stippling.

discussed previously, it is our observation that “oncocytoid RCC following neuroblastoma” (when MiT family translocation carcinomas are excluded) seems to have many similarities with ESC RCC.<sup>268,269</sup>

#### *Renal Cell Carcinoma, Unclassified*

Some RCCs do not precisely fit one of the well-described subtypes and are designated “RCC, unclassified type.”<sup>485</sup> Most of these tumors are large, high grade, and high stage; however, a rare subset of low grade RCCs do not fit a distinct subtype and might be considered “unclassified.” In such cases, it is important to comment on the low grade nature of the tumor, since most urologists equate “unclassified RCC” with very high risk disease. Immunohistochemistry with PAX8 may be useful to confirm renal epithelial origin, but urothelial markers (p63 and high-molecular-weight keratin) are also helpful since up to 25% of upper tract urothelial carcinoma express PAX8, sometimes diffusely. Recent studies suggest distinct molecular subtypes can be identified.<sup>486</sup>

#### *Other Types*

Rare low-grade RCCs made up of well-differentiated, branching tubular glands lined by clear cells with abundant cytoplasm and surrounded and closely intermingled with abundant smooth muscle bundles have been described under various names (Fig. 24.56).<sup>487-493</sup> When clear cell-papillary RCCs are carefully separated from this group, it is thought that this represents a distinct set of clear cell-like renal neoplasms with a more indolent clinical course, currently listed as a WHO provisional entity under the name “RCC with (angio)leiomyomatous stroma.” Unlike clear cell RCC, these tumors have strong and diffuse reactivity for CK7. Recent sequencing studies identified a subset with mutation in the *TCEB1* gene, but not all cases have this alteration.<sup>492</sup> Importantly, they do not show 3p abnormalities.<sup>337</sup> Interestingly, a subset of RCCs in patients with tuberous sclerosis have an identical morphology; therefore, we recommend a careful evaluation of the background kidney for AML tumorlets.<sup>496</sup> Based on the limited data available, these tumors seem to have an indolent clinical course (with no reported metastases) when carefully separated from clear cell RCC.

Other peculiar forms of RCC have been recently described, including a type closely simulating the appearance of a thyroid follicular carcinoma.<sup>494-496</sup> Additionally, renal neoplasms with ALK translocations are reported (separate from the VCL-ALK fusion tumors), but classification of these tumors is still evolving.

## Spread and Metastases

Because of the importance of subtype, most general RCC data are heavily driven by the most common subtype, clear cell RCC. Approximately one-third of RCCs are found to invade perinephric fat and/or regional lymph nodes at the time of operation.<sup>272</sup> Invasion of the main renal vein used to be a common finding, but now it is seen less frequently, likely due to earlier imaging detection. From the renal vein, the tumor may extend into the inferior vena cava and occasionally even into the right atrium. RCC, like Wilms tumor, can invade the *renal sinus* (the adipose tissue compartment located within the confines of the kidney and containing numerous veins and lymphatics), a fact which is likely to increase the risk for metastatic spread.<sup>497</sup> As a matter of fact, it has been claimed that the renal sinus is the *principal* pathway of invasion of RCC and the explanation for the rare cases of tumor-related death in patients with small tumors.<sup>498,499</sup> Therefore, very careful gross examination and sampling of the renal sinus are critical.

Satellite tumors, which may represent intrarenal tumor spread or independent primaries (see earlier), are seen in approximately 6% of the cases.<sup>292</sup>

Approximately one-third of patients with RCC already have distant metastases at the time they seek medical attention.<sup>500</sup> The most common sites of distant metastases are the lung and skeleton. The bones most often involved are the pelvis and femur, but there is also a predilection for the sternum, scapula, and small bones of the hands and feet.<sup>501,502</sup> Metastases can also develop in the adrenal gland, liver, skin, soft tissue, central nervous system, ovary, and almost any other site.<sup>503</sup> RCC is actually notorious (together with malignant melanoma and choriocarcinoma) for metastasizing to the most unusual places, such as the nasal cavity, oral cavity, larynx, parotid, thyroid, heart, bladder, testis, prostate, and pituitary gland.<sup>504-511</sup> These metastases are often solitary, at least at the clinical level.<sup>512</sup> Even at autopsy, 8% of the patients have metastatic involvement of only one or two organs.<sup>513</sup> Because of this and the fact that the primary tumor is often clinically silent, these metastases tend to be confused with primary tumors of the organs in which they lodge. That can be the case when RCC metastasizes to the ovary,<sup>514</sup> and even more so when it metastasizes to the *contralateral* adrenal gland.<sup>515,516</sup> In these instances, detection of EMA, keratin, and PAX-8 positivity favors a diagnosis of RCC.<sup>517</sup> An additional source of misinterpretation stems from the fact that sometimes these metastases develop years or decades after the removal of the primary tumor.<sup>518,519</sup> Several cases have been documented in which these metastases have undergone spontaneous regression.<sup>520,521</sup>

Metastases are extremely rare in tumors that measure 3 cm or less, but they can certainly occur, indicating that the once-popular practice of separating RCC from adenoma on the basis of size alone is unreliable.<sup>522</sup>

## Therapy

The primary treatment of RCC is surgical excision. While transabdominal or thoracoabdominal radical nephrectomy with removal of the entire kidney, surrounding fat, Gerota fascia, and adrenal gland has historically been preferred, a laparoscopic approach with only a segmental resection of the kidney is now more common and yields long-term results comparable to those of open surgery.<sup>523-527</sup> No consistent benefits have yet been demonstrated for administration of adjunctive radiation therapy or chemotherapy; neoadjuvant therapy is sometimes utilized in select cases in an attempt to reduce tumor size prior to surgery.<sup>528</sup>

RCCs that are bilateral, that develop in the setting of VHL disease, or that occur in a solitary kidney are treated with partial nephrectomy, if technically feasible.<sup>529-533</sup> Some authors have proposed this approach for small RCCs in general.<sup>287,534,535</sup>

Various immune-based therapeutic approaches (such as interleukin-2 and  $\alpha$ -interferon) are currently being tried in metastatic RCC; these have met with erratic if occasionally impressive results.<sup>536-538</sup> In recent years, targeted therapy using various agents such as sunitinib (multitargeted receptor tyrosine kinase inhibitor), bevacizumab (antibody-blocking VEGF A), temsirolimus (mTOR inhibitor), and everolimus (mTOR inhibitor) has yielded promising responses for metastatic RCC.<sup>539</sup> Targeted therapies that might selectively treat specific subtypes of RCC are the source of many ongoing studies.

## Prognosis

The overall 5-year survival rate for RCC is approximately 70%. The prognosis is related to several clinicopathologic parameters.

1. *RCC subtype.* The prognostic significance associated with the various microscopic variants of RCC is discussed in connection with those variants.<sup>540</sup>
2. *Staging.* In patients who do not have distant metastases at diagnosis, stage on the basis of surgical findings is one of the strongest prognostic factors. The AJCC 8th edition bases staging on tumor size and spread beyond the kidney.<sup>541</sup> Based on numerous studies by Bonsib, it is clear that the main route of RCC extension outside of the kidney parenchyma involves the blood vessels of the renal sinus.<sup>498,542,543</sup> While renal vein involvement is typically easy to recognize grossly, very careful gross inspection of the tumor/stromal interface where tumor abuts fat is critical (Fig. 24.57).<sup>544</sup> Any separate tumor nodule present in the sinus fat is almost certainly pT3 disease based on involvement of renal sinus blood vessels. A bulging interface at the renal sinus should be carefully sampled to determine if the tumor is microscopically entering a blood vessel. Destructive invasion of adipocytes is actually rare and likely represents late invasion through the wall of a blood vessel. Direct contiguous invasion of the adrenal gland (pT4) should be distinguished from a separate adrenal nodule (pM1). The prognosis seems to be particularly poor in cases with invasion of the adrenal gland.<sup>545</sup>
3. *Distant metastases.* The presence of distant metastasis at the time of operation is, not surprisingly, the single most important unfavorable prognostic parameter.<sup>546</sup>
4. *Tumor size.* Size of the primary tumor relates to prognosis for the very small (<4 cm) and the very large (>10 cm) tumors but not for those between these extremes, which represent the large majority.<sup>547-549</sup> For such tumors (4–10 cm), size seems to be a



**Figure 24.57** Clear cell renal cell carcinoma with definitive macroscopic invasion of renal sinus (pT3).

continuous and therefore relative variable.<sup>550</sup> Out of necessity, an arbitrary size cutoff is needed, and this cutoff has been established to be 7 cm between T1 and T2 tumors in the 2016 TNM staging system; however, it has been suggested that different size cutoffs might be more predictive of the survival of stage I patients after radical nephrectomy.<sup>551,552</sup> As Bonsib has emphasized, increasing tumor size correlates very highly with invasion of the renal sinus, such that it is difficult to identify a pT2 clear cell RCC after very careful gross evaluation.<sup>543</sup>

5. *Renal vein invasion.* Gross invasion of the renal vein has been regarded as a poor prognostic sign and therefore constitutes a criterion for surgical staging.<sup>541,549</sup> Microscopic lymphovascular invasion has also been found to be an important predictor of relapse, but this has been variably defined.<sup>553-555</sup>
6. *Microscopic grade.* Nuclear grade of the tumor as determined in microscopic sections is an important predictor of survival in clear cell carcinoma (but not in chromophobe cell carcinoma, and possibly some rare variants as noted earlier).<sup>400,556-559</sup> It is strongly correlated with surgical staging, but it also maintains statistical validity independently from it.<sup>547,560</sup> Grading is performed using the WHO/ISUP grading system, which has proven utility in clear cell and papillary RCC (see Table 24.3).<sup>559,561,562</sup> Rhabdoid and sarcomatoid differentiation have now been incorporated into the grading system and are regarded as grade 4. Some have advocated for the use of nuclear morphometry to further refine the criteria for nuclear grading, but this is not standard practice.<sup>563-565</sup>
7. *Necrosis.* Coagulative tumor necrosis has been shown to be a strong predictor of outcome, and there has been a proposal to integrate necrosis into the grading system.<sup>566-568</sup>

## Adenomas

Renal papillary adenomas, defined as minute cortical foci of tubular or (more commonly) papillary epithelium, are present in approximately 20% or more of adult kidneys; most of them measure 1–3 mm in diameter and by the latest WHO definition are less than 1.5 cm, lack a tumor capsule, and are no more than nucleolar grade 2.<sup>569-572</sup> The cytoplasm of the proliferating cells is typically acidophilic rather than clear and not particularly abundant.<sup>573</sup> Psammoma bodies may be present. Papillary adenomas are particularly common and numerous in end-stage kidneys in patients on long-term dialysis (*renal adenomatosis*).<sup>574,575</sup> Since these adenomas share the same cytogenetic findings as type 1 papillary RCC, they likely represent early forms of the disease without metastatic potential. In contrast, other subtypes of renal neoplasia are no longer divided into adenomas and carcinomas based on size, such that small clear cell RCCs are still diagnosed as carcinoma.

## Oncocytoma, “Difficult to Classify” Oncocytic Tumors, and Oncocytosis

The diagnosis of renal oncocytoma represents one of the more problematic and controversial topics in renal neoplasia classification today.<sup>380</sup> Renal oncocytomas reportedly make up 5%–9% of all primary nonurothelial epithelial renal neoplasms; however, this number depends largely on the diagnostic criteria employed.<sup>576</sup> Our diagnostic approach is to identify three histologic groups of low-risk oncocytic tumors: classic prototypical oncocytoma, classic prototypical chromophobe RCC, and oncocytic tumors that are “difficult to classify.” This section describes classic oncocytoma, followed by comments on handling problematic cases. Grossly, renal oncocytoma is typically solid and mahogany brown, often has a central stellate scar, and can reach large sizes (Fig. 24.58).<sup>577</sup> They can be multicentric and bilateral.<sup>578</sup> Invasion of the perirenal tissues or renal vein may

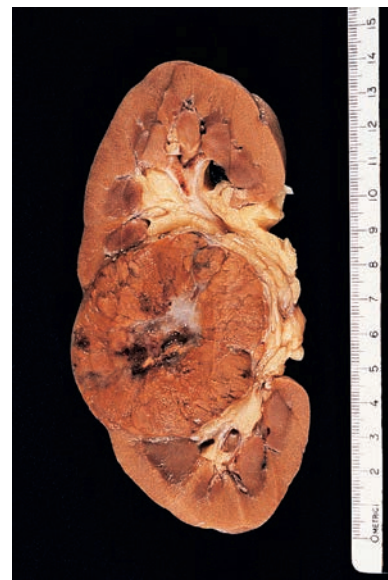


**Figure 24.58** Gross Appearance of Oncocytoma of Kidney. The tumor is characteristically well circumscribed, mahogany brown, and has a central fibrous scar.

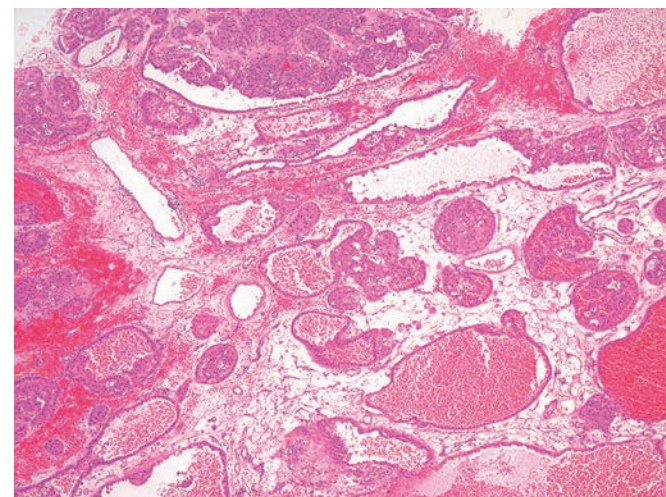


**Figure 24.59** Typical nesting and cystic pattern of renal oncocytoma.

be encountered.<sup>576,579-582</sup> Some of these gross features (particularly the central scar) have been used to distinguish oncocytomas from RCC on CT scan, but the level of accuracy is poor.<sup>583</sup> Microscopically, oncocytomas are composed entirely of cells with abundant acidophilic granular cytoplasm, growing in a nesting (“alveolar”) or tubular fashion (Fig. 24.59). In some foci, nests and tubules often “float” in an edematous stroma. The nuclei of oncocytoma cells are usually small, round, and regular (Fig. 24.60).<sup>584</sup> Pockets of “degenerative type” nuclear atypia can occur, and some scattered binucleate cells may be present.<sup>585,586</sup> Psammoma bodies can be present, most of them in an intraluminal location. A variant of oncocytoma has been described composed of small cells (i.e. “oncoblasts”), which can easily be misinterpreted.<sup>587,588</sup> Renal tumors with oncocytic cytoplasm and a predominant papillary pattern should probably be placed with the papillary RCCs.<sup>589</sup> Immunohistochemically, the tumor cells express pancytokeratin, low-molecular-weight keratins, CD117, S-100A1 protein,<sup>590</sup> and E-cadherin, but show only focal or no

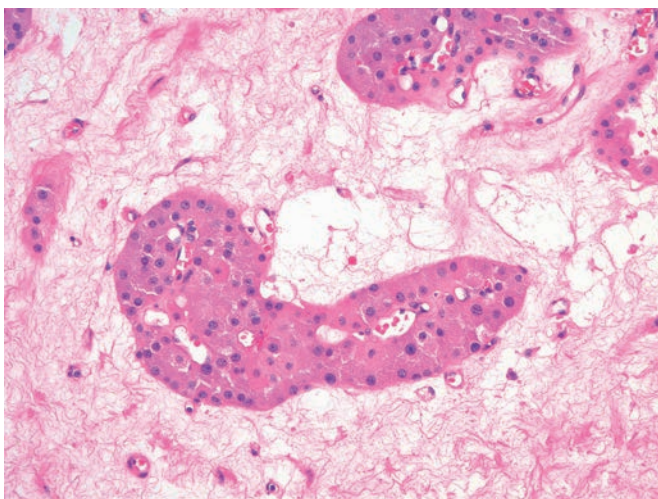


**Figure 24.60** Renal Oncocytoma. Nuclei are round and monomorphic.

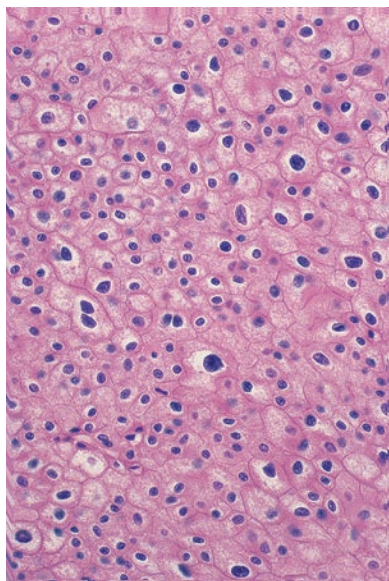


**Figure 24.61** Perinuclear halos, binucleation, and “koilocytotic atypia” are features of a prototypical chromophobe renal cell carcinoma.

reactivity for vimentin.<sup>591-593</sup> Cytokeratin 7 is usually negative or only positive in scattered cells; however, entrapped tumor nests within the central scar (often associated with cytoplasmic clearing) have stronger expression of cytokeratin 7.<sup>594</sup> Hale colloidal iron is typically negative.<sup>379</sup> Ultrastructurally, packing of the cytoplasm by mitochondria is the most striking feature.<sup>595-598</sup> Cytogenetically, oncocytomas lack the 3p abnormalities of clear cell RCC and display different chromosomal alterations, particularly loss of chromosome 1, rearrangements of 11q13, and deletion of chromosome 14.<sup>599,600</sup>

If strict morphologic criteria are employed, the overwhelming majority of oncocytomas will be cured by excision regardless of size<sup>582,584,601-605</sup> and/or the presence of atypical microscopic features such as vascular invasion or perirenal fat infiltration.<sup>606,607</sup> Only exceptional cases of well-documented renal oncocyromas have been reported to metastasize.<sup>576,608</sup>

The main differential diagnosis of renal oncocytoma is with the eosinophilic variant of chromophobe RCC, succinate dehydrogenase-deficient RCC, and less commonly epithelioid AML. The cells of

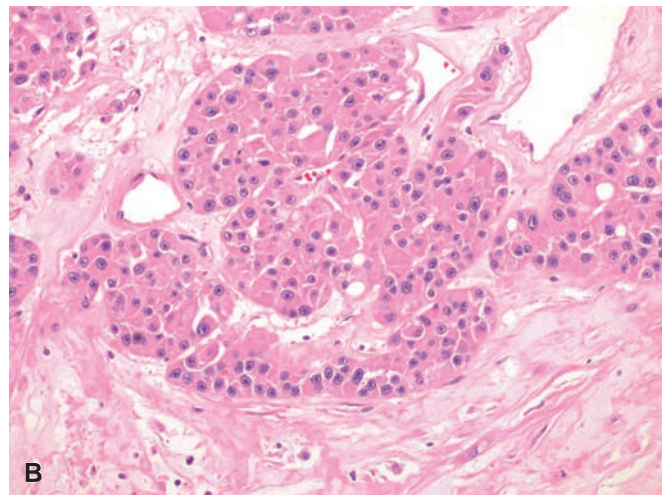
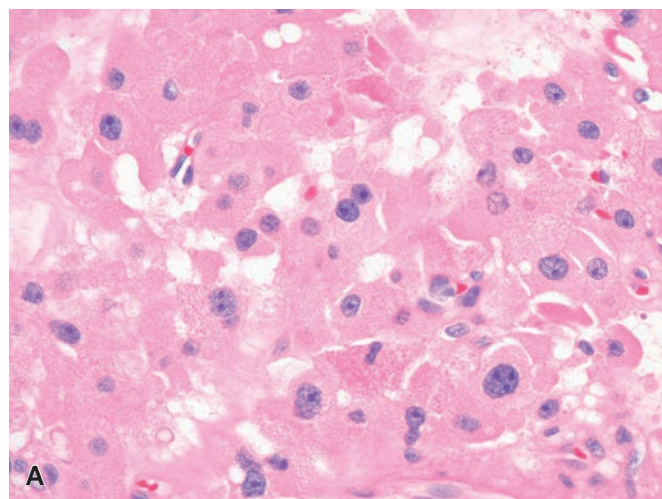


**Figure 24.62** Oncocytic Renal Neoplasms With Features Not Prototypical for Either Oncocytoma or Chromophobe. **A**, This tumor has more variability in nuclear size with multiple nucleoli, but nuclei remain relatively round with no perinuclear clearing. **B**, This case has very prominent and consistent macronucleoli. Other foci showed solid growth. Such tumors have significant variability in diagnosis, even among experts.

chromophobe RCC have wrinkled, raisin-like hyperchromatic nuclei, whereas those of oncocytoma tend to be perfectly round. As stated before, the presence of well-developed perinuclear halos and/or irregular nuclear membranes with frequent binucleation are sufficient for classification as chromophobe RCC (Fig. 24.61).<sup>427</sup>

Some cases are more difficult to classify, and expert consultants often differ in their methods and terminology used to diagnose such cases. There are several approaches: (1) divide all cases into either chromophobe or oncocytoma by morphology, (2) classify difficult cases as chromophobe or oncocytoma using adjunctive immunostains/special stains, or (3) keep strict diagnostic criteria for the diagnosis of chromophobe RCC and oncocytoma by using a separate diagnostic term for “gray zone” cases. Until this diagnostic problem is better addressed by studies, we prefer the latter and have adopted what we find to be a practical diagnostic approach. Most of these “gray zone” cases maintain round nuclear contours without perinuclear clearing (i.e. not classic chromophobe) but have greater variability in nuclear size, greater degree of irregular nuclear chromatin, and variable macronucleoli (Fig. 24.62). To our knowledge, no adjunctive test (whether immunostain, histochemical stain, or cytogenetic test)

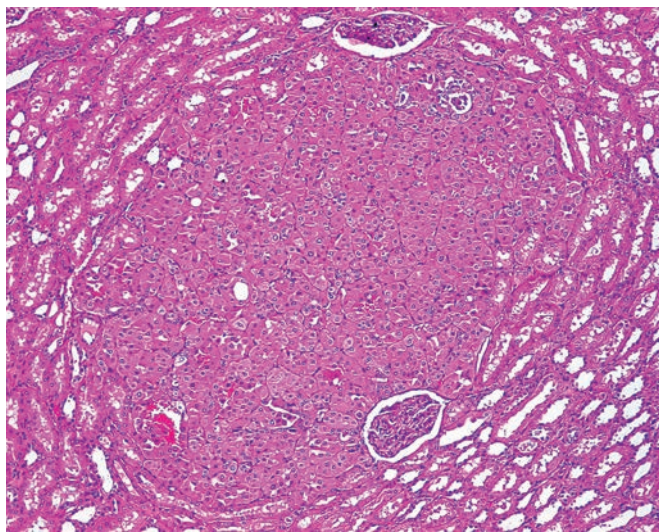


**Figure 24.63** So-called renal oncocytosis. Many similar nodules were scattered throughout the kidney.

has been shown to predict behavior in such tumors. This approach avoids arbitrarily dividing some cases into either a benign or malignant category. Therefore, we prefer to simply utilize the diagnostic term “oncocytic renal neoplasm of low malignant potential,” but other similar terms have been applied. While we have seen extremely rare liver metastases in such cases (far less than 1% based on several hundred cases), it is our anecdotal experience that the vast majority behave in a benign fashion.

As alluded to in the section on unclassified RCC, rare low grade RCCs may have significant overlap with this oncocytic spectrum of neoplasia. We generally reserve the rare diagnosis of “RCC, low-grade oncocytic type” for cases with sheet-like growth and obvious mitotic activity, but without nuclear features of chromophobe RCC.

**Oncocytosis** is the term proposed for a condition characterized by the presence of innumerable oncocytic nodules in one or both kidneys, usually associated with the presence of a dominant nodule (Fig. 24.63). The disease can affect adults and children, and many cases are likely related to Birt-Hogg-Dubé syndrome.<sup>609</sup> Microscopically, the oncocytic tubules intermingle with the normal parenchyma and may be associated with diffuse oncocytic change in the renal tubules and oncocytic cortical cysts.<sup>259</sup> The larger oncocytic nodules/tumors show morphologic features reminiscent of both oncocytoma and chromophobe RCC, but often show immunohistochemical and cytogenetic profiles distinct from them.<sup>610</sup>

## Neuroendocrine Tumors

**Small cell neuroendocrine carcinomas** of the kidney (or other high-grade neuroendocrine carcinomas) with features similar to those of the lung have been described.<sup>611-613</sup> They show evidence of neuroendocrine differentiation ultrastructurally and immunohistochemically.<sup>611,614,615</sup> These should be distinguished from urothelial carcinoma of the renal pelvis with neuroendocrine differentiation.<sup>616-618</sup> The behavior of the few reported cases has been very aggressive.

**Carcinoid tumor** (well-differentiated neuroendocrine neoplasm), which should be sharply segregated from small cell carcinoma, has been reported in a pure form<sup>619-621</sup> and as a component of cystic teratoma.<sup>622-624</sup> Microscopically, the tumor cells are well differentiated at the morphologic, immunohistochemical, and ultrastructural levels.<sup>625-627</sup> The pattern of growth is often trabecular (and therefore similar to that seen in rectal carcinoid and in the carcinoid component

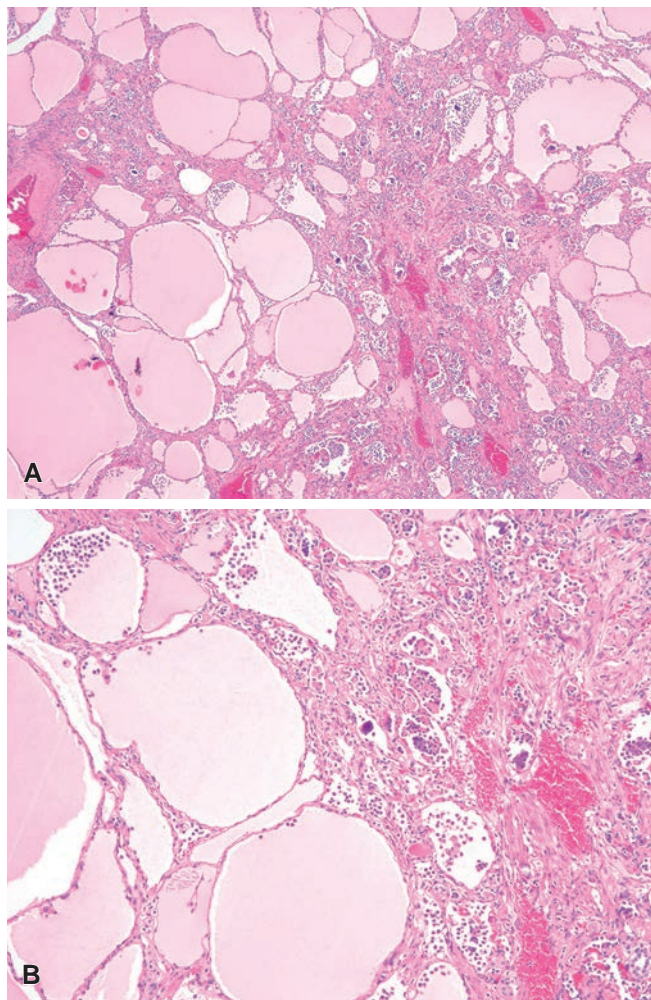


**Figure 24.64** “Atrophic Kidney-Like Tumor.” **A**, Cystically dilated follicles of various sizes are typical, with admixed smaller tubules. **B**, Follicles are lined by a flattened epithelium, and psammoma bodies and amorphous calcifications are present.

of strumal carcinoid of the ovary), but a wide range of appearances has been documented, including nesting (insular) and glandular.<sup>625,628</sup> The cytoplasm of the tumor cells may have an oncocytic quality.<sup>629</sup> Stage at presentation is the most important factor in determining outcome.<sup>627,630</sup> It is important for a metastasis from another anatomic site (e.g. gastrointestinal tract) to be excluded clinically.

**Paraganglioma** may also rarely involve the kidney.<sup>631</sup>

## Other Epithelial Tumors

We have seen several examples of “atrophic kidney-like tumor,” which was described by Hes et al. in 2014 as a “distinctive renal neoplasm simulating atrophic kidneys with 2 types of microcalcifications.”<sup>632</sup> These are characterized by a circumscribed and encapsulated collection of cystically dilated “follicles” filled with eosinophilic secretions and admixed with smaller renal tubular-like structures (Fig. 24.64). The follicles are lined by an atrophic lining epithelium, and the lumina may contain “sloughed” cells. Variable loose to collagenized stroma is present, and psammoma bodies or more amorphous calcifications are numerous. Some similar tumoral masses have been reported as “thyroid-like follicular RCC,” which we believe is a different lesion. These “atrophic kidney-like tumors” have all

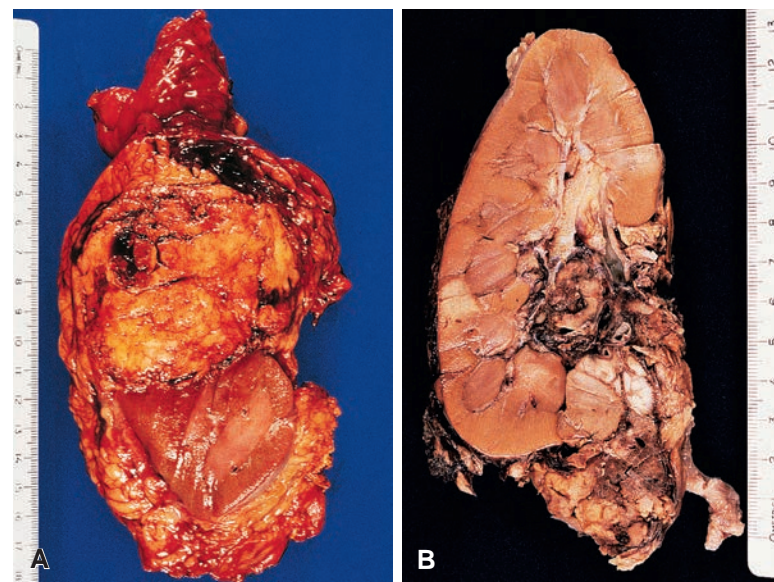


**Figure 24.65 A and B,** Gross appearances of angiomyolipoma of kidney. Both tumors are variegated, with a predominance of yellow areas, admixed with hemorrhagic foci.

occurred in young patients (typically 20–40 years of age but also in young children) and have followed a benign clinical course. Their exact nature is still debated.

Very unusual and as yet not fully characterized morphologic types of renal epithelial neoplasms include *myoepithelioma* and *myoepithelial carcinoma*<sup>633,634</sup>; *spiradenocylindroma* (a sweat gland tumorlike renal neoplasm developing in the wall of a renal cyst and having a somatic mutation in the *CYLD1* gene)<sup>635</sup>; and *papillary tumor of the renal medulla* (a type of carcinoma that is different morphologically and cytogenetically from the usual papillary RCC and from collecting duct carcinoma).<sup>636</sup>

### Angiomyolipoma

AML has undergone a remarkable transformation, from a rare and rather pedestrian tumor type restricted to the kidney to a biologically fascinating and morphologically heterogeneous entity that can occur in a wide variety of extrarenal sites, including liver, pelvic region, retroperitoneum (unconnected to the kidney), uterus, somatic soft tissues, large bowel, nasal cavity, and bone.<sup>637-641</sup> This family of phenotypically similar tumors is now collectively known as PEComa, which include lymphangiomyoma(tosis) of lung and lymph nodes and so-called clear cell tumor ("sugar tumor") of lung.<sup>642-647</sup> This section will focus specifically on primary renal AML.

Most patients are adults. The tumor may be found incidentally or result in retroperitoneal hemorrhage, which can be massive and even fatal.<sup>648</sup> Approximately one-third of the patients with renal AML suffer from tuberous sclerosis, the incidence being higher if the tumors are multiple or bilateral. It has been estimated that approximately 80% of the patients with the complete or severe form of tuberous sclerosis have renal AMLs,<sup>649</sup> and it has been shown that patients with the closely related genetic disease known as *TSC2/PKD1 contiguous gene syndrome* also have an increased incidence of renal AML.<sup>650</sup>

In some cases, the appearance of AML on ultrasonography and CT scan is highly characteristic<sup>651</sup> and the diagnosis can be confirmed by fine-needle aspiration or needle biopsy, supplemented by immunocytochemistry as needed.<sup>652,653</sup>

The gross appearance of the tumor depends on the relative amounts of the various components and may closely simulate RCC

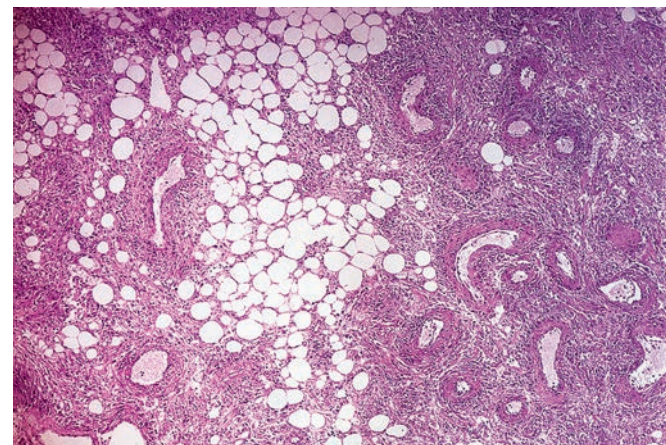


**Figure 24.66 Typical Renal Angiomyolipoma.** The tumor is composed of lipid-rich and myoid-like cells with admixed blood vessels.

because of the admixture of yellow areas (lipid rich) and hemorrhagic areas (vessels) (Fig. 24.65). Capsular invasion is present in one-fourth of the cases, and there can be extension into the perirenal soft tissues. In its conventional form, AML is composed of an intimate admixture of blood vessels and tumor cells; the neoplastic cells are heterogeneous, having either an eosinophilic spindle cell appearance imparting "myoid" features or intracytoplasmic lipid closely mimicking adipocytes (Fig. 24.66).<sup>654,655</sup> Less commonly, epithelioid cells are the predominant cell type. The associated tortuous thick-walled blood vessels lacking elastic tissue lamina often have bundles of tumor cells that seem to emanate from the vessel walls, a very helpful diagnostic feature (Fig. 24.67). Some epithelioid AMLs may have marked cytologic atypia that closely mimics a poorly differentiated RCC (Fig. 24.68). Multicentric microscopic foci are common and suggest tuberous sclerosis; exceptionally, they may be seen involving the glomeruli.<sup>656</sup> In some cases, the AML proliferation is accompanied by cysts lined by cuboidal to hobnail cells resting on a cellular spindle cell stroma with a cambium layer-like appearance. This

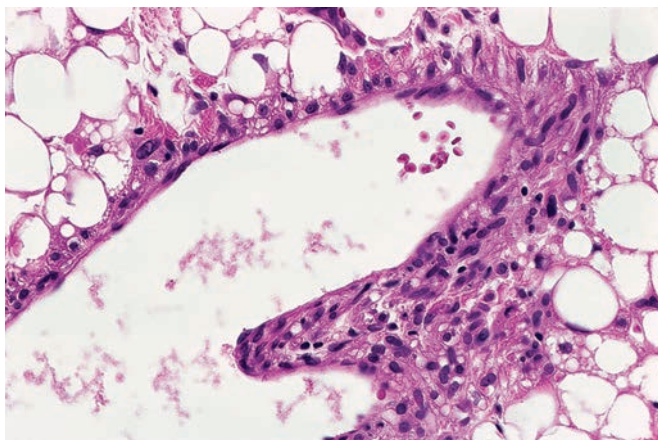


**Figure 24.67** Intimate relationship of the eosinophilic neoplastic cells of angiomyolipoma with a large vessel. This is an important diagnostic clue.

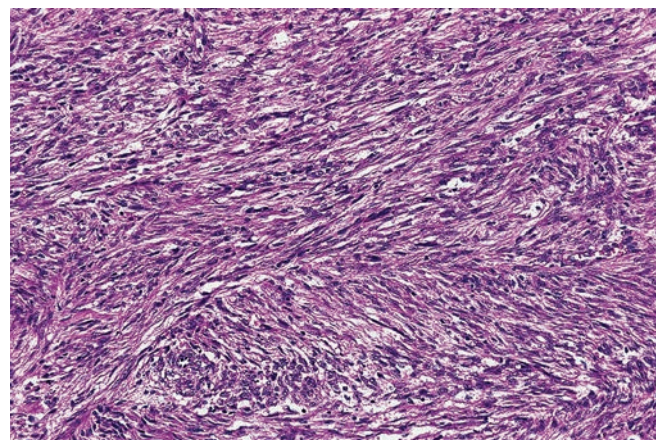


**Figure 24.69** Renal angiomyolipoma showing a predominant myoid appearance.

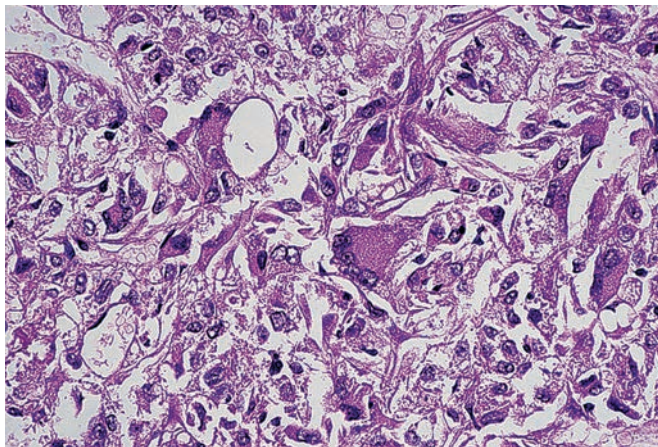


**Figure 24.68** Epithelioid angiomyolipoma of the kidney showing marked pleomorphism of the tumor cells. This tumor recurred locally and later metastasized to lung.

peculiar cystic variant of AML (AMLC) is also characterized by the frequent expression of hormone receptors.<sup>657-658</sup>

Immunohistochemically, AMLs (and all PEComas) are notable because, in addition to the expected smooth muscle markers (such as actin), they regularly express melanocytic markers such as HMB-45, Mart-1/Melan-A, microphthalmia transcription factor, and tyrosinase; however, expression of melanocytic markers may be quite focal.<sup>659-666</sup> Cathepsin-K is strongly and diffusely expressed in AML, and (in the kidney) we find it more useful than other melanocytic markers; however, it is also commonly expressed in MIT family translocation RCC.<sup>667-669</sup> To our knowledge, nuclear PAX8 expression has not been reported in AML; therefore, it has utility in the distinction from RCC. At the ultrastructural level, this immunohistochemical profile is associated with the presence of unique cytoplasmic crystalloids<sup>642</sup> and of organelles consistent with premelanosomes.<sup>670-672</sup> Unfortunately, the renal AMLs of tuberous sclerosis patients with mutation of the TSC1 and TSC2 genes have been found to show inconsistent hamartin and tuberin expression.<sup>673-675</sup>

Recently, our concepts on the nature of PEComas have become ever murkier by the demonstration that a subset of these tumors harbors TFE3 gene fusions and exhibits aberrant immunoreactivity for TFE3 protein (like translocation-associated RCCs and alveolar soft part sarcoma).<sup>676</sup> Apparently, these tumors differ in several

respects from the “conventional” PEComas lacking these molecular features.<sup>677</sup>

AMLs in which spindle cells with a smooth muscle appearance predominate may mimic leiomyomas, leiomyosarcomas, or GISTS (Fig. 24.69).<sup>666,678</sup> Lipid-rich AMLs, in which the adipose tissue is predominant, can be easily confused with an atypical lipomatous tumor (well-differentiated liposarcoma). It should be highlighted that AMLs may express MDM-2 by immunohistochemistry (an adjunctive test for atypical lipomatous tumor/well-differentiated liposarcoma); therefore, FISH evaluation for MDM-2 amplification is more useful in this specific context.<sup>679</sup> Highly pleomorphic AMLs rich in epithelioid cells closely resemble RCC.<sup>680-682</sup> AMLs composed of monomorphic epithelioid cells with homogeneous acidophilic cytoplasm may be mistaken for oncocytomas.<sup>683-685</sup>

The treatment of renal AML is surgical, and excision is usually curative.<sup>686</sup> However, cases resulting in death from massive local recurrence are on record.<sup>687</sup> It is also now abundantly clear that AML is capable of distant metastases; however, the regional lymph node involvement that sometimes accompanies renal AML is an expression of multicentricity rather than true embolic metastases.<sup>688-690</sup> Cases with indisputable metastatic spread in the form of huge retroperitoneal deposits or nodules in the lung and other organs have been documented.<sup>691-694</sup> Practically all of these biologically malignant cases had highly atypical epithelioid features morphologically, which leads to the question as to whether it is possible to make a diagnosis of malignant AML on morphologic grounds.<sup>695,696</sup> It is obvious that a potential for malignant behavior cannot be excluded for AMLs with “aggressive” morphologic features.<sup>682,697</sup> According to a recent study, presence of three or more of the following features is predictive of malignant behavior: (1)  $\geq 70\%$  atypical epithelioid cells (polygonal cells with prominent nucleoli and nuclear size exceeding twice the size of adjacent nuclei); (2)  $\geq 2$  mitotic figures per 10 high-power fields; (3) atypical mitotic figures; and (4) necrosis.<sup>696</sup>

### Juxtaglomerular Cell Tumor

Patients with juxtaglomerular cell tumor usually present clinically with hypertension because of excessive renin production,<sup>698</sup> but some cases are nonfunctioning.<sup>699</sup> Most patients are adult, but cases have also been reported in children.<sup>700</sup> Grossly, all reported cases have been unilateral and solitary. Most have been less than 3 cm in diameter and located in the cortex, but occasional examples have reached 8 cm.<sup>701</sup> They are solid and well circumscribed, with a gray-white to light yellow cut surface.

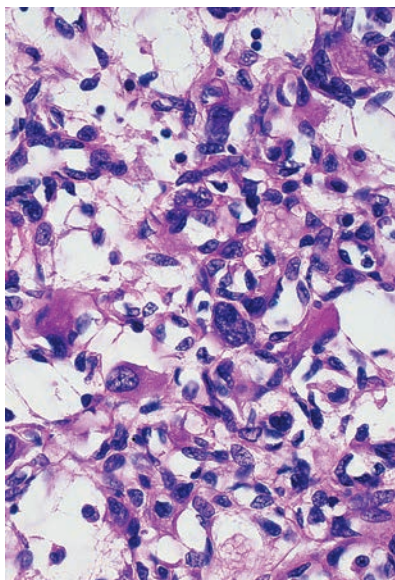


**Figure 24.70** Microscopic Appearance of Juxtaglomerular Cell Tumor. The lesion has a distinct vascular background.

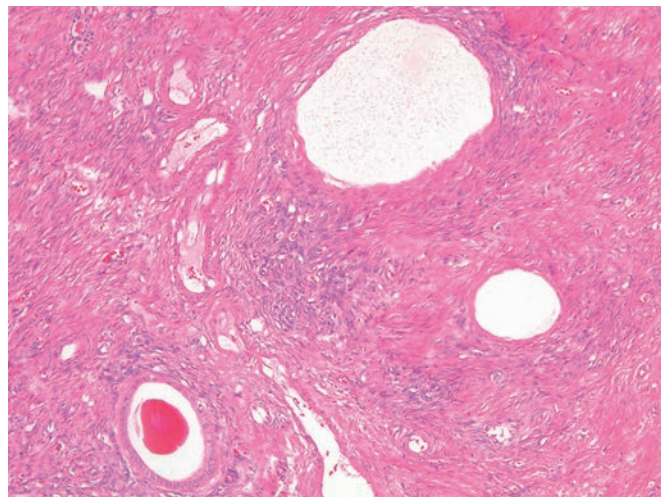


**Figure 24.72** Mixed epithelial and stromal tumor with classic ovarian-like stroma.

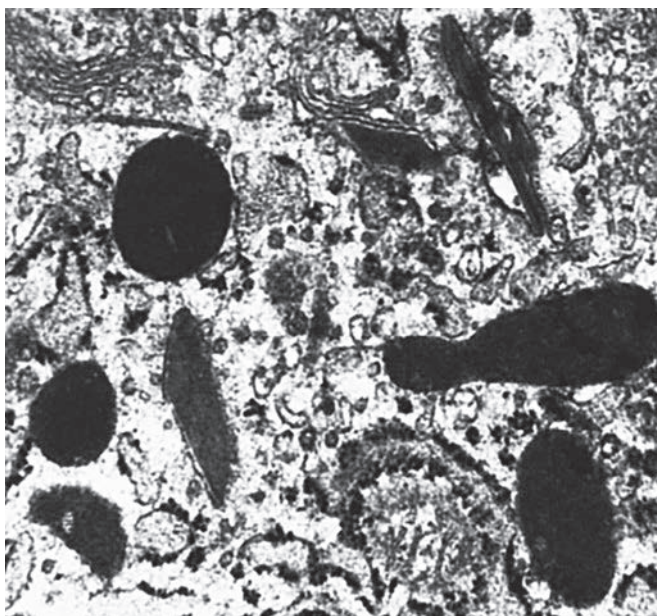


**Figure 24.71** Secretory Granules of Juxtaglomerular Cell Tumor as Seen Ultrastructurally. Some of them are diamond shaped, identical to those seen in normal juxtaglomerular cells. This case has been reported by Conn et al.<sup>848</sup> (Courtesy of Dr. M.R. Abell, Ann Arbor, MI.)

The light microscopic appearance is reminiscent of hemangiopericytoma and glomus tumor, not surprisingly considering the fact that juxtaglomerular cells are specialized vessel-related epithelioid smooth muscle cells.<sup>701,702</sup> The tumor cells are uniform and round to polyhedral and have a granular acidophilic cytoplasm (Fig. 24.70). Mast cells are numerous. In some cases the tumor cells are spindled, and the pattern of growth may be papillary.<sup>703</sup> The intracytoplasmic renin granules may be demonstrated with PAS and Bowie stains, and their nature may be confirmed with immunohistochemical techniques.<sup>698,702,704</sup> In contrast to conventional or epithelioid AML, juxtaglomerular cell tumor is negative for HMB-45.<sup>705</sup> They are consistently positive for

CD34 and CD117 and show focal staining for smooth muscle actin.<sup>706</sup> Ultrastructurally, adrenergic nerve terminals are seen in contact with the tumor cells, which have various types of secretory granules, some of them containing a typical rhomboid crystalline material thought to be renin protogranules (Fig. 24.71).<sup>704,707-709</sup> Cytogenetically, some recurrent chromosome imbalances have been reported.<sup>710,711</sup> All but one of the reported cases have behaved in a benign fashion,<sup>699</sup> but some patients have remained hypertensive following nephrectomy.<sup>701,712</sup>

It should be noted that renin secretion can be associated with other renal and extrarenal neoplasms, such as RCC, Wilms tumor, and pancreatic adenocarcinoma.<sup>713-715</sup>

MEST is the preferred diagnostic term applied to biphasic tumors, generally occurring in middle-aged and older women, that have been called cystic nephroma, MEST, or REST in adults.<sup>716,717</sup> Several recent studies have shown that the similarities, overlaps, and hybrid forms at the clinical, morphologic, phenotypic, and molecular levels are such as to suggest that cystic nephroma and MEST are two different manifestations of the same basic process.<sup>717-720</sup> As discussed in the section on pediatric renal neoplasia, the name cystic nephroma is now preferred for the pediatric cases that often have *DICER1* mutations and frequent syndromic association. MEST may be solid and cystic and may bulge into the renal pelvis. Microscopically, the spindle cell proliferation in between the individual cysts resembles ovarian stroma (Fig. 24.72), including the expression of hormone receptors. The epithelial component is, for the most part, is similar to cystic nephroma (and therefore consistent with renal ductal epithelium, also at the immunohistochemical and ultrastructural level<sup>721</sup>), but is more heterogeneous and may exhibit features suggestive of müllerian-type differentiation, including epithelium of endometrioid, tubal, clear cell, and squamous cell type. In addition, the epithelial component may be more predominant than typically seen in pediatric cases (Fig. 24.73). Cases with great predominance of the stromal or adipose component can be confused with leiomyomas or AMLs.<sup>722</sup> The behavior is generally benign, although a few histologically malignant examples have been reported.<sup>723,724</sup>

## Other Benign Tumors and Tumorlike Conditions

**Medullary fibroma** is also referred to as *renomedullary interstitial cell tumor*, under the assumption that it arises from the medullary interstitial cell.<sup>725</sup> The latter is a specialized stromal element that

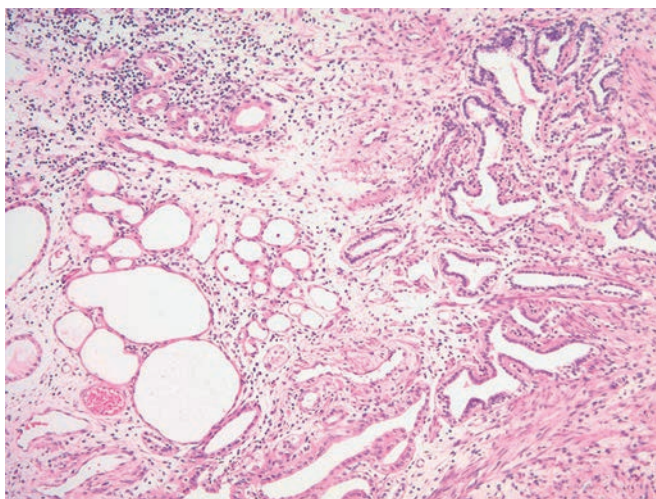


**Figure 24.73** Mixed epithelial and stromal tumor with crowded and various shaped glands.

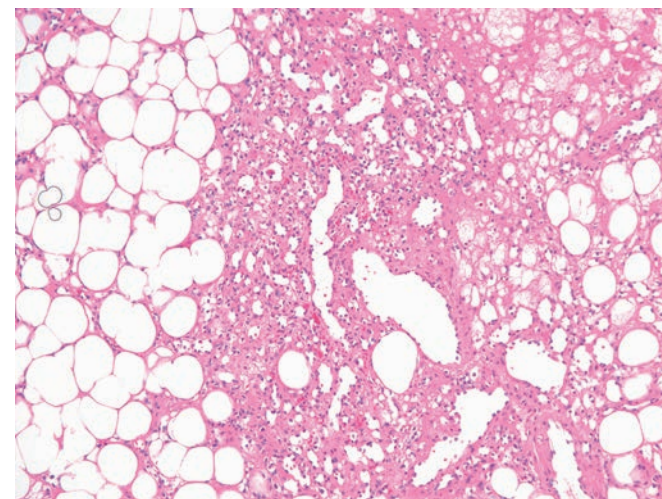


**Figure 24.74** Anastomosing hemangioma in the renal hilum.

produces prostaglandins and is believed to be involved in the regulation of intrarenal blood pressure.<sup>726</sup> The tumors are asymptomatic and invariably found incidentally as minute (usually 3 mm or less) white nodules in the midportion of the medullary pyramids.<sup>727</sup> Microscopically, they are composed of small, stellate, or polygonal cells in a loose stromal background, with entrapped tubules at the periphery.

The rare renal **leiomyoma** is usually located in the cortex or capsule but may also arise in association with hilar blood vessels.<sup>668,728</sup> True leiomyomas occur almost exclusively in women. They may represent an incidental histologic finding at surgery or, as with many tumors, an incidental radiographic finding.<sup>729</sup> In our opinion, many "leiomyomas" reported in the literature represent "lipid-poor" AMLs that closely resemble smooth muscle.<sup>668,730</sup> Immunophenotypically, strong and diffuse desmin expression and absence of cathepsin-K is most helpful since most AMLs show the opposite pattern.<sup>668</sup>

Although reported in the literature, the diagnosis of a renal **lipoma** should be met with great suspicion.<sup>731,732</sup> Before the diagnosis is made, alternative (and more likely) possibilities should be considered: lipid-rich AML or atypical lipomatous tumor of the retroperitoneum (some of which are centered in the perirenal region and which can look very "lipoma-like"). Pelvic/parapelvic lipomatosis could also be considered.

Primary **hemangioblastomas** have been reported in the kidney. These may be difficult to distinguish from clear cell RCC, given the significant overlap in immunophenotype.<sup>733,734</sup>

**Myxoma** presents as a gelatinous intraparenchymal tumor; its appearance is identical to that of myxoma of soft tissue.<sup>735</sup>

**Benign peripheral nerve tumors** of both *schwannoma*<sup>736-738</sup> and *perineurioma* type<sup>739</sup> have been described.

**Vascular tumors and tumorlike conditions** of various types rarely arise in the kidney.<sup>740</sup> **Arteriovenous malformations** are identical to their soft tissue counterparts.<sup>740</sup> **Hemangioma** is frequently located in the medullary portion, where it can give rise to copious hematuria.<sup>727</sup> Microscopically, most are of the capillary type, with a sieve-like pattern reminiscent of splenic pulp.<sup>740</sup> Many exhibit an anastomosing pattern mimicking angiosarcoma (Fig. 24.74).<sup>741</sup> They should be distinguished from RCCs with a prominent angiomyomatoid component. **Lymphangioma** can also involve the kidney,<sup>742,743</sup> but before this diagnosis is made, the more likely possibility of cystic nephroma/MEST should be considered and ruled out. The myopericytoma family of tumors, predominantly *glomus tumor* (some of them with atypical

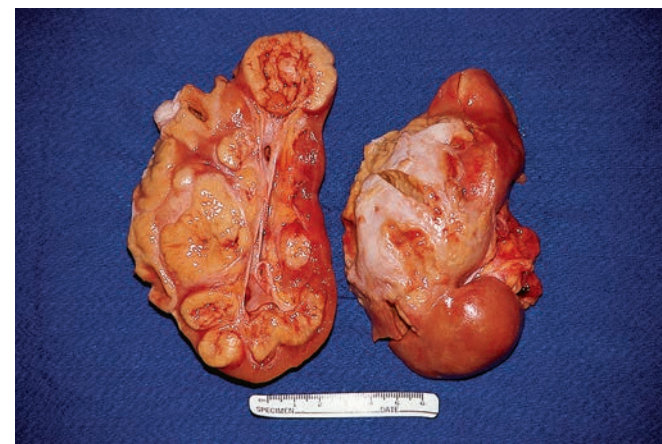


**Figure 24.75** Massive renal involvement by malakoplakia.

features)<sup>744</sup> and the closely related *glomangiomyoma*, can present as intrarenal masses, raising the differential diagnosis with juxtaglomerular cell tumor.<sup>745-747</sup>

**Solitary fibrous tumor (SFT)** has been seen involving the renal parenchyma or the renal capsule, sometimes in association with hypoglycemia.<sup>748-750</sup> Many of the cases historically reported as renal hemangiopericytoma are now considered SFT.<sup>751</sup> As in other sites, most SFTs are benign, with occasional examples behaving aggressively.<sup>752</sup>

**Inflammatory myofibroblastic tumor** may affect primarily the kidney; the behavior is generally indolent.<sup>753</sup>

**Hydatid cyst** can present as an intrarenal mass in countries where this parasitosis is endemic.

**Hematomas** can develop in the kidney or perirenal tissues as a result of trauma, from rupture of hemangiomas, and sometimes for no apparent cause. Some perirenal hematomas may contain peculiar periodic formations ("Liesegang structures") with radial striations that can simulate the appearance of parasites and that have been confused with such.<sup>754</sup>

**Rosai-Dorfman disease (sinus histiocytosis with massive lymphadenopathy)** and **malakoplakia** can result in renal masses (Fig. 24.75).<sup>755-759</sup>

## Sarcomas

**Sarcomas** of various types can arise in the adult kidney, including the renal capsule.<sup>760-762</sup> These include *leiomyosarcoma* (classic or myxoid),<sup>763-765</sup> *synovial sarcoma* (increasingly recognized at this site),<sup>766-769</sup> *fibrosarcoma* (exceptional), *pleomorphic rhabdomyosarcoma* (just as rare),<sup>770</sup> so-called *malignant fibrous histiocytoma* (*pleomorphic undifferentiated sarcoma, NOS*),<sup>771</sup> *liposarcoma* (but need to rule out renal extension of a retroperitoneal tumor),<sup>772</sup> *angiosarcoma*,<sup>740,773,774</sup> *osteosarcoma*,<sup>775-777</sup> *chondrosarcoma*,<sup>778</sup> *malignant mesenchymoma*,<sup>779,780</sup> and *clear cell sarcoma* (malignant melanoma of soft parts, not to be confused with the pediatric-type renal clear cell sarcoma).<sup>781</sup> Some of the chondrosarcomas have been of the mesenchymal variety.<sup>782</sup> Some of the smooth muscle tumors have occurred in immunosuppressed patients in association with Epstein-Barr virus infection.<sup>783</sup> The synovial sarcomas, before the possibility of their intrarenal occurrence was realized and documented by molecular studies, were probably included in the heterogeneous group of embryonal sarcomas of the kidney.<sup>766</sup> The reported cases have been of the monophasic type and some had rhabdoid features.<sup>784</sup> It is well to remember that the entrapment of cystically dilated tubules lined by hobnail epithelium can simulate a biphasic appearance (just as the entrapment of bronchoalveolar epithelium can result in a similar appearance in primary or metastatic monophasic synovial sarcoma in the lung).

An important warning is appropriate at this point: Before a diagnosis of primary sarcoma of the kidney of any type is made, the more common possibilities of sarcomatoid RCC (or urothelial carcinoma) and primary retroperitoneal soft tissue sarcoma (particularly de-differentiated liposarcoma) with secondary renal invasion should be considered.

## Malignant Lymphoma and Related Lymphoid Lesions

**Malignant lymphoma** of the kidney is usually the expression of generalized disease,<sup>785</sup> but sometimes the kidney is the only site of tumor.<sup>786-788</sup> Bilaterality is common in either situation. Renal failure may result from diffuse involvement of the organ.<sup>789,790</sup> The majority of the cases are of large B-cell type.<sup>791</sup> Other types have been described, including low-grade B-cell lymphoma of so-called MALT type (containing lymphoepithelial lesions within renal tubules).<sup>792,793</sup> Some such cases have been reported in the setting of AIDS<sup>794</sup> and others in organ transplant recipients,<sup>795</sup> sometimes with involvement of the renal allograft.<sup>796</sup>

Two varieties of lymphoma with a predilection for secondary renal involvement are thymic large B-cell lymphoma with sclerosis and lymphomatoid granulomatosis/angiotrophic large cell lymphoma.<sup>797</sup>

**Plasmacytomas** may be found within the kidney, usually as a result of dissemination in multiple myeloma but sometimes as an expression of extramedullary tumor.<sup>798</sup>

## Metastatic Tumors

Metastatic carcinoma can affect the kidney as a part of a disseminated process, but the renal involvement is only rarely of clinical significance.<sup>799,800</sup> The metastasis may appear years or decades after the removal of the primary tumor.<sup>801</sup> On CT scan, renal metastases tend to be small, multiple, bilateral, wedge shaped, intracortical, and less exophytic than primary RCC.<sup>802</sup> In contrast to the latter, metastatic tumors are bilateral in a high proportion (over 50%) of cases.<sup>803</sup> About one-third of the patients have microscopic hematuria.<sup>803</sup> Sometimes the metastases are exclusively limited to the renal glomeruli, in an intracapillary or extracapillary fashion, and may

be diagnosed by needle biopsy.<sup>804,805</sup> The most common primary sites are the lung, skin (malignant melanoma), breast, gastrointestinal tract, pancreas, ovary, and testis (nonseminomatous germ cell tumors, particularly choriocarcinoma).<sup>806</sup> Examples of odd types of metastatic tumors to the kidney simulating primary renal tumors include SETTLE, adenoid cystic carcinoma of breast,<sup>807</sup> and the follicular variant of papillary thyroid carcinoma.<sup>808</sup>

## Tumors of Renal Pelvis and Ureter

### Urothelial Carcinoma

Most urothelial carcinomas of the renal pelvis occur in adults (in whom they constitute about 7% of all primary renal carcinomas).<sup>809,810</sup> While a history of analgesic abuse and/or coexistence of renal papillary necrosis,<sup>811,812</sup> Thorotrast exposure for radiographic purposes,<sup>813</sup> or cyclophosphamide therapy<sup>814</sup> may be predisposing factors in a small subset of cases, smoking is likely the greatest risk factor. These tumors have also been reported in horseshoe kidneys; their incidence may actually be increased in this congenital abnormality.<sup>815</sup> Some cases have developed as a manifestation of the hereditary nonpolyposis colorectal cancer syndrome, and these rare cases may show abnormal expression of mismatch repair proteins by immunohistochemistry.<sup>816,817</sup> Hematuria is the most common clinical presentation.<sup>818,819</sup> Synchronous or metachronous tumors elsewhere in the urinary tract (most of them in the bladder) are found in over half of the patients<sup>811,820</sup>; exceptionally, an independent RCC may be found in the same kidney.<sup>821-823</sup> Intravenous and retrograde pyelography provides the most accurate means of diagnosis.<sup>818</sup> The sensitivity and accuracy of cytologic examination are higher than for RCC, particularly for the high-grade tumors.<sup>824</sup>

Grossly, these tumors form soft, gray-to-red masses with smooth, glistening surfaces that resemble the urothelial tumors of the bladder (Fig. 24.76).<sup>812</sup> They often diffusely involve the entire renal pelvis and form arborescent masses that may extend down the ureter. Occasionally, they are circumscribed to a calyx or even to the inside of a calyceal cyst.<sup>825</sup> High-grade lesions can spread massively into the renal parenchyma and even reach the renal capsule. They can be distinguished grossly from RCC because of their granular appearance and extensive pelvic involvement.

Urothelial carcinomas of the ureter may be located anywhere along the length of the organ and usually result in dilation of the proximal portion due to lumen obstruction by the tumor.<sup>826,827</sup>

The microscopic appearance of these urothelial carcinomas, whether located in the renal pelvis or ureter, is identical to that of their more common homologues in the bladder. The majority are high-grade neoplasms, the percentage (about 70%) being much higher than for the same tumor type in the bladder.<sup>828</sup> The pelvic neoplasms sometimes extend proximally along the collecting tubules, a pattern that should not be confused with adenocarcinoma.<sup>829</sup> The adjacent urothelium may show urothelial carcinoma in situ.<sup>830</sup> It should be pointed out that upper tract biopsies are fraught with artifacts that can mimic urothelial neoplasia.<sup>831,832</sup> The similarities with urothelial carcinomas of the bladder also apply to the occurrence of variants such as the *micropapillary type*<sup>833,834</sup> and others,<sup>835</sup> as well as their immunohistochemical profile, including coexpression of keratins 7 and 20<sup>836</sup> and overexpression of p53 protein (particularly in the high-grade tumors).<sup>837</sup> In our experience, up to 25% of upper tract urothelial carcinomas may express nuclear PAX-8.<sup>838,839</sup>

The standard treatment of pyeloureteral urothelial carcinoma is nephroureterectomy. Segmental resection has sometimes been employed for midureteral lesions,<sup>825</sup> and endoscopic removal has been done for low-grade noninvasive lesions, but the high incidence of multicentricity and coexistent carcinoma in situ (particularly with



**Figure 24.76** Gross Appearances of Urothelial Carcinoma of Renal Pelvis. **A** and **B**, The tumor protrudes into the pelvic cavity and has a granular surface. **C**, The tumor coats the pelvis and calyces.

the high-grade tumors) indicates that radical surgery is the treatment of choice for the large majority of cases.<sup>840,841</sup> Furthermore, these tumors have a tendency to implant along the ureter, especially in its terminal (intramural) portion. Therefore a resection of the bladder cuff may be performed to avoid tumor recurrence.<sup>842,843</sup> The overall 5-year survival rate in the surgically resected cases is about 50%.<sup>809,811</sup> The prognosis is largely determined by the stage of the lesion for both the pelvic and ureteral lesions.<sup>844-848</sup> Unfortunately, most of the patients present with locally advanced (pT2 or more) disease at the time of surgery.<sup>828,835</sup>

### Other Carcinoma Types

*Primary squamous cell carcinoma*<sup>813,819,849,850</sup> and *primary adenocarcinoma*<sup>851-854</sup> rarely occur in the upper urinary tract. Essentially all rare subtypes and urothelial carcinoma variants described in the urinary bladder may also be identified in the pelvicalyceal and ureteral system, including hepatoid carcinoma,<sup>855</sup> lymphoepithelioma-like carcinoma,<sup>856</sup> sarcomatoid urothelial carcinoma,<sup>835,857-859</sup> giant cell carcinoma,<sup>860-862</sup> small cell neuroendocrine carcinoma,<sup>618,863</sup> carcinoma with trophoblastic features,<sup>864-867</sup> and carcinoma with rhabdoid features.<sup>868</sup> *Verrucous carcinoma* has been reported in the pelvis of a horseshoe kidney associated with staghorn calculi.<sup>869</sup> Clinicopathologic features are identical to those described in the urinary bladder.

### Other Tumors and Tumorlike Conditions

**Fibroepithelial polyp**<sup>870,871</sup> (Fig. 24.77) and **hypertrophic infundibular stenosis of the calyces**<sup>872</sup> are two rare tumorlike masses of the pelvic region.

**Pelvic lipomatosis** and **fibrolipomatosis** result from excessive proliferation of peripelvic fat with or without accompanying fibrous tissue and may simulate a neoplasm radiographically.<sup>873</sup>

**Amyloidosis** can present as a localized nodule in the wall of one or both ureters (so-called amyloid tumor).<sup>874</sup>

**Myelolipoma** morphologically similar to its more common adrenal counterpart can present as a mass in the renal sinus.<sup>875</sup>

**Malakoplakia** of the pelvis or ureter may result in obstruction and hydronephrosis.<sup>876,877</sup>



**Figure 24.77** Benign fibroepithelial polyp emerging from lower calyx of the left kidney in a 61-year-old woman. The tumor caused hematuria, and total nephrectomy was performed.

**Stone granuloma** is a complication of ureteroscopy and ureteral stone fragmentation; it is characterized by the presence of embedded particles of calcium oxalate associated with macrophages and foreign body giant cells, with surrounding fibrosis and dilation of the proximal ureter.<sup>878</sup>

**Endometriosis** of the ureter presents with hydroureter, often accompanied by hydronephrosis. The disease may be extrinsic to the ureter or present within its wall. As in other sites, endometriosis may rarely be associated with secondary Müllerian neoplasms.

Most patients have a past history of hysterectomy with salpingo-oophorectomy.<sup>879</sup>

**Subepithelial hematoma of the renal pelvis (Antopol-Goldman lesion)** can present with gross hematuria and radiographically simulate a malignant tumor. The etiology is unknown.<sup>880,881</sup>

“Urinoma” results from the extravasation of urine into the renal perihilar and peripelvic fat; in the early stages there is lipolysis with foamy macrophages and multinucleated giant cells, followed by fibrosis and deposition of “urinary precipitates.” Demonstration of Tamm-Horsfall protein by immunostaining confirms the fact that the amorphous extracellular precipitates are derived from uroprotein.<sup>882</sup>

**Benign pyloureteral tumors** include *inverted papilloma* (sometimes multiple),<sup>883,884</sup> *nephrogenic adenoma*,<sup>885-888</sup> *villous adenoma*,<sup>889</sup> *hemangioma*,<sup>890</sup> *leiomyoma*,<sup>891</sup> *SFT*,<sup>892</sup> *neurofibroma*,<sup>893</sup> *granular cell*

*tumor*,<sup>893</sup> and *glomus tumor*.<sup>894</sup> The hemangiomas are often located at the tips of the papillae, are multiple in about 10% of the cases, and may result in recurrent episodes of hemorrhage.<sup>895,896</sup> Owing to their small size, extensive sectioning may be needed to find the lesion. The nephrogenic adenoma may show gastric metaplasia.<sup>897</sup>

**Malignant tumors** of nonepithelial type are exceptional. A few cases of *leiomyosarcoma* have been reported.<sup>898</sup> Non-Hodgkin *malignant lymphoma* of the retroperitoneum can involve the ureter secondarily.<sup>899</sup> A case of primary malignant lymphoma has been reported in the pelvis of a transplanted kidney.<sup>900</sup> A few cases of benign and malignant tumors have been reported in ureteroileal conduits.<sup>901,902</sup>

**Metastatic carcinomas** to the retroperitoneum can invade the ureteral wall and result in obstruction; the breast and lung are the most common sites for the primary tumors.<sup>903,904</sup>

## References

1. Sebire NJ, Vujanic GM. Paediatric renal tumours: recent developments, new entities and pathological features. *Histopathology*. 2009;54(5):516-528.
2. Argani P, Bruder E, Dehner L, Vujanic GM. Nephroblastic and cystic tumours occurring mainly in children. In: Moch H, Humphrey PA, Ulbright TM, Reuter VE, eds. *WHO Classification of Tumours of the Urinary System and Male Genital Organs*. Lyon: IARC Press; 2016.
3. Chevalier G, Yeger H, Martinerie C, et al. novH: differential expression in developing kidney and Wilms' tumors. *Am J Pathol*. 1998;152(6):1563-1575.
4. Li CM, Guo M, Borczuk A, et al. Gene expression in Wilms' tumor mimics the earliest committed stage in the metanephric mesenchymal-epithelial transition. *Am J Pathol*. 2002;160(6):2181-2190.
5. Yashima K, Maitra A, Timmons CF, et al. Expression of the RNA component of telomerase in Wilms tumor and nephrogenic rest recapitulates renal embryogenesis. *Hum Pathol*. 1998;29(5):536-542.
6. Crist WM, Kun LE. Common solid tumors of childhood. *N Engl J Med*. 1991;324(7):461-471.
7. Juberg RC, St Martin EC, Hundley JR. Familial occurrence of Wilms' tumor: nephroblastoma in one of monozygous twins and in another sibling. *Am J Hum Genet*. 1975;27(2):155-164.
8. Webber BL, Parham DM, Drake LG, Wilimans JA. Renal tumors in childhood. *Pathol Ann*. 1992;27(Pt 1):191-232.
9. Hrabovsky EE, Othersen HB Jr, deLorimier A, et al. Wilms' tumor in the neonate: a report from the National Wilms' Tumor Study. *J Pediatr Surg*. 1986;21(5):385-387.
10. Merten DF, Yang SS, Bernstein J. Wilms' tumor in adolescence. *Cancer*. 1976;37(3):1532-1538.
11. Husej J, Grignon DJ, Ro JY, et al. Adult Wilms' tumor: a clinicopathologic study of 11 cases. *Mod Pathol*. 1990;3(3):321-326.
12. Terenziani M, Spreafico F, Collini P, et al. Adult Wilms' tumor: a monoinstitutional experience and a review of the literature. *Cancer*. 2004;101(2):289-293.
13. Williams G, Colbeck RA, Gowing NF. Adult Wilms' tumour: review of 14 patients. *Br J Urol*. 1992;70(3):230-235.
14. Rubin BP, Pins MR, Nielsen GP, et al. Isochromosome 7q in adult Wilms' tumors: diagnostic and pathogenetic implications. *Am J Surg Pathol*. 2000;24(12):1663-1669.
15. Chen I, Pasalic D, Fischer-Valuck B, et al. Disparity in outcomes for adolescent and young adult patients diagnosed with pediatric
- solid tumors across 4 decades. *Am J Clin Oncol*. 2016.
16. Paulino AC, Thakkar B, Henderson WG. Metachronous bilateral Wilms' tumor: the importance of time interval to the development of a second tumor. *Cancer*. 1998;82(2):415-420.
17. Shearer P, Parham DM, Fontanesi J, et al. Bilateral Wilms tumor. Review of outcome, associated abnormalities, and late effects in 36 pediatric patients treated at a single institution. *Cancer*. 1993;72(4):1422-1426.
18. Benatar B, Wright C, Freinkel AL, Cooper K. Primary extrarenal Wilms' tumor of the uterus presenting as a cervical polyp. *Int J Gynecol Pathol*. 1998;17(3):277-280.
19. Ho J, Ma L, Wong KC. An extrarenal Wilms' tumour arising from an undescended testis. *Pathology*. 1981;13(3):619-624.
20. Luchtrath H, de Leon F, Giesen H, Gok Y. Inguinal nephroblastoma. *Virchows Arch A Pathol Anat Histopathol*. 1984;405(1):113-118.
21. Mount SL, Dickerman JD, Taatjes DJ. Extrarenal Wilms' tumor: an ultrastructural and immunoelectron microscopic case report. *Ultrastruct Pathol*. 1996;20(2):155-165.
22. Roberts DJ, Haber D, Sklar J, Crum CP. Extrarenal Wilms' tumors. A study of their relationship with classical renal Wilms' tumor using expression of WT1 as a molecular marker. *Lab Invest*. 1993;68(5):528-536.
23. Wakely PE Jr, Sprague RL, Kornstein MJ. Extrarenal Wilms' tumor: an analysis of four cases. *Hum Pathol*. 1989;20(7):691-695.
24. Ward SP, Dehner LP. Sacrococcygeal teratoma with nephroblastoma (Wilms' tumor): a variant of extragonadal teratoma in childhood. A histologic and ultrastructural study. *Cancer*. 1974;33(5):1355-1363.
25. Clericuzio CL. Clinical phenotypes and Wilms tumor. *Med Pediatr Oncol*. 1993;21(3):182-187.
26. Manivel JC, Sibley RK, Dehner LP. Complete and incomplete Drash syndrome: a clinicopathologic study of five cases of a dysontogenetic-neoplastic complex. *Hum Pathol*. 1987;18(1):80-89.
27. Miller RW, Fraumeni JF Jr, Manning MD. Association of Wilms' tumor with aniridia, hemihypertrophy and other congenital malformations. *N Engl J Med*. 1964;270:922-927.
28. Sotelo-Avila C, Gooch WM 3rd. Neoplasms associated with the Beckwith-Wiedemann syndrome. *Perspect Pediatr Pathol*. 1976;3:255-272.
29. Auber F, Jeanpierre C, Denamur E, et al. Management of Wilms tumors in Drash and Frasier syndromes. *Pediatr Blood Cancer*. 2009;52:55-59.
30. Bolande RP. Neoplasia of early life and its relationships to teratogenesis. *Perspect Pediatr Pathol*. 1976;3:145-183.
31. Olshan AF, Breslow NE, Falletta JM, et al. Risk factors for Wilms tumor. Report from the National Wilms Tumor Study. *Cancer*. 1993;72(3):938-944.
32. Rajfer J. Association between Wilms tumor and gonadal dysgenesis. *J Urol*. 1981;125(3):388-390.
33. Bissig H, Staehelin E, Tolnay M, et al. Co-occurrence of neuroblastoma and nephroblastoma in an infant with Fanconi's anemia. *Hum Pathol*. 2002;33(10):1047-1051.
34. Breslow NE, Takashima JR, Whitton JA, et al. Second malignant neoplasms following treatment for Wilms' tumor: a report from the National Wilms' Tumor Study Group. *J Clin Oncol*. 1995;13(8):1851-1859.
35. Kovalic JJ, Thomas PR, Beckwith JB, et al. Hepatocellular carcinoma as second malignant neoplasm in successfully treated Wilms' tumor patients. A National Wilms' Tumor Study report. *Cancer*. 1991;67(2):342-344.
36. Nakamura Y, Nakashima T, Nakashima H, Hashimoto T. Bilateral cystic nephroblastomas and botryoid sarcoma involving vagina and urinary bladder in a child with microcephaly, arhinencephaly, and bilateral cataracts. *Cancer*. 1981;48(4):1012-1015.
37. Stern M, Longaker MT, Adzick NS, et al. Hyaluronidase levels in urine from Wilms' tumor patients. *J Natl Cancer Inst*. 1991;83(21):1569-1574.
38. Thorner P, McGraw M, Weitzman S, et al. Wilms' tumor and glomerular disease. Occurrence with features of membranoproliferative glomerulonephritis and secondary focal, segmental glomerulosclerosis. *Arch Pathol Lab Med*. 1984;108(2):141-146.
39. Zakowski MF, Edwards RH, McDonough ET. Wilms' tumor presenting as sudden death due to tumor embolism. *Arch Pathol Lab Med*. 1990;114(6):605-608.
40. Lowe LH, Isuani BH, Heller RM, et al. Pediatric renal masses: Wilms tumor and beyond. *Radiographics*. 2000;20:1585-1603.
41. Beckwith JB. Wilms' tumor and other renal tumors of childhood: a selective review from the National Wilms' Tumor Study Pathology Center. *Hum Pathol*. 1983;14(6):481-492.
42. Charles AK, Vujanic GM, Berry PJ. Renal tumours of childhood. *Histopathology*. 1998;32(4):293-309.

43. Marsden HB. The pathology and natural history of childhood tumours. *Recent Results Cancer Res.* 1983;88:11-25.
44. Garvin AJ, Surrette E, Hintz DS, et al. The in vitro growth and characterization of the skeletal muscle component of Wilms' tumor. *Am J Pathol.* 1985;121(2):298-310.
45. Balsaver AM, Gibley CW Jr, Tessmer CF. Ultrastructural studies in Wilms' tumor. *Cancer.* 1968;22(2):417-427.
46. Chatten J. Epithelial differentiation in Wilms' tumor: a clinicopathologic appraisal. *Perspect Pediatr Pathol.* 1976;3:225-254.
47. Mierau GW, Beckwith JB, Weeks DA. Ultrastructure and histogenesis of the renal tumors of childhood: an overview. *Ultrastruct Pathol.* 1987;11(2-3):313-333.
48. Yeger H, Baumal R, Harason P, Phillips MJ. Lectin histochemistry of Wilms' tumor. Comparison with normal adult and fetal kidney. *Am J Clin Pathol.* 1987;88(3):278-285.
49. Hennigar RA, Spicer SA, Sens DA, et al. Histochemical evidence for tubule segmentation in a case of Wilms' tumor. *Am J Clin Pathol.* 1986;85(6):724-731.
50. Kodet R, Marsden HB. Papillary Wilms' tumour with carcinoma-like foci and renal cell carcinoma in childhood. *Histopathology.* 1985;9(10):1091-1102.
51. Edwards O, Chatten J. Hydropic cell variant (clear cell variant) of Wilms' tumor. *Arch Pathol Lab Med.* 1985;109(10):956-958.
52. Hou LT, Azzopardi JG. Muco-epidermoid metaplasia and argytaffin cells in nephroblastoma. *J Pathol Bacteriol.* 1967;93(2):477-481.
53. Delemane JF, Sandstedt B, Tournade MF. Nephroblastoma with fibroadenomatous-like structures. *Histopathology.* 1984;8(1):55-62.
54. Joshi VV, Beckwith JB. Pathologic delineation of the papillonodular type of cystic partially differentiated nephroblastoma. A review of 11 cases. *Cancer.* 1990;66(7):1568-1577.
55. Lindop GB, Fleming S, Gibson AA. Immunocytochemical localisation of renin in nephroblastoma. *J Clin Pathol.* 1984;37(7):738-742.
56. Grimes MM, Wolff M, Wolff JA, et al. Ganglion cells in metastatic Wilms' tumor. Review of a histogenetic controversy. *Am J Surg Pathol.* 1982;6(6):565-571.
57. Masson P. The role of the neural crest in the embryonal adenosarcomas of the kidney. *Am J Cancer.* 1938;33:1-32.
58. Jenkins MC, Allibone EB, Berry PJ. Neuroglial tissue in partially cystic Wilms' tumour. *Histopathology.* 1991;18(4):309-313.
59. Magee JE, Ansari S, McFadden DE, Dimmick J. Teratoid Wilms' tumour: a report of two cases. *Histopathology.* 1992;20(5):427-431.
60. Variend S, Spicer RD, Mackinnon AE. Teratoid Wilms' tumor. *Cancer.* 1984;53(9):1936-1942.
61. Droz D, Rousseau-Merck MF, Jaubert F, et al. Cell differentiation in Wilms' tumor (nephroblastoma): an immunohistochemical study. *Hum Pathol.* 1990;21(5):536-544.
62. Hennigar RA, Garvin AJ, Hazen-Martin DJ, Schulte BA. Immunohistochemical localization of transport mediators in Wilms' tumor: comparison with fetal and mature human kidney. *Lab Invest.* 1989;61(2):192-201.
63. Vasei M, Moch H, Mousavi A, et al. Immunohistochemical profiling of Wilms tumor: a tissue microarray study. *Appl Immunohistochem Mol Morphol.* 2008;16(2):128-134.
64. Magee F, Mah RG, Taylor GP, Dimmick JE. Neural differentiation in Wilms' tumor. *Hum Pathol.* 1987;18(1):33-37.
65. Folpe AL, Patterson K, Cown AM. Antibodies to desmin identify the blastemal component of nephroblastoma. *Mod Pathol.* 1997;10(9):895-900.
66. Bisceglia M, Ragazzi M, Galliani CA, et al. TTF-1 expression in nephroblastoma. *Am J Surg Pathol.* 2009;33(3):454-461.
67. Arva NC, Bonadio J, Perlman EJ, Cajaiba MM. Diagnostic utility of Pax8, Pax2, and NGFR immunohistochemical expression in pediatric renal tumors. *Appl Immunohistochem Mol Morphol.* 2017.
68. Coppes MJ, Haber DA, Grundy PE. Genetic events in the development of Wilms' tumor. *N Engl J Med.* 1994;331(9):586-590.
69. Telerman A, Dodemont H, Degraef C, et al. Identification of the cellular protein encoded by the human Wilms' tumor (WT1) gene. *Oncogene.* 1992;7(12):2545-2548.
70. van Heyningen V, Bickmore WA, Seawright A, et al. Role for the Wilms tumor gene in genital development? *Proc Natl Acad Sci USA.* 1990;87(14):5383-5386.
71. Dowdy SF, Fasching CL, Araujo D, et al. Suppression of tumorigenicity in Wilms tumor by the p15.5-p14 region of chromosome 11. *Science.* 1991;254(5029):293-295.
72. Malik K, Yan P, Huang TH, Brown KW. Wilms' tumor: a paradigm for the new genetics. *Oncol Res.* 2001;12(11-12):441-449.
73. Slater RM, de Kraker J. Chromosome number 11 and Wilms' tumor. *Cancer Genet Cytogenet.* 1982;5(3):237-245.
74. Slater RM, Mannens MM. Cytogenetics and molecular genetics of Wilms' tumor of childhood. *Cancer Genet Cytogenet.* 1992;61(2):111-121.
75. Gerald WL, Gramling TS, Sens DA, Garvin AJ. Expression of the 11p13 Wilms' tumor gene, WT1, correlates with histologic category of Wilms' tumor. *Am J Pathol.* 1992;140(5):1031-1037.
76. Kikuchi H, Akasaka Y, Nagai T, et al. Genomic changes in the WT1 gene (WT1) in Wilms' tumors and their correlation with histology. *Am J Pathol.* 1992;140(4):781-786.
77. Re GG, Hazen-Martin DJ, Sens DA, Garvin AJ. Nephroblastoma (Wilms' tumor): a model system of aberrant renal development. *Semin Diagn Pathol.* 1994;11(2):126-135.
78. Yeger H, Cullinane C, Flenniken A, et al. Coordinate expression of Wilms' tumor genes correlates with Wilms' tumor phenotypes. *Cell Growth Differ.* 1992;3(12):855-864.
79. Fukuzawa R, Holman SK, Chow CW, et al. WTX mutations can occur both early and late in the pathogenesis of Wilms' tumour. *J Med Genet.* 2010;47:791-794.
80. Perotti D, Cambi B, Sardella M, et al. Functional inactivation of the WTX gene is not a frequent event in Wilms' tumors. *Oncogene.* 2008;27:4625-4632.
81. Rivera MN, Kim WJ, Wells J, et al. An X chromosome gene, WTX, is commonly inactivated in Wilms tumor. *Science.* 2007;315(5812):642-645.
82. Ruteshouser EC, Robinson SM, Huff V. Wilms tumor genetics: mutations in WT1, WTX, and CTNNB1 account for only about one-third of tumors. *Genes Chromosomes Cancer.* 2008;47(6):461-470.
83. Wegerl J, Wittmann S, Leuschner I, et al. WTX inactivation is a frequent, but late event in Wilms tumors without apparent clinical impact. *Genes Chromosomes Cancer.* 2009;48(12):1102-1111.
84. Kusafuka T, Miao J, Kuroda S, et al. Codon 45 of the beta-catenin gene, a specific mutational target site of Wilms' tumor. *Int J Mol Med.* 2002;10(4):395-399.
85. Maiti S, Alam R, Amos CI, Huff V. Frequent association of beta-catenin and WT1 mutations in Wilms tumors. *Cancer Res.* 2000;60(22):6288-6292.
86. Royer-Pokora B, Weirich A, Schumacher V, et al. Clinical relevance of mutations in the Wilms tumor suppressor 1 gene WT1 and the cadherin-associated protein beta1 gene CTNNB1 for patients with Wilms tumors: results of long-term surveillance of 71 patients from International Society of Pediatric Oncology Study 9/Society for Pediatric Oncology. *Cancer.* 2008;113(5):1080-1089.
87. Govender D. The genetics of Wilms tumor. *Adv Anat Pathol.* 1997;4:202-206.
88. Sheng WW, Soukup S, Bove K, et al. Chromosome analysis of 31 Wilms' tumors. *Cancer Res.* 1990;50(9):2786-2793.
89. Zhuang Z, Merino MJ, Vortmeyer AO, et al. Identical genetic changes in different histologic components of Wilms' tumors. *J Natl Cancer Inst.* 1997;89(15):1148-1152.
90. el Bahtimi R, Hazen-Martin DJ, Re GG, et al. Immunophenotype, mRNA expression, and gene structure of p53 in Wilms' tumors. *Mod Pathol.* 1996;9(3):238-244.
91. Takeuchi S, Bartram CR, Ludwig R, et al. Mutations of p53 in Wilms' tumors. *Mod Pathol.* 1995;8(5):483-487.
92. Wegerl J, Ishaque N, Vardapour R, et al. Mutations in the SIX1/2 pathway and the DROSHA/DGCR8 miRNA microprocessor complex underlie high-risk blastemal type Wilms tumors. *Cancer Cell.* 2015;9:298-311.
93. Ebb DH, Kerasidis H, Vezina G, et al. Spinal cord compression in widely metastatic Wilms' tumor. Paraplegia in two children with anaplastic Wilms' tumor. *Cancer.* 1992;69(11):2726-2730.
94. Lowis SP, Foot A, Gerrard MP, et al. Central nervous system metastasis in Wilms' tumor: a review of three consecutive United Kingdom trials. *Cancer.* 1998;83(9):2023-2029.
95. D'Angio GJ, Breslow N, Beckwith JB, et al. Treatment of Wilms' tumor. Results of the Third National Wilms' Tumor Study. *Cancer.* 1989;64(2):349-360.
96. D'Angio GJ, Evans A, Breslow N, et al. The treatment of Wilms' tumor: results of the Second National Wilms' Tumor Study. *Cancer.* 1981;47(9):2302-2311.
97. Green DM, Beckwith JB, Breslow NE, et al. Treatment of children with stages II to IV anaplastic Wilms' tumor: a report from the National Wilms' Tumor Study Group. *J Clin Oncol.* 1994;12(10):2126-2131.
98. Tournade MF, Com-Nougues C, Voute PA, et al. Results of the Sixth International Society of Pediatric Oncology Wilms' Tumor Trial and Study: a risk-adapted therapeutic approach in Wilms' tumor. *J Clin Oncol.* 1993;11(6):1014-1023.
99. Perlman EJ. Pediatric renal tumors: practical updates for the pathologist. *Pediatr Dev Pathol.* 2005;8(3):320-338.
100. Vujanic GM, Sandstedt B, Harms D, et al. Revised International Society of Paediatric Oncology (SIOP) working classification of renal tumors of childhood. *Med Pediatr Oncol.* 2002;38:79-82.
101. Vujanic GM, Sandstedt B. The pathology of Wilms' tumour (nephroblastoma): the International Society of Paediatric Oncology approach. *J Clin Pathol.* 2010;63:102-109.
102. D'Angio GJ. Oncology seen through the prism of Wilms tumor. *Med Pediatr Oncol.* 1985;13(2):53-58.
103. Antman KH, Ruxer RL Jr, Aisner J, Vawter G. Mesothelioma following Wilms' tumor in childhood. *Cancer.* 1984;54(2):367-369.
104. Arrigo S, Beckwith JB, Sharples K, et al. Better survival after combined modality care for adults with Wilms' tumor. A report from the National Wilms' Tumor Study. *Cancer.* 1990;66(5):827-830.
105. Breslow NE, Palmer NF, Hill LR, et al. Wilms' tumor: prognostic factors for patients without metastases at diagnosis: results of the National Wilms' Tumor Study. *Cancer.* 1978;41(4):1577-1589.

106. Jereb B, Tournade MF, Lemerle J, et al. Lymph node invasion and prognosis in nephroblastoma. *Cancer*. 1980;45(7):1632-1636.
107. Weeks DA, Beckwith JB, Luckey DW. Relapse-associated variables in stage I favorable histology Wilms' tumor. A report of the National Wilms' Tumor Study. *Cancer*. 1987;60(6):1204-1212.
108. Breslow N, Sharples K, Beckwith JB, et al. Prognostic factors in nonmetastatic, favorable histology Wilms' tumor. Results of the Third National Wilms' Tumor Study. *Cancer*. 1991;68(11):2345-2353.
109. Buchino JJ. Wilms' tumor—the continuing search for the true meaning of anaplasia. *Adv Anat Pathol*. 1997;4:239-243.
110. Bonadio JF, Storey B, Norkool P, et al. Anaplastic Wilms' tumor: clinical and pathologic studies. *J Clin Oncol*. 1985;3(4):513-520.
111. Faria P, Beckwith JB, Mishra K, et al. Focal versus diffuse anaplasia in Wilms tumor—new definitions with prognostic significance: a report from the National Wilms Tumor Study Group. *Am J Surg Pathol*. 1996;20(8):909-920.
112. Zuppan CW. Handling and evaluation of pediatric renal tumors. *Am J Clin Pathol*. 1998;109(4 suppl 1):S31-S37.
113. Zuppan CW, Beckwith JB, Luckey DW. Anaplasia in unilateral Wilms' tumor: a report from the National Wilms' Tumor Study Pathology Center. *Hum Pathol*. 1988;19(10):1199-1209.
114. Kheir S, Pritchett PS, Moreno H, Robinson CA. Histologic grading of Wilms' tumor as potential prognostic factor: results of a retrospective study of 26 patients. *Cancer*. 1978;41(3):1199-1207.
115. Lawler W, Marsden HB, Palmer MK. Wilms' tumor—histologic variation and prognosis. *Cancer*. 1975;36(3):1122-1126.
116. Verschueren AC, Vujanic GM, Van Tinteren H, et al. Stromal and epithelial predominant Wilms tumours have an excellent outcome: the SIOP 93 01 experience. *Pediatr Blood Cancer*. 2010;55:233-238.
117. Gonzalez-Crussi F, Hsueh W, Ugarte N. Rhabdomyogenesis in renal neoplasia of childhood. *Am J Surg Pathol*. 1981;5(6):525-532.
118. Wigger HJ. Fetal rhabdomyomatous nephroblastoma—a variant of Wilms' tumor. *Hum Pathol*. 1976;7(6):613-623.
119. Zuppan CW, Beckwith JB, Weeks DA, et al. The effect of preoperative therapy on the histologic features of Wilms' tumor. An analysis of cases from the Third National Wilms' Tumor Study. *Cancer*. 1991;68(2):385-394.
120. Cheah PL, Looi LM, Chan LL. Immunohistochemical expression of p53 proteins in Wilms' tumour: a possible association with the histological prognostic parameter of anaplasia. *Histopathology*. 1996;28(1):49-54.
121. Lahoti C, Thorner P, Malkin D, Yeger H. Immunohistochemical detection of p53 in Wilms' tumors correlates with unfavorable outcome. *Am J Pathol*. 1996;148(5):1577-1589.
122. Grundy PE, Breslow NE, Li S, et al. Loss of heterozygosity for chromosomes 1p and 16q is an adverse prognostic factor in favorable-histology Wilms tumor: a report from the National Wilms Tumor Study Group. *J Clin Oncol*. 2005;23(29):7312-7321.
123. Grundy PE, Telzrow PE, Breslow N, et al. Loss of heterozygosity for chromosomes 16q and 1p in Wilms' tumors predicts an adverse outcome. *Cancer Res*. 1994;54(9):2331-2333.
124. Messahel B, Williams R, Ridolfi A, et al. Allele loss at 16q defines poorer prognosis Wilms tumour irrespective of treatment approach in the UKW1-3 clinical trials: a Children's Cancer and Leukaemia Group (CCLG) Study. *Eur J Cancer*. 2009;45(5):819-826.
125. Chagtai T, Zill C, Dainese L, et al. Gain of 1q As a prognostic biomarker in Wilms tumors (WTs) treated with preoperative chemotherapy in the International Society of Paediatric Oncology (SIOP) WT 2001 trial: a SIOP renal tumours biology consortium study. *J Clin Oncol*. 2016;34(10):3195-3203.
126. Joshi VV, Beckwith JB. Multilocular cyst of the kidney (cystic nephroma) and cystic, partially differentiated nephroblastoma. Terminology and criteria for diagnosis. *Cancer*. 1989;64:466-479.
127. Bove KE, McAdams AJ. The nephroblastomatosis complex and its relationship to Wilms' tumor: a clinicopathologic treatise. *Perspect Pediatr Pathol*. 1976;3:185-223.
128. Heideman RL, Haase GM, Foley CL, et al. Nephroblastomatosis and Wilms' tumor. Clinical experience and management of seven patients. *Cancer*. 1985;55(7):1446-1451.
129. Stambolic C. Benign epithelial nephroblastoma. A contribution to its histogenesis. *Virchows Arch A Pathol Anat Histopathol*. 1977;376(3):267-272.
130. Perlman M, Levin M, Wittels B. Syndrome of fetal gigantism, renal hamartomas, and nephroblastomatosis with Wilms' tumor. *Cancer*. 1975;35(4):1212-1217.
131. Beckwith JB. Precursor lesions of Wilms tumor: clinical and biological implications. *Med Pediatr Oncol*. 1993;21(3):158-168.
132. Beckwith JB, Kiviat NB, Bonadio JF. Nephrogenic rests, nephroblastomatosis, and the pathogenesis of Wilms' tumor. *Pediatr Pathol*. 1990;10(1-2):1-36.
133. Machin GA, McCaughey WT. A new precursor lesion of Wilms' tumour (nephroblastoma): intralobular multifocal nephroblastomatosis. *Histopathology*. 1984;8(1):35-53.
134. White KS, Kirks DR, Bove KE. Imaging of nephroblastomatosis: an overview. *Radiology*. 1992;182(1):1-5.
135. Benjamin DR, Beckwith JB. Medullary ray nodules in infancy and childhood. *Arch Pathol*. 1973;96:33-35.
136. Hughson MD, McManus JF, Hennigar GR. Studies on "end-stage" kidneys. II. Embryonal hyperplasia of Bowman's capsular epithelium. *Am J Pathol*. 1978;91:71-84.
137. Park S, Bernard A, Bove KE, et al. Inactivation of WT1 in nephrogenic rests, genetic precursors to Wilms' tumour. *Nat Genet*. 1993;5(4):363-367.
138. Vuonovirta R, Sebire NJ, Dallosso AR, et al. Perilobular nephrogenic rests are nonobligate molecular genetic precursor lesions of insulin-like growth factor-II-associated Wilms tumors. *Clin Cancer Res*. 2008;14:7635-7644.
139. Fukuzawa R, Anaka MR, Heathcott RW, et al. Wilms' tumour histology is determined by distinct types of precursor lesions and not epigenetic changes. *J Pathol*. 2008;215:377-387.
140. de Chadarevian JP, Fletcher BD, Chatten J, Rabinovitch HH. Massive infantile nephroblastomatosis: a clinical, radiological, and pathological analysis of four cases. *Cancer*. 1977;39(5):2294-2305.
141. Coppes MJ, Arnold M, Beckwith JB, et al. Factors affecting the risk of contralateral Wilms' tumor development: a report from the National Wilms Tumor Study Group. *Cancer*. 1999;85:1616-1625.
142. Argani P, Dehner L, Leuschner I. Mesenchymal tumours occurring mainly in children. In: Moch H, Humphrey PA, Ulbright TM, Reuter VE, eds. *WHO Classification of Tumours of the Urinary System and Male Genital Organs*. Lyon: IARC Press; 2016.
143. Truong LD, Williams R, Ngo T, et al. Adult mesoblastic nephroma: expansion of the morphologic spectrum and review of literature. *Am J Surg Pathol*. 1998;22(7):827-839.
144. Tulbah A, Kardar AH, Akhtar M. Mesoblastic nephroma in an adult. *J Urol Pathol*. 1997;6:67-74.
145. Drut R. Multicystic congenital mesoblastic nephroma. *Int J Surg Pathol*. 2002;10(1):59-63.
146. Ganick DJ, Gilbert EF, Beckwith JB, Kiviat N. Congenital cystic mesoblastic nephroma. *Hum Pathol*. 1981;12(11):1039-1043.
147. Shen SC, Yunis EJ. A study of the cellular and ultrastructure of congenital mesoblastic nephroma. *Cancer*. 1980;45(2):306-314.
148. Joshi VV, Kasznica J, Walters TR. Atypical mesoblastic nephroma. Pathologic characterization of a potentially aggressive variant of conventional congenital mesoblastic nephroma. *Arch Pathol Lab Med*. 1986;110(2):100-106.
149. Pettinato G, Manivel JC, Wick MR, Dehner LP. Classical and cellular (atypical) congenital mesoblastic nephroma: a clinicopathologic, ultrastructural, immunohistochemical, and flow cytometric study. *Hum Pathol*. 1989;20(7):682-690.
150. Sandstedt B, Delemarre JF, Krul EJ, Tournade MF. Mesoblastic nephromas: a study of 29 tumours from the SIOP nephroblastoma file. *Histopathology*. 1985;9(7):741-750.
151. Carpenter PM, Mascarello JT, Krous HF, Kaplan GW. Congenital mesoblastic nephroma: cytogenetic comparison to leiomyoma. *Pediatr Pathol*. 1993;13(4):435-441.
152. Rubin BP, Chen CJ, Morgan TW, et al. Congenital mesoblastic nephroma t(12;15) is associated with ETV6-NTRK3 gene fusion: cytogenetic and molecular relationship to congenital (infantile) fibrosarcoma. *Am J Pathol*. 1998;153(5):1451-1458.
153. Schofield DE, Yunis EJ, Fletcher JA. Chromosome aberrations in mesoblastic nephroma. *Am J Pathol*. 1993;143(3):714-724.
154. Argani P, Fritsch M, Kadkol SS, et al. Detection of the ETV6-NTRK3 chimeric RNA of infantile fibrosarcoma/cellular congenital mesoblastic nephroma in paraffin-embedded tissue: application to challenging pediatric renal stromal tumors. *Mod Pathol*. 2000;13(1):29-36.
155. Knezevich SR, Garnett MJ, Pysher TJ, et al. ETV6-NTRK3 gene fusions and trisomy 11 establish histogenetic link between mesoblastic nephroma and congenital fibrosarcoma. *Cancer Res*. 1998;58(22):5046-5048.
156. Anderson J, Gibson S, Sebire NJ. Expression of ETV6-NTRK in classical, cellular and mixed subtypes of congenital mesoblastic nephroma. *Histopathology*. 2006;48:748-753.
157. Howell CG, Othersen HB, Kiviat NE, et al. Therapy and outcome in 51 children with mesoblastic nephroma: a report of the National Wilms' Tumor Study. *J Pediatr Surg*. 1982;17(6):826-831.
158. Gonzalez-Crussi F, Sotelo-Avila C, Kidd JM. Mesenchymal renal tumors in infancy: a reappraisal. *Hum Pathol*. 1981;12(1):78-85.
159. Heidelberger KP, Ritchey ML, Dauser RC, et al. Congenital mesoblastic nephroma metastatic to the brain. *Cancer*. 1993;72(8):2499-2502.
160. Vujanic GM, Delemarre JF, Moeslichian S, et al. Mesoblastic nephroma metastatic to the lungs and heart—another face of this peculiar lesion: case report and review of the literature. *Pediatr Pathol*. 1993;13(2):143-153.
161. Gonzalez-Crussi F, Sotelo-Avila C, Kidd JM. Malignant mesenchymal nephroma of infancy.

- report of a case with pulmonary metastases. *Am J Surg Pathol.* 1980;4(2):185-190.
162. Beckwith JB, Weeks DA. Congenital mesoblastic nephroma. When should we worry? *Arch Pathol Lab Med.* 1986;110(2):98-99.
163. Furtwangler R, Reinhard H, Leuschner I, et al. Mesoblastic nephroma—a report from the Gesellschaft für Padiatrische Onkologie und Hämatologie (GPOH). *Cancer.* 2006;106(10):2275-2283.
164. Marsden HB, Lawler W, Kumar PM. Bone metastasizing renal tumor of childhood: morphological and clinical features, and differences from Wilms' tumor. *Cancer.* 1978;42(4):1922-1928.
165. Morgan E, Kidd JM. Undifferentiated sarcoma of the kidney: a tumor of childhood with histopathologic and clinical characteristics distinct from Wilms' tumor. *Cancer.* 1978;42(4):1916-1921.
166. Sotelo-Avila C, Gonzalez-Crussi F, Sadowinski S, et al. Clear cell sarcoma of the kidney: a clinicopathologic study of 21 patients with long-term follow-up evaluation. *Hum Pathol.* 1985;16(12):1219-1230.
167. Oda H, Shiga J, Machinami R. Clear cell sarcoma of kidney. Two cases in adults. *Cancer.* 1993;71(7):2286-2291.
168. Amin MB, de Peralta-Venturina MN, Ro JY. Clear cell sarcoma of kidney in an adolescent and in young adults: a report of four cases with ultrastructural, immunohistochemical, and DNA flow cytometric analysis. *Am J Surg Pathol.* 1999;23:1455-1463.
169. Uzoar I, Podbielski FJ, Chou P, et al. Familial adenomatous polyposis coli and clear cell sarcoma of the kidney. *Pediatr Pathol.* 1993;13(2):133-141.
170. Sandstedt BE, Delemarre JE, Harms D, Tournade MF. Sarcomatous Wilms' tumor with clear cells and hyalinization. A study of 38 tumors in children from the SIOP nephroblastoma file. *Histopathology.* 1987;11(3):273-285.
171. Argani P, Perlman EJ, Breslow NE, et al. Clear cell sarcoma of the kidney: a review of 351 cases from the National Wilms Tumor Study Group Pathology Center. *Am J Surg Pathol.* 2000;24(1):4-18.
172. Kenny C, Bausenwein S, Lazaro A, et al. Mutually exclusive BCOR internal tandem duplications and YWHAE-NUTM2 fusions in clear cell sarcoma of kidney: not the full story. *J Pathol.* 2016;238:617-620.
173. Roy A, Kumar V, Zorman B, et al. Recurrent internal tandem duplications of BCOR in clear cell sarcoma of the kidney. *Nat Commun.* 2015;6:8891.
174. Karlsson J, Valind A, Gisselsson D. BCOR internal tandem duplication and YWHAE-NUTM2B/E fusion are mutually exclusive events in clear cell sarcoma of the kidney. *Genes Chromosomes Cancer.* 2016;55:120-123.
175. Ueno-Yokohata H, Okita H, Nakasato K, et al. Consistent in-frame internal tandem duplications of BCOR characterize clear cell sarcoma of the kidney. *Nat Genet.* 2015;47:861-863.
176. Kao YC, Sung YS, Zhang L, et al. Recurrent BCOR internal tandem duplication and YWHAE-NUTM2B fusions in soft tissue undifferentiated round cell sarcoma of infancy: overlapping genetic features with clear cell sarcoma of kidney. *Am J Surg Pathol.* 2016;40:1009-1020.
177. Weeks DA, Malott RL, Zuppan C, et al. Primitive pelvic sarcoma resembling clear cell sarcoma of kidney. *Ultrastruct Pathol.* 1991;15(4-5):403-408.
178. Kao YC, Sung YS, Zhang L, et al. BCOR overexpression is a highly sensitive marker in round cell sarcomas with BCOR genetic abnormalities. *Am J Surg Pathol.* 2016;40:1670-1678.
179. Kao YC, Sung YS, Zhang L, et al. BCOR upregulation in a poorly differentiated synovial sarcoma with SS18L1-SSX1 fusion-A pathologic and molecular pitfall. *Genes Chromosomes Cancer.* 2017;56:296-302.
180. Berry PJ, Vujanic GM. Malignant rhabdoid tumour. *Histopathology.* 1992;20(2):189-193.
181. Weeks DA, Beckwith JB, Mierau GW, Luckey DW. Rhabdoid tumor of kidney. A report of 111 cases from the National Wilms' Tumor Study Pathology Center. *Am J Surg Pathol.* 1989;13(6):439-458.
182. Mayes LC, Kasselberg AG, Roloff JS, Lukens JN. Hypercalcemia associated with immunoreactive parathyroid hormone in a malignant rhabdoid tumor of the kidney (rhabdoid Wilms' tumor). *Cancer.* 1984;54(5):882-884.
183. Vujanic GM, Sandstedt B, Harms D, et al. Rhabdoid tumour of the kidney: a clinicopathological study of 22 patients from the International Society of Paediatric Oncology (SIOP) nephroblastoma file. *Histopathology.* 1996;28(4):333-340.
184. Haas JE, Palmer NF, Weinberg AG, Beckwith JB. Ultrastructure of malignant rhabdoid tumor of the kidney. A distinctive renal tumor of children. *Hum Pathol.* 1981;12(7):646-657.
185. Weeks DA, Beckwith JB, Mierau GW, Zuppan CW. Renal neoplasms mimicking rhabdoid tumor of kidney. A report from the National Wilms' Tumor Study Pathology Center. *Am J Surg Pathol.* 1991;15(11):1042-1054.
186. Bishu S, Bolton BD, Rajaram B, Chou PM. Malignant rhabdoid tumors: a twelve year experience. *Lab Invest.* 2009;89(suppl 1):345A.
187. Hoot AC, Russo P, Judkins AR, et al. Immunohistochemical analysis of hSNF5/INI1 distinguishes renal and extra-renal malignant rhabdoid tumors from other pediatric soft tissue tumors. *Am J Surg Pathol.* 2004;28(11):1485-1491.
188. Biegel JA, Tan L, Zhang F, et al. Alterations of the hSNF5/INI1 gene in central nervous system atypical teratoid/rhabdoid tumors and renal and extrarenal rhabdoid tumors. *Clin Cancer Res.* 2002;8(11):3461-3467.
189. Sotelo-Avila C, Gonzalez-Crussi F, deMello D, et al. Renal and extrarenal rhabdoid tumors in children: clinicopathologic study of 14 patients. *Semin Diagn Pathol.* 1986;3(2):151-163.
190. Tsokos M, Kourakis G, Chandra RS, et al. Malignant rhabdoid tumor of the kidney and soft tissues. Evidence for a diverse morphological and immunocytochemical phenotype. *Arch Pathol Lab Med.* 1989;113(2):115-120.
191. Tsuneyoshi M, Daimaru Y, Hashimoto H, Enjoji M. Malignant soft tissue neoplasms with the histologic features of renal rhabdoid tumors: an ultrastructural and immunohistochemical study. *Hum Pathol.* 1985;16(12):1235-1242.
192. Li Y, Pawel BR, Hill DA, et al. Pediatric cystic nephroma is morphologically, immunohistochemically, and genetically distinct from adult cystic nephroma. *Am J Surg Pathol.* 2017;41:472-481.
193. Bisceglia M, Creti G. AMR series unilateral (localized) renal cystic disease. *Adv Anat Pathol.* 2005;12(4):227-232.
194. Kajani N, Rosenberg BF, Bernstein J. Multilocular cystic nephroma. *J Urol Pathol.* 1993;1:33-42.
195. Nagao T, Sugano I, Ishida Y, et al. Cystic partially differentiated nephroblastoma in an adult: an immunohistochemical, lectin histochemical and ultrastructural study. *Histopathology.* 1999;35(1):65-73.
196. Baldauf MC, Schulz DM. Multilocular cyst of the kidney. Report of three cases with review of the literature. *Am J Clin Pathol.* 1976;65(1):93-102.
197. Gallo GE, Penchansky L. Cystic nephroma. *Cancer.* 1977;39(3):1322-1327.
198. Vujanic GM, Kelsey A, Perlman EJ, et al. Anaplastic sarcoma of the kidney: a clinicopathologic study of 20 cases of a new entity with polyphenotypic features. *Am J Surg Pathol.* 2007;31(10):1459-1468.
199. Delahunt B, Beckwith JB, Eble JN, et al. *Cancer.* 1998;82:2427-2433.
200. Raney B, Anderson J, Arndt C, et al. Primary renal sarcomas in the Intergroup Rhabdomyosarcoma Study Group (IRSG) experience, 1972-2005: a report from the Children's Oncology Group. *Pediatr Blood Cancer.* 2008;51:339-343.
201. Wu MK, Cotter MB, Pears J, et al. Tumor progression in DICER1-mutated cystic nephroma-witnessing the genesis of anaplastic sarcoma of the kidney. *Hum Pathol.* 2016;53:114-120.
202. Doros LA, Rossi CT, Yang J, et al. DICER1 mutations in childhood cystic nephroma and its relationship to DICER1-renal sarcoma. *Mod Pathol.* 2014;27:1267-1280.
203. Panuel M, Bourliere-Najean B, Gentet JC, et al. Aggressive neuroblastoma with initial pulmonary metastases and kidney involvement simulating Wilms' tumor. *Eur J Radiol.* 1992;14(3):201-203.
204. Nisen PD, Rich MA, Gloster E, et al. N-myc oncogene expression in histopathologically unrelated bilateral pediatric renal tumors. *Cancer.* 1988;61(9):1821-1826.
205. Ellison DA, Parham DM, Bridge J, Beckwith JB. Immunohistochemistry of primary malignant neuroepithelial tumors of the kidney: a potential source of confusion? A study of 30 cases from the National Wilms Tumor Study Pathology Center. *Hum Pathol.* 2007;38(2):205-211.
206. Marley EF, Liapis H, Humphrey PA, et al. Primitive neuroectodermal tumor of the kidney—another enigma: a pathologic, immunohistochemical, and molecular diagnostic study. *Am J Surg Pathol.* 1997;21(3):354-359.
207. Jimenez RE, Folpe AL, Lapham RL, et al. Primary Ewing's sarcoma/primitive neuroectodermal tumor of the kidney: a clinicopathologic and immunohistochemical analysis of 11 cases. *Am J Surg Pathol.* 2002;26(3):320-327.
208. Quezada M, Benjamin DR, Tsokos M. EWS/FLI-1 fusion transcripts in three peripheral primitive neuroectodermal tumors of the kidney. *Hum Pathol.* 1997;28(7):767-771.
209. Sheaff M, McManus A, Scheimberg I, et al. Primitive neuroectodermal tumor of the kidney confirmed by fluorescence in situ hybridization. *Am J Surg Pathol.* 1997;21(4):461-468.
210. Parham DM, Roloson GJ, Feely M, et al. Primary malignant neuroepithelial tumors of the kidney: a clinicopathologic analysis of 146 adult and pediatric cases from the National Wilms' Tumor Study Group Pathology Center. *Am J Surg Pathol.* 2001;25(2):133-146.
211. Mangray S, Somers GR, He J, et al. Primary Undifferentiated Sarcoma of the Kidney Harboring a Novel Variant of CIC-DUX4 Gene Fusion. *Am J Surg Pathol.* 2016;40:1298-1301.
212. Bergerat S, Barthelemy P, Mouracade P, et al. Primary CIC-DUX4 round cell sarcoma of the kidney: a treatment-refractory tumor with poor outcome. *Pathol Res Pract.* 2017;213:154-160.
213. Argani P, Faria PA, Epstein JI, et al. Primary renal synovial sarcoma: molecular and morphologic delineation of an entity previously included among embryonal sarcomas of the kidney. *Am J Surg Pathol.* 2000;24:1087-1096.

214. Kim DH, Sohn JH, Lee MC, et al. Primary synovial sarcoma of the kidney. *Am J Surg Pathol*. 2000;24:1097-1104.
215. Lordello L, Bur ME, Oliva E, Lennerz JK. PAX8-positive biphasic synovial sarcoma expressing hormonal receptors. *Appl Immunohistochem Mol Morphol*. 2017.
216. Karafin M, Parwani AV, Netto GJ, et al. Diffuse expression of PAX2 and PAX8 in the cystic epithelium of mixed epithelial stromal tumor, angiomyolipoma with epithelial cysts, and primary renal synovial sarcoma: evidence supporting renal tubular differentiation. *Am J Surg Pathol*. 2011;35:1264-1273.
217. Davis CJ Jr, Barton JH, Sesterhenn IA, Mostofi FK. Metanephric adenoma. Clinicopathological study of fifty patients. *Am J Surg Pathol*. 1995;19(10):1101-1114.
218. Jones EC, Pins M, Dickersin GR, Young RH. Metanephric adenoma of the kidney. A clinicopathological, immunohistochemical, flow cytometric, cytogenetic, and electron microscopic study of seven cases. *Am J Surg Pathol*. 1995;19:615-626.
219. Strong JW, Ro JY. Metanephric adenoma of the kidney: a newly characterized entity. *Adv Anat Pathol*. 1996;3:172-178.
220. Gatalica Z, Grujic S, Kovatich A, Petersen RO. Metanephric adenoma: histology, immunophenotype, cytogenetics, ultrastructure. *Mod Pathol*. 1996;9(3):329-333.
221. Granter SR, Fletcher JA, Renshaw AA. Cytologic and cytogenetic analysis of metanephric adenoma of the kidney: a report of two cases. *Am J Clin Pathol*. 1997;108(5):544-549.
222. Muir TE, Cheville JC, Lager DJ. Metanephric adenoma, nephrogenic rests, and Wilms' tumor: a histologic and immunophenotypic comparison. *Am J Surg Pathol*. 2001;25:1290-1296.
223. Choueiri TK, Cheville J, Palestro E, et al. BRAF mutations in metanephric adenoma of the kidney. *Eur Urol*. 2012;62:917-922.
224. Pinto A, Signoretti S, Hirsch MS, Barletta JA. Immunohistochemical staining for BRAF V600E supports the diagnosis of metanephric adenoma. *Histopathology*. 2015;66:901-904.
225. Udager AM, Pan J, Magers MJ, et al. Molecular and immunohistochemical characterization reveals novel BRAF mutations in metanephric adenoma. *Am J Surg Pathol*. 2015;39:549-557.
226. Argani P, Beckwith JB. Metanephric stromal tumor: report of 31 cases of a distinctive pediatric renal neoplasm. *Am J Surg Pathol*. 2000;24(7):917-926.
227. Arroyo MR, Green DM, Perlman EJ, et al. The spectrum of metanephric adenofibroma and related lesions: clinicopathologic study of 25 cases from the National Wilms Tumor Study Group Pathology Center. *Am J Surg Pathol*. 2001;25(4):433-444.
228. Hennigar RA, Beckwith JB. Nephrogenic adenofibroma. A novel kidney tumor of young people. *Am J Surg Pathol*. 1992;16:325-334.
229. Chatten J, Cromie WJ, Duckett JW. Ossifying tumor of infantile kidney: report of two cases. *Cancer*. 1980;45(3):609-612.
230. Dehner LP. Intrarenal teratoma occurring in infancy: report of a case with discussion of extragonadal germ cell tumors in infancy. *J Pediatr Surg*. 1973;8(3):369-378.
231. Kumar Y, Bhatia A, Kumar V, Vaiphei K. Intrarenal pure yolk sac tumor: an extremely rare entity. *Int J Surg Pathol*. 2007;15(2):204-206.
232. Collardeau-Frachon S, Ranchere-Vince D, Delattre O, et al. Primary desmoplastic small round cell tumor of the kidney: a case report in a 14-year-old girl with molecular confirmation. *Pediatr Dev Pathol*. 2007;10(4):320-324.
233. Su MC, Jeng YM, Chu YC. Desmoplastic small round cell tumor of the kidney. *Am J Surg Pathol*. 2004;28(10):1379-1383.
234. Wang LL, Perlman EJ, Vujanic GM, et al. Desmoplastic small round cell tumor of the kidney in childhood. *Am J Surg Pathol*. 2007;31(4):576-584.
235. Cohen HT, McGovern FJ. Renal-cell carcinoma. *N Engl J Med*. 2005;353(23):2477-2490.
236. Dehner LP, Leestma JE, Price EB Jr. Renal cell carcinoma in children: a clinicopathologic study of 15 cases and review of the literature. *J Pediatr*. 1970;76(3):358-368.
237. Hartman DS, Davis CJ Jr, Madewell JE, Friedman AC. Primary malignant renal tumors in the second decade of life: Wilms tumor versus renal cell carcinoma. *J Urol*. 1982;127(5):888-891.
238. Lack EE, Cassidy JR, Sallan SE. Renal cell carcinoma in childhood and adolescence: a clinical and pathological study of 17 cases. *J Urol*. 1985;133(5):822-828.
239. Renshaw AA, Granter SR, Fletcher JA, et al. Renal cell carcinomas in children and young adults: increased incidence of papillary architecture and unique subtypes. *Am J Surg Pathol*. 1999;23(7):795-802.
240. Bruder E, Passera O, Harms D, et al. Morphologic and molecular characterization of renal cell carcinoma in children and young adults. *Am J Surg Pathol*. 2004;28(9):1117-1132.
241. Ramphal R, Pappo A, Zielińska M, et al. Pediatric renal cell carcinoma: clinical, pathologic, and molecular abnormalities associated with the members of the mit transcription factor family. *Am J Clin Pathol*. 2006;126(3):349-364.
242. Coughlin SS, Neaton JD, Randall B, Sengupta A. Predictors of mortality from kidney cancer in 332,547 men screened for the Multiple Risk Factor Intervention Trial. *Cancer*. 1997;79(11):2171-2177.
243. Berg S, Jacobs SC, Cohen AJ, et al. The surgical management of hereditary multifocal renal carcinoma. *J Urol*. 1981;126(3):313-315.
244. Friedrich CA. Von Hippel-Lindau syndrome. A pleomorphic condition. *Cancer*. 1999;86(11 suppl):2478-2482.
245. Shen T, Zhuang Z, Gersell DJ, Tavassoli FA. Allelic deletion of VHL gene detected in papillary tumors of the broad ligament, epididymis, and retroperitoneum in von Hippel-Lindau disease patients. *Int J Surg Pathol*. 2000;8(3):207-212.
246. Kragel PJ, Walther MM, Pestaner JP, Filling-Katz MR. Simple renal cysts, atypical renal cysts, and renal cell carcinoma in von Hippel-Lindau disease: a lectin and immunohistochemical study in six patients. *Mod Pathol*. 1991;4(2):210-214.
247. Malek RS, Omess PJ, Benson RCJ, Zincke H. Renal cell carcinoma in von Hippel-Lindau syndrome. *Am J Med Genet A*. 1987;82:236-238.
248. Stornes I, Jorgensen TM. Renal malignancy in von Hippel-Lindau's disease. Case reports. *Scand J Urol Nephrol*. 1993;27(1):139-142.
249. Paraf F, Chauveau D, Chretien Y, et al. Renal lesions in von Hippel-Lindau disease: immunohistochemical expression of nephron differentiation molecules, adhesion molecules and apoptosis proteins. *Histopathology*. 2000;36(5):457-465.
250. George DJ, Kaelin WG Jr. The von Hippel-Lindau protein, vascular endothelial growth factor, and kidney cancer. *N Engl J Med*. 2003;349(5):419-421.
251. Williamson SR, Zhang S, Eble JN, et al. Clear cell papillary renal cell carcinoma-like tumors in patients with von Hippel-Lindau disease are unrelated to sporadic clear cell papillary renal cell carcinoma. *Am J Surg Pathol*. 2013;37(8):1131-1139.
252. Dunnill MS, Millard PR, Oliver D. Acquired cystic disease of the kidneys: a hazard of long-term intermittent maintenance haemodialysis. *J Clin Pathol*. 1977;30:868-877.
253. Hughson MD, Buchwald D, Fox M. Renal neoplasia and acquired cystic kidney disease in patients receiving long-term dialysis. *Arch Pathol Lab Med*. 1986;110(7):592-601.
254. Pan CC, Chen YI, Chang LC, et al. Immunohistochemical and molecular genetic profiling of acquired cystic disease-associated renal cell carcinoma. *Histopathology*. 2009;55(2):145-153.
255. Bernstein J, Evan AP, Gardner KD Jr. Epithelial hyperplasia in human polycystic kidney diseases. Its role in pathogenesis and risk of neoplasia. *Am J Pathol*. 1987;129(1):92-101.
256. Bai SHO. Renal carcinomas arising in patients with autosomal dominant polycystic kidney disease (ADPKD): a clinicopathological review. *Lab Invest*. 2009;89(suppl 1):158A.
257. Toro JR, Wei MH, Glenn GM, et al. BHD mutations, clinical and molecular genetic investigations of Birt-Hogg-Dubé syndrome: a new series of 50 families and a review of published reports. *Cancer Genet Cytogenet*. 2008;184(6):321-331.
258. Pavlovich CP, Walther MM, Eyler RA, et al. Renal tumors in the Birt-Hogg-Dubé syndrome. *Am J Surg Pathol*. 2002;26(12):1542-1552.
259. Tickoo SK, Reuter VE, Amin MB, et al. Renal oncocytosis: a morphologic study of fourteen cases. *Am J Surg Pathol*. 1999;23(9):1094-1101.
260. Kiuru M, Launonen V, Hietala M, et al. Familial cutaneous leiomyomatosis is a two-hit condition associated with renal cell cancer of characteristic histopathology. *Am J Pathol*. 2001;159(3):825-829.
261. Merino MJ, Torres-Cabala C, Pinto P, Linehan WM. The morphologic spectrum of kidney tumors in hereditary leiomyomatosis and renal cell carcinoma (HLRCC) syndrome. *Am J Surg Pathol*. 2007;31(10):1578-1585.
262. Gill AJ, Hes O, Papathomas T. Succinate dehydrogenase (SDH)-deficient renal carcinoma: a morphologically distinct entity: a clinicopathologic series of 36 tumors from 27 patients. *Am J Surg Pathol*. 2014;38(12):1588-1602.
263. Gill AJ, Pachter NS, Chou A, et al. *Am J Surg Pathol*. 2011;35(10):1578-1585.
264. Williamson SR, Eble JN, Amin MB, et al. Succinate dehydrogenase-deficient renal cell carcinoma: detailed characterization of 11 tumors defining a unique subtype of renal cell carcinoma. *Mod Pathol*. 2015;28(1):80-94.
265. Guo J, Tretiakova MS, Troxell ML, et al. Tuberous sclerosis-associated renal cell carcinoma: a clinicopathologic study of 57 separate carcinomas in 18 patients. *Am J Surg Pathol*. 2014;38(11):1457-1467.
266. Yang P, Cornejo KM, Sadow PM, et al. Renal cell carcinoma in tuberous sclerosis complex. *Am J Surg Pathol*. 2014;38(7):895-909.
267. Chowdhuri SR, Vicens J, Teller L, et al. Renal cancer in tuberous sclerosis: an underdiagnosed disease? Molecular, IHC and pathologic correlation. *Lab Invest*. 2009;89(suppl 1):191A.
268. Medeiros LJ, Palmedo G, Krigman HR, et al. Oncoctoid renal cell carcinoma after neuroblastoma: a report of four cases of a distinct clinicopathologic entity. *Am J Surg Pathol*. 1999;23(7):772-780.
269. Falzarano SM, McKenney JK, Montironi R, et al. Renal cell carcinoma occurring in patients with prior neuroblastoma: a heterogeneous group of neoplasms. *Am J Surg Pathol*. 2016;40(7):989-997.
270. Mester JL, Zhou M, Prescott N, Eng C. Papillary renal cell carcinoma is associated

- with PTEN hamartoma tumor syndrome. *Urology*. 2012;79(5):1187.e1-1187.e7.
271. Shuch B, Ricketts CJ, Vocke CD, et al. Germline PTEN mutation Cowden syndrome: an underappreciated form of hereditary kidney cancer. *J Urol*. 2013;190(6):1990-1998.
272. Skinner DG, Colvin RB, Vermillion CD, et al. Diagnosis and management of renal cell carcinoma. A clinical and pathologic study of 309 cases. *Cancer*. 1971;28(5):1165-1177.
273. Dalakas MC, Fujihara S, Askanas V, et al. Nature of amyloid deposits in hypernephroma. Immunocytochemical studies in 2 cases associated with amyloid polyneuropathy. *Am J Pathol*. 1984;116(3):447-454.
274. Fletcher MS, Packham DA, Pryor JP, Yates-Bell AJ. Hepatic dysfunction in renal carcinoma. *Br J Urol*. 1981;53(6):533-536.
275. Maesaka JK, Mittal SK, Fishbane S. Paraneoplastic syndromes of the kidney. *Semin Oncol*. 1997;24(3):373-381.
276. Ramos CV, Taylor HB. Hepatic dysfunction associated with renal carcinoma. *Cancer*. 1972;29(5):1287-1292.
277. Vanatta PR, Silva FG, Taylor WE, Costa JC. Renal cell carcinoma and systemic amyloidosis: demonstration of AA protein and review of the literature. *Hum Pathol*. 1983;14(3):195-201.
278. Aoyagi T, Mori I, Ueyama Y, Tamaoki N. Sinusoidal dilatation of the liver as a paraneoplastic manifestation of renal cell carcinoma. *Hum Pathol*. 1989;20(12):1193-1197.
279. Fan K, Smith DJ. Hypercalcemia associated with renal cell carcinoma: probable role of neoplastic stromal cells. *Hum Pathol*. 1983;14(2):168-173.
280. Goldberg MF, Tashjian AH Jr, Order SE, Dammin GJ. Renal adenocarcinoma containing a parathyroid hormone-like substance and associated with marked hypercalcemia. *Am J Med*. 1964;36:805-814.
281. Hollifield JW, Page DL, Smith C, et al. Renin-secreting clear cell carcinoma of the kidney. *Arch Int Med*. 1975;135(6):859-864.
282. Okabe T, Urabe A, Kato T, et al. Production of erythropoietin-like activity by human renal and hepatic carcinomas in cell culture. *Cancer*. 1985;55(9):1918-1923.
283. Frohmuller HG, Grups JW, Heller V. Comparative value of ultrasonography, computerized tomography, angiography and excretory urography in the staging of renal cell carcinoma. *J Urol*. 1987;138(3):482-484.
284. Aso Y, Homma Y. A survey on incidental renal cell carcinoma in Japan. *J Urol*. 1992;147(2):340-343.
285. Konnak JW, Grossman HB. Renal cell carcinoma as an incidental finding. *J Urol*. 1985;134(6):1094-1096.
286. Brunelli M, Gobbo S, Menestrina F, et al. Core biopsies of renal tumors: accuracy for histopathological evaluation. *Lab Invest*. 2009;89(suppl 1):161A.
287. Campbell S, Uzzo RG1, Allaf ME, et al. Renal mass and localized renal cancer: AJA guideline. *J Urol*. 2017;198(3):520-529.
288. Kovacs G, Akhtar M, Beckwith BJ, et al. The Heidelberg classification of renal cell tumours. *J Pathol*. 1997;183(2):131-133.
289. Storkel S, Eble JN, Adlakha K, et al. Classification of renal cell carcinoma: Workgroup No. 1. Union Internationale Contre le Cancer (UICC) and the American Joint Committee on Cancer (AJCC). *Cancer*. 1997;80(5):987-989.
290. Nguyen DP, Vertosick EA, Corradi RB, et al. Histological subtype of renal cell carcinoma significantly affects survival in the era of partial nephrectomy. *Urol Oncol*. 2016;34:259.e1-259.e8.
291. Moch H, Amin MB, Argani P, et al. Renal cell tumours. In: Moch H, Humphrey PA, Ulbright TM, Reuter VE, eds. *WHO Classification of Tumours of the Urinary System and Male Genital Organs*. Lyon: IARC Press; 2016.
292. Kinouchi T, Mano M, Saiki S, et al. Incidence rate of satellite tumors in renal cell carcinoma. *Cancer*. 1999;86(11):2331-2336.
293. Bonsib SM, Bhalodia A. Retrograde venous invasion in renal cell carcinoma: a complication of sinus vein and main renal vein invasion. *Mod Pathol*. 2011;24(12):1578-1585.
294. Brinker DA, Amin MB, de Peralta-Venturina M, et al. Extensively necrotic cystic renal cell carcinoma: a clinicopathologic study with comparison to other cystic and necrotic renal cancers. *Am J Surg Pathol*. 2000;24(7):988-995.
295. Fleming S, O'Donnell M. Surgical pathology of renal epithelial neoplasms: recent advances and current status. *Histopathology*. 2000;36(3):195-202.
296. Humphrey PA. Clear cell neoplasms of the urinary tract and male reproductive system. *Semin Diagn Pathol*. 1997;14(4):240-252.
297. Montironi R, Mikuz G, Algaba F, et al. Epithelial tumours of the adult kidney. *Virchows Arch*. 1999;434(4):281-290.
298. Thoenes W, Storkel S, Rumpelt HJ. Histopathology and classification of renal cell tumors (adenomas, oncocytomas and carcinomas). The basic cytological and histopathological elements and their use for diagnostics. *Pathol Res Pract*. 1986;181(2):125-143.
299. Steinberg P, Storkel S, Oesch F, Thoenes W. Carbohydrate metabolism in human renal clear cell carcinomas. *Lab Invest*. 1992;67:506-511.
300. Kim MK, Kim S. Immunohistochemical profile of common epithelial neoplasms arising in the kidney. *Appl Immunohistochem Mol Morphol*. 2002;10(4):332-338.
301. Waldherr R, Schwegheimer K. Co-expression of cytokeratin and vimentin intermediate-sized filaments in renal cell carcinomas. Comparative study of the intermediate-sized filament distribution in renal cell carcinomas and normal human kidney. *Virchows Arch A Pathol Anat Histopathol*. 1985;408(1):15-27.
302. Avery AK, Beckstead J, Renshaw AA, Corless CL. Use of antibodies to RCC and CD10 in the differential diagnosis of renal neoplasms. *Am J Surg Pathol*. 2000;24(2):203-210.
303. Al-Ahmadie HA, Alden D, Qin LX, et al. Carbonic anhydrase IX expression in clear cell renal cell carcinoma: an immunohistochemical study comparing 2 antibodies. *Am J Surg Pathol*. 2008;32(3):377-382.
304. Genega EM, Gebremichael M, Najarian R, et al. Carbonic anhydrase IX expression in renal neoplasms: correlation with tumor type and grade. *Am J Clin Pathol*. 2010;134(6):873-879.
305. Mazal PR, Stichenwirth M, Koller A, et al. Expression of aquaporins and PAX-2 compared to CD10 and cytokeratin 7 in renal neoplasms: a tissue microarray study. *Mod Pathol*. 2005;18(4):535-540.
306. Skinner BF, Folpe AL, Hennigar RA, et al. Distribution of cytokeratins and vimentin in adult renal neoplasms and normal renal tissue: potential utility of a cytokeratin antibody panel in the differential diagnosis of renal tumors. *Am J Surg Pathol*. 2005;29(6):747-754.
307. Fetsch PA, Powers CN, Zakowski MF, Abati A. Anti-alpha-inhibin: marker of choice for the consistent distinction between adrenocortical carcinoma and renal cell carcinoma in fine-needle aspiration. *Cancer*. 1999;87(3):168-172.
308. Renshaw AA, Granter SR. A comparison of A103 and inhibin reactivity in adrenal cortical tumors: distinction from hepatocellular carcinoma and renal tumors. *Mod Pathol*. 1998;11(12):1160-1164.
309. Nolan LP, Heatley MK. The value of immunocytochemistry in distinguishing between clear cell carcinoma of the kidney and ovary. *Int J Gynecol Pathol*. 2001;20(2):155-159.
310. Ohta Y, Suzuki T, Shiokawa A, et al. Expression of CD10 and cytokeratins in ovarian and renal clear cell carcinoma. *Int J Gynecol Pathol*. 2005;24(3):239-245.
311. Cameron RI, Ashe P, O'Rourke DM, et al. A panel of immunohistochemical stains assists in the distinction between ovarian and renal clear cell carcinoma. *Int J Gynecol Pathol*. 2003;22:272-276.
312. Ordonez NG. The diagnostic utility of immunohistochemistry in distinguishing between mesothelioma and renal cell carcinoma: a comparative study. *Hum Pathol*. 2004;35(6):697-710.
313. Ingold B, Wild PJ, Nocito A, et al. Renal cell carcinoma marker reliably discriminates central nervous system haemangioblastoma from brain metastases of renal cell carcinoma. *Histopathology*. 2008;52(6):674-681.
314. Jung SM, Kuo TT. Immunoreactivity of CD10 and inhibin alpha in differentiating hemangioblastoma of central nervous system from metastatic clear cell renal cell carcinoma. *Mod Pathol*. 2005;18(6):788-794.
315. MacLennan GT, Farrow GM, Gostwick DG. Immunohistochemistry in the evaluation of renal cell carcinoma: a critical appraisal. *J Urol Pathol*. 1997;6:195-204.
316. Nappi O, Mills SE, Swanson PE, Wick MR. Clear cell tumors of unknown nature and origin: a systematic approach to diagnosis. *Semin Diagn Pathol*. 1997;14(3):164-174.
317. Pan CC, Chen PC, Tsay SH, Ho DM. Differential immunoprofiles of hepatocellular carcinoma, renal cell carcinoma, and adrenocortical carcinoma: a systemic immunohistochemical survey using tissue array technique. *Appl Immunohistochem Mol Morphol*. 2005;13(4):347-352.
318. Sangi AR, Karamchandani J, Kim J, et al. The use of immunohistochemistry in the diagnosis of metastatic clear cell renal cell carcinoma: a review of PAX-8, PAX-2, hKIM-1, RCCMa, and CD10. *Adv Anat Pathol*. 2010;17:377-393.
319. Iqbal MA, Akhtar M, Ali MA. Cytogenetic findings in renal cell carcinoma. *Hum Pathol*. 1996;27(9):949-954.
320. Moch H, Mihatsch MJ. Genetic progression of renal cell carcinoma. *Virchows Arch*. 2002;441(4):320-327.
321. Amo-Takyi BK, Handt S, Gunawan B, et al. A cytogenetic approach to the differential diagnosis of metastatic clear cell renal carcinoma. *Histopathology*. 1998;32(5):436-443.
322. Kim WY, Kaelin WG Jr. Molecular pathways in renal cell carcinoma—rationale for targeted treatment. *Semin Oncol*. 2006;33(5):588-595.
323. Pei J, Feder MM, Al-Saleem T, et al. Combined classical cytogenetics and microarray-based genomic copy number analysis reveal frequent 3;5 rearrangements in clear cell renal cell carcinoma. *Genes Chromosomes Cancer*. 2010;49(7):610-619.
324. Hakimi AA, Reznik E, Lee CH, et al. An integrated metabolic atlas of clear cell renal cell carcinoma. *Cancer Cell*. 2016;29(1):104-116.
325. el-Naggar AK, Batsakis JG, Wang G, Lee MS. PCR-based RFLP screening of the commonly deleted 3p loci in renal cortical neoplasms. *Diagn Mol Pathol*. 1993;2(4):269-276.

326. Fleming S. The impact of genetics on the classification of renal carcinoma. *Histopathology*. 1993;22(1):89-92.
327. Hadaczek P, Podolski J, Toloczko A, et al. Losses at 3p common deletion sites in subtypes of kidney tumours: histopathological correlations. *Virchows Arch*. 1996;429(1):37-42.
328. Kovacs G. Molecular differential pathology of renal cell tumours. *Histopathology*. 1993;22(1):1-8.
329. McCue PA, Gorstein F. Genetic markers in renal cell carcinomas. *Hum Pathol*. 2001;32(10):1027-1028.
330. Presti JC Jr, Reuter VE, Cordon-Cardo C, et al. Allelic deletions in renal tumors: histopathological correlations. *Cancer Res*. 1993;53(23):5780-5783.
331. Teyssier JR, Henry I, Dozier C, et al. Recurrent deletion of the short arm of chromosome 3 in human renal cell carcinoma: shift of the c-ras 1 locus. *J Natl Cancer Inst*. 1986;77(6):1187-1195.
332. Toma MI, Grosser M, Herr A, et al. Loss of heterozygosity and copy number abnormality in clear cell renal cell carcinoma discovered by high-density affymetrix 10K single nucleotide polymorphism mapping array. *Neoplasia*. 2008;10(7):634-642.
333. van der Hout AH, van den Berg E, van der Vlies P, et al. Loss of heterozygosity at the short arm of chromosome 3 in renal-cell cancer correlates with the cytological tumour type. *Int J Cancer*. 1993;53(3):353-357.
334. Weiss LM, Gelb AB, Medeiros LJ. Adult renal epithelial neoplasms. *Am J Clin Pathol*. 1995;103(5):624-635.
335. Foster K, Crossey PA, Cairns P, et al. Molecular genetic investigation of sporadic renal cell carcinoma: analysis of allele loss on chromosomes 3p, 5q, 11p, 17 and 22. *Br J Cancer*. 1994;69(2):230-234.
336. Morita R, Ishikawa J, Tsutsumi M, et al. Allelotype of renal cell carcinoma. *Cancer Res*. 1991;51(3):820-823.
337. Cancer Genome Atlas Research Network. Comprehensive molecular characterization of clear cell renal cell carcinoma. *Nature*. 2013;499:43-49.
338. Dalglish GL, Furke K, Greenman C, et al. Systematic sequencing of renal carcinoma reveals inactivation of histone modifying genes. *Nature*. 2010;463:360-363.
339. Srinivasan SJ, Parwani AV. Molecular pathology of the genitourinary tract: molecular pathology of kidney and testis. *Surg Pathol Clin*. 2009;2:199-223.
340. Sudarshan S, Linehan WM. Genetic basis of cancer of the kidney. *Semin Oncol*. 2006;33(5):544-551.
341. Delahunt B, Eble JN. Papillary renal cell carcinoma: a clinicopathologic and immunohistochemical study of 105 tumors. *Mod Pathol*. 1997;10(6):537-544.
342. Delahunt B, Eble JN, McCredie MR, et al. Morphologic typing of papillary renal cell carcinoma: comparison of growth kinetics and patient survival in 66 cases. *Hum Pathol*. 2001;32(6):590-595.
343. The Cancer Genome Atlas Research Network, Linehan WM, Spellman PT, et al. Comprehensive molecular characterization of papillary renal-cell carcinoma. *N Engl J Med*. 2016;374:135-145.
344. Amin MB, Corless CL, Renshaw AA, et al. Papillary (chromophil) renal cell carcinoma: histomorphologic characteristics and evaluation of conventional pathologic prognostic parameters in 62 cases. *Am J Surg Pathol*. 1997;21(6):621-635.
345. Henn W, Zwerger T, Wullich B, et al. Bilateral multicentric papillary renal tumors with heteroclonal origin based on tissue-specific karyotype instability. *Cancer*. 1993;72(4):1315-1318.
346. Kovacs G, Kovacs A. Parenchymal abnormalities associated with papillary renal cell tumors. A morphological study. *J Urol Pathol*. 1993;1:301-312.
347. Mancilla-Jimenez R, Stanley RJ, Blath RA. Papillary renal cell carcinoma: a clinical, radiologic, and pathologic study of 34 cases. *Cancer*. 1976;38(6):2469-2480.
348. Renshaw AA, Corless CL. Papillary renal cell carcinoma. Histology and immunohistochemistry. *Am J Surg Pathol*. 1995;19(7):842-849.
349. Leroy X, Zini L, Leteurtre E, et al. Morphologic subtyping of papillary renal cell carcinoma: correlation with prognosis and differential expression of MUC1 between the two subtypes. *Mod Pathol*. 2002;15(11):1126-1130.
350. Park BH, Ro JY, Park WS, et al. Oncocytic papillary renal cell carcinoma with inverted nuclear pattern: distinct subtype with an indolent clinical course. *Pathol Int*. 2009;59(3):137-146.
351. Gatalica Z, Kovatch A, Miettinen M. Consistent expression of cytokeratin 7 in papillary renal-cell carcinoma. An immunohistochemical study in formalin-fixed, paraffin-embedded tissues. *J Urol Pathol*. 1995;3:205-211.
352. Corless CL, Aburatani H, Fletcher JA, et al. Papillary renal cell carcinoma: quantitation of chromosomes 7 and 17 by FISH, analysis of chromosome 3p for LOH, and DNA ploidy. *Diagn Mol Pathol*. 1996;5(1):53-64.
353. Jiang F, Richter J, Schraml P, et al. Chromosomal imbalances in papillary renal cell carcinoma: genetic differences between histological subtypes. *Am J Pathol*. 1998;153(5):1467-1473.
354. Kattar MM, Grignon DJ, Wallis T, et al. Clinicopathologic and interphase cytogenetic analysis of papillary (chromophilic) renal cell carcinoma. *Mod Pathol*. 1997;10(11):1143-1150.
355. Allory Y, Ouazana D, Boucher E, et al. Papillary renal cell carcinoma. Prognostic value of morphological subtypes in a clinicopathologic study of 43 cases. *Virchows Arch*. 2003;442(4):336-342.
356. Lubensky IA, Schmidt L, Zhuang Z, et al. Hereditary and sporadic papillary renal carcinomas with c-met mutations share a distinct morphological phenotype. *Am J Pathol*. 1999;155(2):517-526.
357. Chevarie-Davis M, Riazalhosseini Y, Arseneault M, et al. The morphologic and immunohistochemical spectrum of papillary renal cell carcinoma: study including 132 cases with pure type 1 and type 2 morphology as well as tumors with overlapping features. *Am J Surg Pathol*. 2014;38:887-894.
358. Warrick JL, Tsodikov A, Kunju LP, et al. Papillary renal cell carcinoma revisited: a comprehensive histomorphologic study with outcome correlations. *Hum Pathol*. 2014;45:1139-1146.
359. Hes O, Brunelli M, Michal M, et al. Oncocytic papillary renal cell carcinoma: a clinicopathologic, immunohistochemical, ultrastructural, and interphase cytogenetic study of 12 cases. *Ann Diagn Pathol*. 2006;10:133-139.
360. Xia QY, Rao Q, Shen Q, et al. Oncocytic papillary renal cell carcinoma: a clinicopathological study emphasizing distinct morphology, extended immunohistochemical profile and cytogenetic features. *Int J Clin Exp Pathol*. 2013;6:1392-1399.
361. Kunju LP, Woino K, Wolf JS Jr, et al. Papillary renal cell carcinoma with oncocytic cells and nonoverlapping low grade nuclei: expanding the morphologic spectrum with emphasis on clinicopathologic, immunohistochemical and molecular features. *Hum Pathol*. 2008;39:96-101.
362. Baer SC, Ro JY, Ordonez NG, et al. Sarcomatoid collecting duct carcinoma: a clinicopathologic and immunohistochemical study of five cases. *Hum Pathol*. 1993;24(9):1017-1022.
363. Cohen RJ, McNeal JE, Susman M, et al. Sarcomatoid renal cell carcinoma of papillary origin. A case report and cytogenetic evaluation. *Arch Pathol Lab Med*. 2000;124(12):1830-1832.
364. Renshaw AA, Morgan IW, Fletcher JA. A sarcomatoid renal cell carcinoma with a 'hobnail pattern' and immunohistochemical and cytogenetic features of papillary carcinoma. *J Urol Pathol*. 1998;9:93-102.
365. Suzigan S, López-Beltrán A, Montironi R, et al. Multilocular cystic renal cell carcinoma: a report of 45 cases of a kidney tumor of low malignant potential. *Am J Clin Pathol*. 2006;125:217-222.
366. Williamson SR, MacLennan GT, Lopez-Beltran A, et al. Cystic partially regressed clear cell renal cell carcinoma: a potential mimic of multilocular cystic renal cell carcinoma. *Histopathology*. 2013;63:767-779.
367. Bhatt JR, Jewett MA, Richard PO, et al. Multilocular cystic renal cell carcinoma: pathological T staging makes no difference to favorable outcomes and should be reclassified. *J Urol*. 2016;196:1350-1355.
368. Bonsib SM, Lager DJ. Chromophobe cell carcinoma. Analysis of 5 cases. *Am J Surg Pathol*. 1990;14:260-267.
369. Akhtar M, Kardar H, Linjawi T, et al. Chromophobe cell carcinoma of the kidney. A clinicopathologic study of 21 cases. *Am J Surg Pathol*. 1995;19(11):1245-1256.
370. Durham JR, Keohane M, Amin MB. Chromophobe renal cell carcinoma. *Adv Anat Pathol*. 1996;3:336-342.
371. Hes O, Vaneeck T, Perez-Montiel DM, et al. Chromophobe renal cell carcinoma with microcystic and adenomatous arrangement and pigmentation—a diagnostic pitfall. Morphological, immunohistochemical, ultrastructural and molecular genetic report of 20 cases. *Virchows Arch*. 2005;446(4):383-393.
372. Foix MP, Dunatov A, Martinek P, et al. Morphological, immunohistochemical, and chromosomal analysis of multicystic chromophobe renal cell carcinoma, an architecturally unusual challenging variant. *Virchows Arch*. 2016;469:669-678.
373. Peckova K, Martinek P, Ohe C, et al. Chromophobe renal cell carcinoma with neuroendocrine and neuroendocrine-like features. Morphologic, immunohistochemical, ultrastructural, and array comparative genomic hybridization analysis of 18 cases and review of the literature. *Ann Diagn Pathol*. 2015;19:261-268.
374. Granter SR, Renshaw AA. Fine-needle aspiration of chromophobe renal cell carcinoma: analysis of six cases. *Cancer Cytopathol*. 1997;81:122-128.
375. Wiatrowska BA, Zakowski MF. Fine-needle aspiration biopsy of chromophobe renal cell carcinoma and oncocytoma: comparison of cytomorphic features. *Cancer Cytopathol*. 1999;87:161-167.
376. Moreno SM, Benitez IA, Martinez Gonzalez MA. Ultrastructural studies in a series of 18 cases of chromophobe renal cell carcinoma. *Ultrastruct Pathol*. 2005;29(5):377-387.
377. Skinner BF, Jones EC. Renal oncocytoma and chromophobe renal cell carcinoma. A comparison of colloidal iron staining and electron microscopy. *Am J Clin Pathol*. 1999;111(6):796-803.
378. Thoenes W, Storkel S, Rumpelt HJ. Human chromophobe cell renal carcinoma. *Virchows*

- Arch B Cell Pathol Incl Mol Pathol.* 1985;48(3):207-217.
379. Tickoo SK, Amin MB, Zarbo RJ. Colloidal iron staining in renal epithelial neoplasms, including chromophobe renal cell carcinoma: emphasis on technique and patterns of staining. *Am J Surg Pathol.* 1998;22(4):419-424.
380. Williamson SR, Gaddé R, Trpkov K, et al. Diagnostic criteria for oncocytic renal neoplasms: a survey of urologic pathologists. *Hum Pathol.* 2017;63:149-156.
381. Yusenko MV, Kovacs G. Identifying CD82 (KAI1) as a marker for human chromophobe renal cell carcinoma. *Histopathology.* 2009;55(6):687-695.
382. Martignoni G, Pea M, Chilosi M, et al. Parvalbumin is constantly expressed in chromophobe renal carcinoma. *Mod Pathol.* 2001;14(8):760-767.
383. Hornsby CD, Cohen C, Amin MB, et al. Claudin-7 immunohistochemistry in renal tumors: a candidate marker for chromophobe renal cell carcinoma identified by gene expression profiling. *Arch Pathol Lab Med.* 2007;131(10):1541-1546.
384. Osunkoya AO, Cohen C, Lawson D, et al. Claudin-7 and claudin-8: immunohistochemical markers for the differential diagnosis of chromophobe renal cell carcinoma and renal oncocytoma. *Hum Pathol.* 2009;40(2):206-210.
385. Went P, Dirlhofer S, Salvisberg T, et al. Expression of epithelial cell adhesion molecule (EpCam) in renal epithelial tumors. *Am J Surg Pathol.* 2005;29(1):83-88.
386. DeLong WH, Sakr W, Grignon DJ. Chromophobe renal cell carcinoma: a comparative histochemical and immunohistochemical study. *J Urol Pathol.* 1996;41:8.
387. Khouri JD, Abrahams NA, Levin HS, MacLennan GT. The utility of epithelial membrane antigen and vimentin in the diagnosis of chromophobe renal cell carcinoma. *Ann Diagn Pathol.* 2002;6(3):154-158.
388. Kuroda N, Inoue K, Guo L, et al. Expression of CD9/motility-related protein 1 (MRP-1) in renal parenchymal neoplasms: consistent expression in papillary and chromophobe renal cell carcinomas. *Hum Pathol.* 2001;32(10):1071-1077.
389. Taki A, Nakatani Y, Misugi K, et al. Chromophobe renal cell carcinoma: an immunohistochemical study of 21 Japanese cases. *Mod Pathol.* 1999;12(3):310-317.
390. Martignoni G, Pea M, Brunelli M, et al. CD10 is expressed in a subset of chromophobe renal cell carcinomas. *Mod Pathol.* 2004;17(12):1455-1463.
391. Ozcan A, de la Roza G, Ro JY, et al. PAX2 and PAX8 expression in primary and metastatic renal tumors: a comprehensive comparison. *Arch Pathol Lab Med.* 2012;136:1541-1551.
392. Tacha D, Zhou D, Cheng L. Expression of PAX8 in normal and neoplastic tissues: a comprehensive immunohistochemical study. *Appl Immunohistochem Mol Morphol.* 2011;19:293-299.
393. Speicher MR, Schoell B, du Manoir S, et al. Specific loss of chromosomes 1, 2, 6, 10, 13, 17, and 21 in chromophobe renal cell carcinomas revealed by comparative genomic hybridization. *Am J Pathol.* 1994;145(2):356-364.
394. Bugert P, Gaul C, Weber K, et al. Specific genetic changes of diagnostic importance in chromophobe renal cell carcinomas. *Lab Invest.* 1997;76(2):203-208.
395. Akhtar M, Tulbah A, Kardar AH, Ali MA. Sarcomatoid renal cell carcinoma: the chromophobe connection. *Am J Surg Pathol.* 1997;21(10):1188-1195.
396. Davis CE, Ricketts CJ, Wang M, et al. The somatic genomic landscape of chromophobe renal cell carcinoma. *Cancer Cell.* 2014;26:319-330.
397. Wilson EJ, Resnick MI, Jacobs G. Sarcomatoid chromophobe renal cell carcinoma: report of an additional case with ultrastructural findings. *J Urol Pathol.* 1999;11:113-122.
398. Amin MB, Paner GP, Alvarado-Cabreiro I, et al. Chromophobe renal cell carcinoma: histomorphologic characteristics and evaluation of conventional pathologic prognostic parameters in 145 cases. *Am J Surg Pathol.* 2008;32(12):1822-1834.
399. Renshaw AA, Henske EP, Loughlin KR, et al. Aggressive variants of chromophobe renal cell carcinoma. *Cancer.* 1996;78(8):1756-1761.
400. Delahunt B, Sika-Paotonu D, Bethwaite PB, et al. Fuhrman grading is not appropriate for chromophobe renal cell carcinoma. *Am J Surg Pathol.* 2007;31:957-960.
401. Tickoo SK, dePeralta-Venturina MN, Harik LR, et al. Spectrum of epithelial neoplasms in end-stage renal disease: an experience from 66 tumor-bearing kidneys with emphasis on histologic patterns distinct from those in sporadic adult renal neoplasia. *Am J Surg Pathol.* 2006;30:141-153.
402. Aron M, Chang E, Herrera L, et al. Clear cell-papillary renal cell carcinoma of the kidney not associated with end-stage renal disease: clinicopathologic correlation with expanded immunophenotypic and molecular characterization of a large cohort with emphasis on relationship with renal angiomyoadenomatous tumor. *Am J Surg Pathol.* 2015;39:873-888.
403. Aydin H, Chen L, Cheng L, et al. Clear cell tubulopapillary renal cell carcinoma: a study of 36 distinctive low-grade epithelial tumors of the kidney. *Am J Surg Pathol.* 2010;34:1608-1621.
404. Raspollini MR, Montagnani I, Montironi R, et al. A contemporary series of renal masses with emphasis on recently recognized entities and tumors of low malignant potential: a report based on 624 consecutive tumors from a single tertiary center. *Pathol Res Pract.* 2017;213:804-808.
405. Zhou H, Zheng S, Truong LD, et al. Clear cell papillary renal cell carcinoma is the fourth most common histologic type of renal cell carcinoma in 290 consecutive nephrectomies for renal cell carcinoma. *Hum Pathol.* 2014;45:59-64.
406. Hes O, Compérat EM, Rioux-Leclercq N. Clear cell papillary renal cell carcinoma, renal angiomyoadenomatous tumor, and renal cell carcinoma with leiomyomatous stroma relationship of 3 types of renal tumors: a review. *Ann Diagn Pathol.* 2016;21:59-64.
407. Mantilla JG, Antic T, Tretiakova M. GATA3 as a valuable marker to distinguish clear cell papillary renal cell carcinomas from morphologic mimics. *Hum Pathol.* 2017;66:152-158.
408. Brunelli M, Erdini F, Cima L, et al. Proximal CD13 versus distal GATA-3 expression in renal neoplasia according to WHO 2016 classification. *Appl Immunohistochem Mol Morphol.* 2016.
409. Gobbo S, Eble JN, Grignon DJ, et al. Clear cell papillary renal cell carcinoma: a distinct histopathologic and molecular genetic entity. *Am J Surg Pathol.* 2008;32:1239-1245.
410. Rohan SM, Xiao Y, Liang Y, et al. Clear-cell papillary renal cell carcinoma: molecular and immunohistochemical analysis with emphasis on the von Hippel-Lindau gene and hypoxia-inducible factor pathway-related proteins. *Mod Pathol.* 2011;24:1207-1220.
411. Adam J, Couturier J, Molinié V, et al. Clear-cell papillary renal cell carcinoma: 24 cases of a distinct low-grade renal tumor and a comparative genomic hybridization array study of seven cases. *Histopathology.* 2011;58:1064-1071.
412. Diolombi ML, Cheng L, Argani P, Epstein JI. Do clear cell papillary renal cell carcinomas have malignant potential? *Am J Surg Pathol.* 2015;39:1621-1634.
413. Williamson SR. What is the malignant potential of clear cell papillary renal cell carcinoma? *Urol Oncol.* 2016;34:420-421.
414. Matoso A, Chen YB, Rao V, et al. Atypical renal cysts: a morphologic, immunohistochemical, and molecular study. *Am J Surg Pathol.* 2016;40:202-211.
415. Brimo F, Atallah C, Li G, Srigley JR. Cystic clear cell papillary renal cell carcinoma: is it related to multilocular clear cell cystic neoplasm of low malignant potential? *Histopathology.* 2016;68:666-672.
416. Williamson SR, Gupta NS, Eble JN, et al. Clear cell renal cell carcinoma with borderline features of clear cell papillary renal cell carcinoma: combined morphologic, immunohistochemical, and cytogenetic analysis. *Am J Surg Pathol.* 2015;39:1502-1510.
417. Dhakal HP, McKenney JK, Khor LY, et al. Renal neoplasms with overlapping features of clear cell renal cell carcinoma and clear cell papillary renal cell carcinoma: a clinicopathologic study of 37 cases from a single institution. *Am J Surg Pathol.* 2016;40:141-154.
418. Parihar A, Tickoo SK, Kumar S, Arora VK. Xp11 translocation renal cell carcinoma morphologically mimicking clear cell-papillary renal cell carcinoma in an adult patient: report of a case expanding the morphologic spectrum of Xp11 translocation renal cell carcinomas. *Int J Surg Pathol.* 2015;23:234-237.
419. Argani P, Zhong M, Reuter VE, et al. TFE3-fusion variant analysis defines specific clinicopathologic associations among Xp11 translocation cancers. *Am J Surg Pathol.* 2016;40:723-737.
420. Argani P, Antonescu CR, Couturier J, et al. PRCC-TFE3 renal carcinomas: morphologic, immunohistochemical, ultrastructural, and molecular analysis of an entity associated with the t(X;1)(p11.2;q21). *Am J Surg Pathol.* 2002;26(12):1553-1566.
421. Argani P, Ladanyi M. The evolving story of renal translocation carcinomas. *Am J Clin Pathol.* 2006;126(3):332-334.
422. Wu A, Kunju LP, Cheng L, Shah RB. Renal cell carcinoma in children and young adults: analysis of clinicopathological, immunohistochemical and molecular characteristics with an emphasis on the spectrum of Xp11.2 translocation-associated and unusual clear cell subtypes. *Histopathology.* 2008;53(5):533-544.
423. Argani P, Antonescu CR, Illei PB, et al. Primary renal neoplasms with the ASPL-TFE3 gene fusion of alveolar soft part sarcoma: a distinctive tumor entity previously included among renal cell carcinomas of children and adolescents. *Am J Pathol.* 2001;159(1):179-192.
424. Argani P, Olgac S, Tickoo SK, et al. Xp11 translocation renal cell carcinoma in adults: expanded clinical, pathologic, and genetic spectrum. *Am J Surg Pathol.* 2007;31(8):1149-1160.
425. Zhong M, Haberman J, Andraws N, et al. Xp11.2 translocation renal cell carcinoma (RCC) in adults—a TMA study of 120 RCC cases. *Lab Invest.* 2009;89(suppl 1):203A.
426. Argani P, Lal P, Hutchinson B, et al. Aberrant nuclear immunoreactivity for TFE3 in neoplasms with TFE3 gene fusions: a sensitive and specific immunohistochemical assay. *Am J Surg Pathol.* 2003;27(6):750-761.

427. Argani P, Hicks J, De Marzo AM, et al. Xp11 translocation renal cell carcinoma (RCC): extended immunohistochemical profile emphasizing novel RCC markers. *Am J Surg Pathol*. 2010;34(9):1295-1303.
428. Argani P, Zhang L, Reuter VE, et al. RBM10-TFE3 renal cell carcinoma: a potential diagnostic pitfall due to cryptic intrachromosomal Xp11.2 inversion resulting in false-negative TFE3 FISH. *Am J Surg Pathol*. 2017;41:655-662.
429. Xia QY, Wang XT, Zhan XM, et al. Xp11 translocation renal cell carcinomas (RCCs): With RBM10-TFE3 gene fusion demonstrating melanotic features and overlapping morphology with t(6;11) RCC: interest and diagnostic pitfall in detecting a paracentric inversion of TFE3. *Am J Surg Pathol*. 2017;41:663-676.
430. Argani P, Lao M, Hutchinson B, et al. Renal carcinomas with the t(6;11)(p21;q12): clinicopathologic features and demonstration of the specific alpha-TFEB gene fusion by immunohistochemistry, RT-PCR, and DNA PCR. *Am J Surg Pathol*. 2005;29(2):230-240.
431. Suzigan S, Drut R, Faria P, et al. Xp11 translocation carcinoma of the kidney presenting with multilocular cystic renal cell carcinoma-like features. *Int J Surg Pathol*. 2007;15(2):199-203.
432. Williamson SR, Grignon DJ, Cheng L, et al. Renal cell carcinoma with chromosome 6p amplification including the TFE3 gene: a novel mechanism of tumor pathogenesis? *Am J Surg Pathol*. 2017;41:287-298.
433. Argani P, Reuter VE, Zhang L, et al. TFE3-amplified renal cell carcinomas: an aggressive molecular subset demonstrating variable melanocytic marker expression and morphologic heterogeneity. *Am J Surg Pathol*. 2016;40:1484-1495.
434. Peckova K, Vanecek T, Martinek P, et al. Aggressive and nonaggressive translocation t(6;11) renal cell carcinoma: comparative study of 6 cases and review of the literature. *Ann Diagn Pathol*. 2014;18:351-357.
435. Argani P, Aulmann S, Karanjawala Z, et al. Melanotic Xp11 translocation renal cancers: a distinctive neoplasm with overlapping features of PEComa, carcinoma, and melanoma. *Am J Surg Pathol*. 2009;33(4):609-619.
436. Fleming S, Lewi HJ. Collecting duct carcinoma of the kidney. *Histopathology*. 1986;10(11):1131-1141.
437. Morell-Quadreny L, Gregori-Romero A, Carda-Batalla C, Llombart-Bosch A. Collecting duct carcinoma of the kidney: a morphologic and DNA flow cytometric study of seven cases. *J Urol Pathol*. 1998;8:69-84.
438. Gupta R, Billis A, Shah RB, et al. Carcinoma of the collecting ducts of Bellini and renal medullary carcinoma: clinicopathologic analysis of 52 cases of rare aggressive subtypes of renal cell carcinoma with a focus on their interrelationship. *Am J Surg Pathol*. 2012;36:1265-1278.
439. Fuzesi L, Cober M, Mittermayer C. Collecting duct carcinoma: cytogenetic characterization. *Histopathology*. 1992;21(2):155-160.
440. Osunkoya AO, Young AN, Wang W, et al. Comparison of gene expression profiles in tubulocystic carcinoma and collecting duct carcinoma of the kidney. *Am J Surg Pathol*. 2009;33(7):1103-1106.
441. Amin MB, Gupta R, Osunkoya AO, et al. Carcinoma of collecting ducts of Bellini: analysis of 27 distinctive cases of renal cell carcinoma with aggressive clinical behaviour. *Lab Invest*. 2009;89(suppl 1):157A.
442. Srigley JR, Eble JN. Collecting duct carcinoma of kidney. *Semin Diagn Pathol*. 1998;15(1):54-67.
443. Sirohi D, Smith SC, Ohe C, et al. Renal cell carcinoma, unclassified with medullary phenotype: poorly-differentiated adenocarcinomas overlapping with renal medullary carcinoma. *Hum Pathol*. 2017;[epub ahead of print].
444. Colombo P, Smith SC, Massa S, et al. Unclassified renal cell carcinoma with medullary phenotype versus renal medullary carcinoma: lessons from diagnosis in an Italian man found to harbor sickle cell trait. *Urol Case Rep*. 2015;3:215-218.
445. Amin MB, Smith SC, Agaimy A, et al. Collecting duct carcinoma versus renal medullary carcinoma: an appeal for nosologic and biological clarity. *Am J Surg Pathol*. 2014;28:871-874.
446. Chen YB, Brannon AR, Toubaji A, et al. Hereditary leiomyomatosis and renal cell carcinoma syndrome-associated renal cancer: recognition of the syndrome by pathologic features and the utility of detecting aberrant succination by immunohistochemistry. *Am J Surg Pathol*. 2014;38:627-637.
447. Toro JR, Nickerson ML, Wei MH, et al. Mutations in the fumurate hydratase gene cause hereditary leiomyomatosis and renal cell cancer in families in North America. *Am J Hum Genet*. 2003;73:95-106.
448. Trpkov K, Hes O, Agaimy A, et al. Fumarate hydratase-deficient renal cell carcinoma is strongly correlated with fumurate hydratase mutation and hereditary leiomyomatosis and renal cell carcinoma syndrome. *Am J Surg Pathol*. 2016;40:865-875.
449. Smith SC, Trpkov K, Chen YB, et al. Tubulocystic carcinoma of the kidney with poorly differentiated foci: a frequent morphologic pattern of fumurate hydratase-deficient renal cell carcinoma. *Am J Surg Pathol*. 2016;40:1457-1472.
450. Smith SC, Sirohi D, Ohe C, et al. A distinctive, low-grade oncocytic fumurate hydratase-deficient renal cell carcinoma, morphologically reminiscent of succinate dehydrogenase-deficient renal cell carcinoma. *Histopathology*. 2017;71:42-52.
451. Linehan WM, Spellman PT, Ricketts CJ, et al. Comprehensive molecular characterization of papillary renal-cell carcinoma. *N Engl J Med*. 2015;374(2):135-145.
452. Adsay NV, deRoux SJ, Sakr W, Grignon D. Cancer as a marker of genetic medical disease: an unusual case of medullary carcinoma of the kidney. *Am J Surg Pathol*. 1998;22(2):260-264.
453. Bruno D, Wigfall DR, Zimmerman SA, et al. Genitourinary complications of sickle cell disease. *J Urol*. 2001;166(3):803-811.
454. Eble JN. Renal medullary carcinoma: a distinct entity emerges from the confusion of 'collecting duct carcinoma'. *Adv Anat Pathol*. 1996;3:233-238.
455. Rodriguez-Jurado R, Gonzalez-Crussi F. Renal medullary carcinoma: immunohistochemical and ultrastructural observations. *J Urol Pathol*. 1996;4:191-203.
456. Liu Q, Wrathall L, Galli S, et al. Renal medullary carcinoma: molecular, IHC, and pathologic correlation. *Lab Invest*. 2009;89(suppl 1):179A.
457. Davis CJ Jr, Mostofi FK, Sesterhenn IA. Renal medullary carcinoma. The seventh sickle cell nephropathy. *Am J Surg Pathol*. 1995;19(1):1-11.
458. Cheng JX, Tretiakova M, Gong C, et al. Renal medullary carcinoma: rhabdoid features and the absence of INI1 expression as markers of aggressive behavior. *Mod Pathol*. 2008;21(6):647-652.
459. Debelenko LV, Raimondi SC, Daw N, et al. Renal cell carcinoma with novel VCL-ALK fusion: new representative of ALK-associated tumor spectrum. *Mod Pathol*. 2011;24:430-442.
460. Mariño-Enríquez A, Ou WB, Weldon CB, et al. ALK rearrangement in sickle cell trait-associated renal medullary carcinoma. *Genes Chromosomes Cancer*. 2011;50:146-153.
461. Smith NE, Deyrup AT, Mariño-Enríquez A, et al. VCL-ALK renal cell carcinoma in children with sickle-cell trait: the eighth sickle-cell nephropathy? *Am J Surg Pathol*. 2014;38:858-863.
462. Amin MB, MacLennan GT, Gupta R, et al. Tubulocystic carcinoma of the kidney: clinicopathologic analysis of 31 cases of a distinctive rare subtype of renal cell carcinoma. *Am J Surg Pathol*. 2009;33(3):384-392.
463. Yang XJ, Zhou M, Hes O, et al. Tubulocystic carcinoma of the kidney: clinicopathologic and molecular characterization. *Am J Surg Pathol*. 2008;32:177-187.
464. Al-Hussain TO, Cheng L, Zhang S, Epstein JI. Tubulocystic carcinoma of the kidney with poorly differentiated foci: a series of 3 cases with fluorescence in situ hybridization analysis. *Hum Pathol*. 2013;44:1406-1411.
465. Ulamec M1, Skenderi F, Zhou M, et al. Molecular genetic alterations in renal cell carcinomas with tubulocystic pattern: tubulocystic renal cell carcinoma, tubulocystic renal cell carcinoma with heterogenous component and familial leiomyomatosis-associated renal cell carcinoma. Clinicopathologic and molecular genetic analysis of 15 cases. *Appl Immunohistochemistry Mol Morphol*. 2016;24:521-530.
466. Chen N, Nie L, Gong J, et al. Gains of chromosomes 7 and 17 in tubulocystic carcinoma of kidney: two cases with fluorescence in situ hybridisation analysis. *J Clin Pathol*. 2014;67:1006-1009.
467. Zhou M, Yang XJ, Lopez JL, et al. Renal tubulocystic carcinoma is closely related to papillary renal cell carcinoma: implications for pathologic classification. *Am J Surg Pathol*. 2009;33:1840-1849.
468. Aubert S, Duchene F, Augusto D, et al. Low-grade tubular myxoid renal tumors: a clinicopathological study of 3 cases. *Int J Surg Pathol*. 2004;12(2):179-183.
469. Ferlicot S, Allory Y, Comperat E, et al. Mucinous tubular and spindle cell carcinoma: a report of 15 cases and a review of the literature. *Virchows Arch*. 2005;447(6):978-983.
470. Parwani AV, Husain AN, Epstein JI, et al. Low-grade myxoid renal epithelial neoplasms with distal nephron differentiation. *Hum Pathol*. 2001;32(5):506-512.
471. Fine SW, Argani P, DeMarzo AM, et al. Expanding the histologic spectrum of mucinous tubular and spindle cell carcinoma of the kidney. *Am J Surg Pathol*. 2006;30(12):1554-1560.
472. Jung SJ, Yoon HK, Chung JI, et al. Mucinous tubular and spindle cell carcinoma of the kidney with neuroendocrine differentiation: report of two cases. *Am J Clin Pathol*. 2006;125(1):99-104.
473. Paner GP, Srigley JR, Radhakrishnan A, et al. Immunohistochemical analysis of mucinous tubular and spindle cell carcinoma and papillary renal cell carcinoma of the kidney: significant immunophenotypic overlap warrants diagnostic caution. *Am J Surg Pathol*. 2006;30(1):13-19.
474. Cossu-Rocca P, Eble JN, Delahunt B, et al. Renal mucinous tubular and spindle carcinoma lacks the gains of chromosomes 7 and 17 and losses of chromosome Y that are prevalent in papillary renal cell carcinoma. *Mod Pathol*. 2006;19(4):488-493.
475. Argani P, Netto GJ, Parwani AV. Papillary renal cell carcinoma with low-grade spindle cell foci: a mimic of mucinous tubular and

- spindle cell carcinoma. *Am J Surg Pathol*. 2008;32(9):1353-1359.
476. Shen SS, Ro JY, Tamboli P, et al. Mucinous tubular and spindle cell carcinoma of kidney is probably a variant of papillary renal cell carcinoma with spindle cell features. *Ann Diagn Pathol*. 2007;11(1):13-21.
477. Mehra R, Vats P, Cieslik M, et al. Biallelic alteration and dysregulation of the hippo pathway in mucinous tubular and spindle cell carcinoma of the kidney. *Cancer Discov*. 2016;6:1258-1266.
478. Dhillon J, Amin MB, Selbs E, et al. Mucinous tubular and spindle cell carcinoma of the kidney with sarcomatoid change. *Am J Surg Pathol*. 2009;33(1):44-49.
479. Gehrig JJ Jr, Gottheiner TI, Swenson RS. Acquired cystic disease of the end-stage kidney. *Am J Med*. 1985;79:609-620.
480. Rioux-Leclercq NC, Epstein JI. Renal cell carcinoma with intratumoral calcium oxalate crystal deposition in patients with acquired cystic disease of the kidney. *Arch Pathol Lab Med*. 2003;127:E89-E92.
481. Sule N, Yakupoglu U, Shen SS, et al. Calcium oxalate deposition in renal cell carcinoma associated with acquired cystic kidney disease: a comprehensive study. *Am J Surg Pathol*. 2005;29:443-451.
482. Kuroda N, Tamura M, Hamaguchi N, et al. Acquired cystic disease-associated renal cell carcinoma with sarcomatoid change and rhabdoid features. *Ann Diagn Pathol*. 2011;15:462-466.
483. Trpkov K, Hes O, Bonert M, et al. Eosinophilic, solid, and cystic renal cell carcinoma: clinicopathologic study of 16 unique, sporadic neoplasms occurring in women. *Am J Surg Pathol*. 2016;40:60-71.
484. Trpkov K, Abou-Ouf H, Hes O, et al. Eosinophilic solid and cystic renal cell carcinoma (ESC RCC): further morphologic and molecular characterization of ESC RCC as a distinct entity. *Am J Surg Pathol*. 2017;41(10):1299-1308.
485. Cheng L, Amin MB, Lopez-Beltran A, Montironi R. Unclassified renal cell carcinoma. In: Moch H, Humphrey PA, Ulbright TM, Reuter VE, eds. *WHO Classification of Tumours of the Urinary System and Male Genital Organs*. Lyon: IARC Press; 2016.
486. Chen YB, Xu J, Skanderup AJ, et al. Molecular analysis of aggressive renal cell carcinoma with unclassified histology reveals distinct subsets. *Nat Commun*. 2016;7:13131.
487. Kuhn E, De Andra J, Manoni S, et al. Renal cell carcinoma associated with prominent angiomyoimoma-like proliferation: report of 5 cases and review of the literature. *Am J Surg Pathol*. 2006;30(11):1372-1381.
488. Brunelli M, Menestrina F, Segala D, et al. Renal cell carcinoma associated with prominent leiomyomatous proliferation appears not to be a variant of clear cell renal cell carcinoma. *Lab Invest*. 2009;89(suppl 1):160A.
489. Michal M, Hes O, Nemcova J, et al. Renal angiomyoadenomatous tumor: morphologic, immunohistochemical, and molecular genetic study of a distinct entity. *Virchows Arch*. 2009;454(1):89-99.
490. Shannon BA, Cohen RJ, Segal A, et al. Clear cell renal cell carcinoma with smooth muscle stroma. *Hum Pathol*. 2009;40(3):425-429.
491. Lan TT, Keller-Ramey J, Fitzpatrick C, et al. Unclassified renal cell carcinoma with tubulopapillary architecture, clear cell phenotype, and chromosome 8 monosomy: a new kid on the block. *Virchows Arch*. 2016;469:81-91.
492. Hakimi AA, Tickoo SK, Jacobsen A, et al. TCEB1-mutated renal cell carcinoma: a distinct genomic and morphological subtype. *Mod Pathol*. 2015;28:845-853.
493. Williamson SR, Cheng L, Eble JN, et al. Renal cell carcinoma with angiomyoimoma-like stroma: clinicopathological, immunohistochemical, and molecular features supporting classification as a distinct entity. *Mod Pathol*. 2015;28:279-294.
494. Amin MB, Gupta R, Ondrej H, et al. Primary thyroid-like follicular carcinoma of the kidney: report of 6 cases of a histologically distinctive adult renal epithelial neoplasm. *Am J Surg Pathol*. 2009;33(3):393-400.
495. Jung SJ, Chung JI, Park SH, et al. Thyroid follicular carcinoma-like tumor of kidney: a case report with morphologic, immunohistochemical, and genetic analysis. *Am J Surg Pathol*. 2006;30(3):411-415.
496. Sterlacci W, Verderfer I, Gabriel M, Mikuz G. Thyroid follicular carcinoma-like renal tumor: a case report with morphologic, immunophenotypic, cytogenetic, and scintigraphic studies. *Virchows Arch*. 2008;452(1):91-95.
497. Bonsib SM, Gibson D, Mhoon M, Greene GF. Renal sinus involvement in renal cell carcinomas. *Am J Surg Pathol*. 2000;24(3):451-458.
498. Bonsib SM. The renal sinus is the principal invasive pathway: a prospective study of 100 renal cell carcinomas. *Am J Surg Pathol*. 2004;28(12):1594-1600.
499. Thompson RH, Blute ML, Krambeck AE, et al. Patients with pT1 renal cell carcinoma who die from disease after nephrectomy may have unrecognized renal sinus fat invasion. *Am J Surg Pathol*. 2007;31(7):1089-1093.
500. Holland JM. Proceedings: cancer of the kidney—natural history and staging. *Cancer*. 1973;32(5):1030-1042.
501. Gurney H, Larcos G, McKay M, et al. Bone metastases in hypernephroma. Frequency of scapular involvement. *Cancer*. 1989;64(7):1429-1431.
502. Troncoso A, Ro JY, Grignon DJ, et al. Renal cell carcinoma with acrometastasis: report of two cases and review of the literature. *Mod Pathol*. 1991;4(1):66-69.
503. Insabato L, De Rosa G, Franco R, et al. Ovarian metastasis from renal cell carcinoma: a report of three cases. *Int J Surg Pathol*. 2003;11(4):309-312.
504. Datta MW, Ulbright TM, Young RH. Renal cell carcinoma metastatic to the testis and its adnexa: a report of five cases including three that accounted for the initial clinical presentation. *Int J Surg Pathol*. 2001;9(1):49-56.
505. Leung CS, Srigley JR, Robertson AR. Metastatic renal cell carcinoma presenting as solitary bleeding prostatic metastasis. *J Urol Pathol*. 1997;7:127-132.
506. Marlowe SD, Swartz JD, Koenigsberg R, et al. Metastatic hypernephroma to the larynx: an unusual presentation. *Neuroradiology*. 1993;35(3):242-243.
507. Matias-Guiu X, Garcia A, Curell R, Prat J. Renal cell carcinoma metastatic to the thyroid gland: a comparative molecular study between the primary and the metastatic tumor. *Endocr Pathol*. 1998;9(3):255-260.
508. Melnick SJ, Amazon K, Dembrow V. Metastatic renal cell carcinoma presenting as a parotid tumor: a case report with immunohistochemical findings and a review of the literature. *Hum Pathol*. 1989;20(2):195-197.
509. Nishio S, Tsukamoto H, Fukui M, Matsubara T. Hypophyseal metastatic hypernephroma mimicking a pituitary adenoma. Case report. *Neurosurg Rev*. 1992;15(4):319-322.
510. Okabe Y, Ohoka H, Miwa T, et al. View from beneath: pathology in focus. Renal cell carcinoma metastasis to the tongue. *J Laryngol Otol*. 1992;106(3):282-284.
511. Sim SI, Ro JY, Ordonez NG, et al. Metastatic renal cell carcinoma to the bladder: a clinicopathologic and immunohistochemical study. *Mod Pathol*. 1999;12(4):351-355.
512. Radley MG, McDonald JV, Pilcher WH, Wilbur DC. Late solitary cerebral metastases from renal cell carcinoma: report of two cases. *Surg Neurol*. 1993;39(3):230-234.
513. Saitoh H, Hida M, Nakamura K, et al. Metastatic processes and a potential indication of treatment for metastatic lesions of renal adenocarcinoma. *J Urol*. 1982;128(5):916-918.
514. Young RH, Hart WR. Renal cell carcinoma metastatic to the ovary: a report of three cases emphasizing possible confusion with ovarian clear cell adenocarcinoma. *Int J Gynecol Pathol*. 1992;11(2):96-104.
515. Foucar E, Dehner LP. Renal cell carcinoma occurring with contralateral adrenal metastasis: a clinical and pathological trap. *Arch Surg*. 1979;114(8):959-963.
516. Preview SR, Wilscher MK, Burke CR. Renal cell carcinoma with solitary contralateral adrenal metastasis: experience with 2 cases. *J Urol*. 1982;128(1):132-134.
517. Wick MR, Cherwitz DL, McGlennen RC, Dehner LP. Adrenocortical carcinoma. An immunohistochemical comparison with renal cell carcinoma. *Am J Pathol*. 1986;122(2):343-352.
518. McNichols DW, Segura JW, DeWeerd JH. Renal cell carcinoma: long-term survival and late recurrence. *J Urol*. 1981;126(1):17-23.
519. Shah IA, Haddad FS, Wheeler L, Chinichian A. Metastatic renal cell carcinoma: late recurrence and prolonged survival. *J Urol Pathol*. 1996;4:289-298.
520. Fairlamb DJ. Spontaneous regression of metastases of renal cancer: a report of two cases including the first recorded regression following irradiation of a dominant metastasis and review of the world literature. *Cancer*. 1981;47(8):2102-2106.
521. Garfield DH, Kennedy BJ. Regression of metastatic renal cell carcinoma following nephrectomy. *Cancer*. 1972;30(1):190-196.
522. Aizawa S, Suzuki M, Kikuchi Y, et al. Clinicopathological study on small renal cell carcinomas with metastases. *Acta Pathol Jpn*. 1987;37(6):947-954.
523. Berger A, Brandina R, Atalla MA, et al. Laparoscopic radical nephrectomy for renal cell carcinoma: oncological outcomes at 10 years or more. *J Urol*. 2009;182(5):2172-2176.
524. Bissada NK. Renal cell adenocarcinoma. *Surg Gynecol Obstet*. 1977;145(1):97-104.
525. deKernion JB, Berry D. The diagnosis and treatment of renal cell carcinoma. *Cancer*. 1980;45(7 suppl):1947-1956.
526. Robson CJ, Churchill BM, Anderson W. The results of radical nephrectomy for renal cell carcinoma. *Trans Am Assoc Genitourin Surg*. 1968;60:122-129.
527. Waters WB, Richie JP. Aggressive surgical approach to renal cell carcinoma: review of 130 cases. *J Urol*. 1979;122(3):306-309.
528. Rini BI, Garcia J, Elson P, et al. The effect of sunitinib on primary renal cell carcinoma and facilitation of subsequent surgery. *J Urol*. 2012;187:1548-1554.
529. Frydenberg M, Malek RS, Zincke H. Conservative renal surgery for renal cell carcinoma in von Hippel-Lindau's disease. *J Urol*. 1993;149(3):461-464.
530. Lund GO, Fallon B, Curtis MA, Williams RD. Conservative surgical therapy of localized renal cell carcinoma in von Hippel-Lindau disease. *Cancer*. 1994;74(9):2541-2545.
531. Marshall FF, Walsh PC. In situ management of renal tumors: renal cell carcinoma and transitional cell carcinoma. *J Urol*. 1984;131(6):1045-1049.

532. Novick AC. Partial nephrectomy for renal cell carcinoma. *Urol Clin North Am*. 1987;14(2):419-433.
533. Topley M, Novick AC, Montie JE. Long-term results following partial nephrectomy for localized renal adenocarcinoma. *J Urol*. 1984;131(6):1050-1052.
534. Steinbach F, Stockle M, Muller SC, et al. Conservative surgery of renal cell tumors in 140 patients: 21 years of experience. *J Urol*. 1992;148(1):24-29, discussion 29-30.
535. Stephens R, Graham SD Jr. Enucleation of tumor versus partial nephrectomy as conservative treatment of renal cell carcinoma. *Cancer*. 1990;65(12):2663-2667.
536. Atkins MB, Dutcher J, Weiss G, et al. Kidney cancer: the Cytokine Working Group experience (1986-2001): part I. IL-2-based clinical trials. *Med Oncol*. 2001;18(3):197-207.
537. Nathan PD, Eisen TG. The biological treatment of renal-cell carcinoma and melanoma. *Lancet Oncol*. 2002;3(2):89-96.
538. Pantuck AJ, Zisman A, Belldegrun A. Gene and immune therapy for renal cell carcinoma. *Int J Urol*. 2001;8(7):S1-S4.
539. Herrmann E, Bierer S, Wulffing C. Update on systemic therapies of metastatic renal cell carcinoma. *World J Urol*. 2010;28(3):303-309.
540. Cheville JC, Lohse CM, Zincke H, et al. Comparisons of outcome and prognostic features among histologic subtypes of renal cell carcinoma. *Am J Surg Pathol*. 2003;27(5):612-624.
541. Rini B, McKiernan JM, Chang SS, et al. Amin MB, ed. *AJCC Cancer Staging Manual*. 8th ed. New York: Springer; 2017.
542. Bonsib SM, Gibson D, Mhoon M, Greene GE. Renal sinus involvement in renal cell carcinomas. *Am J Surg Pathol*. 2000;24:451-458.
543. Bonsib SM. T2 clear cell renal cell carcinoma is a rare entity: a study of 120 clear cell renal cell carcinomas. *Am J Surg Pathol*. 2005;174:1199-1202.
544. Trpkov K, Grignon DJ, Bonsib SM, et al. Handling and staging of renal cell carcinoma: the International Society of Urological Pathology Consensus (ISUP) conference recommendations. *Am J Surg Pathol*. 2013;37:1505-1517.
545. Jung SJ, Ro JY, Truong LD, et al. Reappraisal of T3N0/NxM0 renal cell carcinoma: significance of extent of fat invasion, renal vein invasion, and adrenal invasion. *Hum Pathol*. 2008;39(11):1689-1694.
546. Sell C, Hinshaw WM, Woodard BH, Paulson DF. Stratification of risk factors in renal cell carcinoma. *Cancer*. 1984;52:270-275.
547. Fuhrman SA, Lasky LC, Limas C. Prognostic significance of morphologic parameters in renal cell carcinoma. *Am J Surg Pathol*. 1982;6(7):655-663.
548. Kay S. Renal carcinoma. A 10-year study. *Am J Clin Pathol*. 1968;50(4):428-432.
549. Medeiros LJ, Gelb AB, Weiss LM. Renal cell carcinoma. Prognostic significance of morphologic parameters in 21 cases. *Cancer*. 1988;61:1639-1651.
550. Delahunt B, Kittelson JM, McCredie MR, et al. Prognostic importance of tumor size for localized conventional (clear cell) renal cell carcinoma: assessment of TNM T1 and T2 tumor categories and comparison with other prognostic parameters. *Cancer*. 2002;94(3):658-664.
551. Elmore JM, Kadesky KT, Koeneman KS, Sagalowsky AI. Reassessment of the 1997 TNM classification system for renal cell carcinoma: a 5-cm T1/T2 cutoff is a better predictor of clinical outcome. *Cancer*. 2003;98:2329-2334.
552. Kinouchi T, Saiki S, Meguro N, et al. Impact of tumor size on the clinical outcomes of patients with Robson Stage I renal cell carcinoma. *Cancer*. 1999;85(3):689-695.
553. Herrera LP, Jorda M, Reis I, et al. The potential value of a simple two-level grading system for renal cell carcinomas. *Lab Invest*. 2009;89(suppl 1):172A.
554. Mrstil C, Salamon J, Weber R, Stoger Mayer F. Microscopic venous infiltration as predictor of relapse in renal cell carcinoma. *J Urol*. 1992;148(2 Pt 1):271-274.
555. Van Poppel H, Vandendriessche H, Boel K, et al. Microscopic vascular invasion is the most relevant prognosticator after radical nephrectomy for clinically nonmetastatic renal cell carcinoma. *J Urol*. 1997;158(1):45-49.
556. Lanigan D, Conroy R, Barry-Walsh C, et al. A comparative analysis of grading systems in renal adenocarcinoma. *Histopathology*. 1994;24(5):473-476.
557. Medeiros LJ, Jones EC, Aizawa S, et al. Grading of renal cell carcinoma: Workgroup No. 2. Union Internationale Contre le Cancer and the American Joint Committee on Cancer (AJCC). *Cancer*. 1997;80(5):990-991.
558. Minervini A, Lilas L, Minervini R, Sell C. Prognostic value of nuclear grading in patients with intracapsular (pT1-pT2) renal cell carcinoma. Long-term analysis in 213 patients. *Cancer*. 2002;94(10):2590-2595.
559. Sika-Paotonu D, Bethwaite PB, McCredie MR, et al. Nucleolar grade but not Fuhrman grade is applicable to papillary renal cell carcinoma. *Am J Surg Pathol*. 2006;30:1091-1096.
560. Gelb AB, Shibuya RB, Weiss LM, Medeiros LJ. Stage I renal cell carcinoma. A clinicopathologic study of 82 cases. *Am J Surg Pathol*. 1993;17(3):275-286.
561. Delahunt B, Cheville JC, Martignoni G, et al. The International Society of Urological Pathology (ISUP) grading system for renal cell carcinoma and other prognostic parameters. *Am J Surg Pathol*. 2013;37:1490-1504.
562. Dagher J, Delahunt B, Rioux-Leclercq N, et al. Clear cell renal cell carcinoma: validation of WHO/ISUP grading. *Histopathol*. 2017.
563. Lohse CM, Blute ML, Zincke H, et al. Comparison of standardized and nonstandardized nuclear grade of renal cell carcinoma to predict outcome among 2,042 patients. *Am J Clin Pathol*. 2002;118(6):877-886.
564. Montironi R, Santinelli A, Pomante R, et al. Morphometric index of adult renal cell carcinoma. Comparison with the Fuhrman grading system. *Virchows Arch*. 2000;437(1):82-89.
565. Pound CR, Partin AW, Epstein JI, et al. Nuclear morphometry accurately predicts recurrence in clinically localized renal cell carcinoma. *Urology*. 1993;42(3):243-248.
566. Sengupta S, Lohse CM, Leibovich BC, et al. Histologic coagulative tumor necrosis as a prognostic indicator of renal cell carcinoma aggressiveness. *Cancer*. 2005;104(3):511-520.
567. Khor LY, Dhakal HP, Jia X, et al. Tumor necrosis adds prognostically significant information to grade in clear cell renal cell carcinoma: a study of 842 consecutive cases from a single institution. *Am J Surg Pathol*. 2016;40:1224-1231.
568. Delahunt B, McKenney JK, Lohse CM, et al. A novel grading system for clear cell renal cell carcinoma incorporating tumor necrosis. *Am J Surg Pathol*. 2013;37:311-322.
569. Delahunt B, Eble JN. Papillary adenoma of the kidney: an evolving concept. *J Urol Pathol*. 1997;7:99-112.
570. Grignon DJ, Eble JN. Papillary and metanephric adenomas of the kidney. *Semin Diagn Pathol*. 1998;15(1):41-53.
571. Ligato S, Ro JY, Tamboli P, et al. Benign tumors and tumor-like lesions of the adult kidney. Part I: benign renal epithelial neoplasms. *Adv Anat Pathol*. 1999;6(1):1-11.
572. Eble J, Moch H, Amin MB, et al. Papillary adenoma. In: Moch H, Humphrey PA, Ulbright TM, Reuter VE, eds. *WHO Classification of Tumours of the Urinary System and Male Genital Organs*. Lyon: IARC Press; 2016.
573. Suzuki M, Nikaido T, Ikegami M, et al. Renal adenoma. Clinicopathological and histochemical studies. *Acta Pathol Jpn*. 1989;39(11):731-736.
574. Hughson MD, Hennigar GR, McManus JF. Atypical cysts, acquired renal cystic disease, and renal cell tumors in end stage dialysis kidneys. *Lab Invest*. 1980;42(4):475-480.
575. Kobs DGI, Crotty K, Orihuela E, Cowan DF. Renal adenomatosis in acquired renal cystic disease without dialysis. *J Urol Pathol*. 1996;4:273-282.
576. Perez-Ordonez B, Hamed G, Campbell S, et al. Renal oncocytoma: a clinicopathologic study of 70 cases. *Am J Surg Pathol*. 1997;21(8):871-883.
577. Choi H, Almagro UA, McManus JT, et al. Renal oncocytoma. A clinicopathologic study. *Cancer*. 1983;51(10):1887-1896.
578. Kadesky KT, Fulgham PF. Bilateral multifocal renal oncocytoma: case report and review of the literature. *J Urol*. 1993;150(4):1227-1228.
579. Hes O, Michal M, Sima R, et al. Renal oncocytoma with and without intravascular extension into the branches of renal vein have the same morphological, immunohistochemical and genetic features. *Virchows Arch*. 2008;452(3):285-293.
580. Trpkov K, Yilmaz A, Uzer D, et al. Renal oncocytoma revisited: a clinicopathological study of 109 cases with emphasis on problematic diagnostic features. *Histopathol*. 2010;57:893-906.
581. Wobker SE, et al. Renal oncocytoma with vascular invasion: a series of 22 cases. *Hum Pathol*. 2016;58:1-6.
582. Amin MB, Crotty TB, Tickoo SK, Farrow GM. Renal oncocytoma: a reappraisal of morphologic features with clinicopathologic findings in 80 cases. *Am J Surg Pathol*. 1997;21:1-12.
583. Davidson AJ, Hayes WS, Hartman DS, et al. Renal oncocytoma and carcinoma: failure of differentiation with CT. *Radiology*. 1993;186(3):693-696.
584. Lieber MM, Tomera KM, Farrow GM. Renal oncocytoma. *J Urol*. 1981;125:481-485.
585. Barnes CA, Beckman EN. Renal oncocytoma and its congeners. *Am J Clin Pathol*. 1983;79(3):312-318.
586. Merino MJ, Livolsi VA. Oncocytomas of the kidney. *Cancer*. 1982;50(9):1852-1856.
587. Hes O, Michal M, Boudova L, et al. Small cell variant of renal oncocytoma—a rare and misleading type of benign renal tumor. *Int J Surg Pathol*. 2001;9(3):215-222.
588. Shimazaki H, Tanaka K, Aida S, et al. Renal oncocytoma with intracytoplasmic lumina: a case report with ultrastructural findings of “oncoblasts”. *Ultrastruct Pathol*. 2001;25(2):153-158.
589. Lefevre M, Couturier J, Sibony M, et al. Adult papillary renal tumor with oncocytic cells: clinicopathologic, immunohistochemical, and cytogenetic features of ten cases. *Am J Surg Pathol*. 2005;29:1576-1581.
590. Li G, Barthelemy A, Feng G, et al. S100A1: a powerful marker to differentiate chromophobe renal cell carcinoma from renal oncocytoma. *Histopathology*. 2007;50(5):642-647.
591. Hes O, Michal M, Kuroda N, et al. Vimentin reactivity in renal oncocytoma: immunohistochemical study of 234 cases. *Arch Pathol Lab Med*. 2007;131(12):1782-1788.

592. Pitz S, Moll R, Storkel S, Thoenes W. Expression of intermediate filament proteins in subtypes of renal cell carcinomas and in renal oncocytomas. Distinction of two classes of renal cell tumors. *Lab Invest*. 1987;56(6):642-653.
593. Zhou M, Roma A, Magi-Galluzzi C. The usefulness of immunohistochemical markers in the differential diagnosis of renal neoplasms. *Clin Lab Med*. 2005;25:247-257.
594. Wu SL, Kothari P, Wheeler TM, et al. Cytokeratins 7 and 20 immunoreactivity in chromophobe renal cell carcinomas and renal oncocytomas. *Mod Pathol*. 2002;15(7):712-717.
595. Chang A, Harawi SJ. Oncocytes, oncocytosis, and oncocytic tumors. *Pathol Ann*. 1992;27(Pt 1):263-304.
596. Eble JN, Hull MT. Morphologic features of renal oncocytoma: a light and electron microscopic study. *Hum Pathol*. 1984;15(11):1054-1061.
597. Lloreta-Trull J, Serrano S. Biology and pathology of the mitochondrion. *Ultrastruct Pathol*. 1998;22(5):357-367.
598. Tallini G. Oncocytic tumours. *Virchows Arch*. 1998;433(1):5-12.
599. Paner GP, Lindgren V, Jacobson K, et al. High incidence of chromosome 1 abnormalities in a series of 27 renal oncocytomas: cytogenetic and fluorescence in situ hybridization studies. *Arch Pathol Lab Med*. 2007;131(1):81-85.
600. Brunelli M1, Delahunt B, Gobbo S, et al. Diagnostic usefulness of fluorescent cytogenetics in differentiating chromophobe renal cell carcinoma from renal oncocytoma: a validation study combining metaphase and interphase analyses. *Am J Clin Pathol*. 2010;133:116-126.
601. Alanen KA, Efkors TO, Lipasti JA, Nurmi MJ. Renal oncocytoma: the incidence of 18 surgical and 12 autopsy cases. *Histopathology*. 1984;8(5):731-737.
602. Davis CJ, Sesterhenn IA, Mostofi FK, Ho CK. Renal oncocytoma. Clinicopathological study of 166 patients. *J Urogen Pathol*. 1991;1:41-52.
603. Klein MJ, Valensi QJ. Proximal tubular adenomas of kidney with so-called oncocytic features. A clinicopathologic study of 13 cases of a rarely reported neoplasm. *Cancer*. 1976;38(2):906-914.
604. Lewi HJE, Alexander CA, Fleming S. Renal oncocytoma. *Br J Urol*. 1986;58:12-15.
605. Medeiros LJ, Gelb AB, Weiss LM. Low-grade renal cell carcinoma. A clinicopathologic study of 53 cases. *Am J Surg Pathol*. 1987;11(8):633-642.
606. Dishong KM, Quick CM, Gokden N. Renal oncocytomas with atypical features: a clinicopathologic analysis of 34 cases. *Lab Invest*. 2009;89(suppl 1):166A.
607. Ulzer D, Yilmaz A, Bismar T, Trpkov K. Worrisome and atypical features in renal oncocytoma: clinicopathological analysis of 76 cases. *Lab Invest*. 2009;89(suppl 1):199A.
608. Tickoo SK, Amin MB. Discriminant nuclear features of renal oncocytoma and chromophobe renal cell carcinoma. Analysis of their potential utility in the differential diagnosis. *Am J Clin Pathol*. 1998;110(6):782-787.
609. Chen TS, McNally M, Hulbert W, et al. Renal oncocytoma presenting in childhood: a case report. *Int J Surg Pathol*. 2003;11(4):325-329.
610. Gobbo S, Eble JN, Delahunt B, et al. Renal cell neoplasms of oncocytosis have distinct morphologic, immunohistochemical, and cytogenetic profiles. *Am J Surg Pathol*. 2010;34(5):620-626.
611. Capella C, Eusebi V, Rosai J. Primary oat cell carcinoma of the kidney. *Am J Surg Pathol*. 1984;8(11):855-861.
612. Gonzalez-Lois C, Madero S, Redondo P, et al. Small cell carcinoma of the kidney: a case report and review of the literature. *Arch Pathol Lab Med*. 2001;125(6):796-798.
613. Lane BR, Chery F, Jour G, et al. Renal neuroendocrine tumours: a clinicopathological study. *BJU Int*. 2007;100:1030-1035.
614. Morgan KG, Banerjee SS, Eyden BP, Barnard RJ. Primary small cell neuroendocrine carcinoma of the kidney. *Ultrastruct Pathol*. 1996;20(2):141-144.
615. Tetu B, Ro JY, Ayala AG, et al. Small cell carcinoma of the kidney. A clinicopathologic, immunohistochemical, and ultrastructural study. *Cancer*. 1987;60(8):1809-1814.
616. Essenfeld H, Manivel JC, Benedette P, Albores-Saavedra J. Small cell carcinoma of the renal pelvis. A clinicopathologic, morphologic and histochemical study of 2 cases. *J Urol*. 1991;144:344-347.
617. La Rosa S, Bernasconi B, Micello D, et al. Primary small cell neuroendocrine carcinoma of the kidney: morphological, immunohistochemical, ultrastructural, and cytogenetic study of a case and review of the literature. *Endocr Pathol*. 2009;20(1):24-34.
618. Mills SE, Weiss MA, Swanson PE, Wick MR. Small cell undifferentiated carcinoma of the renal pelvis. A light microscopic, immunocytochemical, and ultrastructural study. *Surg Pathol*. 1988;1:83-88.
619. Bégin LR, Jamison BM. Renal carcinoid—a tumor of probable hindgut neuroendocrine phenotype. Report of a case and literature review. *J Urol Pathol*. 1993;3:269-282.
620. Unger PD, Russell A, Thung SN, Gordon RE. Primary renal carcinoid. *Arch Pathol Lab Med*. 1990;114(1):68-71.
621. Zaki FG, Jindra K, Capozzi F. Carcinoidal tumor of the kidney. *Ultrastruct Pathol*. 1983;4(1):51-59.
622. Fetisoff F, Benatre A, Dubois MP, et al. Carcinoid tumor occurring in a teratoid malformation of the kidney. An immunohistochemical study. *Cancer*. 1984;54(10):2305-2308.
623. Kojiro M, Ohishi H, Isobe H. Carcinoid tumor occurring in cystic teratoma of the kidney: a case report. *Cancer*. 1976;38(4):1636-1640.
624. Yoo J, Park S, Jung Lee H, et al. Primary carcinoid tumor arising in a mature teratoma of the kidney: a case report and review of the literature. *Arch Pathol Lab Med*. 2002;126(8):979-981.
625. Huettner PC, Bird DJ, Chang YC, Seiler MW. Carcinoid tumor of the kidney with morphologic and immunohistochemical profile of a hindgut endocrine tumor: report of a case. *Ultrastruct Pathol*. 1991;15(6):655-661.
626. Murali R, Kneale K, Lalak N, Delprado W. Carcinoid tumors of the urinary tract and prostate. *Arch Pathol Lab Med*. 2006;130(11):1693-1706.
627. Raslan WF, Ro JY, Ordonez NG, et al. Primary carcinoid of the kidney. Immunohistochemical and ultrastructural studies of five patients. *Cancer*. 1993;72(9):2660-2666.
628. Takeshima Y, Inai K, Yoneda K. Primary carcinoid tumor of the kidney with special reference to its histogenesis. *Pathol Int*. 1996;46(11):894-900.
629. Hannah J, Lippe B, Lai-Goldman M, Bhuta S. Oncocytic carcinoid of the kidney associated with periodic Cushing's syndrome. *Cancer*. 1988;61(10):2136-2140.
630. Hansel DE, Epstein JI, Berbescu E, et al. Renal carcinoid tumor: a clinicopathologic study of 21 cases. *Am J Surg Pathol*. 2007;31(10):1539-1544.
631. Pagni F, Galbiati E, Bono F, Di Bella C. Renal hilus paraganglioma: a case report and brief review. *Pathologica*. 2009;101:89-92.
632. Hes O, de Souza TG, Pivovarcikova K, et al. Distinctive renal cell tumor simulating atrophic kidney with 2 types of microcalcifications. Report of 3 cases. *Ann Diagn Pathol*. 2014;18:82-88.
633. Pacchioni D, Volante M, Casetta G, et al. Myxoid renal tumor with myoepithelial differentiation mimicking a salivary gland pleomorphic adenoma: description of a case. *Am J Surg Pathol*. 2007;31(4):632-636.
634. Cajaiba MM, Jennings LJ, Rohan SM, et al. Expanding the spectrum of renal tumors in children: primary renal myoepithelial carcinomas with a novel EWSR1-KLF15 fusion. *Am J Surg Pathol*. 2016;40:386-394.
635. Strobel P, Zettl A, Ren Z, et al. Spiradenocylindroma of the kidney: clinical and genetic findings suggesting a role of somatic mutation of the CYLD1 gene in the oncogenesis of an unusual renal neoplasm. *Am J Surg Pathol*. 2002;26(1):119-124.
636. Renshaw AA, Shapiro C, Fletcher JA, Pinsky M. An unusual papillary tumor of the renal medulla. Distinction from usual papillary renal cell carcinoma and collecting duct carcinoma. *J Urol Pathol*. 1998;8:121-133.
637. Ditonno P, Smith RB, Koyle MA, et al. Extrarenal angiomyolipomas of the perinephric space. *J Urol*. 1992;147(2):447-450.
638. Hruban RH, Bhagavan BS, Epstein JI. Massive retroperitoneal angiomyolipoma. A lesion that may be confused with well-differentiated liposarcoma. *Am J Clin Pathol*. 1989;92(6):805-808.
639. Righi A, Dimosthenous K, Rosai J. PEComa: another member of the MiT tumor family? *Int J Surg Pathol*. 2008;16(1):16-20.
640. Hornick JL, Fletcher CD. PEComa: what do we know so far? *Histopathology*. 2006;48(1):75-82.
641. Martignoni G, Pea M, Reghellin D, et al. PEComas: the past, the present and the future. *Virchows Arch*. 2008;452(2):119-132.
642. Mukai M, Torikata C, Iri H, et al. Crystalloids in angiomyolipoma. 1. A previously unnoticed phenomenon of renal angiomyolipoma occurring at a high frequency. *Am J Surg Pathol*. 1992;16(1):1-10.
643. Monga G, Ramponi A, Falzoni PL, Boldorini R. Renal and hepatic angiomyolipomas in a child without evidence of tuberous sclerosis. *Pathol Rev Pract*. 1994;190(12):1208-1211, discussion 1212-1213.
644. Chan JK, Tsang WY, Pau MY, et al. Lymphangiomyomatosis and angiomyolipoma: closely related entities characterized by hamartomatous proliferation of HMB-45-positive smooth muscle. *Histopathology*. 1993;22(5):445-455.
645. Monteforte WJ Jr, Kohen PW. Angiomyolipomas in a case of lymphangiomyomatosis syndrome: relationships to tuberous sclerosis. *Cancer*. 1974;34(2):317-321.
646. Fetsch PA, Fetsch JE, Marincola FM, et al. Comparison of melanoma antigen recognized by T cells (MART-1) to HMB-45: additional evidence to support a common lineage for angiomyolipoma, lymphangiomyomatosis, and clear cell sugar tumor. *Mod Pathol*. 1998;11(8):699-703.
647. Yavuz E, Cakr C, Tuzlal S, et al. Uterine perivascular epithelial cell tumor coexisting with pulmonary lymphangioleiomyomatosis and renal angiomyolipoma: a case report. *Appl Immunohistochem Mol Morphol*. 2008;16(4):405-409.
648. Steiner MS, Goldman SM, Fishman EK, Marshall FF. The natural history of renal angiomyolipoma. *J Urol*. 1993;150(6):1782-1786.
649. Bernstein J, Robbins TO, Kissane JM. The renal lesions of tuberous sclerosis. *Semin Diagn Pathol*. 1986;3(2):97-105.

650. Martignoni G, Bonetti F, Pea M, et al. Renal disease in adults with TSC2/PKD1 contiguous gene syndrome. *Am J Surg Pathol*. 2002;26(2):198-205.
651. Daughtry JD, Rodan BA. Renal angiomyolipoma: definitive diagnosis by ultrasonography and computerized tomography. *South Med J*. 1985;78(2):195-197.
652. Bonzanini M, Pea M, Martignoni G, et al. Preoperative diagnosis of renal angiomyolipoma: fine needle aspiration cytology and immunocytochemical characterization. *Pathology*. 1994;26(2):170-175.
653. Granter SR, Renshaw AA. Cytologic analysis of renal angiomyolipoma: a comparison of radiologically classic and challenging cases. *Cancer*. 1999;87(3):135-140.
654. Eble JN. Angiomyolipoma of kidney. *Semin Diagn Pathol*. 1998;15(1):21-40.
655. Hayashi T, Tsuda N, Chowdhury PR, et al. Renal angiomyolipoma: clinicopathologic features and differential diagnosis. *J Urol Pathol*. 1999;10:121-140.
656. Kilicaslan I, Culluoglu MG, Dogan O, Uysal V. Intraglomerular microlesions in renal angiomyolipoma. *Hum Pathol*. 2000;31(10):1325-1328.
657. Davis CJ, Barton JH, Sesterhenn IA. Cystic angiomyolipoma of the kidney: a clinicopathologic description of 11 cases. *Mod Pathol*. 2006;19(5):669-674.
658. Fine SW, Reuter VE, Epstein JI, Argani P. Angiomyolipoma with epithelial cysts (AMLEC): a distinct cystic variant of angiomyolipoma. *Am J Surg Pathol*. 2006;30(5):593-599.
659. Hoon V, Thung SN, Kaneko M, Unger PD. HMB-45 reactivity in renal angiomyolipoma and lymphangiomyomatosis. *Arch Pathol Lab Med*. 1994;118(7):732-734.
660. Jungbluth AA, Iversen K, Coplan K, et al. Expression of melanocyte-associated markers gp-100 and Melan-A/MART-1 in angiomyolipomas. An immunohistochemical and rt-PCR analysis. *Virchows Arch*. 1999;434(5):429-435.
661. Makhoul HR, Ishak KG, Shekar R, et al. Melanoma markers in angiomyolipoma of the liver and kidney: a comparative study. *Arch Pathol Lab Med*. 2002;126(1):49-55.
662. Pea M, Bonetti F, Zamboni G, et al. Melanocyte-marker-HMB-45 is regularly expressed in angiomyolipoma of the kidney. *Pathology*. 1991;23(3):185-188.
663. Roma AA, Magi-Galluzzi C, Zhou M. Differential expression of melanocytic markers in myoid, lipomatous, and vascular components of renal angiomyolipomas. *Arch Pathol Lab Med*. 2007;131(1):122-125.
664. Stone CH, Lee MW, Amin MB, et al. Renal angiomyolipoma: further immunophenotypic characterization of an expanding morphologic spectrum. *Arch Pathol Lab Med*. 2001;125(6):751-758.
665. Weeks DA, Chase DR, Malott RL, et al. HMB-45 staining in angiomyolipoma, cardiac rhabdomyoma, other mesenchymal processes, and tuberous sclerosis-associated brain lesions. *Int J Surg Pathol*. 1994;1:191-198.
666. Zamecnik M, Majercik M, Gomolcak P. Renal angiomyolipoma resembling gastrointestinal stromal tumor with skeinoid fibers. *Ann Diagn Pathol*. 1999;3(2):88-91.
667. Martignoni G, Pea M, Gobbo S, et al. Cathepsin-K immunoreactivity distinguishes MiTF/TFE family renal translocation carcinomas from other renal carcinomas. *Mod Pathol*. 2009;22:1016-1022.
668. Patil PA, McKenney JK, Trpkov K, et al. Renal leiomyoma: a contemporary multi-institution study of an infrequent and frequently misclassified neoplasm. *Am J Surg Pathol*. 2015;39:349-356.
669. Martignoni G, Bonetti F, Chilos M, et al. Cathepsin K expression in the spectrum of perivascular epithelioid cell (PEC) lesions of the kidney. *Mod Pathol*. 2012;25:100-111.
670. Barnard M, Lajoie G. Angiomyolipoma: immunohistochemical and ultrastructural study of 14 cases. *Ultrastruct Pathol*. 2001;25(1):21-29.
671. Kaiserling E, Krober S, Xiao JC, Schaumburg-Lever G. Angiomyolipoma of the kidney. Immunoreactivity with HMB-45. Light- and electron-microscopic findings. *Histopathology*. 1994;25(1):41-48.
672. Ljwnicz BH, Weeks DA, Zuppan CW. Extrarenal angiomyolipoma with melanocytic and hibernoma-like features. *Ultrastruct Pathol*. 1994;18(4):443-448.
673. Plank TL, Logginidou H, Klein-Szant A, Henske EP. The expression of hamartin, the product of the TSC1 gene, in normal human tissues and in TSC1- and TSC2-linked angiomyolipomas. *Mod Pathol*. 1999;12(5):539-545.
674. Johnson SR, Clelland CA, Ronan J, et al. The TSC-2 product tuberin is expressed in lymphangiomyomatosis and angiomyolipoma. *Histopathology*. 2002;40(5):458-463.
675. Bonsib SM, Boils C, Gokden N, et al. Tuberous sclerosis complex: hamartin and tuberin expression in renal cysts and its discordant expression in renal neoplasms. *Pathol Res Pract*. 2016;212:972-979.
676. Argani P, Aulmann S, Illei PB, et al. A distinctive subset of PEComas harbors TFE3 gene fusions. *Am J Surg Pathol*. 2010;34(10):1395-1406.
677. Malinowska I, Kwiatkowski DJ, Weiss S, et al. Perivascular epithelioid cell tumors (PEComas) harboring TFE3 gene rearrangements lack the TSC2 alterations characteristic of conventional PEComas: further evidence for a biological distinction. *Am J Surg Pathol*. 2012;36:783-784.
678. Eble JN, Amin MB, Young RH. Epithelioid angiomyolipoma of the kidney: a report of five cases with a prominent and diagnostically confusing epithelioid smooth muscle component. *Am J Surg Pathol*. 1997;21(10):1123-1130.
679. Asch-Kendrick RJ, Shetty S, Goldblum JR, et al. A subset of fat-predominant angiomyolipomas label for MDM2: a potential diagnostic pitfall. *Hum Pathol*. 2016;57:7-12.
680. Delgado R, de Leon Bojorge B, Albores-Saavedra J. Atypical angiomyolipoma of the kidney: a distinct morphologic variant that is easily confused with a variety of malignant neoplasms. *Cancer*. 1998;83(8):1581-1592.
681. Mai KT, Perkins DG, Collins JP. Epithelioid cell variant of renal angiomyolipoma. *Histopathology*. 1996;28(3):277-280.
682. Nesi N, Martignoni G, Fletcher CD, et al. Renal perivascular epithelioid cell tumors [(PEComa)], so called epithelioid angiomyolipoma (EAML): analysis of 61 cases including 44 with pure/predominant epithelioid (P-PEComa) morphology and parameters associated with malignant outcome. *Lab Invest*. 2009;89(suppl 1):186A.
683. Hes O, Michal M. Renal oncocytic angiomyolipoma. *Int J Surg Pathol*. 2004;12(4):421, author reply 422.
684. Martignoni G, Pea M, Bonetti F, et al. Oncocytoma-like angiomyolipoma. A clinicopathologic and immunohistochemical study of 2 cases. *Arch Pathol Lab Med*. 2002;126(5):610-612.
685. Sironi M, Spinelli M. Oncocytic angiomyolipoma of the kidney: a case report. *Int J Surg Pathol*. 2003;11(3):229-234.
686. Oesterling JE, Fishman EK, Goldman SM, Marshall FF. The management of renal angiomyolipoma. *J Urol*. 1986;135(6):1121-1124.
687. Kragel PJ, Toker C. Infiltrating recurrent renal angiomyolipoma with fatal outcome. *J Urol*. 1985;133(1):90-91.
688. Ansari SJ, Stephenson RA, Mackay B. Angiomyolipoma of the kidney with lymph node involvement. *Ultrastruct Pathol*. 1991;15(4-5):531-538.
689. Brecher ME, Gill WB, Straus FH 2nd. Angiomyolipoma with regional lymph node involvement and long-term follow-up study. *Hum Pathol*. 1986;17(9):962-963.
690. Ro JY, Ayala AG, el-Naggar A, et al. Angiomyolipoma of kidney with lymph node involvement. DNA flow cytometric analysis. *Arch Pathol Lab Med*. 1990;114(1):65-67.
691. Cibas ES, Goss GA, Kulke MH, et al. Malignant epithelioid angiomyolipoma ('sarcoma ex angiomyolipoma') of the kidney: a case report and review of the literature. *Am J Surg Pathol*. 2001;25(1):121-126.
692. Ferry JA, Malt RA, Young RH. Renal angiomyolipoma with sarcomatous transformation and pulmonary metastases. *Am J Surg Pathol*. 1991;15(11):1083-1088.
693. Kawaguchi K, Oda Y, Nakanishi K, et al. Malignant transformation of renal angiomyolipoma: a case report. *Am J Surg Pathol*. 2002;26(4):523-529.
694. Martignoni G, Pea M, Rigaud G, et al. Renal angiomyolipoma with epithelioid sarcomatous transformation and metastases: demonstration of the same genetic defects in the primary and metastatic lesions. *Am J Surg Pathol*. 2000;24(6):889-894.
695. He W, Cheville JC, Sadow PM, et al. Epithelioid angiomyolipoma of the kidney: pathological features and clinical outcome in a series of consecutively resected tumors. *Mod Pathol*. 2013;26:1355-1364.
696. Brimo F, Robinson B, Guo C, et al. Renal epithelioid angiomyolipoma with atypia: a series of 40 cases with emphasis on clinicopathologic prognostic indicators of malignancy. *Am J Surg Pathol*. 2010;34(5):715-722.
697. Aydin H, Magi-Galluzzi C, Lane BR, et al. Renal angiomyolipoma: clinicopathologic study of 194 cases with emphasis on the epithelioid histology and tuberous sclerosis association. *Am J Surg Pathol*. 2009;33(2):289-297.
698. Conn JW, Cohen EL, Lucas CP, et al. Primary reninism. Hypertension, hyperreninemia, and secondary aldosteronism due to renin-producing juxtaglomerular cell tumors. *Arch Int Med*. 1972;130(5):682-696.
699. Duan X, Bruneval P, Hammadeh R, et al. Metastatic juxtaglomerular cell tumor in a 52-year-old man. *Am J Surg Pathol*. 2004;28(8):1098-1102.
700. Koder R, Taylor M, Vachalova H, Pycha K. Juxtaglomerular cell tumor. An immunohistochemical, electron-microscopic, and in situ hybridization study. *Am J Surg Pathol*. 1994;18(8):837-842.
701. Martin SA, Mynderse LA, Lager DJ, Cheville JC. Juxtaglomerular cell tumor: a clinicopathologic study of four cases and review of the literature. *Am J Clin Pathol*. 2001;116(6):854-863.
702. Gherardi GJ, Arya S, Hickler RB. Juxtaglomerular body tumor: a rare occult but curable cause of lethal hypertension. *Hum Pathol*. 1974;5(2):236-240.
703. Tetu B, Vaillancourt L, Camilleri JP, et al. Juxtaglomerular cell tumor of the kidney.

- report of two cases with a papillary pattern. *Hum Pathol.* 1993;24(11):1168-1174.
704. Camilleri JP, Hinglais N, Bruneval P, et al. Renin storage and cell differentiation in juxtaglomerular cell tumors: an immunohistochemical and ultrastructural study of three cases. *Hum Pathol.* 1984;15(11):1069-1079.
705. Bonsib SM, Hansen KK. Juxtaglomerular cell tumors: a report of two cases with HMB-45 immunostaining. *J Urol Pathol.* 1998;9:61-72.
706. Kim HJ, Kim CH, Choi YJ, et al. Juxtaglomerular cell tumor of kidney with CD34 and CD117 immunoreactivity: report of 5 cases. *Arch Pathol Lab Med.* 2006;130(5):707-711.
707. Hasegawa A. Juxtaglomerular cells tumor of the kidney: a case report with electron microscopic and flow cytometric investigation. *Ultrastruct Pathol.* 1997;21(2):201-208.
708. Kim CH, Park YW, Ordonez NG, et al. Juxtaglomerular cell tumor of the kidney: case report with immunohistochemical and electron microscopic investigations and review of the literature. *Int J Surg Pathol.* 1999;7:115-123.
709. Lindop GB, Stewart JA, Downie TT. The immunocytochemical demonstration of renin in a juxtaglomerular cell tumor by light and electron microscopy. *Histopathology.* 1983;7(3):421-431.
710. Bandal P, Busund LT, Heim S. Chromosome abnormalities in juxtaglomerular cell tumors. *Cancer.* 2005;104(3):504-510.
711. Capovilla M, Couturier J, Molinie V, et al. Loss of chromosomes 9 and 11 may be recurrent chromosome imbalances in juxtaglomerular cell tumors. *Hum Pathol.* 2008;39(3):459-462.
712. Squires JP, Ulbright TM, DeSchryver-Kecskemeti K, Engleman W. Juxtaglomerular cell tumor of the kidney. *Cancer.* 1984;53(3):516-523.
713. Lindop GB, Leckie B, Winearls CG. Malignant hypertension due to a renin-secreting renal cell carcinoma—an ultrastructural and immunocytochemical study. *Histopathology.* 1986;10(10):1077-1088.
714. Ruddy MC, Atlas SA, Salerno FG. Hypertension associated with a renin-secreting adenocarcinoma of the pancreas. *N Engl J Med.* 1982;307(16):993-997.
715. Tomita T, Poisner A, Inagami T. Immunohistochemical localization of renin in renal tumors. *Am J Pathol.* 1987;126(1):73-80.
716. Michal M, Hes O, Bisciglia M, et al. Mixed epithelial and stromal tumors of the kidney. A report of 22 cases. *Virchows Arch.* 2004;445(4):359-367.
717. Turbiner J, Amin MB, Humphrey PA, et al. Cystic nephroma and mixed epithelial and stromal tumor of kidney: a detailed clinicopathologic analysis of 34 cases and proposal for renal epithelial and stromal tumor (REST) as a unifying term. *Am J Surg Pathol.* 2007;31(4):489-500.
718. Antic T, Perry KT, Harrison K, et al. Mixed epithelial and stromal tumor of the kidney and cystic nephroma share overlapping features: reappraisal of 15 lesions. *Arch Pathol Lab Med.* 2006;130(1):80-85.
719. Eble JN, Bonsib SM. Extensively cystic renal neoplasms: cystic nephroma, cystic partially differentiated nephroblastoma, multilocular cystic renal cell carcinoma, and cystic hamartoma of renal pelvis. *Semin Diagn Pathol.* 1998;15(1):2-20.
720. Zhou M, Kort E, Hoekstra P, et al. Adult cystic nephroma and mixed epithelial and stromal tumor of the kidney are the same disease entity: molecular and histologic evidence. *Am J Surg Pathol.* 2009;33(1):72-80.
721. Picken MM, Fresco R. Mixed epithelial and stromal tumor of the kidney: preliminary immunohistochemical and electron microscopic studies of the epithelial component. *Ultrastruct Pathol.* 2005;29(3-4):283-286.
722. Parikh P, Chan TY, Epstein JI, Argani P. Incidental stromal-predominant mixed epithelial-stromal tumors of the kidney: a mimic of intraparenchymal renal leiomyoma. *Arch Pathol Lab Med.* 2005;129(7):910-914.
723. Jung SJ, Shen SS, Tran T, et al. Mixed epithelial and stromal tumor of kidney with malignant transformation: report of two cases and review of literature. *Hum Pathol.* 2008;39(3):463-468.
724. Nakagawa T, Kanai Y, Fujimoto H, et al. Malignant mixed epithelial and stromal tumors of the kidney: a report of the first two cases with a fatal clinical outcome. *Histopathology.* 2004;44(3):302-304.
725. Glover SD, Buck AC. Renal medullary fibroma: a case report. *J Urol.* 1982;127(4):758-760.
726. Lerman RJ, Pitcock JA, Stephenson P, Muirhead EE. Renomedullary interstitial cell tumor (formerly fibroma of renal medulla). *Hum Pathol.* 1972;3(4):559-568.
727. Tamboli P, Ro JY, Amin MB, et al. Benign tumors and tumor-like lesions of the adult kidney. Part II: benign mesenchymal and mixed neoplasms, and tumor-like lesions. *Adv Anat Pathol.* 2000;7(1):47-66.
728. Gupta S, et al. *Am J Surg Pathol.* 2016;40:1557-1563.
729. Bossart MI, Spjut HJ, Wright JE, Pranke DW. Multilocular cystic leiomyoma of the kidney. *Ultrastruct Pathol.* 1982;3(4):367-374.
730. Calio A, Warfel KA, Eble JN. Pathological features and clinical associations of 58 small incidental angiomyolipomas of the kidney. *Hum Pathol.* 2016;58:41-46.
731. Dineen MK, Venable DD, Misra RP. Pure intrarenal lipoma—report of a case and review of the literature. *J Urol.* 1984;132(1):104-107.
732. Stone NN, Cherry J. Renal capsular lipoma. *J Urol.* 1985;134(1):118-119.
733. Ip YT, Yuan JQ, Cheung H, Chan JK. Sporadic hemangioblastoma of the kidney: an underrecognized pseudomalignant tumor? *Am J Surg Pathol.* 2010;34:1695-1700.
734. Zhou M, Williamson SR, Yu J, et al. PAX8 expression in sporadic hemangioblastoma of the kidney supports a primary renal cell lineage: implications for differential diagnosis. *Hum Pathol.* 2013;44:2247-2255.
735. Melamed J, Reuter VE, Erlandson RA, Rosai J. Renal myxoma. A report of two cases and review of the literature. *Am J Surg Pathol.* 1994;18(2):187-194.
736. Alvarado-Cabreiro I, Folpe AL, Srigley JR, et al. Intrarenal schwannoma: a report of four cases including three cellular variants. *Mod Pathol.* 2000;13(8):851-856.
737. Gobbo S, Eble JN, Huang J, et al. Schwannoma of the kidney. *Mod Pathol.* 2008;21(6):779-783.
738. Ma KF, Tse CH, Tsui MS. Neurilemmoma of kidney—a rare occurrence. *Histopathology.* 1990;17(4):378-380.
739. Kahn DG, Duckett T, Bhuta SM. Perineurioma of the kidney. Report of a case with histologic, immunohistochemical, and ultrastructural studies. *Arch Pathol Lab Med.* 1993;117(6):654-657.
740. Brown JG, Folpe AL, Rao P, et al. Primary vascular tumors and tumor-like lesions of the kidney: a clinicopathologic analysis of 25 cases. *Am J Surg Pathol.* 2010;34(7):942-949.
741. Montgomery E, Epstein JI. Anastomosing hemangioma of the genitourinary tract: a lesion mimicking angiomyoma. *Am J Surg Pathol.* 2009;33(9):1364-1369.
742. Anderson C, Knibbs DR, Ludwig ME, Ely MG. 3rd. Lymphangioma of the kidney: a pathologic entity distinct from solitary multilocular cyst. *Hum Pathol.* 1992;23(4):465-468.
743. Levine E. Lymphangioma presenting as a small renal mass during childhood. *Urol Radiol.* 1992;14(3):155-158.
744. Gill J, Van Vliet C. Infiltrating glomus tumor of uncertain malignant potential arising in the kidney. *Hum Pathol.* 2010;41(1):145-149.
745. Al-Ahmadi HA, Yilmaz A, Olgac S, Reuter VE. Glomus tumor of the kidney: a report of 3 cases involving renal parenchyma and review of the literature. *Am J Surg Pathol.* 2007;31(4):585-591.
746. Siddiqui NH, Rogalska A, Basil IS. Glomangiomyoma (glomus tumor) of the kidney. *Arch Pathol Lab Med.* 2005;129(9):1172-1174.
747. Sirohi D, Smith SC, Epstein JI, et al. Pericytic tumors of the kidney—a clinicopathologic analysis of 17 cases. *Hum Pathol.* 2017;64:106-117.
748. Fain JS, Eble J, Nascimento AG, et al. Solitary fibrous tumor of the kidney: report of three cases. *J Urol Pathol.* 1996;4:227-238.
749. Gelb AB, Simmons ML, Weidner N. Solitary fibrous tumor involving the renal capsule. *Am J Surg Pathol.* 1996;20(10):1288-1295.
750. Wang J, Arber DA, Frankel K, Weiss LM. Large solitary fibrous tumor of the kidney: report of two cases and review of the literature. *Am J Surg Pathol.* 2001;25(9):1194-1199.
751. Richard GK, Freeborn WA, Zaatari GS. Hemangiopericytoma of the renal capsule. *J Urol Pathol.* 1996;4:85-98.
752. Fine SW, McCarthy DM, Chan TY, et al. Malignant solitary fibrous tumor of the kidney: report of a case and comprehensive review of the literature. *Arch Pathol Lab Med.* 2006;130(6):857-861.
753. Kapusta LR, Weiss MA, Ramsay J, et al. Inflammatory myofibroblastic tumors of the kidney: a clinicopathologic and immunohistochemical study of 12 cases. *Am J Surg Pathol.* 2003;27(5):658-666.
754. Sneege N, Dekmezian RH, Silva EG, et al. Pseudoparasitic Liesegang structures in perirenal hemorrhagic cysts. *Am J Clin Pathol.* 1988;89(2):148-153.
755. Afzal M, Baez-Giangreco A, al Jaser AN, Onuora VC. Unusual bilateral renal histiocytosis. Extranodal variant of Rosai-Dorfman disease. *Arch Pathol Lab Med.* 1992;116(12):1366-1367.
756. August C, Holzhausen HJ, Schroder S. Renal parenchymal malakoplakia: ultrastructural findings in different stages of morphogenesis. *Ultrastruct Pathol.* 1994;18(5):483-491.
757. Esperanza AR, McKay DB, Cronan JJ, Chazan JA. Renal parenchymal malakoplakia. Histologic spectrum and its relationship to megalocytic interstitial nephritis and xanthogranulomatous pyelonephritis. *Am J Surg Pathol.* 1989;13(3):225-236.
758. Harik L, Nassar A. Extranodal Rosai-Dorfman disease of the kidney and coexistent poorly differentiated prostatic adenocarcinoma. *Arch Pathol Lab Med.* 2006;130(8):1223-1226.
759. Lloreta J, Canas MA, Munne A, et al. Renal malakoplakia: report of a case with multifocal involvement. *Ultrastruct Pathol.* 1997;21(6):575-585.
760. Farrow GM, Harrison EG Jr, Utz DC. Sarcomas and sarcomatoid and mixed malignant tumors of the kidney in adults. 3. *Cancer.* 1968;22(3):556-563.
761. Grignon DJ, Ayala AG, Ro JY, et al. Primary sarcomas of the kidney. A clinicopathologic and DNA flow cytometric study of 17 cases. *Cancer.* 1990;65(7):1611-1618.
762. Vogelzang NJ, Fremgen AM, Guinan PD, et al. Primary renal sarcoma in adults. A natural history and management study by the

- American Cancer Society, Illinois Division. *Cancer*. 1993;71(3):804-810.
763. Deyrup AT, Montgomery E, Fisher C. Leiomyosarcoma of the kidney: a clinicopathologic study. *Am J Surg Pathol*. 2004;28(2):178-182.
764. Miller JS, Zhou M, Brimo F, et al. Primary leiomyosarcoma of the kidney: a clinicopathologic study of 27 cases. *Am J Surg Pathol*. 2010;34(2):238-242.
765. Yokose T, Fukuda H, Ogiwara A, et al. Myxoid leiomyosarcoma of the kidney accompanying ipsilateral ureteral transitional cell carcinoma. A case report with cytological, immunohistochemical and ultrastructural study. *Acta Pathol Jpn*. 1991;41(9):694-700.
766. Argani P, Faria PA, Epstein JI, et al. Primary renal synovial sarcoma: molecular and morphologic delineation of an entity previously included among embryonal sarcomas of the kidney. *Am J Surg Pathol*. 2000;24(8):1087-1096.
767. Chen S, Bhuiya T, Liatsikos EN, et al. Primary synovial sarcoma of the kidney: a case report with literature review. *Int J Surg Pathol*. 2001;9(4):335-339.
768. Divietro M, Karpate A, Basak R, Desai SB. Synovial sarcoma of the kidney. *Ann Diagn Pathol*. 2008;12(5):333-339.
769. Kim DH, Sohn JH, Lee MC, et al. Primary synovial sarcoma of the kidney. *Am J Surg Pathol*. 2000;24(8):1097-1104.
770. Dalfior D, Echer A, Gobbo S, et al. Primary pleomorphic rhabdomyosarcoma of the kidney in an adult. *Ann Diagn Pathol*. 2008;12(4):301-303.
771. Scriven RR, Thrasher TV, Smith DC, Stewart SC. Primary renal malignant fibrous histiocytoma: a case report and literature review. *J Urol*. 1984;131(5):948-949.
772. Mayes DC, Fechner RE, Gillenwater JY. Renal liposarcoma. *Am J Surg Pathol*. 1990;14(3):268-273.
773. Cerilli LA, Huffman HT, Anand A. Primary renal angiosarcoma: a case report with immunohistochemical, ultrastructural, and cytogenetic features and review of the literature. *Arch Pathol Lab Med*. 1998;122(10):929-935.
774. Tsuda N, Chowdhury PR, Hayashi T, et al. Primary renal angiosarcoma: a case report and review of the literature. *Pathol Int*. 1997;47(11):778-783.
775. Eble JN, Young RHJ, Störkel CS, Thoenes W. Primary osteosarcoma of the kidney. A report of three cases. *J Urogen Pathol*. 1991;1:83-88.
776. Miclough TS, Liang D, Schwartz S. Primary osteogenic sarcoma of the kidney. *J Urol*. 1984;131(6):1164-1166.
777. O'Malley FP, Grignon DJ, Shepherd RR, Harker LA. Primary osteosarcoma of the kidney. Report of a case studied by immunohistochemistry, electron microscopy, and DNA flow cytometry. *Arch Pathol Lab Med*. 1991;115(12):1262-1265.
778. Nativ O, Horowitz A, Lindner A, Many M. Primary chondrosarcoma of the kidney. *J Urol*. 1985;134(1):120-121.
779. Mead JH, Herrera GA, Kaufman MF, Herz JH. Case report of a primary cystic sarcoma of the kidney, demonstrating fibrohistiocytic, osteoid, and cartilaginous components (malignant mesenchymoma). *Cancer*. 1982;50(10):2211-2214.
780. Quinn CM, Day DW, Waxman J, Krausz T. Malignant mesenchymoma of the kidney. *Histopathology*. 1993;23(1):86-88.
781. Rubin BP, Fletcher JA, Renshaw AA. Clear cell sarcoma of soft parts: report of a case primary in the kidney with cytogenetic confirmation. *Am J Surg Pathol*. 1999;23(5):589-594.
782. Malhotra CM, Doolittle CH, Rodil JV, Vezeridis MP. Mesenchymal chondrosarcoma of the kidney. *Cancer*. 1984;54(11):2495-2499.
783. Creager AJ, Maia DM, Funkhouser WK. Epstein-Barr virus-associated renal smooth muscle neoplasm: report of a case with review of the literature. *Arch Pathol Lab Med*. 1998;122(3):277-281.
784. Jun SY, Choi J, Kang GH, et al. Synovial sarcoma of the kidney with rhabdoid features: report of three cases. *Am J Surg Pathol*. 2004;28(5):634-637.
785. Richmond J, Sherman RS, Diamond HD, Craver LF. Renal lesions associated with malignant lymphomas. *Am J Med*. 1962;32:184-207.
786. Ferry JA, Harris NL, Papanicolaou N, Young RH. Lymphoma of the kidney. A report of 11 cases. *Am J Surg Pathol*. 1995;19(2):134-144.
787. Okuno SH, Hoyer JD, Ristow K, Witzig TE. Primary renal non-Hodgkin's lymphoma. An unusual extranodal site. *Cancer*. 1995;75(9):2258-2261.
788. Osborne BM, Brenner M, Weitzner S, Butler JJ. Malignant lymphoma presenting as a renal mass: four cases. *Am J Surg Pathol*. 1987;11(5):375-382.
789. Ellman L, Davis J, Lichtenstein NS. Uremia due to occult lymphomatous infiltration of the kidneys. *Cancer*. 1974;33(1):203-205.
790. Randolph VL, Hall W, Bramson W. Renal failure due to lymphomatous infiltration of the kidneys. *Cancer*. 1983;52(6):1120-1121.
791. Schniederjan SD, Osunkoya AO. Lymphoid neoplasms of the urinary tract and male genital organs: a clinicopathological study of 40 cases. *Mod Pathol*. 2009;22(8):1057-1065.
792. Parveen T, Navarro-Roman L, Medeiros LJ, et al. Low-grade B-cell lymphoma of mucosa-associated lymphoid tissue arising in the kidney. *Arch Pathol Lab Med*. 1993;117(8):780-783.
793. Qiu L, Unger PD, Dillon RW, Strauchen JA. Low-grade mucosa-associated lymphoid tissue lymphoma involving the kidney: report of 3 cases and review of the literature. *Arch Pathol Lab Med*. 2006;130(1):86-89.
794. Tsang K, Kneafsey P, Gill MJ. Primary lymphoma of the kidney in the acquired immunodeficiency syndrome. *Arch Pathol Lab Med*. 1993;117(5):541-543.
795. Weissmann DJ, Ferry JA, Harris NL, et al. Posttransplantation lymphoproliferative disorders in solid organ recipients are predominantly aggressive tumors of host origin. *Am J Clin Pathol*. 1995;103(6):748-755.
796. Randhawa PS, Magnone M, Jordan M, et al. Renal allograft involvement by Epstein-Barr virus associated post-transplant lymphoproliferative disease. *Am J Surg Pathol*. 1996;20(5):563-571.
797. D'Agati V, Sablai LB, Knowles DM, Walter L. Angiotropic large cell lymphoma (intravascular malignant lymphomatosis) of the kidney: presentation as minimal change disease. *Hum Pathol*. 1989;20(3):263-268.
798. Kandel LB, Harrison LH, Woodruff RD, et al. Renal plasmacytoma: a case report and summary of reported cases. *J Urol*. 1984;132(6):1167-1169.
799. Davis RI, Corson JM. Renal metastases from well differentiated follicular thyroid carcinoma: a case report with light and electron microscopic findings. *Cancer*. 1979;43(1):265-268.
800. Herzberg AJ, Bossen EH, Walther PJ. Adenoid cystic carcinoma of the breast metastatic to the kidney. A clinically symptomatic lesion requiring surgical management. *Cancer*. 1991;68(5):1015-1020.
801. Johnson MW, Morettin LB, Sarles HE, Zaharopoulos P. Follicular carcinoma of the thyroid metastatic to the kidney 37 years after resection of the primary tumor. *J Urol*. 1982;127(1):114-116.
802. Honda H, Coffman CE, Berbaum KS, et al. CT analysis of metastatic neoplasms of the kidney. Comparison with primary renal cell carcinoma. *Acta Radiol*. 1992;33(1):39-44.
803. Wagle DG, Moore RH, Murphy GP. Secondary carcinomas of the kidney. *J Urol*. 1975;114(1):30-32.
804. Belghiti D, Hirbec G, Bernaudin JF, et al. Intraglomerular metastases. Report of two cases. *Cancer*. 1984;54(10):2309-2312.
805. Toth T. Extracapillary tumorous metastatic crescents in glomeruli of the kidney. *Pathol Res Pract*. 1987;182(2):240-243.
806. Bates AW, Baithun SI. The significance of secondary neoplasms of the urinary and male genital tract. *Virchows Arch*. 2002;440(6):640-647.
807. Colome MI, Ro JY, Ayala AG, et al. Adenoid cystic carcinoma of the breast metastatic to the kidney: an unusual site of initial distant metastasis, mimicking a primary renal tumor. *J Urol Pathol*. 1996;4:69-78.
808. Gamboa-Dominguez A, Tenorio-Villalvazo A. Metastatic follicular variant of papillary thyroid carcinoma manifested as a primary renal neoplasm. *Endocr Pathol*. 1999;10(3):256-268.
809. Guinan P, Vogelzang NJ, Randazzo R, et al. Renal pelvic cancer: a review of 611 patients treated in Illinois 1975-1985. Cancer Incidence and End Results Committee. *Urology*. 1992;40(5):393-399.
810. Koyanagi T, Sasaki K, Arikado K, et al. Transitional cell carcinoma of renal pelvis in an infant. *J Urol*. 1975;113(1):114-117.
811. Johansson S, Angervall L, Bengtsson U, Wahlqvist L. Uroepithelial tumors of the renal pelvis associated with abuse of phenacetin-containing analgesics. *Cancer*. 1974;33(3):743-753.
812. Johansson S, Angervall L, Bengtsson U, Wahlqvist L. A clinicopathologic and prognostic study of epithelial tumors of the renal pelvis. *Cancer*. 1976;37(3):1376-1383.
813. Verhaak RL, Harmsen AE, van Unnik AJ. On the frequency of tumor induction in a thororast kidney. *Cancer*. 1974;34(6):2061-2068.
814. McDougal WS, Cramer SE, Miller R. Invasive carcinoma of the renal pelvis following cyclophosphamide therapy for nonmalignant disease. *Cancer*. 1981;48(3):691-695.
815. Murphy DM, Zincke H. Transitional cell carcinoma in the horseshoe kidney: report of 3 cases and review of the literature. *Br J Urol*. 1982;54(5):484-485.
816. Blaszyk H, Wang L, Dietmaier W, et al. Upper tract urothelial carcinoma: a clinicopathologic study including microsatellite instability analysis. *Mod Pathol*. 2002;15(8):790-797.
817. Harper HL, McKenney JK, Heald B, et al. Upper tract urothelial carcinomas: frequency of association with mismatch repair protein loss and lynch syndrome. *Mod Pathol*. 2017;30:146-156.
818. Raabe NK, Fossa SD, Bjerkehagen B. Carcinoma of the renal pelvis. Experience of 80 cases. *Scand J Urol Nephrol*. 1992;26(4):357-361.
819. Strobel SL, Jasper WS, Gogate SA, Sharma HM. Primary carcinoma of the renal pelvis and ureter. Evaluation of clinical and pathologic features. *Arch Pathol Lab Med*. 1984;108(9):697-700.
820. Holmang S, Johansson SL. Synchronous bilateral ureteral and renal pelvic carcinomas: incidence, etiology, treatment and outcome. *Cancer*. 2004;101(4):741-747.
821. Hart AP, Brown R, Lechago J, Truong LD. Collision of transitional cell carcinoma and renal cell carcinoma. An immunohistochemical study and review of the literature. *Cancer*. 1994;73(1):154-159.

822. Wegner HE, Bornhoft G, Dieckmann KP. Renal cell cancer and concomitant transitional cell cancer of the renal pelvis and ureter in the same kidney—report of 4 cases and review of the literature. *Urol Int*. 1993;51(3):158-163.
823. Yokoyama I, Berman E, Rickert RR, Bastidas J. Simultaneous occurrence of renal cell adenocarcinoma and urothelial carcinoma of the renal pelvis in the same kidney diagnosed by preoperative angiography. *Cancer*. 1981;48(12):2762-2766.
824. Potts SA, Thomas PA, Cohen MB, Raab SS. Diagnostic accuracy and key cytologic features of high-grade transitional cell carcinoma in the upper urinary tract. *Mod Pathol*. 1997;10(7):657-662.
825. Mai KT, Gerridson RG, Millward SF. Papillary transitional cell carcinoma arising in a calyceal cyst and masquerading as a renal cyst. *Arch Pathol Lab Med*. 1996;120(9):879-882.
826. Bloom NA, Vidone RA, Lytton B. Primary carcinoma of the ureter: a report of 102 new cases. *J Urol*. 1970;103(5):590-598.
827. McIntyre D, Pyrah LN, Raper FP. Primary ureteric neoplasms. Report of 40 cases. *Br J Urol*. 1965;37:160-191.
828. Olgac S, Mazumdar M, Dalbagni G, Reuter VE. Urothelial carcinoma of the renal pelvis: a clinicopathologic study of 130 cases. *Am J Surg Pathol*. 2004;28(12):1545-1552.
829. Balslev E, Fischer S. Transitional cell carcinoma of the renal collecting tubules ("renal urothelioma"). *Acta Pathol Microbiol Immunol Scand [A]*. 1983;91(6):419-424.
830. Mahadevia PS, Karwa GL, Koss LG. Mapping of urothelium in carcinomas of the renal pelvis and ureter. A report of nine cases. *Cancer*. 1983;51(5):890-897.
831. Wobker SE, Aron M, Epstein JI. Mechanical implantation of urothelium into periureteral soft tissue: a series of 4 cases mimicking high-stage urothelial carcinoma. *Am J Surg Pathol*. 2016;40:1564-1570.
832. Tavora F, Fajardo DA, Lee TK, et al. Small endoscopic biopsies of the ureter and renal pelvis: pathologic pitfalls. *Am J Surg Pathol*. 2009;33:1540-1546.
833. Guo CC, Tamboli P, Czerniak B. Micropapillary variant of urothelial carcinoma in the upper urinary tract: a clinicopathologic study of 11 cases. *Arch Pathol Lab Med*. 2009;133(1):62-66.
834. Perez-Montiel D, Hes O, Michal M, Suster S. Micropapillary urothelial carcinoma of the upper urinary tract: clinicopathologic study of five cases. *Am J Clin Pathol*. 2006;126(1):86-92.
835. Perez-Montiel D, Wakely PE, Hes O, et al. High-grade urothelial carcinoma of the renal pelvis: clinicopathologic study of 108 cases with emphasis on unusual morphologic variants. *Mod Pathol*. 2006;19(4):494-503.
836. Han AC, Duszak R Jr. Coexpression of cytokeratins 7 and 20 confirms urothelial carcinoma presenting as an intrarenal tumor. *Cancer*. 1999;86(11):2327-2330.
837. Rey A, Lara PC, Redondo E, et al. Overexpression of p53 in transitional cell carcinoma of the renal pelvis and ureter. Relation to tumor proliferation and survival. *Cancer*. 1997;79(11):2178-2185.
838. Young A, Kunju LP. High-grade carcinomas involving the renal sinus: report of a case and review of the differential diagnosis and immunohistochemical expression. *Arch Pathol Lab Med*. 2012;136:907-910.
839. Albadine R, Schultz L, Illei P, et al. PAX8 (+)/p63 (-) immunostaining pattern in renal collecting duct carcinoma (CDC): a useful immunoprofile in the differential diagnosis of CDC versus urothelial carcinoma of upper urinary tract. *Am J Surg Pathol*. 2010;34:965-969.
840. Auld CD, Grigor KM, Fowler JW. Histopathological review of transitional cell carcinoma of the upper urinary tract. *Br J Urol*. 1984;56(5):485-489.
841. McCarron JP Jr, Chasko SB, Gray GF Jr. Systematic mapping of nephroureterectomy specimens removed for urothelial cancer: pathological findings and clinical correlations. *J Urol*. 1982;128(2):243-246.
842. Strong DW, Pearse HD. Recurrent urothelial tumors following surgery for transitional cell carcinoma of the upper urinary tract. *Cancer*. 1976;38(5):2173-2183.
843. Wagle DG, Moore RH, Murphy GP. Primary carcinoma of the renal pelvis. *Cancer*. 1974;33(6):1642-1648.
844. Akaza H, Koiso K, Niijima T. Clinical evaluation of urothelial tumors of the renal pelvis and ureter based on a new classification system. *Cancer*. 1987;59(7):1369-1375.
845. Batata MA, Whitmore WF, Hilaris BS, et al. Primary carcinoma of the ureter: a prognostic study. *Cancer*. 1975;35(6):1626-1632.
846. Melamed MR, Reuter VE. Pathology and staging of urothelial tumors of the kidney and ureter. *Urol Clin North Am*. 1993;20(2):333-347.
847. Mills C, Vaughan ED Jr. Carcinoma of the ureter: natural history, management and 5-year survival. *J Urol*. 1983;129(2):275-277.
848. Werth DD, Weigel JW, Mebstub WK. Primary neoplasms of the ureter. *J Urol*. 1981;125(5):628-631.
849. Hertle L, Androulakakis P. Keratinizing desquamative squamous metaplasia of the upper urinary tract: leukoplakia—cholesteatoma. *J Urol*. 1982;127(4):631-635.
850. Nativ O, Reiman HM, Lieber MM, Zincke H. Treatment of primary squamous cell carcinoma of the upper urinary tract. *Cancer*. 1991;68(12):2575-2578.
851. Kobayashi S, Ohmori M, Akaeda T, et al. Primary adenocarcinoma of the renal pelvis. Report of two cases and brief review of literature. *Acta Pathol Jpn*. 1983;33(3):589-597.
852. Aufderheide AC, Streitz JM. Mucinous adenocarcinoma of the renal pelvis. Report of two cases. *Cancer*. 1974;33(1):167-173.
853. Shibahara N, Okada S, Onishi S, et al. Primary mucinous carcinoma of the renal pelvis. *Pathol Res Pract*. 1993;189(8):946-949, discussion 950.
854. Spires SE, Banks ER, Cibull ML, et al. Adenocarcinoma of renal pelvis. *Arch Pathol Lab Med*. 1993;117(11):1156-1160.
855. Ishikura H, Ishiguro T, Enatsu C, et al. Hepatoid adenocarcinoma of the renal pelvis producing alpha-fetoprotein of hepatic type and bile pigment. *Cancer*. 1991;67(12):3051-3056.
856. Fukunaga M, Ushigome S. Lymphoepithelioma-like carcinoma of the renal pelvis: a case report with immunohistochemical analysis and in situ hybridization for the Epstein-Barr viral genome. *Mod Pathol*. 1998;11(12):1252-1256.
857. Genega E, Ittmann M, Wieczorek R, Sidhu G. Carcinosarcoma of the renal pelvis with immunohistochemistry and review of the literature. *J Urol Pathol*. 1997;6:205-212.
858. Suster S, Robinson MJ. Spindle cell carcinoma of the renal pelvis. Immunohistochemical and ultrastructural study of a case demonstrating coexpression of keratin and vimentin intermediate filaments. *Arch Pathol Lab Med*. 1989;113(4):404-408.
859. Wick MR, Perrone TI, Burke BA. Sarcomatoid transitional cell carcinomas of the renal pelvis. An ultrastructural and immunohistochemical study. *Arch Pathol Lab Med*. 1985;109(1):55-58.
860. Akhtar M, Aslam M, Lindstedt E, et al. Osteoclast-like giant cell tumor of renal pelvis. *J Urol Pathol*. 1999;11:181-194.
861. Molinie V, Pouchot J, Vinceneux P, Barge J. Osteoclastoma-like giant cell tumor of the renal pelvis associated with papillary transitional cell carcinoma. *Arch Pathol Lab Med*. 1997;121(2):162-166.
862. Zanella M, Falconieri G. Sarcomatoid urothelial carcinoma of the renal pelvis: report of two cases with extensive osteoclast-like giant cell component. *J Urol Pathol*. 2000;12:13-28.
863. Guillou L, Duvoisin B, Chobaz C, et al. Combined small-cell and transitional cell carcinoma of the renal pelvis. A light microscopic, immunohistochemical, and ultrastructural study of a case with literature review. *Arch Pathol Lab Med*. 1993;117(3):239-243.
864. Deodhare S, Leung CS, Bullock M. Choriocarcinoma associated with transitional cell carcinoma in-situ of the ureter. *Histopathology*. 1996;28(4):363-365.
865. Grammatico D, Grignon DJ, Eberwein P, et al. Transitional cell carcinoma of the renal pelvis with choriocarcinomatous differentiation. Immunohistochemical and immunoelectron microscopic assessment of human chorionic gonadotropin production by transitional cell carcinoma of the urinary bladder. *Cancer*. 1993;71(5):1835-1841.
866. Vahlensieck W Jr, Riede U, Wimmer B, Ihling C. Beta-human chorionic gonadotropin-positive extragonadal germ cell neoplasia of the renal pelvis. *Cancer*. 1991;67(12):3146-3149.
867. Zettl A, Konrad MA, Polzin S, et al. Urothelial carcinoma of the renal pelvis with choriocarcinomatous features: genetic evidence of clonal evolution. *Hum Pathol*. 2002;33(12):1234-1237.
868. Kumar S, Kumar D, Cowan DF. Transitional cell carcinoma with rhabdoid features. *Am J Surg Pathol*. 1992;16(5):515-521.
869. Sheaff M, Fociani P, Badenoch D, Baithun S. Verrucous carcinoma of the renal pelvis: case presentation and review of the literature. *Virchows Arch*. 1996;428(6):375-379.
870. Macksood MJ, Roth DR, Chang CH, Perlmuter AD. Benign fibroepithelial polyps as a cause of intermittent ureteropelvic junction obstruction in a child: a case report and review of the literature. *J Urol*. 1985;134(5):951-952.
871. Nowak MA, Marzich CS, Scheetz KL, McElroy JB. Benign fibroepithelial polyps of the renal pelvis. *Arch Pathol Lab Med*. 1999;123(9):850-852.
872. MacMahon HE. Hypertrophic infundibular stenosis of the calyces of the kidney. *Hum Pathol*. 1974;5(3):363-364.
873. Hurwitz RS, Benjamin JA, Cooper JF. Excessive proliferation of peripelvic fat of the kidney. *Urology*. 1978;11(5):448-456.
874. Farrands PA, Tribe CR, Slade N. Localized amyloid of the ureter—case report and review of the literature. *Histopathology*. 1983;7(4):613-622.
875. Amin MB, Tickoo SK, Schultz D. Myelolipoma of the renal sinus. An unusual site for a rare extra-adrenal lesion. *Arch Pathol Lab Med*. 1999;123(7):631-634.
876. Matthews PN, Greenwood RN, Hendry WF, Cattell WR. Extensive pelvic malacoplakia: observations on management. *J Urol*. 1986;135(1):132-134.
877. Rudd EG, Matthews MD. Malacoplakia: an unusual etiology of ureteral obstruction. *Obstet Gynecol*. 1982;60(1):134-136.
878. Dretler SP, Young RH. Stone granuloma: a cause of ureteral stricture. *J Urol*. 1993;150(6):1800-1802.

879. Al-Khawaja M, Tan PH, MacLennan GT, et al. Urteral endometriosis: clinicopathological and immunohistochemical study of 7 cases. *Hum Pathol.* 2008;39(6):954-959.
880. Demirkiran NC, Tuncay L, Duzcan E, et al. Subepithelial haematoma of the renal pelvis (Antopol-Goldman lesion). *Histopathology.* 1999;35(3):282-283.
881. Kim SJ, Ahn HS, Chung DY, et al. Subepithelial hematoma of the renal pelvis simulating neoplasm (Antopol-Goldman lesion). *Urol Int.* 1997;59(4):260-262.
882. Carr RA, Newman J, Antonakopoulos GN, Parkinson MC. Lesions produced by the extravasation of urine from the upper urinary tract. *Histopathology.* 1997;30(4):335-340.
883. Fromowitz FB, Steinbook ML, Lautin EM, et al. Inverted papilloma of the ureter. *J Urol.* 1981;126(1):113-116.
884. Kyriakos M, Royce RK. Multiple simultaneous inverted papillomas of the upper urinary tract. A case report with a review of ureteral and renal pelvic inverted papillomas. *Cancer.* 1989;63(2):368-380.
885. Fernandez PL, Nogales FF, Zuluaga A. Nephrogenic adenoma of the ureter. *Br J Urol.* 1991;68(1):104-105.
886. Gokaslan ST, Krueger JE, Albores-Saavedra J. Symptomatic nephrogenic metaplasia of ureter: a morphologic and immunohistochemical study of four cases. *Mod Pathol.* 2002;15(7):765-770.
887. Kunze E, Fischer G, Dembowski J. Tubulo-papillary adenoma (so-called nephrogenic adenoma) arising in the renal pelvis. Report of a case with a critical consideration of histogenesis and terminology. *Pathol Res Pract.* 1993;189(2):217-225, discussion 225-227.
888. Martinez-Pineiro L, Hidalgo L, Picazo ML, et al. Nephrogenic adenoma of the renal pelvis. *Br J Urol.* 1991;67(1):101.
889. Seibel JL, Prasad S, Weiss RE, et al. Villous adenoma of the urinary tract: a lesion frequently associated with malignancy. *Hum Pathol.* 2002;33(2):236-241.
890. Cubillo E, Hesker AE, Stanley RJ. Cavernous hemangioma of the kidney: an angiographic-pathologic correlation. *J Can Assoc Radiol.* 1973;24(3):254-256.
891. Uchida M, Watanabe H, Mishina T, Shimada N. Leiomyoma of the renal pelvis. *J Urol.* 1981;125(4):572-574.
892. Fukunaga M, Nikaido T. Solitary fibrous tumour of the renal peripelvis. *Histopathology.* 1997;30(5):451-456.
893. Madi R, Gokden N, Greene G. Granular cell tumour of the ureter: first case reported. *Can Urol Assoc J.* 2009;3:156-158.
894. Herawi M, Parwani AV, Edlow D, et al. Glomus tumor of renal pelvis: a case report and review of the literature. *Hum Pathol.* 2005;36(3):299-302.
895. Chabrel CM, Hickey BB, Parkinson C. Pericaliceal haemangioma-a cause of papillary necrosis? Case report and review of 7 similar vascular lesions. *Br J Urol.* 1982;54(4):334-340.
896. Edward HG, Deweerd JH, Woolner LB. Renal hemangiomas. *Proc Staff Meetings Mayo Clin.* 1962;37:545-551.
897. Nasu M, Hamasaki K, Kishi H, Matsubara O. Nephrogenic adenoma of the ureter with gastric metaplasia. *J Urol Pathol.* 1997;7:63-69.
898. Werner JR, Klingensmith W, Denko JV. Leiomyosarcoma of the ureter: case report and review of literature. *J Urol.* 1959;82(1):68-71.
899. Scharifker D, Chalasani A. Ureteral involvement by malignant lymphoma. Ten years' experience. *Arch Pathol Lab Med.* 1978;102(10):541-542.
900. Maeda K, Hawkins ET, Oh HK, et al. Malignant lymphoma in transplanted renal pelvis. *Arch Pathol Lab Med.* 1986;110(7):626-629.
901. Kochevar J. Adenocarcinoid tumor, goblet cell type, arising in a ureteroileal conduit: a case report. *J Urol.* 1984;131(5):957-959.
902. Peterson NE. Adenoma of ileal urinary conduit. *J Urol.* 1984;131(6):1171-1172.
903. Geller SA, Lin C. Ureteral obstruction from metastatic breast carcinoma. *Arch Pathol.* 1975;99(9):476-478.
904. Recloux P, Weiser M, Piccart M, Sculier JP. Ureteral obstruction in patients with breast cancer. *Cancer.* 1988;61(9):1904-1907.